GPO PRICE $ _____

CSFTI PRICE(S) $ _____

Hard copy (HC) 8.51

Microfiche (MF) 2.75

ff 653 July 65

NASA TT F-9378

NASA TT F-9378

AUTOMATIC CONTROL OF GUIDED MISSILES

Yu. P. Dobrolenskiy, V. I. Ivanova
and G. S. Pospelov

Translation of "Avtomatika upravlyayemykh snaryadov"
Oborongiz, 548 pp., Moscow, 1963

FACILITY FORM 602

N65-32957 (ACCESSION NUMBER)	(THRU)
551 (PAGES)	1 (CODE)
(NASA CR OR TMX OR AD NUMBER)	31 (CATEGORY)

NATIONAL AERONAUTICS AND SPACE ADMINISTRATION
WASHINGTON APRIL 1965

AUTOMATIC CONTROL OF GUIDED MISSILES

Yu. P. Dobrolenskiy
V. I. Ivanova
G. S. Pospelov

OBORONGIZ
Moscow 1963

UDC 62-50(075.8):623.451.8

ANNOTATION

32957

/2

This book is concerned with the automatic control of guided missiles. The problems associated with the automatic control of guided missiles of various classes are solved by the application of engineering design methods developed by the theory of automatic control for linear and nonlinear dynamic systems.

Various principles are considered for obtaining control signals using different methods of tracking. The fundamentals of missile control dynamics and typical control systems are described. Analytical expressions are presented for designing tracking systems and for determining the errors of these systems.

The book is designed to serve as a textbook for university students. At the same time it will be useful to engineers and technicians who specialize in the field of the automatic control of guided missiles.

author

Numbers given in the margin indicate the pagination in the original foreign text.

CONTENTS

		Page
PREFACE		vii
CHAPTER 1.	GENERAL INFORMATION ON GUIDED MISSILES	1
1.1.	Basic Concepts and Definitions	1
1.2.	Methods of Generating the Control Force	5
1.3.	Engines for Guided Missiles	13
1.4.	Modern Guided Missiles	16
CHAPTER 2.	SOME MATHEMATICAL METHODS FOR INVESTIGATING AUTOMATIC CONTROL SYSTEMS	26
2.1.	General Information	26
2.2.	The Method of Standard Coefficients	27
2.3.	The Method of Logarithmic Amplitude-Frequency Characteristics	34
2.4.	Brief Remarks on the Theory of Nonstationary Linear Systems	54
2.5.	Statistical Dynamics of Linear Systems	57
2.6.	Method of the Phase Plane for Analyzing Relay Systems	71
CHAPTER 3.	CONTROL SIGNALS FOR HOMING GUIDANCE	96
3.1.	Forms of Energy Which Can be Utilized. Active, Semiactive and Passive Homing Devices	96
3.2.	Sensors Used in Infrared Homing Guidance Heads	97
3.3.	Coordinates of the Infrared Homing Guidance Head	105
3.4.	Comparison of the Passive, Active and Semiactive Radar Homing Heads	110
3.5.	Obtaining the Error Signal in Radar Heads	111
3.6.	Formation of the Control Signal	113
3.7.	Interferences in Radar Heads	117
3.8.	Generation of Control Signals for Various Methods of Homing Guidance	119
CHAPTER 4.	CONTROL SIGNALS IN EXTERNAL GUIDANCE	127
4.1.	Radio Beam Guidance of Missiles	127
4.2.	Command Guidance System	135
4.3.	Radar Stations for Detecting Aerial Targets	143
4.4.	Missile Guidance Using the Methods of Radio Navigation	150

		Page
CHAPTER 5.	CONTROL SIGNALS IN SELF-CONTAINED GUIDANCE	154
5.1.	General Information	154
5.2.	Sensors for Measuring the Angular Position of the Missile's Axes	155
5.3.	Angular Velocity Sensors	159
5.4.	Combined Gyroscope Sensors	162
5.5.	Sensors for Linear Accelerations of the Missile's Center of Gravity (Accelerometers)	164
5.6.	Air Speed Sensors or Sensors of Ram Compression	165
5.7.	Altitude Sensors	166
5.8.	Determining the Ground Speed	170
5.9.	Inertial Systems of Navigation	178
CHAPTER 6.	THE HANDLING OF CONTROL SIGNALS ABOARD MISSILES	192
6.1.	General Information	192
6.2.	Smoothing and Filtering of Signals	192
6.3.	Differentiation and Integration of Signals	198
6.4.	Summation of Signals	205
6.5.	Transformation of Coordinates	208
CHAPTER 7.	AMPLIFIERS AND ACTUATORS USED IN MISSILE GUIDANCE SYSTEMS	210
7.1.	Magnetic Amplifiers	210
7.2.	Vacuum Tube and Semiconductor Amplifiers	213
7.3.	Actuators with Electric Motors	216
7.4.	Hydraulic Actuators	220
7.5.	Pneumatic Actuators	223
CHAPTER 8.	MATHEMATICAL DESCRIPTION OF MOTION	226
8.1.	Systems of Coordinates	226
8.2.	General Equations of Motion of a Missile Assuming That It Is a Rigid Body	229
8.3.	Reduction of Generation Equations of Motion of a Missile to a Simpler Form	234
8.4.	Equations for the Longitudinal Motion of the Missile Obtained by the Method of Linearization and Their Analysis	239
8.5.	Equations and Analysis for the Lateral Motion of a Missile Obtained by the Method of Linearization	251
8.6.	Equations for the Longitudinal Motion of a Missile Obtained by the Method of Grouping	259
8.7.	Equations for the Lateral Motion of a Missile Obtained by the Method of Grouping	261

		Page
CHAPTER 9.	THE STRUCTURE OF AUTOMATIC PILOTS	264
9.1.	General Information	264
9.2.	Functional Diagrams of Automatic Pilots	265
9.3.	Examples of Automatic Pilot Systems for Controlling Missiles	271
9.4.	Automatic Pilot Using Relays	275
CHAPTER 10.	CONTROL OF MOTION OF A MISSILE WITH RESPECT TO ITS CENTER OF GRAVITY	277
10.1.	General Information	277
10.2.	Lateral Motion of a Missile with Cruciform Wings When the Control Surface is Deflected	277
10.3.	Longitudinal Motion of a Missile When the Control Surface is Deflected	286
10.4.	Lateral Movement of a Tilted Missile with Plane Wings	288
10.5.	Control of the Yaw Angle of a Missile with Cruciform Wings	293
10.6.	Control of the Pitch Angle of a Missile	302
10.7.	Control of a Yaw Angle of a Missile with Plane Wings	305
10.8.	Control of Motion with Respect to the Center of Gravity of a Missile with Variable Velocity	309
10.9.	Control of the Tilt Angle of a Missile by Means of Relay Automatic Pilots	314
10.10.	Self-Adaptive Missile Guidance Systems	326
CHAPTER 11.	CONTROL OF THE MOTION OF THE CENTER OF GRAVITY OF A MISSILE WITH RESPECT TO A GIVEN TRAJECTORY	334
11.1.	General Information	334
11.2.	Control of the Center of Gravity of a Missile with Cruciform Wings during Lateral Motion	334
11.3.	Control of the Center of Gravity of a Plane-Winged Missile during Lateral Motion	347
11.4.	Control of the Longitudinal Motion of the Missile's Center of Gravity	355
11.5.	Control of the Center of Gravity when the Velocity of the Missile is Variable	360
CHAPTER 12.	THE MOTION OF A MISSILE IN A DISTURBED ATMOSPHERE	364
12.1.	General Information	364
12.2.	Mathematical Description of a Disturbed Atmosphere	364
12.3.	Controlling the Motion of a Missile in a Disturbed Atmosphere	373

Page

12.4. The Effect of the Constant Wind Component on the Motion of a Missile 380
12.5. The Effect of a Random Wind Component on the Motion of the Missile 391

CHAPTER 13. DYNAMICS OF HOMING MISSILES 402

13.1. Kinematic Trajectories of Homing Guidance 402
13.2. The Equation of Motion for Missiles with Homing Guidance 420
13.3. The Dynamics of Missile Homing Guidance during Parallel Approach 425
13.4. The Dynamics of Homing Guidance in the Pursuit Method 441

CHAPTER 14. THE DYNAMICS OF EXTERNALLY GUIDED MISSILES 455

14.1. Formulation of the Problem 455
14.2. The Kinematic Trajectories of the Beam Method 456
14.3. Dynamics of Guiding the Missile Along the Beam 458
14.4. Dynamics of the Beam Method during Visual Sighting 461
14.5. Placing the Missile on the Beam 465
14.6. Missile Guidance by Means of Radar Stations and Radio Navigation Systems 472

CHAPTER 15. THE DYNAMICS OF MISSILES WITH SELF-CONTAINED GUIDANCE SYSTEMS 484

15.1. Control and Guidance of Airplane Missiles by Means of Inertial Systems 484
15.2. The Flight Trajectory of a Short Range Ballistic Rocket (L = 500-1000 km) 491
15.3. Flight Trajectories of Long-Range Ballistic Rockets (L > 1000 km) 494
15.4. The Range of a Ballistic Rocket 500
15.5. Errors in Range of Long-Range Ballistic Missiles 502
15.6. The Active Region of the Ballistic Rocket Trajectory 505
15.7. Automatic Control of Rocket Flight over the Active Region 513
15.8. Controlling the Range of a Ballistic Missile 520

CHAPTER 16. MISSILE GUIDANCE SYSTEMS AND METHODS OF EVALUATING THE FIRING ACCURACY 523

16.1. General Information 523
16.2. Homing Guidance Systems 524
16.3. External Missile Guidance Systems 531

REFERENCES 541

PREFACE /3

At the present time, missiles of the most diverse types have control systems which improve their firing accuracy. The control system forms a closed loop for the control signals and for the feedback signals. This loop is characteristic of automatic control systems whose theory has been developed with sufficient completeness. In evaluating the effectiveness of any control system, the nature of the dynamic processes which take place in it is of paramount significance. The methods developed in the theory of automatic control make it possible to solve problems associated with the analysis of missile control systems.

The book presents the theoretical principles associated with automatic control systems. The first two chapters present general information on guided missiles and consider briefly the basic mathematical methods necessary to solve the problems of automatic control.

Chapters 3-7 present methods for obtaining control signals during various methods of tracking missiles and the transformation and amplification of these signals. Finally, the driving mechanisms for the control elements of missiles are described, based on data published in the Soviet and foreign literature.

Chapters 8-12 generalize the problems associated with the dynamics of missile motion with respect to its center of gravity, as well as the dynamics of controlling the missile's center of gravity with respect to a given trajectory.

Chapters 13-15 analyze the motion of the missile's center of gravity for different methods of tracking; the purpose of this analysis is to obtain expressions for the miss distance of a missile.

The concluding Chapter 16 describes integrated missile control systems /4
and the method of establishing their accuracy.

Specific examples of control systems are taken from the foreign literature.

Chapters 1, 8, 11, 12 and sections 1-5 of Chapter 2, sections 1-3 of Chapter 9 and sections 1-9 of Chapter 10 were written by Dobrolenskiy. Chapters 3, 4, 6, 7 and sections 1-8 of Chapter 5 were written by Ivanova. Chapters 13-16, section 9 of Chapter 5 and section 10 of Chapter 10 were written by Pospelov; section 6 of Chapter 2, section 4 of Chapter 9 and section 9 of Chapter 10 were written by Pospelov in collaboration with N. K. Bodunov.

The authors request that reader comments concerning this work be addressed to: Moscow I-51 Petrovka, 24, Oborongiz.

CHAPTER 1. GENERAL INFORMATION ON GUIDED MISSILES /5

Section 1.1. Basic Concepts and Definitions

In the last decade the rapid development of automation, electrical engineering and other scientific and engineering disciplines has produced a new powerful weapon--the guided missile. Guided missiles were first used during World War II.

Every missile, whether it is controlled or not, is fired from a special launching device. In the case of an artillery shell, this launching device is the gun barrel, for an aerial bomb it is the bomb shackle, while for a rocket it is a launching pad, etc. The firing accuracy for unguided missiles is determined by the accuracy of aiming, i.e., the accuracy in computing and realizing the required direction of the missile during firing. While aiming, insofar as possible, all of the factors are considered which determine the impact point of the missile: the velocity of the target and of the missile, wind velocity, temperature and density of the air along the trajectory, etc. Nevertheless, in the majority of cases the firing accuracy for unguided missiles is insufficient. The impact errors may be classified in the following manner:

(1) sighting errors; these include methodical errors which occur because most of the sights give only an approximate solution to the problem of missile impact at the target. This class also includes instrument errors due to imperfections in sights;

(2) random errors due to many reasons of a random nature with respect to the sighting process; these include errors due to unavoidable spread in the parameters of the missiles and of their launching ramps, human error and unaccounted external factors (change in wind, temperature and air density), /6
which affect the missile after it is fired and also the possible maneuvers of the target after firing, which differ from those assumed during sighting.

The frequent insufficient accuracy of unguided missiles may be confirmed by the following examples:

(1) the low probability with which antiaircraft shells hit an airplane;

(2) low effectiveness of the gun armament of an airplane; for this reason the firing from one airplane to another is effective only over a short distance;

(3) low accuracy of bombing surface targets from an airplane; to destroy a small target, e.g., a bridge, it is necessary to drop several tens and sometimes several hundreds of bombs.

When guided missiles are used, the firing accuracy is substantially increased. We define a guided missile as one equipped with a control system which can vary its trajectory after the missile has been launched. The control system is defined to include all technical devices used to measure the trajectory of the missile in order to increase its accuracy. This system includes various sensing means, both on the missile and at the surface, which determine the missile's position in space with respect to its target, methods of transforming and transmitting signals as well as control elements which directly affect the flight of the missile. In some cases the control system operates during the entire period of flight, while in others it is operative only over definite regions of the trajectory. The operation of the control system results in sharp increase in firing accuracy.

Thus, the combat effectiveness of guided missiles is substantially greater than that of unguided missiles. However, the application of guidance makes the missiles more complicated and increases their cost. But with the high accuracy of guided missiles the total cost of hitting certain targets becomes substantially less than is the case with unguided missiles.

The application of guided missiles also has certain additional advantages. For example, the increase in firing accuracy makes it possible to hit targets with guided missiles from substantially greater distances than with unguided missiles. The large firing range makes it difficult to destroy launching pads or objects (airplanes, ships, mobile launchers) used to launch the guided missiles. As a second example of the additional advantages of guided missiles, we cite the possibility of decreasing the sighting accuracy in some cases, which is particularly important when firing from airplanes. Finally, when we /7
fire on moving targets, the probability of hitting the targets with an unguided missile may be so small that it is impossible to fire enough shots to hit it while within range of the weapon. Due to the higher probability of hitting a target with a guided missile, the number of shots and the time necessary to hit a target are decreased.

As we have pointed out, the control system changes the trajectory of the missile to approach the target as closely as possible. To change the trajectory of any body, it is necessary to apply an additional force to this body, which in our case we shall call the control force. Figure 1.1, e.g., shows the trajectory of an uncontrolled (broken line) and controlled (solid line) aircraft rocket. Due to sighting error, the uncontrolled missile would miss the target (ship). The variation in the trajectory of the guided missile is due to control force F produced by the control system. The methods of producing the control force and their technical realization are considered in section 1.2.

In spite of the diversity of technical methods used to control missiles, /8
we can name only three methods of control which differ in principle: self-contained guidance, external guidance and homing guidance. These methods differ in how and where signals are obtained to control the flight of the missile.

In a system with self-contained guidance, the control signals are developed by equipment contained entirely within the missile; after launching,

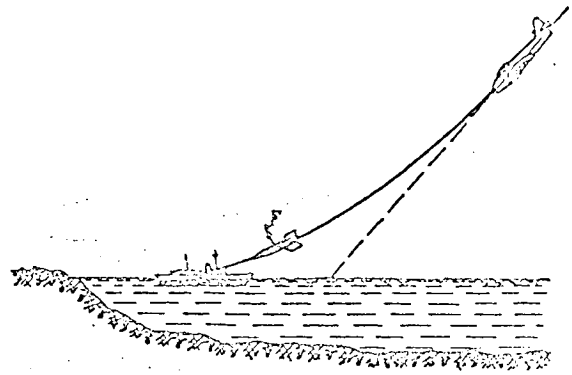

Figure 1.1. Variation in trajectory of missile under action of controlling force.

this equipment receives no information from the point of launching or from the target. In self-contained guidance systems, two principles for obtaining the control signals can be used. It is possible to compute the variation of certain parameters (velocity, slope of the trajectory, course, etc.) with time; these determine the trajectory of the missile as it moves to its target. The functions of time which are obtained are introduced into the control system of the missile in the form of a program. The true values of these parameters are measured continuously by means of sensors, and the control system eliminates the discrepancy between the programmed and actual parameters of motion. In particular, the missile may be assigned a definite flight trajectory, and the control system will keep the missile on this trajectory. Self-contained control of this type is called programmed control.

However, the self-contained guidance of a missile may be carried out by using a different principle. Let us assume that the missile is equipped with instruments to measure continuously its coordinates in space. This equipment may be purely inertial or it may be inertial with compensation, achieved by using terrestrial or astronomical points of reference. The coordinates of this missile, which are established by this equipment, are introduced into a computer aboard the missile and form the control signals which guide the missile to its target when the coordinates of the latter are known.

This method of obtaining control signals differs from programmed control by the absence of preassigned time functions at the input to the control system. In this case, a fixed trajectory is not assigned and a new trajectory passing through the target is computed in each case, depending on the true coordinates of the missile.

As we can see from this description, the method of self-contained control is applicable to missiles which are primarily concerned with fixed targets. When the target moves, its future coordinates must be known beforehand with sufficient accuracy for the period of missile flight.

In the method of external guidance, the coordinates of the target and of the missile are measured continuously at the control point, where signals are developed for the control of the missile guidance system. This system must vary the trajectory of the missile in such a way that it meets its target. In a variation of this method the control signals are formed on the missile itself, but always by the energy received from the control point. It is clear that the use of external guidance to obtain control signals does not, in principle, create any limitations on the movement of the target or of the control point. /9

In homing guidance the control signals are developed in the missile itself by radiation or reflection of some form of energy by the target. This isolates the target on the surrounding background. Thus, in homing guidance the coordinates of the target with respect to the missile are measured by equipment on the missile, and the control system uses these data to direct the missile to its target.

These methods of missile guidance may be applied over the entire trajectory of the missile or over part of it. In some cases different methods are used over different regions of the trajectory. Thus, over a large part of its trajectory the missile may be subjected to self-contained control, while at the final stage of flight homing guidance may be used to increase accuracy. Finally, it is possible to have a case using different methods to control various parameters of motion over the same region of the trajectory.

In concluding this section, we present the common classification of guided missiles associated with the launching point and the target point. The launching point determines the general conditions for using a missile. The location of the target determines to some extent its nature and consequently the practical assignment of the missile. On the basis of this principle, guided missiles are divided into the following classes:

(1) surface-to-surface missiles

(2) surface-to-air missiles

(3) air-to-surface missiles

(4) air-to-air missiles.

The first word in each class refers to the launching point of the missile, while the last word refers to the location of the target. In this classification the term "surface" refers to dry land as well as to water.

The need for the classification of guided missiles stems from the fact that there is a very large number of different types of missiles in existence today. Guided missiles are used in all forms of warfare and are designed to solve the most diverse strategic and tactical problems.[1] To illustrate this we enumerate various forms of guided missiles:[2]

---

[1] V. I. Marisov and I. K. Kucherov, "Guided Missiles," Voyenizdat, 1959.
[2] Examples of specific missiles are presented in section 1.4.

(1) ballistic rockets /10

(2) airplane missiles

(3) guided aerial bombs

(4) guided antiaircraft missiles

(5) aerial combat guided missiles

(6) guided missiles used on the battlefield (antitank missiles, anti-infantry missiles).

In addition to these guided missile types, whose trajectory passes through the Earth's atmosphere, there are several types of guided missiles which move to their target underwater. These missiles are not considered in this book.

Section 1.2. Methods of Generating the Control Force

Any moving body describes some trajectory in space whose form is determined entirely by the initial conditions and by the forces acting on the body during its motion. In the general case, a missile in flight is subjected to the following forces: thrust of the engine, force of gravity and aerodynamic forces.[1] To change the flight trajectory of a missile it is necessary to vary the magnitude or direction of these forces (or both at the same time), because it is not possible to apply any other kind of a force to a missile in flight. The variation of forces acting on a missile is performed by the control system, which supplies a control force of desired magnitude and direction. This force must be perpendicular to the flight trajectory and thus be situated in a plane in which the flight trajectory of the missile must be changed.

Because most of the guided missiles fly in the lower layers of the atmosphere where the aerodynamic forces play the principal role in developing a control force, we shall briefly consider the basic aerodynamic forms of missiles. As a rule, modern missiles travel at supersonic velocities. The frame of the missile, therefore, usually has the form of a body of revolution with a sharp nose. Missiles may be without wings (but with stabilizers), with flat wings, with cruciform wings or with annular wings. The various forms of missiles are shown in figure 1.2.

A missile is said to be aerodynamically symmetric if the aerodynamic forces /11
do not vary when it rotates around its longitudinal axis. It is clear that wingless missiles and missiles with annular wings possess complete aerodynamic symmetry. In the case of a missile with cruciform wings, the aerodynamic forces vary insignificantly when the missile rotates around its longitudinal axis. The greatest asymmetry is characteristic of missiles with plane wings.

---

[1] In principle the thrust is also an aerodynamic force, and it is listed separately merely to make our presentation more convenient.

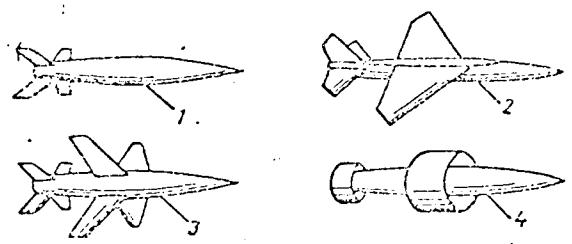

Figure 1.2. Aerodynamic forms of missiles: 1--wingless, 2--with plane wings, 3--with cruciform wings, 4--with annular wings.

At the present time two methods are used to generate a control force:

(1) rotation of the missile frame around the center of gravity by means of control surfaces;

(2) rotation of the wings with respect to the frame or use of an auxiliary engine whose thrust is normal to the flight trajectory (direct method).

The first method is most commonly used. Its technical realization depends on the aerodynamic shape of the missile. As a first example, let us consider the missile with cruciform wings for obtaining the control force. Figure 1.3 shows the forces acting on a missile in horizontal flight with constant velocity V. The sum of thrust P, gravity G, lift force of the wings and of fuselage Y and of control surface Y_c and of drag X is equal to zero. The moment produced by all forces with respect to the missile's center of gravity is also equal to zero. Due to these conditions, the missile undergoes a uniform rectilinear flight. The lift force Y is produced by the angle of attack α of the wings and the fuselage, while the lift force of the control surface is due to the angle of attack of the control surface, which is equal to $\delta - \alpha$.

If the control surfaces of the missile are deflected by some angle $\Delta\delta$ in clockwise direction (fig. 1.4), the negative lift force of the control surface will be increased by an amount ΔY_c. The missile will begin to rotate around its center of gravity and increase its angle of attack. This rotation will stop when the angle of attack has increased by an amount $\Delta\alpha$, such that the increase in the lift force of the wing and of the fuselage ΔY[1] again reduces the moment of forces, with respect to the missile's center of gravity, to zero. However, the projection of the forces along the normal to the direction of flight will /12 no longer be equal to zero, but will be equal to $\Delta Y - \Delta Y_c$.[2] Since the area of the

[1]To simplify our presentation flight velocity V is assumed to be constant.
[2]We do not take into account the small increase in the projection of thrust P on the normal to the flight trajectory.

wings is usually much greater than the area of the control surfaces, the increase in the lift force produced by the wing turns out to be much greater than the increase in the lift force of the control surfaces. It is precisely this increase in the lift force of the wing ΔY (which may exceed weight G of the missile by several times and which is directed perpendicularly to the missile flight velocity vector), that is the control force in our case. By means of this force, which is obtained by the rotation of the missile with respect to its center of gravity, the flight trajectory of a plane-winged missile is changed in the vertical plane.

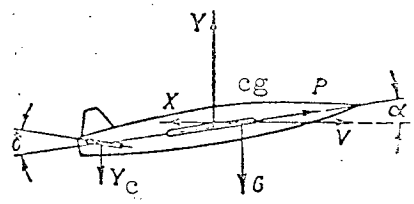

Figure 1.3. Forces acting on plane-winged missile in rectilinear flight (cg = center of gravity).

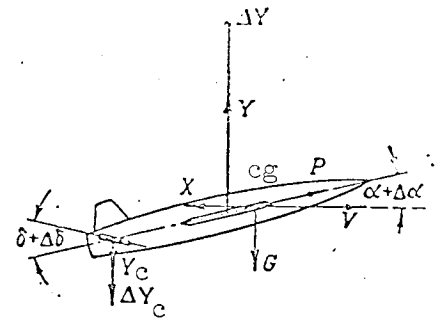

Figure 1.4. Forces acting on plane-winged missile when control surfaces are deflected.

In addition to the conventional position of control surfaces behind the wings, shown in figures 1.3 and 1.4, wide application is made of control surfaces placed in front of the wings. A plane-winged missile with a forward position of control surfaces is shown schematically in figure 1.5. The forward position of the control surface on the missile is convenient purely from the standpoint of design considerations: the control equipment and the drive for the control surfaces are situated in the forward part of the missile, because the tail end is usually occupied by the engine. The second advantage of having the control surfaces in front is that their lift forces and those of the wings are added rather than subtracted in this case.

For plane-winged missiles the control force in a horizontal plane is produced by rotation with respect to the longitudinal axis, i.e., by the tilt of the missile. Figure 1.6 shows the forces which act on a missile whose tilt angle is γ. Due to the tilt, the lift force produces a horizontal component ($Y \sin \gamma$), which is the control force changing the trajectory of the missile in the horizontal plane. It is clear that when the missile has a tilt moment, the vertical component of the lift force ($Y \cos \gamma$) decreases. To retain horizontal flight when the tilt angle γ is increased, it is also necessary to increase the angle of attack α, so that the resultant force is always equal to the weight of the missile G. Thus, in the final analysis control in the horizontal plane takes place because of increase in the angle of attack, i.e., because of the rotation of the missile with respect to its center of gravity. /13

To produce the tilt angle, both ailerons and control surfaces may be used if they are deflected in opposite directions. Sometimes the control surfaces of

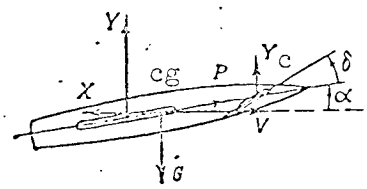

Figure 1.5. Forces acting on plane-winged missile with control surfaces placed in front of wings.

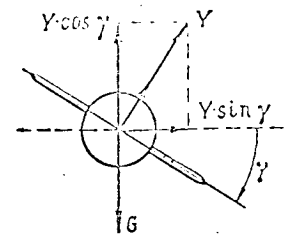

Figure 1.6. Forces acting on plane-winged missile during tilt.

plane-winged missiles are combined with ailerons (fig. 1.7). Such control elements are known as elevons. When the elevons are displaced in the same direction, they perform the function of the elevator, and when they are deflected in different directions, they perform the functions of ailerons.

Missiles with cruciform wings have wings and control surfaces situated in the horizontal and vertical plane (fig. 1.2). The control surfaces may be placed in front of the wings or behind them. It is clear that for missiles of this type the control force in the vertical and horizontal plane is actuated in the same manner as that of the plane-winged missile in the vertical plane.

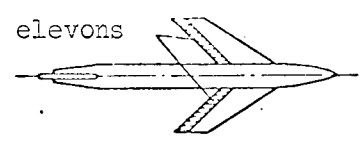

Figure 1.7. Plane-winged missile with elevons.

Missiles with annular wings use the same method of control as those with cruciform wings. The control surfaces of missiles with annular wings may also be of annular shape (fig. 1.2), which is free to rotate in two planes, due to the use of a Cardan's suspension, and to control the angle of rotation of the missile with respect to its center of gravity. It is possible to have a combination consisting of an annular wing with cruciform control surfaces.

In the case of a wingless missile, the control force is generated in a different manner (fig. 1.8). It is necessary to point out that wingless missiles are used as ballistic missiles, i.e., as missiles which move along the principal part of their trajectory because of inertia obtained by acceleration to a high velocity over an initial, relatively short section of the trajectory. Over this section of the trajectory (called active) the rocket engine, which accelerates the missile, is operative. The thrust of the engine is substantially greater than the atmospheric drag, so that the missile is accelerated. /14

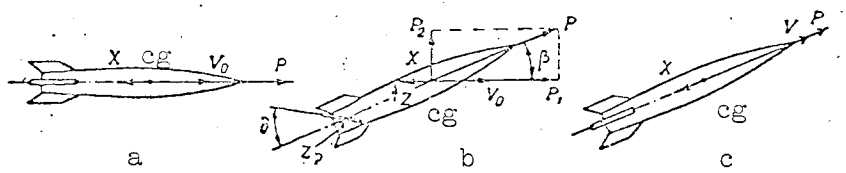

Figure 1.8. Forces acting on wingless missile.

Figure 1.8 shows three positions of a wingless missile and the corresponding forces which act on the missile. To make the presentation simple, we consider the motion in a horizontal plane where the force of gravity does not act. Therefore, during the rectilinear motion of the missile, the angles of attack and the deflection of the control surfaces are equal to zero (fig. 1.8a). By using the control surface, we rotate the frame of the missile by some angle, so that there is an angle of attack in the horizontal plane β (fig. 1.8b). As a result of this angle, a lateral aerodynamic force Z is produced, which is quite small because the missile has no wings. We do not consider the effect of this force on the motion of the missile, because it does not play a principal role in the control of a wingless missile. After the missile has turned, the control surface should be moved back into the neutral position. If the frame of the missile turns rapidly, then, initially, the velocity vector $\overline{V}_0$ retains its magnitude and position (fig. 1.8b).

In the following instant of time, due to the force component P_2, which is perpendicular to the velocity vector V_0, this vector will rotate until the missile moves in a straight line along a new direction (fig. 1.8c). It is clear that the condition for the rectilinear motion of the missile is the one in which the projection of all forces perpendicular to velocity vector V is equal to zero.

Thus, in the present case, the control force which changes the trajectory of a wingless missile is primarily the thrust component P_2, which is produced when the missile is rotated with respect to its center of gravity. This rotation of the missile in the dense layers of the atmosphere may be accomplished by means /15 of conventional aerodynamic control surfaces (fig. 1.8). However, the active section of the trajectory of ballistic missiles may terminate at a very high altitude. As the altitude is increased and the air density decreases, the effectiveness of aerodynamic control surfaces is decreased, and they cannot be used to control the rotation of the missile with respect to its center of gravity. In this case, the missile is equipped with a jet control surface, which operates in the gas jet of the reactive engine.

A control surface, made of heat-resistant material and placed in a gas jet, is subjected to the aerodynamic forces produced by this jet (fig. 1.9). The lift force of the control surface Y_{cs} produces a moment around the center of

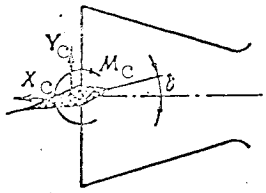

Figure 1.9. Forces acting on control surface in gas jet.

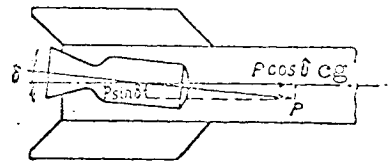

Figure 1.10. Generation of moment with respect to center of gravity of missile by rotating combustion chamber of engine.

gravity of the missile. The drag X_{cs} characterizes the loss in thrust produced by the control surface in the gas jet. The moment M_{cs} is the hinge moment, which is overcome by the driving force on the control surface and does not produce an effect on the missile. Sometimes a wingless missile is controlled by rotating the combustion chamber by means of an auxiliary rocket engine (fig. 1.10), which produces a force component P sin δ. This component produces a moment, with respect to the center of gravity, which causes the missile to rotate, as in the case where the control surface in the gas jet is deflected.

In both cases the force produced by the deflection of the gas control surface or by the rotation of the combustion chamber is directed perpendicular to the trajectory of flight. However, it cannot be considered the control force: this force is too small and therefore produces no significant change in the trajectory. The principal role of this force, as we have indicated, is to rotate the missile with respect to its center of gravity.

All of these principles for producing a control force are associated with the initial rotation of the missile with respect to its center of gravity. This rotation produces a control force and changes the direction of motion of the missile. When a direct method is used to produce a controlling force, it is not /16 necessary to change the angular position of the missile, and it is not, therefore, necessary to have control surfaces. The control force may be produced by aerodynamic as well as by reactive forces. The aerodynamic forces are used to guide missiles with trajectories not outside the relatively dense layers of the atmosphere.

To regulate the control force, the wings of the missile are designed so that they can be rotated (fig. 1.11). They are situated in such a way that their lift force is as close as possible to the center of gravity of the missile. The wings are rotated by a powerful actuator which responds to control signals. Such missiles are equipped with a sufficiently developed empennage, so that the longitudinal axis of the missile practically coincides with the direction of the velocity vector. During rectilinear flight in a horizontal plane the wings are situated along the axis of the frame, and their angle of attack as well as the angle of attack of the frame are equal to zero. When the wings are rotated with respect to the frame, an angle of attack is developed together with the control

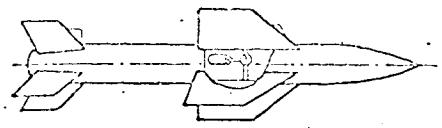

Figure 1.11. Missile with rotatable wings.

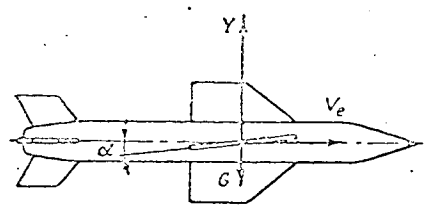

Figure 1.12. Control force of missile with rotatable wings.

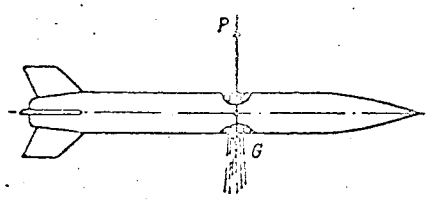

Figure 1.13. Missile with lateral reactive thrust.

force, which is normal to the velocity vector of the missile (fig. 1.12). This force produces the rotation of the missile's velocity vector and changes its trajectory. In this case the longitudinal axis of the missile is continuously oriented with respect to the velocity vector.

At high altitudes the wings, like the control surfaces, become ineffective and cannot produce a substantial control force. In this case, to produce a control force, we may use a reactive engine with a lateral thrust (fig. 1.13). The axis of the side nozzles is placed as near as possible to the center of gravity, so that the operation of the engine does not produce a moment which turns the frame with respect to the center of gravity. The magnitude of the side force is controlled by the distribution of the ejected gases through the side nozzles. It is important to point out that the control of a missile by means of lateral /17 thrust is the only method that can be used at high altitudes, if the main reactive engine is no longer operating and the missile is moving due to its inertia. This method of controlling the trajectory is used by cosmic rockets.

The principal advantage of regulating the control force directly, compared with the method of control where the missile is rotated with respect to its center of gravity, is the small delay in the generation of the control force after the control signal is received. The time required to rotate the wings of a missile or to change the flow of gas through the side nozzles is substantially less than the time required to rotate the missile with respect to its center of gravity. For certain types of highly maneuverable missiles, this advantage may be quite significant.

The disadvantage of the control system which rotates the wings is the high power required to actuate the wings. In addition, it is difficult in either method to get this force to coincide with the center of gravity during the entire flight period of the missile.

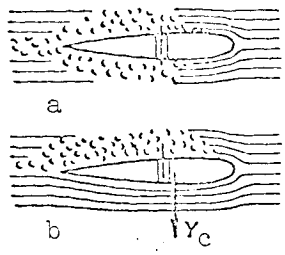

Figure 1.14. Schematic representation of lift force developed when spoiler is moved out.

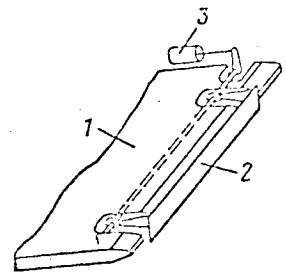

Figure 1.15. Spoiler installed behind trailing edge of profile. 1--profile, 2--spoiler, 3--actuator.

In addition to these conventional control elements, missiles are sometimes equipped with special control devices--flow interruptors or spoilers. The principle of operation of a spoiler is illustrated in figure 1.14. A spoiler, installed on the profile of the missile stabilizer, may be moved out into either direction by means of some driving mechanism. When its position is symmetric (fig. 1.14a), the spoiler impairs the flow around the profile and increases its drag, but does not produce a lift force on the profile. When the position of the spoiler is asymmetric (fig. 1.14b), the flow over one side of the profile (where the spoiler is removed) is improved and the pressure on this side is decreased, while on the other side (where the spoiler comes out further) the disruption of the flow and the pressure increase. As a result of this, a lift force Y_{cs} is produced which causes the missile to rotate just like a conventional control surface. Sometimes a spoiler is installed behind the trailing edge and not inside the profile (fig. 1.15), but in this case its action is the same as in the first case. If the spoiler is installed behind the wings and not behind the stabilizer, then its displacement will produce an effect which is analogous to the rotation of the wing, i.e., we have a direct regulation of the force which controls the missile.

Usually spoilers are deflected into their extreme positions, which makes it possible to use simple drivers of the relay type. The power required to actuate spoilers as a rule is substantially less than the power required to actuate control surfaces. The disadvantages of spoilers include the increase in the drag of the missile, associated with the deterioration of the flow around the profile containing the spoiler. /18

The control of a missile in two planes--vertical and horizontal--is purely conditional for some types of missiles. This operation is significant for plane-winged missiles and for missiles with tilt stabilization when the rotation of the missile around its longitudinal axes is not permissible. However, many missiles do not have stabilization of this type and may occupy an arbitrary position with respect to their longitudinal axes. For missiles of this type, the control planes coincide with the planes containing the control elements at the particular instant of time. Finally, some missiles spin around their longitudinal axes. In this case, it is rational to consider one spatial picture of the forces acting on the missile, rather than the forces in two planes.

Section 1.3. Engines for Guided Missiles

All types of guided missiles (except aerial bombs) are equipped with engines designed either to accelerate the missile to a definite velocity or to maintain a given velocity during the entire flight of the missile. The large variety of guided missiles and of the conditions for their use has resulted in the application of all known types of reaction engines. A reaction engine is one in which the thrust is produced directly, without mechanical elements between the engine and the ejected air mass. In reaction engines, this force is the reaction of the jet leaving the nozzle of the engine at high velocity. In /19 nonreaction engines, the thrust is produced indirectly, because an intermediate element (the air propeller) exists between the engine and the ejected air mass. Missiles utilize reaction engines exclusively, because only these can provide the high flight velocities. In addition, at altitudes where air density is low, the reaction engine (in particular a rocket engine) is the only type of engine capable of developing the large thrust necessary to control the missile.

Reaction engines may be divided into two basic groups: air-breathing jet engines and rocket engines. In air-breathing engines, fuel combustion is accomplished by using the oxygen obtained from the atmosphere surrounding the engine. At high altitudes and in air-free space, engines of this type cannot operate. In a rocket engine, the fuel contains both components necessary for combustion: the combustible material and the oxidizer. Therefore, the origin of the gas jet which produces the thrust of a rocket engine is not associated with the presence of surrounding air. The largest thrust is obtained in air-free space.

Each of the two groups of reaction engines in turn consists of several types of engines. Air-breathing jet engines are of three types: turbojet engines, ramjet engines, and pulsejet engines. Rocket engines are subdivided into two types: engines utilizing solid fuel and engines utilizing liquid fuel.

Let us consider the principle of operation and the basic characteristics of each of these reaction engines. Figure 1.16 shows the schematic diagram of a turbojet engine. The air which enters through diffusor 1 is compressed by compressor 2. At the present time, axial and centrifugal compressors are used. Part of the compressed air enters combustion chamber 4, where it is mixed with the fuel (usually kerosene) introduced through fuel injection nozzle 3, where the mixture is burned. The products of combustion are mixed with the remaining part of the colder air flowing from the compressor and are directed to turbine buckets 5. As the gaseous products of combustion pass through the turbine, it begins to rotate and drives the compressor mounted on the same shaft. The hot gases passing through the turbine are ejected at high velocities into the atmosphere through nozzle 6. The reaction of the jet flowing from the nozzle of the engine produces the thrust of the engine.

The schematic diagram of a ramjet engine is shown in figure 1.17. A ramjet engine has no moving parts and is the simplest of the air-breathing jet engines. In a ramjet engine, the air is compressed due to the velocity of the air entering the engine. Consequently, it can begin to operate only when the

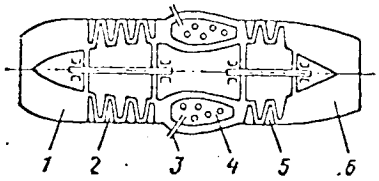

Figure 1.16. Schematic diagram of turbojet engine. 1--diffusor, 2--compressor, 3--fuel injection nozzle, 4--combustion chamber, 5--turbine, 6--nozzle.

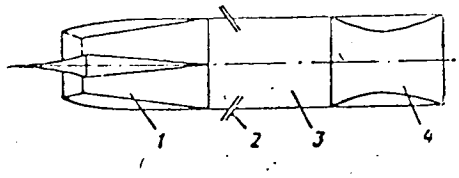

Figure 1.17. Schematic diagram of ramjet engine. 1--diffusor, 2--fuel injection nozzle, 3--combustion chamber, 4--nozzle.

flying machine on which it is installed already has a substantial velocity. Diffusor 1 decreases the air velocity entering the engine and converts a large part of the kinetic energy of the air into potential energy in the form of dynamic pressure. After being compressed in the diffusor, the air enters combustion chamber 3, in which fuel is injected simultaneously through nozzle 2. The mixture of air and fuel burns continuously in the combustion chamber. The hot gases formed in the combustion chamber flow out into the atmosphere through nozzle 4 at a velocity higher than the flow velocity past the engine. As a result the engine produces a thrust. /20

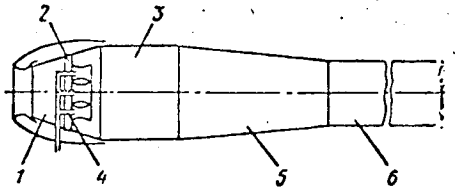

Figure. 1.18. Schematic diagram of pulsejet engine. 1--diffusor, 2--series of valves, 3--combustion chamber, 4--fuel injection nozzle, 5--nozzle, 6--exhaust tube.

The third type of jet engine is the pulsejet, represented schematically in figure 1.18. Input diffusor 1 compresses the air entering the engine during flight. As a result the air passes into combustion chamber 3 through a series of valves 2, which permit it to flow in only one direction. In the combustion chamber the air is mixed with the fuel flowing from fuel injection nozzle 4, and the mixture burns, forming hot gases. The pressure in the combustion chamber increases, which causes the valves to close. The products of combustion flow through nozzle 5 and exhaust tube 6 into the atmosphere with a velocity greater than that of the air entering the engine. Due to this, the engine develops thrust. As the gases leave through the exhaust tube, the pressure in the combustion chamber decreases until the valves open again, and the cycle is repeated. The pulsation frequency of an engine depends on its dimensions and varies from 40-250 cps. Unlike the ramjet engine, the pulsejet may develop a thrust even when the flight velocity is zero, i.e., during the launching of the device in which it is installed. This special feature of a pulsating engine is due to the presence of valves and the inertia of the gas mass which moves along a rather long exhaust tube.

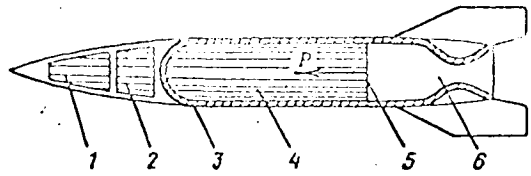

Figure 1.19. Rocket engine utilizing solid fuel installed in missile. 1--control system, 2--warhead, 3--engine case, 4--solid fuel, 5--combustion surface, 6--nozzle.

The principal shortcoming of a jet engine is that it requires surrounding air. The air density decreases rapidly with altitude. The limiting altitude at which any type of air-breathing jet engine can be used is of the order of 30-40 km.

A rocket engine utilizing solid fuel is the simplest type of reaction engine. The solid fuel consists of a homogeneous mixture of combustible material with an oxidizer. Existing engines use solid fuels of various chemical composition. Figure 1.19 shows a rocket engine utilizing solid fuel installed /21 in a missile. The case of engine 3, filled with solid fuel 4, simultaneously serves as the combustion chamber of the engine. As the solid fuel burns, the products of combustion are ejected with high velocity through nozzle 6 and thrust force P is exerted on the surface of solid fuel 5 (or on the front wall of the combustion chamber). Usually the burning time and, therefore, the operation time of the engine using solid fuel is 10-30 sec. The combustion chamber is therefore not cooled, even though the temperature in the combustion chamber is high. Sometimes the internal surface of the combustion chamber is covered with heat-resistant thermal insulation.

Liquid rocket engines usually use a two-component mixture consisting of a liquid combustible material and a liquid oxidizer. Such engines have two principal parts:

(1) one or several combustion chambers in which the liquid fuels undergo chemical reaction forming gases at high pressure and temperature, which flow out of the nozzle and produce the thrust;

(2) devices for supplying and atomizing the combustible mixture in the combustion chamber.

The combustible material and the oxidizer are supplied by means of turbine pumps or by utilizing the pressure of an inert gas in a gas accumulator. Figure 1.20 shows the schematic diagram of a liquid rocket engine installed in a missile. The combustible material 1 and oxidizer 2 are supplied to the fuel injection nozzle 6 of combustion chamber 7 by means of pumps 4. The pumps 4 are driven by gas turbine 3. The gases for driving the turbine are formed in the combustion chamber of turbogas generator 5, which is also supplied with a small /22 portion of fuel and oxidizer. To cool the combustion chamber walls, both fuel

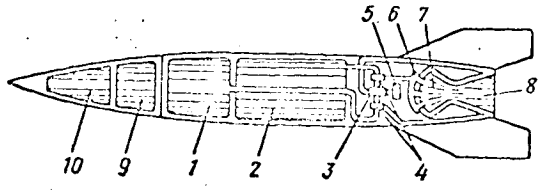

Figure 1.20. Liquid rocket engine installed in missile. 1--combustible substance, 2--oxidizer, 3--turbine, 4--fuel pumps, 5--turbine gas generator, 6--fuel injection nozzle, 7--combustion chamber, 8--nozzle, 9--warhead, 10--control system.

components are used. As shown in figure 1.20, these are supplied to the fuel injection nozzles through recesses in the walls of the combustion chamber. This cooling decreases thermal losses, and the engine is capable of operating for a longer period of time without damage to the combustion chamber. In addition to this method, liquid rocket engines use other cooling systems(e.g., evaporation system).

We pointed out that the basic advantage of rocket engines compared with jet engines is that their thrust does not depend on the presence of atmosphere. Consequently, rocket engines are not limited in altitude and are the only practical engines suitable for flight at high altitudes and for flight into cosmic space. The second significant advantage of a rocket engine, compared with all other engines, is its highest thrust per unit frontal area.

However, rocket engines have a substantial shortcoming which eliminates their use in aviation as the principal source of thrust. This shortcoming consists of high fuel consumption, associated with the necessity of carrying both fuel and oxidizer. Compared with jet engines which are used at low altitudes, rocket engines consume substantially more fuel for producing the same thrust.

Section 1.4. Modern Guided Missiles

Guided missile technology is developing very rapidly. In this section we give a brief description of some guided missiles developed in capitalistic nations.[1]

1. Ballistic Rockets. The term ballistic rocket is used for a missile whose trajectory is that of a freely thrown body (fig. 1.21), except over a short region when the rocket engine is operating. The launching of ballistic missiles is done from launching pads, usually in the vertical direction in order /23 to reduce the portion of the flight in the dense layers of the atmosphere. When

[1] V. I. Marisov and I. K. Kucherov, "Guided Missiles," Voyenizdat, 1959.

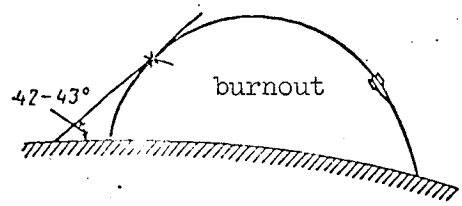

Figure 1.21. Trajectory of ballistic rocket.

the rocket achieves sufficient velocity, the control system produces rotation of the velocity vector in the firing plane by an angle of approximately 45° with respect to the horizon (for short-range rockets). When preassigned velocity and flight direction are achieved, the engine is turned off and the rocket continues its flight along a ballistic trajectory.

A large number of ballistic rockets has already been developed for various purposes. The range of ballistic missiles varies from several tens and several hundreds of km (tactical missiles) up to several thousand km (strategic missiles). Ballistic missiles may be launched from the ground, from ships and from submarines. It is also possible to launch such missiles from carrier airplanes.

Figure 1.22 shows the Atlas Intercontinental Ballistic Missile (USA).

Basic Data on the Atlas Intercontinental Ballistic Missile

Launching mass--90,000 kg

Mass of warhead--1,360 kg

Mass of fuel--80,000 kg

Total length--24.4 m

Frame diameter--2.75 m

Velocity (maximum)--20,000 km/hr

Range--9,000 km.

At the forward part, the cylindrical frame of rocket 3 is transformed into cone 2 which contains the warhead (thermonuclear charge). The cone is terminated with a spherical nose, having an aerodynamic endpiece 1. The endpiece serves to transfer the compression shock from the spherical nose ahead to decrease the drag of the missile and the aerodynamic heating of the nose. The control system is contained within cowlings 4. The main engine, with a thrust of approximately 300 kilonewtons (kN) is placed in tail funnel 7. The nozzle of engine 6 protrudes at the end of the missile. Booster engines 5, with a thrust of 600 kN each, are situated diametrically opposite on the sides of the missile frame. In

addition, there are two small engines 8 to control and stabilize the missile over the initial part of the passive trajectory. Antenna 9 is designed to transmit data on the parameters of motion to the control point.

The rocket has a self-contained control system augmented by remote control from the launching site by radio. During launching, the booster and the sustainer engines operate and the same fuel is used (kerosene and liquid oxygen). When a large part of the fuel has been consumed, booster engines 5 together with funnel 7 are jettisoned, and the remaining acceleration of the rocket is carried out by the sustainer engine. The Atlas rocket is controlled by rotating the combustion chambers of the engines, attached to the frame by means of Cardan's suspensions.

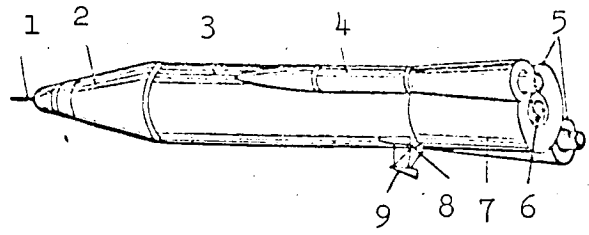

Figure 1.22. Atlas Ballistic Missile. 1--aerodynamic endpiece, 2--cone, 3--frame, 4--cowling of control system, 5--booster engines, 6--nozzle of sustainer engine, 7--tail funnel, 8--auxiliary engines, 9--antenna.

When covering the maximum range (9,000 km), the rocket moves along an elliptic trajectory and reaches an altitude of approximately 1,200 km. The flight time in this case is approximately 30 min. On the descending branch of the trajectory, cone 2 with the warhead separates from the frame of the rocket. When this cone enters the dense regions of the atmosphere, its velocity is more than 15 times the velocity of sound. To preserve this part of the rocket from intense aerodynamic heating, it is provided with a multilayer heat-resistant covering. /24

2. Airplane-Missiles. Airplane-missiles have the same aerodynamic configuration as piloted airplanes. As a rule the sustainer engine is operative over the entire trajectory of the airplane-missile. Usually, flight to the target is accomplished at constant altitude determined by the ceiling of a given airplane-missile.

Like the ballistic missiles, the airplane-missiles have a variety of purposes with corresponding ranges. They are launched from the ground, from ships and from airplanes. Compared with ballistic missiles, the airplane-missiles are more economical because, for the same range, the quantity of fuel required is several times less. However, they are substantially more vulnerable than rockets because their velocities and altitudes are much smaller.

As an example, we consider the Snark strategic airplane-missile (USA), shown in figure 1.23.

Basic Data on the Snark Airplane-Missile

Take-off mass (without the booster engine and the suspended tanks)--22,000 kg

Mass of the warhead--1,300 kg

Total length--21 m

Wing span--13 m

Fuselage diameter--1.6 m

Velocity--960 km/hr

Range--8,000 km.

The forward section of fuselage 1 contains the warhead (thermonuclear charge). The middle part 2 contains the fuel tanks and the control equipment. The tail section 4 of the fuselage is occupied by the sustainer turbojet engine. The fuel consists of kerosene. The missile is self-controlled by means of an inertial and a celestial navigation system. The control elements consist of elevons 3 and course rudder 5.

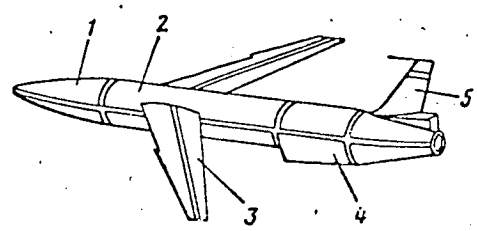

Figure 1.23. Snark airplane-missile. 1--forward section, 2--middle section, 3--elevons, 4--tail section, 5--course rudder.

The Snark airplane-missile is launched by means of two booster, solid fuel engines at some angle with respect to the horizon. When the definite velocity is reached at which the wings of the missile develop the necessary lift force, flight is continued by means of the sustainer engine at an altitude of 15 km. As fuel is consumed, the flight altitude is slightly increased. Over the target the airplane-missile is placed into a dive by the control system. During /25
this course the forward section with the warhead separates from the airplane-missile. The significant shortcoming of the Snark airplane-missile is its low flight velocity, which makes its interception easy.

3. Guided Aerial Bombs. Guided bombs are used to hit small targets (bridges, ships, command points, etc.) whose antiaircraft defense is ineffective, permitting the bomber to pass over the target.

Aerial bombs are controlled by aerodynamic forces which act on their wings, and which differentiate them from unguided bombs. In view of the conditions which restrict the manner in which the bomb can be carried in an airplane, the wings cannot be made too large. Therefore, the control force of such bombs is small, and it is for this reason that there is only a small difference in the trajectories of guided and unguided aerial bombs.

Figure 1.24 shows these trajectories. The bomb which is dropped at point O first falls to point O_1 without guidance. The broken line O_1O_2 shows the trajectory of the bomb when it is not guided. Trajectory 1 corresponds to the maximum deflection of the control surfaces of the guided bomb in one direction,

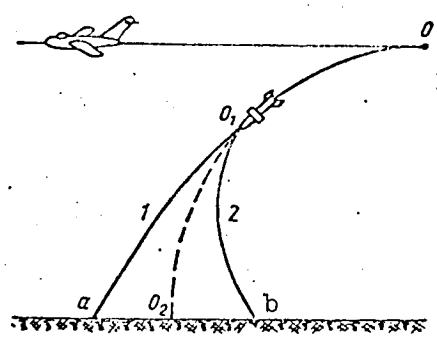

Figure 1.24. Trajectory of guided and unguided aerial bombs.

while trajectory 2 corresponds to their maximum deflection in the opposite direction. Thus the possible impact range which can be controlled in one plane is given by segment ab. It is clear that the situation is the same in any other plane, and consequently there is a certain area on the ground within which the impact point of the bomb may be controlled. The shape of this area depends on the aerodynamic scheme of the bomb. If, e.g., the bomb has an annular wing, which is most advantageous from the standpoint of size, the shape of the impact area will be close to a circle. Aerial bombs are controlled by external guidance (from the carrier airplane) and by homing guidance. In the latter case, the target must exhibit some type of contrast on its surrounding background. /26

As an example, figure 1.25 shows the Tarzan aerial bomb (USA). The total mass of the bomb is approximately 6,000 kg, while its total length is 8.5 m. The warhead of bomb 4 is a blockbuster. The bomb is aimed by external guidance from the carrier airplane. The receiving part of the control system is situated in tail section 2 which has a developed stabilizer 1. The annular wing 3 can be rotated in two perpendicular planes which produce the control forces.

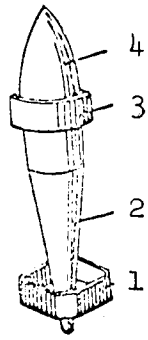

Figure 1.25. Tarzan guided aerial bomb. 1--stabilizer, 2--tail section, 3--annular wing, 4--warhead.

A significant shortcoming of guided aerial bombs is the necessity for the carrier airplane to fly over the target or close to it, which takes it within the range of antiaircraft weapons.

4. Guided antiaircraft missiles protect various objects (populated areas, industrial installations, warehouses, ships) from air attack. Since this problem is very broad, there is a large number of various modifications of such missiles. These modifications differ in range and power of warhead. The minimum ranges for missiles designed to be fired at aircraft near a protected area are 20 to 40 km. As a rule, such missiles have a warhead which produces a fragmentation effect and utilizes a time fuse. At the same time, missiles are being developed to destroy the intercontinental rockets of the enemy. It is obvious that these missiles must have a range of hundreds and thousands of km. Antiaircraft missiles are used against rapidly flying and highly maneuverable targets. Therefore, the missiles must have high maneuverability and a control system which guides them to the target with high accuracy. To achieve this high accuracy, the antiaircraft missiles, particularly those of long range, are equipped with a combined control system: external guidance at the initial and middle sections of the trajectory and homing guidance at the terminal section of the trajectory.

As an example, let us consider the Nike-Hercules antiaircraft missile (USA) shown in figure 1.26.

Basic Data on the Nike-Hercules Missile

Launching mass--4,500 kg

Mass without booster engines--2,270 kg

Total length--12.7 m

Length without booster engines--8.2 m

Wing span--1.9 m

Velocity--3,700 km/hr

Inclined range--80 km.

Frame 1 of the missile contains the warhead and the combined guidance system (external guidance along the initial section of the trajectory and homing guidance close to the target) and a solid fuel sustainer engine. The warhead may contain a charge of ordinary explosive or an atomic charge of various trotyl equivalents. To produce the control force, the missile is equipped with cruciform wings 2 with elevons 3 as the control elements. The four solid propellant booster engines 4 with stabilizer 5 are jettisoned after the missile has been accelerated and the propellant has been burned. /27

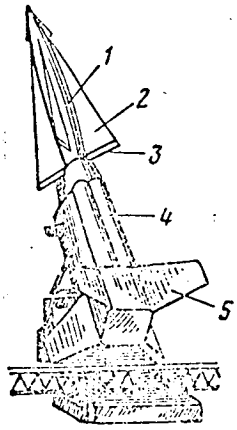

Figure 1.26. Nike-Hercules antiaircraft guided missile. 1--missile frame, 2--wings, 3--elevons, 4--booster engines, 5--stabilizer.

The launching site and the tracking site are outfitted to control a battery of four missiles (fig. 1.27). The launching site has two firing pads (with a diameter of 150 m) to launch the missiles and underground installations: the control point for launching, storage space for missiles, space for assembling and checking out the missiles. At the tracking site, which is situated several km from the launching site, three radars are installed: long-range radar for detecting the targets, radar for tracking the target and radar for guiding the missile. The last two radars are connected to a computer, which controls the guidance radar in such a way that the missile moving in the equisignal zone of the radar beam is directed to intercept the target. As the missile approaches the target, it switches to a homing guidance system.

5. Guided Missiles for Aerial Combat. Guided missiles for aerial combat are designed to be launched from an airplane towards aerial targets: aircraft and guided missiles. This demands special requirements for such missiles: relatively small weight and size, high speed, maneuverability and accuracy. High speed with small size is only possible because the range of these missiles is very small. The range of modern missiles for aerial combat is several tens of km. Due to their short range, these missiles are sometimes equipped only with a booster engine, which accelerates the projectile to a high velocity, usually /28

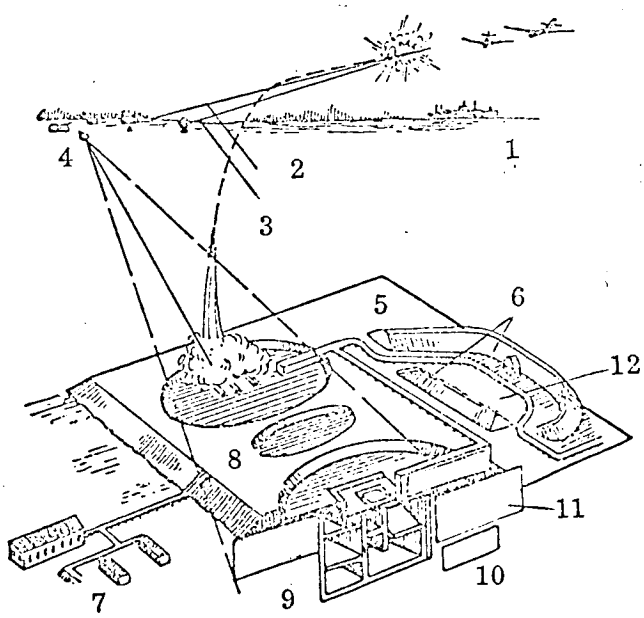

1--protected area;
2--guidance of missile to target;
3--target tracking;
4--guidance point;
5--embankment;
6--fortification;
7--administrative buildings and personnel housing;
8--firing pads;
9--launching control;
10--storage;
11--maintenance;
12--fuel storage.

Figure 1.27. Launching site and tracking site for Nike-Hercules missile.

two to three times the velocity of sound. After the booster engine has stopped operating, the velocity of such a shell begins to decrease due to air resistance. However, at the maximum range it must still be sufficient to achieve the required maneuverability and rapid pursuit of the target. The control systems for aerial combat missiles use external guidance or homing guidance.

Figure 1.28 shows the Sidewinder missile (USA) for aerial combat.

Basic Data on the Sidewinder Missile

Launching mass--70 kg

Total length--2.87 m

Wing span--0.48 m

Frame diameter--0.114 m

Velocity--2,800 km/hr

Range--5.5 km.

The forward part of fuselage 3 contains the sensing element of the homing guidance system which reacts to the thermal radiation of the target airplane. This sensing element is covered with a transparent aerodynamic shield 1. The

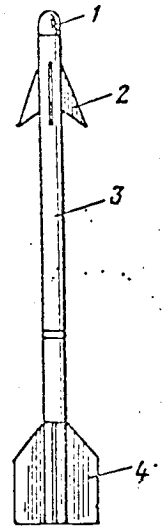

Figure 1.28. Sidewinder guided missile for aerial combat. 1--cowling, 2--control surfaces, 3--frame, 4--wings.

other components of the control system are also situated here. The actuators control surfaces 2, which are placed ahead of cruciform wings 4. The middle part of frame 3 contains the warhead with time fuses. The ends of the wings also have contact fuses. The tail part of the missile contains the booster, solid propellant motor which operates for a period of two sec.

6. Battlefield Guided Missiles. Missiles of this type are the weapons of infantry and are used directly on the battlefield against maneuverable and small targets. Initially, these missiles were developed as antitank missiles; however, their high accuracy and firing effectiveness makes them universal. The characteristic features of these missiles are their small range and relatively low flight velocity as well as simplicity of the control system. Missiles of this type can be made quite light. /29

As an example, we consider the Nord-5200 externally guided antitank missile (France).

Basic Data on the Nord-5200 Missile

Launching mass--18 kg

Total length--1.22 m

Wing span--0.63 m

Frame diameter--0.17 m

Velocity--700 km/hr

Range--3.5 km.

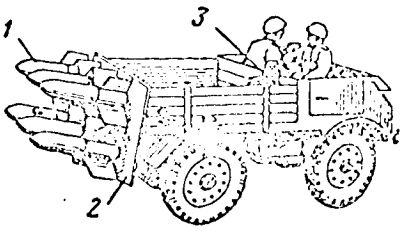

Figure 1.29. Rocket launcher "Nord-5200." 1--rockets, 2--launching platform, 3--controls.

Figure 1.29 shows the launcher for the Nord-5200 missiles mounted on a truck. Six missiles 1 are placed on the collapsible launching platform 2. The missiles are equipped with booster and sustainer, solid propellant engines. The large wing area provides for good maneuverability of the missile. The operator controls the flight of the missile by means of command device 3, which generates the control signals. These signals are transmitted to the missile over wires. The control line is made of two thin, insulated steel wires wound on reels and situated in the frame of the missile. As the missile flies, this wire is unwound from the coils. The control elements of the missile consist of spoilers placed at the trailing edge of the wings.

CHAPTER 2. SOME MATHEMATICAL METHODS FOR INVESTIGATING AUTOMATIC CONTROL SYSTEMS /30

Section 2.1. General Information

Missile guidance systems are systems with feedback. Figure 2.1 shows a functional diagram of such a system. The methods of the theory of automatic control may be used to analyze missile guidance systems. These methods fall into two large groups. The first group contains the methods based on investigating the characteristics of the system during the transient processes produced by the action of standard control signals (unit function or δ-function). The second group refers to the frequency methods of system analysis, which may be called the methods of stationary state. In principle, both methods are equivalent; however, in specific problems, the solution may be obtained more rapidly or simply by one or the other method.

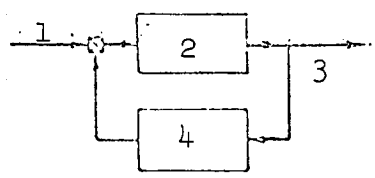

1. control signal
2. missile
3. coordinates of missile with respect to target
4. feedback network

Figure 2.1. General functional diagram for a missile guidance system.

In the present book wide application will be made of two methods for analyzing missile guidance systems: the method of standard coefficients and the method of logarithmic amplitude-frequency characteristics. The method of standard coefficients refers to the first group, while the method of logarithmic amplitude-frequency characteristics refers to the second group. These methods are simple and easy to visualize, and it is for this reason that they are widely used in engineering practice for designing automatic systems.

The methods of standard coefficients and of the logarithmic amplitude-frequency characteristics are applicable to stationary linear systems, i.e., systems which are described by linear differential equations with constant coefficients. At the same time, missile control systems are frequently nonstationary and nonlinear. For this reason the present chapter introduces the methods /31
of analyzing linear nonstationary systems and nonlinear systems as well as methods of analyzing stationary and nonstationary systems subject to random perturbations. Such perturbations are characteristic of missile control systems.

Section 2.2. The Method of Standard Coefficients

Let us assume that we have a single closed loop scheme with fixed negative feedback over an arbitrary linear transmitting system (fig. 2.2).

First let us consider the transfer function of an open loop system by disconnecting the feedback loop (fig. 2.2). Let us assume that the input and output quantities of this system are given by a differential equation with constant coefficients

$$a_0 \frac{d^n y}{dt^n} + a_1 \frac{d^{n-1} y}{dt^{n-1}} + \ldots + a_{n-1} \frac{dy}{dt} + a_n y =$$
$$= b_0 \frac{d^m \varepsilon}{dt^m} + b_1 \frac{d^{m-1} \varepsilon}{dt^{m-1}} + \ldots + b_{m-1} \frac{d\varepsilon}{dt} + b_m \varepsilon. \qquad (2.1)$$

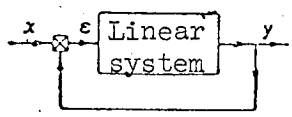

Figure 2.2. Functional diagram of single closed loop automatic control system. x--is assigned or input quantity, y--is true or output quantity.

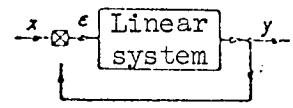

Figure 2.3. Functional diagram of single open loop automatic control system.

It is clear that when the feedback loop is opened $x = \varepsilon$. The system of linearized missile equations or of equations with constant or quasiconstant coefficients is reduced to such a system. By adopting the symbolic designation $p = d/dt$, this equation may be written in the form

$$N(p)\, y = M(p)\, \varepsilon, \qquad (2.2)$$

where

$$\left.\begin{aligned} N(p) &= a_0 p^n + a_1 p^{n-1} + \ldots + a_{n-1} p + a_n, \\ M(p) &= b_0 p^m + b_1 p^{m-1} + \ldots + b_{m-1} p + b_m. \end{aligned}\right\} \qquad (2.3)$$

The transfer function of a system is the ratio of the instantaneous value of the output quantity to the input quantity. In accordance with this definition, the transfer function of the system described by equation (2.2) has the form /32

$$W_{y/\varepsilon}(p) = \frac{y}{\varepsilon} = \frac{M(p)}{N(p)}. \qquad (2.4)$$

It follows from equation (2.4) that the transfer function is a fractional-rational function of symbol p.

If the feedback loop is closed, i.e., if we return to the simplest automatic control system (fig. 2.2), the following relationship (fig. 2.3) will hold between the input and output quantities: $\epsilon = x - y$. Substituting this relationship into equation (2.2), which remains valid for a system with feedback, we obtain a new differential equation for the closed loop system having the following symbolic form

$$[M(p) + N(p)]\,y = M(p)\,x. \tag{2.5}$$

The transfer function of a closed loop system is a ratio of polynomials

$$\Phi_{y/x}(p) = \frac{M(p)}{M(p) + N(p)} = \frac{W(p)}{1 + W(p)}. \tag{2.6}$$

The dynamic properties of this system are best illustrated by means of the transient function H(t), which represents the reaction of the system or the output quantity when a unit function is applied at the input.

In a system with satisfactory dynamic characteristics, the transient function must have a form close to that of the curves shown in figure 2.4, and the allowable overcontrol (overshoot) and control time are determined by the specific operating conditions of the system. There is a rather complex, but definite relationship between the nature of the transfer function and the transient function. The form of the transient function is determined by the value of zeros (roots of the numerator) and of the poles (roots of the denominator) of the transfer function. It is clear that for any specific form of the transfer function, we can find an optimum distribution of zeros and poles for which the transfer function will be most advantageous from the standpoint of the dynamics of the system in

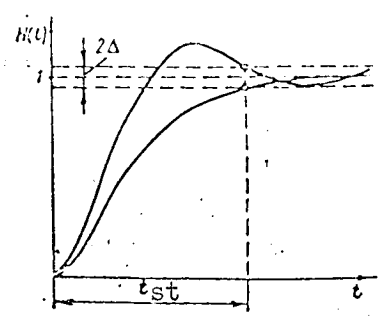

Figure 2.4. Graph of transient functions.

question. For each such optimum distribution of zeros and poles, there is a definite value for the coefficients of the polynomials in the numerator and denominator of the transfer function which we shall call standard. We present the values of these standard coefficients for several typical transfer functions. Any polynomial of the form (2.3) may be reduced to /33

$$N'(p) = p^n + A_1\Omega_0 p^{n-1} + \ldots + \\ + A_{n-1}\Omega_0^{n-1} p + \Omega_0^n, \tag{2.7}$$

where Ω_0 is conditionally called the natural frequency of the system under investigation.

It is clear that the coefficients of the polynomials N(p) and N'(p) are related by the following equations

$$A_1 = \frac{a_1}{a_0\Omega_0}; \quad A_2 = \frac{a_2}{a_0\Omega^2}; \quad \ldots; \quad A_{n-1} = \frac{a_{n-1}}{a_0\Omega_0^{n-1}}; \quad \Omega_0 = \sqrt[n]{\frac{a_n}{a_0}}.$$

As a first typical function we take the transfer function of a closed loop system which contains no zeros

$$\Phi(p) = \frac{\Omega_0^n}{p^n + A_1\Omega_0 p^{n-1} + \ldots + A_{n-1}\Omega_0^{n-1} p + \Omega_0^n}. \tag{2.8}$$

For a system with such a function we obtain a transient process without overshoot when the roots of the numerator (the poles of the transfer function) are all real. For all real roots and for Ω_0^n = const the control time will be a minimum, if all of the roots are multiples. We call this process optimum. In this case the coefficients A_1, A_2 ..., A_{n-1} turn out to be the coefficients of Newton's binomial $(p + 1)^n$. Table 2.1 shows the values of these coefficients for n = 1, 2, 3, 4, 5, and 6.

TABLE 2.1. STANDARD COEFFICIENTS FOR MULTIPLE ROOTS.

n	Coefficients of denominator
1	1 1
2	1 2 1
3	1 3 3 1
4	1 4 6 4 1
5	1 5 10 10 5 1
6	1 6 15 20 15 6 1

Figure 2.5 shows the graph of transient functions for systems which are determined by the standard coefficients given in table 2.1. All the curves are shown as functions of the dimensionless time $\tau = \Omega_0 t$. The true time is given by the expression

$$t = \frac{\tau}{\Omega_0}. \tag{2.9}$$

The broken lines in figure 2.5 show the control time for systems of different order. The transient process is considered to be practically finished when the value of the quantity $|1-H(t)|\cdot 100$ percent does not exceed $\Delta = 5$ percent. /34

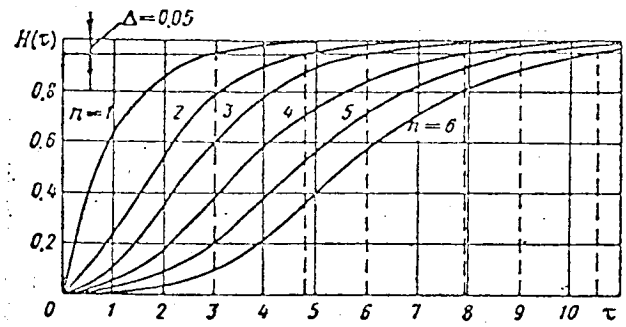

Figure 2.5. Graph of transient functions for system with transfer function of type (2.8) and with coefficients given in table 2.1.

If it is permissible to have some overcontrol over the transient function, the roots may be taken to be complex, which also decreases the control time. Let us represent the polynomial of the transfer function denominator (2.8) as a product of n/2 identical quadratic trinomials

$$\left(p^2 + 2\zeta\Omega_0 p + \Omega_0^2\right)^{n/2} = p^n + A_1\Omega_0 p^{n-1} + \ldots + A_{n-1}\Omega_0^{n-1}p + \Omega_0^n \tag{2.10}$$

and select a value $\zeta = 0.75$. When n is odd, the denominator of the transfer function (2.8) consists of $(n - 1)/2$ quadratic trinomials and one binomial of the first degree. The free term of this binomial is assumed to be equal to 1. The values of the coefficients $A_1, A_2 \ldots, A_{n-1}$ for this distribution of roots are shown on table 2.2.

TABLE 2.2. STANDARD COEFFICIENTS FOR MULTIPLE COMPLEX ROOTS.

n	Coefficients of denominator						
2			1	1.5	1		
3		1	2.5	2.5	1		
4	1	3	4.25	3	1		
5	1	4	7.25	7.25	4	1	
6	1	4.5	9.75	12.375	9.75	4.5	1

Figure 2.6 shows the graph of transient functions for systems which are determined by the standard coefficients of table 2.2. The broken lines show the control time for systems of different order. Comparing this time with its

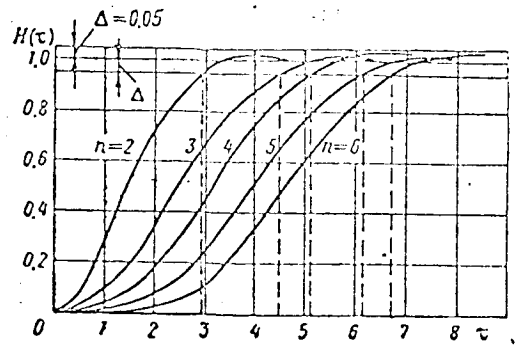

Figure 2.6. Graph of transient functions for systems with transfer function of type (2.8) and with coefficients given in table 2.2.

value for systems, which have coefficients given by table 2.1 (curves in fig. 2.5), we see that for the same n the control time in the latter case is substantially less. /35

Let us now consider a transfer function which has one zero equal to $-\frac{\Omega_0}{A_{n-1}}$

$$\Phi(p) = \frac{A_{n-1}\Omega_0^{n-1}p + \Omega_0^n}{p_n + A_1\Omega_0 p^{n-1} + \ldots + A_{n-1}\Omega_0^{n-1}p + \Omega_0^n}. \qquad (2.11)$$

When the transfer function has a zero, the multiple roots, obtained for standard coefficients from tables 2.1 and 2.2, no longer provide a satisfactory transient function. This function develops a large initial overshoot over the stationary value (overcontrol). To decrease the overshoot produced by the effect of the zero, it becomes necessary to decrease the rise time of the transient function. This can only be done by spreading out the roots of the denominator polynomial along the real axis. There are guidelines[1] for the distribution of the roots along the real axis which gives a satisfactory transient function when zeros are present in the transfer function. For a transfer function with one zero, equation (2.11), it is recommended that the roots be distributed on the negative real semiaxis in arithmetic progression. The values of the coefficients of the polynomial in the denominator of equation (2.11) are shown in table 2.3 for this distribution. /36

Figure 2.7 shows the graphs of the transient functions for systems determined by the standard coefficients of table 2.3.

---

[1]A. A. Krasovskiy and G. S. Pospelov, "Principles of Automation and Engineering Cybernetics," Gosenergoizdat, 1962: G. S. Pospelov and Yu. P. Dobrolenskiy, The Method of Standard Coefficients for Selecting the Parameters of Linear Automatic Control Systems. Collected Articles on Automation and Electrical Engineering, Izd. AN SSSR, 1956.

TABLE 2.3. STANDARD COEFFICIENTS WHEN ROOTS ARE DISTRIBUTED IN ARITHMETIC PROGRESSION.

n	First term	Difference	Coefficients of denominator
2	0.5	1.5	1 2.5 1
3	0.183	1.517	1 5.1 6.35 1
4	0.098	1.138	1 7.22 16.3 11.8 1
5	0.063	0.867	1 9 29 38 18 1
6	0.039	0.717	1 11 43 83 73 25 1

As in the previous graphs, the broken lines designate the relative control time. /37

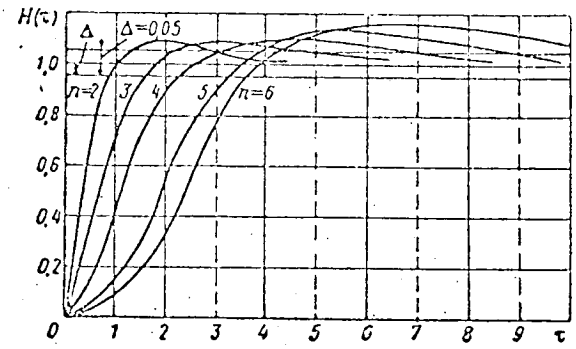

Figure 2.7. Graph of transient functions for systems with transfer function of type (2.11) and coefficients given in table 2.3.

Finally, let us consider a transfer function with two zeros

$$\Phi(p) = \frac{A_{n-2}\Omega_0^{n-2}p^2 + A_{n-1}\Omega_0^{n-1}p + \Omega_0^n}{p^n + A_1\Omega p^{n-1} + \ldots + A_{n-2}\Omega_0^{n-2}p^2 + A_{n-1}\Omega_0^{n-1}p + \Omega_0^n} \tag{2.12}$$

To decrease the effect of zeros in this case, it is recommended that the roots of the polynomial in the denominator be distributed on the negative real semiaxis according to the law of geometric progression. Table 2.4 shows the values of the coefficients of the polynomial in the denominator A_1, A_2,..., A_{n-1} for such a distribution of roots.

Figure 2.8 shows the graph of transient functions for systems determined by standard coefficients listed in table 2.4.

The values of standard coefficients presented in tables 2.1 - 2.4 provide optimum dynamic properties of systems with transfer functions of the form (2.8), (2.11) or (2.12). The method of utilizing these standard coefficients to select the parameters of control systems consists of the following. The coefficients /38

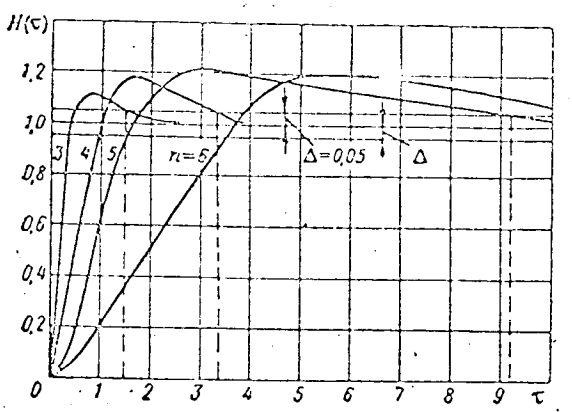

Figure 2.8. Graph of transient functions for systems with transfer functions of type (2.12) and coefficients determined in table 2.4.

TABLE 2.4. STANDARD COEFFICIENTS WHEN ROOTS ARE DISTRIBUTED ACCORDING TO LAW OF GEOMETRIC PROGRESSION.

n	First term	Denominator	Coefficients of denominator
3	0.182	5.5	1 6.7 6.7 1
4	0.185	3.08	1 7.9 15 7.9 1
5	0.075	3.63	1 18 69 69 18 1
6	0.038	3.7	1 36 251 485 251 36 1

A_1, A_2, ..., A_{n-1} of the transfer functions or of the initial differential equations used to obtain these functions depend on the parameters of the individual elements of the system a, b, c, ... Mathematically this may be formulated in the following manner

$$\left.\begin{aligned} A_1\Omega_0 &= f_1(a, b, c, \ldots), \\ A_2\Omega_0^2 &= f_2(a, b, c, \ldots), \\ &\cdots\cdots\cdots\cdots \\ A_{n-1}\Omega_0^{n-1} &= f_{n-1}(a, b, c, \ldots), \\ \Omega_0^n &= f_n(a, b, c, \ldots), \end{aligned}\right\} \qquad (2.13)$$

where f_i (a, b, c, ...) is the expression for the ith coefficient of the transfer function or of the initial differential equation in terms of parameters a, b, c, ... of its individual elements.

The equations will form a system consisting of n algebraic equations, if the number of variable parameters a, b, c, ... is equal to n. If the number of

variable parameters is greater than n, then some of the parameters are assigned so that we obtain a system of n equations with n variables. In this case the selection of values for the variable parameters is reduced to the solution of the indicated system. This cannot always be carried out analytically because the system of equations (2.13) may be nonlinear. However, if by some method or other, all of the n roots of system (2.13) are found and are real numbers, the problem of selecting the parameters, which would provide for a preassigned optimum transient function, may be considered solved. In this case, the assignment of Ω_0 means the assignment of the duration of the transient process or of the control time.

In cases when the number of parameters a, b, c, ... is less than n or when some of the roots are imaginary, the analysis of equations (2.13) may be quite useful, particularly because small deviations of coefficients A_1, A_2, ... A_{n-1} from standard values do not produce a substantial effect on the dynamic characteristics of the investigated system.

Section 2.3. The Method of Logarithmic Amplitude-Frequency Characteristics

In some cases the method of standard coefficients presented in the preceding sections is insufficiently flexible. Indeed, the transfer functions of some closed loop circuits in missile control systems may not coincide with any of the standard functions (2.8) - (2.12). In another case, the system of equations (2.13), used to determine the parameters of the system, may not have any real roots. Finally, the number of variable parameters of a system may turn out to be less than n, and the system of equations (2.13) in this case becomes incomplete and sometimes incompatible. In those cases where the method of standard coefficients cannot be applied, the problem can usually be solved by another method, which is sufficiently simple and more flexible. This method of logarithmic amplitude-frequency characteristics is widely known and will not be presented here. It is only necessary to recommend them for application to the selection of the control system parameters, which will be widely used later. Let us consider the relations between the logarithmic amplitude-frequency characteristics and the transient functions by considering systems which are described by equations of the first and second order. As we know, the method of logarithmic amplitude-frequency characteristics permits evaluation of the dynamic properties of a closed loop system from the characteristics of the open loop system. /39

First we consider the simplest automatic control system represented in figure 2.9. When the feedback loop is closed, this system is described by the following differential equation of the first order

$$\frac{dy}{dt} + ky = kx. \tag{2.14}$$

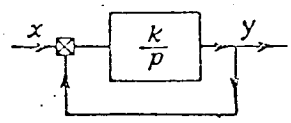

Figure 2.9. Functional diagram of automatic control system described by a differential equation of the first order.

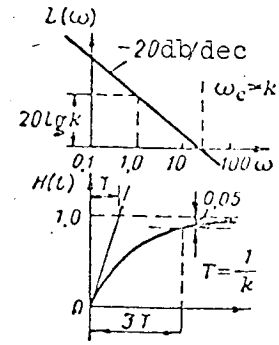

Figure 2.10. Logarithmic amplitude-frequency characteristics (LAC) and graph of transient function of system shown in figure 2.9.

The transfer function of the open loop system, shown in figure 2.9, is given by expression

$$W(p) = \frac{k}{p}. \tag{2.15}$$

Finally, the logarithmic amplitude-frequency characteristics of this system are given by /40

$$L(\omega) = 20 \lg k - 20 \lg \omega. \tag{2.16}$$

Figure 2.10 shows the logarithmic amplitude-frequency characteristics and the transient function constructed on the basis of equations (2.16) and (2.14). These graphs illustrate the following basic relations between these characteristics of the system, which is described by a differential equation of the first order:

(1) the cutoff frequency ω_c is equal to amplification factor k;

(2) the cutoff frequency is inversely proportional to time constant T of the closed loop system.

Thus, the higher the cutoff frequency ω_c, the faster will the system respond to a control signal.

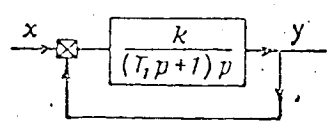

Figure 2.11. Functional representation of automatic control system described by differential equation of the second order.

Figure 2.11 shows the schematic diagram of a system described by a differential equation of the second order. When the feedback loop is closed, this system is described by equation

$$T_1 \frac{d^2y}{dt^2} + \frac{dy}{dt} + ky = kx. \tag{2.17}$$

The transfer function of an open loop system is determined by the expression

$$W(p) = \frac{k}{(T_1 p + 1)p}. \tag{2.18}$$

Finally, the logarithmic amplitude-frequency characteristics for this system are given by

$$L(\omega) = 20 \lg k - 20 \lg \omega - 20 \lg \sqrt{T_1^2 \omega^2 + 1}. \tag{2.19}$$

Figure 2.12 shows the logarithmic amplitude-frequency characteristics and the transient functions constructed on the basis of (2.17) and (2.19) for various values of the relative attenuation coefficient $\zeta = 0.5/\sqrt{T_1 k}$. For a system described by an equation of the second order, this coefficient will be less than 0.5, if the reciprocal frequency $\omega_1 = 1/T_1$ is less than the cutoff frequency ω_c. In this case, the transient function has an oscillatory nature. When $\omega_1 = \omega_c$, the relative attenuation coefficient is equal to 0.5 and becomes greater than 0.5 when $\omega_1 > \omega_c$. The greater the value of ω_1, compared with ω_c, the closer is the transient function of the second order system to the exponent with the time constant $T = 1/\omega_c$. On the basis of what we have presented we may establish the /41 following basic relations between the logarithmic amplitude-frequency characteristics and the transient function for a system described by a differential equation of the second order.

(1) to accelerate the transient process, we must increase the cutoff frequency ω_c;

(2) to obtain a transient function with good attenuation, the cutoff frequency must correspond to the region of the logarithmic amplitude-frequency characteristics with a slope of 20 db/decade;

(3) the greater the region with a slope 20 db/decade near the frequency ω_c (i.e., the greater ω_1 is compared with ω_c), the greater is the relative attenuation coefficient.

The conclusions obtained for the second order system turn out to be valid for more complex systems.

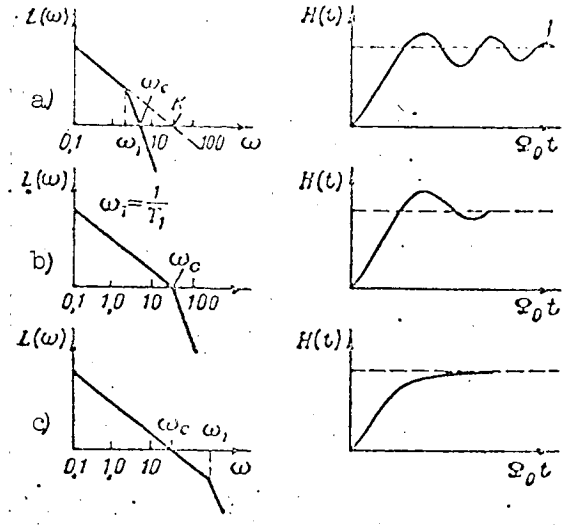

Figure 2.12. LAC and graph of transient functions of system shown in figure 2.11.

As an example, figure 2.13 shows the logarithmic amplitude-frequency characteristics which correspond to the following transfer function of an open loop system

$$W(p) = \frac{k(T_2 p + 1)}{p(T_1 p + 1)(T_3 p + 1)} = \frac{T_2}{T_1 T_3} \cdot \frac{k(p + \omega_2)}{p(p + \omega_1)(p + \omega_3)}. \qquad (2.20)$$

In any system, the cutoff frequency characterizes the response of a system. To obtain the necessary characteristics for the transient function of a closed loop system, the logarithmic amplitude-frequency characteristics of an open loop system must have a sufficient region near the cut-off frequency (approximately one decade) with a slope of 20 db/decade. In addition, the ratio of frequencies /42

$\frac{\omega_3}{\omega_c}$ should be within limits $2 < \omega_3/\omega_c < 4$. The wider the middle region of the logarithmic amplitude-frequency characteristics with a slope of 20 db/decade, the closer is the transient process to an exponent when a unit function is applied at the input.

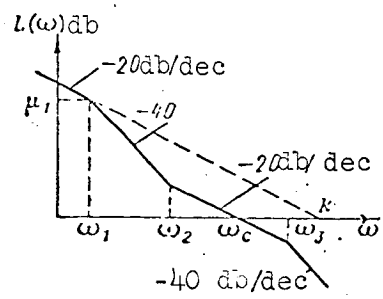

Figure 2.13. LAC corresponding to transfer function (2.20).

Sometimes the logarithmic amplitude-frequency characteristics of an investigated system in the regions from ω_1 to ω_2 and from ω_3 to infinity has a slope greater than that shown in figure 2.13. For these logarithmic amplitude-frequency characteristics, the recommendations made concerning the behavior in the region of the cutoff frequency are also valid. However, in all cases when the differential equation is of a higher order than 2, these recommendations are qualitative in nature. A more accurate relation between the logarithmic amplitude-frequency characteristics and the transient function of the system is given by special nomograms[1] shown in figures 2.14a - 2.14i. On these nomograms typical logarithmic amplitude-frequency characteristics are determined by frequencies ω_1, ω_3 and by the ordinate μ_1. Frequencies ω_1 and ω_3 are given with respect to the cutoff frequency ω_c. It follows from figure 2.13 that the assignment of μ_1 and ω_1 for a selected frequency ω_c means the assignment of ω_2. An increase in any one of the parameters (μ_1 or ω_1), when the second one is constant, leads to an increase in ω_2 and to a decrease in the middle region where the slope is 20 db/decade. In this case overcontrol and oscillations of the transient process increase.

The following characteristics of a closed loop system (fig. 2.15) are determined by means of the nomograms in figure 2.14:

t_c -- control time during which the transient function of the output quantity reaches a value which differs from the stationary value by not more than 5 percent;

t_0 -- time required to reach the first overshoot;

H_m -- maximum value of the transient function;

ω_t -- frequency of oscillation of the transient function near the stationary value;

ω_m -- frequency of the maximum value of the amplitude-frequency characteristics of a closed loop system;

Φ_m -- magnitude of this maximum.

The characteristics of parameters shown on the nomograms in figure 2.14 are given as a function of the ratio ω_1/ω_c for various values of μ_1 (db) and of the ratio ω_3/ω_c. The nomograms give the relative and not the absolute value of the /43

[1] Handbook on Automatic Control, edited by J. Traksel, Gosenergoizdat, 1962.

parameters t_c, t_0, ω_t and ω_m, which are shown in the following form: $t_c\,\omega_c/10$, $t_0\,\omega_c/10$, ω_t/ω_c, ω_m/ω_c.

In designing a control system for some object it usually turns out that the frequency response characteristics of the object in a simple control system or regulator are insufficient to provide for the necessary dynamic properties of the system. Thus, it becomes necessary to include a compensating device into the circuit to damp out the initial frequency response characteristics and obtain the necessary dynamic characteristics of the system. These devices may be of the most diverse physical form. However, the most common compensating /52 devices used in automatic control systems are composed of active resistances and capacitors. Such systems may be connected into the transfer circuit of a control signal, if the latter is a dc signal.

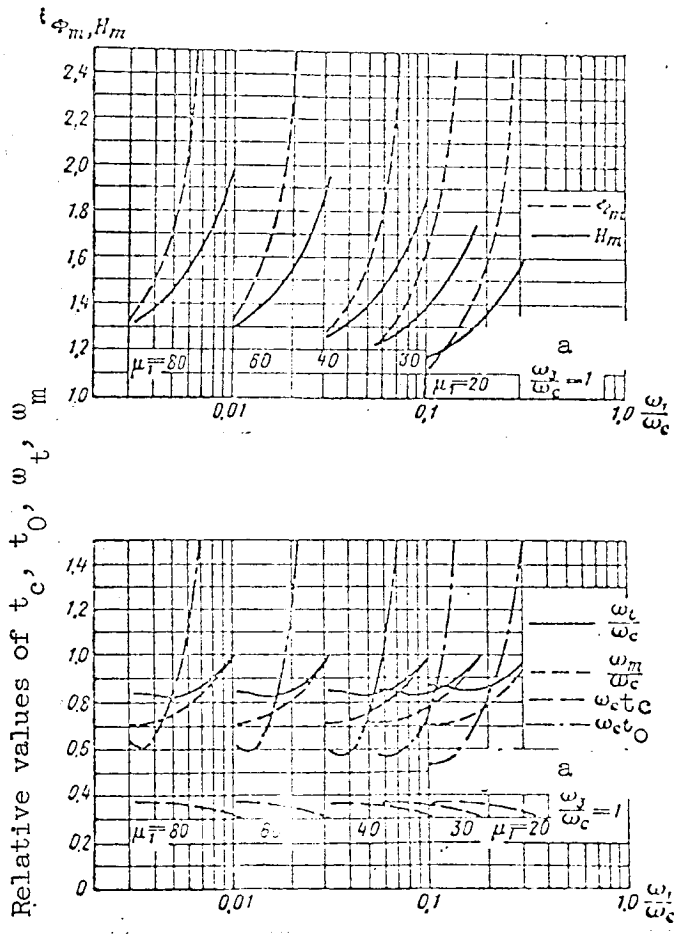

Figure 2.14a. Nomograms of typical LAC; a is: ω_1 to ω_2 = 40 db/dec; ω_3 to ∞ = 40 db/dec.

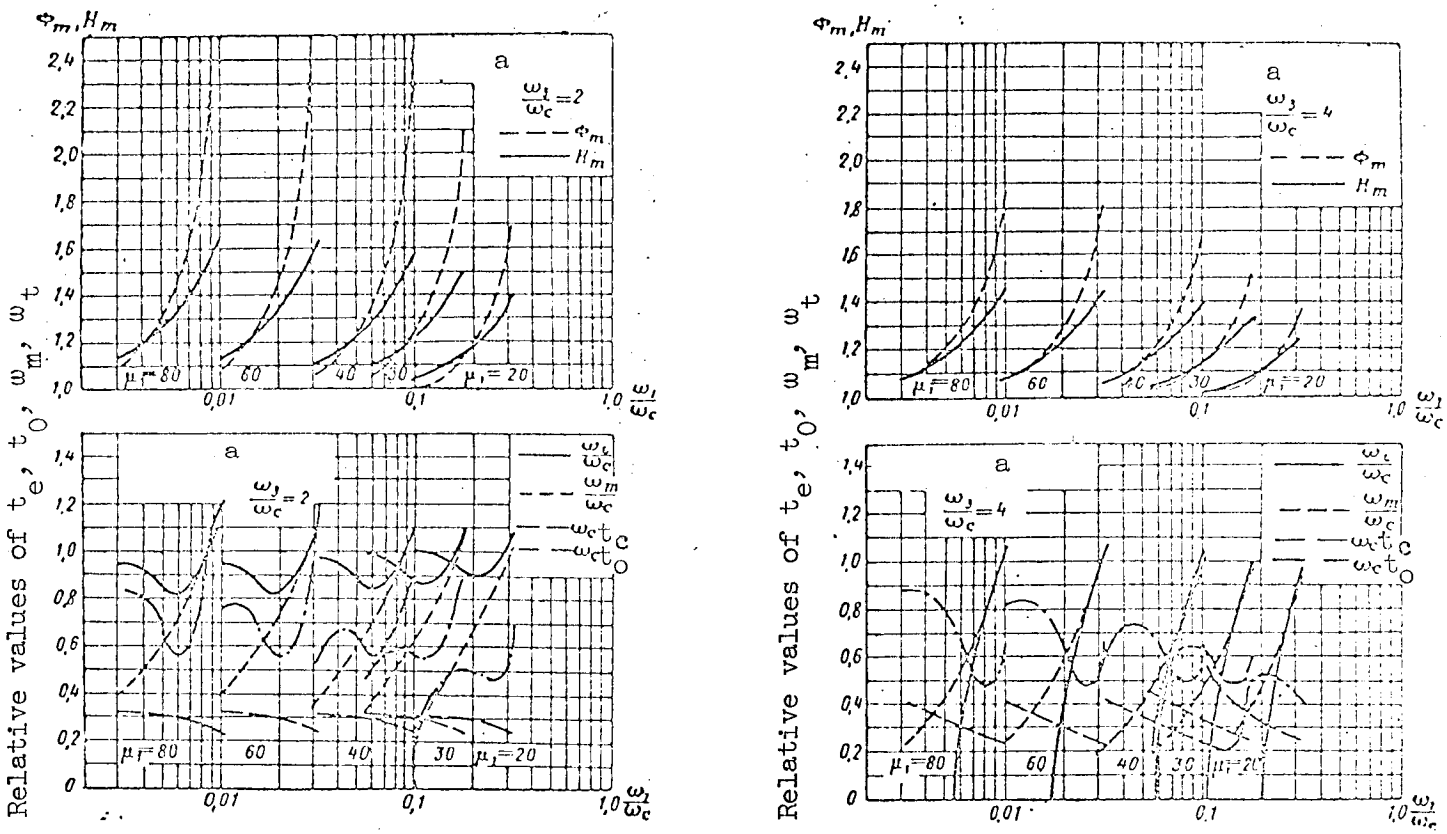

Figure 2.14b. Nomograms of typical LAC.
a is: ω_1 to ω_2 = 40 db/dec; ω_3 to ∞ = 40 db/dec.

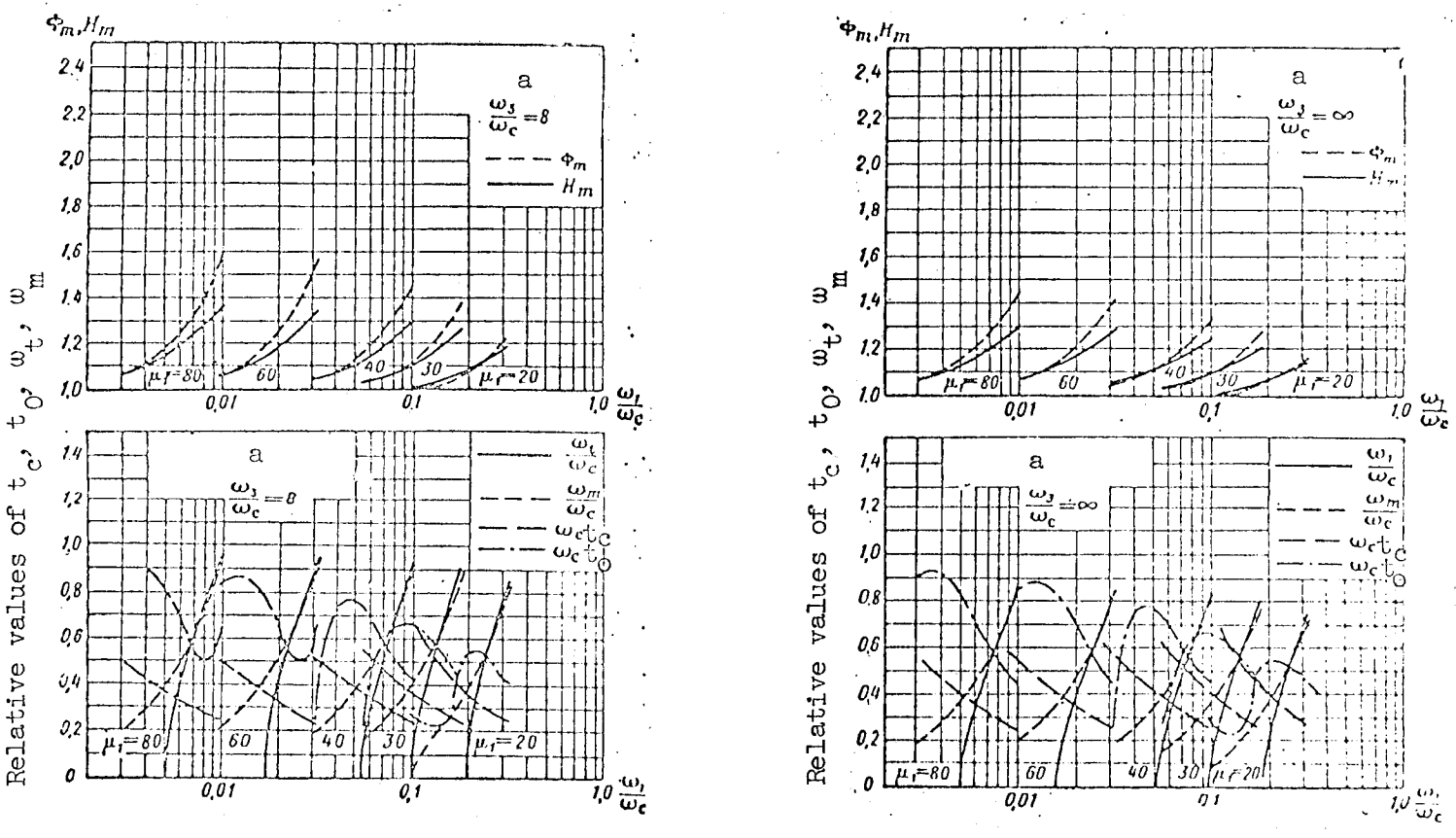

Figure 2.14c. Nomograms of typical LAC.
a is: ω_1 to ω_2 = 40 db/dec; ω_3 to ∞ = 40 db/dec.

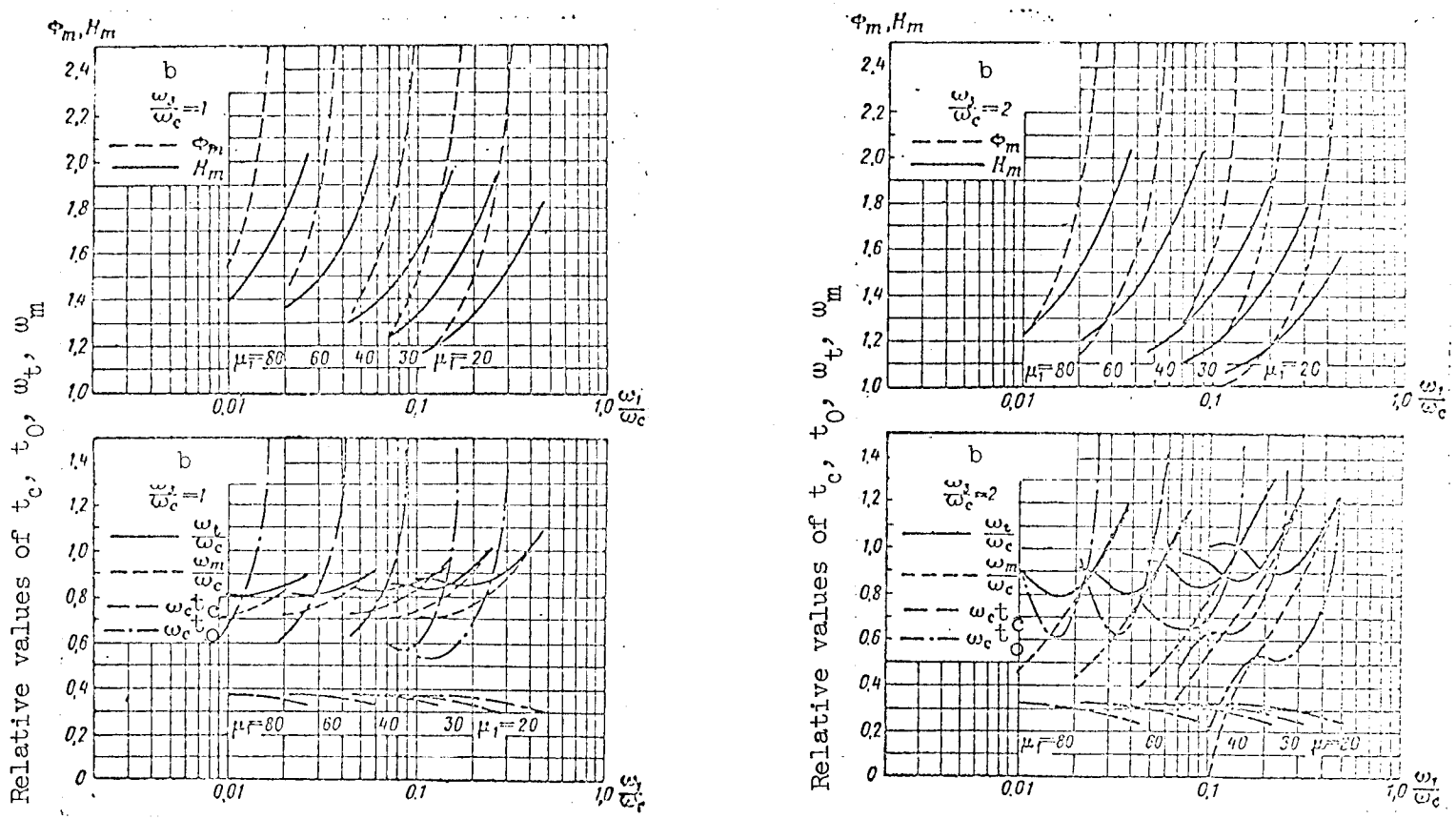

Figure 2.14d. Nomograms of typical LAC.
b is: ω_1 to ω_2 = 60 db/dec; ω_3 to ∞ = 40 db/dec.

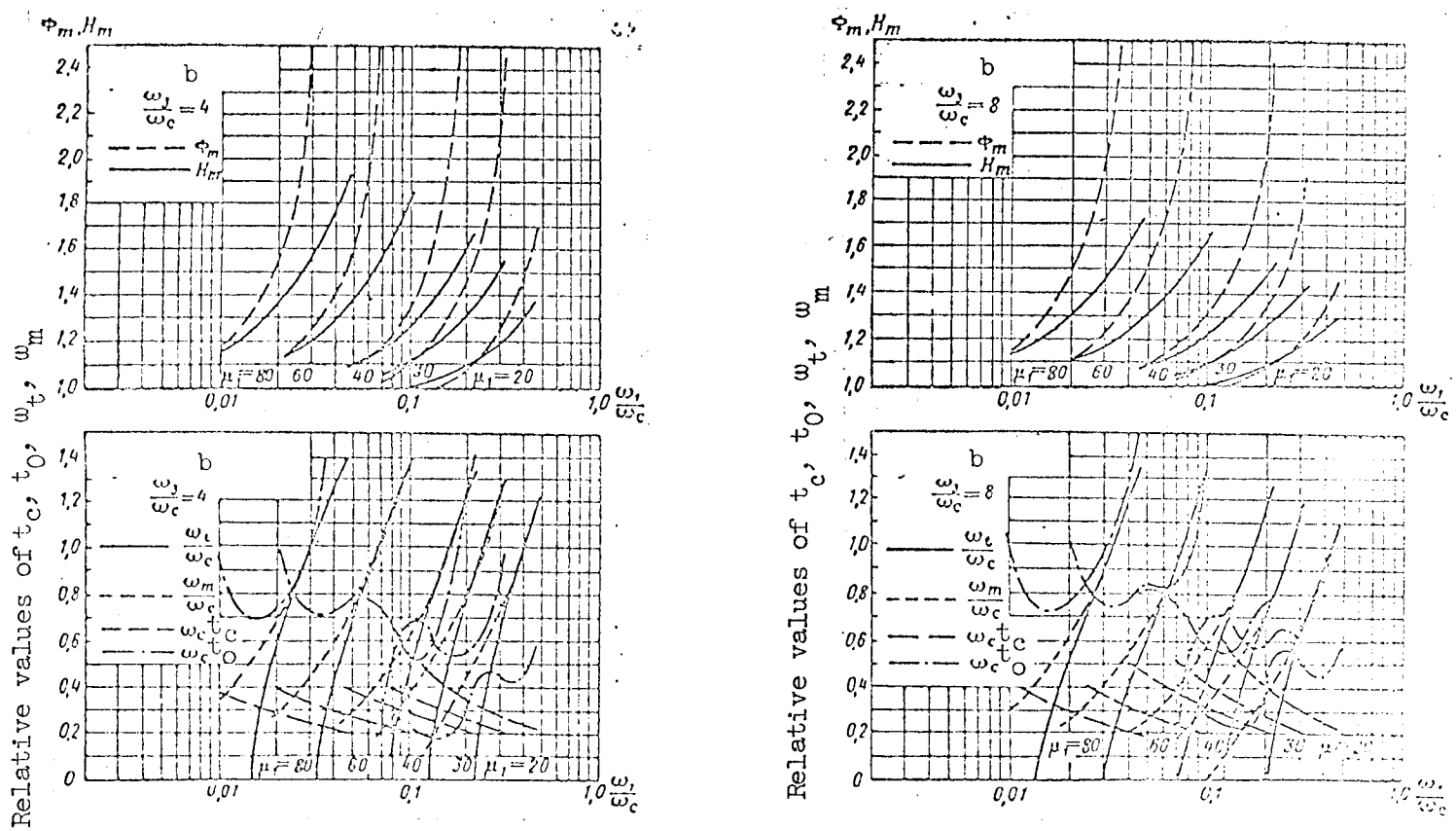

Figure 2.14e. Nomograms of typical LAC.
b is: ω_1 to ω_2 = 60 db/dec; ω_3 to ∞ = 40 db/dec.

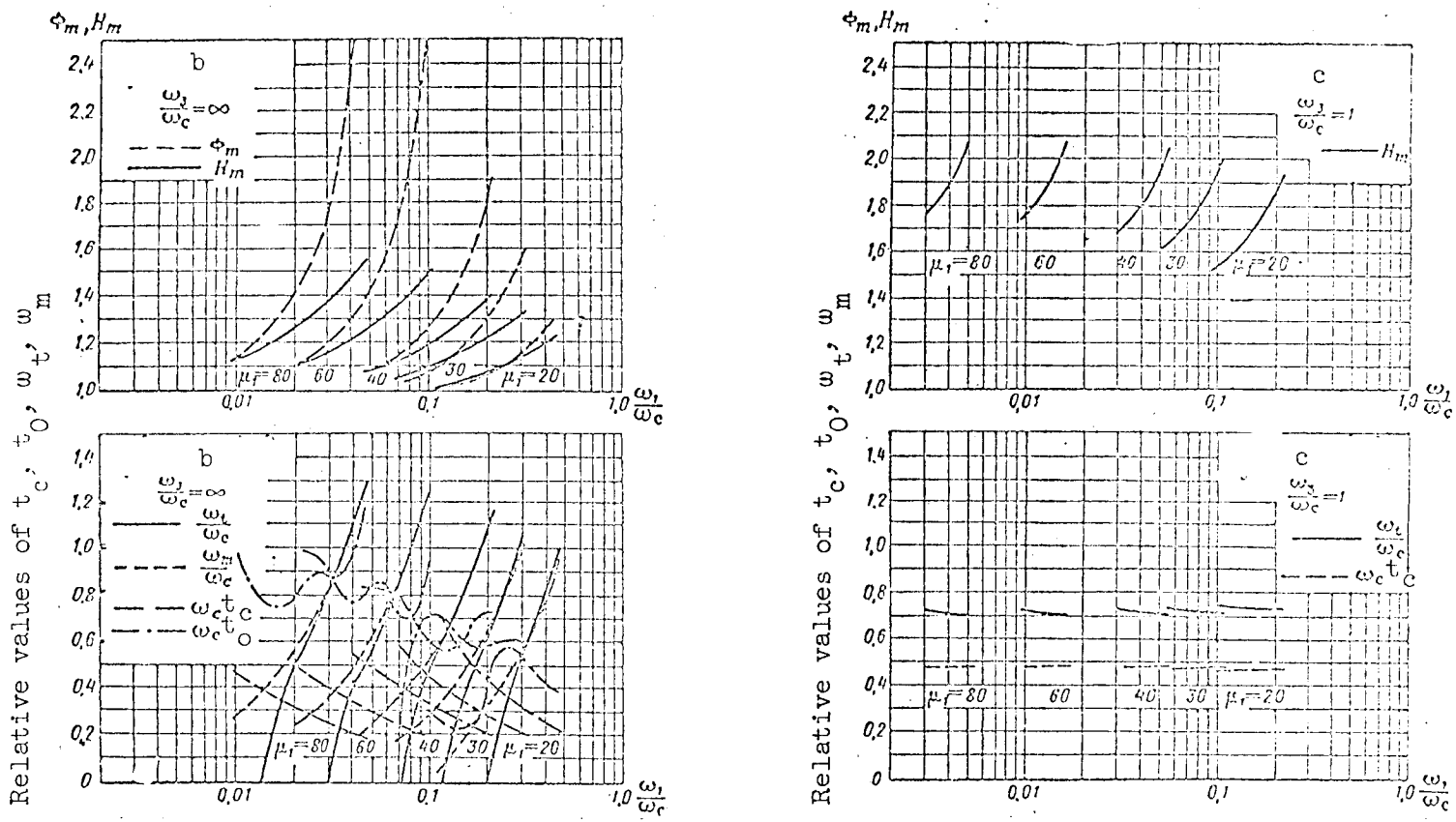

Figure 2.14f. Nomograms of typical LAC. b is: ω_1 to ω_2 = 60 db/dec; ω_3 to ∞ = 40 db/dec; c is: ω_1 to ω_2 = 40 db/dec; ω_3 to ∞ 60 db/dec.

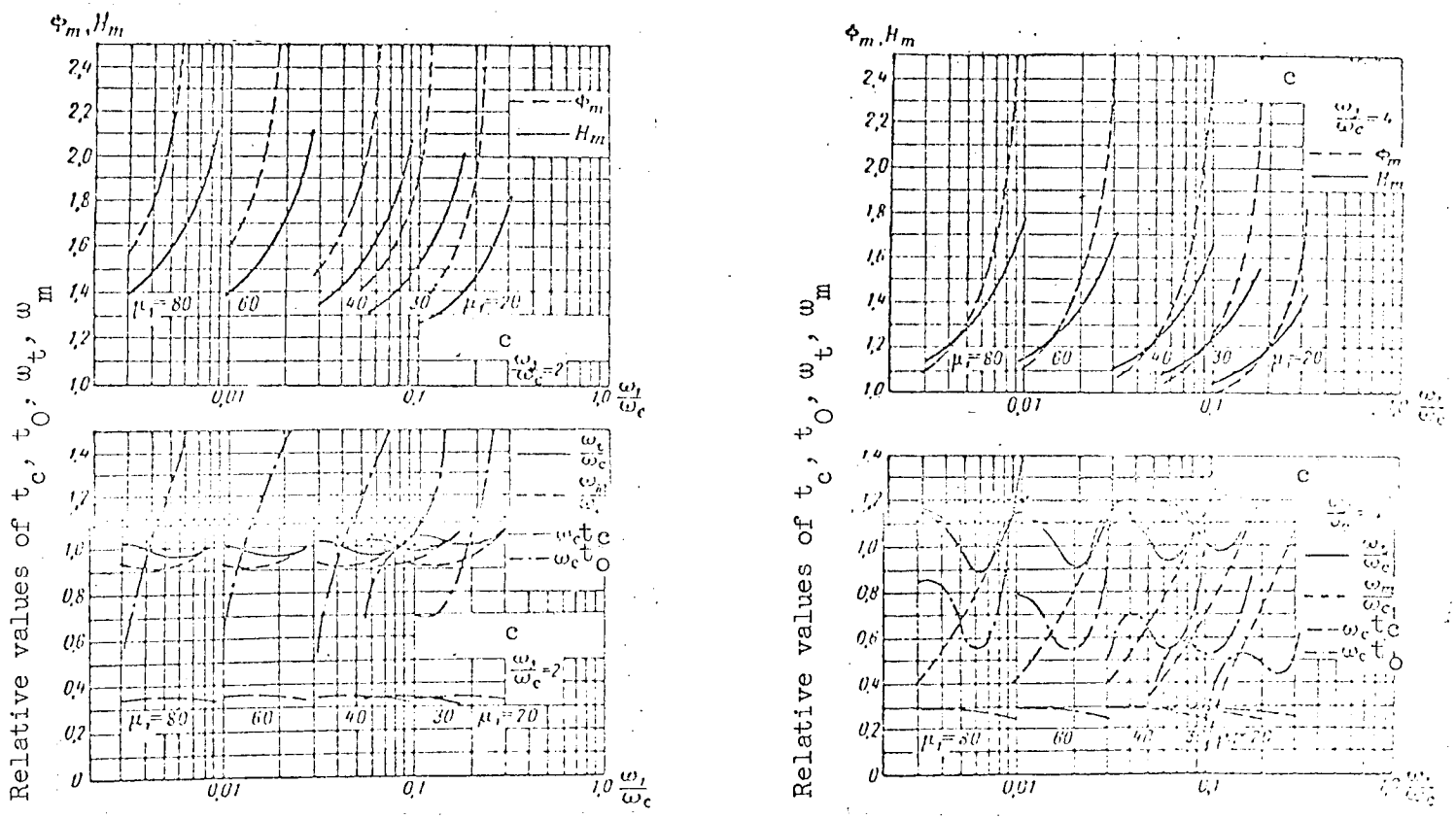

Figure 2.14g. Nomograms of typical LAC.
c is: ω_1 to ω_2 = 40 db/dec; ω_3 to ∞ = 60 db/dec.

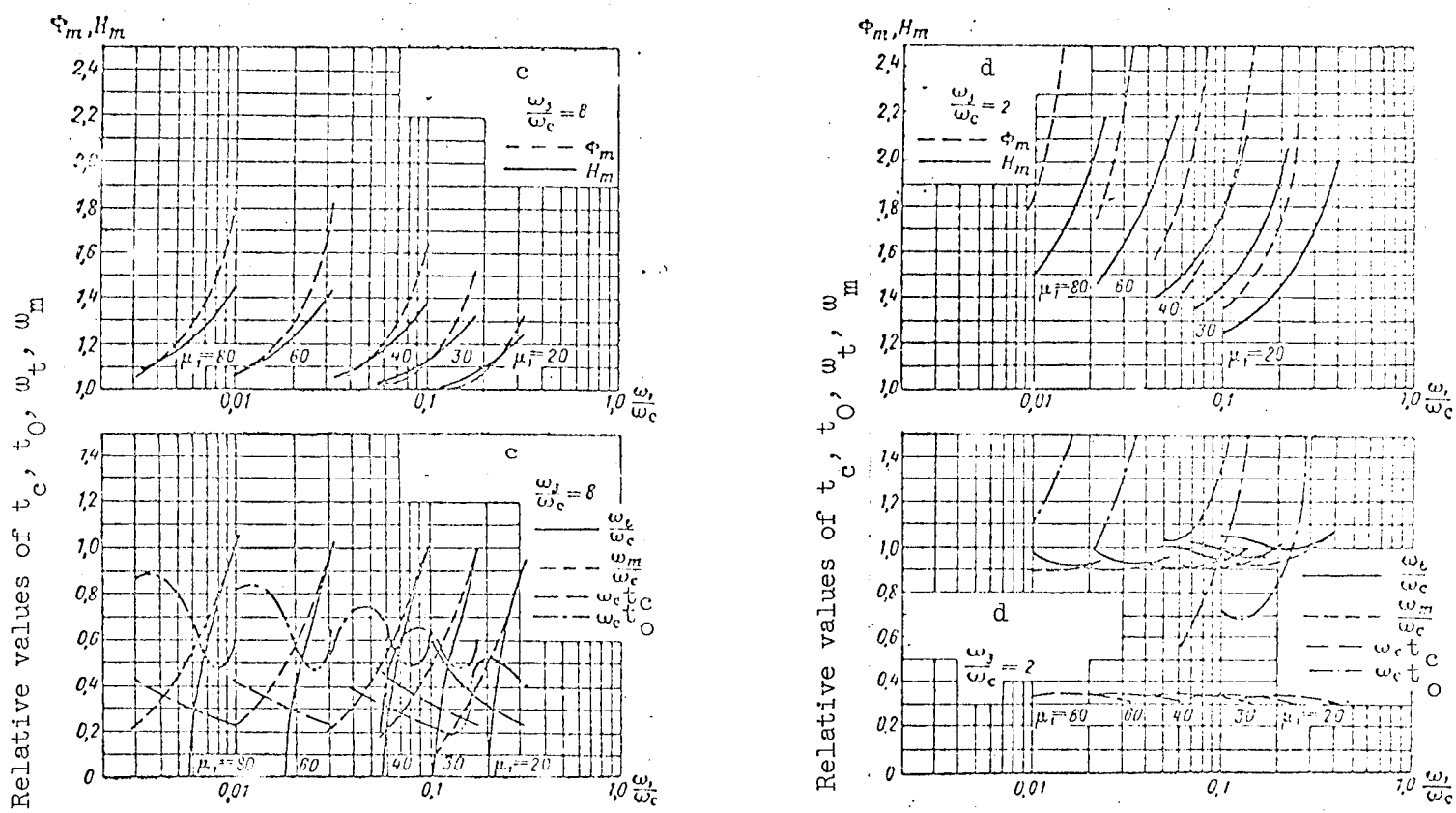

Figure 2.14h. Nomograms of typical LAC.
c is: ω_1 to ω_2 = 40 db/dec; ω_3 to ∞ = 60 db/dec; d is: ω_1 to ω_2 = 60 db/dec; ω_3 to ∞ = 60 db/dec.

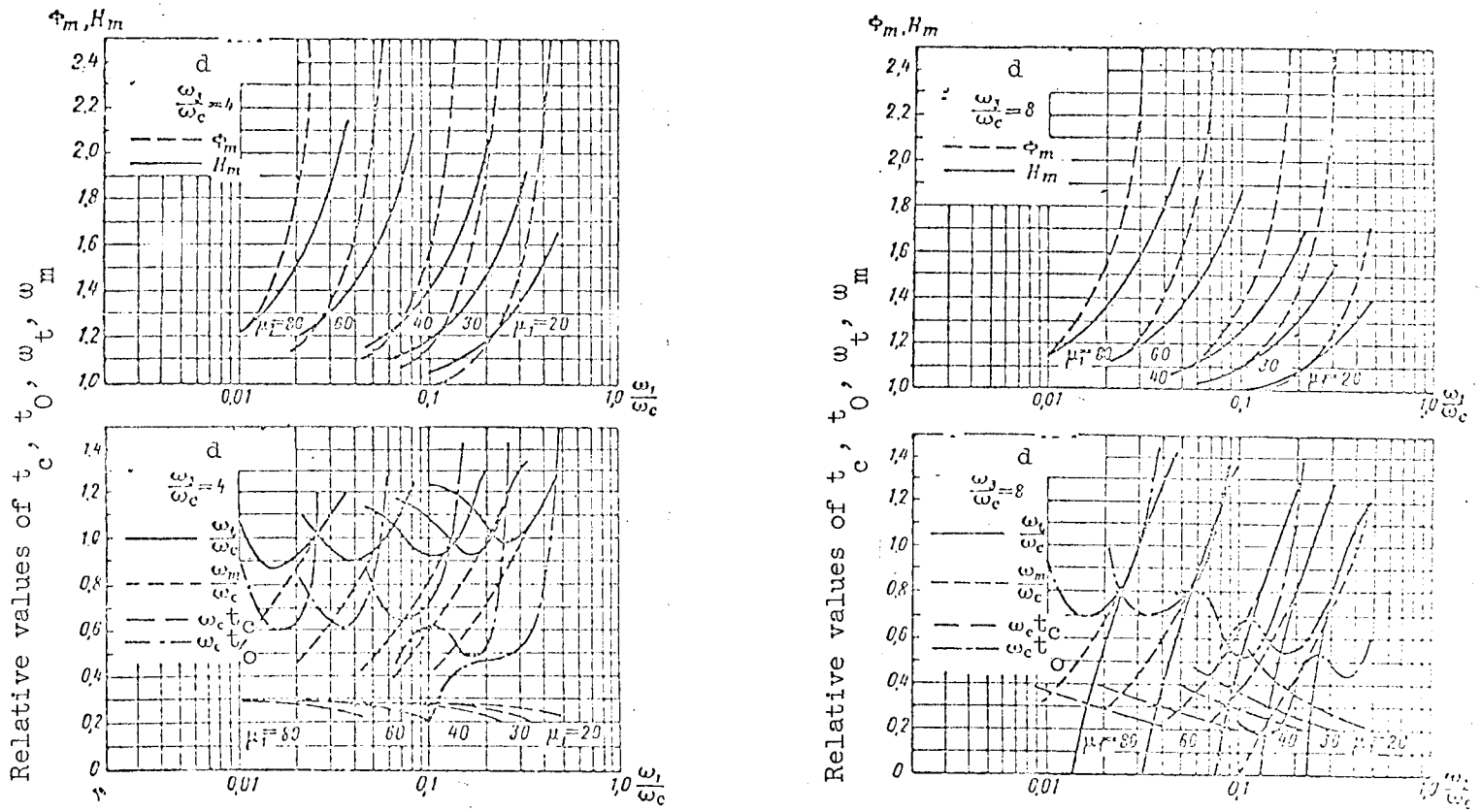

Figure 2.14i. Nomograms of typical LAC.
d is: ω_1 to ω_2 = 60 db/dec; ω_3 to ∞ = 60 db/dec.

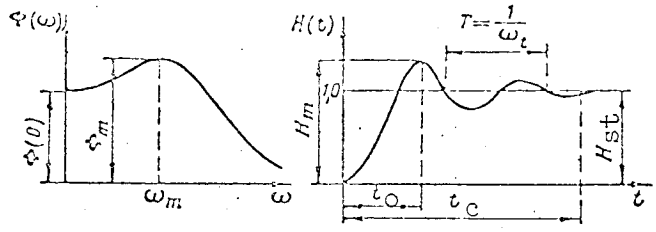

Figure 2.15. Graph of typical transient function of closed loop system.

Table 2.5 shows the most common schemes used for compensation, their transfer functions and frequency response characteristics. It should be pointed out that these tables can be used for compensating devices which are of a different physical nature (mechanical, hydraulic, pneumatic), if their transfer functions coincide with those shown in table 2.5. The method of logarithmic amplitude-frequency characteristics for selecting the automatic control system parameters consists of the following. Let us assume that we have an automatic control system of a definite structure with known parameters, which may be used as a basis to construct the logarithmic amplitude-frequency characteristics of the system. If the dynamic characteristics of the system are unsatisfactory, we can change the frequency response characteristics of the system and provide the necessary dynamic properties by using a compensating device. This device should be selected in such a way that the response of the system agrees with these recommendations. The selection of the compensating device parameters by means of frequency response characteristics is clarified in the following example.

Example 2.1. Let us assume that we have a control system which, in its open loop state has the following transfer function

$$W_1(p) = \frac{k}{p(T_3 p + 1)(T_4 p + 1)}. \tag{2.21}$$

Figure 2.16 shows the frequency response characteristics corresponding to the transfer function (2.21) when the parameters have the following values: $k = 30$; $T_3 = 0.1$ sec; $T_4 = 0.02$ sec; $\omega_3 = 1/T_3 = 10$ 1/sec and $\omega_4 = 1/T_4 = 50$ 1/sec. This frequency response characteristic (curve 1) has a cutoff frequency in the region with a slope 40 db/decade, which agrees with the recommendations presented for the unfavorable characteristics of the transient process--weak attenuation of the oscillations. This proposition is confirmed by the transient function of the closed loop system shown in figure 2.17 (curve 1).

The typical desired frequency response characteristics for this system (curve 2, fig. 2.16) are constructed on the basis of these recommendations. These frequency response characteristics have an amplification factor of $k = 30$, but have the following conjugate frequencies: $\omega_1 = 0.1$ /53

TABLE 2.5. COMPENSATING NETWORKS (dc).

Diagram of network and asymptotic logarithmic amplitude-frequency characteristics.	$W(p)$	$W(0)$	$W(\infty)$	T_1	T_2
	Differentiating networks				
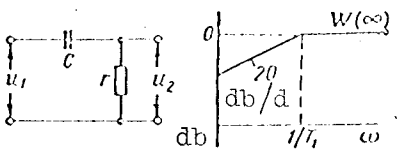	$\frac{T_1 p}{T_1 p + 1}$	0	1	rC	--
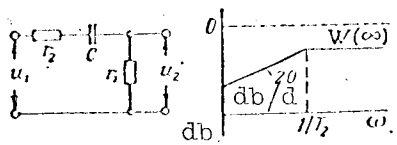	$\frac{T_1 p}{T_2 p + 1}$	0	$\frac{r_1}{r_1 + r_2}$	$r_1 C$	$(r_1 + r_2) C$
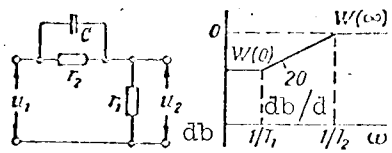	$W(0)\frac{T_1 p + 1}{T_2 p + 1}$	$\frac{r_1}{r_1 + r_2}$	1	$r_2 C$	$\frac{r_1 T_1}{r_1 + r_2}$
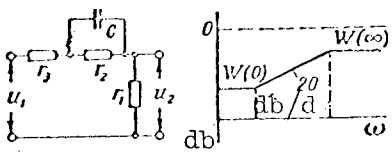	$W(0)\frac{T_1 p + 1}{T_2 p + 1}$	$\frac{r_1}{r_1 + r_2 + r_3}$	$\frac{r_1}{r_1 + r_2}$	$r_2 C$	$\frac{r_1 + r_2}{r_1 + r_2 + r_3} T_1$
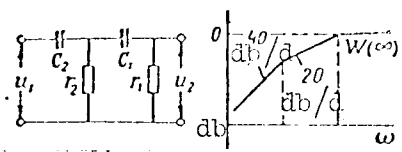	$\frac{T_1 T_2 p^2}{T_1 T_2 p^2 + \left(\frac{r_1 + r_2}{r_1} T_1 + T_2\right) p + 1}$	0	1	$r_1 C_1$	$r_2 C_2$

TABLE 2.5. (cont'd)

Diagram of network and asymptotic logarithmic amplitude-frequency characteristics.	$W(p)$	$W(0)$	$W(\infty)$	T_1	T_2
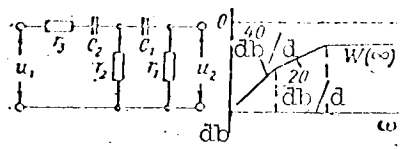	$\frac{(T_1p+1)(T_2p+1)}{T_1T_2p^2+\left[1+\frac{(r_1+r_2)r_3}{r_1r_2}\right]+\left[T_1\left(1+\frac{r_2}{r_1}\right)+T_2\left(1+\frac{r_3}{r_2}\right)\right]p+1}$	0	$\frac{r_1r_2}{r_1r_2+(r_1+r_2)r_3}$	r_1C_1	r_2C_2
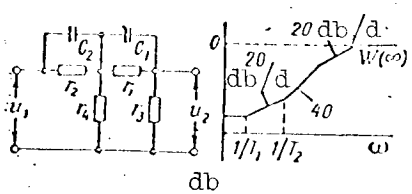	$\frac{(T_1p+1)(T_2p+1)}{T_1T_2p^2+\left\{T_1\left(1+\frac{r_2}{r_1}\right)+T_2\left[1+\frac{(r_1+r_3)r_4}{r_1r_3}\right]\right\}p+\frac{1}{W(0)}}$	$\frac{r_3r_4}{(r_1+r_3)r_4+(r_1+r_3+r_4)r_2}$	1	r_2C_2	r_1C_1
Integrating networks					
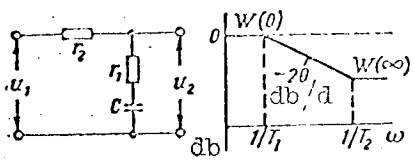	$\frac{T_2p+1}{T_1p+1}$	1	$\frac{r_1}{r_1+r_2}$		r_1C
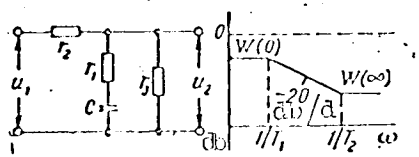	$W(0)\frac{T_2p+1}{T_1p+1}$	$\frac{r_3}{r_2+r_3}$	$\frac{r_1r_3}{r_1r_2+r_2r_3+r_3r_1}$	$\left[1+\frac{r_2r_3}{r_1(r_2+r_3)}\right]T_2$	r_1C

/57

/56

TABLE 2.5. (cont'd)

Diagram of network and asymptotic logarithmic amplitude-frequency characteristics.	$W(p)$	$W(0)$	$W(\infty)$	T_1	T_2
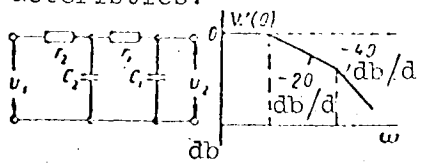	$\dfrac{1}{T_1T_2p^2+\left[T_1\left(1+\dfrac{r_2}{r_1}\right)+T_2\right]p+1}$	1	0	r_1C_1	r_2C_2
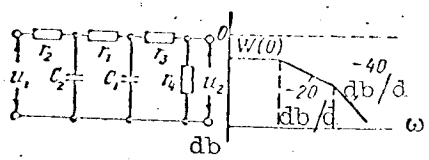	$\dfrac{1}{T_1T_2p^2+\left[T_1\left(1+\dfrac{r_2}{r_1}\right)+T_2\left(1+\dfrac{r_2}{r_4}+\dfrac{r_3}{r_4}\right)\right]p+1}$	$\dfrac{r_4}{r_1+r_2+r_3+r_4}$	0	$\dfrac{r_3+r_4}{r_4}r_1C_1$	r_2C_2
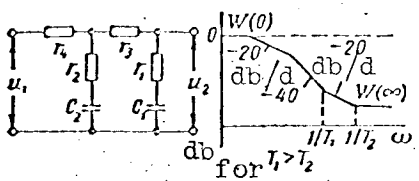	$\dfrac{(T_1p+1)(T_2p+1)}{T_1T_2\left[\left(1+\dfrac{r_3}{r_1}\right)\left(1+\dfrac{r_4}{r_2}\right)+\dfrac{r_4}{r_1}\right]p^2+\left[T_1\left(1+\dfrac{r_3}{r_1}+\dfrac{r_4}{r_1}\right)+T_2\left(1+\dfrac{r_4}{r_2}\right)\right]p+1}$	1	$\dfrac{1}{\left(1+\dfrac{r_3}{r_1}\right)\left(1+\dfrac{r_4}{r_2}\right)+\dfrac{r_4}{r_1}}$	r_1C_1	r_2C_2
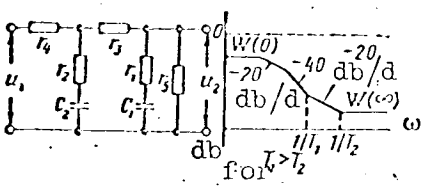	$\dfrac{\dfrac{r_5}{r_3+r_5}(T_1p+1)(T_2p+1)}{T_1T_2\left\{\left[1+\dfrac{r_3r_5}{r_1(r_3+r_5)}\right]\left(1+\dfrac{r_4}{r_2}\right)+\dfrac{r_4(r_1+r_5)}{r_1(r_3+r_5)}\right\}p^2+\left\{T_1\left[1+\dfrac{r_3r_5}{r_1(r_3+r_5)}+\dfrac{r_4(r_1+r_5)}{r_1(r_3+r_5)}\right]+T_2+1+\dfrac{r_4}{r_3}+\dfrac{r_4}{r_3+r_5}\right\}p+1+\dfrac{r_4}{r_3+r_5}}$	$\dfrac{r_5}{r_3+r_4+r_5}$	$\dfrac{r_1r_5}{[r_1(r_3+r_5)+r_3r_5]\left(1+\dfrac{r_4}{r_2}\right)+r_4(r_1+r_5)}$	r_1C_1	r_2C_2

TABLE 2.5. (cont'd)

Diagram of network and asymptotic logarithmic amplitude-frequency characteristics.	$W(p)$	$W(0)$	$W(\infty)$	T_1	T_2
	Integrating-differentiating networks				
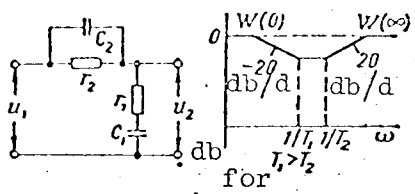	$\frac{(T_1p+1)(T_2p+1)}{T_1T_2p^2+\left[T_1\left(1+\frac{r_2}{r_1}\right)+T_2\right]p+1}$	1	1	r_1C_1	r_2C_2
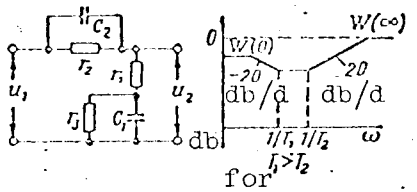	$\frac{(T_1p+1)(T_2p+1)}{T_1T_2p^2+\left[T_1\left(1+\frac{r_2}{r_1}\right)+T_2\right]p+\frac{r_1+r_2+r_3}{r_1+r_3}}$	$\frac{r_1+r_3}{r_1+r_2+r_3}$	1	$\frac{r_1r_3}{r_1+r_3}C_1$	r_2C_2
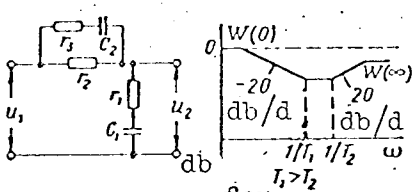	$\frac{(T_1p+1)(T_2p+1)}{T_1T_2\left[1+\frac{r_2r_3}{r_1r_2+r_1r_3}\right]p^2+\left[T_1\left(1+\frac{r_2}{r_1}\right)+T_2\right]p+1}$	1	$\frac{r_1r_2+r_1r_3}{r_1r_2+r_2r_3+r_3r_4}$	r_1C_1	$(r_2+r_3)C_2$
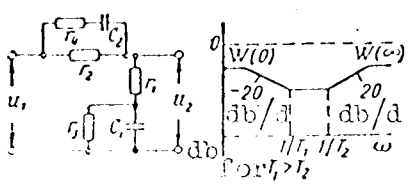	$\frac{(T_1p+1)(T_2p+1)}{T_1T_2\left(1+\frac{r_2r_4}{r_1r_2+r_1r_4}\right)p^2+\left\{T_1\left(1+\frac{r_2}{r_1}\right)+1+\frac{r_2r_4}{(r_1+r_3)(r_2+r_4)}\right\}p+\frac{r_1+r_3}{r_1+r_2+r_3}}$	$\frac{r_1+r_3}{r_1+r_2+r_3}$	$\frac{r_1r_2+r_1r_4}{r_1r_2+r_2r_4+r_4r_1}$	$\frac{r_1r_3}{r_1+r_3}C_1$	$(r_2+r_4)C_2$

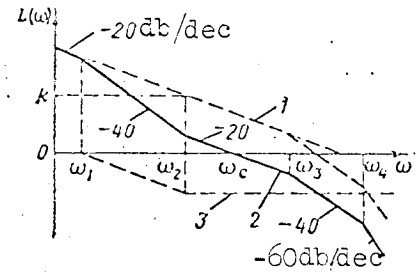

Figure 2.16. Frequency response characteristics corresponding to transfer function (2.21).

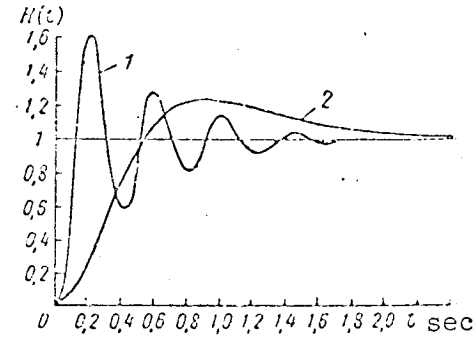

Figure 2.17. Graph of transient functions of system. 1--uncompensated, 2--compensated.

1/sec; ω_2 = 1.0 1/sec; ω_3 = 10.0 1/sec and ω_4 = 50 1/sec. The cutoff frequency ω_c is in the region where the slope is 20 db/decade and ω_3/ω_c = 3.16. The difference between curve 1 and 2 on figure 2.16 gives the characteristics of the compensating network which change the characteristics from those shown by curve 1 to those shown by curve 2. Comparing curve 3 (fig. 2.16) with the typical response characteristics of compensating networks shown in table 2.5, we note that it represents an integrating network (see drawing No. 8 in table 2.5). The circuit has a transfer function

$$W_k(p) = \frac{T_2 p + 1}{T_1 p + 1}, \tag{2.22}$$

where

$$T_1 = (r_1 + r_2)c; \quad T_2 = r_1 c. \tag{2.23}$$

Comparing these values of the compensating network's constants with those required on the bases of curve 3, we obtain the relations $\omega_1 = 0.1 = 1/T_1$ and $\omega_2 = 1.0 = 1/T_2$. Substituting the values of T_1 and T_2 from equation (2.23), we obtain: $r_1 c = 1$; $(r_1 + r_2)\, c = 10$ and, finally, $r_2/r_1 = 9$. By assuming a value for any of the three parameters of the compensating network, the remaining two are obtained from these relations. Let us assume, e.g., that $c = 10^{-5}$ φ = 10 μφ; then $r_1 = 10^5$ ohm and $r_2 = 9 \cdot 10^5$ ohm.

When a compensating network is present, the transfer function of the system under consideration takes on the form

$$W_2(p) = \frac{k(T_1 p + 1)}{p(T_2 p + 1)(T_3 p + 1)(T_4 p + 1)}. \tag{2.24}$$

Figure 2.17 shows the transient function of a closed loop system (curve 2), which has a compensating network with parameters which have been determined. Compared with the uncompensated system (curve 1), the transient function of the compensated network has a form which is different in principle.

When we selected the parameters of the compensating network in the example 2.1, we set forth only one requirement--an increase in damping. This requirement is satisfied because the cutoff frequency of the compensated system in substantially lower than that of the uncompensated system. If this is undesirable, a different type of compensating network may be used. Thus, the selection of any compensating network is determined by the specific requirements of the control system in question. /62

In conclusion we should point out that the method of logarithmic amplitude-frequency characteristics in the form presented here is applicable only to the minimum phase systems. A system is known as a minimum phase system if its transfer function (when the feedback loop is open) does not contain zeros and poles in the right semiplane of the complex plane. For minimum phase systems, it is characteristic to have a single-valued relation between the amplitude and phase characteristics, so that it is only necessary to know one of these characteristics. Therefore, the method of logarithmic amplitude-frequency characteristics operates only with amplitude characteristics. If the logarithmic amplitude-frequency characteristics have a sufficiently large region with a slope of 20 db/decade, this provides the necessary stability in phase. In synthesizing nonminimum phase systems, it is necessary to consider simultaneously the amplitude and the phase-frequency characteristics of open loop systems.

Section 2.4. Brief Remarks on the Theory of Nonstationary Linear Systems

The methods for analyzing linear systems presented in sections 2.2 and 2.3 are applicable only to stationary systems described by linear differential equations with constant coefficients. At the same time, the motion of a guided missile in the general case is described by nonlinear equations with variable coefficients. The variations in the parameters of the missile itself are due to change in its weight, caused by fuel consumption, and change in its velocity and flight altitude. In subsequent chapters we shall show that the characteristics of some control systems depend a great deal on the distance between the missile and the target. In some cases it is convenient to consider these characteristics as depending on the flight time of the missile. By using various approximation techniques, which are presented when specific examples are considered, it is sometimes possible to reduce nonlinear equations with variable coefficients to linear equations, also with variable coefficients. However, even with this simplification of the problem some difficulties still arise.

The basic difficulty in investigating systems described by linear differential equations with variable coefficients is that the solution of such

equations, which are of an order greater than one, does not contain elementary functions. The integration of this class of equations cannot be carried out by quadrature in the general case. At the same time, in solving missile guidance problems (and many others), the principal objective of the investigation is to determine the effect of the control system parameters on the characteristics of missile motion and in the selection of optimum values of these parameters. Obviously, this problem can be most completely solved in the case when we have the general solution of the equations which describe the motion of the missile, and when the relationship between the parameters and the characteristics of motion are expressed in analytical form. In the general case, in order to obtain the general solution of the problem, it is necessary to make simplifications and sometimes to neglect very significant factors. Of course, the general solution obtained in this way will be very approximate in describing the true system.

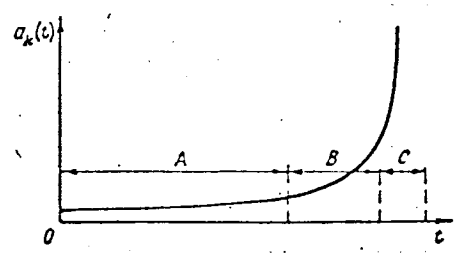

Figure 2.18. Typical graph showing variation in coefficients of the equations of motion for missile with homing guidance.

It is necessary to point out, however, that in connection with the tremendous new possibilities of solving the problem exactly by means of computers, the role of such analytical methods becomes more and more important. These methods give, although with some difficulty, at least a true qualitative solution of the problem in the general form, which gives us a basis for selecting the direction of more accurate investigations by means of computers.

The behavior of a linear nonstationary system is described by an equation of form (2.1), but the coefficients a_K and b_K of this equation are functions of time. The variation in the variable coefficients of the equation as a function of time describing, e.g., the motion of missiles with homing guidance, may be expressed by a graph, as shown in figure 2.18. Over region A, which corresponds to a long range to the target, the coefficients vary slowly. In analyzing the dynamics of the missile along this section, it is possible to use the method of fixed coefficients such that the value of these coefficients is taken to be different for different instants of time. The nature of missile motion for different values of the coefficients shows qualitatively how the variation in the coefficients affects the dynamics of the system. Along region B, where /65
the variation of the coefficients is more appreciable, we use the method of quasistationary coefficients. These coefficients are constant but are not equal to the fixed coefficients for a given instant of time. The quasistationary coefficients are computed by means of special equations. One of the methods

TABLE 2.6. TRANSFORMATION OF NONSTATIONARY COEFFICIENTS INTO QUASISTATIONARY.

Initial equation	Transformed equation	Value of quasistationary coefficients
$a\frac{dx}{dt}+bx=0$	$A\frac{dx}{dt}+Bx=0$	$A=a_0;\ B=b_0$
$a\frac{d^2x}{dt^2}+b\frac{dx}{dt}+cx=0$ $a=\text{const}$	$A\frac{d^2x}{dt^2}+B\frac{dx}{dt}+Cx=0$	$A=a_0;\ B=b_0+\frac{1}{2}a_0\frac{c_1}{c_0};$ $C=c_0$
$a\frac{d^2x}{dt^2}+b\frac{dx}{dt}+cx=0$ $c=\text{const}$	$A\frac{d^2x}{dt^2}+B\frac{dx}{dt}+Cx=0$	$A=a_0\cdot B=b_0-\frac{1}{2}a_1;$ $C=c_0$
$a\frac{d^3x}{dt^3}+b\frac{d^2x}{dt^2}+c\frac{dx}{dt}+$ $+dx=0$ $a=\text{const}$	$A\frac{d^3x}{dt^3}+B\frac{d^2x}{dt^2}+$ $+C\frac{dx}{dt}+Dx=0$	$A=a_0,\ B=b_0+a_1\frac{d_1}{d_0};$ $C=c_0-\frac{1}{3}b_1+\frac{4}{9}b_0\times$ $\times\frac{d_1}{d_0}+\frac{2}{9}\frac{d_1^2}{d_0^2};\ D=d_0$
$a\frac{d^3x}{dt^3}+b\frac{d^2x}{dt^2}+c\frac{dx}{dt}+$ $+dx=0$ $d=\text{const}$	$A\frac{d^3x}{dt^3}+B\frac{d^2x}{dt^2}+$ $+C\frac{dx}{dt}+Dx=0$	$A=a_0;\ B=b_0-a_1;$ $C=c_0-\frac{1}{3}b_1-\frac{1}{9}b_0\times$ $\times\frac{a_1}{a_0}+\frac{2}{9}\frac{a_1^2}{a_0^2};$ $D=d_0;$
$a\frac{d^4x}{dt^4}+b\frac{d^3x}{dt^3}+c\frac{d^2x}{dt^2}+$ $+d\frac{dx}{dt}+ex=0$ $a=\text{const}$	$A\frac{d^4x}{dt^4}+B\frac{d^3x}{dt^3}+C\frac{d^2x}{dt^2}+$ $+D\frac{dx}{dt}+Ex=0$	$A=a_0;\ B=b_0+\frac{3}{2}a_0\frac{e_1}{e_0};$ $C=c_0-\frac{2}{3}b_1+\frac{11}{12}b_0\frac{e_1}{e_0};$ $D=d_0-\frac{1}{4}c_1-\frac{1}{24}\frac{b_0}{a_0}b_1+$ $+\frac{3}{8}c_0\frac{e_1}{e_0};\ E=e_0.$

Note: $a_0=a(t)_{t=t_0};\ b_0=b(t)_{t=t_0}$, etc.

$a_1=\left(\frac{da}{dt}\right)_{t=t_0};\ b_1=\left(\frac{db}{dt}\right)_{t=t_0}$ etc.

for calculating these coefficients is shown below. Thus, along regions A and B missile dynamics is described by linear equations with constant coefficients, whose analysis was carried in sections 2.2 and 2.3. Along region C, when the missile is close to its target, the variable coefficients of equations which describe its motion vary so rapidly that, except in the rare cases pertaining

to the equation of the first or second order, the solution may only be obtained by numerical methods or by simulation with analog computers.

We present data for one method of calculating the quasistationary coefficients for region B.[1] These coefficients are computed by means of special equations which take into account the rate of change of the variable coefficients of the initial equation (first derivative).

Table 2.6 gives formulas for calculating quasistationary coefficients for the differential equations from the first to the fourth order.

Section 2.5. Statistical Dynamics of Linear Systems

When investigating missile guidance systems, it is always necessary to evaluate the behavior of these systems when subjected to random fluctuations. The sources of fluctuations are the internal noise sources aboard the guidance system, the fluctuation of signals which carry information concerning the coordinates of the target and the disturbances produced by the atmosphere. Specific problems on the effect of various random disturbances on the motion of a missile will be considered in subsequent chapters. In the present section we present, in condensed form, the necessary general facts concerning the behavior of linear systems when subjected to random perturbations. The random perturbations which act on the missile are usually random functions of time. A random function is one whose realization as a result of experiment has a random character, i.e., cannot be predicted in advance.

1. Stationary Random Processes. Let us first consider one class of random functions which is of prime importance in most of the applied problems--the class of stationary random functions. A random function is called stationary if all /66 of its probability characteristics (determined below) do not depend on time. The mathematical analysis of stationary functions is relatively simple, and the calculations which are based on this method can be carried out rapidly. It is sometimes convenient to assume that the function is stationary over small intervals of time, when we analyze nonstationary random functions which vary slowly.

An additional limitation, placed on stationary random functions and considered later, is the assumption that these functions are ergodic. A random function has ergodic properties when the probability characteristics, obtained by averaging out over the period of one realization (over a sufficiently large interval of observations), coincide approximately with characteristics obtained by averaging over a multiplicity of realizations (when the time is fixed).

The basic probability characteristics of a stationary random function $x(t)$ with ergotic properties are determined by the following expressions.

The mathematical expectation or the average value is equal to

---

[1] P. E. W. Grensted, Stability Criteria for Linear Equations with Time--Varying Coefficients, R. A. S., No. 3, 1956.

$$\bar{x}(t) = \lim_{T\to\infty} \frac{1}{2T} \int_{-T}^{T} x(t)\,dt \tag{2.25}$$

(when T is sufficiently large).

The dispersion or the average square of the function is

$$\overline{x_0^2}(t) = \sigma_x^2 = \lim_{T\to\infty} \frac{1}{2T} \int_{-T}^{T} x_0^2(t)\,dt, \tag{2.26}$$

where $x_0(t) = x(t) - \bar{x}(t)$ is the balanced random function.

Later in this section we shall consider only balanced random functions; therefore, for convenience, the subscript used to designate these functions will be dropped.

The correlation function which characterizes the degree of coupling between the values of the random function at the instant of time t and $t + \tau$ is equal to

$$R_x(\tau) = \overline{x(t)\cdot x(t+\tau)} = \lim_{T\to\infty} \frac{1}{2T} \int_{-T}^{T} x(t)\,x(t+\tau)\,dt. \tag{2.27}$$

By comparing equations (2.26) and (2.27) we see that

$$R_x(0) = \sigma_x^2. \tag{2.28}$$

A direct Fourier transformation of the correlation function gives the spectral density of the random function.[1] /67

$$S_x(\omega) = \frac{1}{\pi} \int_{-\infty}^{\infty} R_x(\tau)\,e^{-j\omega\tau}\,d\tau = \frac{2}{\pi} \int_{0}^{\infty} R_x(\tau)\cos\omega\tau\,d\tau. \tag{2.29}$$

The spectral density characterizes the frequency distribution of the power of random function x(t). Since power cannot be negative, the spectral density too is a positive function in the entire range of frequencies from 0 to $\pm\infty$. If we know the spectral density of a random function, we can use the inverse Fourier transformation to obtain the correlation function

$$R_x(\tau) = \frac{1}{2} \int_{-\infty}^{\infty} S(\omega)\,e^{j\omega\tau}\,d\omega = \int_{0}^{\infty} S(\omega)\cos\omega\tau\,d\omega. \tag{2.30}$$

---

[1] It is necessary to point out that in Fourier transformation equations other coefficients are frequently used in front of the integral; this should be taken into account when carrying out calculations.

In equations (2.29) and (2.30) the lower limit of integration is replaced by zero (in place of $-\infty$) with a simultaneous decrease by 2 in the averaging interval. This is possible because the correlation function and the spectral density are even functions. By comparing equations (2.30) and (2.28) we obtain the relationship

$$\sigma_x^2 = \int_0^\infty S(\omega)\, d\omega. \tag{2.31}$$

The analytical expressions for the correlation functions and the spectral densities of random stationary processes may be quite diverse. As an example we introduce the random process known as "white noise" or "the absolutely random process." The spectral density of such a process is constant in the entire region of frequencies, i.e.,

$$S_a(\omega) = S_a(0) = \text{const.} \tag{2.32}$$

Equation (2.32) clarifies the origin of the term "white noise." Indeed, the physical analogy of such a random process is the "white light," whose spectrum contains the oscillations of all the frequencies with the same amplitude.

The correlation function of "white noise" may be obtained from its spectral density by using equation (2.30). This gives us /68

$$R_a(\tau) = \pi S_a(0)\, \delta(\tau). \tag{2.33}$$

Equation (2.33) clarifies the origin of the second term used to describe this process--"absolutely random process." The correlation functions of the δ-function type points to the absence of correlation between any arbitrarily close values of the random process.

It is necessary to point out that a random process of the "white noise" type is a mathematical idealization of a real process, because physically it is impossible to realize such a process. The dispersion of this process, as follows from equation (2.31), will be infinitely large. Consequently, the power required to produce such a process is also infinite. In spite of this, in those problems where the spectrum of random reaction substantially exceeds the bandpass of the system under investigation, the true spectrum may be replaced quite successfully with "white noise." However, if this relation between the spectra of reaction and of the system is not satisfied, the necessary spectrum may be obtained by passing "white noise" through a shaping filter.

Now let us analyze the reaction of linear stationary systems to perturbations of the random stationary function type. This reaction may be determined

by utilizing the expression for both the correlation function and the spectral density of random perturbation. The respective equations are presented here without proof.[1]

The stationary linear systems are described by an equation of type (2.1). If the input or perturbed quantity x(t) is a unit function, the output quantity or the reaction of the system y(t) is called the transient function and is designated by H(t). However, if input quantity x(t) is a δ function, the reaction of system y(t) is called the pulse transient function or the weighting function and is designated by K(t). Functions H(t) and K(t) are associated by the following relation

$$K(t) = \frac{dH(t)}{dt}. \tag{2.34}$$

If an arbitrary function of time x(t) is applied to the input of the system, reaction y(t) of a stationary system is determined by Duhamel's integral

$$y(t) = \int_{-\infty}^{t} K(t-\tau)\, x(\tau)\, d\tau. \tag{2.35}$$

The lower integration limit (2.35) shows that in the general case signal x(t) may start to act on the system when $\tau = -\infty$. The upper integration limit shows that the reaction of the system is due only to those values of x(t) for which $\tau \leq t$. This limit may be replaced with infinity if it is convenient, because for any real system $K(t - \tau) = 0$ when $\tau > t$. /69

In subsequent discussionsit is more convenient to use a form of Duhamel's integral obtained from (2.35) by changing variables (with the associated change in the limits of integration)

$$y(t) = \int_{0}^{\infty} K(\tau)\, x(t-\tau)\, d\tau. \tag{2.36}$$

Expression (2.36) will clarify the meaning of the term "weighting function." Indeed, y(t) at the instant of time t is a weighed sum (or integral) with respect to values x(t), which exist τ seconds before the instant of time t.

---

[1] V. S. Pugachev, The Theory of Random Functions and Its Application to the Problems of Automatic Control, Fizmatgiz, 1961;
J. Kh. Lening and R. G. Bettin, Random Processes in Automatic Control Problems, Foreign Literature (I. L.), 1958;
V. V. Solodovnikov, Statistical Dynamics of Linear Automatic Control Systems, Fizmatgiz, 1960.

If we apply to the input of a stationary linear system a random stationary function x(t), whose correlation function is $R_y(\tau)$, the correlation function of the output quantity $R_y(\tau)$ is given by the expression

$$R_y(\tau) = \int_0^\infty K(\tau_1)\, d\tau_1 \int_0^\infty K(\tau_2) R_x(\tau - \tau_2 + \tau_1)\, d\tau_2. \tag{2.37}$$

Using equations (2.28) and (2.37), when $\tau = 0$, we obtain the dispersion of the output quantity of the system

$$\overline{y^2}(t) = \sigma_y^2 = \int_0^\infty K(\tau_1)\, d\tau_1 \int_0^\infty K(\tau_2) R_x(\tau_1 - \tau_2)\, d\tau_2. \tag{2.38}$$

If input function x(t) is applied to the system when $t \geq 0$, i.e., the lower limit in (2.35) is zero, the upper limit in (2.36), (2.37) and (2.38) may be replaced by t. It is possible to retain infinity as the upper limit under these conditions, because this will not affect the results of the calculations.

The relation between the spectral density of input perturbation $S_x(\omega)$ and /70
output quantity $S_y(\omega)$ has a much simpler form

$$S_y(\omega) = \Phi_y(j\omega)\Phi_y(-j\omega) S_x(\omega) = |\Phi_y(j\omega)|^2 S_x(\omega), \tag{2.39}$$

where $\Phi_y(j\omega)$ is the complex transfer closed loop function of the system to which the random perturbation x(t) is applied.

If the system has no feedback (if the feedback loop is open or does not exist), then in expression (2.39) instead of $\Phi_y(j\omega)$ we substitute the transfer function of the system without feedback, designated by $W(j\omega)$, equation (2.4).

On the basis of equations (2.39) and (2.31), the dispersion of the output quantity is equal to

$$\sigma_y^2 = \int_0^\infty |\Phi_y(j\omega)|^2 S_x(\omega)\, d\omega. \tag{2.40}$$

The calculations used to determine dispersion in accordance with equations (2.38) or (2.40) are rather complicated. The amount of time required to perform these calculations increases substantially if it is necessary to determine the dispersion by using the different parameter variations of the system. Therefore, it is of interest to describe a method of determining the dispersion in stationary linear systems by means of analog computers (simulation).

Simulation is a method of studying any phenomena in which the true system is replaced by a simpler system (model), and when some of the phenomena in the model satisfy the same analytical relations as the true system. Usually simulation is performed by using conventional electronic or electromechanical computers--integrators. These computers comprise a collection of units which perform the functions of addition, subtraction, multiplication and division and also integration and differentiation. Special units are used to reproduce quantities which vary in time in accordance with a preestablished law, and also to reproduce various nonlinear characteristics.

Simulation of missile guiding systems may be purely mathematical or may be hybrid, when one part of the system is simulated while the other is a true prototype. When simulation is purely mathematical, all elements of the control system and of the coupling between them are replaced by mathematical relations. In this case it is possible to take into account both the nonlinear characteristics of individual elements of the system as well as the variation in its parameters with time. The mathematical relations obtained, which represent a conventional system of integral-differential equations, are reproduced by selecting corresponding units of the integrator; then the behavior of the entire control system is investigated for different initial conditions and external forces. If the operator so desires, he may examine by oscilloscope or record the nature of variation of any coordinate of the system.

The mathematical principles for utilizing analog computers to determine the /71
dispersion of any output quantity of the dynamic system under consideration follow from comparison of expression (2.40) with the Parseval equation, sometimes known as Rayleigh's theorem

$$\int_{-\infty}^{\infty} y^2(t)\,dt = \frac{1}{\pi}\int_{0}^{\infty} |\Phi_y(j\omega)|^2\,d\omega, \tag{2.41}$$

where $y(t)$ and $\Phi_y(t)$ must be related by the Fourier transformation.

Since the spectral density is a real, even, and nonnegative function of ω, it may always be approximated by the fractional-rational function with real coefficients containing only even powers of ω. Consequently, the spectral density of the input quantity may be represented in the form

$$S_x(\omega) = \sigma_x^2 |W_x(j\omega)|^2, \tag{2.42}$$

where $W_x(j\omega)$ is the transfer function of the element used to obtain the image of the spectral density in the region of the prototypes.[1] Substituting (2.42) into (2.40) we obtain the following expression for dispersion

[1]This element is known as the shaping filter.

$$\sigma_y^2 = \int_0^\infty |\Phi_y(j\omega)|^2 \sigma_x^2 |W_x(j\omega)|^2 d\omega. \tag{2.43}$$

By applying Parseval's formula to equation (2.43), we establish a relation between the unknown dispersion of the output quantity of the system and the integral quadratic evaluation of function y(t)

$$\sigma_y^2 = \frac{1}{\pi} \int_0^\infty |\sigma_x \sqrt{\pi}\, W_x(j\omega)\, \Phi_y(j\omega)|^2 d\omega = \int_{-\infty}^{\infty} y^2(t)\, dt. \tag{2.44}$$

Expression (2.44) shows that y(t) is a pulse transient function of the system whose transfer function is given by expression /72

$$W_y'(p) = \sigma_x \sqrt{\pi}\, W_x(p)\, \Phi_y(p). \tag{2.45}$$

When carrying out simulation by means of analog computers, it is convenient to use the unit function as the perturbation instead of the δ-function. On the basis of (2.34) we may state that y(t) will be the transient function of the system whose transfer function is obtained from equation (2.45) by multiplying it by p, i.e.,

$$W_y(p) = \sigma_x \sqrt{\pi}\, p W_x(p)\, \Phi_y(p). \tag{2.46}$$

The functional diagram showing the simulation of y(t) is shown in figure 2.19a. To obtain dispersion σ_y^2, as follows from expression (2.44), it is sufficient to square y(t) and to integrate it. The corresponding functional diagram consisting of a multiplying unit and an integrator is shown in figure 2.19b.

In conclusion, it is necessary to consider the methods of simulating a system whose transfer function contains zeros. Such transfer functions usually include the function of the investigated system $\Phi_y(p)$, and sometimes the function

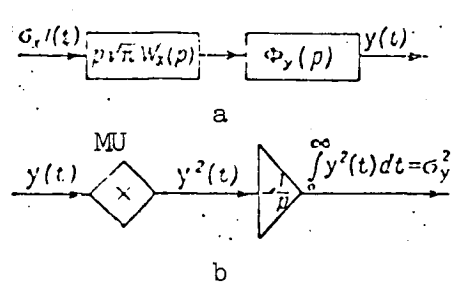

Figure 2.19. Functional diagram showing simulation of the system with a random input signal. a--functional diagram for obtaining output quantity; b--functional diagram for squaring and integrating.

of the shaping filter $W_x(p)$. As we know, the presence of zeros in transfer functions of a system, whose input is subjected to a unit function, is associated with the occurrence of the δ-function and its derivatives in the right side of the differential equation of the system. A solution of this type of equation by means of analog computers is usually reduced to the solution of homogeneous equations with nonzero initial conditions. The inconvenience of this method is that when the parameters of the system are varied the control coefficients vary, and consequently the initial conditions also vary, because they are related by recurrent relationships with the coefficients. When the number of zeros is large, the calculations and the introduction of initial conditions become very difficult. We shall describe a simulation technique free of these disadvantages.

Let us assume that the investigated dynamic system is described by nonhomogeneous differential equations written in symbolic form. /73

$$(p^n + a_{n-1}p^{n-1} + \ldots + a_1 p + a_0)\, y(t) = \\ = (b_m p^m + b_{m-1}p^{m-1} + \ldots + b_1 p + b_0)\, x(t),$$

where n > m.

If we divide the left side and the right side of this equation into a characteristic polynomial, we obtain

$$y(t) = \left(b_m \frac{1}{p^{n-m}} + b_{m-1}\frac{1}{p^{n-m+1}} + \ldots + b_1 \frac{1}{p^{n-1}} + b_0 \frac{1}{p^n}\right) z(t), \qquad (2.47)$$

where z(t) is an auxiliary function given by expression

$$z(t) = \frac{p^n x(t)}{p^n + a_{n-1}p^{n-1} + \ldots + a_1 p + a_0}$$

or

$$z(t) = x(t) - \left(a_{n-1}\frac{1}{p} + \ldots + a_1 \frac{1}{p^{n-1}} + a_0 \frac{1}{p^n}\right) z(t). \qquad (2.48)$$

Equation (2.48) is used to construct the functional diagram whose output contains auxiliary function z(t). Then, on the basis of equation (2.47), a general functional diagram is prepared for obtaining the output quantity of the system y(t). This diagram is shown in figure 2.20. This method makes it possible to simulate systems whose transfer functions contain zeros without introducing nonzero initial conditions.

2. Nonstationary Random Processes. Let us consider the general expression for the output quantity of a nonstationary linear system, subjected to nonstationary random forces. For any reaction /74

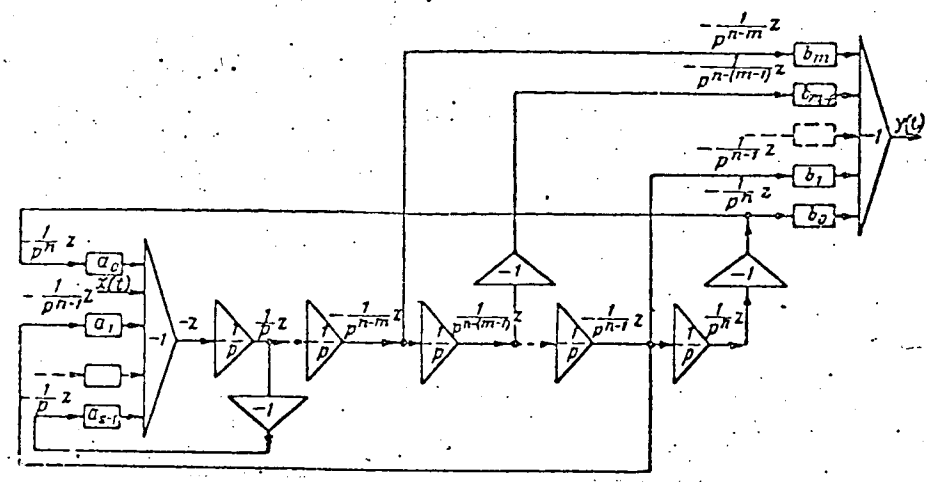

Figure 2.20. Functional diagram showing simulation of a system whose transfer function contains zeros.

$$y(t) = \int_{-\infty}^{t} K(t, \tau)\, x(\tau)\, d\tau, \tag{2.49}$$

where input quantity x(t) may be determined in the interval $-\infty \leq t \leq \infty$. The output quantity may be any coordinate of the guided missile which is of interest to us, in particular it may be one of the coordinates of the center of gravity, which can be used to measure the miss of the missile.

It is necessary to point out that equation (2.49) for nonstationary systems is different from equation (2.35) for stationary systems. In the case of stationary systems, the pulse transient function depends only on the difference between running time t and instant of time τ at which the δ-function is applied to the system. It is obvious that in the nonstationary system the pulse transient function is not a function of the difference $(t - \tau)$, but of both these variables, because in this system the nature of the system's reaction depends on the time when the δ-function is applied to the system. The pulse transient function $K(t,\tau)$ may be represented in the form of a surface in the rectangular system of coordinates t, τ (fig. 2.21). Since in real systems the output signal cannot appear before the input signal, the following identity is valid

$$K(t, \tau) \equiv 0 \quad \text{when} \quad t < \tau.$$

If x(t) is a random function of time, the mathematical expectation of the output quantity is given by expression

$$\overline{y(t)} = \int_{-\infty}^{\infty} K(t, \tau)\, \overline{x(\tau)}\, d\tau, \tag{2.50}$$

where $\overline{x(t)}$ is the mathematical expectation of the input perturbing function.

The correlation function of output quantity $R_y(t_1,t_2)$ may be computed by means of the following equation from the known correlation function of input quantity $R_x(t_1,t_2)$[1]

$$R_y(t_1, t_2) = \int_{-\infty}^{t_1} K(t_1, \tau_1)\, d\tau_1 \int_{-\infty}^{t_1} K(t_2, \tau_2) R_x(\tau_1, \tau_2)\, d\tau_2. \tag{2.51}$$

To obtain the dispersion of the output quantity, it is sufficient to let /75
$t_1 = t_2 = t$ in equation (2.51)

$$\sigma_y^2(t) = \int_{-\infty}^{t} K(t, \tau_1)\, d\tau_1 \int_{-\infty}^{t} K(t, \tau_2) R_x(\tau_1, \tau_2)\, d\tau_2. \tag{2.52}$$

Equations (2.50) - (2.52) refer to the case when one input signal is applied to the system. For a missile control system it is of interest to determine the output quantity (e.g., the miss) when a large number of input signals are applied simultaneously--random signals and nonrandom signals.

If n input signals $x_1(t)$, $x_2(t)$,..., $x_n(t)$ are applied to a nonstationary linear system, the output quantity, if we use the principle of superposition as applied to linear systems, will be given by the expression

$$y(t) = \sum_{k=1}^{n} \int_{-\infty}^{t} K_k(t, \tau)\, x_k(\tau)\, d\tau.$$

The correlation function of output quantity $R_y(t_1, t_2)$ may be determined by means of the following equation in terms of the correlation functions $R_{xk}(t_1,t_2)$ and reciprocal correlation functions $R_{xjk}(t_1,t_2)$

$$R_y(t_1, t_2) = \sum_{j=1}^{n} \sum_{k=1}^{n} \int_{-\infty}^{t_1} K_j(t_1, \tau_1)\, d\tau_1 \int_{-\infty}^{t_2} K_k(t_2, \tau_2) R_{xk}(\tau_1, \tau_2)\, d\tau_2. \tag{2.53}$$

If all n of the input functions are statistically independent and have zero mathematical expectations, then in equation (2.53) the terms with various subscripts ($j \neq k$) will be equal to zero

---

[1] Equation (2.51) is analogous in principle to equation (2.37) for stationary systems.

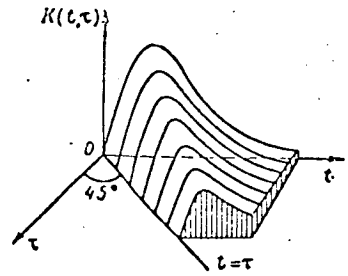

Figure 2.21. Curves of pulse transient function of nonstationary system.

$$R_y(t_1, t_2) = \sum_{k=1}^{n} \int_{-\infty}^{t_1} K_k(t_1, \tau_1)\, d\tau_1 \int_{-\infty}^{t_2} K_k(t_2, \tau_2)\, R_{xk}(\tau_1, \tau_2)\, d\tau_2. \tag{2.54}$$

Assuming that in equation (2.54) $t_1 = t_2 = t$, we obtain the dispersion for /76 a special case when the reactions perturbing the system are statistically independent

$$\sigma_y^2(t) = \sum_{k=1}^{n} \int_{-\infty}^{t} K_k(t, \tau_1)\, d\tau_1 \int_{-\infty}^{t} K_k(t, \tau_2)\, R_{xk}(\tau_1, \tau_2)\, d\tau \tag{2.55}$$

or

$$\sigma_y^2(t) = \sigma_{y_1}^2(t) + \sigma_{y_2}^2(t) + \ldots + \sigma_{y_n}^2(t). \tag{2.56}$$

Expression (2.56) shows that in this special case the dispersion of the output quantity is equal to the sum of the dispersions due to the individual reaction of each input signal.

Finally, let us consider the case when a nonstationary system having nonzero, but random initial conditions is subjected, at instant $t = 0$, to a random perturbing function $x(t)$. The correlation function for the output quantity in this case is given by expression

$$\begin{aligned} R_y(t_1, t_2) = {} & \sum_{j=1}^{n} \sum_{k=1}^{n} u_j(t_1)\, u_k(t_2)\, \overline{c_j c_k} + \sum_{j=1}^{n} u_j(t_1) \int_0^{t_2} K(t_2, \tau)\, \overline{c_j x(\tau)}\, d\tau + \\ & + \sum_{j=1}^{n} u_j(t_2) \int_0^{t_1} K(t_1, \tau)\, \overline{c_j x(\tau)}\, d\tau + \\ & + \int_0^{t_1} K(t_1, \tau_1)\, d\tau_1 \int_0^{t_2} K(t_2, \tau_2)\, R_x(\tau_1, \tau_2)\, d\tau_2, \end{aligned} \tag{2.57}$$

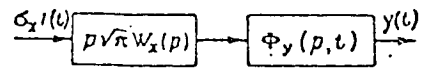

Figure 2.22. Functional diagram showing simulation of nonstationary system.

where $u_j(t)$ is the output function of the system due to the jth nonzero initial condition, which is equal to unity when the other initial conditions are equal to zero; and c_j is the random value of the jth initial condition.

Averaging in (2.57) is carried out over a multiplicity of possible combinations of initial conditions. In a special case, when the initial conditions are statistically independent and also do not depend on the perturbing function and have zero average values, the expression for the dispersion of the output quantity has the form

$$\sigma_y^2(t) = \sum_{k=1}^{n} (\bar{c}_k)^2 u_k^2(t) + \int_0^t K(t, \tau_1)\, d\tau_1 \int_0^t K(t, \tau_2) R_x(\tau_1, \tau_2)\, d\tau_2. \qquad (2.58)$$

The equations which we have presented for the analysis of nonstationary linear systems, subjected to random perturbations, are extremely complicated and in practice do not make it possible to carry out an analytical investigation of these systems. Therefore, these equations are usually used to substantiate some method of statistical analysis by means of analog or digital computers.[1] The following is one of the methods of simulating such systems. The simulator of the system is fed with a sequence of a large number of realizations of random reactions, and the realizations of the random process showing the variation of the output quantity of interest to us is recorded. By reducing the large number of realizations of the output quantity obtained, it is possible to obtain the desired probability characteristics of this quantity. In the problem concerning the flight of a guided missile, the greatest interest obviously will be in the probability characteristics (mathematical expectation, dispersion) of the miss distance of the missile with respect to the target. /77

The method which we have described for studying the reaction of random perturbations on a nonstationary system has a series of definite advantages. It may be applied to a system of any class, including a nonlinear system, and makes it possible to obtain accurate data on the characteristics of the investigated system. The disadvantage of the method is the necessity of having a large number of realizations of perturbing reactions and some complexity in introducing these realizations into the simulator.

In conclusion let us consider a simulation method for obtaining the dispersions of a nonstationary system, subjected to a stationary random perturbation.

---

[1] N. P. Buslenko, The Method of Statistical Investigation, Fizmatgiz, 1962.

The functional diagram of a system using a machine simulator is shown in figure 2.22. Because the parameters of the system vary with time, instead of the transfer function, we introduce the operator of the system $\overline{\Phi}_y(p,t)$. The transfer function is a special case of the operator when the system changes from a nonstationary one to a stationary one. Because the input signal is stationary, the transfer function of the shaping filter $\overline{W}_x(p)$, remains as a fractional-rational function p and is determined from the spectral density of the input signal by means of (2.42). This transfer function (fig. 2.22) is multiplied by p; therefore, the pulse transient function at the output of the system will be obtained when a unit function rather than a δ-function is introduced at the input. A perturbation of the unit function type is easier to realize in simulators. /78

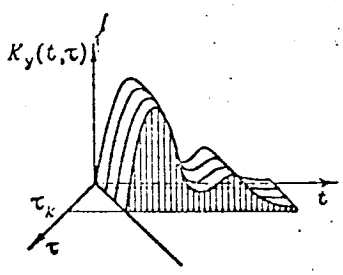

Figure 2.23. Intersection of surface $K_y(t, \tau)$ by plane τ_k = const.

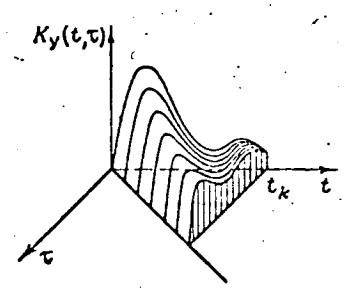

Figure 2.24. Intersection of surface $K_y(t, \tau)$ by plane t_k = const.

Let us designate by $K_y(t, \tau)$ the pulse transient function for a system consisting of a shaping filter and the investigated nonstationary system. Such pulse transient function may, in principle, be obtained for any output quantity of the system y(t). The dispersion for this output quantity is obviously given by equation

$$\sigma_y^2(t) = \int_{-\infty}^{t} K_y^2(t, \tau)\, d\tau. \tag{2.59}$$

To determine dispersion $\sigma_y^2(t)$ by the method of numerical integration, it is necessary to obtain function $K_y(t, \tau)$. For this purpose, in the schematic diagram of figure 2.22 we shall introduce a unit function $\sigma_x\, 1(\tau)$ at different instants of time τ. The physical introduction of a unit function at various instants of time τ means that as time τ changes, the parameters of the system $\overline{\Phi}_y(p, \tau)$ also change. At the instant of time τ_k for each application of the unit function at the input of this scheme we obtain a reaction at the output

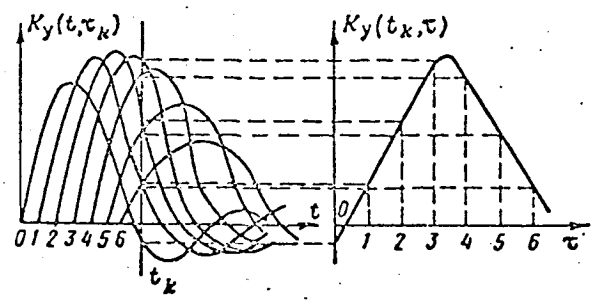

Figure 2.25. Graphical method for obtaining characteristics of $K_y(t_k, \tau)$.

which is equal to the pulse transient function $K_y(t, \tau_k)$. Such a reaction is a function of time t and of time instant τ_k when the unit function is applied. What we have stated is clarified in figure 2.23, where the intersections of surface $K_y(t, \tau)$ are shown by vertical planes parallel to the t axis. For each value of τ_k there is a different intersection and consequently a different curve $K_y(t, \tau_k)$. According to equation (2.59), to compute the dispersion of the output quantity for a given $t = t_k$, it is necessary to obtain curve $K_y(t_k, \tau)$, i.e., the intersection of surface $K_y(t, \tau)$ by a vertical plane parallel to the τ axis (fig. 2.24). Figure 2.25 illustrates how this curve is obtained graphically from a family of curves $K_y(t, \tau_k)$, recorded experimentally (fig. 2.22). Function $K_y(t_k, \tau)$, obtained graphically, is squared and integrated. In accordance with /79
(2.59), integration gives us

$$\sigma_y^2(t_k) = \int_0^{t_k} K_y^2(t_k, \tau)\, d\tau. \tag{2.60}$$

The lower limit of integration in (2.60) is taken equal to zero because, during the experimental investigations, it was assumed that $t \geq 0$.

When investigating a missile control system, it is usually interesting to know some coordinate of the missile on a definite plane which contains the target. In this case, the final purpose of the calculation is to obtain the dispersion of the output quantity of the system for a definite instant of time $t = t_k$ by means of expression (2.60), if t_k is the missile's flight time through the indicated plane. If we are to determine σ_y^2 as a function of time, the calculations in question must be repeated by as many times as there are points required to obtain the function $\sigma_y(t)$.

Section 2.6. Method of the Phase Plane for Analyzing Relay Systems

In missile control systems, relay amplifying devices or other elements are used which have characteristics of the relay type. If a control system has even one such element, it is impossible to use the methods of analysis presented for linear systems.

The method of the phase plane is widely used in investigating control processes in relay systems. This method is descriptive and provides for high accuracy. The principal limitation of this method is that it can only be used to describe nonlinear differential equations not greater than second order. The investigation of systems, described by equations of higher orders, makes it necessary to represent the processes taking place in them in the phase space, which becomes very difficult to visualize. /80

Let us consider the basic principles of this method. The phase plane is a plane which contains two coordinate axes (z,y), along which the variables characterizing the transient behavior of the system are plotted. For these variables it is convenient to take the deviation of the controlled quantity y, and the rate of change of this deviation z = dy/dt. Let us assume that the behavior of some system is described by a nonlinear equation of the second order

$$\frac{d^2y}{dt^2} = f\left(y, \frac{dy}{dt}\right). \tag{2.61}$$

We introduce the notation z = dy/dt, and represent this equation in the form of two equations of the first order

$$\left.\begin{aligned} \frac{dy}{dt} &= f_1(y, z), \\ \frac{dz}{dt} &= f_2(y, z), \end{aligned}\right\} \tag{2.62}$$

where in the general case f_1, f_2 are nonlinear functions.

The solution of (2.62) gives the law for the time variation of the deviation y and its velocity z. Both expressions may be considered as differential equations in the parametric form of some curve in the plane y, z, where the parameter is time t. By dividing equation (2.62) term by term (eliminating the parameter t), we obtain the differential equation of this curve on the phase plane.

$$\frac{dz}{dy} = \frac{f_2(y, z)}{f_1(y, z)}. \tag{2.63}$$

Integrating equation (2.63), we obtain the equation for the integral curve z = F(y, c) on the plane. Curve z = F(y, c) is called the phase curve or the

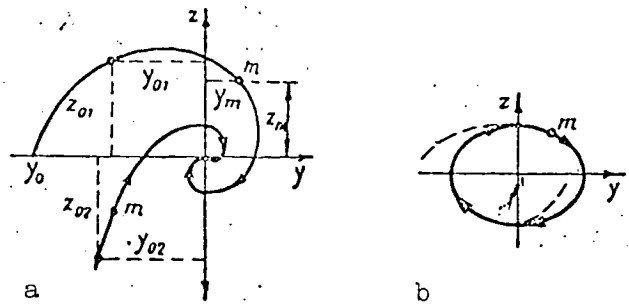

Figure 2.26. Phase trajectory. a--damped oscillations; b--selfsustained oscillations.

phase trajectory of the system's motion, where c is the integration constant which is determined from the initial conditions. The possible form of phase trajectory is shown in figure 2.26. Some point m on the phase plane with co- /81
ordinates y_m, z_m, known as the image point, characterizes the state of the sys-

tem at the particular instant of time. The transient process in the system will be characterized by the movement of point m which describes a curve--phase trajectory--as the transient process takes place in the system (fig. 2.26a). Countless numbers of initial conditions determine a countless number of phase trajectories. Because the differential equations have a single-valued solution for definite initial conditions, the point tracing the phase trajectory will move along a definite curve, and when external forces are absent, it may go over to another trajectory.

In a stable system, whether linear or nonlinear, the transient process is damped out and for $t \to \infty$ $y \to 0$ and $z \to 0$. This means that in a stable system the tracing point will always move along the phase trajectory towards the origin of the coordinate system. Figure 2.26a shows the phase trajectories of a stable system.

If the transient process has an oscillatory type of damped motion, then the tracing point will approach the center of coordinates in a spiral, because the magnitudes of the deviations and the velocities change their signs and decrease in absolute value. If the system can sustain undamped oscillations, i.e., if the equation of the system has a periodic solution, the tracing point will move continuously along some close loop (fig. 2.26b). One revolution of the tracing will obviously be equal to one period of the selfsustained oscillations. In an unstable system the tracing point moves from the origin of the coordinates, i.e., the deviation and velocity increase without limit.

Having presented these general principles, we shall analyze the control /82
processes in specific systems by using the method of the phase plane. Let us consider a nonlinear (relay) system, schematically represented in figure 2.27. This system occurs, in particular, in a tracking system with a relay amplifier, in a system for stabilizing the tilt angle of a missile with relay control and in a series of other systems.

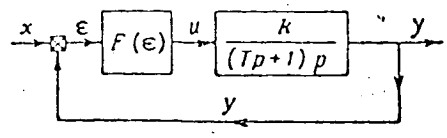

Figure 2.27. Functional diagram of a system with a transfer function in the linear part, given by (2.64).

In figure 2.27 F(ε) designates the characteristics of the nonlinear element from which the signal is applied to the linear part of the system with a transfer function

$$W(p) = \frac{k}{(Tp+1)p}, \tag{2.64}$$

where T and k are the time constant and the amplification factor of the system, respectively.

1. Analysis of Simplest Relay Servosystem with Ideal Characteristics. Let us consider the processes in a system containing a nonlinear element with idealized characteristics (fig. 2.28). A relay device will have such a characteristic, if its sensitivity is large. We shall neglect the delay in the operation of the relay. The functional diagram of a system with these characteristics is shown in figure 2.29.

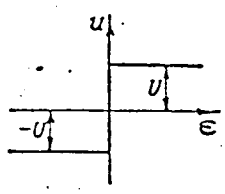

Figure 2.28. Idealized relay characteristic.

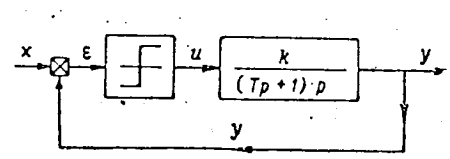

Figure 2.29. Functional diagram of system with relay characteristics (fig. 2.28).

Let us write the equations of motion of the system and analyze the effect produced by input signal x. The equation of the linear part of the system has the form

$$T\frac{d^2y}{dt^2} + \frac{dy}{dt} = ku. \tag{2.65}$$

Signal u, applied to the linear part of the system is constant in magnitude, and its sign is determined by the sign of the mismatch, i.e., /83

$$u = U \operatorname{sign} \varepsilon. \tag{2.66}$$

This expression is a symbolic designation of the step function shown in figure 2.28. We note that equation (2.66) may be represented in the form

$$u = U\frac{\varepsilon}{|\varepsilon|}. \tag{2.67}$$

If we add to equations (2.65) and (2.66) the equation which determines the mismatch

$$\varepsilon = x - y, \tag{2.68}$$

we obtain a system of equations for a simple relay system.

If we eliminate ε and u from equations (2.65), (2.66) and (2.68), we obtain a relationship between the input and output quantities of the servosystem in the form of a nonlinear differential equation

$$T\frac{d^2y}{dt^2} + \frac{dy}{dt} - kU\,\mathrm{sign}\,(x - y) = 0. \tag{2.69}$$

First let us consider the case x = const. In this case, without disrupting the general nature of the investigation, we may assume that x = 0. Also, if we note that sign (x - y) is an odd function, i.e., sign $(-\varepsilon)$ = - sign (ε), we obtain the equation of the system in the following form

$$T\frac{d^2y}{dt^2} + \frac{dy}{dt} + \omega_0\,\mathrm{sign}\,y = 0, \tag{2.70}$$

where $\omega_0 = kU$.

Equation (2.70) contains the specific parameters of the system T and ω_0. In order that the subsequent investigation retain its general character, it is necessary to write it in standard form.

If we take into account the obvious property of the function sign (ay) = sign (y), where a is any positive number, we obtain

$$\frac{d^2\bar{y}}{d\tau^2} + \frac{d\bar{y}}{d\tau} = \varkappa, \tag{2.71}$$

where $\tau = \frac{t}{T}$ is the dimensionless time; $\bar{y} = \frac{y}{T\omega_0}$ is the dimensionless value of the output quantity; $\frac{d\bar{y}}{d\tau} = \frac{1}{\omega_0}\frac{dy}{dt}$ is the dimensionless velocity; $\frac{d^2\bar{y}}{d\tau^2} = \frac{T}{\omega_0}\frac{d^2y}{dt^2}$ is the /84 dimensionless acceleration and χ = - sign $\bar{y}$.

We note that

$$\varkappa = 1 \quad \text{when} \quad \bar{y} < 0,$$
$$\varkappa = -1 \quad \text{when} \quad \bar{y} > 0.$$

Also, noting that $d\bar{y}/d\tau = \bar{z}$, we obtain two equations of the first order in place of (2.71)

$$\left.\begin{aligned} \frac{d\bar{z}}{d\tau} + \bar{z} &= \varkappa, \\ \frac{d\bar{y}}{d\tau} &= \bar{z}, \end{aligned}\right\}. \tag{2.72}$$

If we eliminate the independent variable τ from (2.71), we find the equation which relates $\bar{z}$ and $\bar{y}$

$$\frac{d\bar{z}}{d\bar{y}} = \frac{\varkappa - \bar{z}}{\bar{z}}. \tag{2.73}$$

After integrating (2.73) with initial conditions $\tau = 0$, $\bar{y} = \bar{y}_0$ and $\bar{z} = \bar{z}_0$, we obtain the equation of the phase trajectories

$$\bar{y} = \bar{y}_0 + \bar{z}_0 - \bar{z} + \varkappa \ln \frac{\bar{z}_0 - \varkappa}{\bar{z} - \varkappa}. \tag{2.74}$$

When $\bar{y} < 0$ $\chi = 1$, i.e., for the entire left part of the phase plane, we have

$$\bar{y} = \bar{y}_0 + \bar{z}_0 - \bar{z} + \ln \frac{1 - \bar{z}_0}{1 - \bar{z}}. \tag{2.75}$$

When $\bar{y} > 0$ $\chi = -1$, i.e., for the entire right side of the phase plane, we have

$$\bar{y} = \bar{y}_0 + \bar{z}_0 - \bar{z} - \ln \frac{1 + \bar{z}_0}{1 + \bar{z}}. \tag{2.76}$$

Figure 2.30 shows the phase trajectories constructed in accordance with equations (2.75) and (2.76) with initial conditions $\bar{Z}_0 = 0$ and $\bar{y}_0 = 0a_0$. Region /85
a_0b_1 is constructed in accordance with equation (2.75), and region $b_1a_1b_2$ is constructed from equation (2.76), while region $b_2a_2b_3$ is constructed from (2.75). The initial conditions for the second region are $\bar{y}_0 = 0$, $\bar{Z}_0 = 0b_1$ and for the third region they are $\bar{y}_0 = 0$, $\bar{Z}_0 = 0b_2$, etc. As we continue to construct the phase trajectory in sections, we note that we obtain a curve which converges towards the origin of the coordinate system. This means that the system is stable, and that it has a transient process with damped oscillations. The phase trajectory of the process has breaks on the axis of the ordinates. These breaks are due to the change in the sign of control signal U at the output of the relay element.

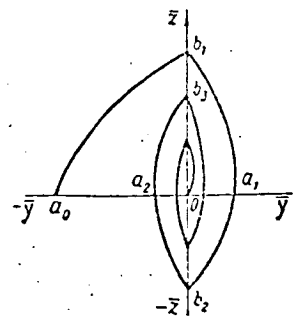

Figure 2.30. Phase trajectories constructed in accordance with equations(2.75) and(2.76).

Let us find the relationship between output quantity $\bar{y}$ and its rate of change $\bar{z}$ with time. The solution of the first equation of system (2.72) with initial conditions $\tau = 0$, $\bar{z} = \bar{z}_0$ will have the following form

$$\bar{z} = \bar{z}_0 e^{-\tau} + \varkappa(1 - e^{-\tau}). \tag{2.77}$$

If we integrate the value of $\bar{z}$ obtained by means of this equation, we find $\bar{y}$ as a function of τ

$$\bar{y} = \int \bar{z}\, d\tau + c = -\bar{z}_0 e^{-\tau} + \varkappa\tau + \varkappa e^{-\tau} + c.$$

We determine the arbitrary constant from the initial conditions, assuming that for $\tau = 0$ $\bar{y} = \bar{y}_0$, $\bar{z} = \bar{z}_0$. In this case

$$c = \bar{y}_0 + \bar{z}_0 - \varkappa$$

and

$$\bar{y} = \bar{y}_0 + \bar{z}_0(1 - e^{-\tau}) + \varkappa[\tau - (1 - e^{-\tau})]. \tag{2.78}$$

On the basis of (2.77) and (2.78), by aligning the initial conditions, we may construct a curve showing the variation in $\bar{y}$ and $\bar{z}$ as a function of time.

The time variables $\bar{z} = \bar{z}(\tau)$ and $\bar{y} = \bar{y}(\tau)$ may also be obtained from the phase picture of the system's motion. To determine the time it takes for the tracing point to move from position 1 (coordinates $\bar{y}_1$, $\bar{z}_1$) to position 2 (coordinates $\bar{y}_2$, $\bar{z}_2$) (fig. 2.31), we add equations (2.77) and (2.78) replacing, respectively, $\bar{z}_0$, $\bar{y}_0$ by $\bar{z}_1$, $\bar{y}_1$ and $\bar{z}$, $\bar{y}$ by $\bar{z}_2$, $\bar{y}_2$. Then we obtain /86

$$\tau_2 - \tau_1 = \Delta\tau_{1.2} = \frac{1}{\varkappa}\left[(\bar{y}_2 - \bar{y}_1) + (\bar{z}_2 - \bar{z}_1)\right]$$

or

$$\Delta\tau_{1.2} = \frac{1}{\varkappa}(\Delta\bar{y} + \Delta\bar{z}). \tag{2.79}$$

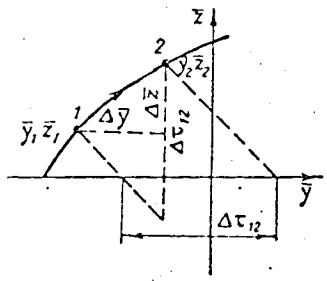

Figure 2.31. Determining time variation from phase picture of system.

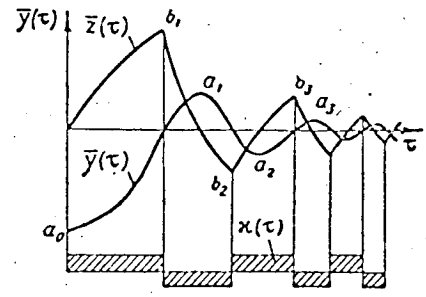

Figure 2.32. Transient process in system with phase picture shown in figure 2.30.

The time increment $\Delta\tau_{1,2}$ is equal to the sum of the increments in coordinates $\Delta\bar{y}$ and $\Delta\bar{z}$. Coordinated $\Delta\bar{y}$ and $\Delta\bar{z}$ must be taken with corresponding signs. From expression (2.79) we also obtain a method for determining graphically the time during which the tracing point is displaced from position 1 to position 2. To do this, it is merely necessary to draw two straight lines to points 1 and 2 (in any quadrant) at an angle of 135° with respect to the $\bar{y}$ axis. These two straight lines will intercept a segment on the $\bar{y}$ or $\bar{z}$ axis whose value will be equal to the unknown time $\Delta\tau_{1,2}$, if the scale of the $\bar{z}$ axis is the same as the scale of the $\bar{y}$ axis.

Figure 2.32 shows the variation in $\bar{y}$ and $\bar{z}$ as a function of time. These curves correspond to the phase picture shown in figure 2.30. Figure 2.32 also shows the variation in χ, i.e., the switching of the relay amplifier of the system. It also follows from these graphs that the switching frequency increases continuously and tends to infinity in the limit. Thus, in the state of rest, the system will be characterized by oscillations of infinitely high frequency and infinitely small amplitude. This result is explained by our assumption concerning the instantaneous response of the relay element.

2. Processes in a Relay System with Delay. Real relay elements are unable to reproduce an input signal of infinite frequency. Each relay element has a limiting frequency at which it still operates. The time which elapses from the application of the signal to the input of a relay element until a signal appears at the output is called the delay time and is designated by t_3. /87

The functional diagram of a system taking into account the delay produced by the relay element is shown in figure 2.33. Here $e^{-t_3 p}$ is the transfer function of the member with constant delay.

As before, we write the equation of motion of the system in dimensionless form

$$\frac{d^2\bar{y}}{d\tau^2} + \frac{d\bar{y}}{d\tau} + \mathrm{sign}_{\Delta\tau}(\bar{y}) = 0, \tag{2.80}$$

where $\Delta\tau = \frac{t_3}{T}$ is the dimensionless delay time; and $\mathrm{sign}_{\Delta\tau}(\bar{y})$ is the step function analogous to the one shown in figure 2.28, but delayed by time $\Delta\tau$.

If we let $\mathrm{sign}_{\Delta\tau}(\bar{y}) = -\chi$ in (2.80), we obtain the same equations as in the preceding case, i.e., equations of the form (2.72).

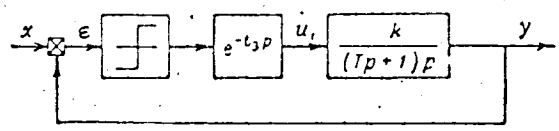

Figure 2.33. Functional diagram of system with delay.

The effect of delay causes χ to vary from -1 to +1, not on the axis of the ordinates, but at some point b_1 (fig. 2.34). If we know the delay time, we can always use this method (fig. 2.31) to determine the switching point. The phase trajectory, constructed by taking into account the delay (fig. 2.34), does not tend towards the origin of the coordinate system, but converges to some cycle. This means that the system will be subject to selfsustained oscillations. The curve in figure 2.34 was constructed with an initial deviation, greater than the amplitude of the steady state oscillations. If the initial deviation is less than the amplitude of the selfsustained oscillations (less than $\bar{y}_m$), the phase trajectory curve will unwind, and the same cycle will be reestablished. Regardless of the initial conditions, the phase trajectory will converge towards the same cycle, which is therefore known as the limiting cycle. /88

Due to delay, the breaks in the phase trajectory are displaced to the right in a clockwise direction with respect to the axis of the ordinates. It is possible to show that the switching line (the line containing the breaks in the trajectories) also remains straight (fig. 2.35), with a slope φ, and intersects the $\bar{z}$ axis at a distance a from the origin of the coordinates.

By using the methods for measuring time on the phase plane, we can proceed from the picture in the phase plane (fig. 2.34) to curves showing the variation in the processes with time. The processes corresponding to such a phase picture are shown in figure 2.36. These curves, as well as the phase pictures, show the principal parameters of selfsustained oscillations:

period of selfsustained oscillations θ or frequency $\frac{1}{\theta}$;

maximum value of deviation $\bar{y}_m$;

maximum value of velocity $\bar{z}_m$;

value of velocity $\bar{z} = \bar{z}_1$, at the time when $\bar{y} = 0$;

value of deviation $\bar{y} = \bar{y}_1$ when $\bar{z} = \bar{z}_m$.

The cycle of selfsustained oscillations is formed by two curves, described by equations (2.75) and (2.76). In view of this, all of the parameters of selfsustained oscillations are associated by single-valued relations. It is sufficient to know one of them to determine the other four.

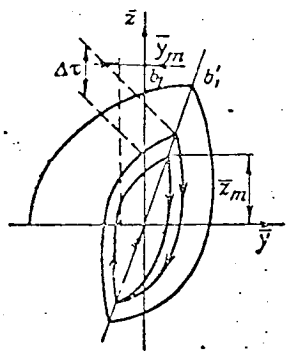

Figure 2.34. Phase trajectory of system with delay.

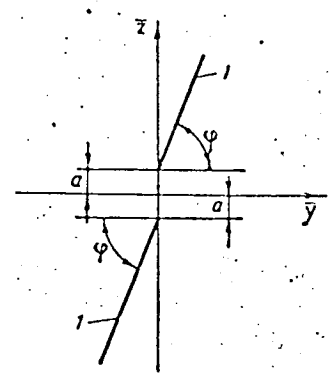

Figure 2.35. Switching lines. z axis--switching line without delay; 1--switching line with delay.

To determine the parameter of the selfsustained oscillations, it is necessary to express one of the parameters in terms of the delay. It is simplest to express velocity $\bar{z}_1$ in terms of the delay at the time when $\bar{y} = 0$. By making /89

a more detailed analysis of how these selfsustained oscillations are established, it is possible to obtain the relationship between $\Delta\tau$ and $\bar{z}_1$ in the form

$$\Delta\tau = \ln \frac{1 + \sqrt{1 - (1 - \bar{z}_1)^2 e^{2\bar{z}_1}}}{(1 - \bar{z}_1) e^{2\bar{z}_1}}. \tag{2.81}$$

If we know $\bar{z}_1$ and make use of (2.75), we obtain $\bar{z}_m$

$$\bar{z}_m = 1 - (1 - \bar{z}_1)\, e^{-\Delta\tau}. \tag{2.82}$$

If we consider the cycle of selfsustained oscillations, using the rules for measuring the segments of time on the phase plane, we obtain an expression for the period of the selfsustained oscillation θ

$$\theta = 4(\bar{z}_1 + \Delta\tau). \tag{2.83}$$

We find the amplitude of deviation y_m by making use of expression (2.75), substituting the initial values $\bar{y}_0 = -\bar{y}_m$ and $\bar{z}_0 = 0$ and the final values $\bar{y} = 0$ and $\bar{z} = \bar{z}_1$

$$\bar{y}_m = \ln\frac{1}{1-\bar{z}_1} - \bar{z}_1. \tag{2.84}$$

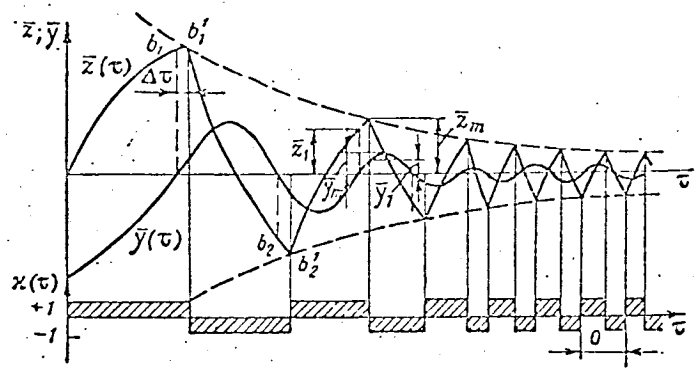

Figure 2.36. Transient processes in system with self-sustained oscillations.

Figure 2.37 shows $\bar{y}_m$, $\bar{z}_m$ and $1/\theta$ and the delay function on the basis of these /90 equations. The parameters of the selfsustained oscillations were computed under the assumption that a closed cycle has been formed on the phase plane, corresponding to the selfsustained oscillations in the system. However, actually we may have only stable selfsustained oscillations, which are represented on the phase plane by the stable cycle. In the present simple case, the stability of selfsustained oscillations is obvious from the fact that all of the phase trajectories, which have been constructed graphically, converge to the same cycle, whose parameters are determined uniquely by the delay.

From the curves in figure 2.37 it follows that when the delay is small, the period and amplitude are small. In most cases we may assume that the system has such small oscillations. However, the magnitude of the delay in relay devices is usually such that selfsustained oscillations occur with low frequency and high amplitude. The systems become inoperative, and we must take measures to damp out the selfsustained oscillations, decrease their amplitude or increase their frequency. This can be done by the following methods:

--by introducing an element with a region of insensitivity into the system;

--by introducing compensating devices--negative feedbacks and differentiating networks.

Let us consider these methods.

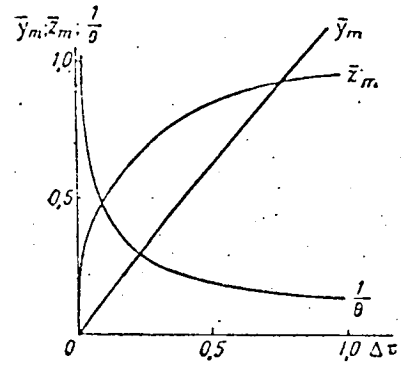

Figure 2.37. Graphs of $\bar{y}_m$, $\bar{z}_m$ and $1/\theta$ in delay function.

3. Effect of Zone of Insensitivity. Let us assume that the characteristics of a relay amplifier have the form shown in figure 2.38. Here $\Delta\varepsilon$ represents the zone of insensitivity. The schematic diagram of the system remains unchanged, and only the characteristics of the nonlinear element are different. First, let us neglect the effect of delay in the relay element. The equation of the system with a region of insensitivity may be written

$$
\begin{aligned}
&T\frac{d^2y}{dt^2}+\frac{dy}{dt}=ku;\\
&u=F(\varepsilon);\quad \varepsilon=x-y;\\
&u=U \quad \text{when} \quad \varepsilon>\Delta\varepsilon;\\
&u=-U \quad \text{when} \quad \varepsilon<-\Delta\varepsilon;\\
&u=0 \quad \text{when} \quad -\Delta\varepsilon<\varepsilon<\Delta\varepsilon.
\end{aligned}
\tag{2.85}
$$

In the case x = 0, the equation of the system will have a form which is analagous to that of equation (2.71) /91

$$
\frac{d^2\bar{y}}{d\tau^2}+\frac{d\bar{y}}{d\tau}+F(\bar{y})=0. \tag{2.86}
$$

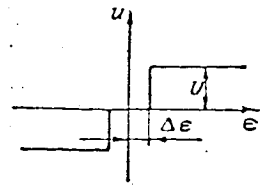

Figure 2.38. Relay characteristic with region of insensitivity.

The function $F(\bar{y})$ has the following properties

$$\left.\begin{aligned} F(\bar{y}) &= 1 \quad \text{when} \quad \bar{y} < -\eta, \\ F(\bar{y}) &= 0 \quad \text{when} \quad -\eta < \bar{y} < \eta, \\ F(\bar{y}) &= -1 \quad \text{when} \quad y > \eta. \end{aligned}\right\} \tag{2.87}$$

where $\eta = \frac{\Delta\varepsilon}{T\omega_0} = \frac{\Delta\bar{y}}{T\omega_0}$ is the dimensionless value of the region of insensitivity $\Delta\varepsilon$, equal in this case to $\Delta\bar{y}$.

Outside the region of insensitivity, we designate as before $F(\bar{y}) = \chi$. Then, for the region where $|\bar{y}| > |\eta|$, we have

$$\frac{d^2\bar{y}}{d\tau^2} + \frac{d\bar{y}}{d\tau} = \chi. \tag{2.88}$$

For the region of insensitivity $|\bar{y}| < |\eta|$ we obtain

$$\frac{d^2\bar{y}}{d\tau^2} + \frac{d\bar{y}}{d\tau} = 0. \tag{2.89}$$

The solution of equation (2.88) has already been obtained, and all of the results will be valid in this case, but only in region $|\bar{y}| > |\eta|$. It remains to examine the behavior of the system in the region of insensitivity, i.e., to analyze the solution of equation (2.89). Because $\frac{d\bar{y}}{d\tau} = \bar{z}$, equation (2.89) may be written in the form

$$\frac{d\bar{z}}{d\tau} + \bar{z} = 0; \tag{2.90}$$

$$\frac{dy}{d\tau} = \bar{z}. \tag{2.91}$$

The integral of equation (2.90) has the form /92

$$\bar{z} = \bar{z}_0 e^{-\tau}, \tag{2.92}$$

and, consequently,

$$\bar{y} = \bar{y}_0 + \bar{z}_0 (1 - e^{-\tau}). \tag{2.93}$$

Expression (2.93) shows that in this case both $\bar{z}$ and $\bar{y}$ are exponential functions of time.

To clarify the nature of the phase curves in the region of insensitivity, we eliminate time τ from equations (2.92) and (2.93), which gives us

$$\bar{z} = \bar{y}_0 + \bar{z}_0 - \bar{y}. \tag{2.94}$$

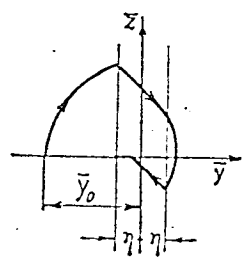

Figure 2.39. Phase picture of system with region of insensitivity.

From equation (2.94) we can see that in the region of insensitivity the phase trajectories have straight lines, with a slope of 135° with respect to the $\bar{y}$ axis. Figure 2.39 shows the phase picture of the system's motion, when the initial conditions are $\bar{z}_{\tau=0} = 0$, $\bar{y}_{\tau=0} = -|y_0|$. Outside this region of insensitivity the phase trajectories are constructed in accordance with equation (2.74). From this figure, it follows that there is a sharp drop in the velocity in the region of insensitivity; when the region of insensitivity is large, the system rapidly comes to a state of rest. The state of equilibrium is characterized on the phase plane, not by the point with coordinate $\bar{z} = 0$; $\bar{y} = 0$ as in the preceding case, but by a segment on the axis of the abscissas

$$-\eta \leqslant \bar{y} \leqslant \eta.$$

The appearance of delay in this case increases the tendency of the system to oscillate. Depending on the relationship between region of insensitivity η and delay $\Delta\tau$, selfsustained oscillations may occur in the system or oscillations

may become impossible. Figure 2.40a and b show the phase picture for both cases. In figure 2.40a, the region of insensitivity is too small to prevent oscillations. In figure 2.40b, on the other hand, the region of insensitivity is sufficient to prevent oscillations. Thus, in a nonlinear system of this type, it is always possible to suppress selfsustained oscillations by increasing the region of insensitivity. Of course, this is associated with the introduction of errors in the reproduction of the output quantity. In the steady state form x = const, the error may be equal to the width of the region on insensitivity ($\pm\ \eta$).

4. Lowering the Amplitude and Increasing the Frequency of Selfsustained Oscillations by Means of a Compensating Scheme. Rate feedback is widely used as a compensating scheme in automatic control systems. To achieve rate feedback, signal generating tachometers, rate gyros and differentiating networks are usually used. As an example let us consider the processes in a nonlinear system with an ideal relay element and with rate feedback. The schematic of this system is shown in figure 2.41. The rate feedback, in this case, is produced by the differentiation of the output signal y and summation at the auxiliary winding of the relay with a mismatch signal ϵ. /93

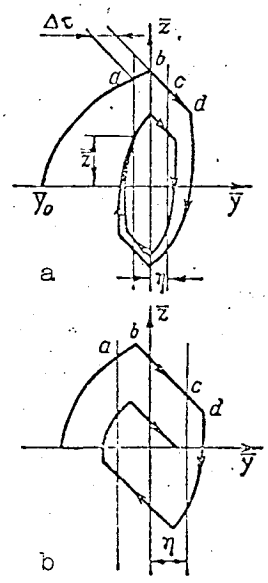

Figure 2.40. Phase picture of the system. a--system with selfsustained oscillations when region of insensitivity is present; b--system with oscillations damped out in region of insensitivity.

Let us write equations of the system

$$\left.\begin{aligned} T\frac{d^2y}{dt^2}+\frac{dy}{dt}&=ku,\\ u&=U\operatorname{sign}\left[\varepsilon-b\frac{dy}{dt}\right].\end{aligned}\right\} \qquad (2.95)$$

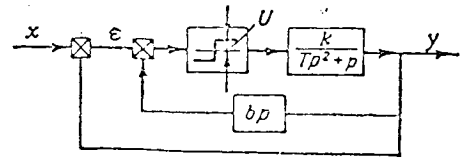

Figure 2.41. Functional diagram of system with rate feedback.

As before, we consider the case x = 0, and obtain

$$T\frac{d^2y}{dt^2}+\frac{dy}{dt}+\omega_0\,\mathrm{sign}\left(y+b\frac{dy}{dt}\right)=0. \qquad (2.96)$$

In this equation, the argument of the nonlinear function sign consists of a sum of the deviation and its derivative with coefficient b. In dimensionless form, equation (2.96) becomes /94

$$\frac{d^2\bar{y}}{d\tau^2}+\frac{d\bar{y}}{d\tau}+\mathrm{sign}\left(\bar{y}+\zeta\frac{d\bar{y}}{d\tau}\right)=0, \qquad (2.97)$$

where $\zeta = \frac{b}{T}$ is the relative value of the rate feedback coefficient; and $\frac{d\bar{y}}{d\tau}=\bar{z}$.

The modulus of the last term in equation (2.97) is equal to 1 and changes its sign when the sum $\bar{y} + \zeta\bar{z}$ passes through zero. In connection with this we can let sign $(\bar{y} + \zeta\bar{z}) = -\varkappa$ and correspondingly change the condition for varying the sign of $\varkappa$. Then equation (2.97) will become identical to equations (2.72). Thus expressions (2.74), (2.75) and (2.78) are valid for the present system. It is only necessary to remember that if the sign of $\varkappa$ previously changed, when deviation y passed through zero, it now changes when the sum $\bar{y} + \zeta\bar{z}$ passes through zero. If switching previously took place on the straight line $\bar{y} = 0$, it now takes place on the straight line $\bar{y} + \zeta\bar{z} = 0$. The switching line $\bar{y} = 0$ has turned by an angle $\arctan\frac{1}{\zeta}$ counterclockwise. With this rotation of the switching line, selfsustained oscillations occur in the same manner as in the system shown in figure 2.29. However, when the rate feedback is switched on, it changes the nature of the system's motion to a state of rest, decreases its tendency to oscillate and lowers the period of motion.

The effect of switching in a compensating scheme is also quite pronounced when the relay element has a delay. As we have shown, delay caused the switching line to turn clockwise, resulting in oscillations. However, the rotation of the switching line counterclockwise will, in some sense, compensate for the delay and produce a decrease in amplitude and an increase in frequency of oscillations, to a greater degree when ζ is large. However, there are no values of ζ for which selfsustained oscillations can be eliminated, if the system has no regions of insensitivity.

Figure 2.42 shows the phase picture for establishment of selfsustained oscillations, when the values of ζ are relatively small. Switching would occur

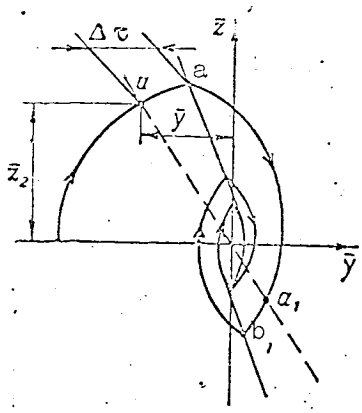

Figure 2.42. Phase picture of system with delay and rate feedback.

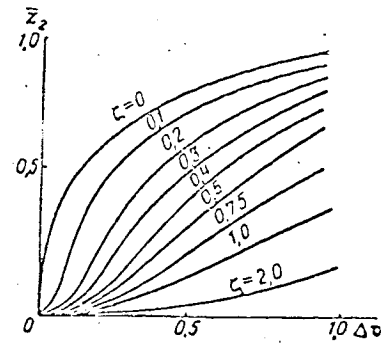

Figure 2.43. Variation in parameter $\bar{z}_2$ as function of relative delay.

on the switching line at point a, but due to delay the switching process (variation in the sign of $\varkappa$) takes place at point b, which may be determined for a known value of $\Delta\tau$ by the method described below. The position of point b_1 with respect to a_1 is determined in the same way. Finally, as already pointed out, /95 the phase trajectory will coincide with some cycle of selfsustained oscillations whose parameters will be a function of both $\Delta\tau$ and ζ. The simplest expression in terms of $\Delta\tau$ and ζ is the oscillation parameter $\bar{z}_2$ (the value of the velocity for which the sum $\bar{y} + \zeta y$ becomes equal to zero). If we know z_2, we may use equations analogous to (2.81)--(2.84) to obtain the other parameters of oscillations.

The relationship $\bar{z}_2 = \bar{z}_2\ (\Delta\tau,\ \zeta)$ is shown in figure 2.43. As we can see from this figure, when the coefficient of rate feedback ζ increases, there is a substantial decrease in $\bar{z}_2$, and there is consequently a decrease in the amplitude of selfsustained oscillations. Quantity ζ affects not only the amplitude and frequency of oscillations, but also the transient process in the relay system. For small values of ζ (fig. 2.42), the general transient process differs little from the case $\zeta = 0$, considered above. For small values of ζ, the transient process retains an oscillatory nature. When ζ is increased (when ζ is of the order of unity or greater), the nature of the transient process changes. As an example, figure 2.44a shows the phase picture of the system when ζ is relatively large. Curves $\bar{z} = \bar{z}\ (\tau)$ and $\bar{y} = \bar{y}\ (\tau)$, corresponding to the phase picture, are shown in figure 2.44b. As we can see, the system pulses towards the equilibrium position. This form of motion is called the sliding state. Due to this, the /96 transient process may be substantially prolonged. For this reason, excessive values of ζ cannot be recommended. Coefficient ζ must be selected so that on the one hand the amplitude of oscillations is sufficiently small, and on the other

hand the transient process is not too prolonged. The optimum value of ζ may be selected, depending on the delay by means of the following equation[1]

$$\zeta_{\text{optimum}} = 1 - \ln 2 \cdot e^{-\Delta\tau} \tag{2.98}$$

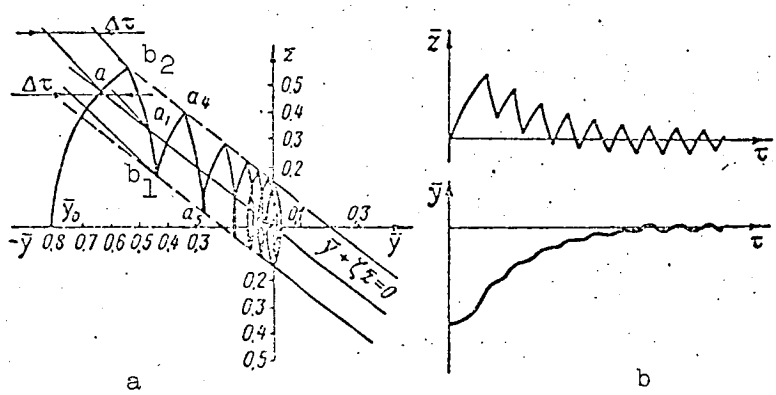

Figure 2.44. Phase picture (a) and transient processes (b) when values of ζ are large.

When ζ is selected in accordance with (2.98), we can guarantee a sufficiently small oscillation amplitude and a minimum duration of the transient process. When the region of insensitivity is small and when $\zeta \neq 0$, the oscillations are easily damped. In this case, the damping of oscillations can be achieved with a substantially smaller region of insensitivity than in the case of $\zeta = 0$.

In conclusion, we note that instead of differentiating the output quantity, we could use some method to introduce the derivative of the mismatch. In this case, the transient process during initial deviation and the selfsustained oscillations in the system may be changed by selecting the parameters of the differentiating device. From the standpoint of accuracy, in servosystems, the last variation is preferred to the introduction of the derivative of the output quantity.

5. Vibratory Linearization of Relay Systems /97

The Reaction of Relay Systems to Slowly Varying Inputs. The presence of oscillations in a relay system, whose frequency spectrum is substantially higher than the control spectrum x(t) and the spectrum of perturbations F(t), produces the effect of vibratory linearization. This means that the reaction to inputs F(t) and x(t), which are slowly varying functions compared with the oscillations in the

[1] A. A. Krasovskiy and G. S. Pospelov, The Principles of Automatic Control and Engineering Cybernetics, Gosenergoizdat, 1962.

relay system, turns out to be close to the reaction linear systems. In the same way, transient processes with limited initial deviations turn out to be close to transient processes in linear systems. High frequency oscillations in a linear system may be forced or of the selfsustaining type. Let us consider these methods of vibratory linearization.

Vibratory Linearization by Means of Forced Oscillations. Let us assume that the input to the relay element is a slowly varying function $x(t)$ and a periodic signal $\varphi(t)$. We shall select the frequency of this signal so that it is sufficiently high, but such that the relay element has time to operate every half-period. Signal $x(t)$ and the signal from the source of high frequency oscillations may be added by different methods. Let us see how linearization is achieved when these signals are added at the windings of the polarized relay. A voltage which is proportional to signal $x(t)$ is fed to the winding with ampere-turns AW_I, while the voltage from the source of high frequency oscillations is fed to the second winding with ampere-turns AW_{II}.

Since the source of ac current is usually a saw-tooth oscillator, we assume that the current we are using has a triangular form. In this case, when the signal is $x(t) = 0$, the switching diagram, i.e., the output signal of the relay element, has the form shown in figure 2.45. The diagram is constructed with the assumption that the delay of the relay is equal to zero, and the sign of signal u changes when the current in the second winding passes through zero (the current in the first winding is equal to zero because signal $x(t)$ is equal to zero). The average value of the signal u in this case will be equal to zero. The switching frequency of the relay's contacts must be such that the oscillations of the output quantity $y(t)$ due to it have a negligibly small amplitude. Therefore, in the future we shall consider only the average value of this signal.

Now let us consider the case when signal $x(t)$ is different from zero. The value of the ampere-turns AW_I in winding I of the polarized relay (fig. 2.46) /98 will be proportional to signal $x(t)$. The sign of signal u will vary at the instant of time when the sum of the ampere-turns of winding I and winding II will pass through zero. The diagram showing the variation in signal u for this case is shown in figure 2.46.

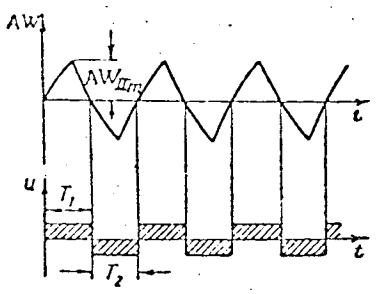

Figure 2.45. Switching diagram for a zero mismatch.

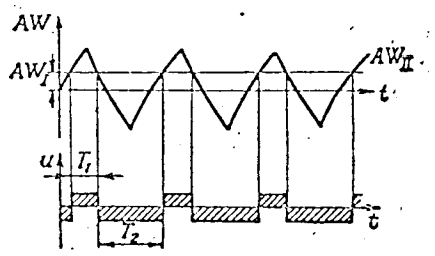

Figure 2.46. Switching diagram for a nonzero mismatch.

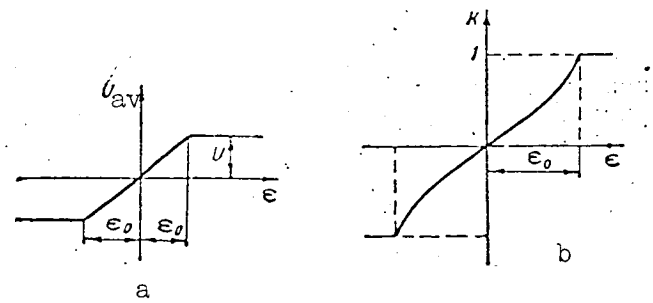

Figure 2.47. Linearized characteristics of relay systems. a--with saw-tooth signal, b--with sinusoidal signal.

From these diagrams we determine the average value of the voltage at the output of the relay device.

$$U_{av} = UK, \tag{2.99}$$

where K is the command coefficient equal to

$$K = \frac{T_1 - T_2}{T_1 + T_2}. \tag{2.100}$$

The value of coefficient K may be expressed in terms of the ampere-turns of windings I and II of the relay

$$K = \frac{AW_I}{AW_{IIm}}, \tag{2.101}$$

where AW_{IIm} is the amplitude value of the ampere-turns of winding II.

Because AW_I is proportional to signal x(t), which in an automatic control system may be the error signal or the mismatch signal ε, we obtain from (2.101)

$$K = \frac{k_\varepsilon \varepsilon}{AW_{IIm}}. \tag{2.102}$$

The law (2.102) is valid only in the range $\varepsilon < \varepsilon_0$, and

$$\varepsilon_0 = \frac{AW_{IIm}}{k_\varepsilon}. \tag{2.103}$$

Expression (2.103) shows that the region of proportionality is determined by the amplitude of the saw-tooth oscillations. Figure 2.47 shows the variation /99

in the average voltage $U_{average}$ as a function of mismatch ϵ. If saw-tooth waves are not acting, this relationship would have the form shown in figure 2.28. Thus, due to the action of saw-tooth oscillations, the nonlinear characteristics become linear in a certain range. In this range the relay system may be considered a linear system. The relay amplifier in the diagram in this case is replaced by a linear amplifier with an amplification factor equal to k_ϵ/AW_{IIm}.

Previously we assumed that delay Δt of the relay device is equal to zero. If we take into account the delay, the position of the relay amplifier must be occupied by a linear amplifier with delay, whose transfer function has the following form

$$W(p) = \frac{k_\epsilon}{AW_{IIm}} e^{-\Delta t p}. \tag{2.104}$$

If selfsustained oscillations exist in the relay system, then for the case of linearization they are damped by the applied external oscillations. The frequency of external oscillations must be several times greater than the frequency of selfsustained oscillations, because this provides negligible amplitude of oscillations in the output quantity of the system.

In some cases sinusoidal oscillations are used for linearization. In this case, the relationship between K and mismatch ϵ is nonlinear and is given by expression[1]

$$K = \frac{2}{\pi} \arcsin \frac{k_\epsilon \epsilon}{AW_{IIm}}. \tag{2.105}$$

This relationship is shown graphically in figure 2.47b. This law is valid only in the range $|\epsilon| < \epsilon_0$, where /100

$$\epsilon_0 = \frac{AW_{IIm}}{k_\epsilon}.$$

However, for small values of mismatch, this relationship may be assumed to be linear and we may consider that

$$K = \frac{2}{\pi} \frac{k_\epsilon \epsilon}{AW_{IIm}}. \tag{2.106}$$

Vibratory Linearization Due to Delayed Feedback Around the Relay Element. Let us assume that the relay element system has the characteristic shown in figure 2.48. This characteristic is typical of a two-position polarized relay.

---

[1] See footnote on p. 87.

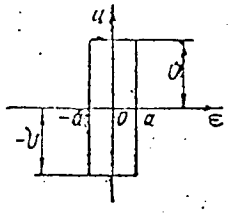

Figure 2.48. Relay characteristic with loop.

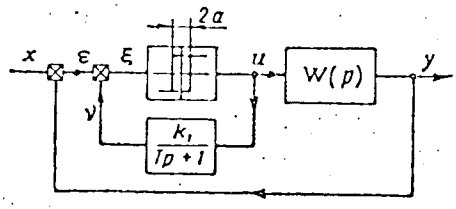

Figure 2.49. Functional diagram of system with delayed feedback.

Free play in mechanical transmissions of a nonlinear system also produce loop characteristics. Let us place a feedback loop around the relay element which contains an inertial member with time constant T and amplification factor k_1 (fig. 2.49). Selfsustained oscillations occur in the circuit consisting of the relay element and the inertial element. Sometimes these are called relaxation oscillation and the circuit itself is called a relaxation generator. The oscillation frequency of the circuit is selected so that it is sufficiently high and permits us to neglect its component in the output signal y(or error ε). When the problem is formulated in this manner, we must determine the transfer characteristics of the relaxation circuit for the slowly varying error signal ε.

We write the equation of the circuit using the designation shown in figure 2.49 /101

$$\left.\begin{aligned} u &= F(\xi), \\ \xi &= \varepsilon - \nu, \\ T\frac{d\nu}{dt} + \nu &= k_1 u. \end{aligned}\right\} \qquad (2.107)$$

The presence of high frequency selfsustained oscillations in the circuit makes it possible to write the system of equations (2.107) for average values of the signals. We shall designate these values with asterisks

$$\left.\begin{aligned} u^* &= \frac{\omega_a}{2\pi}\int_0^{\frac{2\pi}{\omega_a}} F(\varepsilon)\,dt = \psi(\varepsilon), \\ \xi^* &= \varepsilon - u^*, \\ T\frac{d\nu^*}{dt} + \nu^* &= k_1 u^*, \end{aligned}\right\} \qquad (2.108)$$

where ω_a is the frequency of selfsustained oscillations.

The average value of the output signal of the circuit $u^* = \Psi(\epsilon)$ is a function only of input signal ϵ, and for the case of a relay element (fig. 2.48) is equal to the command coefficient K, i.e.,

$$\psi(\varepsilon) = \frac{T_1 - T_2}{T_1 + T_2}, \tag{2.109}$$

where T_1 is the positive pulse duration and T_2 is the negative pulse duration.

Both quantities T_1, T_2 and, consequently, the period of selfsustained oscillations $T_1 + T_2 = 2\pi/w_a$ are functions of input signal ϵ. The form of the oscillations in the circuit is shown in figure 2.50 for value ν. When $\epsilon = 0$, the circuit contains symmetric selfsustained oscillations $T_1 = T_2$. When $\epsilon \neq 0$, the selfsustained oscillations become nonsymmetric. The sign of ϵ determines the relationship between T_1 and T_2 and hence the sign of u^*. In the intervals T_1 and T_2 the laws for the variation of $\nu_{a1}(t)$ and $\nu_{a2}(t)$ are described by the exponents' equations $\pm k_1 U(1 - 2e^{-t/T})$. Therefore, for the interval $0 \leq t \leq T_1$

$$\nu_{a1}(t) = (\varepsilon - a)\, e^{-t/T} + k_1 U (1 - e^{-t/T}). \tag{2.110}$$

while for the interval $0 \leq t \leq T_2$

$$\nu_{a2}(t) = (\varepsilon + a)\, e^{-t/T} - k_1 U (1 - e^{-t/T}). \tag{2.111}$$

In equations (2.110) and (2.111), time is measured from the beginning of the intervals. /102

The half-period T_1 terminates and switching occurs when $\xi = \epsilon - \nu_{a1}(t)$ reaches a value -a. The half-period T_2 terminates and switching occurs when $\xi = \epsilon - \nu_{a2}(t)$ is equal to + a. By using these relationships, T_1 and T_2 may be expressed in terms of ϵ, a and, consequently, we can obtain relationship $y^* = \Psi/\epsilon, a)$. The graphs of the functions $y^* = \Psi(\epsilon)$ for various values of a are shown in figure 2.51. For $a \to 0$ when the relay element with characteristics shown in figure 2.48 is transformed into a relay element with characteristics shown in figure 2.28, the frequency of selfsustained oscillations becomes infinite, and $\Psi(\epsilon)$ in the range $-k_1, U \leq \epsilon \leq k_1 U$ transforms into a linear function with an amplification factor $\frac{1}{k_1}$, i.e., $\Psi(\epsilon) = \frac{1}{k_1}\epsilon$. If $|\epsilon \pm a| \ll k_1 U$, then, as follows from figure 2.51, we may assume approximately that $\psi(\epsilon) = \frac{1}{k_1}\epsilon$ also, when $a \neq 0$.

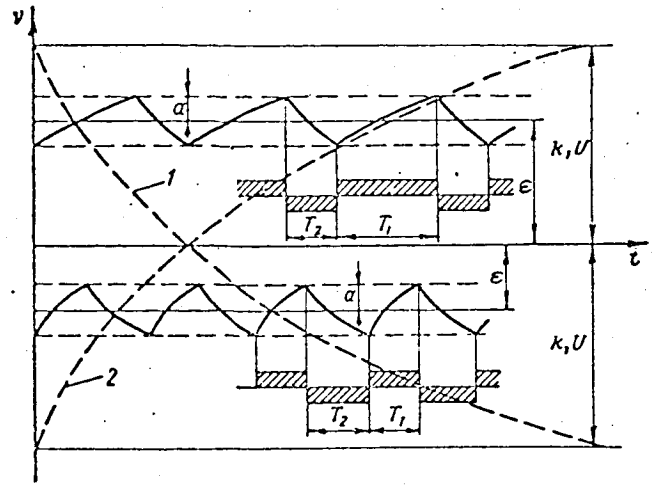

Figure 2.50. Curves showing oscillations in feedback circuit of system functionally represented in figure 2.49. 1 and 2--limiting exponents.

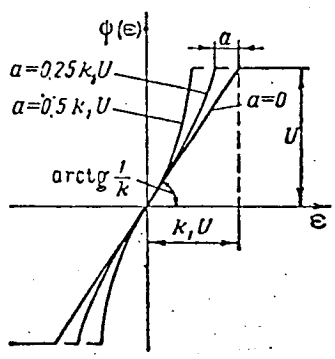

Figure 2.51. Linearized characteristics of relay element with delayed feedback.

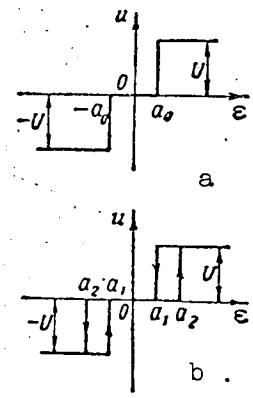

Figure 2.52. Relay characteristics with region of insensitivity (a) and with loop (b).

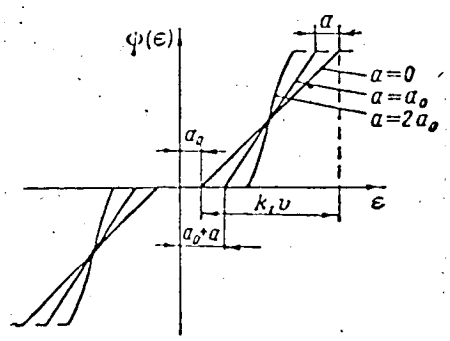

Figure 2.53. Linearized characteristics of relay element (fig. 2.52) with delayed feedback.

A relaxation circuit may also be formed by producing a feedback with delay over the three-position polarized relay with characteristics shown in figure 2.52. The function $\Psi(\epsilon)$ for this case may be determined analytically. The graphs of the function $\Psi(\epsilon)$ for various values of a are shown in figure 2.53. /103
It follows from these graphs that the function $\Psi(\epsilon)$ is close to a linear function in the range

$$(a_0 + a) \leqslant \epsilon \leqslant (k_1 U + a_0 - a)$$

for positive values of ϵ and in the range $-(a_0+a) \geqslant \epsilon \geqslant (k_1 U + a_0 - a)$, for negative values, where $a_0 = \frac{a_1 + a_2}{2}$, $a = \frac{a_2 - a_1}{2}$. In the limiting case when $a \to 0$, i.e., the characteristics shown in figure 2.52b are transformed into characteristics given by figure 2.52a, we have

$$\psi(\epsilon) = -\frac{a_0}{k_1} + \frac{1}{k_1}\epsilon. \tag{2.112}$$

In the range $|\epsilon| < (a_0 + a)$ the characteristics of figure 2.53 have a region of /104
insensitivity. If ϵ lies in this range, there are no selfsustained oscillations in the circuit. The graphs of functions $\Psi(\epsilon)$, shown in figures 2.51 and 2.53, are the statistical characteristics of relaxation circuits and are valid for different constant values of ϵ. We consider only the transmitting function of relaxation contours, correct for the dynamic region when $\epsilon = \epsilon(t)$, limited there only by the limiting relay characteristics shown in figures 2.28 and 2.52a. In the limiting cases when $a \to 0$, while the frequency of oscillation is $\omega_a \to \infty$, the input signal of the relay element also tends to zero. Consequently, in the limiting case $\nu^* = \epsilon$, and we find from the last equation of system (2.108) that

$$u^* = \frac{1}{k_1}\left(\epsilon + T\frac{d\epsilon}{dt}\right). \tag{2.113}$$

Expression (2.113) shows that in the limiting case the transfer function of a relaxation circuit consists of a transfer function pertaining to an ideal forcing element of the first order

$$W_{\epsilon/u^*}(p) = \frac{1}{k_1}(Tp + 1). \tag{2.114}$$

We note that the same transfer function is characteristic of an amplifier with an infinite amplification factor which has an inertial element in its feedback loop (fig. 2.54). In the limiting case, a linear amplifier which has

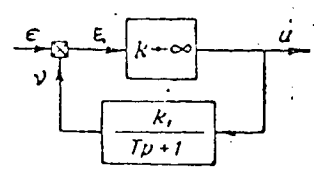

Figure 2.54. Functional diagram of amplifier with infinite amplification factor.

undergone vibratory linearization indeed has an amplification factor which is infinite, because $k = u^* / \xi$ and since $\xi \to 0$, $k \to \infty$. The forcing properties of a relay amplifier with feedback (relaxation circuit) are accompanied by delay in the transformation of input signal ϵ. The delay is determined by the time it takes the relay to operate and to release and also by the width of the loop a in its characteristics. When signal ϵ is sinusoidal, the operation and release of the /105 relay produces a phase shift in the output signal u^* with respect to input signal ϵ, which is proportional to the frequency, and the presence of a loop in the characteristics gives the same phase shift at any frequency. If the forcing properties of a circuit are to be substantial, it is necessary to select large values for constant T. To avoid a very low frequency of oscillation, it is necessary to have a relay amplifier with high dynamic properties, small width of loop a and small values for the operating and release time.

CHAPTER 3. CONTROL SIGNALS FOR HOMING GUIDANCE /106

Section 3.1. Forms of Energy Which Can Be Utilized. Active, Semiactive and Passive Homing Devices

Devices which can be used to determine the position of a missile with respect to its target are called homing devices.

It is necessary to have energy coupling between the missile and the target for proper operation of sensors in the homing heads. The coupling energy may be electromagnetic (light waves, infrared rays and radio waves) and acoustic. The target must have a higher energy than the surrounding medium, i.e., it must present a contrast on the background medium. The use of sound waves for aerial missiles moving in air has not become widespread because the missile itself is a source of high level noise which interferes with the detection of sounds emitted by the target. Acoustic contrast is used only in the heads of homing torpedoes. Light contrast is also seldom used in homing missile systems. This is true because a large number of targets do not exhibit sufficient contrast and /107
it is difficult to isolate them from the background. In principle, the missile homing heads may use radiation in the much shorter wave part of the electromagnetic spectrum--gamma rays.

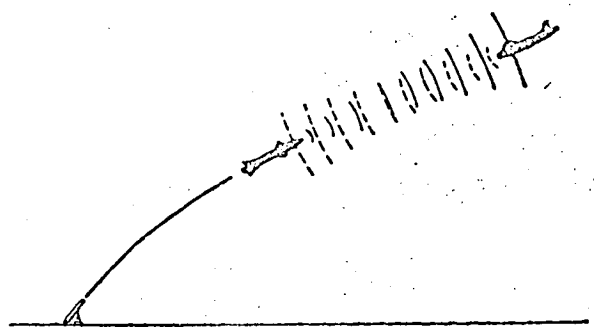

Figure 3.1. Schematic diagram of active homing guidance. ——— Incident radiation front. ------ Reflected radiation front.

The most common form of energy used is that of infrared rays and radio waves. There are three types of homing guidance heads, depending on the location of the energy source:

(1) active--the source of energy for illuminating the target is on the missile, and part of the energy reflected by the target falls on the sensor in the homing head (fig. 3.1);

(2) semiactive--the source of energy for illuminating the target is situated outside the missile. Part of the energy reflected by the target falls on the sensitive element in the head (fig. 3.2);

(3) passive--the target serves as the source of energy: the energy radiated by the target falls on the sensitive element in the head (fig. 3.3).

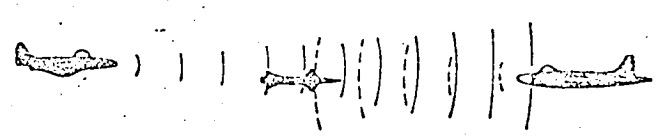

Figure 3.2. Schematic diagram of semiactive homing guidance.

Table 3.1 shows the regions of the electromagnetic spectrum and the corresponding wavelengths which can be used in various types of homing guidance heads.

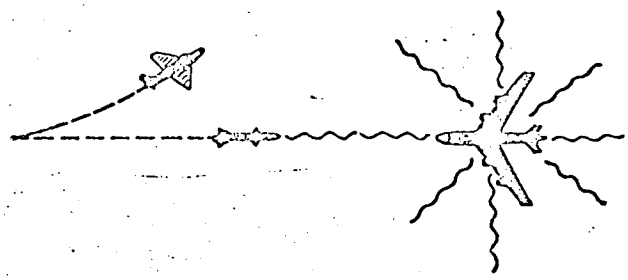

Figure 3.3. Schematic representation of passive homing guidance.

Section 3.2. Sensors Used in Infrared Homing Guidance Heads /108

Before considering the operating principles of infrared homing heads, it is necessary to consider the properties of infrared radiation sources and the propagation of these rays in the atmosphere. Any body whose temperature is above absolute zero ($T = -273.15^{\circ}C$) is a source of infrared rays.

The wavelength of infrared rays depends on the temperature of the radiating body which establishes the region in the infrared spectrum, and the type of sensor used in the homing guidance head. The higher the temperature of an object, the smaller is the range of waves radiated by it. The quantity of radiated energy corresponding to a definite wavelength for a given temperature of the object is called the intensity of radiation. Figure 3.4 shows the variation

TABLE 3.1. CLASSIFICATION OF ELECTROMAGNETIC SPECTRUM BY REGIONS OF WAVELENGTHS.

Region of Spectrum		Wavelength
Radio Waves	Long	20 000-2000 m
	Medium	2 000-200 m
	Short	200-10 m
	Ultrashort	10-0.5 m
	Microwave	Shorter than 0.5 m
Infrared rays	Long wave	750-25 μ
	Medium wave	25-2.5 μ
	Short wave	2.5-0.76 μ
Visible rays		0.76-0.4 μ
Ultraviolet rays		4000-50 Å
X-rays		50-0.04 Å
Gamma rays		40 X and shorter

Remarks: $1\ \mu = 10^{-6}$ m; $1\ \text{Å} = 10^{-10}$ m, $1\ X = 10^{-13}$ m.

in the intensity of longwave infrared radiation as a function of the body's temperature. The infrared radiation produced by the jet of hot gases flowing from a reaction or rocket engine lies in a very narrow band of the spectrum, whose average wavelength is determined by the characteristics of the molecular resonance of the products of combustion. Thus, e.g., carbon dioxide and water vapor, which are contained in exhaust gases, produce radiation with wavelengths (2.5 - 3.2 μ) and (4.2 - 4.5 μ), respectively.

The direction of the maximum radiation energy of infrared rays coincides approximately with the direction of motion of exhaust gases from the engine of the target airplane. The radiated energy depends not only on the temperature of the body, but on the condition of its surface. The cleaner and lighter this surface, the smaller is the percentage of infrared energy which can be radiated by an object at a given temperature. Thus, an airplane with a well-polished surface will radiate only 10 percent of that energy which would be radiated at the same temperature by an airplane painted black. To express the effectiveness of radiation of an object, we use the concept of emission power. It is characterized by the radiation coefficient ϵ, i.e., the ratio of power actually radiated by an object to the power which would be radiated if the object were an absolutely black body. This ratio is always less than unity. /109

On the basis of the Stefan-Boltzmann law we may find the radiation energy

$$E_T = \epsilon\sigma T^4 \text{ watt/cm}^2 \tag{3.1}$$

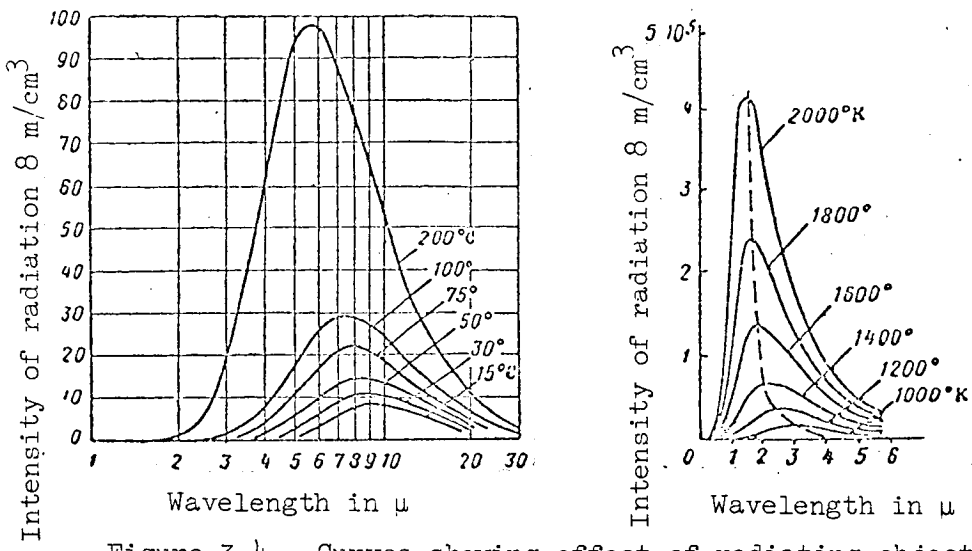

Figure 3.4. Curves showing effect of radiating object temperature on intensity and wavelength of infrared radiation.

where E_T is the energy per unit area radiated by a body over the solid angle 2π: σ is the radiation constant equal to $5.6686 \cdot 10^{-12}$ watt/cm^2 deg^4; T is the temperature of the body in $^{\circ}$K; and ϵ is the radiation coefficient.

Equation (3.1) is used to determine the energy which is radiated by an object. Only part of the energy will reach the sensor. Energy will decrease due to scattering and due to losses in the optical system. Scattering is inversely proportional to the square of the distance between the source of energy and the sensor. Thus, the magnitude of the power which arrives from an object at the homing guidance head, when the distance between them is 1600 m and the temperature of the object is 900°C and the radiation coefficient is $\epsilon = 0.1$, /110

constitutes $35 \cdot 10^{-12}$ watt/1 cm^2 of the sensing surface from each square centimeter of the object's surface.

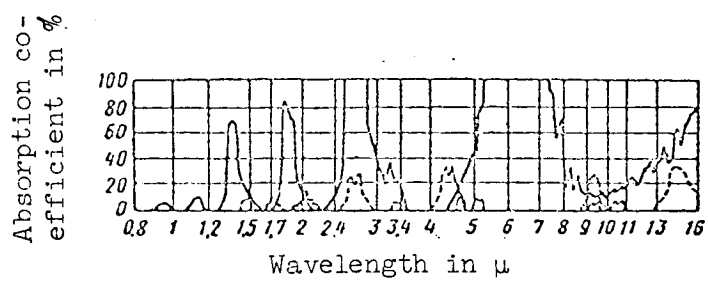

Figure 3.5. Curves illustrating regions of absorption of infrared energy by atmosphere. ——— Water vapor. ------ Carbon dioxide. ..... Ozone.

In addition to the scattering of infrared rays during their passage through the atmosphere, there is a particularly pronounced absorption over some regions of the spectrum. Infrared rays are absorbed by water vapor in the atmosphere and by carbon dioxide. Thus, carbon dioxide is responsible for intense absorption bands for wavelengths 2.05, 2.6, 4.3 and particularly 12.8 - 17.3 μ.[1]

The most intense absorption of infrared rays is accomplished by water vapor, which has intense absorption bands at various wavelengths. The strongest absorption by water vapor takes place at the following wavelengths (the figures indicate the centers of the absorption bands): 0.94; 1.13; 1.38; 1.46; 1.87; 2.66; 3.15; 6.26; 11.7; 12.6; 13.5 and 14.3 μ. Figure 3.5 shows curves which illustrate water vapor absorption regions and absorption regions of carbon dioxide. The relative amplitudes of the absorption bands corresponding to these components of the atmosphere are represented by an arbitrary scale, because the percentage of these components in the atmosphere may vary. The regions of the spectrum where infrared energy is transmitted without distortion are called windows. /111

As the altitude is increased, the width of windows increases due to lower air density and lower water vapor density. At an altitude of approximately 10 km and higher, the absorption of infrared radiation practically ceases, except in narrow bands of the spectrum, one of which is in the region of wavelengths 2.8 μ, while the other is in the region of wavelengths 4.4 μ, corresponding to the absorption bands of carbon dioxide and water vapor, respectively.

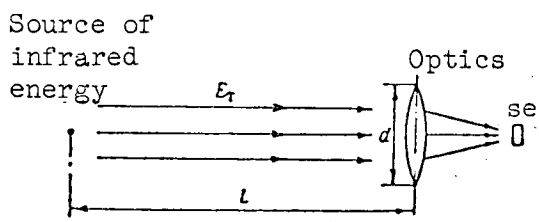

Figure 3.6. Schematic representation of infrared energy sensor. se--sensing element.

As a result, the quantity of energy which arrives at the sensor (fig. 3.6) may be computed by means of equation

$$E_u = E_T \frac{1}{L^2} S k_1 k_2, \tag{3.2}$$

where E_u is the entire energy which has arrived at the sensor in watts; L is the distance from the energy source to the sensor in cm; S is the area of the input pupil which projects the infrared rays on the sensor, in cm^2; k_1 is a coefficient

[1] I. A. Margolin and N. P. Rumyantsev, Principles of Infrared Engineering, Gosenergoizdat, 1955.

which characterizes losses in the atmosphere. The magnitude of the coefficient depends on the state of the atmosphere, and k_2 is a coefficient which characterizes the losses in the optical system.

The sensors of infrared radiation may be divided into two groups--selective and nonselective. Nonselective sensors have a uniform sensitivity in a sufficiently wide region of the spectrum. They are based on the principle of transforming the energy of infrared rays into heat. The surface of a nonselective sensor must have an absorption coefficient which is constant over the given region of the spectrum. Usually the coating consists of platinum black, soot or /112 other substances with a high absorption coefficient for infrared rays. Bolometers are used as nonselective sensors in homing guidance heads. The sensitive layer absorbs the radiant flux, is heated and causes a change in the resistance of the bolometer. This makes it possible to detect a radiant flux of power as low as 10^{-10} watts.

The sensing element of the bolometer is fabricated from a thin layer of various materials, semiconductors and dielectrics with a high temperature coefficient of resistance. The layer of metal has a thickness of 0.1 - 10 μ. In practice, two such sensors are used and are connected in the arms of a bridge with an equal bias voltage (fig. 3.7). One of the sensing elements (se) is subjected to infrared rays, while the other (ce) is screened to provide compensation for the variation in the resistance due to changes in ambient temperature.

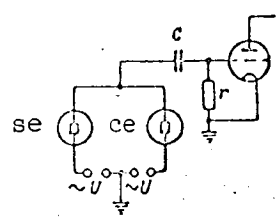

Figure 3.7. Schematic diagram showing arrangement of sensors in infrared detector. ce--compensating element.

Photoresistive cells are used as selective sensors of infrared radiation. Their resistance changes under the action of infrared radiation. Semiconductive materials are used to fabricate photoresistive cells, including lead sulphide, lead telluride, indium antimonide and others.

Let us compare the characteristics of these two basic types of sensors which use the infrared radiation of the target.

Sensitivity. An increase in sensitivity leads to an increase in the detection range of a target. The concept of spectral sensitivity is widely applied, i.e., the distribution of sensitivity over the regions of the infrared spectrum.

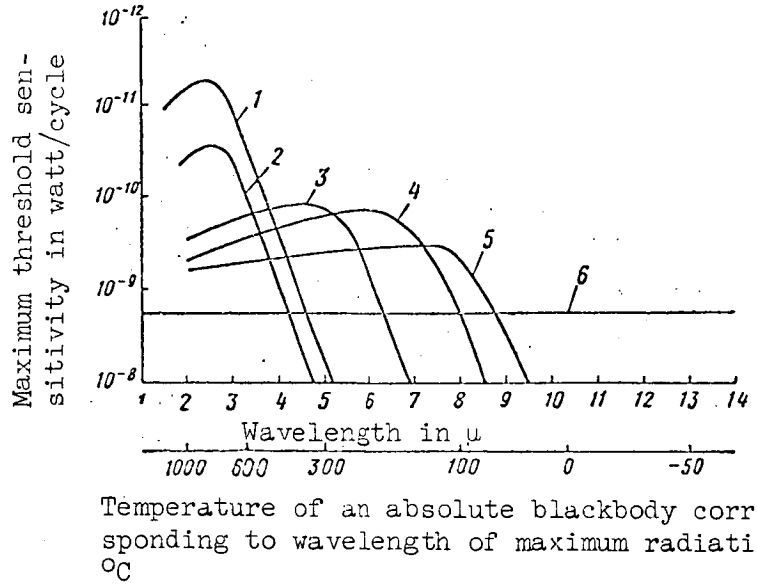

Figure 3.8. Curve showing spectral sensitivity of infrared detectors. 1--cooled lead sulphide (-80°C); 2--uncooled lead sulphide; 3--cooled lead telluride (-80°C); 4--cooled lead selenide (-183°C); 5--cooled indium antimonide (-183°C), and 6--thermal (bolometric) detectors.

Bolometers are equally sensitive to all wavelengths in the infrared spectrum; however, to obtain an equivalent signal level at the output, they require at least 100 times more infrared radiation energy compared to photoresistive cells fabricated from lead sulphide. In view of its low sensitivity, the application of the bolometer would have ceased a long time ago, if the high sensitivity of photoresistive cells were not limited by the relatively narrow band in the infrared spectrum.

Figure 3.8 compares the maximum threshold sensitivities of various detectors.[1] If we examine the curves shown in this figure, we see that the sensitivity of lead sulphide at a wavelength of 3 μ drops sharply at room temperature, at wavelength 4.0 - 4.5 μ the sensitivity of a lead sulphide cell is less than the sensitivity of a bolometer. The spectral sensitivity of photoresistive cells may be increased somewhat by lowering their temperature. By cooling a lead sulphide element with dry ice to a temperature of approximately -80°C, its spectral response is widened by 0.5 μ and its sensitivity increases by more than 15 times. However, when sensitive elements are cooled, their response time decreases. Other materials such as lead telluride and lead antimonide have a high sensitivity to radiation at the long wavelength end of the infrared spectrum compared with lead sulphide, but are less sensitive to radiation in other regions of the spectrum. /113

[1] M. A. Bramson and A. Ye. Kalikeyev, Infrared Technology of Capitalist Nations, "Soviet Radio", 1960.

Lead telluride cooled to a temperature of 90°K (-183°C) is sensitive to radiation with wavelengths greater than 7 μ, while cooled lead antimonide is sensitive to wavelengths of approximately 8 μ. The maximum sensitivity of cooled lead telluride reaches only 10-20 percent of the sensitivity of lead sulphide, while the sensitivity of lead antimonide is equal only to half the sensitivity of lead telluride. /114

Photoelectric Current. The photoelectric current depends not only on the illumination, but also on the applied voltage. Figure 3.9 shows the volt-ampere characteristics for dark current (i_T) and for current during illumination (i_c). As we can see from this figure, when the applied voltage varies, the photoelectric current at constant illumination also varies. The variation in the photoelectric current during constant illumination is called noise. In addition to the useful signal, each sensor is a source of various noise. In bolometers the principal role is played by thermal noise which is produced by molecular fluctuations in the sensitive layer. Another form of interference in bolometers is the noise produced by the variation of the current which flows through the sensitive layer of the detector. Compared with thermal noise, the level of this noise is relatively small when the bias voltage is of normal value.

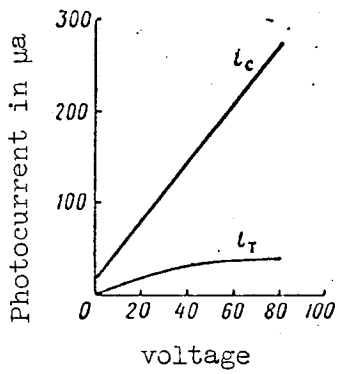

Figure 3.9. Volt-ampere characteristics of bismuth sulphide photoresistive cell.

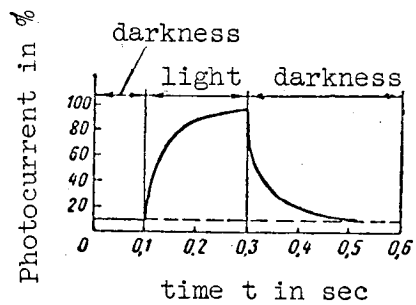

Figure 3.10. Transient process in selenium photoresistive cell.

To decrease the noise which originates when air penetrates the sensitive layer during vibration, thermal detectors are placed in a vacuum. The magnitude of the sensor's noise is evaluated by the equivalent noise power which corresponds to the infrared power (in watts) at the input, which produces an output signal equal to the mean square value of the noise signal in the corresponding band of frequencies. Thus, e.g., the equivalent noise power of a thermal bolometer in a band of 1 cycle is approximately equal to 10^{-10} watt, while for a cooled lead sulphide cell it is equal to approximately 10^{-11} watts when the band is 1 cycle. The sensor will produce a clear signal only if the power (energy), which falls on the sensor from the target, is greater than the

equivalent noise power. From these considerations we may evaluate the detection range of a homing guidance thermal head by means of equation (3.2): /115

$$L_{max} = \sqrt{\frac{E_1 k_1 k_2 S}{E_{ne}\ k_3}},$$

where $E_{noise\ equivalent}$ is the equivalent noise energy and k_3 is the safety factor $k_3 > 1$.

Frequency and Time Characteristics. All sensors which respond to infrared rays have a lag in their response: the photoelectric current which occurs when they are illuminated or darkened does not change instantaneously, but with some delay in time. The delay time is the time necessary to achieve a photoelectric current, which is 95 percent of the maximum value. The delay encountered when the photoelectric current decreases is different from the delay encountered when it increases: usually the rise time is less than the decay time.

Figure 3.10 shows the transient process in a circuit with a selenium photoresistive cell. As we can see from the figure, the rise time and the decay time of the photoelectric current is approximately 0.2 sec. For lead sulphide, the delay time is approximately 3×10^{-4} sec.

In a photoresistive cell of the same chemical composition, the spread in the delay time may be ± 50 percent of the average typical value. Bolometers with a metallic film of gold have a delay time of the order of 4×10^{-3} sec.[1] /116

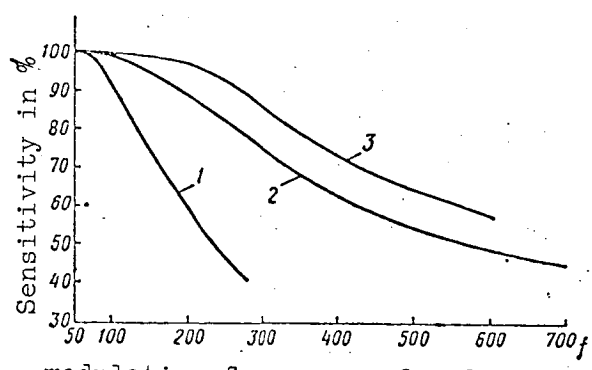

Figure 3.11. Amplitude-frequency characteristics. 1--bolometer made of gold and covered with a thin film; 2--thallium sulphide photoresistance; 3--lead sulphide photocell.

[1] P. Smith, F. Jones and P. Chessmer, The Detection and Measurement of Infrared Radiation, I. L., 1959.

When the sensors are illuminated with a modulated light flux, the amplitude of the output signal is decreased as the modulation frequency f is increased. Figure 3.11 shows the amplitude characteristics of certain infrared sensors.

Section 3.3. Coordinates of the Infrared Homing Guidance Head

Parabolic mirrors may be used in infrared detection systems, tracking systems or control systems to collect and focus the infrared radiation. As in the case of visible light, the focused flux of infrared radiation is directly proportional to the square of the diameter and inversely proportional to the square of the focal distance of the mirror. The greater the power of infrared radiation focused by the mirror, the smaller is the required area for the sensitive layer of the detector, which in turn decreases its delay time.

For the best focusing of infrared radiation (in addition to that achieved by the mirror), lenses are sometimes used in front of the sensor. These lenses are made of materials which are transparent to infrared rays. To increase the efficiency of a mirror in the infrared region of the spectrum, its surface is covered with a thin layer of gold or aluminum.

The sensors, the focusing system, the amplifiers and other elements which comprise the homing guidance head, are placed in the nose of the missile. To protect the sensor and the optics from external mechanical disturbances, the nose of the missile is covered with a cowling. The material of the cowling must satisfy the following condition:

(1) it must be sufficiently rigid and durable;

(2) it must be highly transparent to that part of the infrared spectrum which is used for the operation of the homing guidance head;

(3) it must have high thermal conductivity to carry the heat to the rim of the cowling.

To increase the transparency, the cowling is coated like photographic lenses, which makes it possible to increase the transmitted infrared energy by 20 - 50 percent.

The sensor and the optical system only permit determination of the existence of an infrared radiation source (target). However, in addition, it is also necessary to determine the position of this source (target) with respect to the missile. Figure 3.12 shows the relative positions of the target and the missile. /117

The position of the target with respect to the missile may be determined in a system of polar coordinates, if we compute ϵ = arc sin R/L and μ, or in a system of Cartesian coordinates

$$\epsilon_y = \arcsin \frac{R\cos\mu}{L}; \qquad \epsilon_z = \arcsin \frac{R\sin\mu}{L}. \tag{3.3}$$

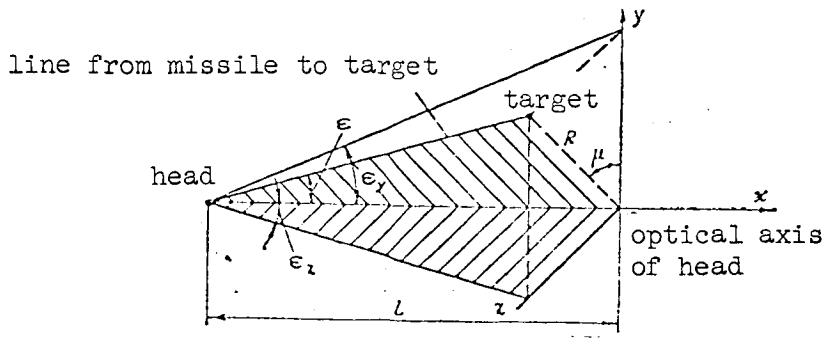

Figure 3.12. Geometric relation between position of missile and target.

The selection of the coordinate system is dictated by the method used in guiding the missile. In determining the relative position, the radiation flux is modulated in the homing heads. Figure 3.13 shows one of the circuits used in a homing head.[1] Sensor 1 is situated at the focus of parabolic reflector 3. Modulating disk 2 rotates between the mirror and the sensor. The current produced by the sensor is amplified by amplifier 5 and enters the missile control system. For some types of modulating disks, (fig. 3.14a) it is necessary to provide a commutator for output signals 4 (fig. 3.13), which is placed on the disk of the drive shaft and provides for four switches during one revolution.

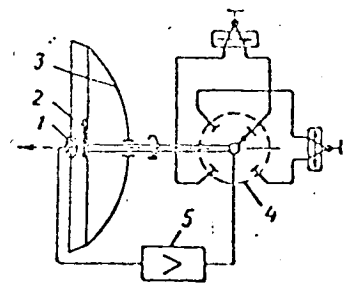

Figure 3.13. Schematic diagram of homing head. 1--sensor; 2--modulating disk; 3--reflector; 4--commutator of output signals; 5--amplifier.

Figure 3.14 shows modulation disks coated with various substances which do not transmit infrared rays.

When the disks shown in figures 3.14a and b are used, the optical axis passes through the center of the disk. When the optical axis deviates from the direction to the target, the image of the target is displaced along the radius of the disk and during different intervals of time current pulses are read from the sensor. In practice the application of such disks makes it possible to obtain /119

[1]F. Muller, Remote Control, I. L., 1957.

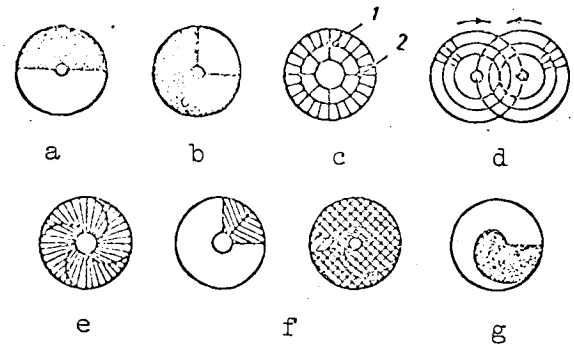

Figure 3.14. Modulating disk of infrared homing head.

control signals of the type "yes - no." The magnitude of the current depends on the radiation of thermal energy by the target, and it increases as the range to the target decreases. The basic disadvantage of such a system is that it is highly susceptible to interference. All the irregularities in the background radiation which surrounds the target produce false signals difficult to distinguish from the useful signals.

If disks are used (fig. 3.14c) with radial graduation lines which differ in frequency and are covered with a material that does not transmit infrared rays, the modulation frequency increases. The photocell is placed behind the modulation disk. If the optical axis is not directed towards the target, then, depending on which row of slots is subjected to the focused optical energy flux from the target, the signal at the output of the amplifier will shift in frequency and will be transmitted to the missile control systems through a corresponding filter. In this manner the displacement of the target in one plane may be determined. By installing a second optical system and another sensor, which is rotated by 90° with respect to the first (points 1 and 2 in figure 3.14c show the projection of the optical axes), it becomes possible to measure displacement in another plane. In this way we can obtain signals which are proportional to deviations in two mutual perpendicular planes by installing two disks with a different number of slots (fig. 3.14d). In this way we obtain four overlapping fields, each of which determines two frequencies from the four possible modulation frequencies. This mixture of frequencies from the output of the photoelectric amplifier is transmitted to the filter stages. From the frequencies which are filtered out it is possible to establish the direction of the optical axis of the device and of the direction of the line between the missile and the target. When the disks shown in figures 3.14c and d are used, it is also possible to obtain the signals "yes - no." Proportional control signals may be obtained by using disks shown in figure 3.14e.

As the image of the target is displaced along the radius, the modulation time of the light flux by frequencies f_1 and f_2 is varied. The ratio of the times is proportional to ϵ_y or ϵ_z. The circuit, which can be used to determine the signal which is proportional to the time ratio, is shown in figure 3.15. The photoelectric current of the sensor is amplified and is then transmitted to the primary winding of transformer Tr. During period T_1 the voltage

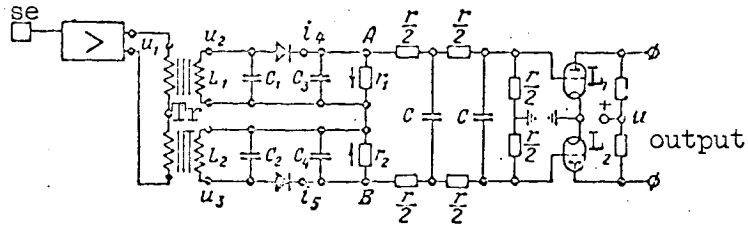

Figure 3.15. Schematic diagram of homing head.

varies with frequency f_1, while during period T_2 it varies with frequency f_2. The secondary windings of the transformer with inductances L_1 and L_2 and with capacitors c_1 and c_2 form resonant filters which are tuned, respectively, to /120 frequencies f_1 and f_2. When the signal at frequency f_1 is applied, the current passes through the upper half of the circuit, and when the applied signal has frequency f_2, it passes through the lower part of the circuit. A rectifier in each part of the circuit transmits the current for only half a period. By means of capacitors c_3 and c_4, the dc component of the current is isolated and is fed to resistances r_1 and r_2. The currents in resistances r_1 and r_2 are directed towards each other, and the voltage between points AB is equal to the difference in voltages across the resistances r_1 and r_2.

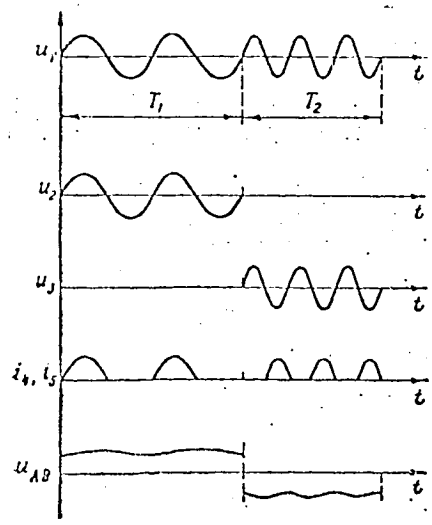

Figure 3.16. Variations in voltage which clarify operation of scheme shown in figure 3.15.

The curves in figure 3.16 show the variation in voltage at different points of the circuit. Due to the filtering of the voltage in the two-element filter, dc voltages are fed to tubes L_1 and L_2 (fig. 3.15). The increments of voltage on the grids of tubes L_1 and L_2 have the same signs. The modulus of the difference in the increments of the voltages depends on the value of the difference $T_1 - T_2$. The value of voltage u_{out} is proportional to the ratio $\left|\frac{T_1 - T_2}{T_1 + T_2}\right|$, and the sign of u_{out} is determined by the sign of the difference $T_1 - T_2$. Figure 3.17 shows the variation in the output voltage of the homing head as a function of the mismatch signal from the angle ϵ between the optical axis of the head and the direction from the missile to the target.

Some shapes of modulating disks (figs. 3.14c, d, e) make it possible to obtain control signals in a Cartesian system of coordinates, while the disks represented in figures 3.14f and g make it possible to obtain control signals in the polar system of coordinates. Two disks with cutouts (fig. 3.14f) rotate in the same direction, but with different velocities; one of them has a cutout in /121
the form of a sector, while the other has a cutout in the form of a spiral slit. The cutout in the form of a sector determines angle μ, while the spiral slit determines angle ϵ. The amplified photoelectric current is distributed by a commutator, which rotates with the disks, to corresponding control channels.

On the disk shown in figure 3.14g, a layer which does not transmit infrared rays is applied along an Archimedean spiral. Therefore the photocell generates current pulses whose duration is proportional to the departure of the target image from the center of the slit. The image of the slit is obtained in the form of a luminous point focused in the plane of the disk. An ac current generator is synchronized with the rotating disk. The phase of the photoelectric current pulses, with respect to the phase of the sinusoidal voltage produced by the generator, determines angles ϵ and μ by means of a computer.

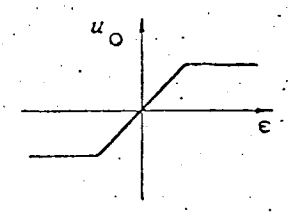

Figure 3.17. Characteristics of homing head.

These remarks are valid when the image of the target represents a point. As the missile approaches the target, its image increases and the sensor is subjected to infrared rays which are modulated simultaneously by two frequencies, i.e., the clear establishment of the angle between the optical axis and the direction to the target is disrupted--"the head goes blind."

One of the principal component parts of an infrared homing head is the electronic amplifier. As the range decreases, the amount of infrared energy which falls on the sensor increases, and consequently the photoelectric current also increases. Therefore the gain of the amplifier must be varied--it must be decreased proportionately to the square of the range. For this purpose an automatic gain control (agc) is used. Nevertheless, at a certain distance from target the photoelectric current will be so large that the operating point of the amplifier will pass over to the region of saturation, and the head will generate a maximum signal regardless of the displacement of the missile. This will be the second reason for the "blinding" of the head.

It is desirable to reduce the internal noise of the head to a minimum.

The noise sources capable of suppressing a weak signal from the detector are tubes, resistances and conductors. When the signal frequencies are relatively low, due to the slow rotation of the coordinate disks, it is necessary to have a precise control and thorough filtering of the supply voltage which feeds the heaters and other elements of the tubes. To decrease the effect of induction pickup, the first stage of the amplifier is placed as close as possible to the infrared radiation detector.

Section 3.4. Comparison of the Passive, Active and Semiactive Radar Homing Heads /122

A passive radar homing head does not have a device for illuminating the target; it is, therefore, simple and its operation is unknown to the enemy. A passive radar homing head is used if the target is a radar or some other object having a continuously operating radio transmitter in the range of wavelengths suitable for homing guidance.

Semiactive heads have the advantage that the powerful energy source is situated at the tracking point and does not perish with the missile. Therefore, the equipment aboard the missile, equipped with a semiactive head, is simpler, cheaper and lighter than in an active head. Since the power and directionality of a radar transmitter aboard a missile cannot be made as large as at the tracking point, the range of a missile equipped with an active tracking system is smaller than that of the one with a semiactive system.

Active homing heads make homing guidance independent of the operation of the tracking point, which is expedient for the case of any other mobile tracking point. In addition, when an active radar head is in operation, only the missile is decamouflaged and not the tracking point. The active radar head may be more expedient in those cases when the process of homing guidance does not start at launching, but only close to the target, i.e., at a large distance from the tracking point. From these considerations it follows that the type of radar homing head is selected on the basis of technical considerations and is limited by the technical mission of the missile.

Section 3.5. Obtaining the Error Signal in Radar Heads

To measure the angle between the axis of the homing head and the direction to the target, any of the known methods of direction finding may be used: the method of equisignal zone, direction finding according to the maximum, direction finding according to the minimum, etc. However, the method of the equisignal zone is more widely used in the homing guidance heads because it satisfies, to a large extent, the basic requirements presented to these heads.

The method of equisignal zones is based on the comparison of signals received by several or by one antenna, but for different positions of its radiation pattern. The equisignal zone may be spatial or it may be plane. A combination of two plane equisignal zones to measure, respectively, the deviations ϵ_y and ϵ_z (fig. 3.12) form a spatial equisignal zone. A spatial equisignal zone may be formed by rotating the radiation pattern. /123

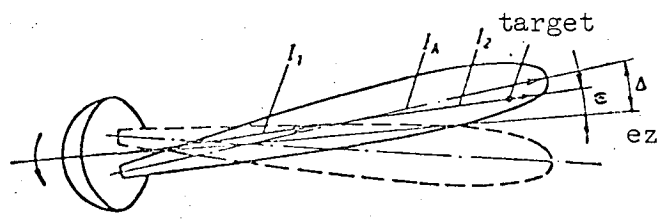

Figure 3.18. Principle of generating an equisignal zone (ez).

This principle is used most frequently in homing guidance heads.[1] The antenna and reflector of an active head are shown in figure 3.18, which also shows two positions of the radiation pattern. The antenna rotates with a constant angular velocity Ω and the I_A axis of the radiation pattern is inclined at an angle Δ with respect to the axis of rotation of the antenna, which is also the axis of the equisignal zone. Thus, for any position of the antenna, the same quantity of energy is radiated in the direction of the equisignal zone (ez) by the active head and received by the active, semiactive and passive head. If the equisignal zone is directed towards the target and the angle ϵ between the equisignal zone and the direction to the target is small, the amplitude of the received signal, when the antenna rotates, varies according to the law

$$u_m(t) = u_{0m}[1 + m\cos(\Omega t + \mu)], \qquad (3.4)$$

where $m = k\,\epsilon$; k is a constant which depends on the parameters of the antenna; and μ is the angle formed by the plane containing the target with the plane yx (fig. 3.12).

---

[1] L. S. Gutkin, The Principles of Radio Control of Pilotless Objects, "Soviet Radio," 1959.

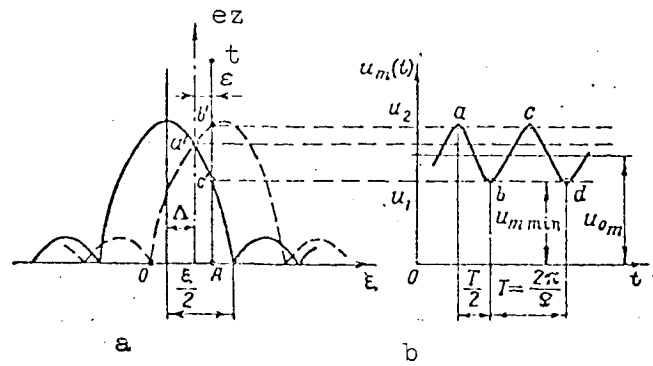

Figure 3.19. Section of the radiation pattern and formation of control signal.

Let us show the validity of expression (3.4). Figure 3.19a shows the section of the radiation pattern by the plane of the drawing. The solid line shows the section of the radiation pattern at the instant of time t, while the broken line shows it after a period of time $T/2 = \pi/\omega$, i.e., when the radiation pattern is rotated by 180°. The side lobes of the radiation pattern are also shown. Figure 3.19b shows the variation in the intensity of the signal received by the antenna as a function of time. It is obvious that when angle ϵ is larger, the difference $u_2 - u_1$, equal to twice the amplitude of the periodic component of the signal, is also greater. When $\epsilon < \Delta$ we may assume, for practical purposes, that the amplitude of this periodic component is proportional to mismatch ϵ. The receiver of the head has an automatic gain control which makes the output voltage independent of the quantity u_{0m}. The amplitude of the input signal for a passive /124

and semiactive head depends on the square of the range, while for an active head the amplitude of the input signal varies as the fourth power of the range. After amplification and detection of the signal received by the antenna, we obtain the following voltage at the output of the receiver

$$u_\epsilon = k_1 \varepsilon \cos(\Omega t + \mu), \tag{3.5}$$

where k_1 is a constant.

The voltage u_ϵ is called the error signal. Figure 3.20 shows the variation in the amplitude of the error signal as a function of the mismatch. When $\epsilon < \frac{\xi}{2} - \Delta$ (where ξ is the angle of the radiation pattern), we may assume that the characteristics are practically linear. For $\epsilon \geq \frac{\xi}{2} - \Delta$ after the maximum value is achieved, /125 u_ϵ begins to decrease. Thus, the magnitude of the linear zone of error signal amplitude variation depends on the width ξ of the antenna radiation pattern and on the Δ-angle of inclination of the pattern with respect to the antenna axis of rotation. As we know, when the width of the radiation pattern decreases, the range, freedom from interference and the gain of a radar system increase.

However, when the radiation pattern becomes narrow and the angle Δ becomes narrow, it is difficult to capture the target. Therefore, the magnitude of the sighting angle and the equivalent width of the linear region for the variation in the amplitude of the output voltage as a function of mismatch angle ϵ in most cases constitutes $\pm$ 5 to 10°.

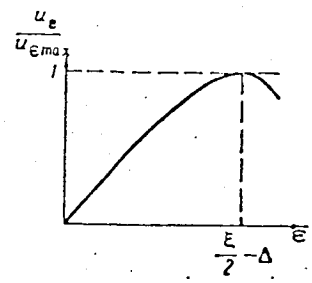

Figure 3.20. Variation in error signal amplitude as function of mismatch.

Section 3.6. Formation of the Control Signal

As indicated by equation (3.5), the error signal contains two parameters ϵ and μ which characterize the relative position of the missile and the target. To control plane-winged missiles the signals must be proportional to ϵ and μ, while for missiles with cruciform wings the signals must be proportional to $-\epsilon_y$ and ϵ_z.

Let us see how control signals are obtained for each of the aerodynamic missile forms.

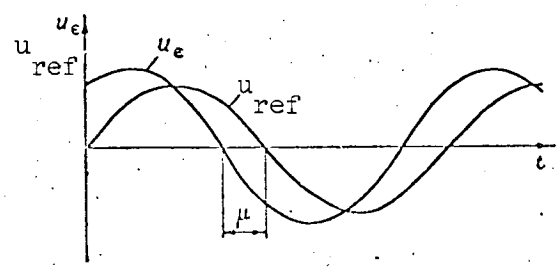

Figure 3.21. Phase of the error signal.

Missiles with Plane Wings. In controlling missiles with plane wings it is necessary to determine the amplitude and phase of the error signal. In order to obtain a control signal proportional to the phase, the error signal u_ϵ is compared with a reference voltage (fig. 3.21). The reference voltage u_{ref} is produced by a sine wave generator whose rotation is synchronized with the rotation of the radiation pattern. By feeding both of these voltages to a phase-sensitive bridge, it is possible to determine phase μ. /126

Missiles with Cruciform Wings. Figure 3.22 shows the schematic diagram for obtaining control signals for axially-symmetric missiles. The signal from antenna

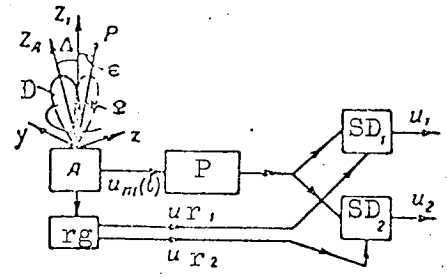

Figure 3.22. Schematic diagram showing generation of missile control signals. rg--reference generator.

A passes through receiver P and is fed to a synchronous detector SD. To obtain control signals in this case the signals of the reference generators are used. In addition to the error signal, the input of the synchronous detectors is also subjected to the reference voltages

$$\left.\begin{aligned} u_{ref\ 1} &= U_{ref} \cos \Omega t, \\ u_{ref\ 2} &= U_{ref} \sin \Omega t. \end{aligned}\right\} \qquad (3.6)$$

In some cases the sine-wave generator of reference voltages and the electronic synchronous detectors are replaced by mechanical commutators which are synchronized with the rotation of the pattern.

When the error signals are compared with reference voltages, the synchronous detectors develop voltages u_y and u_z, which are proportional to ϵ_y and ϵ_z. The synchronous detectors may have different circuits. Figure 3.23 shows the schematic diagrams of synchronous detectors (for one control channel) when a sine-wave generator of reference voltages is used. The diagram shown in figure 3.23a is the simplest. The reference voltage is applied to the grids of tubes L_1 and L_2, together with the error signal. The error signal is out of phase, while the reference voltage is in phase.

As a result the variable voltages on the grids of the tubes will be /127

$$\left.\begin{aligned} u_1 &= u_{ref\ 1} + u_\epsilon \\ u_2 &= u_{ref\ 1} - u_\epsilon . \end{aligned}\right\} \qquad (3.7)$$

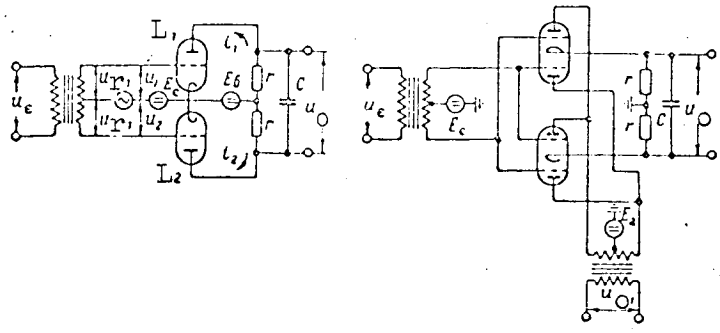

Figure 3.23. Diagram of synchronous detector.

In our analysis we shall assume tubes L_1 and L_2 are identical. When the load resistance is small ($r \ll r_i$), the plate currents of the tube may be written in the following form

$$\left.\begin{aligned} i_1 &= I_a + au_1 + bu_1^2, \\ i_2 &= I_a + au_2 + bu_2^2, \end{aligned}\right\} \tag{3.8}$$

where a and b are coefficients in the expansion showing the variation in the plate current of the tube as a function of grid voltage.

The terms in the expansion which are greater than second order are not considered. If we neglect the effect of capacity c on the transmission of dc and the low frequency component of the output signal, we may write

$$u_{\text{output 1}} = i_1 r - i_2 r = r(i_1 - i_2) = r\Delta i. \tag{3.9}$$

By using equations (3.7) and (3.8) we can express the difference in the currents Δi in terms of the signal error voltage and the reference voltages in the following manner

$$\Delta i = 2au_\varepsilon + 4bu_\varepsilon u_{\text{ref 1}}. \tag{3.10}$$

By taking into account expressions (3.5) and (3.6) and carrying out some transformations, we obtain /128

$$\begin{aligned} \Delta i = {} & 2ak_1\varepsilon\cos(\Omega t + \mu) + 4bu_0k_1\varepsilon\frac{1}{2}\cos\mu + \\ & + 4bu_0k_1\varepsilon\frac{1}{2}\cos(2\Omega t + \mu). \end{aligned} \tag{3.11}$$

However,

$$\varepsilon_y = \varepsilon \cos \mu, \tag{3.12}$$

Therefore,

$$\Delta i = 2ak_1\varepsilon \cos(\Omega t + \mu) + 2bu_0k_1\varepsilon_y + 2bu_0k_1\varepsilon \cos(2\Omega t + \mu). \tag{3.13}$$

The quantity Ω depends on the frequency of rotation of the radiation pattern, i.e.,

$$\Omega = 2\pi f_a, \tag{3.14}$$

where f_a is the frequency of rotation of the antenna in cps.

Usually $f_a \approx$ 20-100 cps. The functions ϵ and ϵ_y vary slowly with time. The spectrum of frequencies for these signals lies in the range 0 to 5 cps. Therefore, to isolate a signal which is proportional to ϵ_y it is sufficient to place a filter with a bandpass of 0 to 5 cps at the output of the phase detector. It is obvious that if the frequency of rotation of the antenna f_a is increased, it is possible to decrease the time constant of the filter, i.e., to decrease the delay in the channel which generates the control signal. The increase in the frequency of rotation of the antenna is limited by the mechanical strength of the entire system. When disturbances are present the error signal may develop low frequency components and we are faced with the problem of filtering them. In this case a push-pull synchronous detector is used. The possible scheme of such a detector is shown in figure 3.23b.

To decrease the mutual effect of the reference voltages and error signal voltages, these are fed to different electrodes of each tube--to the grid and to the anode. When the circuit is completely symmetrical, the resulting current in the first and the second detector may be expressed in the form

$$\left.\begin{aligned} \Delta i &= ku_{\varepsilon}u \quad \text{ref 1} \\ \Delta i &= ku_{\varepsilon}u \quad \text{ref 1} \end{aligned}\right\} \tag{3.15}$$

where k is a coefficient which depends on the parameters of the circuit and the tubes.

It can be shown that the voltage at the output of the filter, which is placed after the synchronous detector, is equal to

$$\left.\begin{aligned} u_{\text{output 1}} &= r\Delta i = r2bu_0k_1\varepsilon_y, \\ u_{\text{output 2}} &= r\Delta i = r2bu_0k_1\varepsilon_z. \end{aligned}\right\} \tag{3.16}$$

The control signals may be obtained in this manner. In considering the operation of the circuits we did not take into account disturbances or the additional circuits used to decrease their effect. /129

Section 3.7. Interferences in Radar Heads

Interferences which affect the operation of radar heads may be produced in the target control channel, i.e., in the channel which receives signals reflected by the target. Reflections from the target are rather weak, while the illumination of the target is carried out with a powerful radio beam which makes it easier for the enemy to recognize the technical features of the target control system and to generate interference. In addition to the interference produced by the enemy, there are several other forms of interference, of which the following are most important:

(1) interference produced by the internal noise of the radar receiver, i.e., by the fluctuation of electrons in tubes and in the circuits of the receiver, and

(2) interference produced by the pulsation of the signal reflected by the target.

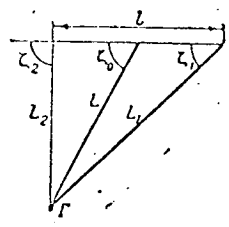

Figure 3.24. Generation of interference.

The internal noise of the receiver is present regardless of the target range, and when the range is very large the received signal becomes comparable to the noise signal. Thus, if we know the magnitude of the noise we may establish the limiting range of the head.

Interferences produced by the pulsation of the signal reflected by the target added to the interference from the internal noise decrease the range of the head. These interferences also decrease the strike accuracy of the missile, because they produce its oscillations not due to the realization of tracking. Let us briefly consider the reasons for the pulsation of the signal reflected by the target. At centimeter and decimeter waves, the wavelength is small compared with the linear dimensions of the target l and reflection pattern from the target in any plane is of a complex multilobe nature.

In theory the reflection from the target is assumed to be a reflection from a point, but actually the electromagnetic oscillations are reflected by the target under different angles ζ (fig. 3.24). The pulsation frequency of the reflected signal depends on wavelength λ, on the dimensions of target l and also on the rate of variation of angle ζ_0

$$f = \frac{2l}{\lambda}\left|\frac{d\zeta_0}{dt}\sin\zeta_0\right|. \qquad (3.17)$$

Therefore, error signal pulsations may occur even when the variation in the angle of incidence ζ_0 is uniform. If we note that in most cases the angle ζ_0 does not /130

vary uniformly and has random components, the true spectrum of the pulsations may contain an appreciable number of components with a wide frequency range--from units to hundreds of cycles.

The variations in the angle ζ_0 may be due to the following basic causes:

(1) the rotation of the target with respect to the equisignal zone; in particular, this motion may be of two forms in airplane targets: turning during evasion maneuvers and oscillations with respect to the center of gravity; and

(2) the forward motion of the target.

It is easy to evaluate the signal error pulsation frequency when the airplane is undergoing evasion maneuvers. When the target is turning with an angular velocity of 10-20 °/sec, we obtain the following values when l = 15-30 meters, $\lambda \leq 10$ cm and $\zeta_0 = 90°$

$$f_{max} = \frac{3000}{10}\left|\frac{10}{57.3}\right| \approx 50 \text{ cps},$$

$$f_{max} = \frac{6000}{10}\left|\frac{20}{57.3}\right| \approx 200 \text{ cps}.$$

When the target is moving forward, the angular rate of change will be given by

$$\frac{d\zeta_0}{dt} \approx \frac{V}{L}\sin\zeta_0. \qquad (3.18)$$

Substituting this expression into equation (3.17) we obtain

$$f = \frac{2V}{\lambda}\frac{l}{L}\sin^2\zeta_0. \qquad (3.19)$$

For the same value of l and λ when $V \leq 300$ meters/sec, we obtain

$$f_{max} \leqslant \frac{60 - 200}{L_{\text{км}}} \text{ cps}.$$

Consequently, when the target is moving forward the pulsation frequency depends on the range, and for large ranges ($L \approx 10$-15 km) lies within the limits $f_{max} \leq 4$-20 cps.

It is clear that pulsation frequencies close to the frequencies of rotation of the radiation pattern will have a particularly pronounced effect on the head and introduce large errors. If we bear this in mind, we may conclude that at long ranges the principal interference is produced by pulsations due to the rotation of the target, while at short ranges it is produced by the forward motion of the target.

Figure 3.25 shows a typical curve for the pulsation of the radar receiver signal produced by reflection from a long range flying target which does not undergo sharp maneuvers. Figure 3.26 shows the frequency spectrum of this curve. /131

To decrease the pulsation of the signal, it is possible to increase the wavelength. However, this method is not used because it is necessary to keep the size of the antenna small.

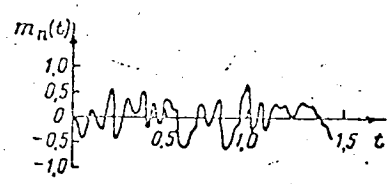

Figure 3.25. Variation in error signal as function of time.

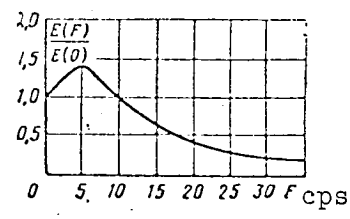

Figure 3.26. Frequency spectrum of error signal.

An increase in the frequency of rotation of the radiation pattern also leads to a decrease in the effect of signal pulsation, however, when the antenna is rotated mechanically, this frequency is limited by the mechanical strength of the system. Thus, in a series of cases a substantial lowering of pulsation may be quite difficult because the performance of the radar head will decrease.

Filters before and after the detector are also used to decrease the pulsation of the signal. The parameters of the filter are selected in such a way that the noise frequencies are not passed by it. When filters are used, a lag is introduced into the radar head.[1]

Section 3.8. Generation of Control Signals for Various Methods of Homing Guidance

In preceding sections we have shown how to obtain a signal proportional to the angle between the optical axis of the head and the line joining the missile

---

[1] L. S. Gutkin, The Theory of Optimum Reception of Radio Waves in the Presence of Fluctuating Noise. Gosenergoizdat, 1961.

and the target (see sections 3.3 and 3.6). To accomplish various methods of homing guidance, which will be analyzed in Chapter 13, it is necessary to have a control signal proportional to the angle between the line of sight from the missile to the target and the longitudinal axis of the missile, or the air speed vector, or to have a signal proportional to the angular velocity of the line joining the missile and the target.

It is clear that the simplest signal is one proportional to the angle between the line joining the missile and the target and the longitudinal axis of the missile. In this case the optical axis of the head must coincide with the longitudinal axis of the missile, i.e., the homing head is rigidly attached to the frame of the missile. /132

Let us consider in more detail the generation of the control signal proportional to the angle ϵ_y between the line joining the missile and the target and the velocity vector in the vertical plane. The geometric relations for this problem are shown in figure 3.27. A signal which is proportional to the angle ϵ_y may be obtained in several ways:

(1) aboard the missile the optical axis of the head always coincides with the direction of the missile's longitudinal axis; angle ϵ_y is the sum of two angles(fig. 2.7)

$$\epsilon_y = \epsilon_{head} + \alpha.$$

The sum of the signals which are proportional to angles ϵ_{head} and α is fed to the control systems;

(2) by using a servosystem which rotates the head with respect to the missile frame and by using a sensor which gives the value of the angle of attack α.

If the servosystem rotates the optical axis of the head by the angle of attack with respect to the longitudinal axis of the missile, the control signal taken from the head will be proportional to the angle between the line joining the missile and the target and the velocity vector. Before considering the operating principle of a servosystem, we pause briefly to examine the sensors used to measure the angle of attack.

A signal proportional to the angle of attack may be obtained by means of a sensor which detects the angle of attack and the angle of slip. To measure the angles of attack and slip accurately, the rod must be secured in the nose of the missile, which is impossible in most cases due to the presence of the homing head. Therefore, the sensor which detects the angle of attack and the angle of slip is usually used in preliminary testing of the missiles without the control system. The value of the angle of attack may be obtained indirectly by using an accelerometer or a damping gyroscope.[1]

[1]These devices are considered in more detail in section 5.5.

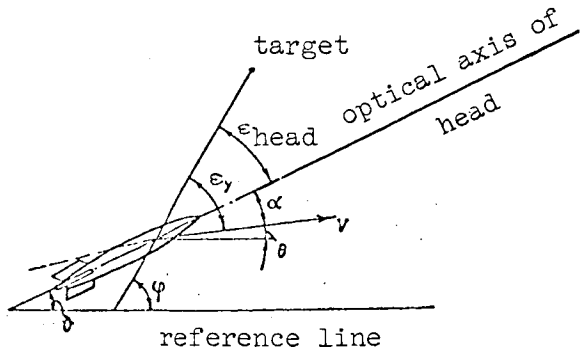

Figure 3.27. Relative position of missile and target in pursuit method.

In the vertical plane the missile is constantly subjected to acceleration due to gravity and acceleration due to aerodynamic forces. Let us establish the relationship between the acceleration normal to the flight trajectory and the angle of attack of the missile. The normal acceleration is given by ex- /133
pression

$$j_y = V\frac{d\theta}{dt} = \frac{Y - G\sin\theta}{m}, \tag{3.20}$$

where Y is the lift force of the missile; m, G are the mass and weight of the missile, respectively, and θ is the slope of the trajectory, as shown in figure 3.27.

The variation in lift force Y over a definite range of the angle of attack is linear. Consequently, expression (3.20) may be represented in the form

$$j_y = k\alpha - g\sin\theta, \tag{3.21}$$

where g is the acceleration due to gravity; and $k = k(V, \rho, m)$ is the coefficient of proportionality for a given missile which depends on the flight velocity.

From equation (3.21) we obtain an expression which relates the angle of attack of the missile and the normal acceleration

$$\alpha = \frac{j_y + g\sin\theta}{k}. \tag{3.22}$$

In the horizontal plane the relation between the slip angle and acceleration will be even simpler, since the force of gravity does not affect the motion of the missile in this plane

$$\beta = \frac{j_z}{k_1}, \tag{3.23}$$

where $j_z = V\frac{d\theta_s}{dt}$ is the acceleration normal to the trajectory in the horizontal

plane; θ_s is the slope of the trajectory in the horizontal plane, and $k_1 = k_1$ (V, ρ, m) is a coefficient of proportionality.

It follows from expressions (3.22) and (3.23) that when the flight velocity, air density, mass of the missile and the slope of the trajectory are constant or vary slowly, the accelerometer may be graduated in terms of the angle of attack and the slip angle. If the above parameters vary within wide limits, it is always possible to measure them in principle and to use a special computer to take into account their effect on the relationship between the normal acceleration in the vertical and horizontal plane and between the angles of attack and slip.

Let us consider the problem of using a gyroscope with two degrees of freedom for measuring the angle between the velocity vector and the longitudinal axis of the missile. We shall limit ourselves to the determination of the relation between the deviation of such a gyroscope and the slip angle. A gyroscope with two degrees of freedom gives a signal proportional to the angular velocity of the /134 longitudinal axis of the missile in the horizontal plane. In this case, the axis of the gyroscope pattern is directed along the z axis, while the axis of the frame is directed along the longitudinal axis of the missile. This angular velocity may be determined from expression

$$\frac{d\psi}{dt} = \frac{d\theta_s}{dt} + \frac{d\beta}{dt} = \frac{j_z}{V} + \frac{d\beta}{dt} = \frac{k_1}{V}\beta + \frac{d\beta}{dt}, \qquad (3.24)$$

where θ_s is the slope of the trajectory in the horizontal plane, and ψ is the slope of the missile's axis in the same plane.

If we let $\frac{k_1}{V} = \frac{1}{T}$, we obtain

$$T\frac{d\beta}{dt} + \beta = T\frac{d\psi}{dt}. \qquad (3.25)$$

As we can see from expression (3.25), the slip angle β lags the angular velocity $d\psi/dt$ of the longitudinal axis of the missile. Therefore, the signal which is taken from the damping gyroscope, and which has passed through an inertial element (filter) with a time constant T, will correspond to the value of the slip angle β. On the basis of equation (3.24) the time constant must vary with flight velocity, air density and mass of the missile. But in many cases the variation in the time constant is insignificant, and in practice it may be assumed to be constant.

The servosystem for rotating the optical axis of the head must be designed in line with the diagram shown in figure 3.28, regardless of whether the sensor is for the angle of attack or the slip angle. The comparison element 1 is used to obtain a signal proportional to the angle between the direction of the longitudinal axis of the missile and the optical axis of the head $\psi-\mu$ (fig. 3.30). A signal proportional to slip angle β is fed to the second comparison element 2 (fig. 3.28). The difference between these signals is fed to the head turn

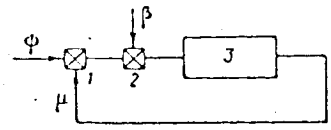

Figure 3.28. Functional diagram of servosystem for rotating head. 1 and 2--comparison elements; 3--head actuator.

actuator and when it operates, the head turns in the direction of the velocity vector. The signal from the head is proportional to angle ϵ_y and is fed to the missile control system. The rotation of the head must be sufficiently rapid, if the optical axis is to follow the velocity vector accurately. This requirement is fully met by gyroscopic systems which stabilize the head with compensation. In practice a system of this type may be considered to be free of inertia.

Figure 3.29 shows a simplified diagram of a system for stabilizing the head. Its principle of operation consists of the following. The homing head is secured to the internal frame of a gyroscope with three degrees of freedom. Compensating devices produce moments with respect to the axes of the internal and external frames. This causes the gyroscope to precess, and the optical axis turns in the desired direction. The rate of precession is proportional to the applied moment which, in turn, is proportional to the control signal. /135

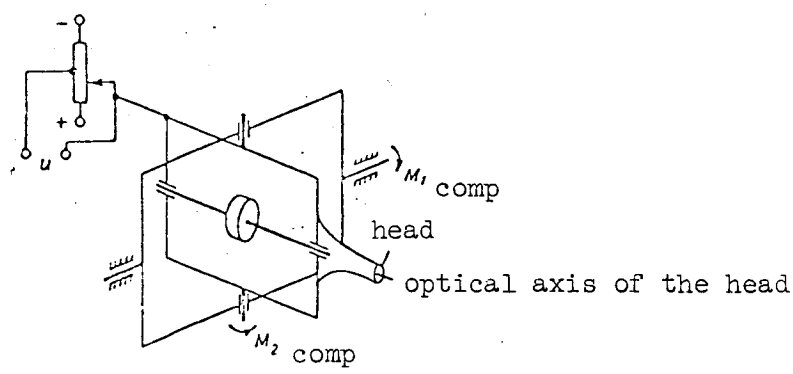

Figure 3.29. Schematic representation of head system.

On this basis we may write (motion in a plane)

$$M_{comp} = k\eta, \tag{3.26}$$

where η is the control signal; k is a coefficient of proportionality, and M_{comp} is the compensating moment.

At the same time

$$\eta = \dot{\psi} - \mu - \beta = \theta_s - \mu, \tag{3.27}$$

where μ is the position of the optical axis.

Let us write the variation in the rate of precession as a function of the compensating moment

$$\frac{d\mu}{dt} = k_1 M_{\text{comp}}. \tag{3.28}$$

By transforming equations (3.26), (3.27), (3.28), we find

$$T\frac{d\mu}{dt} + \mu = \theta_s, \tag{3.29}$$

where

$$T = \frac{1}{kk_1}.$$

From analysis of equation (3.29) it follows that upon the termination of the transient process the optical axis will be directed along the velocity vector, if θ_s = const, or that it will track with sufficient accuracy in this direction when the variations in the angle θ_s are small. The tracking accuracy increases /136

as the time constant T decreases, which corresponds to an increase in the amplification factor (gain). The derivation of the equations did not take into account the lag in the generation of the compensating moment and of the control signal, or the nonlinear variation in the rate of precession as a function of the compensating moment. As we can see from equation (3.27), it is necessary to measure the angle between the longitudinal axis of the missile and the optical axis of the head, if the system is to operate properly. To do this, we may use a potentiometer rigidly attached to the frame of the missile. The brush of the potentiometer is fixed to the corresponding frame (fig. 3.29). The voltage u taken from the potentiometer will be proportional to the angle between the longitudinal axis of the missile and the optical axis of the head.

From a similar system for the stabilization of the head we may obtain a signal which is proportional to the angular velocity of rotation of the line joining the missile and the target. In this case, the homing head tracks the target, i.e., the optical axis of the head is always directed towards the target. To achieve this, it is necessary that during the deviation of the optical axis from the direction to the target the compensating moments be proportional to this deviation. When the compensating moment acts, the homing head points towards the target.

In line with what we have said, we formulate an equation of motion for the stabilization system. The signal from the head is proportional to the angle between the line joining the missile and the target and the optical axis of the head (fig. 3.30), i.e.,

$$\varepsilon_{\text{head}} = \varphi - \mu. \tag{3.30}$$

The compensating moment is proportional to the signal from the homing guidance head, i.e.,

$$M_{comp} = k\epsilon_{head}. \tag{3.31}$$

The angular velocity of the optical axis is proportional to the compensating moment /137

$$\frac{d\mu}{dt} = k_1 M_{comp}. \tag{3.32}$$

By eliminating the variables from equations (3.30) - (3.32), we find

$$T_1 \frac{d\mu}{dt} + \mu = \varphi, \tag{3.33}$$

where

$$T_1 = \frac{1}{kk_1} \text{ (sec)}.$$

If angle φ is constant, then after the transient process is over $\mu = \varphi$, i.e., the optical axis of the head is directed along the line joining the missile and the target, and tracking is accomplished. When angle φ is varied slowly, it is obvious that angle μ also varies with approximately the same velocity, i.e., $d\mu/dt \approx d\varphi/dt$. This identity is also valid when the missile is far from the target when $d^2\varphi/dt^2$ is small. As the missile approaches the target, the angular acceleration $d^2\varphi/dt^2$ may increase radically, and then the equality $d\mu/dt \approx d\varphi/dt$ is no longer satisfied. If the angular velocities $d\mu/dt$ and $d\varphi/dt$ are close to each other, then it follows from equation (3.32) that

$$\frac{d\varphi}{dt} \approx k_1 M_{comp}. \tag{3.34}$$

Finally, by using equation (3.31) we obtain

$$k_1 k\varepsilon_{head} = \frac{d\varphi}{dt}. \tag{3.35}$$

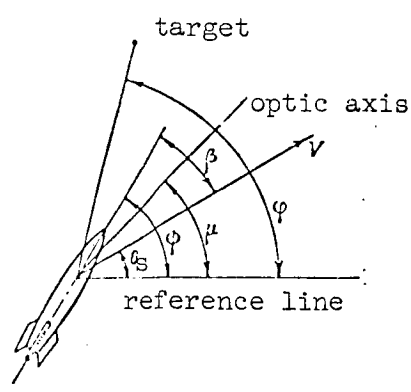

Figure 3.30. Relative position of missile and of target in method of parallel approach.

Expression (3.35) shows that the signal from the homing head is proportional to the angular velocity of the line joining the missile and the target. Therefore, the signal from the homing head after amplification by a factor of k_1k is fed to the missile control channel. Since the coefficients k and k_1 also determine the time constant T_1 of the tracking system, they are selected on the basis of stability and performance. It is necessary to point out that when the homing head is tracking, the requirements for the angle of vision are radically reduced and the range is, therefore, extended.

Above, we have considered the simplest scheme for rotating and stabilizing homing heads. It is clear that any gyro stabilization system may be used. In selecting a system, the basic requirements are reliable operation, accuracy and cost. The cost of a head which is gyro-stabilized is several times higher than /138 the cost of a head rigidly attached to the frame of the missile. We should add that an introduction of a stabilizing system, as an introduction of any additional components, decreases the reliability, i.e., increases the probability of failure of the entire system. For this reason, tracking heads as a rule are used only to measure the angular rate of rotation of the line joining the missile and the target.

CHAPTER 4. CONTROL SIGNALS IN EXTERNAL GUIDANCE /139

Section 4.1. Radio Beam Guidance of Missiles

A radio beam is a region of space which has the shape of a body of revolution within which electromagnetic energy from the transmitter of a radar station is propagated. Since the radio beam is formed by the rotation of the radiation pattern of the radar transmitter, its axis is the equisignal zone of the radar.

The guidance of a missile along a beam produces control signals aboard the missile directly, without auxiliary communication channels. The radar station, which produces the radio beam pointing to the target, is situated at the missile control site. The missile contains a receiver which picks up the signals from the radar transmitter at the control site. This receiver determines the magnitude and direction of missile deviation from the equisignal zone in a system of coordinates fixes with respect to this zone. The signal from the output of the receiver is fed to the missileborne control system. When the control surfaces are actuated, a force is produced which keeps the missile on the beam.

The equisignal zone which is produced by the rotation of the radiation pattern, makes it possible to obtain control signals on the missile in any two mutually perpendicular planes, whose line of intersection coincides with the direction of the equisignal zone. If the position of the equisignal zone is not too close to the vertical, the missile receives "up-down" and "right-left" control signals (fig. 4.1). When the direction of the beam approaches the vertical, the signals "up-down" are designated as "forward-backward." This principle is used to guide antiaircraft missiles, to guide aerial combat missiles and short range airplane-missiles, which are dropped from the carrier-airplane. If it is necessary to control the missile with respect to a plane (usually with respect to the firing plane), the equisignal zone is produced not by rotation, but by the displacement of the radiation pattern in one plane. In this case the missile will only receive signals of the type "right-left." This method /140 is used to guide tactical and strategic airplane-missiles and long range rockets. Different versions of missile guidance are shown in figure 4.2.

In the general case, when the control point and the target are in motion along arbitrary trajectories, the radio beam which contains the missile may be displaced at very high velocity. Therefore, the trajectory acquires a substantial curvature so that the missile is on the beam at all times. If the missile is to follow this trajectory, it must have a substantial control force, which can only be achieved by increasing the size of the wings and the dimensions of the missile. Increase in the size is in turn associated with increase in drag, and consequently affects the power of the engine and the mass of the missile. By making the tracking equipment more complicated, it is possible to guide the missile along a trajectory with low curvature.

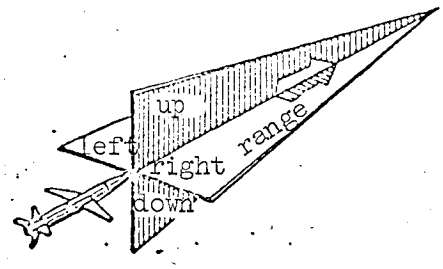

Figure 4.1. Control signals which act on missile control system.

For example, let us install two radars producing two independent radar beams at the control point. We let one radar track the target, which gives us the range and direction to the target, as well as the velocity of rotation of the radio beam axis. The second beam must be directed to the point of interception where the missile and the target meet, if they move uniformly along a /141

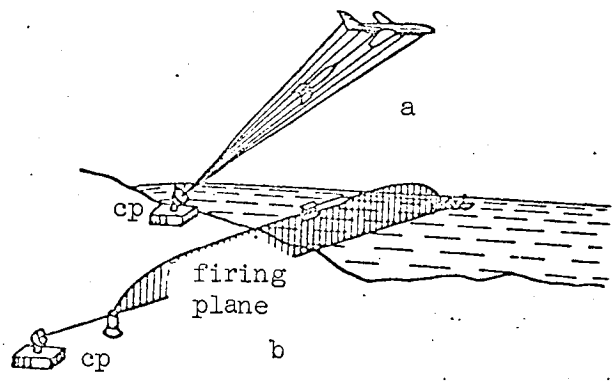

Figure 4.2. Missile guidance by means of radio beam (a) and by means of radio track (b).

straight line. The missile must fly along the axis of the second beam until it hits the target. A deflection angle forms between both beams, and its instantaneous value depends on the velocity of the target and the velocity of the missile. Information on the velocity of the missile and of the target is obtained by processing the data obtained from the radars tracking the target and the missile. On the basis of these data, the deflection angle is continuously calculated by means of a computer at the control point and is processed by the servosystem controlling the second beam. If the motion of the target is rectilinear and uniform, the trajectory of the missile in the two-beam guidance system will be a straight line. If the target undergoes evasive maneuvers, the trajectory is somewhat distorted, but its curvature will be less than in the case when only one beam is used for control. The schematic diagram of the control system which can guide a missile to a predicted point is shown in figure 4.3.

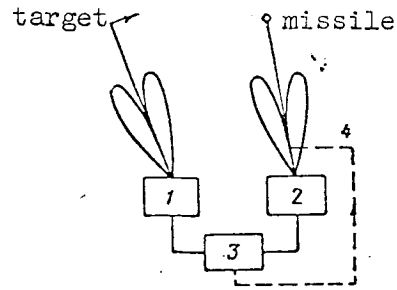

Figure 4.3. Block diagram of two-beam system which guides missile to predicted point. 1--target tracking station; 2--missile tracking station; 3--computer; 4--line for transmitting commands.

The disadvantage of a double beam control system compared with a single beam system is the substantial increase in the complexity of the control equipment. A two-beam system requires two radars and a complicated computer. We should also point out that when a missile is guided from a mobile control point (e.g., from an airplane), by selecting a corresponding law of motion for the control point we can provide for a low turning velocity of the radio beam and consequently for small curvature in the trajectory of the missile. The range of a tracking system using a radio beam is determined by the range of the radar at the control point.

Since the launching site for the missile and the radar site for control are situated at different points, it is necessary to bring the missile into the radio beam. To achieve this in a simple manner, it is frequently necessary that the cross section of the beam be considerable at relatively short distances from the radar antenna. This condition can also be satisfied by widening the radiation pattern of the radar antenna. It is clear that this can only be achieved by decreasing the range or increasing the power of the radar. However, the cross section area of the radio beam increases proportionately to the square of the distance from the radar. Near the target, the missile is reliably retained inside the beam whose radiation pattern is of a smaller width /142 than that required to bring the missile reliably into the beam. A decrease in the sighting angle increases the range of the radar and the accuracy and freedom from interference of the system. Therefore, in a series of cases, a discontinuous or uniform variation in the sighting angle of the radar at the control point is introduced as the missile flies to its target. Initially, the sighting angle is set for a maximum value, and as the missile flies to its target, this angle is decreased.

The radar at the control point tracks the target automatically. This principle has already been described in the preceding chapter when we discussed the tracking heads used in homing guidance. Therefore, we shall consider only the generation of the control signal aboard the missile which flies along a radio beam. The tail part of the missile contains an antenna and a receiver. If the missile is on the radio beam (fig. 4.4a), the magnitude of the signal received by the receiver on the missile will be constant because the

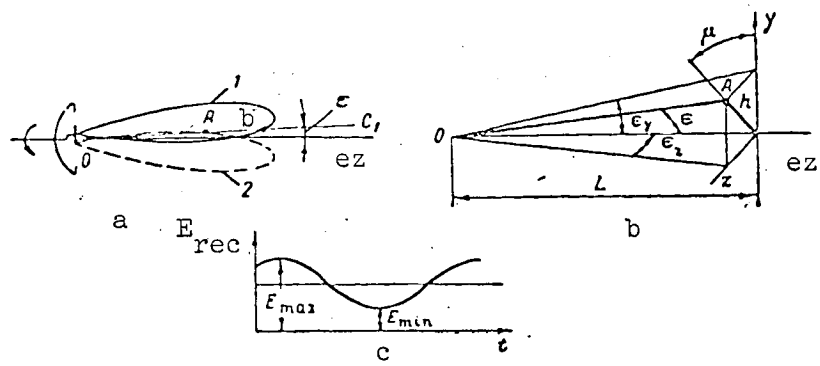

Figure 4.4. Generation of control signal by an equisignal zone; (subscript rec = receiver; ez = equisignal zone).

radiation power of the radar is constant in the direction of the equisignal zone. If the missile deviates from the axis of the radio beam (e.g., towards point A in figure 4.4b), the signal received by the antenna of the missile will oscillate with a frequency of rotation of the radar radiation pattern. The maximum value of the signal corresponds to position 1 of the radiation pattern, while the minimum value corresponds to position 2, because in the first case the signal is proportional to segment OB, while in the second case it is proportional to segment OA. The amplitude of the field intensity will be proportional to angle ε between the direction of the radio beam axis and line OC_1.

From figure 4.4b we can obtain /143

$$\operatorname{tg}\varepsilon = \frac{h}{L}, \tag{4.1}$$

where h is the deviation of the missile from the axis of the radio beam in the plane yz which is perpendicular to this axis, and L is the distance of the missile from the control point.

The form of the signal at the output of the receiver in the missile is shown in figure 4.4c. The phase of the ac component of the signal is determined by angle μ between radius-vector h, showing the deviation of the missile from the axis of the radio beam and the axis y (or z) in a plane perpendicular to this axis (fig. 4.4b). Thus, after the dc component is separated, the signal has the form

$$u_{receiver} = k\varepsilon \cos(\Omega t + \mu), \tag{4.2}$$

where k is a constant which takes into account the parameters of the signal transmission channel, and Ω is the angular frequency of rotation of the radiation pattern.

As the missile moves away from the control point, the field intensity drops off as the square of the distance, and for this reason the receiver has automatic gain control making the output voltage independent of the range.

Equations (4.2) and (3.5) are identical. Consequently, the form of the voltage at the output of the receiver in the missile guided by the radio beam is analogous to the form of voltage at the output of the receiver in the homing guidance radar head.

To control missiles with cruciform wings we require signals proportional to the components of deviation h on the vertical y and the lateral z surfaces (fig. 4.4b). To obtain signals of this type it is necessary to compare the signal received by the missile with the reference voltage in the synchronous detector (the diagrams of synchronous detectors have been considered in section 3.6). The reference voltage developed aboard the missile must correspond in frequency and phase to the rotation of the radiation pattern of the radar at the control point producing the equisignal zone. Therefore, reference signals are sent to the missile and are used to synchronize the generator of reference voltages aboard the missile with the rotation of the radiation pattern of the radar. As a result the output of the synchronous detector contains error signals which are proportional, respectively, to ϵ_y and ϵ_z (section 3.6). However, to control the missile, it is necessary to have signals proportional to y and z. From figure 4.4b we obtain /144

$$y = L \operatorname{tg} \epsilon_y, \qquad (4.3)$$

$$z = L \operatorname{tg} \epsilon_z.$$

Since the deviations from the axis of the radio beam are small during missile control, we have

$$y \approx L\epsilon_y, \qquad (4.4)$$

$$z \approx L\epsilon_z.$$

As we can see from equation (4.4), when the deviation from the axis of the radio beam h is constant, angle ϵ decreases with range. Therefore, the signal from the output of the synchronous detector must be varied proportionately to the range in order to provide for control by linear rather than angular deviation. When the velocity of the missile is constant, the change in the range is almost a linear function of time, and the signal is controlled by means of a potentiometer with a clock mechanism (fig. 4.5). As the distance between the missile and the control point changes, an increasing portion of the voltage supplied to the potentiometer is picked up from it. The moving wiper of the potentiometer is displaced by a clock mechanism. If the velocity of the missile is not constant, the potentiometer is shaped accordingly.

We note that when a radio beam is used for homing we cannot permit the rotation of the missile with respect to its longitudinal axis (if the missile does

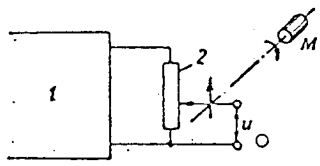

Figure 4.5. Scheme for taking into account distance between missile and target: 1--phase detector, 2--potentiometer.

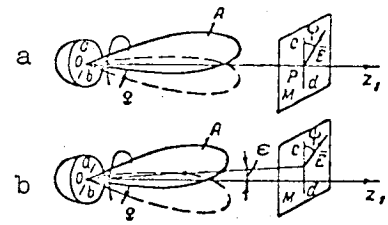

Figure 4.6. Arrangement of transmitting dipole and receiving dipole when missile is controlled with radio beam.

not contain a special transducer for control signals). If the missile rotates, the normal operation of the control channels will be disrupted. For example, if the missile turns by 90° with respect to its longitudinal axis, the control channels "up-down" and "left-right" will change their roles and the operation of the control system will become impossible.

The signal which is received by the missile may also become distorted due to the rotation of the radiation polarization plane produced by the radar at the control point. In the simple case the transmitting and receiving antennas consist of dipoles. The mutual position of the transmitting dipole ab and the receiving dipole cd is shown in figure 4.6. We assume that the receiving dipole is situated in a plane perpendicular to the axis of the equisignal zone (axis of the beam). At each instant of time the electric field intensity vector E is /145 parallel to the transmitting dipole ab and rotates with it at an angular velocity Ω. The polarization plane of the radiated energy also rotates in this fashion. When the polarization plane coincides with the receiving dipole cd, the amplitude of the signal received by the antenna will be a maximum. However, if the dipole cd is perpendicular to the polarization plane, the amplitude is equal to zero. Thus the amplitude of the signal voltage at the antenna of the receiver is given by the following equation

$$u_m(t) = h_{eh} \; E \left|\cos \Omega t\right|, \tag{4.5}$$

where E is the field intensity produced by the transmitting antenna along the axis of the beam, and h_{eh} is the effected height of the receiving antenna.

If the missile is on the axis of the radio beam (fig. 4.6a), the rotation of the radiation pattern does not affect the field intensity E which in this case may be represented by E_0. If we expand the function (4.5) by means of Fourier series, we obtain the following expression

$$u_m(t) = h_{eh} \; E_0 \left[\frac{2}{\pi} + \frac{4}{\pi}\left(\frac{\cos 2\Omega t}{1\cdot 3} - \frac{\cos 4\Omega t}{1\cdot 3\cdot 5} + \dots\right)\right]. \tag{4.6}$$

As we can see from equation (4.6), the amplitude of the voltage at the antenna of the receiver contains a dc component and even harmonics at the frequency of rotation of the radar radiation pattern. Therefore, if there is a sufficient number of narrow bandpass filters in the amplifier of the receiver, the parasitic modulation does not produce a signal at the output of the receiver if the missile is on the axis of the radio beam.

If the missile deviates from the axis of the radio beam (fig. 4.6b), the rotation of the radiation pattern changes the value (modulus) of the field intensity E at the reception point

$$E = E_0[1 + k\varepsilon \cos(\Omega t + \mu)]. \tag{4.7}$$

Due to the modulation of the field intensity expressed by equation (4.7), we obtain a useful modulation of the signal with which we can determine the magnitude and direction of the angular deviation ε (or the corresponding value of h). However, when parasitic modulation is present, the resulting amplitude modulation of this voltage is determined from equations (4.6) and (4.7) and has the form /146

$$u_m(t) = h_{eh}\frac{2}{\pi}\left[1 + \frac{2}{3}\cos 2\Omega t - \frac{2}{15}\cos 4\Omega t + \dots\right] \times \\ \times [1 + k\varepsilon \cos(\Omega t + \mu)]. \tag{4.8}$$

After removing the brackets, we obtain

$$u_m(t) = \frac{2}{\pi} h_{eh}\left[1 + k\varepsilon \cos(\Omega t + \mu) + \frac{1}{3} k\varepsilon \cos(\Omega t - \mu) + \right. \\ \left. + \frac{2}{3}\cos 2\Omega t + \frac{1}{3} k\varepsilon \cos(3\Omega t + \mu) - \frac{2}{15}\cos 4\Omega t + \dots\right]. \tag{4.9}$$

The dc component and the higher harmonics may be filtered out, and two components will appear at the output of the receiver: the useful component $k\varepsilon \cos(\Omega t + \mu)$ and the parasitic component $1/3\, k\varepsilon \cos(\Omega t - \mu)$. The parasitic component distorts both the amplitude and the phase of the control signal.

The receiver in the missile may use an antenna with circular polarization. Let us consider how circular polarization is achieved by the application of two mutually perpendicular dipoles cd and c'd', whose axes are directed as shown in figure 4.7. When the dipoles are thus situated, the voltage picked up from

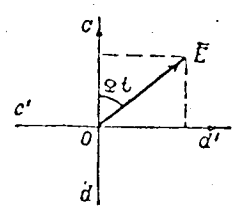

Figure 4.7. Distribution of receiving antenna dipoles.

them is displaced 90° in phase. The amplitude of the total voltage will not depend on the rotation of the receiving antenna's polarization plane, and the parasitic modulation due to this rotation will not take place. The received signal will be modulated only when the missile deviates from the beam axis; its amplitude is given by equation (4.2). Since the antenna is rigidly attached to the missile, when the missile moves with respect to the beam axis, the plane of the dipoles becomes nonperpendicular to the axis of the radio beam. When the plane of the dipoles is rotated, parasitic modulation again appears. The angle of rotation of the dipole plane usually does not exceed 30°-40°, and the distortion of the error signal caused by parasitic modulation turns out to be substantially less than in the case when we use an antenna consisting of one dipole. Therefore, the antennas of the missile receiver must have circular polarization when the missile is guided by the beam.

We can now compare the method of beam guidance with the method of homing guidance. The basic advantages of beam guidance are: /147

--long range, and

--relative simplicity. (The equipment aboard the missile is less complicated.)

We shall clarify our statement by considering figure 4.8. Since the transmitters illuminating the target are situated at the control point in both cases, in principle they may be identical. Thus the difference in the range is due to the fact that in radio beam guidance the signal reflected by the target is received by the control point, while in homing guidance it is received by the missile. The receiver at the control point may be made considerably more sensitive (by increasing the size of the antenna) and more efficient than the receiver in the missile. This situation remains true for a passive homing head when the target serves as a source of ultrashort radio waves. It is clear that in this case too the range of the beam guidance system can be much greater than the range of the homing guidance system. Finally, for active homing guidance the range of the head is small, because it is impossible to install a sufficiently powerful radar on the missile.

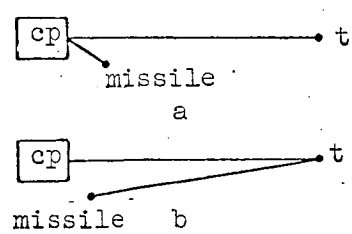

Figure 4.8. Schematic representation of radio beam guidance (a) and homing guidance (b).

The second advantage of a missile guided by a radio beam is obvious, since in this case the receiver on board the missile is less efficient and has less gain than the receiver in the homing head. This is true because the latter

receives weak reflections from the target, while the receiver in a missile guided by the radio beam receives a powerful signal from the control point. The principal disadvantages of a beam guidance system compared with the radar homing guidance systems are as follows:

--lower accuracy at long ranges between the control point and the missile and

--continuous participation of the control point in guidance of the missile.

As the range is increased, the presence of the angular error in the direction of the radio beam leads to an increase in the linear deviation of this axis from the center of the target. Another disadvantage becomes apparent when air-to-air missiles are tracked. The necessity of tracking the target by means of radar installed on the airplane limits the maneuvers of the airplane. During active homing guidance the control point does not participate in the tracking. In semi-active homing guidance the control point must only illuminate the target, which no longer limits the maneuvers of the airplane containing the receiver. /148

To utilize the positive properties of both methods, a combined system is sometimes used. In this system beam guidance is conducted over the initial section of the trajectory, and homing guidance is used when the target is approached by the missile.

Section 4.2. Command Guidance System

In the preceding section we considered beam guidance where the control signals were developed directly by the equipment aboard the missile, although a control point was present. Now let us consider methods of generating control signals in external guidance, when the control signals or the "commands" are developed at the control point and sent to the missile by means of a special communications channel.

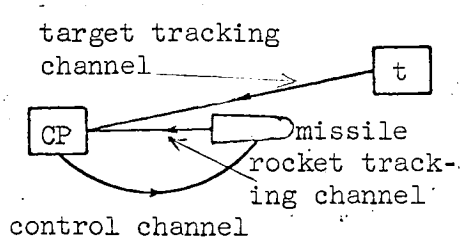

Figure 4.9. System for controlling relative position of missile with respect to target by equipment installed at control point.

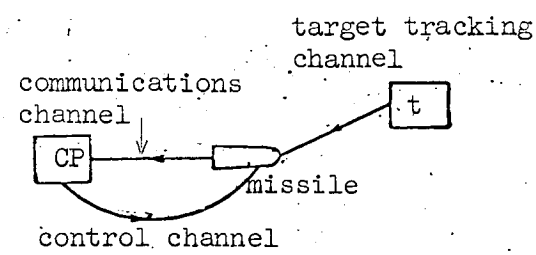

Figure 4.10. Control system for position of missile with respect to target by equipment aboard missile.

Two principal methods of controlling the missile with respect to the target may be used in developing command guidance systems:

--control by means of equipment installed at the control point (fig. 4.9), and

--control by means of equipment installed in the missile (fig. 4.10).

In systems of the first type an operator is usually used to track the position of the missile and the target and to develop control commands. As an example of the first system we consider the guidance of an aerial bomb by means of an optical bomb sight (fig. 4.11). The operator uses the bomb sight to observe the target and the missile continuously. The magnitude and direction of the deviation of the missile from the target is represented in the form of a segment which connects their images. The control commands are generated by the operator by turning the control lever and are transmitted to the missile. The operator who controls the missile tries to superpose the image of the target and of the missile. This method is called the method of "three points" because three points--the control point (operator), the missile and the target--in the ideal case are on one straight line at all times. Obviously this method of guidance cannot be considered automatic because the control loop uses an operator. /149

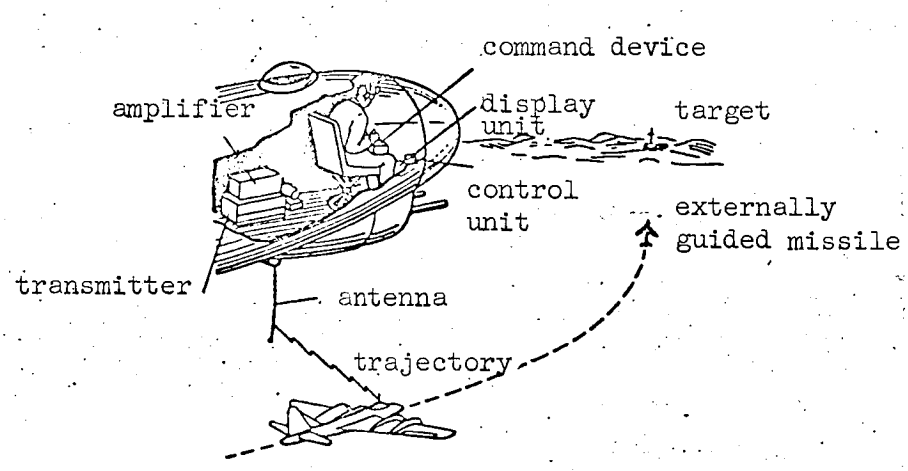

Figure 4.11. System of guiding missile H_s-293 by optical sight.

As an example of a system in which the control commands are formed automatically we can consider the system for the control of antiaircraft missiles (fig. 4.12). The coordinates of the target and of the missile are determined at the command point. From these data a computer develops a command which is transmitted to the missile over the radio channel.

The method of tracking the missile is somewhat different from the method of tracking the target, because the missile has special equipment facilitating this tracking. The systems for controlling the position of the missile may be passive, semiactive or active, depending on the location of the energy source.

Passive systems use the radiation of the missile (e.g., the radiation of the missile's engine) or the energy of a natural source (Sun) reflected by the missile. /150

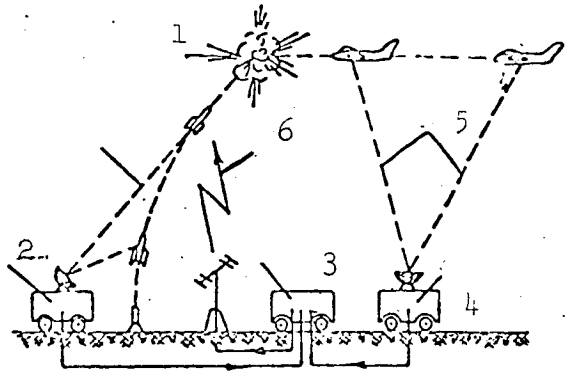

1--radar beam tracking missile; 2--missile tracking radar; 3--computer; 4--target tracking radar; 5--radar beam tracking target; 6--control command.

Figure 4.12. Functional diagram of system for guiding antiaircraft missiles.

A semiactive system utilizes the signal reflected by the missile.

Active systems utilize the energy of a radiator installed on the missile. In the visual control, the radiators are tracers installed in the tail of the missile. In radio control, the radiator is the transmitter installed on the missile and tracked from the control point. This disadvantage of the active system is that the missile is not camouflaged.

An example of this system in which the position of the missile with respect to the target is controlled by equipment contained in the missile is a control system which uses a television head or a radar set. The functional diagram of this system is shown in figure 4.13. The missile contains a television transmitter and the lens of the television camera obtains the image of the target. This image is transmitted over the communication channel to the control point, where it is reproduced on a television screen. The operator who observes the screen generates the control signals by manipulating control levers. These signals are transmitted back to the missile over the radio channel.

The presence of additional channels for transmitting information concerning the target and control signals substantially complicates the control system as a whole and decreases the resistance of the system to interference. /151
Thus this guidance system appears to be unsuccessful. However, the presence of a human operator in this system gives it new characteristics not available in fully automatic systems. The human operator utilizes his excellent visual perception as well as his ability to adapt himself to the behavior of the missile and may provide effective control over the system when automatic systems do not work. Conditions of this type arise, e.g., when the target exhibits very weak contrast on the background, when the image of the target disappears for a while and when there are many targets and it is necessary to select the most important one. Therefore, to utilize the valuable properties of a human operator in a missile control system, it is necessary to have a natural image of the target. Such an image can be obtained only by means of television equipment, because radar screens and direction finding stations represent the target in the form of a dot or of a spot of varying brightness.

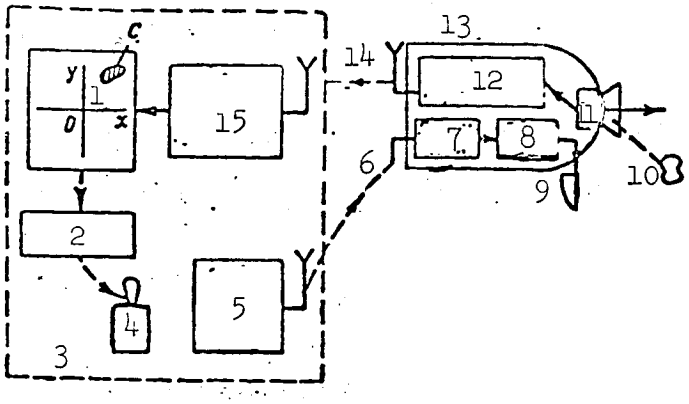

1--screen; 2--operator; 3--control point; 4--control lever; 5--radio transmitter; 6--control channel; 7--receiver; 8--automatic pilot; 9--control surface; 10--target; 11--TK; 12--TV transmitter; 13--missile; 14--communications channel; 15--TV receiver.

Figure 4.13. Missile guidance system using television head.

The disadvantages of using a human operator in a missile control system involve the necessity of expending a considerable amount of time and expense to train him, and also the fact that the performance of a human operator depends on his subjective characteristics.

The command guidance systems, regardless of whether they are completely automatic or contain a human operator, always have a communication channel to transmit control signals to the missile. For the sake of brevity, we shall call this channel the control channel. The schematic diagram of a control channel is shown in figure 4.14. The control commands which are developed by the command unit are coded and transmitted over the communication link to the missile. On the missile the received signals are decoded and transmitted to the control system on the missile. /152

The coding of the control signals increases:

--freedom from interference in the control channel, and

--the capacity of the link.

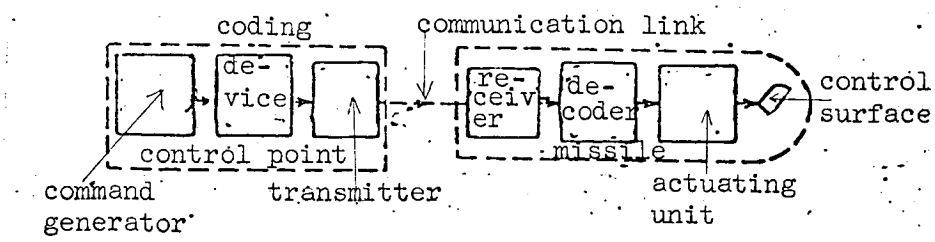

Figure 4.14. Schematic diagram of missile control channel.

To transmit the control commands, in principle it is possible to use a wire link or a radio link as well as infrared radiation and light radiation. The basic advantage of wire communication is its high resistance to interference.

However, when wires are used it is difficult to achieve reliability when the missile moves at high speeds, because the wires break. The resistance to interference of a radio link is much less than of a wire link, but the radius of action is substantially greater. Infrared radiation and invisible light radiation do not provide a sufficient range and, more important, they do not always provide reliable operation in every environment. Therefore, to date they have not been used for the guidance of missiles.

Let us consider in more detail, by means of examples, the technical realization of wire and radio communication links.

1. Wire Communication Links. The communication link consists of a steel wire of small diameter, which is unwound from a spool installed on the missile or at the control point or at the missile and the control point simultaneously. In the latter version the unwinding rate of the wire from each spool decreases, which reduces the probability of breakage.

It is rational to use a wire link for missiles which are guided from a stationary control point to mobile surface targets, because when a missile is guided from a mobile point (e.g., from an airplane) the probability of wire breakage increases. The range of a wire communication link does not exceed /153 several kilometers. Figure 4.15 shows the schematic diagram of an external guidance system with a wire communication link. The command-coding unit I consists of control lever 1 and two rollers 2 and 3, which are driven by a constant speed electric motor D. Roller 2 is fabricated from current conducting material and is divided by a dielectric material into two parts, fed with voltages from the opposite terminals of battery B by means of brushes br_1 and br_2. Brush br_3 is connected to the control lever and is displaced from its middle position along the generatrix of the roller, when the control lever is displaced from its average position (e.g., to the right or to the left). When brush br_3 is in the middle position, its period of contact with both halves of roller 2 during each of its revolutions is the same, and is equal to half the period of each revolution. Since the dielectric which separates roller 2 into two parts is situated at an angle with respect to its axis, when brush br_3 is displaced from its average position, its period of contact with each half of the roller becomes different. The generation of a command is produced by another roller 3 in a different plane. Roller 3 is also divided into two parts, one of which is made of a conducting material, while the other is made from a dielectric. A voltage from the middle point of supply battery B is fed to the current conducting part through brush br_5. Brush br_4 is connected to the control lever and is displaced from the middle position along the generatrix of the roller if the control level is moved forward or backward from the vertical. The plane separating the conducting and insulating part of roller 3 passes at an angle with respect to its axis. When brush br_4 is displaced, the period of time it spends on the conductive part of the roller and on the insulated part of the roller varies. Brush br_4 is connected with the middle point on battery B through a resistance /154 r_1. The control signals picked up by brushes br_3 and br_4 are fed to the wire transmission link II.

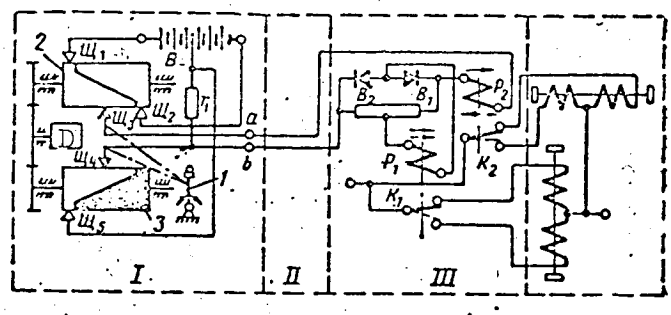

Figure 4.15. Schematic diagram of the H_s-293 missile guidance system utilizing wires; (Щ = br).

The command decoding unit III in the missile consists of polarized relays R_1 and R_2 and a bridge with rectifiers D_1 and D_2. Relay R_2 is a three-position relay, and its contact k_2 is in the middle position when the wire is dead. The deflection of the contact into one of the extreme positions depends on the direction of the current in the winding. Thus, relay R_2 reacts to the polarity of the signal. Relay R_1 is a two-position relay and its contact k_1 is in the lower position, if the relay winding is dead or if the magnitude of the current is below the value necessary to close the relay. The presence of a bridge rectifier scheme makes it possible to obtain a dc current in the winding of relay R_1 which does not depend on the polarity of the current in the communication link. Consequently relay R_1 reacts to the amplitude of a signal.

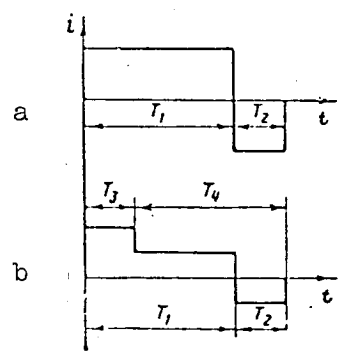

Figure 4.16. Current diagrams in wire communication link.

Let us determine the form of the signals which enter the communication line. Let us designate by T_1 and T_2 the periods of time which brush br_3 spends on the halves of roller 2 and designate by T_3 and T_4 the period of time which brush br_4

spends on the halves of roller 3. In this case the following expression is valid

$$T_1 + T_2 = T_3 + T_4 = T, \tag{4.10}$$

where T is the period of rotation of rollers 2 and 3.

Each of the intervals of time T_1, T_2, T_3 and T_4 may vary from zero to T. During the interval of time T_1 brush br_3 is connected to the negative terminal, while during the interval of time T_2 it is connected to the positive terminal of battery B. Brush br_4, during the interval of time T_3, is connected to the middle point of battery B directly, and during the interval of time T_4 it is connected through resistance r_1.

Figure 4.16 shows the currents in the communication link (the position of brushes br_3 and br_4 is arbitrary). Let us explain this figure. Initially we shall assume that roller 3 is fixed (fig. 4.15). Then the current in the line will have the form shown in figure 4.16a. The polarity of the current changes in accordance with the position of brush br_3 on the roller generatrix. If we neglect the delay in the operation of relay R_2, it will also close and open its contacts as shown schematically in figure 4.16a. During each period of rotation of roller 3 (figs. 4.15 and 4.16), an additional resistance r_1 will be switched into the signal current circuit for a period of time T_4 and will decrease this current. During the interval of time T_3 there will be no variations in the signal current. Thus the signal current assumes the form shown in figure 4.16b. /155
Since relay R_1 reacts only to current amplitude (regardless of its polarity), this relay will close during intervals T_3 and will be released during intervals T_4.

Let us introduce the concept of the command coefficient to designate the average value of the reaction produced by relay R_1 and R_2 on the subsequent members of the equipment aboard the missile. It is obvious that the command coefficient in this sense is characterized by the equations

$$K_1 = \frac{T_3 - T_4}{T_3 + T_4}, \tag{4.11}$$

$$K_2 = \frac{T_1 - T_2}{T_1 + T_2}. \tag{4.12}$$

The graph for command coefficients K_1 and K_2 as a function of the angular displacement of the control lever from its vertical position is shown in figure 4.17.

In the diagram of the external guidance system shown in figure 4.15, relays R_1 and R_2 of the decoder react on the electromagnetic spoilers which control the rotation of the missile in two planes. If the time required for the electromagnets to operate is neglected, their deviations in one plane will be determined by T_1 and T_2 while, in the other plane, they will be determined by T_3 and T_4. Consequently, the command coefficients K_1 and K_2 will characterize the average value of the control forces applied to the missile in the firing plane (up, down), and in a plane perpendicular to it (right, left).

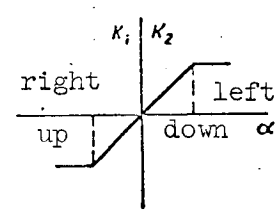

Figure 4.17. Graph of command coefficients K_1 and K_2 as function of angular deviation of control lever from its vertical position.

2. Radio Communication Link. Radio communication may be carried out at any wavelength. The factor to be considered is that when the wavelength decreases, the antenna size becomes small.

As an example of a radio transmission link for commands we shall describe briefly a scheme whose principle of operation is analogous to that of the wire communication link previously described. The schematic diagram of the equipment at the control point is shown in figure 4.18. The control commands are formed in a command device which contains two rollers driven by a motor, a lever for displacing the brushes along the generatrixes of the rollers, a modulator which contains an audiogenerator of frequencies f_1, f_2, f_3 and f_4 and a trans- /156 mitter with an antenna. The audio-frequency voltages of the modulator are fed through the brushes br_1, br_2, br_3 and br_4 to the half-rollers, and at each instant of time two of these voltages act on the transmitter modulating the carrier frequency. Aboard the missile there is a receiver with an antenna, a decoder and an amplifier.

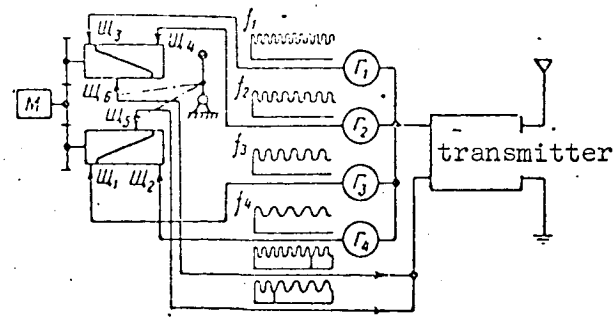

Щ = brush; M = motor.

Figure 4.18. Schematic representation of equipment at control point used to guide missile H_2-293.

The decoder consists of a system of resonant circuits which are used to select the voltages of the modulating frequencies f_1 and f_2 in one channel and f_3 and f_4 in the other channel. After rectification and amplification, the output of both channels of the decoder produce a succession of polar pulses shown in figure 4.19. The intervals of time T_1, T_2, T_3 and T_4 which characterize these successions are determined by the magnitude and direction of deviation from the vertical position of the control lever in two perpendicular planes. The average value of the voltage at the output of each channel is determined by the command coefficients which are known from equations (4.11) and (4.12). Later these voltages may be fed to the subsequent elements of the control system, either directly or after they are smoothed out by an appropriate filter.

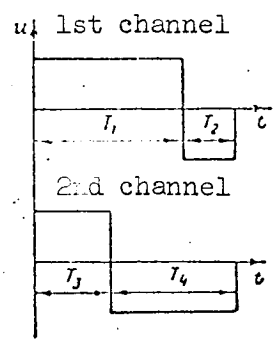

Figure 4.19. Diagram of voltages at output of decoder, which control missile.

Section 4.3. Radar Stations for Detecting Aerial Targets

Radar stations which detect aerial targets as a rule are stations with circular scanning. Chapter 14 considers one of the methods for realizing the external guidance, in which information on the coordinates of the target and of the /157

missile is obtained by means of radar stations with circular scanning. In this section we consider the different principles for measuring the coordinates of the target by means of radar stations. Obviously the same principles may be used to detect the coordinates of the missile.[1]

Stations for detecting the position of the target in space usually utilize a spherical system of coordinates. In this system the coordinates are the inclined range L, azimuth φ and the elevation ε (fig. 4.20). The region of space which is examined by the radar station is characterized by the detection range of the target, the bearing sector and the elevation sector. The aperture angle of the radiation pattern of the radar station is substantially less than the scanning sector in the corresponding plane. Therefore, to detect a target, the radiation pattern of the station must be displaced within the limits of the given region of space. This displacement of the radiation pattern which is subject to a definite law is called the radar scan of space.

The scanning systems must have the following properties:

(1) the targets must not be missed during scanning, in other words, every point inside a given region must be illuminated;

(2) minimum duration for scanning a given region; when scanning is of long duration the target may have time to move a substantial distance between successive scans and data concerning its position may become quite inaccurate;

(3) for each illumination of the target the number of pulses which hit the target must not be less than a certain minimum to make the detection of the target reliable;

(4) the necessary accuracy for determining the coordinates of the detected target.

Radar stations may operate as search stations or may automatically track the target or the missile. Information on the detection of targets during search is /158 transmitted to the display unit of the station, where two coordinates of the target (usually range and azimuth) are reproduced on a cathode-ray tube. The third coordinate is reproduced on the screen of a second tube. During automatic tracking the equisignal zone of the station's antenna is directed towards the target by means of a servosystem. As a result, the position of the antenna determines the magnitude of the azimuth and of elevation.

We shall consider briefly the principle of measuring the coordinates. The pulse method is usually used to determine the range to the target. The radar transmitter generates short pulses of high frequency, called main pulses. During the quiescent intervals between these pulses, the weak reflected signals are received. The distribution of pulses in time is shown in figure 4.21. The time between pulses T is known as the repetition rate of the pulses. The range is determined by Δt--the time between the transmission of the main pulse and the reception of the reflected pulse. During time Δt the main pulse and the reflected

[1] B. M. Stepanov, Radar Survey, Voyenizdat, 1959.

pulse must cover the distance to the target (range L), which is given by equation

$$L = \frac{c}{2}\Delta t, \tag{4.13}$$

where c is the propagation velocity of radio waves--velocity of light, approximately equal to 300,000 km/sec.

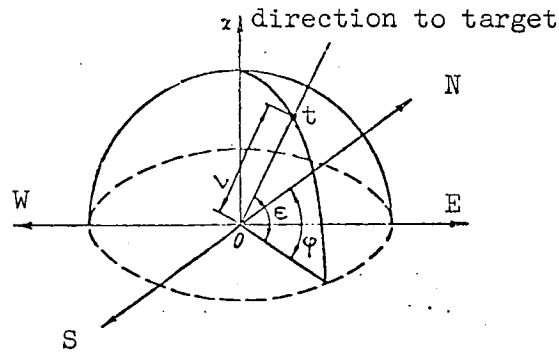

Figure 4.20. Spherical system of coordinates of target.

One disadvantage of the pulse method is the impossibility of detecting and determining the range of objects closer to the radar station than $L = c\tau/2$, because in this case the reflected pulse arrives when the radiation of the main pulse has not ended. The pulse method provides an accurate determination of the range. The average error in a pulse range finder reaches a value of several meters, and this accuracy is retained for target ranges of tens of kilometers (40-60 km).

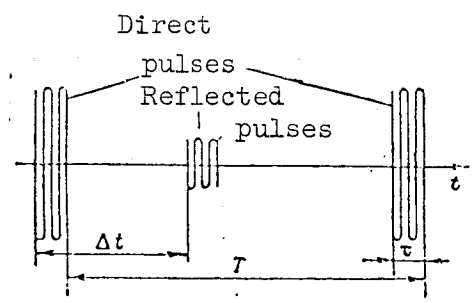

Figure 4.21. Direct and reflected pulses of radar station.

To determine bearing and elevation the directional properties of the antenna are utilized. In this case, to determine the bearing the antenna system must have sharply defined directional properties in the horizontal plane, and to determine the elevation it must have these properties in the vertical plane. When one antenna is used, it is common to use the maximum of the reflected signal. Figure 4.22 shows the radiation pattern of an antenna in one plane and the envelope of the pulse amplitude reflected by the target. When the antenna is rotated, the radiation pattern passes through the target. When the radiation /159

pattern is symmetric, the line O target will be the energy center of the point of pulses. If the received signals are displayed, the pulse with the maximum amplitude will correspond to a spot with maximum brightness. The operator tries to direct the antenna in such a way that a spot of maximum brightness appears on the display tube. The greater the curvature of the radiation pattern, the higher is the accuracy in determining the direction to the target. The direction to the target may also be obtained by rotating the antenna with a constant velocity. It is clear that the pulses reflected from the target will form luminous spots. Since the frequency of pulses is very high, the spots blend together and form an arc. The center of the arc corresponds to the direction to the target. In some cases, the direction to the target is determined by means of two antennas with a narrow radiation pattern (fig. 4.23). In this case the direction to the target is determined by varying the position of the radiation pattern in the vertical plane to achieve a minimum amplitude for the reflected signal (in this case the minimum of the radiation pattern is directed towards the target), and by measuring the elevation.

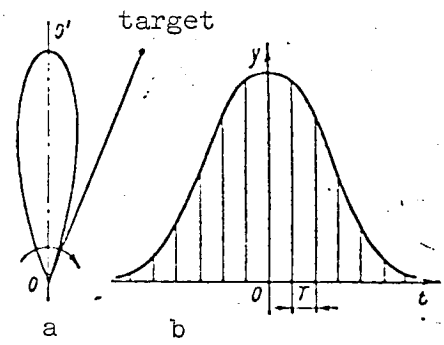

Figure 4.22. Radiation pattern of antenna (a) and envelope of reflected signal amplitudes (b).

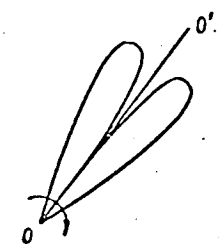

Figure 4.23. Radiation pattern with sharply defined minimum.

V-beam radiation patterns (fig. 4.24), which have a complex form, are most commonly used to determine the azimuth and the elevation. The pattern consists of two plane lobes, one of which is vertical and the second is at some angle to it. The width of the lobes in the horizontal plane is made as small as possible (0.5 - 2.0°). The aximuth of the target is determined by the vertical lobe from the maximum amplitude of the reflected signal. Both lobes are used to measure the elevation. The greater the elevation of target ϵ, the greater is the distance /160

tt' and the angle ρ. Consequently, as the altitude increases, the interval of time between the maxima of the reflected signal amplitudes also increases. If we know angle ρ and inclined range L, we can determine the altitude of target (t). In accordance with the geometry shown in figure 4.24, we obtain

$$H = tt' \operatorname{tg} \mu; \tag{4.14}$$

$$tt' = BA = L \cos \epsilon \sin \rho; \tag{4.15}$$

$$L \cos \epsilon = \sqrt{L^2 - H^2}, \tag{4.16}$$

where μ is the flare of the radiation pattern.

After transformation we obtain

$$H = L \frac{\sin \rho \operatorname{tg} \mu}{\sqrt{1 + \sin^2 \rho \operatorname{tg}^2 \mu}}. \tag{4.17}$$

When the flare is $\mu = 45^\circ$ we have

$$H = L \frac{\sin \rho}{\sqrt{1 + \sin^2 \rho}}. \tag{4.18}$$

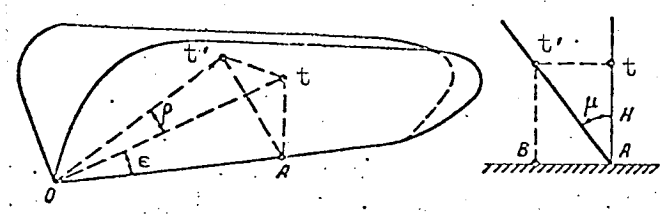

Figure 4.24. V-beam radiation pattern.

The coordinates of the target are determined with the highest accuracy when the principle of the equisignal zone is utilized. The principle of obtaining signals proportional to the angles of deviation of the equisignal zone from the line joining the radar station and the target is analogous to the principle of obtaining a control signal in the radar homing heads (sec. 3.5). The average error in the angular coordinates of the target varies in the limits 0.2' - 7.2'. The principle of the equisignal zone is used in automatic tracking. Figure /161
4.25 shows the diagram of an automatic tracking system. One of the operating characteristics of a radar station is the magnitude of space in which the target can be detected and the principle of scanning this space.

The scanning period of a radar station (T_{scan}) is the interval of time between two successive passages of the radiation pattern through the same point in space. Space may be scanned by using any complex trajectory (fig. 4.26). The maximum angle between the adjoining elements of the trajectory of the radiation pattern is known as its pitch (ξ). The radiation pattern must be displaced with a definite angular velocity Ω so that all given space is scanned in a given period of time. Thus, angle Δ will be scanned during the period

$$t = \frac{\Delta}{\Omega} \text{ (sec)}. \tag{4.19}$$

Illumination time (T_{ill}) is the time during which the target is within the limits of the radiation pattern. The illumination time is equal to

$$T_{ill} = \frac{\Phi}{\Omega}, \tag{4.20}$$

where Φ is the flare of the radiation pattern.

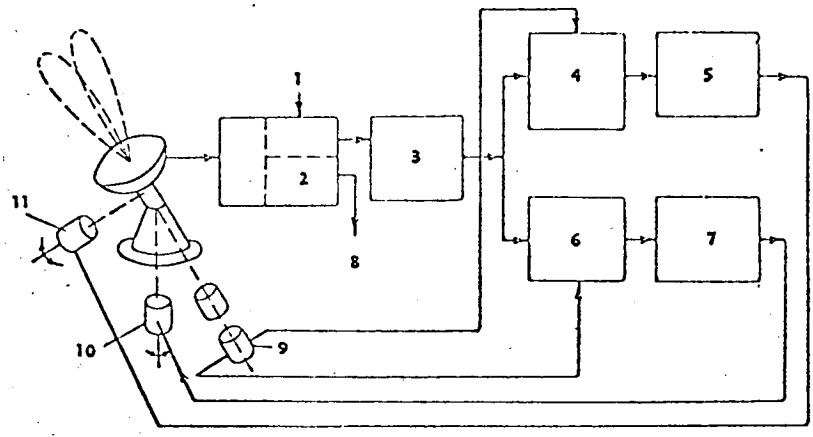

Figure 4.25. Functional diagram of automatic tracking system. 1--strobing pulses; 2--range channel; 3--amplifier and detector; 4--synchronous detector for elevation; 5--servosystem for elevation; 6--synchronous detector for azimuth; 7--servosystem for azimuth; 8--to range tube; 9--generator of reference voltages; 10--azimuth motor; 11--elevation motor.

During time T_{ill} n pulses are reflected by the target. For reliable detection of the target, minimum number of pulses must not be less than $n_{min} \approx$ 5-6. Several reflected pulses are required because the background noise of the receiver may mask a single weak reflected pulse. If, however, during each illumination of the target several reflected pulses with approximately constant amplitude are received, and the time of their arrival corresponds to the position of the electron beam at the same point on the display tube, their integrated action will produce a much brighter spot than noise. If the position of the target is determined automatically rather than visually, it is possible to decrease n_{min} to 1-2, and the scanning period can be decreased (to increase angular velocity Ω).

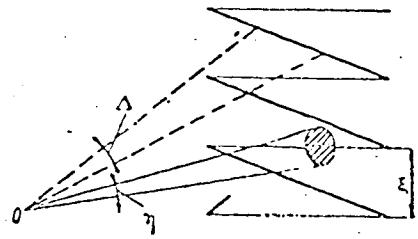

Figure 4.26. Schematic diagram of zig-zag scanning.

The scanning period is determined on the basis of tactical requirements. Since the radar station is used to detect mobile targets, the target must not move a great distance during one scanning period, otherwise the spot on the display tube will appear to jump. When the spot jumps the conditions for observing the targets deteriorate, there is a decrease in the accuracy of the coordinates and the orientation of operators becomes difficult.

The evaluation of the maximum allowable scanning period is made by means of equation

$$T_{scan} \leq k \frac{Q}{V_{max}}, \tag{4.21}$$

where Q is the linear dimension of the spot showing the target (scale); V_{max} is the maximum velocity of the target, and k is a coefficient which varies from 1/3 to 3, depending on the tactical mission of the radar station.

The minimum scanning period is a function of the dimensions of the scanned region, the flare of the radiation pattern of the antenna and the minimum number of pulses necessary for a clear detection of the target

$$(T_{scan})_{min} = \frac{n_{min} T \Delta_\varepsilon \Delta_\varphi}{\eta_\varepsilon \eta_\varphi}, \tag{4.22}$$

where T is the repetition period of the pulses; Δ_ε, Δ_φ are the angular dimensions /163
of the region in terms of its elevation and bearing, and η_ε, η_φ are the angular dimensions of the radiation pattern of the antenna in elevation and bearing.

The pulse repetition period is determined by the maximum range of the radar station

$$T = k \frac{2L_{max}}{c}, \tag{4.23}$$

where k is a factor of safety approximately equal to 1.25.

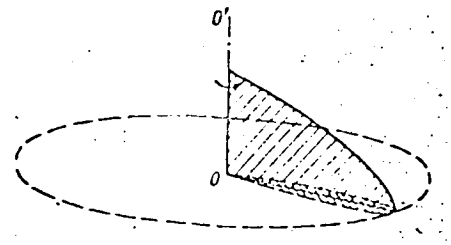

Figure 4.27. Schematic diagram of circular scanning.

Substituting the value of T into equation (4.22) we obtain

$$(T_{scan})_{min} = 2.5 \frac{n_{min} L_{max} \Delta_\varepsilon \Delta_\varphi}{\eta_\varepsilon \eta_\varphi}. \qquad (4.24)$$

The theoretical minimum scanning period is obtained from equation (4.24). However, during scanning some points in the scanning region are illuminated during two positions of the radiation pattern (fig. 4.26), and it is necessary to increase the value for the scanning time $(T_{scan})_{min}$ slightly. As we have pointed out, there are several methods of scanning space, and these are determined by the movement of the antenna radiation pattern. The simplest of all these scanning forms is circular scanning, which is most common in the guidance of missile. In circular scanning the plane radiation pattern rotates around a vertical axis (fig. 4.27). This provides for high accuracy in determining range and bearing. When the V-type radiation pattern is used, the elevation is also determined (fig. 4.24). A particular case of circular scanning is sector scanning--the scanning of part of the circumference by plane radiation patterns.

When a needle-like radiation pattern is used (symmetric with respect to the direction of maximum radiation), scanning is of the zig-zag, screw, spiral, combined rectilinear-conic and conic types. In these cases the radiation pattern undergoes complex motion. Of all these scanning methods the one of particular /164 significance for missile guidance is conic scanning. In conic scanning of a narrow sector an equisignal zone is formed which is used in the systems of homing guidance, beam guidance and automatic target tracking.

Section 4.4. Missile Guidance Using the Methods of Radio Navigation

Various radio navigation systems are used for airplanes. In the simplest case these systems make it possible to carry out the flight to and from a radio beacon and, in combination with a radio range finder, to determine the distance to the beacon continuously. There are also systems which can determine the bearing of an airplane with respect to the beacon. By finding the direction of two beacons from an airplane or, conversely, by finding the direction of an

transceiver which interrogates, while stations A and B have transceivers operating as responders. The transmitter on the missile transmits a pulse, which is received by stations A and B. These stations in turn send back pulses, which are received by the missile. The missile must move towards the target along one of the hyperbolas determined by the assigned values for the time interval between the reception of pulses from stations A and B. By measuring this interval

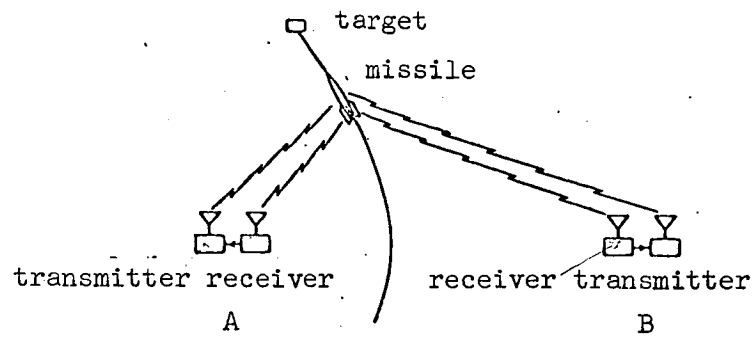

Figure 4.29. Schematic diagram of hyperbolic navigation system for guidance of missiles.

at the missile we can obtain a control signal, where this interval is greater or less than the given interval. This signal, when fed to the control system, provides for the return of the missile to the given trajectory. The system makes it possible to have the missile move along a preselected hyperbola passing through the target. The flight altitude is kept constant, and the sensor for stabilizing the flight altitude may be some type of an altimeter. /166

To determine the time when the missile is above the target, a second pair of stations may be used, which forms a family of hyperbolas for determining the range. To increase the accuracy in range determination it is desirable that the family of range hyperbolas in the region of the target intersect with the family of course hyperbolas at angles close to right angles. When a missile reaches a given range hyperbola which passes through the target, the homing guidance system is turned on (if it is used) or the missile is placed into a dive towards the target.

Another method in measuring the range consists of determining the time at the missile between the transmission of a pulse by the missile and the arrival of the responding pulse from one of the stations (A or B). In this way the distance to the station is determined. When this distance achieves a given value, the missile is placed into a dive towards the target. The latter method may be used to guide the missile by the method of circular navigation shown in figure 4.30. In this case only one station is used to assign a trajectory. If the time between transmission and reception of the responder pulse at the missile is constant, it will move along a circle with station A at the center. This time is assigned in such a way that the trajectory of the missile (the /167

airplane by means of two ground stations with subsequent transmission of the results to the airplane, we can determine the position of the airplane with respect to the Earth's surface. Finally, there is an ever-increasing application of hyperbolic radio navigation systems which can determine the position of the airplane by measuring the time intervals between the arrival of signals from two radio stations transmitting pulses.[1]

All of these systems of radio navigation do not determine the flight altitude of the airplane; this must be determined by an independent barometric device or by a radio altimeter. In guiding missiles by the method of external guidance, it is possible, in principle, to utilize the same radio navigation means, provided the information on the position of the missile with respect to the ground is recorded automatically.

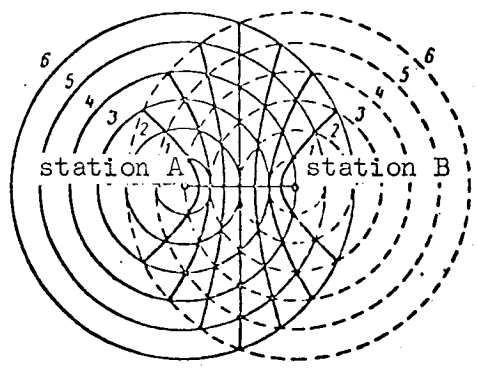

Figure 4.28. Generation of a family of hyperbolas. 1-6, circles of equal ranges.

As an example, let us consider in more detail the principle of obtaining guidance signals by utilizing the hyperbolic system of radio navigation. Figure 4.28 clarifies the principle used to form a family of hyperbolas by two radio stations A and B radiating short pulses of high frequency electromagnetic energy. The circles with the station at the center represent the geometric position of points to which the propagation time of the pulse from the station is the same. If two stations generate pulses simultaneously, and if the latter are received at some point simultaneously, this point is at an equal distance from both stations. If along some curve the time between reception of pulses from stations A and B is the same, then, due to the constant velocity of radio wave propagation, the difference in the distances to both stations is also constant at any point on this curve. It is easy to see that this curve is a hyperbola with its focuses at points A and B.

One of the possible methods of obtaining a hyperbolic navigation system for guiding missiles is clarified in figure 4.29. The missile is equipped with a

[1] A. S. Lokk, Guided Missiles, Gostekhizdat, 1957.

transceiver which interrogates, while stations A and B have transceivers operating as responders. The transmitter on the missile transmits a pulse, which is received by stations A and B. These stations in turn send back pulses, which are received by the missile. The missile must move towards the target along one of the hyperbolas determined by the assigned values for the time interval between the reception of pulses from stations A and B. By measuring this interval

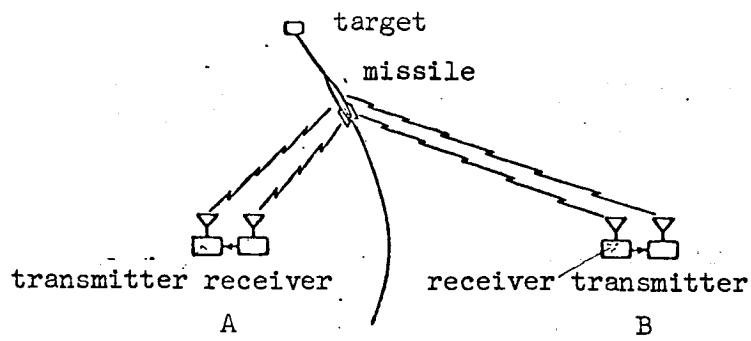

Figure 4.29. Schematic diagram of hyperbolic navigation system for guidance of missiles.

at the missile we can obtain a control signal, where this interval is greater or less than the given interval. This signal, when fed to the control system, provides for the return of the missile to the given trajectory. The system makes it possible to have the missile move along a preselected hyperbola passing through the target. The flight altitude is kept constant, and the sensor for stabilizing the flight altitude may be some type of an altimeter. /166

To determine the time when the missile is above the target, a second pair of stations may be used, which forms a family of hyperbolas for determining the range. To increase the accuracy in range determination it is desirable that the family of range hyperbolas in the region of the target intersect with the family of course hyperbolas at angles close to right angles. When a missile reaches a given range hyperbola which passes through the target, the homing guidance system is turned on (if it is used) or the missile is placed into a dive towards the target.

Another method in measuring the range consists of determining the time at the missile between the transmission of a pulse by the missile and the arrival of the responding pulse from one of the stations (A or B). In this way the distance to the station is determined. When this distance achieves a given value, the missile is placed into a dive towards the target. The latter method may be used to guide the missile by the method of circular navigation shown in figure 4.30. In this case only one station is used to assign a trajectory. If the time between transmission and reception of the responder pulse at the missile is constant, it will move along a circle with station A at the center. This time is assigned in such a way that the trajectory of the missile (the /167

circle) passes through the target. When the stated interval of time deviates from the assigned value, a signal is generated which is fed to the control system and returns the missile to the assigned circle. Station B in this case is used to determine the position of the missile along the circular trajectory by measuring the time that it takes for pulses from the station to arrive at the missile. When a given point is achieved on the circular orbit, the missile is placed into a dive.

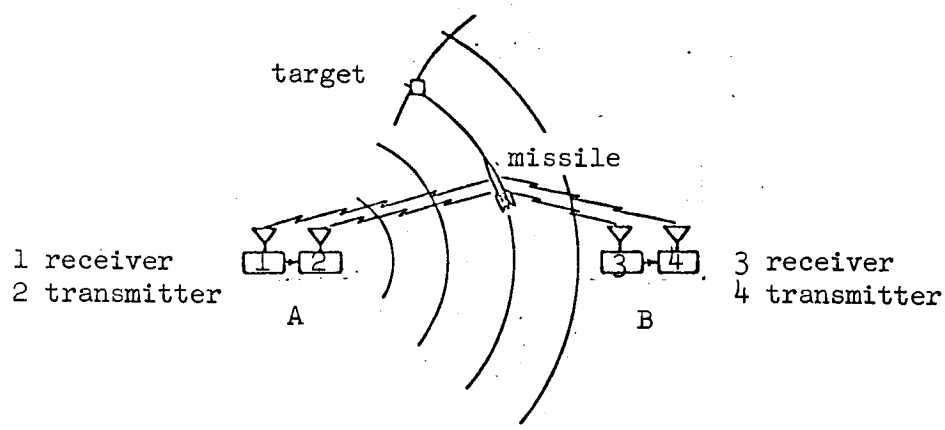

Figure 4.30. Schematic diagram of circular navigation system for missile guidance.

The range of hyperbolic and circular navigation systems depends on the frequency used in transmitting the pulses. When ultrashort waves are used, this distance is limited by the line of sight propagation of these waves and depends on the flight altitude of the missile. When medium waves and long waves are used, the range is several thousands of km.

The advantage of using hyperbolic and circular navigation systems for guiding missiles is the possibility of using one pair of stations to control many missiles launched from the most diverse launching pads scattered over a large area. After launching, the missile follows a programed trajectory until it reaches the zone of a given hyperbola, after which the control system, which depends on the radio navigation system, is turned on. The accuracy of hyperbolic navigation systems is high.

CHAPTER 5. CONTROL SIGNALS IN SELF-CONTAINED GUIDANCE /168

Section 5.1. General Information

The control signals which are used in a self-contained guidance system depend on the type of missile. Thus, for example, the ballistic rocket must move over a given trajectory during the active portion of its flight. The active portion of this trajectory in the vertical plane, as provided by the programing unit, is shown in figure 5.1a. In practice the programing units do not assign a trajectory, but rather the direction of the rocket's longitudinal axis as a function of time. As the rocket flies, the action of various external perturbations (wind, dissymmetry of aerodynamic forces, etc.) may cause its trajectory to deviate from the assigned one. Therefore, the rocket control system must provide for a comparison of the true position of the mass center with the assigned position and to generate a control signal when there is a discrepancy between the two.

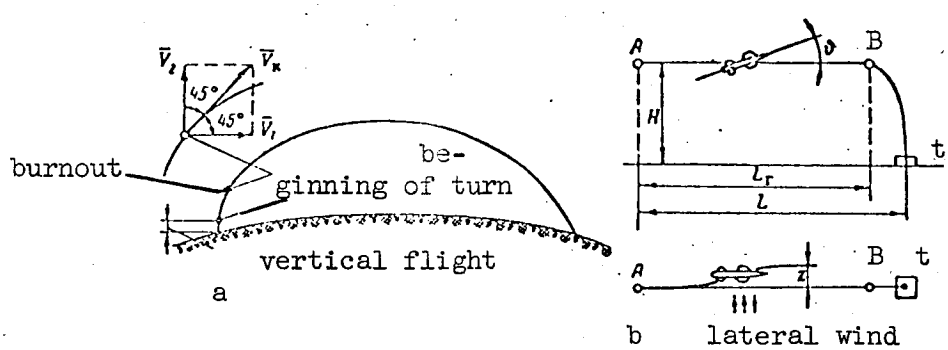

Figure 5.1. Forms of programed trajectories.

The rocket may deviate from the firing plane assigned to it. Consequently it is necessary to measure and eliminate the lateral deviations of the rocket from this plane. Finally, when the rocket has reached a certain speed, its engine must be turned off by the control system which continuously compares the true value of the velocity with the given computed value. /169

In the self-contained guidance of airplane-missiles, the composition of the control signals depends on the range of the missile. Airplane-missiles of short range have a rectilinear trajectory which is sometimes subdivided into regions of different altitude. Here we again have the problem of measuring the direction of the longitudinal axis of the missile as well as its flight altitude. To

place the missile into a dive towards the target, it is necessary to measure its flight range.

Airplane-missiles which fly over a short distance have a rectilinear horizontal trajectory. In order that the rectilinear trajectory pass at a certain altitude (fig. 5.1b), it is necessary to measure the position of the longitudinal axis and the actual flight altitude of the missile. The flight range may be assigned by the flight time, in which case the missile must contain a time sensor. As the flight range is increased, the guidance error increases because the program assigned at the launching site does not take into account the random variations in the state of the atmosphere over the entire flight trajectory. In addition to measuring the position of the longitudinal axis of the missile, it is also necessary to determine the altitude, the lateral displacement and the range.

Guidance systems must provide for good dynamic characteristics of the missiles and, therefore, require the introduction of signals which are proportional, not only to the angular and linear coordinates of the missile, but also to the first and sometimes to the second derivatives of these coordinates. Thus, we are faced with the problem of measuring the angular and linear velocities and accelerations of the missile with respect to its three axes.

When missiles with self-contained guidance fly over a long range, we are faced with the problem of continuously sampling or measuring their coordinates with respect to the ground. Then we can determine the position of the missile with respect to the target with coordinates assigned on the missile.

From experience in the navigation of piloted airplanes means were developed for determining the position of the aircraft with respect to the Earth's surface. Based on the geographic charts developed from study of the Earth's motion with respect to heavenly bodies, terrestrial and astronomical coordinates and reference systems have been established for use in navigation.

To increase the accuracy of missile guidance, inertial-gyro systems are used by which we can determine the position of the missile with respect to the ground. These systems must contain accelerometers which measure the acceleration of the missile's center of gravity with respect to the Earth; for this purpose they are mounted on a platform stabilized in space.

In subsequent sections we shall consider devices and systems used in missiles with self-contained guidance systems. Some of these devices are also used in homing guidance and external guidance systems. /170

Section 5.2. Sensors for Measuring the Angular Position of the Missile's Axes

An astatic gyroscope with three degrees of freedom (fig. 5.2) is used to determine the angles which are formed by the axes fixed with respect to the missile and the axes of the "stationary" system of coordinates. The center of gravity of the astatic gyroscope's rotor coincides with the center of gravity of

the suspension which eliminates the moments of force produced by gravity. The variation in the position of the gyroscope's rotor takes place only as a result of friction in the suspension axes and due to some residual unbalance in the rotor. The rate of variation in the position of the gyroscope's rotor is small, when it has the proper kinetic moment. Therefore, in cases when it is necessary to establish a definite direction during a short period of time (up to 2-3 min), it is quite feasible to use an astatic gyroscope for these purposes. An astatic gyroscope may be installed in any position; it may be used for short term determination of any direction with respect to a fixed system of coordinates. The astatic gyroscope must be present in the required direction, since the gyroscope itself does not establish this direction.

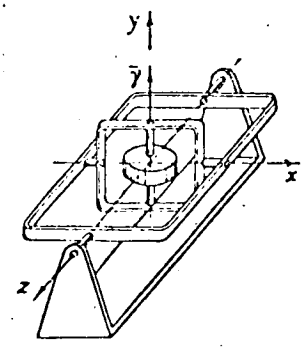

Figure 5.2. Astatic gyroscope.

The sensors which produce angular displacement signals may be potentiometers fixed to the frame of the gyroscope. The brushes are attached on the axis of the respective gyroscope frame. A gyroscope with three degrees of freedom may be assumed, with a sufficient degree of accuracy, to be an element without inertia. The transfer function of such an element has the form

$$W(p) = \frac{u}{\vartheta} = k, \tag{5.1}$$

where u is the voltage picked up from the potentiometer, and ϑ is the angle of rotation of the missile's axis.

If the operation of the gyroscope is sufficiently prolonged, or if the effect of friction on the suspension axes is such that it produces a substantial precession and, consequently a noticeable change in the position of the gyroscope's axes, the gyroscope is compensated. The compensation of a gyroscope is most frequently achieved by means of two independent systems, each of which is designed for a specific suspension frame. It is possible to compensate for the position of only one suspension frame when it changes its position more rapidly or when it is loaded more. /171

The functional diagram of a compensation scheme for maintaining the perpendicular position of a gyroscope's frames is shown in figure 5.3. The relation between the signal sensor and a moment sensor in each compensating system is crossed, i.e., the compensation of the first frame is achieved by applying

a moment to the second frame. Compensation may be achieved by a linear (proportional) system or by a nonlinear system.

The sensors used in navigational systems are integrating floating gyroscopes which provide accuracy of measurements and increased resistance to vibration and to shocks.

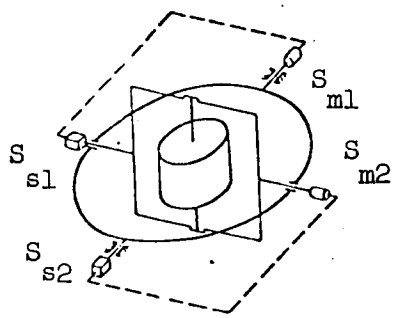

Figure 5.3. Functional diagram showing gyroscope compensation. S_{s1}, S_{s2}--signal sensors of compensating system; S_{m1}, S_{m2}--moment sensors of the compensating system; subscript "1" refers to first (internal) and subscript "2" refers to the second (external) suspension frame.

The frame of the device is filled with a heavy liquid. The volume of the frame and the specific weight of the liquid are selected in such a way that the buoyancy force of the liquid is equal to the weight of the gyro assembly and, in practice, completely unloads its bearings. The small load on the bearings produces a decrease in the friction moment to a negligible value and avoids transmission of shocks and vibrations. The center of gravity of the gyro assembly and the center of pressure of the liquid must coincide to prevent the occurrence of an unbalancing moment. Damping is achieved by friction between the cylindrical surface of the gyro assembly's case and the thin layer of viscous fluid which occupies the small gap between the cylindrical surfaces of the gyro assembly's case and the case of the device. With this type of damping, there is no dry friction. The size of the gap between the case of a floating gyro and the case of the device is selected so that for all angular velocities (encountered during operation) of the floating gyro assembly with respect to the case of the device, the damping moment is strictly proportional to the turning rate of the floating gyro assembly. The device is placed in a chamber of constant temperature. Constant temperature is required, first, to preserve the constant viscosity of the liquid and, consequently, a constant coefficient of the damping moment, secondly, to maintain a constant specific weight of the liquid and, finally, to preserve the stationary position of the liquid's center of pressure with respect to the axis of rotation of the gyro assembly. /172

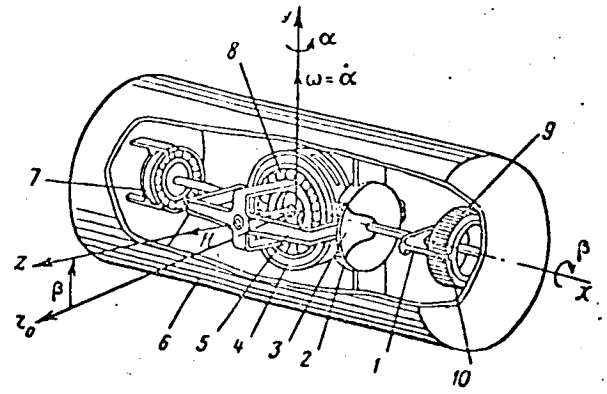

Figure 5.4. Simplified drawing of integrating gyroscope. 1--brushes of the potentiometer; 2--case of the damper (rigidly attached to the case of the gyroscope); 3--the damper disk (rigidly attached to frame of gyroscope); 4--the gyroscope rotor; 5--gyroscope frame; 6--gyroscope case; 7--exciter; 8--stator of gyro motor; 9--potentiometer; 10--center tap on potentiometer.

Figure 5.4 shows a simplified scheme of an integrating gyroscope. Here β designates the deviation angle of the frame (of the gyroscope axis z) from its initial position (z_0 axis), and α is the angle of rotation of the gyroscope's frame about its measurement (input) axis y. We shall show that the angle of rotation of the frame β is proportional to angle α. When the frame rotates around the y axis with angular velocity ω, a gyroscopic moment is produced causing the frame to rotate. The rotation of the frame is prevented by the moment produced by the damper. When the frame rotates, a moment due to inertial forces is also produced. The axis of the frame is also subject to the friction moment; however, as we have pointed out, this moment is very small and may be neglected. On the basis of Newton's second law, the motion of the gyroscope may be described by the following equation

$$J\frac{d^2\beta}{dt^2} + K_d\frac{d\beta}{dt} = H\frac{d\alpha}{dt}, \tag{5.2}$$

where $J\frac{d^2\beta}{dt^2}$ is the moment due to the forces of inertia; $K_d\frac{d\beta}{dt}$ is the damping moment, /173 and $H\frac{d\alpha}{dt}$ is the gyroscopic moment.

Integrating equation (5.2) for zero initial conditions $\alpha = \beta = d\beta/dt = 0$, we obtain

$$T\frac{d\beta}{dt} + \beta = \frac{H}{K_d}\alpha, \tag{5.3}$$

where $T = \frac{J}{K_d}$ (0.0015 - 0.003) sec is the time constant of the integrating gyroscope.

Integrating equation (5.3) under the same initial conditions we obtain

$$\beta = \frac{H}{K_d} \alpha (1 - e^{-t/T}). \tag{5.4}$$

If time constant T of the device is very small, the second term in the brackets of equation (5.4) attenuates more rapidly and we may assume that

$$\beta = \frac{H}{K_d} \alpha. \tag{5.5}$$

Thus the accuracy of expression (5.5) will be greater when the time constant of the device is less. This must be taken into account when designing the device.

The application of the integration gyroscope to measure angle α by measuring directly the variation in angles β of rotation of the gyro's frame with respect to the case of the device is feasible only in cases when the possible values of angles α and the parameters of the device are such that angle β remains small during the entire period of operation. However, if angle β achieves values for which we cannot assume that $\cos \beta \approx 1$, the gyroscopic moment will be equal to $H \frac{d\alpha}{dt} \cos \beta$, which will cause a nonlinear relationship between β and α. Also, in this case, we cannot assume that $\sin \beta \approx 0$, and the magnitude of angle β will be affected by the angular velocity of the device's case about the initial position of the z axis, i.e., about the z_0 axis. Therefore, if it is necessary to measure arbitrary angles α, the integrating gyro must be used together with a servodrive which controls the integrating gyroscope in such a way that the angular rate of its operation is equal to $d\alpha/dt$, and then $\beta \approx 0$ (the accuracy is determined by the transient processes). Such a system as a whole represents an integrator of angular velocity operating on the principle of an integrating drive with the gyroscope as the sensing element. /174

Section 5.3. Angular Velocity Sensors

Angular velocity is usually sensed by rate or two stage gyroscopes with the degree of freedom of the suspension restricted by the centering spring and a damper (fig. 5.5). The direction of the axis along which the gyroscope is not free (z axis), coincides with the direction of the axis used as a reference to measure the angular velocity of motion. Rotor 2 rotates with respect to the z axis, may overcome the force of spring 1 and of damper 4 and may rotate with respect to the y axis. Frame 3 rotates until the gyroscopic moment is balanced by the opposing moment of the spring. The gyroscopic moment is proportional to the angular turn rate. On the basis of Newton's second law, the motion of the rate gyro may be described by the following equation:

$$J \frac{d^2\mu}{dt^2} + h_d \frac{d\mu}{dt} + K_d \mu = H\omega_c, \tag{5.6}$$

where J is the moment of inertia with respect to the axis of the frame; μ is the angle of rotation of the frame; $h_d \frac{d\mu}{dt}$ is the damping moment; $K_s\mu$ is the spring (s) moment; $H\omega_c$ is the gyroscopic moment, and ω_c is the missile's angular rate of turn.

When the transient process ends (when $d^2\mu/dt^2 = d\mu/dt = 0$), the turn angle of the gyroscope's frame becomes proportional to the angular rate of turn of the missile

$$\mu_{ss} = \frac{H\omega_c}{K_s} \tag{5.7}$$

Dividing equation (5.6) by K_s we obtain /175

$$T^2 \frac{d^2\mu}{dt^2} + 2T \frac{d\mu}{dt} + \mu = \frac{H\omega_c}{K_s}, \tag{5.8}$$

where $T = \sqrt{\frac{J}{K_s}} = \frac{1}{\omega_0}$; ω_0 is the natural frequency of oscillations of the device, and $\zeta = \frac{h_d}{2\sqrt{K_s J}}$ is the relative damping coefficient.

Equation (5.8) shows that the rate gyro is an oscillating element. As we know from the theory of automatic control, the transfer functions of an oscillating element are completely characterized by the quantities ω_0 and ζ. When the magnitude of ζ is small and when the output signal varies with frequency ω /176
close to ω_0, resonance occurs when the amplitude of the output quantity (in this case of angle μ) turns out to be very large. When $\zeta \geq 0.75$, resonance does not occur.

Figure 5.6 shows the logarithmic amplitude-frequency and phase-frequency characteristics of the oscillating element. As we can see from the amplitude characteristics, the relative damping coefficient must lie in the limits ζ = 0.6 - 0.8, because the horizontal region of the amplitude characteristics is greatest under these conditions. From the phase characteristics it follows that as the signal frequency increases, the phase distortions increase. Consequently, the natural frequency of a gyroscope must be substantially higher than the frequencies of the possible input signals, i.e., the frequencies of the angular oscillations of the missiles. The region of possible output signal frequencies lies in the range 0 - 2.5 cps. It is not rational to increase the frequency of the natural oscillations of the device appreciably, because it may turn out to be close to the vibration frequency of the missile structure and the device may react to these. The natural frequency of a gyroscope with an air damper must be 8 - 10 cps.

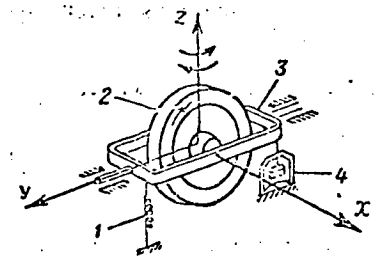

Figure 5.5. Schematic diagram of rate gyroscope.
1--spring; 2--rotor; 3--frame; 4--damper.

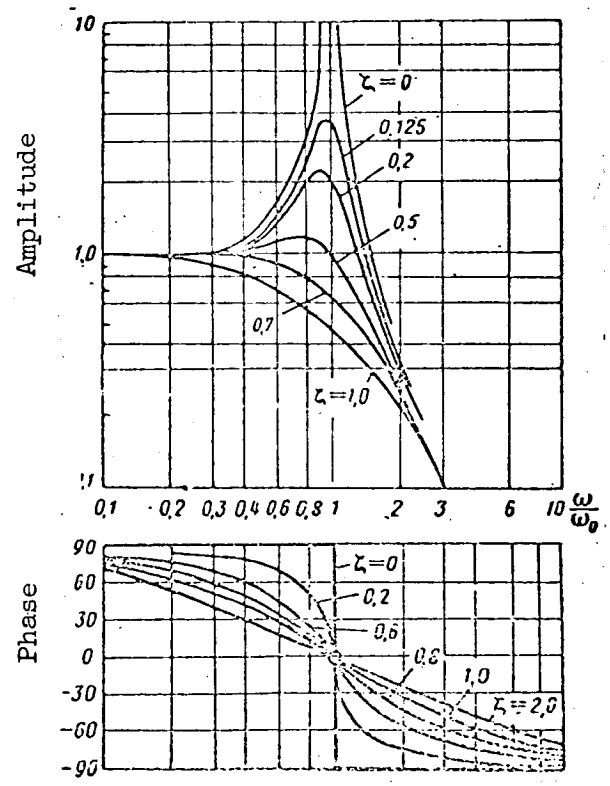

Figure 5.6. Amplitude-frequency and phase-frequency characteristics of oscillating element.

Friction in the support bearings of gyroscopic devices generates noise in the output signal. As the loading on the ball bearings decreases, the amplitude noise also decreases, and so does its effect on the output signal. To decrease the loading on the bearings, the rotor on the gyroscope is placed into a viscous liquid, i.e., a floating gyroscope is used. The position of the gyroscope in the viscous liquid also makes it possible to increase the damping

moment and, hence, to increase the degree of damping of the device ζ. The use of temperature control for the liquid of a floating gyroscope will retain the characteristics of the device during the entire period of flight.

Section 5.4. Combined Gyroscope Sensors

A signal which is proportional to the angular velocity and acceleration of the missile may be obtained by means of an acceleration-rate gyroscope, represented schematically in figure 5.7. The acceleration-rate gyroscope consists of a gyroscope with three degrees of freedom, in which one degree of freedom (rotation around the axis of the external frame) is limited by means of an elastic coupling with the housing of the device, while the other is limited as in the case of the rate gyro.

When the missile rotates at constant velocity ω_c with respect to the axis which coincides with the axis of the external frame, the elastic coupling causes the outer frame to rotate with the same angular velocity. The internal frame of the gyroscope will react to the angular velocity ω_c, just as in the case of the two-stage rate gyroscope, i.e., it will turn by an angle proportional to the angular velocity. When the angular velocity of the missile ω_c is constant, /177 the spring of the outer frame is not deformed, while the moment produced by the spring of the inner frame causes the precession of the outer frame in the direction of rotation of the case with an angular velocity equal to the angular velocity of the case.

When the angular velocity of rotation ω_c changes, the angle of rotation of the inner frame varies, and the faster the variation in the angular velocity ω_c, the greater is the velocity of rotation of the inner frame. When this rotation is present, a gyroscopic moment appears whose vector is directed along the axis of the external frame. The modulus of the moment is proportional to the rate of rotation of the inner frame, i.e., to the angular acceleration of the missile. When this gyroscopic moment acts, the external frame will turn until the moment is counterbalanced by the spring moment. This causes the external frame to rotate by an angle proportional to the angular acceleration.

A signal which is proportional to the angular velocity and the angular acceleration may be obtained by using only one spring (fig. 5.8), which would produce moments both around the axis of the inner frame and around the axis of the outer frame. One end of the spring is secured to the internal frame, while the other is secured to the housing of the device. When the angular velocity of the inner frame around its axis is stabilized, the spring is stretched and a moment is produced, both with respect to the axis of the inner frame and with respect to the axis of the outer frame. The moment with respect to the axis of the outer frame rotates it by an angle proportional to the angle of turn of the inner frame, i.e., proportional to the angular turn velocity of the missile. /178 When the missile is subjected to angular acceleration, the inner frame begins

LW

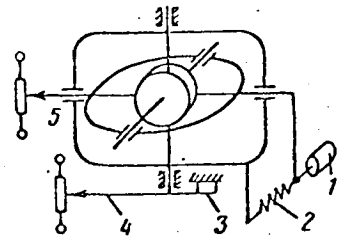

Figure 5.7. Schematic diagram of acceleration-rate gyroscope. 1--damper; 2--counter-acting spring of internal frame; 3--counter-acting spring of external frame; 4--angular acceleration sensor; 5--angular velocity sensor.

to turn and a gyroscopic moment appears producing additional deviation of the outer frame, with respect to the housing of the device, by an angle at which the gyroscopic moment will be balanced by the spring. Thus, the external frame will turn by an angle which is proportional both to the angular velocity and to the angular acceleration. The ratio of the signals will depend on the design parameters, i.e., on the ratio of the arms R_1 and R_2.

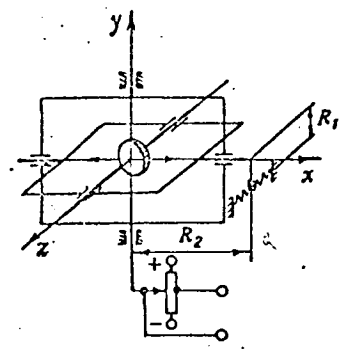

Figure 5.8. Schematic diagram of acceleration-rate gyroscope with one spring.

To decrease the weight and size of the control system carried aboard the missile and also to make the system less expensive, the differentiation and integration of the signals from a three-stage or a two-stage gyroscope is frequently performed by means of RC networks. It is rational to carry out integration only when the flight duration of the missile is short because, in the case of long range flight, the accuracy of missile guidance is decreased. This is true because the integration of the signals, which correspond to the drift of the null point of the device, produces signals of substantial magnitude causing the inaccuracies. A more detailed examination of differentiating and integrating networks will be carried out in Chapter 6.

Section 5.5. Sensors for Linear Accelerations of the Missile's Center of Gravity (Accelerometers)

Linear accelerations are measured by means of accelerometers using the inertial properties of a freely suspended mass. Figure 5.9 shows the schematic diagram of an accelerometer with a potentiometric sensor. When acceleration occurs, the inertial forces of the mass overcome the elasticity of springs 1 and 2 and displace the brush along potentiometer 3.

The equation of motion of the mass has the following form

$$m\frac{d^2x_1}{dt^2} + h\frac{dx_1}{dt} + kx_1 = m\frac{d^2x}{dt^2}, \tag{5.9}$$

where x is the linear displacement of the missile at the point where the device is installed; x_1 is the displacement of the mass of the device with respect to the missile; $h\frac{dx_1}{dt}$ is the damping force; kx_1 is the spring force, and $m\frac{d^2x_1}{dt^2}$ is the force of inertia which acts on the mass of the device.

Rewriting equation (5.9) and dividing it by coefficient k we obtain

$$T^2\frac{d^2x_1}{dt^2} + 2\zeta T\frac{dx_1}{dt} + x_1 = \frac{m}{k}\frac{d^2x}{dt^2}, \tag{5.10}$$

where $T = \sqrt{\frac{m}{k}}$; $2\zeta T = \frac{h}{k}$.

Equation (5.10) is the equation of an oscillating element. Consequently, the accelerometer, like any oscillating element, will reproduce with sufficient accuracy the slowly varying acceleration of the missile, and the error will increase as the frequencies of these accelerations increase. If we take this into account, the natural frequency of an accelerometer $\omega_0 = 1/T$ should be selected so that it is 4 - 10 times higher than the frequency of variation in the missile's acceleration. /179

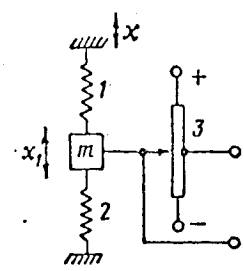

Figure 5.9. Schematic diagram of accelerometer. 1,2--springs; 3--potentiometer.

To obtain an electrical signal proportional to the displacement of the accelerometer's mass, inductive sensors as well as potentiometers are used. The advantage of inductive sensors is that they have no current contacts and hence produce no additional loading due to friction, as in the case of a potentiometric scheme.

Section 5.6. Air Speed Sensors or Sensors of Ram Compression

Data on the magnitude of the air velocity or of the ram compression are used in guidance systems of airplane-missiles and many other types of missiles. Data on the air speed are frequently used instead of data on ground speed, which requires complex equipment on the missile for its determination.

The simplest sensor of ram compression is shown in figure 5.10. The pressure force on plate 1 which is in the air stream is balanced by the force of spring 3. When the ram compression increases, the spring is stretched and the brush is displaced along the potentiometer by a distance proportional to the ram compression. The tension of the spring corresponds to the average value of the ram compression.

Some of the missiles use a propeller ("wind turbine") installed in the nose of the missile. The angular rotation of the wind turbine is proportional to the air speed, and the number of turns is proportional to the traveled path. The principal disadvantage of these sensors is that they increase the drag of the missile and are of insufficient accuracy.

Manometric sensors do not have these disadvantages. Figure 5.11 shows the schematic diagram of such a sensor. The manometric chamber 1 is subjected to the total pressure equal to the sum of the dynamic and static pressures. The intake orifice for the total pressure is situated in the nose of the missile. /180
The missile frame has an orifice for picking up the static pressure. Chamber 1 is subjected to static pressure from the outside, and its displacement is proportional to the pressure difference, i.e., $(p_{total} - p_{static}) = p_{dynamic}$ to the dynamic pressure or the ram compression. The displacement of the chamber is transmitted to the brush which slides along the potentiometer. In

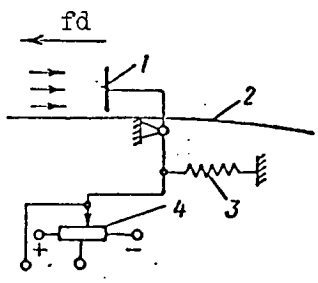

Figure 5.10. Ram compression sensor. 1--plate; 2--missile frame; 3--spring; 4--potentiometer; fd--flight direction.

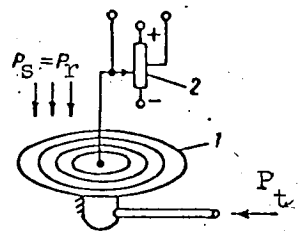

Figure 5.11. Simplest sensor of air velocity. 1--barometric chamber; 2--potentiometer; subscripts s = static, r = ram, t = total.

many cases inductive sensors which measure the displacement of the movable center of the membrane chamber are used to obtain an electric signal proportional to velocity or to the ram compression.

Section 5.7. Altitude Sensors

Barometric altimeters and radio altimeters are used to sense the flight altitude of a missile. The barometric altimeter measures the relative flight altitude, i.e., the flight altitude with respect to the launching site, while the radio altimeter measures the true flight altitude. The difference in the values of the flight altitude is clarified in figure 5.12.

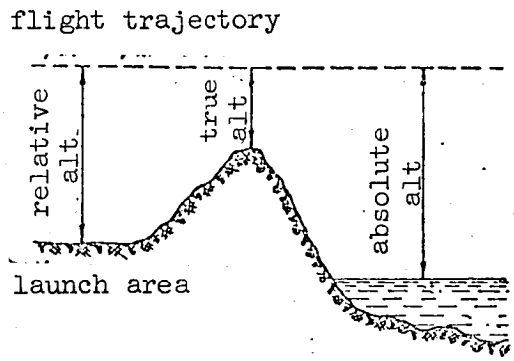

Figure 5.12. Relative, true and absolute flight altitudes.

Barometric Altimeter. The barometric method of measuring flight altitude is based on the law governing the variation of air density with altitude.

For altitudes from 0 - 11,000 m

$$H = \left[1 - \left(\frac{p_r}{p_0}\right)^{\tau R}\right] \frac{T_0}{\tau}, \tag{5.11}$$

while for altitude above 11,000 m

$$H = 11\,000 + RT_{11} \ln \frac{p_{11}}{p_r}, \tag{5.12}$$

where R = 29.27 is the gas constant in m/deg; T_0 is the absolute temperature at the surface; τ is the temperature gradient; p_0 is the absolute pressure at the surface in Newtons/m^2; T_{11} is the absolute temperature at the altitude of 11,000 m, and p_{11} is the absolute pressure at an altitude of 11,000 m. /181

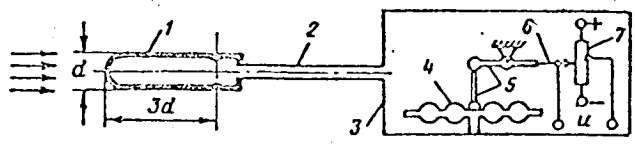

Figure 5.13. Schematic diagram of barometric altimeter. 1--static pressure receiver; 2--intake pipe; 3--hermetically sealed case; 4--membrane chamber; 5--transmitter; 6--brush; 7--potentiometer.

If we assume that the parameters p_0, T_0, τ are constant, $H = f(p_{ram})$ may be measured by means of a barometer. The schematic diagram of a barometric altimeter is shown in figure 5.13. From the static pressure receiver 1 the air enters the hermetically sealed case 3, where the membrane chamber 4 is installed. When the pressure (altitude) varies, the movable center of the chamber is displaced and moves brush 6 (which slides along potentiometer 7 through transmitter 5. Voltage u is proportional to the displacement of the brush and, consequently, to the variation in the flight altitude relative to the altitude at the launching point. The static pressure may also be picked up at the fuselage of the missile. In this case, a point may be found on the surface of /182 the fuselage where the pressure is equal to the static pressure. An intake pipe is placed at this point with a line leading to the altimeter.

If the altimeter is connected to the flight stabilization system and the technical mission of the missile requires that it fly at different altitudes, an altitude preselector is introduced into the altimeter scheme. The simplest altitude preselector consists of a device to vary the elasticity of the membrane chamber. This device may consist of a spring which is compressed by a calibrating screw. The screw is set by means of a scale graduated in units of altitude.

When flight takes place over large distances, the assumption that the parameters p_0, T_0 and τ are constant leads to an increase in the methodical error of the altimeter. In such cases it is rational to use radio altimeters.

Radio Altimeter. The operation of the radio altimeter is based on the reflection of electromagnetic waves by the surface of the Earth. The source of electromagnetic waves is a transmitter of the altimeter installed on the missile. Electromagnetic waves are radiated into space (primarily towards the Earth) by the antenna of the transmitter and after reflection by the Earth's surface are picked up by the antenna of the altimeter's receiver (fig. 5.14).

The time it takes the radio waves to move from the missile to the Earth and back again depends on the flight altitude

$$t = \frac{2H}{c}, \tag{5.13}$$

where $c = 3 \cdot 10^8$--the velocity of radio wave propagation equal to the velocity of light in m/sec.

The velocity of electromagnetic wave propagation is not commensurable with the velocity of the missile; therefore, the time which it takes for the wave to move from the missile to the ground and back is practically independent of flight velocity.

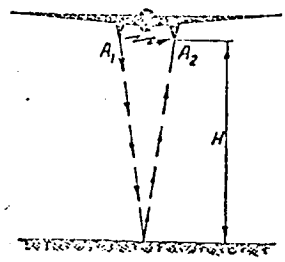

Figure 5.14. Path of electromagnetic waves when radio altimeter is used.

Existing radio altimeters may be divided into two types:

radio altimeters operating with continuous radiation

radio altimeters with pulse radiation.

Radio altimeters with continuous radiation are used for altitudes less than 1,500 m, because the required power increases proportionately to the fourth power of the measured altitude and becomes prohibitively large for high altitudes. The principle of operation of a radio altimeter with continuous radiation consists of the following: the antenna of the radio transmitter radiates electromagnetic waves into space, whose frequency is continuously varied within certain limits from its average value. The variation in frequency as a function of time has the form of a saw-tooth wave (fig. 5.15). As shown in figure 5.15a, the frequency of radio waves reflected from the ground and received by the altimeter varies according to the same law, but incorporates a delay time (broken line) whose magnitude is /183

$$\tau = \frac{2H}{c}. \tag{5.14}$$

At each instant of time the frequency of the transmitted signal differs from the frequency of the reflected signal by a value equal to the change in the frequency of the transmitter during the travel of the radio wave from the missile to the surface and back (with the exception of time intervals 1--points

1, 2, 3, etc., where the difference in frequency decreases to zero). The difference in frequencies $\nu = f_1 - f_2$ is easy to determine, if the analytical law for the variation of frequencies f_1 and f_2 has the form

$$f_1 = f_0(1 \pm at) \quad \text{and} \quad f_2 = f_0[1 \pm a(t-\tau)].$$

The high frequency oscillations f_1 and f_2 are detected, and as a result a voltage of low frequency ν is obtained (fig. 5.15b)

$$\nu = f_1 - f_2 = f_0 a\tau = f_0 a \frac{2H}{c}.$$

The frequency is measured with a frequency meter and the signal, proportional to the change in frequency, will be proportional to flight altitude H. A radio altimeter of this type can measure the true altitude with an accuracy up to 5 percent.

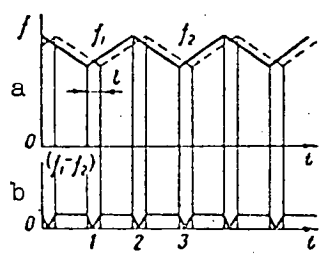

Figure 5.15. Measurement of frequency of radio altimeter signal.

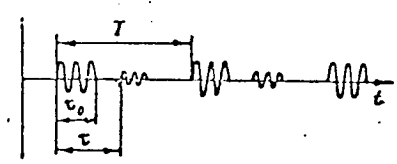

Figure 5.16. Curves characterizing pulses of radio altimeter.

For higher altitudes (above 1,500 m), pulse type radio altimeters are used (fig. 5.16) which send periodic short-time pulses of high power while maintaining the average power of the transmitter at a relatively low level. The ratio of the instantaneous power radiated into space as a pulse to the average power of the transmitter is equal to /184

$$\frac{P_{pulse}}{P_{av}} = \frac{T}{\tau_0}, \tag{5.15}$$

where T is the interval between pulses, and τ_0 is the pulse duration.

The reflected pulses are received by the antenna in the intervals between transmitted pulses. The interval of time between the transmitted and the reflected pulse $\tau = 2H/c$ corresponds to the flight altitude.

Section 5.8. Determining the Ground Speed

For missiles with a self-contained control system it is necessary to determine the ground velocity and from it the traveled path. From the navigation triangle of velocities (fig. 5.17), we can see that ground velocity vector $\overline{V}$ is equal to the geometric sum of two vectors--the true air speed V_{air} (velocity of the missile with respect to the air) and the wind velocity $\overline{W}$ (velocity of the wind with respect to the ground). For navigation of the missile we must know the components of the ground velocity along two mutually perpendicular directions, for example, north-south and east-west (fig. 5.17). The ground velocity can be determined by using an inertial system of navigation, described in detail in section 5.9. However, in some cases it is only necessary to determine one component of the ground speed, for example, if the operation of the engine of a long-range rocket is to be stopped when the rocket reaches a computed flight velocity in the firing plane.

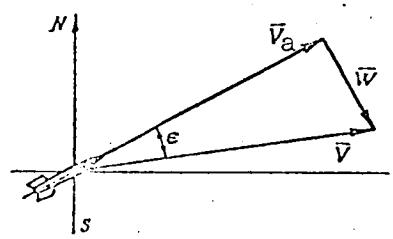

Figure 5.17. Navigation triangle of velocities.

A gyroscopic integrator of acceleration is most frequently used for this purpose (fig. 5.18). It consists of a 3-stage gyroscope, in which the axis of suspension for the inner frame does not pass through the center of gravity of the gyroscope. The axis of the internal frame is directed along the longitudinal axis of the rocket when it is necessary to determine the velocity in the firing plane. When acceleration takes place, a moment with respect to the axis of the inner frame appears and as a result the external frame of the gyroscope precesses. The angular velocity of precession is proportional to the moment applied to the axis of the frame /185

$$\omega_{pr} = \frac{Fl}{J\Omega}, \tag{5.16}$$

(subscript pr = precession),

where F is the force applied to the center of gravity of the gyroscope; l is the force lever arm, and $J\Omega$ is the kinetic moment of the gyroscope.

The moment may be computed as the product of forces applied to the gyroscope's center of gravity by a lever equal to the distance between the suspension axis of the internal frame and its center of gravity. The force applied to the center of gravity will be the resultant of the gravity force and inertial force components in the direction perpendicular to the axis of the internal gyroscope frame.

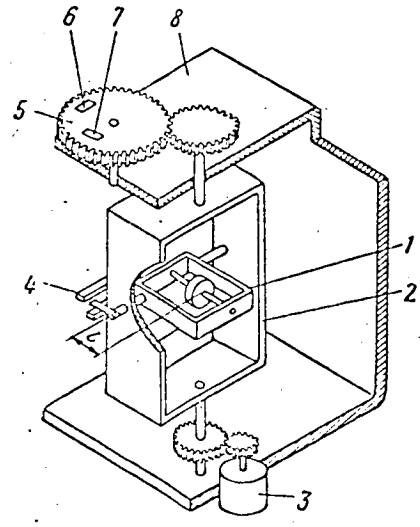

Figure 5.18. Integr ting gyroscope. 1--internal frame; 2--external frame; 3--compensating motor; 4--compensating contacts; 5--contact disk; 6--cam for partial disengagement of motor; 7--cam for total disengagement of motor; 8--housing of device.

Figure 5.19 shows the accelerations which act on the missile. As we can see, the apparent force of gravity applied to the center of gravity of the gyroscope will be equal to

$$F = m\left[\frac{dV}{dt}\cos\alpha + V\frac{d\theta}{dt}\sin\alpha + g\sin(\theta+\alpha)\right]. \qquad (5.17)$$

where m is the mass of the gyroscope's rotor with housing; α is the angle of attack; θ is the slope of the velocity vector; g is the acceleration due to gravity, and V is the velocity of the missile.

The angle of rotation of the external frame with respect to the x axis may be obtained from equation /186

$$\mu = \int_0^t \omega_{pr}\,dt = \int_0^t \frac{ml}{J\Omega}\left[\frac{dV}{dt}\cos\alpha + V\frac{d\theta}{dt}\sin\alpha + g\sin(\theta+\alpha)\right]dt. \qquad (5.18)$$

When the kinetic moment of the gyroscope, lever arm l and mass m are constant and when the angle of attack α is small, the angle of rotation of the frame is the resultant of two components:

$\mu_1 = \frac{ml}{J\Omega}V$ --the angle proportional to the magnitude of the flight velocity at the given instant of time;

$$\mu_2 = \frac{ml}{J\Omega} g \int_0^t \sin\theta \, dt$$ --the angle of rotation of the frame due to the force of gravity;

$$\mu_3 = \frac{ml}{J\Omega} \int_0^t V \frac{d\theta}{dt} \alpha \, dt$$ --the angle of rotation of the frame due to acceleration directed perpendicular to the velocity vector.

Angle θ varies in accordance with the flight program, and therefore the readings of the gyroscopic integrator must be corrected on the basis of the given program for θ, and also on the basis of the computed law for the variation of the angle of attack α along the trajectory. The necessity of taking into account the flight program leads to a methodical error of the integrator. Since the program is carried out with errors, these errors affect rocket velocity V determined by the integrator.

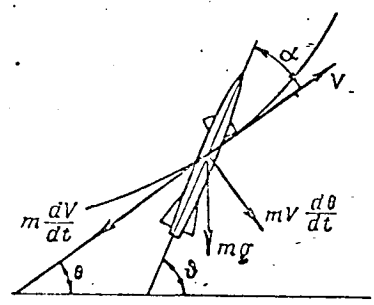

Figure 5.19. Schematic diagram showing forces which act on missile.

To increase the accuracy of the integrator, it is necessary that lever arm l remain fixed in flight; to achieve this, the frames must remain perpendicular. To satisfy this condition, the integrator is equipped with a compensating device. If the axis of the gyroscope is deflected up or down, the lower or upper contact is closed, and a corresponding signal is transmitted to the moment motor. When this happens, a moment is transmitted to the axis of the gyroscope's external frame through a gear drive. This moment produces the precession of the inner frame and the perpendicular position of the frames is reestablished. The flight velocity at which the motor is turned off is determined by the rotation of the disk which carries the contacts. The drive gear, connected to the axis of the external frame through the transmission, contains cams. One of the cams will close a contact for partial disengagement of the motor, while the second will close a contact for complete disengagement.

The ground speed is determined by means of a Doppler radar. As we know, the Doppler effect is observed when the source and the receiver of energy (sound, light and electromagnetic) are displaced with respect to each other. /187

The Doppler effect consists of a variation in the frequency of the received signals compared with the frequency of the transmitted signals, when there is relative displacement of transmitter and receiver. If receiver and transmitter are fixed with respect to each other, then, obviously, these frequencies are the same. The magnitude of the frequency shift is known as the Doppler shift.

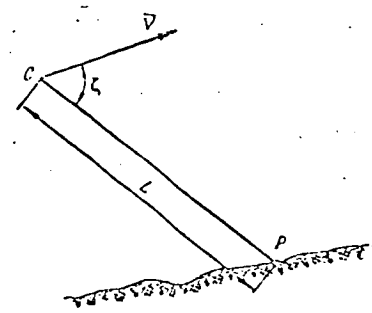

Figure 5.20. Use of Doppler effect to determine velocity.

In systems which determine the ground speed of the missile, the source of ultrahigh-frequency is located on the missile, which moves with velocity V with respect to the ground (fig. 5.20). The electromagnetic waves are propagated towards the Earth to point P, and part of them are reflected back to the receiver located at point C. To obtain quantitative relations, we assume that the process transmission--reflection--reception is a single one.

The signal of the transmitter is given by expression

$$E_{tr} = A \sin 2\pi f t, \tag{5.19}$$

while the received signal is given by the expression

$$E_{re} = B \sin (2\pi f t - \varphi), \tag{5.20}$$

where A and B are constants characterizing the signal amplitude; f is the frequency of the transmitter, and φ is the phase shift of the received signal with respect to the transmitted signal due to finite propagation time.

The phase shift is equal to

$$\varphi = 2\pi \frac{2L}{\lambda}, \tag{5.22}$$

where L is the distance from receiver-transmitter to point P; $\lambda = c/f$ is the wavelength of the electromagnetic energy, and c is the velocity of light.

Since the period of time between transmission and reception of the reflected signal is small, distance L may be computed by means of an approximate equation /188

$$L(t) = L_0 - Vt \cdot \cos\zeta, \tag{5.23}$$

where L_0 is the distance when t = 0, and ζ is the angle between velocity $\bar{V}$ and the propagation direction of the electromagnetic waves.

If we take into account expressions (5.22) and (5.23), equation (5.20) may be written in the form

$$\begin{aligned} E_{re} &= B \sin\left[2\pi f t - \frac{4\pi}{c} f (D_0 - Vt\cos\zeta)\right] = \\ &= B \sin\left[\left(2\pi f + \frac{4\pi}{c} V \cos\zeta f\right) t - \varphi_0\right], \end{aligned} \tag{5.24}$$

where $\varphi_0 = \frac{4\pi D_0}{c} f$ is the constant phase lag.

From expression (5.24) we determine the frequency of the received signal

$$f_{re} = f + \frac{2V\cos\zeta}{c} f = f\left(1 + \frac{2V\cos\zeta}{c}\right). \tag{5.25}$$

Consequently, the Doppler frequency is given by expression

$$\nu = f_{re} - f = \frac{2V\cos\zeta}{c} f. \tag{5.26}$$

The quantity V cos ζ represents the ground speed component in the propagation direction. To determine the total value of vector V, it is necessary to make use of at least three beams which are not coplanar. The velocity of the missile determined by means of the multibeam system represents the ground speed in a system of coordinates fixed with respect to the missile.

Let us consider the case when the antenna system is stabilized in the horizontal plane. The antennas are rotated in the horizontal plane by means of servosystems in such a way that the horizontal projection of the ground velocity vector is along the line bisecting the angle between the rays K and L (fig. 5.21). If the four beams K, L, M and N are directed symmetrically with respect to the x and z axes, we have

$$\begin{aligned} k_x &= l_x = -m_x = -n_x = \cos\gamma, \\ k_y &= l_y = m_y = n_y = -\cos\mu, \\ k_z &= -l_z = -m_z = n_z = \cos\sigma, \end{aligned} \tag{5.27}$$

where k, l, m and n are unit vectors in the direction of the four rays, and k_x, k_y, k_z, etc., are components of the vector k, etc., along axes which are orthogonal to the x, y, z coordinate system. /189

If the condition of symmetry is fulfilled, we have

$$\begin{aligned} V_{ho} = V_x &= V\cos\theta, \\ V_y &= V\sin\theta, \\ V_z &= 0, \end{aligned} \tag{5.28}$$

where θ is the slope of the trajectory.

From equations (5.26), (5.27) and (5.28) it follows that

$$\left.\begin{aligned} \nu_k = \nu_l &= \frac{2}{\lambda} V(\cos\gamma\cos\theta - \cos\mu\sin\theta), \\ \nu_m = \nu_n &= \frac{2}{\lambda} V(-\cos\gamma\cos\theta - \cos\mu\sin\theta). \end{aligned}\right\} \tag{5.29}$$

As a result we obtain

$$(\nu_k - \nu_m) = (\nu_l - \nu_n) = \frac{4}{\lambda} V\cos\gamma\cos\theta = \frac{4}{\lambda}\cos\gamma V_{ho} \tag{5.30}$$

Expression (5.30) shows that the difference in the Doppler frequencies for beams directed towards the nose and the tail of the missile is proportional to the horizontal component of the ground velocity vector. A single integration of the signal, which is proportional to the horizontal component of the ground speed, makes it possible to determine the path traveled by the missile over the surface of the Earth.

If the frequency difference $\nu_k - \nu_l$ or $\nu_m - \nu_n$ is not equal to zero, then the angle between beam K and the horizontal projection of the ground velocity vector and the angle between the beam L and the same projection are not equal to each other. Let us show that the Doppler frequency difference $\nu_k - \nu_l$ is proportional to the angle between the horizontal projection of the velocity vector and the x axis (fig. 5.21). From geometric considerations we have

$$\left.\begin{aligned} V_x &= V\cos\theta\cos\beta, \\ V_y &= V\sin\theta, \\ V_z &= -V\cos\theta\sin\beta, \end{aligned}\right\} \tag{5.31}$$

where β is the angle between the horizontal projection of the velocity vector and the x axis.

By making use of equations (5.23), (5.24) and (5.25) we obtain

$$\left.\begin{aligned} \nu_k &= \frac{2}{\lambda} V [\cos\theta \cos\beta \cos\gamma - \sin\theta \cos\mu - \cos\theta \sin\beta \cos\sigma], \\ \nu_l &= \frac{2}{\lambda} V [\cos\theta \cos\beta \cos\gamma - \sin\theta \cos\mu + \cos\theta \sin\beta \cos\sigma]. \end{aligned}\right\} \quad (5.32)$$

The difference $\nu_k - \nu_l$ is equal to /190

$$\nu_k - \nu_l = -\frac{4}{\lambda} V \cos\theta \sin\beta \cos\sigma = -\frac{4}{\lambda} \cos\sigma \sin\beta V_{ho} \quad (5.33)$$

When angle β is small, $\sin\beta$ may be replaced by angle β. Then the difference of the Doppler frequencies for rays directed towards the nose or towards the tail of the missile is proportional to the angle between the axis of symmetry of the

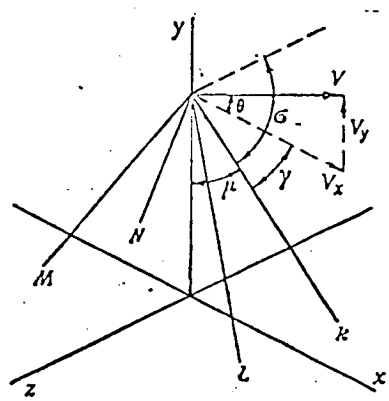

Figure 5.21. Determination of horizontal component of ground speed.

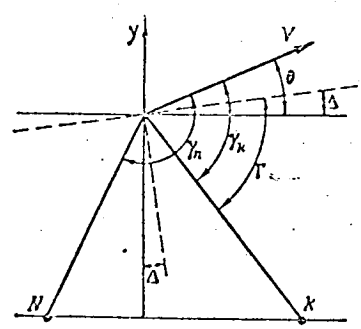

Figure 5.22. Determination of errors in velocity.

rays and the horizontal projection of the ground speed vector. If it is obvious that $\cos\sigma$ and V cannot be equal to zero, while the difference $\nu_k - \nu_l = 0$ only when $\beta = 0$. On this basis the signal proportional to $\nu_k - \nu_l$ is used by the servosystem to rotate the antennas with respect to the vertical axis.

To determine the components of the ground velocity, we may use antennas which are fixed with respect to the missile and a computer to record the true position of the missile and, consequently, of the antennas with respect to the Earth's surface. The accuracy achieved in maintaining the Doppler antenna system for measuring the ground velocity in the horizontal plane or the accuracy of

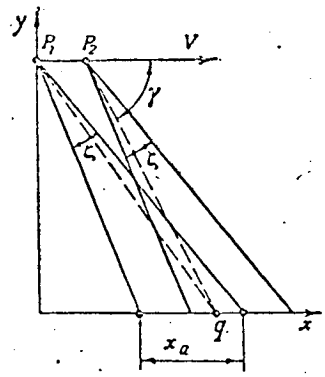

Figure 5.23. Determination of signal from individual surface element.

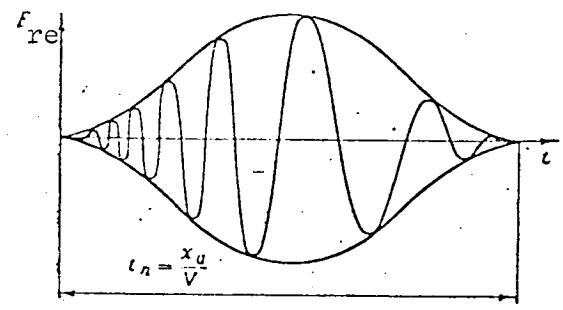

Figure 5.24. Form of signal reflected from individual surface element; re = receiver.

recording the position of the antenna system with respect to the Earth's surface, has a substantial effect on the errors introduced by this system.

Let us evaluate the errors produced by the deviation of the antenna from the horizontal plane. To simplify calculations we shall consider the two-dimensional problem. Let us assume that a vertical plane passes through the ground speed vector (fig. 5.22). The angle Δ characterizes the error of stabilizing the antenna along the vertical. If the error Δ is not equal to zero, then

$$\nu = \nu_k - \nu_n = \frac{2V}{\lambda}(\cos\gamma_k - \cos\gamma_n) = \frac{2V}{\lambda}[\cos(\Gamma + \theta - \Delta) + \cos(\Gamma - \theta + \Delta)] = \frac{4V}{\lambda}\cos\Gamma\cos(\theta - \Delta). \quad (5.34)$$

When θ = 0 and Δ = 1°, the error incurred in determining the velocity is approximately 0.015 percent. When θ = 15° and Δ = 1°, Δ V = 0.0196 percent.

All of these expressions are derived for the case of an infinitely thin radio beam. Actually, electromagnetic energy is radiated by an antenna whose radiation pattern is not infinitely narrow. The radiation pattern determines the radiation power level in a given direction. The maximum illumination energy is directed along the line bisecting angle ζ (fig. 5.23). As the missile moves from point P_1 to point P_2, the element of surface q is illuminated with /191

varying power. Also, angle γ changes with time, which causes a change in the Doppler frequency. Figure 5.24 shows the form of the signal reflected from an individual surface element. The average value of the Doppler frequency corresponds to the direction of the beam maximum to the reflecting element q. The total signal reflected by element q consists of a sum of many signals, similar to one shown in figure 5.24. Since at each instant of time the antenna illuminates an infinitely large number of surface elements, the reflection of the signal will also consist of an infinitely large number of signals, and the amplitudes and phases of the signals reflected from each element will be different.

The properties of such a signal are subject to statistical laws. It has been determined that the spectrum of the reflected signal is continuous and that its middle point corresponds to the Doppler frequency $\nu = \frac{2V}{\lambda} \cos \gamma_0$ (γ_0 is the angle between the maximum of the radiation pattern and the velocity vector).

Section 5.9. Inertial Systems of Navigation

Inertial navigation consists of determining the fix of an object near the surface of the Earth by measuring the acceleration of a flying vehicle with equipment carried aboard and performing a double integration of the signals obtained. The sensors of inertial systems of navigation are of two types. Sensors of the first type consist of three accelerometers oriented along the known system of coordinates; to orient the accelerometers, it is necessary to have a stable platform of a certain type. In the sensor of the second type, six accelerometers /192 are rigidly attached to the frame of the missile. Sensors of the first type are widely used while sensors of the second type are not too well known. In the following discussions we shall be concerned with inertial systems operating with sensors of the first type. These inertial systems in turn are divided into several types, depending on the system of coordinates used for the orientation of the accelerometers and the structural relationships between the accelerometers and the stable platform. Let us consider two principal types of these inertial systems. In systems of the first type, two accelerometers are oriented in the horizontal plane in two mutually perpendicular directions, while the axis of the third accelerometer coincides with the ground acceleration vector. In systems of the second type, the Cartesian system of coordinates, in which the accelerometers are oriented, is fixed in universal space.

1. Inertial Systems of the First Type. Inertial systems of this type are known as the Schuler type. This is the name given to a pendulum with a suspension equal to the radius of the Earth and a period of oscillations equal to

$T = 2\pi\sqrt{R/g} = 84.5$ min.

Let us assume that a flying vehicle, carrying a stable platform with accelerometers, moves near the surface of the Earth (fig. 5.25) with an acceleration $j = \frac{dV}{dt} = \frac{d^2x}{dt^2}$ in a direction corresponding to one of the axes of the accelerometers. If the platform is deflected by a small angle β from the horizon /193 (local), the signal produced by the accelerometer will be equal to

$$j + g\beta.$$

To rotate the platform so that it follows the horizontal plane we generate a compensating signal proportional to the integral of the accelerometer's signal

$$M_к = k\int_0^t (j + g\beta)\,dt.$$

We obtain the rate of turn of the platform $\dot{\beta}_g$, if we divide the compensating moment by the kinetic moment H

$$\dot{\beta}_g = \frac{k}{H}\int_0^t (j + g\beta)\,dt, \tag{5.35}$$

where β_g is the central angle of rotation of the platform.

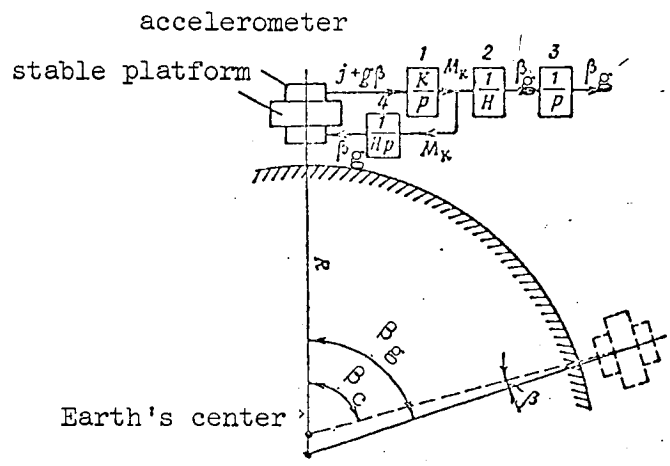

Figure 5.25. Position of stable platform of first type during movement of missile; subscript g = gyro, subscript c = central.

The path x traveled by the missile may be represented in the form of the central angle $\beta_c = x/R$, where R is the Earth's radius. If at any instant of time angles β_g and β_c coincide, this means that the stable platform coincides with the line of the local horizon and that angle $\beta = 0$. Consequently, the following relation is always true

$$\beta = \beta_c - \beta_g. \tag{5.36}$$

The angle

$$\beta_c = \frac{1}{R}\int_0^t\int_0^t j\,dt\,dt \tag{5.37}$$

is determined by the flight characteristics of the missile and consequently is some function of time.

Let us rewrite equations (5.35) - (5.37) in operational form

$$\left.\begin{aligned} \beta_g &= \frac{k}{H}\frac{1}{p^2}(j+g\beta), \\ \beta &= \beta_c - \beta_g, \\ \beta_c &= \frac{1}{R}\frac{1}{p^2}j. \end{aligned}\right\} \tag{5.38}$$

The system of equation (5.38) corresponds to the diagram shown in figure 5.26. This schematic represents a combined servosystem with an auxiliary control of the second derivative by input quantity β_c.

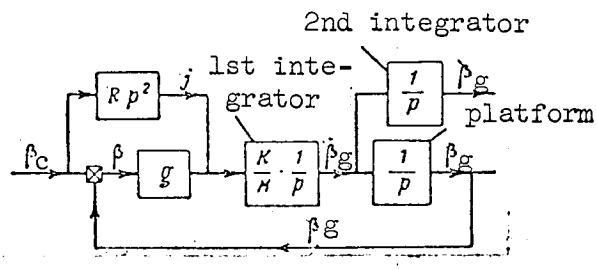

Figure 5.26. Diagram of system for stabilizing platform with accelerometers.

The transfer functions for output quantity β_g and for error β have the following form /194

$$\Phi(p) = \frac{(Rp^2+g)\frac{k}{H}}{p^2+\frac{k}{H}g}; \tag{5.39}$$

$$S(p) = \frac{\left(\frac{1}{R}-\frac{k}{H}\right)Rp^2}{p^2+\frac{k}{H}g}. \tag{5.40}$$

From transfer functions (5.39) and (5.40) or from system (5.38), we obtain equations for the closed loop system

$$\ddot\beta_g + \frac{k}{H}g\beta_g = \frac{k}{H}R\ddot\beta_c + \frac{k}{H}g\beta_c; \tag{5.41}$$

$$\ddot{\beta} + \frac{k}{H} g\beta = \left(\frac{1}{R} - \frac{k}{H}\right) j. \tag{5.42}$$

If we select

$$\frac{k}{H} = \frac{1}{R}, \tag{5.43}$$

transfer function (5.39) will become equal to unity, while transfer function (5.40) will become equal to zero. This result shows that there is an ideal tracking of the horizontal plane by the stable platform. Since angle β turns out to be equal to zero, the normal to the platform will always coincide with the Earth's acceleration vector. With this adjustment, the missile contains a vertical which is not perturbed.

Where $\frac{k}{H} = \frac{1}{R}$, equation (5.42) takes the form /195

$$\ddot{\beta} + \frac{g}{R}\beta = 0. \tag{5.44}$$

It follows from equation (5.44) that if we have an initial error in the local vertical β_0 and if $\dot{\beta}_0 = 0$, the platform will be subjected to undamped oscillations

$$\beta = \beta_0 \cos \omega_0 t, \tag{5.45}$$

where $\omega_0 = \sqrt{\frac{g}{R}}$ is the angular frequency of oscillation of the Schuler pendulum.

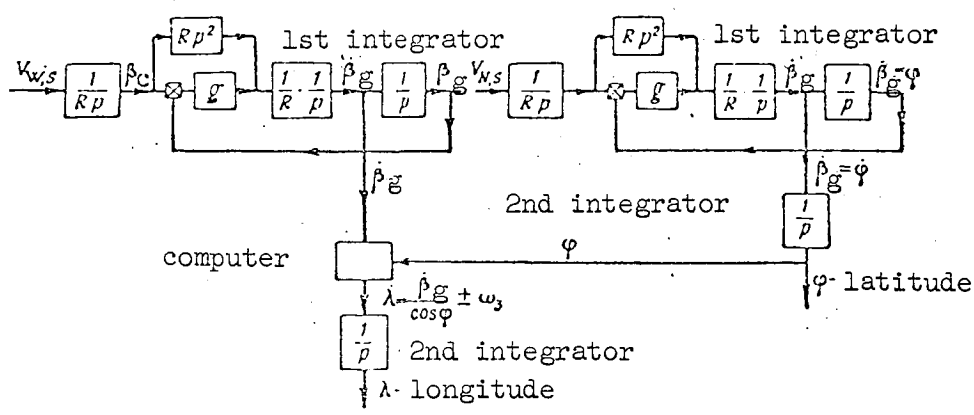

Figure 5.27. Diagram of gyroscopic navigation system giving fix of missile in geographic system of coordinates.

If the initial errors are $\beta_0 = \dot{\beta}_0 = 0$, the platform will always be horizontal and the accelerometers will produce a signal equal to the acceleration of the missile. The output of the first integrator (fig. 5.27) multiplied by R will, in this case, yield the ground speed of the missile, while the second integrator will show the traveled distance. If the accelerometer shown in figure 5.27 and figure 5.28 is oriented in the north-south direction, the output of the second integrator β_g, when $k/H = 1/R$, will show the actual latitude of the missile φ. In a similar manner, but with some special features, a system is designed to indicate the longitude.

Figure 5.27 shows the diagram of a gyroscopic navigation system which gives the fix of the missile in the geographic system of coordinates. After the readings of the accelerometer j_{NS}, oriented in north-south direction, are integrated, we obtain the angular velocity of latitude $\dot{\varphi}$ and latitude φ. The first integral $\dot{\beta}_g$ of the signal from the accelerometer, which is in the west-east direction j_{WE}, does not constitute the angular rate of change of the longitude $\dot{\lambda}$. To obtain $\dot{\lambda}$ it is necessary to divide $\dot{\beta}_g$ by $\cos\varphi$ and to take into account the angular diurnal rotation of the Earth ω_e /196

$$\dot{\lambda} = \frac{\dot{\beta}_g}{\cos\varphi} \pm \omega_e. \tag{5.46}$$

The mathematical operations designated by equation (5.46) are carried out by means of a special computer. After the signal $\dot{\lambda}$ is computed, it is integrated and the true longitude is obtained. The gyroscopic navigation system represented schematically in figure 5.27 is not suitable for navigation in the polar regions, because expression (5.46) has a singularity when $\varphi = \pi/2$. It is possible to construct a gyroscopic navigation system using other coordinate systems without this shortcoming.

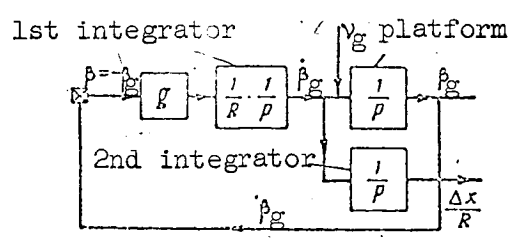

Figure 5.28. Simplified diagram of system for stabilizing platform with accelerometers.

Let us pause briefly to consider the accuracy of these gyroscopic navigation systems. The initial error β_0 in the orientation of the platform according to (5.45) will produce a harmonic component in the signal of the accelerometer

equal to $-g\beta_0 \cos \omega_0 t$. This component, after it is integrated twice, will produce a harmonic component in the error of the traveled path

$$\Delta x = \int_0^t \int_0^t g\beta_0 \cos \omega_0 t \, dt \, dt = \frac{g\beta_0}{\omega_0^2} (1 - \cos \omega_0 t) =$$

$$= \beta_0 R (1 - \cos \omega_0 t). \tag{5.47}$$

Equation (5.47) shows that for every angular minute of initial error β_0 the harmonic component of the error in the traveled path is equal to 1 nautical mile (1.84 km). Since the sign of the error Δx coincides with the sign of β_0, the maximum value of the error will be equal to 2 nautical miles for each angular minute β_0.

A more annoying error is produced by the drift of the stable platform. Let us assume that we have, at the instant of time $t = 0$, an initial drift of the stable platform with constant angular velocity ν_g. In this case equation (5.35) takes the following form (when $k/H = 1/R$) /197

$$\dot{\beta}_g = \frac{1}{R} \int_0^t (j + g\beta) \, dt + \nu_g 1(t). \tag{5.48}$$

Since we are considering only the error produced by the drift ν_g, we shall assume that $j = 0$ and $\beta = 0$. In this case $\beta = \beta_g$, and expression (5.48) after differentiation takes the form

$$\ddot{\beta}_g + \frac{g}{R} \beta_g = \nu_g \delta(t), \tag{5.49}$$

where

$$\delta(t) = \frac{d}{dt} 1(t) \text{ is the Dirac function.}$$

If we solve (5.49) by using the Laplace transformation, we find

$$\beta_g = \frac{\nu_g}{\omega_0} \sin \omega_0 t. \tag{5.50}$$

The drift of the stable platform also produces its oscillation with the Schuler period. As a result, the output of the accelerometer will have a signal $g\beta_g$ which, after double integration, will give the error in the traveled path or in the range

$$\Delta x = \frac{g\nu g}{\omega_0} \int_0^t \int_0^t \sin \omega_0 t \, dt \, dt = R\nu_g \left(t - \frac{1}{\omega_0} \sin \omega_0 t \right). \tag{5.51}$$

Errors in range have a component which increases in a linear manner and an oscillating component.

The requirements for small drift in the stable platform are very critical. Thus, when the drift is $\nu_g = 0.1$ deg/hr, the platform begins to oscillate with an amplitude of 1.35', which corresponds to a distance of 2.5 km. With the same drift, the error which increases linearly becomes equal to 8.4 nautical miles (15.6 km) during an 84 min flight.

For missiles with a short flight duration (several min) $\sin \omega_0 t$ in equation (5.51) can be replaced by the first two terms of the series

$$\sin \omega_0 t \approx \omega_0 t - \frac{(\omega_0 t)^3}{6}.$$

Then equation (5.51) for the deviation error of the gyroscope takes the form

$$\Delta x = g\nu_g \frac{t^3}{6}. \tag{5.52}$$

Equation (5.52) may be obtained from two considerations. For short intervals of time, the diagram of figure 5.28 may be considered to be of the open loop type. In this case, the drift of the platform with a constant velocity produces an accelerometer signal which increases in a linear manner. A double integration of this quantity leads to expression (5.52). /198

In conclusion we note that equation (5.51) may be obtained from an analysis of the diagram shown in figure 5.28. The drift ν_g may be considered a perturbation acting at the input of the platform. The transfer function for the output of the second integrator $\Delta x/R$ in terms of the perturbation ν_g will have the form

$$\Phi(p) = \frac{\omega_0^2}{p^2 + \omega_0^2} \frac{1}{p},$$

where

$$\omega_0^2 = \frac{g}{R}.$$

For a step function $\nu_g(t) = \nu_g \cdot 1(t)$ we obtain the following transform of the output from the second integrator

$$L\left(\frac{\Delta x}{R}\right) = \frac{\omega_0^2}{p^2+\omega_0^2}\frac{\nu_g}{p}.$$

The original of this transform is precisely expression (5.51) previously derived.

2. Compensation and Damping of Inertial Systems of the First Type. When auxiliary sources of information on the coordinates of the missile are available, the readings of the inertial system of navigation may be compensated, i.e., the accumulated errors may be eliminated. The method for eliminating error depends on the manner in which the external information is fed into the system. If the missile contains equipment which can recognize ground objects with known coordinates, the errors are eliminated as these surface objects are identified. Frequently, the external information is supplied continuously. In these cases, the compensation of the self-contained guidance system may take place continuously. The sources of external information for compensating inertial systems may be in the form of astronavigation and radionavigation methods. As an example let us consider the compensation of an inertial system 2 (fig. 5.29) by an electronic device 1 for measuring the ground speed vector of the missile based on the Doppler effect. This device produces a signal V + f, where V is the ground speed and f is the interference whose spectrum is of a high frequency nature and whose mathematical expectation is equal to zero. However, the inertial system produces a signal $V + \dot{\alpha} = \beta_g R$, where V is also the value of the true ground speed while $\dot{\alpha}$ is a slowly varying error. If we take into account the initial error β_0 and the drift of the platform with constant velocity, we have /199

$$\dot{\alpha} = \dot{\alpha}_0 + \dot{\alpha}_m \sin(\omega_0 t - \varphi),$$

where

$\dot{\alpha}_0 = \frac{g\nu_g}{\omega_0^2} = \nu_g R$ is the constant component of the error;

$\dot{\alpha}_m = R\sqrt{\beta_0^2\omega_0^2 + \nu_g^2}$ is the amplitude of the error's harmonic component, and

$\varphi = \operatorname{arc\,tg}\frac{\nu_g}{\beta_0\omega_0}$ is the phase of the error's harmonic component.

The compensation of the inertial system is accomplished by mixing V + f and $V + \dot{\alpha}$ at the single integration servosystem with two inputs 1 and 2 (fig. 5.29). The composite signal V_0 (subscript o = output) from output 3 is fed to the second integrator of the inertial system which computes the path. The key K_{ey} in front of the servosystem integrator is used to turn the compensating signal, which is fed from the Doppler sensor off and on.

At input 1, the servosystem has a transfer function in the form of a low frequency filter

$$W_1(p) = \frac{1}{T_\kappa p + 1},$$

while at input 2, it has the form of a high frequency filter

$$W_2(p) = \frac{T_\kappa p}{T_\kappa p + 1}.$$

The composite signal V_0 at the input of the servosystem is obtained from the principle of superposition /200

$$V_0 = \frac{1}{T_\kappa p + 1}(V + f) + \frac{T_\kappa p}{T_\kappa p + 1}(V + \dot{\alpha}) = \tag{5.53}$$

$$= V + \frac{f}{T_\kappa p + 1} + \frac{T_\kappa p}{T_\kappa p + 1}\dot{\alpha}.$$

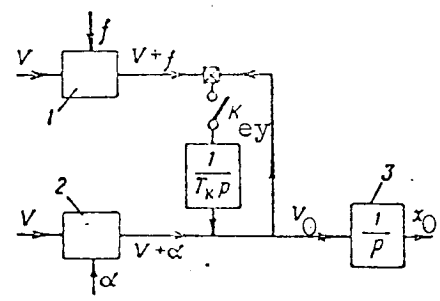

Figure 5.29. Functional diagram showing compensation of inertial system by single integration.

Expression (5.53) shows that output 3 contains a much cleaner signal of the ground speed than the one available from the acceleration integrator, because the high frequency interference is eliminated by the low frequency filter, while the slowly varying error is eliminated by the high frequency filter.

Let us compute the error in the traveled path Δx due to the inaccuracies in the inertial system when operating in conjunction with the compensating system described. If we neglect the transfer component in the compensating servosystem, we have

$$\Delta x = \frac{1}{p}\left[T_\kappa p\dot{\alpha}\right] = T_\kappa\dot{\alpha}_0 + T_\kappa\dot{\alpha}_m \sin(\omega_0 t + \varphi).$$

Thus, the error which increases linearly is absent. We have a constant component $T_k \dot{\alpha}_0 = T_k \nu_g R$ and an oscillating component with an amplitude $T_k \nu_g R$,

which is due to the deviation of the platform, and a constant component with an amplitude $T_k \beta_0 \sqrt{gR}$ due to the initial error β_0. The error due to the deviation of the platform is equal to

$$\Delta x_0 = 31 T_k \nu_g \text{ deg/hr} \cdot 10^{-3}$$

when $\nu_g = 0.1$ deg/hr and $T_k = 30$ sec, the quantity $\Delta x_0 = 93$ m. The amplitude error due to initial conditions will be

$$\Delta x_m = 0.14 T_k \beta_0^\circ \text{ км.}$$

When $\beta_0^\circ = 1^\circ/60$ and $T_k = 30$ sec, the quantity $\Delta x_m = 70$ m.

For long range flights, these errors are insignificant. This situation makes it possible to relax the requirements for the values β_0 and ν_g substantially and to apply less accurate and, consequently, cheaper inertial systems when compensation is used. The constant error Δx_0 may be eliminated completely by changing the schematic of the compensating servosystem. The signal from the Doppler sensor is first integrated and fed to the input of a double integrating servosystem, as shown in figure 5.30. One of the integrators of this system is the second integrator of the inertial system. From this diagram it is easy to /201

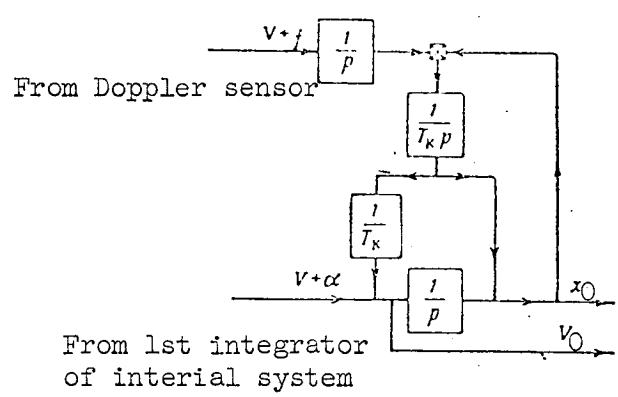

Figure 5.30. Diagram of double integral compensation of inertial system.

find the transfer function of the servosystem and to determine the values of the output signals x_0 and V_0.

The oscillating component of the error may be eliminated by damping the inertial system. By using the signal from the Doppler sensor of the ground speed, we may damp the system without disturbing the conditions which eliminate

perturbations, i.e., we can obtain a Schuler pendulum with damping. Figure 5.31 shows how the Doppler signal for the velocity is used to damp and compensate the inertial system. The damping signal is mixed with the output of the first integrator by means of a servosystem, similar to the one used for compensation (in particular, this is done to decrease the effect of interference on the circuit of the gyroscopic inertial system). It follows from the diagram shown in figure 5.31 that there is one other control circuit which can be used in addition to the one shown in figure 5.28. As in the preceding case, let us derive the expression for the transfer functions for β_g and β.

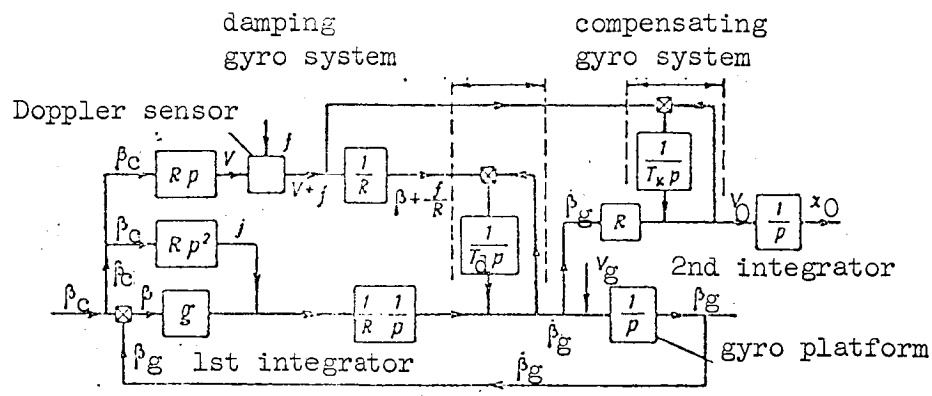

Figure 5.31. Functional diagram showing damping of inertial system.

The transfer function for β_g has the following components: a component at output 1 /202

$$\Phi_1(p)=\frac{\dfrac{T_d\omega_0^2}{(T_d p+1)p}}{1+\dfrac{T_d\omega_0^2}{(T_d p+1)p}}=\frac{\omega_0^2}{p^2+\dfrac{1}{T_d}p+\omega_0^2}; \tag{5.54}$$

(subscript d = damping);

a component at output 2

$$\Phi_2(p)=\frac{\dfrac{T_d p^2}{(T_d p+1)p}}{1+\dfrac{T_d\omega_0^2}{(T_d p+1)p}}=\frac{p^2}{p^2+\dfrac{1}{T_d}p+\omega_0^2}; \tag{5.55}$$

a component at output 3

$$\Phi_3(p)=\frac{\dfrac{p}{(T_d p+1)p}}{1+\dfrac{T_d\omega_0^2}{(T_d p+1)p}}=\frac{\dfrac{1}{T_d}p}{p^2+\dfrac{1}{T_d}p+\omega_0^2}. \tag{5.56}$$

As a result, the transfer function for β_g has the form

$$\Phi(p) = \Phi_1(p) + \Phi_2(p) + \Phi_3(p) = \frac{p^2 + \frac{1}{T_d}p + \omega_0^2}{p^2 + \frac{1}{T_d}p + \omega_0^2} = 1. \tag{5.57}$$

Thus, signal β_c is passed without distortion, i.e., in the same manner as when compensation due to the Doppler device is absent. By following the same argument, we can see that the transfer function for β will be equal to zero. Thus, the property of the inertial system of freedom of perturbation has been retained, while the equation for the free oscillations has the form

$$\ddot{\beta} + \frac{1}{T_d}\dot{\beta} + \omega_0^2\beta = 0$$

or

$$\ddot{\beta} + 2\zeta\omega_0\dot{\beta} + \omega_0^2\beta = 0,$$

where /203

$$\omega_0^2 = \frac{g}{R},\ 2\zeta\omega_0 = \frac{1}{T_d},\ \zeta = \frac{\sqrt{R}}{2T_d\sqrt{g}}.$$

The initial error will now be damped according to the law

$$\beta = \beta_0 \frac{e^{-\zeta\omega_0 t}}{\sqrt{1-\zeta^2}} \sin(\omega_0\sqrt{1-\zeta^2}\,t + \varphi),$$

where

$$\varphi = \operatorname{arc\,tg}(\sqrt{1-\zeta^2}/\zeta).$$

As we know, the optimum damping coefficient ζ is equal to $\sqrt{2}/2$. With this damping coefficient, the damping of the initial error β_0 will be lowered to 5 percent of its initial value during the half period of the natural oscillations, i.e., in this case, during a period of 42.2 min. The constant T_d for $\zeta = \sqrt{2}/2$ is equal to $\sqrt{R/2g} \approx 470$ sec. The large value of T_d means that the gain of the integrating element $1/T_d$ is small. When integrating motors are used, the small value for the coefficient $1/T_d$ is obtained when the transfer number of the reducer is high.

3. Inertial Systems of the Second Type. In systems of this type the stable platform with accelerometers remains stationary in universal space. In this connection, as the missile moves close to the surface of the Earth, the components

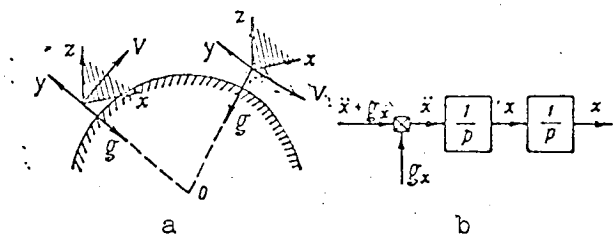

Figure 5.32. Variations in position of gyrostable platform of second type during missile motion; b, structural diagram.

of acceleration due to gravity g_x, g_y and g_z, which are sensed by the accelerometers, will vary continuously (fig. 5.32a). The readings of each accelerometer will be $\ddot{x} + g_x$; $\ddot{y} + g_y$ and $\ddot{z} + g_z$, respectively. To obtain velocity components $\dot{x}$, $\dot{y}$, $\dot{z}$ and missile coordinates x, y, z, it is necessary to eliminate components g_x, g_y and g_z from the readings of the accelerometers (fig. 5.32b).

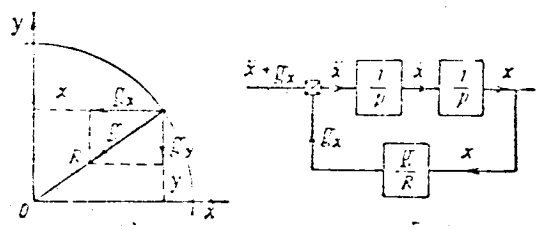

Figure 5.33. Diagram for determining missile coordinates using stable platform of second type.

These components may be computed if we know g and the coordinates x, y, z. By placing the coordinate system x, y, z at the center of the Earth (fig. 5.33a), we note that $g_x = g\,x/R$; $g_y = g\,y/R$ and $g_z = g\,z/R$. We can see that the analytical exclusion of component g_x (and similarly g_y and g_z) again leads us to a closed loop circuit with two integrating elements and a gain of $g/R = \omega_0^2$ (fig. 5.33b). Under initial deviations, the circuit again undergoes undamped oscillations with the Schuler period.

Thus, the compensation for the acceleration due to gravity in the readings of the accelerometers from the standpoint of dynamics is equivalent to the simulation of the Schuler pendulum by the stable platform with accelerometers. In this connection, all of the considerations concerning the accuracy

and compensation of inertial systems remain valid. We note that for a flight of short duration and a steep trajectory, like the one encountered in ballistic missiles or defensive missiles, we do not have to consider the variations in g_x, g_y and g_z. In this case, the integration scheme turns out to be an open loop system.

CHAPTER 6. THE HANDLING OF CONTROL SIGNALS ABOARD MISSILES /205

Section 6.1. General Information

In Chapters 3-5 we considered the methods of obtaining control signals for various methods of missile guidance. In many cases, these control signals contain noise as well as the useful component. To combat noise, special filters are used which transmit the useful signal without appreciable distortion and which eliminate noise to a large degree. As a rule, the automatic pilot of a missile is fed with several control signals. Thus, the problem of signal summation arises. In the course of summation, the specific weight of each signal is determined by the control law.

To provide for high dynamic properties and for impact accuracy, the control law incorporates signals which are proportional to the derivatives and to the integral of control signal components. Sometimes these signals, proportional to derivatives with respect to different quantities, may be obtained directly (rate gryroscope, accelerometer). If this cannot be achieved, then the signals proportional to derivatives may be obtained by differentiating the corresponding signal. Integration of some signal is achieved by various electrical or electromechanical devices. In some cases the missiles are not stabilized in space with respect to the longitudinal axis and may occupy an arbitrary position. If the control signals are sent from the ground or from an airplane, they are associated with the ground coordinate system. To utilize these signals properly aboard the missile, they must be transformed from the ground system of coordinates into a system of coordinates fixed with respect to the missile. This operation is carried out by special devices.

These problems, associated with some form of signal transformation, are considered in the present chapter.

Section 6.2. Smoothing and Filtering of Signals /206

The control signals which are fed from the sensors of the missile tracking system frequently contain harmful high frequency components in addition to the slowly varying useful component. In some cases a high frequency component may be due to some form of modulation of the control signal produced, for example, by the rotation of the radar antennas polarization plane, which is part of the missile control system. In other cases, the high frequency component is due to a combination of noise, produced by the most diverse sources in the control system. In both cases the problem arises of isolating the useful signal from a background of high frequency noise. Below we shall consider filters which reduce noises of frequencies in a definite range.

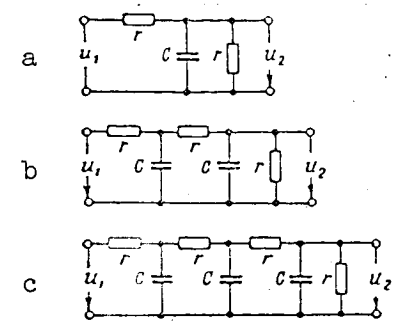

Figure 6.1. Diagrams of smoothing filters. a--single-stage filter; b--two-stage filter, c--three-stage filter.

Let us consider the simplest and most common filters which utilize RC elements. Figure 6.1 shows the schematic diagrams of smoothing filters consisting of one, two or three stages. The transfer functions of these filters have the form

single-stage filter

$$W_1(p) = \frac{1}{T_\Phi p + 2}; \tag{6.1}$$

($T_\Phi = T_{filter}$);

two-stage filter

$$W_2(p) = \frac{1}{T_\Phi^2 p^2 + 4 T_\Phi p + 3}; \tag{6.2}$$

three-stage filter

$$W_3(p) = \frac{1}{T_\Phi^3 p^3 + 6 T_\Phi^2 p^2 + 10 T_\Phi p + 4}. \tag{6.3}$$

In all of these equations, the time constant T_Φ is given by the relationship

$$T_\Phi = rc. \tag{6.4}$$

To define the characteristics of filters, we introduce the concept of transfer coefficient. The transfer coefficient is equal to the ratio of the active output sinusoidal signal to the active input sinusoidal signal. For the filters shown in figure 6.1 the transfer coefficient is given by equations /207

single-stage filter

$$k_1 = \frac{u'_{2\sim}}{u_{1\sim}} = \frac{1}{\sqrt{\mu^2 + 4}}; \tag{6.5}$$

two-stage filter

$$k_2 = \frac{u'_{2\sim}}{u_{1\sim}} = \frac{1}{\sqrt{\mu^4 + 10\mu^2 + 9}}; \tag{6.6}$$

three-stage filter

$$k_3 = \frac{u'_{2\sim}}{u_{1\sim}} = \frac{1}{\sqrt{\mu^6 + 16\mu^4 + 52\mu^2 + 16}}. \tag{6.7}$$

In equations (6.5) - (6.7) μ is the dimensionless signal frequency given by expression

$$\mu = T_{\Phi}\omega. \tag{6.8}$$

If, in equations (6.5) - (6.7) we let $\mu = 0$, we obtain the value of transfer coefficients for constant voltage. As we have already stated, the control signals aboard missiles usually consist of a useful signal due to the deviation of the missile from a given flight trajectory and a noise signal, which usually is of a higher frequency. For simplicity we shall assume that the useful signal is constant in magnitude and consider how the smoothing filter transforms the voltage consisting of a constant component and a sinusoidal component. The signal at the input to the filter is characterized by the ripple ratio, which defines the ratio of the active value of the variable voltage component to the constant component

$$q_1 = \frac{u_{1\sim}}{u_{1=}}. \tag{6.9}$$

The signal at the output of the filter is also characterized by the ripple ratio

$$q_2 = \frac{u'_{2\sim}}{u'_{2=}}. \tag{6.10}$$

The ripple ratio at the output may be expressed in terms of the ripple ratio at the input and the transfer coefficient of the filter by means of equation /208

$$q_2 = q_1 \cdot \frac{k_\sim}{k_=}, \tag{6.11}$$

where

$$k_\sim = \frac{u_{2\sim}}{u_{1\sim}}$$

and

$$k_{=} = \frac{u_{2=}}{u_{1=}}.$$

Substituting into equation (6.11) the values of the transfer coefficient of various filters, we can obtain, on the basis of expressions (6.5) - (6.7), the values of the ripple ratios at the output

single-stage filter

$$q_2 = q_1 \frac{2}{\sqrt{\mu^2 + 4}}; \tag{6.12}$$

two-stage filter

$$q_2 = q_1 \frac{3}{\sqrt{\mu^3 + 10\mu^2 + 9}}; \tag{6.13}$$

three-stage filter

$$q_2 = q_1 \frac{4}{\sqrt{\mu^6 + 16\mu^4 + 52\mu^2 + 16}}. \tag{6.14}$$

Equations (6.12) - (6.14) may be represented in brief form

$$q_2 = q_1 k. \tag{6.15}$$

Figure 6.2 shows the graph for the constant k as a function of the dimensionless frequency μ. These graphs are constructed on the basis of equations (6.12) - (6.14). Knowing the frequency of the variable component and of the ripple ratio at the input to the filter, and also the required value of the ripple ratio in the output signal, we can use the graphs in figure 6.2 to determine the necessary filter constant T_{Φ}. The calculations are carried out in the following order:

(1) from the known value q_1 and the assigned value q_2 we find the required value $k = q_2/q_1$;

(2) from the graphs in figure 6.2 we obtain the value of μ corresponding to a given k; in this case, as the value of k becomes smaller, the necessary filter scheme becomes more complex; /209

(3) knowing μ and ω, we use equation (6.8) to determine the time constant of the filter: $T_{\Phi} = \mu/\omega$.

This method of selecting the parameters of smoothing filters may be extended to passive smoothing filters of any type.

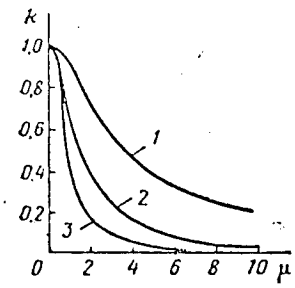

Figure 6.2. Characteristics of smoothing filters. 1--single-stage filter; 2--two-stage filter; 3--three-stage filter.

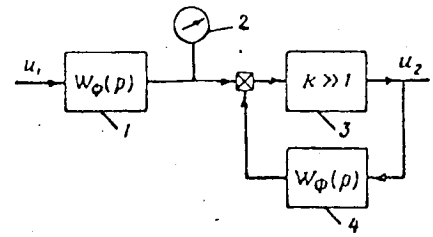

Figure 6.3. Diagram of active smoothing filter. 1 and 4--filters; 2--indicator; 3--amplifier.

In complex control systems, it is sometimes necessary to smooth a signal at a specific point in the control circuit, but in doing so, it is undesirable to introduce a time delay associated with the smoothing filter. This situation arises, for example, in systems where a human operator participates in the control of the missile. High frequency noise may produce undesirable oscillations of the instrument needle being used by the operator. By using a filter, a signal may be smoothed out quite effectively before it is fed to the indicating instrument. In order that the introduction of such a filter does not increase the delay in the control circuit, the system shown in figure 6.3 is used. The noise is reduced to a desired degree by filter 1 and the signal is fed to indicator 2. The indicator is followed by an electronic amplifier 3 with high gain k and with a feedback loop containing filter 4, analogous to filter 1. The transfer function of the entire system shown in figure 6.3 is given by expression

$$W(p) = \frac{k W_\Phi(p)}{1 + k W_\Phi(p)} = \frac{1}{\frac{1}{k W_\Phi(p)} + 1} \approx 1, \qquad (6.16)$$

i.e., for large values of k the system has no phase shift. It is obvious that as k becomes larger, equality W(p) = 1 is fulfilled more accurately. Thus, the diagram of an active filter shown in figure 6.3 solves the problem, smoothing out the signal without introducing any delay in the transmission of the signal. /210

In a series of cases, the reduction of noise contained in the control signal is simplified if sensors are available which measure directly the first and sometimes the second derivative of the control signal. Thus, for example, in controlling the flight altitude, the signal of a variometer is proportional to the first derivative with respect to altitude while the signal of a normal load factor is proportional to the second derivative.

Let us consider the operation of a smoothing filter whose input contains both the control signal and its derivatives. In the future we shall call such

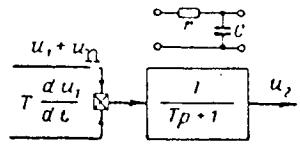

Figure 6.4. Functional diagram of operational smoothing filter with a first derivative.

filters operational. Figure 6.4 shows the schematic diagram of the simplest operational filter with one smoothing stage. The transfer function of this stage differs from the transfer function (6.1), because the free term in the numerator is reduced by half. This is explained by the fact that the load resistance of the filter is assumed to be infinitely large. The input signal of an operational filter shown in figure 6.4 consists of a useful signal u_1, its derivative and a noise signal u_n. The signal of the derivative must be introduced with a coefficient of proportionality

$$T = rc.$$

The relation between the input signal and the output signal for the diagram shown in figure 6.4 is determined by means of a differential equation

$$T\frac{du_2}{dt} + u_2 = T\frac{du_1}{dt} + u_n + u_1. \tag{6.17}$$

If the noise has a frequency ω, in the steady state the voltage at the output of the filter will be equal to

$$u_2 = u_1 + \frac{u_n}{\sqrt{(T\omega)^2 + 1}}. \tag{6.18}$$

Expression (6.18) shows that the control signal passes through this filter without distortion (this is also true for transient states), while the noise is reduced by a factor $(\sqrt{(T_\omega)^2 + 1})$. The diagram shown in figure 6.4 makes it possible to achieve the necessary smoothing, because the control signal is transmitted to the output of the filter without additional delay, and there is nothing to prevent an increase in the time constant of the filter. The principal difference between operational-smoothing filters and conventional filters is that the former provide for the smoothing of noise irrespective of the useful signal frequency, even when it is greater than the noise frequency. This is due to the derivative of the control signal obtained by an independent detector. This is, of course, not always feasible. /211

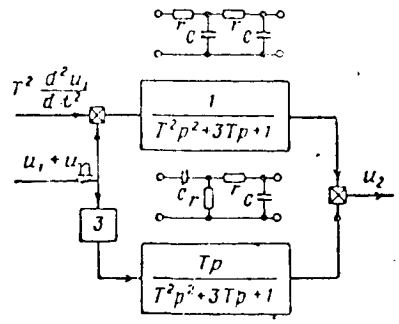

Figure 6.5. Schematic diagram of operational smoothing filter with a second derivative.

If, instead of the signal due to the first derivative, we have an independent signal proportional to the second derivative of the control signal, we may also obtain an intense attenuation of noise by using the filter shown in figure 6.5. In the steady state the voltage at the output has the form

$$u_2 = u_1 + \frac{u_n \sqrt{(3T\omega)^2 + 1}}{\sqrt{(1-T^2\omega^2)^2 + 9T^2\omega^2}}, \tag{6.19}$$

where T = rc and ω is the noise frequency.

If the noise has a definite fixed band of frequencies, it can be attenuated quite effectively by rejection filters. The filtration of the control signal, i.e., the selection of a required band of frequencies, is usually achieved by a resonant filter or a bandpass filter.

Section 6.3. Differentiation and Integration of Signals

In section 2.1 we presented two basic groups of methods used to analyze automatic control systems: methods associated with the investigation of transient processes in systems and frequency methods. As a result of this division there are also two approaches to the analysis of devices used to obtain signals which improve the stability and accuracy of automatic control systems. In the first case the analysis consists of establishing the methods and accuracies for differentiating and integrating various signals to improve the dynamic and static characteristics of the system. In the second case, similar devices are analyzed by the frequency methods and, as shown in section 2.3, the /212 effect of these devices on the general frequency characteristics of the system is considered. In the present section we shall develop both of these approaches.

1. Differentiation of Signals. If the control signals are realized in the form of a dc current, their transformation is usually achieved by the use of RC networks. Figure 6.6 shows the diagram of a differentiating network, in which the output voltage is proportional to the input voltage and to its derivative. The differential equation which relates the output and input voltages has the form

$$T_2 \frac{du_2}{dt} + u_2 = k\left(u_1 + T_1 \frac{du_1}{dt}\right), \tag{6.20}$$

where

$$\begin{aligned} T_1 &= r_1 c; \\ T_2 &= kT_1; \\ k &= \frac{r_2}{r_1 + r_2}. \end{aligned} \tag{6.21}$$

It follows from equation (6.20) that, if T_2 is equal to 0, the output voltage is proportional to u_1 and du_1/dt, which is what is required. Since the fulfillment of the condition $T_2 = 0$ is impossible, the term T_2 du/dt is added to the output voltage, causing a dynamic error in the scheme. The error will be smaller for smaller values of k, which is usually selected in the range 0.1 - 0.2. Due to this, the signal is attenuated during differentiation, which requires an amplifier following the differentiating network. We shall show how we can use a high gain dc amplifier to produce a scheme which differentiates the signal with sufficient accuracy and without signal attenuation. The schematic diagram of such an operational amplifier is shown in figure 6.7. The transfer function of this scheme has the form

$$W(p) = \frac{k}{1 + kW_f(p)} = \frac{1}{\frac{1}{k} + W_f(p)} \approx \frac{1}{W_f(p)}. \tag{6.22}$$

(subscript f = feedback).

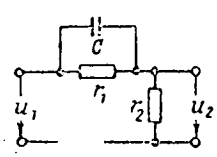

Figure 6.6. Functional diagram of differentiating network.

When a circuit with phase shift and with a transfer function $W_f(p) = \frac{1}{T_p + 1}$ is connected into the feedback loop, the scheme shown in figure 6.7 produces effective differentiation and simultaneously transmits the main signal. In this case the output signal is given by equation /213

$$u_2 = u_1 + T\frac{du_1}{dt}. \tag{6.23}$$

Since gain k of the dc amplifier may be of the order of several thousands or even several ten thousands, equation (6.23) may be realized with a high degree of accuracy.

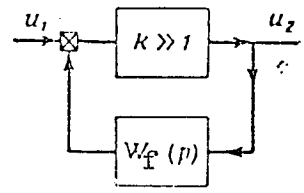

Figure 6.7. Functional diagram of operational amplifier.

In ac circuits it is also possible to obtain a derivative of the control signal. Let us assume that the control signal modulates the amplitude of a definite carrier frequency. As the sign of the control signal varies, the phase of the carrier voltage jumps through 180°. The control signal may be written in the following form

$$u = A(t)\sin\omega_0 t, \tag{6.24}$$

where ω_0 is the carrier frequency; and A(t) is the control signal.

For a sufficiently accurate reproduction of the control system, the frequency of this signal must be substantially less than the carrier frequency.

If we represent the control signal by the expression $A(t) = A \sin \omega t$, voltage u may be written in the form

$$u = A\sin\omega t\sin\omega_0 t = \frac{A}{2}\left[\cos(\omega_0 - \omega)t + \cos(\omega_0 + \omega)t\right]. \tag{6.25}$$

Expression (6.25) shows that the signal voltage is composed of two components with different frequencies. The difference of frequencies $(\omega_0 - \omega) = \Omega_1$ is known as the lower side band, while the sum $(\omega_0 + \omega) = \Omega_2$ is known as the upper side band.

The derivative of a control signal is achieved by means of a twin-T network (fig. 6.8) tuned to the frequency ω_t (tune). The output frequency of the T-network is fed to the input of the phase detector which detects the voltage with a specific phase. At the tuning frequency ω_t the circuit is closed, i.e.,

the voltage at the output of the circuit is equal to 0. Most frequently the tuning frequency is selected equal to the carrier frequency. The complex transfer function of the circuit shown in figure 6.8 may be represented in the following form

$$W(j\xi) = \frac{1}{1 + j\frac{k\xi}{1-\xi^2}}, \tag{6.26}$$

where

$$\xi = \frac{\Omega}{\omega_t}; \qquad k = \frac{\mu + nm^2}{\mu nm}; \qquad \mu = \frac{r_2}{r};$$

$$n = \frac{\frac{1}{\Omega c_2}}{\frac{1}{\Omega c_1} + \frac{1}{\Omega c_2}}; \quad m = \frac{\frac{1}{\omega_t c_1} + \frac{1}{\omega_t c_2}}{r}; \quad r = r_1 + r_2.$$

If the network is symmetric, $r_1 = r_2$; $c_1 = c_2$, i.e., $\mu = n = 1/2$; $m = 1$, /214
the frequency to which the network is tuned is given by the expression $\omega_t = 1/r_1c_1$. When $\Omega = \omega_t$, we have $\xi = 1$ and a transfer function $W(j\xi) = 0$, i.e., the network is blocked. According to equation (6.25) the signal at the input

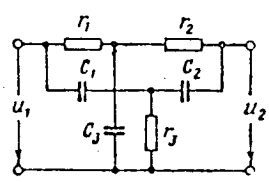

Figure 6.8. Schematic diagram of T network.

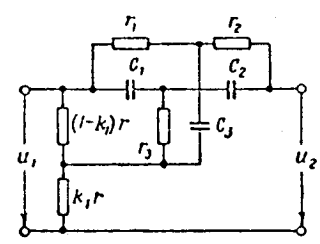

Figure 6.9. Twin-T network with voltage divider.

of the above network consists of two components with frequencies $\Omega_1 = \omega_0 - \omega$ and $\Omega_2 = \omega_0 + \omega$, respectively. Substituting the values of Ω_1 and Ω_2 into expression (6.25), we find that the transfer function for frequency Ω_1 has the form

$$W(j\Omega_1) \approx j\Omega_1 T, \tag{6.27}$$

where

$$T = \frac{2}{k\omega_t} .$$

Due to the phase sensitive detector, the signal component with frequency Ω is not transmitted. Equation (6.27) shows that the voltage at the output of the scheme is a derivative of one of the component input voltages described by equation (6.25). To obtain the sum of a signal and its derivative, it is necessary to use a twin-T network with a voltage divider (fig. 6.9) and to follow it with a phase sensitive detector. The transfer function of this network may be written in the form

$$W(j\Omega_1) = k_1(1 + j\Omega_1 T'), \tag{6.28}$$

where

$$T' = \frac{1 - k_1}{k_1} T;$$

k_1 is the attenuation coefficient.

When $k_1 \ll 1$

$$T' \cong \frac{1}{k_1} T = \frac{1}{k_1} \frac{2}{k\omega_t} .$$

If the control signal is of a mechanical nature (e.g., rotation), the derivative of this signal is obtained quite simply by means of a dc or ac tachometer generator. The tachometer generator represents a dc or ac current generator with independent excitation. The schematic diagram of a dc tachometer generator with the field winding is shown in figure 6.10. The excitation current remains constant and the output voltage u picked up by the brushes of the

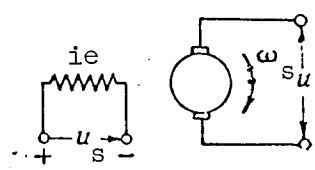

Figure 6.10. Schematic diagram of dc tachometer generator; ie = independent excitation.

tachometer generator is proportional to the angular velocity of its shaft ω_s (shaft). When the direction of rotation changes, the polarity of the output voltage also changes. The tachometer generator is attached to the shaft whose velocity of rotation is to be measured. If we neglect the transient processes

in the armature circuit of the tachometer generator, the voltage picked up by its brushes is given by equation

$$u = k\omega_s = k\frac{d\alpha}{dt}, \tag{6.29}$$

where α is the angular displacement of the tachometer generator. If we must differentiate a slowly varying electric signal, we may use a low power servosystem and transform it into the angular displacement of the servosystem shaft, and then connect this shaft to a tachometer generator by means of a gear box.

2. Integration of Signals. Figure 6.11 shows the diagram of an integrating circuit whose output voltage within certain limits of accuracy is proportional to the sum of the input voltage and its integral. The relationship between the output and input voltage of the circuit shown in figure 6.11 is determined by the following differential equation /216

$$T_2\frac{du_2}{dt} + u_2 = T_1\frac{du_1}{dt} + u_1, \tag{6.30}$$

where

$$T_1 = r_1 c \quad \text{and} \quad T_2 = (r_1 + r_2)c.$$

Integrating (6.30) from 0 to t so that when t = 0 $\dot{u}_1 = u_1 = 0$, we obtain

$$u_2 = k\left(u_1 + \frac{1}{T_1}\int_0^t u_1 dt\right) - \frac{1}{T_2}\int_0^t u_2 dt, \tag{6.31}$$

where

$$k = \frac{r_1}{r_1 + r_2}.$$

It follows from expression (6.31) that this network performs its functions with an error proportional to the integral of the output quantity. This error becomes smaller as T_2 increases compared with T_1. As in the case of the differentiating network shown in figure 6.6, the error decreases as the coefficient k decreases.

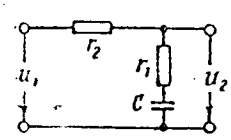

Figure 6.11. Schematic diagram of the integrating network.

By using the operational amplifier shown in figure 6.7 the error produced by the integrating network may be reduced to an insignificant value. If a capacity is placed in the feedback network of this amplifier, the voltage at the output will be given, very accurately, by expression

$$u_2 = \int_0^t u_1 dt. \tag{6.32}$$

The operating range of an integrating amplifier is limited by the nonlinearity of its characteristics. If, in addition to the integral of the input signal we must obtain the signal itself at the output, then the feedback network of the amplifier must include a differentiating network, shown schematically in figure 6.6.

The ac signal is integrated by an amplifier with a feedback loop containing a twin-T network (fig. 6.8). The equivalent complex transfer function of such an operational amplifier may be represented with a high degree of accuracy

$$W(j\Omega_1) = \frac{1}{j\Omega_1 T}. \tag{6.33}$$

The integration of slowly varying signals is frequently accomplished by /217
means of an integrating dc or ac motor. The velocity of rotation of such motors must be a linear function of the applied signal voltage over a wide range. To reduce the zone of insensitivity of the integrator, the starting voltage of the motor must be as low as possible. Figure 6.12 shows the schematic diagram of an integrating dc motor. The motor with independent excitation rotates due to signal voltage u_1 which must be integrated. The shaft moves a reducing gear and displaces the brush of the potentiometer which picks up output voltage u_2, approximately equal to the integral of input voltage u_1. The differential equation of motion for the dc motor with independent excitation has the form

$$T_M \frac{d^2\alpha}{dt^2} + \frac{d\alpha}{dt} = k_m u_1, \tag{6.34}$$

where T_M is the electromechanical time constant; k_m (meter) is the amplification factor of the motor, and α is the angular displacement of the motor shaft.

If we neglect the time constant of the motor, which is permissible when the variation in the signal voltage u_1 is slow, the angular displacement of the motor shaft is given by the following expression (on the basis of equation (6.34))

$$\alpha = k_m \int_0^t u_1 dt. \tag{6.35}$$

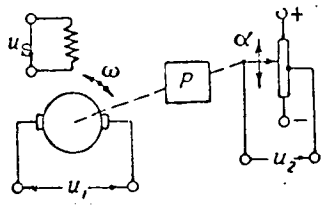

Figure 6.12. Diagram of integrating dc motor.

Since the angular displacement of the motor shaft and the voltage are proportional to each other, we finally have

$$u_2 = k \int_0^t u_1 dt. \tag{6.36}$$

The range of the integrator with the motor is limited by the angular displacement of the brush in the output potentiometer. /218

To integrate the angular velocity of rotation of a missile with respect to its center of gravity, integrating gyroscopes are used whose principle of operation was considered in Chapter 4. In this section we consider the physical and mathematical principles of simple differentiating and integrating devices. In actual systems, particularly those with dc control signals, the dynamic properties of these systems are improved by means of rather complex combinations of simple networks. Such combinations of differentiating and integrating networks are known as compensating circuits. A summary of diagrams and characteristics of compensating networks is given in table 2.5.

Section 6.4. Summation of Signals

As pointed out in section 6.1, the signal which is transferred to the actuator of control surfaces of a missile is usually the sum of signals from various sensors in the control system. The control system network performing the summation of several signals is called the summator. These signals are added algebraically in the summator, and there should be a provision for varying the strength of each signal over a wide range. The types of summators depend on the physical nature of the signals. In electric control systems, summation is accomplished by means of special circuits as well as by means of magnetic amplifiers.

Figure 6.13 shows a scheme for summation which uses resistors. This scheme makes it possible to add several voltages u_1 ..., u_n, each of which is proportional to a corresponding signal.

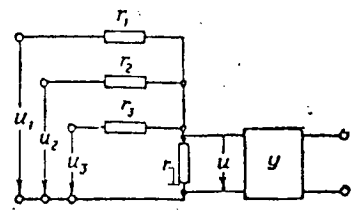

Figure 6.13. Schematic diagram showing summation by means of resistors; subscript 1 = load.

The total voltage is picked up across the resistance r_1 (load). Resistances $r_1, \ldots, r_n$ are called input resistances. If we write a system of equations for this scheme and solve it with respect to output voltage u, we find

$$u = \sum_{i=1}^{n} k_i u_i, \tag{6.37}$$

where

$$k_i = \frac{r_1}{r_i\left[1 + r_1 \sum_{i=1}^{n} \frac{1}{r_i}\right]}. \tag{6.38}$$

By varying resistances r_1 we can obtain the necessary coefficient in front /219 of each component. The disadvantage of this scheme is that a portion of signals k_i depends on all of the resistances of the scheme, equation (6.3). Therefore, a variation in any of these resistances produces a variation in all coefficients k_i. This shortcoming may be eliminated in practice if all of the input resistances are selected so that they are greater than the load resistance. In this case $r_1 \sum_{i=1}^{n} \frac{1}{r_i} \ll 1$ and expression (6.38) may be represented in the form

$$k_i \approx \frac{r_1}{r_i}. \tag{6.39}$$

We note that when condition $r_1 \sum_{i=1}^{n} \frac{1}{r_i} \ll 1$ is satisfied there is a decrease in all of the component signals, so that after a summator of this type we must use an amplifier, shown in figure 6.13. This scheme for adding electric signals is suitable both for dc and ac currents.

If a magnetic amplifier is present in the control system, it is rational to use it as a summator of control signals. Depending on the number of signals which must be added, the magnetic amplifier must contain the same number of control windings. The advantage of a magnetic amplifier consists of the possibility of adding signals which are taken from sensors electrically coupled, because the control windings are insulated from each other. The disadvantage of adding signals by means of a magnetic amplifier is the presence of delay in the reproduction of the input signals. A more detailed consideration of the magnetic amplifier will be conducted in the following chapter.

In missile control systems it is sometimes necessary to add signals which represent mechanical displacements of some elements of the sensors. Sensors for the position and angular velocity of a missile (gyroscopes), the sensors of velocity head, integrating motors, etc., produce output signals which have the form of angular or linear displacement. To add such signals, various bridge schemes are used. /220

As an example, figure 6.14 shows a bridge scheme with two bridges for adding three signals. If more signals are to be added, the number of bridges in the scheme must increase. The mechanical displacements x_1, x_2 and x_3 are transmitted to the brushes of three potentiometers r. The fourth potentiometer with a middle point is used to null all schemes. In the given scheme, all of the potentiometers are identical. The rheostats r_1 are used to control the bridge schemes. The displacement of the sliding arms of rheostats r_1 in different directions changes the proportion of the added signals. If the scheme does not

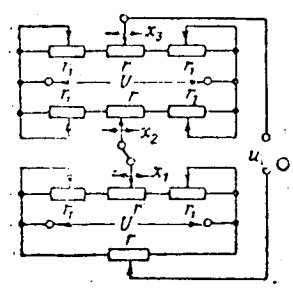

Figure 6.14. Schematic diagram of summation by bridge schemes; subscript o = output.

require this control during its exploitation, the proportion of signals may be established by varying the lengths of potentiometers r, while the null point is displaced by the mechanical movement of sliding arms with respect to their center point and it is not necessary to have rheostats r_1. The output voltage of the scheme is equal to the sum of voltages picked up by each of the sliding arms with respect to the middle point of the lower potentiometer:

$$u_0 = u_1 + u_2 + u_3. \tag{6.40}$$

Each of the added voltages in turn is determined by equation

$$u_i = \frac{rU}{r + 2\alpha_i r_1}\left[\frac{x_i}{l} + 2\frac{r_1}{r}\beta_i\right], \tag{6.41}$$

where x_i is the displacement of the sliding arm of the i-th potentiometer with respect to the middle point; l is the total linear or angular length of the potentiometer; α_i is part of the rheostat resistance r_1 introduced into the scheme when the sliding arms are displaced opposite directions, and β_i is part of the rheostat resistance r_1 introduced into the scheme when the sliding arms are displaced in the same direction.

The coefficient α_i is a substantially positive quantity, while coefficient β_i, depending on the direction of displacement of the sliding arms, may be positive or negative. Equation (6.41) shows that by varying the value of α_i we can vary the proportion of each signal within a wide range. The magnitude and sign of the null displacement of the potentiometer depends on coefficient β_i. This /221 displacement is determined by the voltage taken from the potentiometer when its sliding arm is at the middle point ($x_i = 0$).

Section 6.5. Transformation of Coordinates

In some cases it is necessary to transform control signals obtained in one system of coordinates into control signals corresponding to the position of the missile in another system of coordinates. As an example we may consider missiles guided by a radio beam. The control signal is obtained aboard the missile and is determined by the position of the missile's center of gravity, with respect to a system of coordinates fixed to the radar control point. When the missile rotates with respect to the longitudinal axis, the control signals must vary as functions of the tilt angle.

Figure 6.15 shows the mutual position of the coordinates: y_g, z_g are Earth axes, fixed with respect to the radar at the control point and y_1, z_1 are axes fixed with respect to the missile. The angle γ is the tilt angle of the missile. The vector showing the mismatch in the center of gravity of the missile with respect to the axis of the equisignal zone is shown by the corresponding voltage

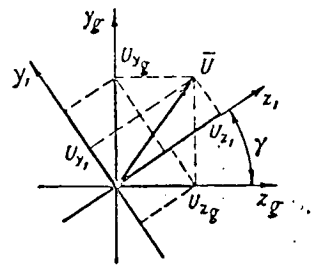

Figure 6.15 Projection of vector in two coordinate systems.

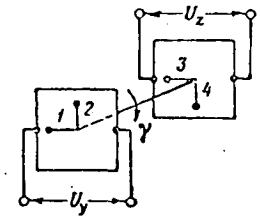

Figure 6.16. Schematic of device for transforming coordinates. 1, 2, 3, and 4--brushes.

vector of control signal $\bar{u}$. On the missile this voltage is measured as the projection of the voltage vector on the axis of the Earth coordinate system. To control the missile, it is necessary to transform them to system y_1, z_1. The relation between the projections of the vector in the two systems is given by the following expression

$$\left.\begin{aligned} u_{y_1} &= u_{yg}\cos\gamma - u_{zg}\sin\gamma, \\ u_{z_1} &= u_{zg}\cos\gamma + u_{yg}\sin\gamma. \end{aligned}\right\} \qquad (6.42)$$

To realize the transformation of signals given by expressions (6.42), we can use sine-cosine potentiometers (fig. 6.16). Most frequently these potentiometers have the form of ceramic plates covered with a thin layer of metal. To minimize brush friction, the metalized surface must be very smooth. To carry out the transformation of signals in accordance with equation (6.42), it is necessary to have two potentiometers, each with two brushes. The plates of the potentiometers are fixed to the frame of the missile, while the brushes are fixed to the frame axis of the position gyroscope. The signals u_{yg} and u_{zg} generated by the sensor aboard the missile are fed to the potentiometers shown in figure 6.16. When the missile is rotated with respect to the longitudinal axis by a tilt angle, the following signals are taken from the middle points of the potentiometers and from each of the brushes /222

brush 1--$U_{yg}\cos\gamma$,

brush 2--$U_{yg}\sin\gamma$,

brush 3--$U_{zg}\cos\gamma$,

brush 4--$U_{zg}\sin\gamma$.

By adding these signals we obtain the transformed control signals u_{y1} and u_{z1}.

CHAPTER 7. AMPLIFIERS AND ACTUATORS USED IN MISSILE GUIDANCE SYSTEMS /223

Section 7.1. Magnetic Amplifiers

Due to their high reliability, magnetic amplifiers are widely used in missile guidance systems. The input signal is introduced into the magnetic amplifier in the form of a dc current, while the output amplified signal is obtained as an ac current. At the present time three types of magnetic amplifiers are used: differential, bridge and transformer.

Figure 7.1 shows the schematic of a differential amplifier. The signal is fed to the control winding W_y which encompasses two cores. The same cores are wound with biasing windings W_b (bias). The biasing windings and the control windings are connected in such a way that the magnitizing forces which they produce with a signal of given polarity are added in one pair of ferromagnetic cores and subtracted in the other pair. The output signal u_2 is taken from the load impedance Z_1, which is installed between the middle point of the feeding transformer T and the ac current winding $W_\sim$ of both pairs of cores. When $u_1 = 0$, both pairs of cores of the amplifier are magnitized by the same amount, and the inductance of the ac windings is also the same. The currents in these windings are equal, and the voltage across the load impedance is equal to zero. When $u_1 \neq 0$, the magnetization in one pair of the cores is increased, while in the second pair it is decreased. A current flows through the load impedance. When the sign of the input voltage u_1 changes, the phase of the output voltage u_2 shifts by 180°.

Figure 7.2 shows the variation in the current through the load impedance as a function of the control current in a magnetic amplifier. The excitation currents are selected in such a way that the characteristics of the amplifier have a maximum steepness. This steepness determines the current amplification factor $k_i = dI_2/dI_1$. In cases where the element of the control system which receives a signal from the output of the magnetic amplifier must be fed with a dc current, a scheme with rectification is used, as shown in figure 7.3. The disadvantage of this scheme is the presence of additional resistances r_a (additional), which decrease the power amplification. In the scheme of figure 7.3 these resistances /224

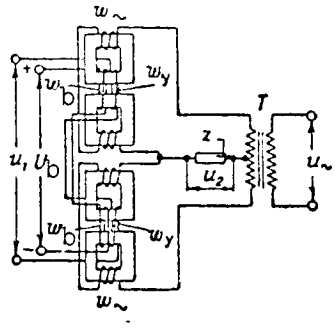

Figure 7.1. Schematic diagram of a differential amplifier.

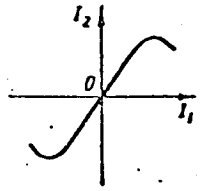

Figure 7.2. Characteristic curve of magnetic amplifier.

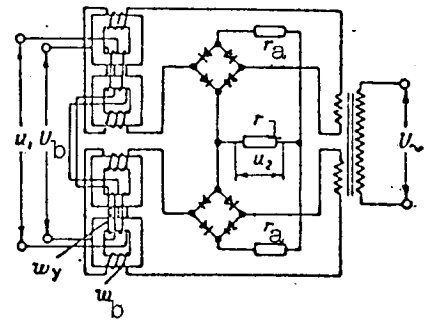

Figure 7.3. Schematic diagram of differential magnetic amplifier with dc current output.

are necessary, because when they are absent the rectifying bridges shunt the load resistance and only a small portion of the rectified current will flow in this resistance. To eliminate the shortcoming in the scheme shown in figure 7.3, which is associated with the presence of resistance r_a, it is necessary that the element powered by the amplifier have two identical and isolated windings. Then the subtraction of output currents may be replaced by the subtraction of magnetic fluxes in the power element, and it becomes unnecessary to have resistances r_a.

The differential scheme of a magnetic amplifier is most convenient for introducing positive current feedback, which causes an increase in the gain. To achieve feedback it is necessary to rectify the ac current in the load and transmit it through the feedback winding W_f which is wound on the same core as the control winding. This current produces an additional excitation of the core, so that the same value of load current is obtained with a smaller control current.

Let us consider the dynamic properties of a magnetic amplifier. Since the number of windings and consequently the inductance of the ac winding is small, we

may assume that the current at the output of the amplifier is proportional to the control current and experiences practically no delay. However, due to the large inductance of the control winding, the control current i_1 always lags behind voltage u_1. The relationship between the control winding and the signal voltage is given by the equation

$$L_y \frac{di_1}{dt} + r_y i_1 = u_1, \tag{7.1}$$

where L_y, r_y are the inductance and resistance of the control winding, respectively.

The output current I_2 is proportional to the current i_1 and, consequently, the output voltage is also proportional to i_1

$$u_2 = I_2 r_1 = k_i r_1 i_1. \tag{7.2}$$

If in equation (7.1) we substitute the value of the current i_1 from (7.2), we obtain

$$T \frac{du_2}{dt} + u_2 = k u_1, \tag{7.3}$$

where $T = \frac{L_y}{r_y}$ is the time constant of the magnetic amplifier

$$k = r_1 k_i \frac{1}{r_y}.$$

The solution of equation (7.3) for zero initial conditions and with u_1 = const has the form

$$u_2 = k u_1 \left(1 - e^{-\frac{t}{T}}\right). \tag{7.4}$$

Thus, when voltage jump u_1 appears at the input to the amplifier, output voltage u_2 varies according to the exponential law with time constant T. The time constant may be expressed in terms of the power gain by equation

$$T = \frac{k_W}{4f}, \tag{7.5}$$

where k_W is the power gain; and f is the frequency of the ac current in cps.

Expression (7.5) shows that with a given power gain the time constant of a magnetic amplifier and, consequently, the lag which it introduces in the transmission of signals, may be decreased only by increasing the frequency of the ac current. A magnetic amplifier may have several control windings. The simplicity of adding signals by placing several control windings is one of the basic advantages of a magnetic amplifier compared with a vacuum tube amplifier. /226

Section 7.2. Vacuum Tube and Semiconductor Amplifiers

1. Vacuum Tube Amplifiers. Vacuum tube amplifiers are used in control schemes as well as in the magnetic amplifiers. They must have an odd characteristic for the relationship between the output voltage and the input voltage. This requirement is satisfied by the push-pull schemes. An example of such a scheme is the dc bridge amplifier shown in figue 7.4. Tubes L_1 and L_2 and the resistances r_a make up a bridge with the plate voltage U_a applied to one of the arms. The second arm has the load resistor r_1. If the parameters of the tube are the same and the input voltage is equal to zero, the currents in the tubes are equal, and the output voltage is also equal to zero. When an input voltage appears, the grid of one tube is positive, while the grid of the other tube becomes negative. The currents in the tubes will be different, the bridge becomes unbalanced and a current appears in the load. When the polarity of the input voltage is changed, the polarity of the output voltage also changes.

Balanced systems are characterized by improved stability in the drift of the null point. The null drift of an amplifier occurs due to a variation in the plate supply voltage, in the heater current, and in the tube parameters when the temperature varies, etc. In a balanced scheme, the drift produced by external factors, which have the same effect on both tubes, will be compensated because the output voltage is determined as a difference of the plate currents of the tubes. Because the characteristics of the tubes are not exactly the same, external factors will, nevertheless, produce some drift in the null point. A drift in the null point of an amplifier is equivalent to a false signal at the input of the amplifier and is a serious shortcoming of the dc amplifier. To decrease it, it is possible to use negative feedback, although this decreases the gain of the amplifier.

An example of an amplifier with substantial feedback is the cathode follower, in which the load resistance is connected into the cathode circuit (fig. 7.5). The voltage gain of a cathode follower is always less than unity, while the current gain and the power gain may be quite large. Therefore, cathode followers are used basically as stable power amplifiers. The characteristic of the cathode follower shown in figure 7.5 is even. To obtain an odd characteristic, it is /227 necessary to use cathode followers in a balanced scheme.

To amplify an ac voltage, whose phase varies by 180° when the sign of the control signal changes, phase sensitive ac tube amplifiers are used. A dc voltage is obtained at the output of the amplifier whose value is proportional to the input ac signal and whose polarity is determined by the phase of the input voltage.

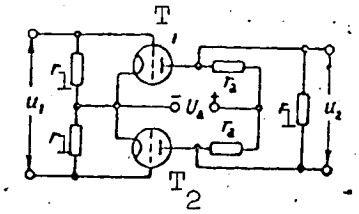

Figure 7.4. A dc bridge amplifier; T = tube.

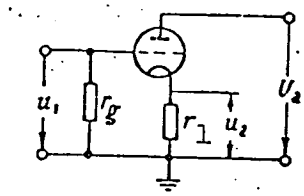

Figure 7.5. Cathode follower.

Figure 7.6 shows the schematic of a phase sensitive amplifier. When there is no input signal ($u_1 = 0$) the plate circuits of the tubes have pulsating currents whose average values are equal.

Currents through the tubes flow only when the plate voltage is positive. Because the average values of the plate currents are equal, the value of the voltage across the load resistance is equal to zero. The phases of the voltage on the grids of the tubes are opposite. If the phase of the input signal at the grid of one tube coincides with the phase of the plate voltage, the grid voltage of the other tube will be out of phase with the plate voltage. Therefore, the average value of the current in the first tube will increase, while in the second tube it will decrease, and a difference in the average values of plate currents will appear. The output voltage will be proportional to this difference. When the input voltage increases, the difference between the currents will increase and consequently, the voltage at the output will also increase. The input /228 signal which is fed to a phase sensitive amplifier must be obtained in a scheme which has the same power supply as the amplifier. Only in this case will there be the necessary phase relationship between the grids and the plates of the tubes.

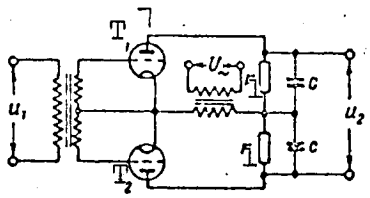

Figure 7.6. Phase sensitive amplifier with plate supply in phase.

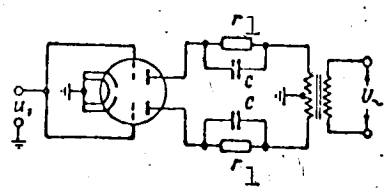

Figure 7.7. Phase sensitive amplifier in which plates are powered out-of-phase.

Figure 7.7 shows another diagram of a phase sensitive amplifier. Unlike the scheme shown in figure 7.6, in this amplifier the phases of the voltages on the grids of both tubes are the same, while the phases of the voltages on the plates are opposite. The principle of operation of such an amplifier will be the same as that shown in figure 7.6.

The dynamic properties of vacuum tube amplifiers are very high and it can be assumed that in a missile guidance system they introduce no phase shift.

2. Transistor Amplifiers. Transistors may be connected as low frequency amplifiers in three different ways from the standpoint of input and output connections. Figure 7.8 shows the schematic of an amplifier with a common base. Such amplifiers have an input impedance much less than the output impedance. They have a current gain equal to unity, but a large voltage gain. The common emitter circuit (fig. 7.9) is more advantageous because, in this case, the current gain and the voltage gain are approximately equal and of substantial value. The advantage of this scheme is the higher input impedance and the lower output impedance. The scheme with a common collector (fig. 7.10) is analogous to a cathode follower. The voltage amplification of the scheme is slightly less than

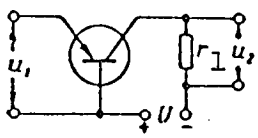

Figure 7.8. Amplifier with common base.

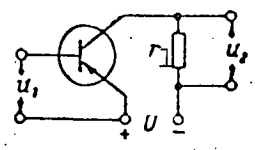

Figure 7.9. Amplifier with common emitter.

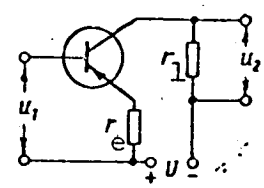

Figure 7.10. Amplifier with common collector.

unity. The input impedance depends considerably on the resistance r_e in the emitter circuit and may vary from hundreds of ohms to a fraction of an ohm. The output impedance depends on the source impedance of the signal. The advantage of the scheme is that the gain depends little on the collector voltage and on the variation in the parameters of the transistor.

The drift of the zero point for transistors is much greater than for vacuum tubes. To stabilize the parameters of the amplifier, it is necessary to introduce negative feedback, which decreases the gain. Figure 7.11 shows the diagram of a bridge amplifier. The diagram of a phase sensitive amplifier using transistors is shown in figure 7.12. The signals fed to the bases are out-of-phase while the collectors are fed in-phase. The use of a rectifier prevents the direct current from passing through the transistor. When the input signal is absent, the currents in the load resistances are equal to zero.

If the input voltage is not equal to zero, the voltage on the base of one transistor is in phase with the supply voltage, while on the base of the other transistor it is out-of-phase. In this case, a current pulse appears in the circuit of the first collector, while the second collector does not conduct. The average value of the current will be proportional to the input voltage. When the phase of the input voltage changes by 180°, the current will pass through the second collector, which will cause a change in the polarity of the output voltage.

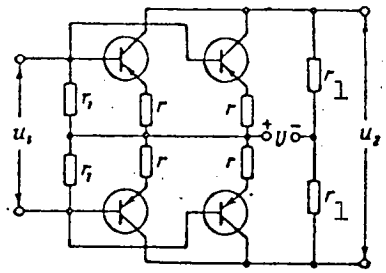

Figure 7.11. Bridge amplifier using transistors.

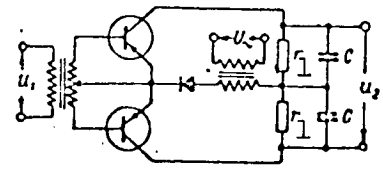

Figure 7.12. Diagram of phase sensitive amplifier using transistors.

Section 7.3. Actuators with Electric Motors

After the necessary transformation of the control signals and after their power amplification, these signals will act on the actuators aboard the missile. The actuators displace the control elements. Missiles usually utilize three types of actuators: with electrical motors, hydraulic motors and pneumatic motors. Recently, actuators have appeared which use powder gases. The present section considers acutators of all types except those using powder gases.

The dc electric motors with independent excitation and two-phase asynchronous motors are used to drive control surfaces. The application of an electric motor is convenient from the standpoint of supplying it with energy, as well as from the standpoint of exploiting a missile guidance system. /230

1. Actuator Using a dc Motor with Independent Excitation. The schematic diagram of this actuator is shown in figure 7.13. The armature A of the motor drives the control surface through a gear reduction box P. The excitation winding EW carries a dc current of magnitude I_e. The velocity of rotation is controlled by varying the voltage U which is fed to the armature A of the motor from some amplifier. The static characteristics of the motor are determined by its external characteristics, i.e., the variation in the torque as a function of angular velocity. A family of such characteristics for different values of voltage applied to the armature are shown in figure 7.14. These characteristics do not take into account the reaction of the armature and are therefore approximate.

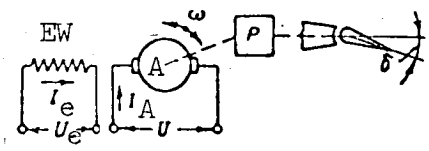

Figure 7.13. Schematic diagram of actuator with dc motor.

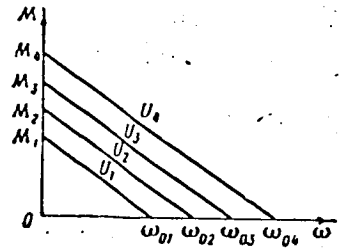

Figure 7.14. External characteristics of dc motor with independent excitation.

Let us consider the dynamic characteristics of a drive using a motor with independent excitation. On the basis of Newton's Second Law, the equations of motion for the armature of a motor can be written in the form

$$J\frac{d\omega}{dt}=M_M+M_L, \tag{7.6}$$

where J is the moment of inertia of the moving parts; M_M (motor) is the torque developed by the motor, and M_L is the load moment.

The basic component of the moment of inertia is the moment of inertia of the armature, because the moment of inertia of the remaining moving parts is reduced to the shaft of the motor with a coefficient inversely proportional to the square of the transfer coefficient of the speed reducer, which usually varies from 200 to 1,000. The load moment is composed of the friction moment in the reducer and of the damping and hinge moments of the control surface. To decrease the hinge moment, the control surface is suspended in such a way that the aerodynamic pressure center, which acts on the control surface, is as close as possible to the axis of rotation. The damping moment and the friction moment are usually less than the hinge moment. Proceeding from these considerations, we shall neglect the load moment in equation (7.6) to make the presentation easier. The rotating moment M_M developed by the motor with independent excitation is given by the expression /231

$$M_M=k\Phi I_A, \tag{7.7}$$

where Φ is the magnetic flux of the excitation winding, and I_A is the armature current.

To clarify the variation in the armature current I_A as a function of control voltage U and of the parameters of motion, we consider Kirchhoff's for the

Second Law for the armatured circuit of the motor, which is written without taking into account the small inductance of the armature

$$I_A r_A + E = U, \tag{7.8}$$

where r_A is the resistance of the armature winding, and E is the counter emf of the armature due to its rotation in the magnetic field of the excitation winding.

The counter emf of the armature is given by the following equation

$$E = c\omega\Phi, \tag{7.9}$$

where ω is the angular velocity of the armature, and c is a coefficient determined by the structural parameters of the motor.

Using equations (7.8) and (7.9) and substituting the values of I_A and E into equation (7.7) we obtain

$$M_M = \frac{k_i}{r_A} U - \frac{k_i k_E}{r_A} \omega, \tag{7.10}$$

where

$$k_i = k\Phi \quad \text{and} \quad k_E = c\Phi.$$

Equation (7.10) may be written in a different form

$$M_M = M_k - \frac{M_k}{\omega_0} \omega, \tag{7.11}$$

where $M_k = \frac{k_i U}{r_A}$ is the starting torque developed by the motor when the armature /232 is at rest, and $\omega_0 = \frac{U}{k_E}$ is the ideal idling speed, i.e., the velocity of the motor when the load moments are absent.

Equation (7.11) is an analytical expression for the family of characteristics shown in figure 7.14. Substituting the value of M_M from equation (7.11) into equation (7.6), setting $M_L = 0$ and carrying out elementary transformations, we find the equation of motion for the armature of the motor

$$T_M \frac{d\omega}{dt} + \omega = k_M U, \tag{7.12}$$

where $T_M = \frac{J\omega_0}{M_k}$ is the time constant of the motor, and $k_M = \frac{1}{k_E}$ is the gain of the motor.

For a low power motion the time constant is a few one hundredths of a second.

The output quantity of the actuator is the angle of rotation of the control surface. The relationship between the velocities of rotation of the armature and of the control surface is obvious

$$\omega = i\frac{d\delta}{dt}, \tag{7.13}$$

where i is the transfer ratio of the speed reducer.

Substituting the value of ω, given by expression (7.13) into equation (7.12), we obtain a differential equation for the entire drive

$$T_d\frac{d^2\delta}{dt^2} + \frac{d\delta}{dt} = k_d U, \tag{7.14}$$

where $T_d = T_M$ is the time constant of the drive, and $k_d = \frac{k_M}{i}$ is the gain of the drive.

On the basis of equation (7.14) we find the transfer function of the drive

$$W_d(p) = \frac{k_d}{(T_L p + 1)p}. \tag{7.15}$$

(subscript d = drive).

2. An Actuator with a Two-Phase Asynchronous Motor. Two-phase asynchronous motors of low power are used as drivers in control systems. Such a motor incorporates a short-circuited rotor or a hollow rotor with thin walls. A schematic diagram of an actuator with a two-phase motor is shown in figure 7.15. The stator of the motor has two windings--the excitation winding and the control winding. The excitation winding is fed from a phase-shift circuit or through a condensor c directly from the ac source. The control voltage is supplied to the control winding W_y. The magnitude of this voltage and the sign of its phase vary in accordance with the magnitude and sign of the control signal. Thus, the currents in the two windings are shifted in phase with respect to each other by 90°. In addition to this, the axes of the windings in space are also perpendicular. Under these conditions, the windings on the stator produce a rotating magnetic field. This field induces currents in the shorted rotor or in the hollow rotor. The interaction of the field due to the induced currents with the rotating field produces the driving torque. A change in the /233

phase of the current in the control winding by 180° changes the direction of rotation of the motor.

Figure 7.16 represents a family of external characteristics for a two-phase motor for different values of the control voltage U_y. In a rather large range of angular velocities the variation in the moment and in the velocity of rotation is linear as in the case of the dc motor.

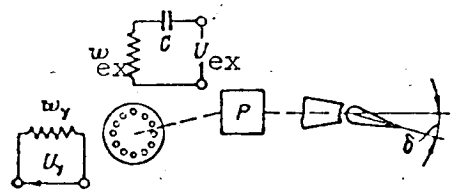

Figure 7.15. Schematic diagram of actuator with two-phase asynchronous motor; subscript ex = excitation.

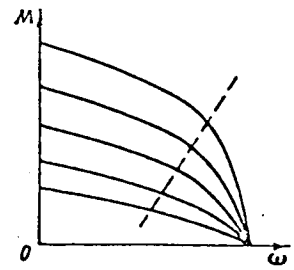

Figure 7.16. External characteristics of two-phase asynchronous motor.

The equation for the actuator using the same assumptions will obviously have the same form as equation (7.14) for a mechanism with a dc motor.

Section 7.4. Hydraulic Actuators /234

Hydraulic actuators are used in the control systems of airplanes and missiles. One of the advantages of a hydraulic system is the large force which can be applied to a unit moving mass compared with that which can be applied by means of an electric motor. The latter situation in turn provides for the rapid operation of a hydraulic actuator. The constructions of hydraulic actuators are quite diverse, but the most common actuator is of the piston type with a distribution value. Figure 7.17 shows the schematic diagram of a hydraulic actuator. The working fluid is pumped into the central channel of a distribution box, and when the valve is displaced from its middle position, it enters the respective cavity of the operating cylinder. The other cavity of the operating cylinder becomes connected with the overflow tank. The resulting pressure difference causes the piston to move and to rotate the control surface of the missile.

Let us derive the equation of motion for the piston. Let us assume that the valve has been displaced from its neutral position to the right by a distance y. Then the fluid will flow through the slit into the cavity to the right of the piston and will flow out of the cavity to the left of the piston. The volumetric consumptions Q_1 and Q_2 of the fluid through the input and output openings of the valve per unit time are given by expressions

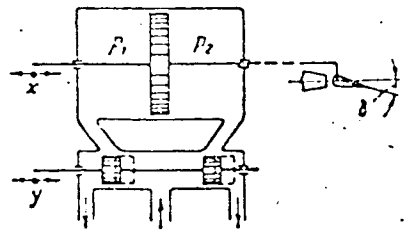

Figure 7.17. Schematic diagram of a hydraulic actuator.

$$\left.\begin{aligned} Q_1 &= \xi b y \sqrt{p_1 - p_0}\,; \\ Q_2 &= \xi b y \sqrt{p_0 - p_2}\,, \end{aligned}\right\} \tag{7.16}$$

where ξ is the consumption coefficient; b is the width of the window at the input and at the output[1]; p_1 and p_2 are the fluid pressures at the input and the output; p_0 is the fluid pressure in the cavities of the cylinder, and y is the displacement of the valve.

From the condition for the continuity of fluid flow we have /235

$$Q_1 = Q_2 = Q. \tag{7.17}$$

Since Q_1 is equal to Q_2, the right sides of equation (7.16) are equal

$$p_1 - p_0 = p_0 - p_2 \quad \text{or} \quad p_0 = \frac{p_1 + p_2}{2}. \tag{7.18}$$

Substituting the value of p_0 into the first equation (7.16), we obtain

$$Q = \xi b y \sqrt{\frac{p_1 - p_2}{2}}. \tag{7.19}$$

---

[1] The shape of the valve window is assumed to be rectangular. The width of the valve shoulder is equal to the width of the window.

The volumetric consumption per unit time through the valve window is equal to the volumetric consumption in the cavity of the operating cylinder when the piston is displaced. This equality is expressed by the following obvious equation

$$Q = S\frac{dx}{dt}, \tag{7.20}$$

where S is the area of the piston, and x is the displacement of the piston.

By substituting into equation (7.20) the value of the consumption per unit time from (7.19), we obtain the final expression for the characteristics of the hydraulic actuator

$$\frac{dx}{dt} = k_h y, \tag{7.21}$$

(subscript h = hydraulic),

where $k_h = \frac{\xi b \sqrt{p_1 - p_2}}{\sqrt{2}\, S}$ is the amplification factor of the hydraulic actuator.

The angular displacement of the control surface differs from the linear displacement of the piston only by the transfer number i, which depends on the geometric relations in the transformation system of these motions. Therefore, the equation for the entire hydraulic drive has the form

$$\frac{d\delta}{dt} = k_{hds} y, \tag{7.22}$$

(subscript hds = hydraulic driving system),

where

$$k_{hds} = \frac{k_h}{i}.$$

Equation (7.22) is the analytic expression for the static characteristics of a hydraulic drive. These characteristics are shown in figure 7.18 (broken line), taking into account the limitation in the displacement of the valve due to the width of the window. When the windows of the valve are completely open, piston has maximum velocity. The actual characteristics have a "dead zone," because the collars of the valve are made somewhat wider than the windows. These characteristics are shown in figure 7.18 by a solid line. A construction of this type makes it difficult to adjust the valve when the dimensions of the windows and of the collars are the same. In some cases the collars of the valve are narrower than the windows. In this case the "dead zone" is absent, but fluid is consumed all the time. /236

On the basis of equation (7.22) the transfer function of a hydraulic drive has the form

$$W_{hds}(p) = \frac{k_{hds}}{p}. \tag{7.23}$$

We note that in deriving equation (7.22) we made the following assumption: we did not take into account the inertia of the fluid and of all moving parts connected to the piston, nor did we take into account the external forces applied to the coupling rod--the hinge moment and the forces of friction.

If we take into account the inertia of the moving parts, then the piston will not achieve its velocity instantaneously when the valve is displaced, as stipulated by equation (7.22). The velocity will build up with some delay, and the equation and the transfer function of the hydraulic drive will take on the same form as the drive with an electric motor, equations (7.14) and (7.15). However, the time constant T_{hds} for the hydraulic drive is very small and it usually is neglected.

Section 7.5. Pneumatic Actuators

Pneumatic actuators are widely used in missile control systems. The use of a compressed gas as a source of energy is convenient in the missile guidance systems, when the flight time to the target is short. The compressed gas is contained in cylinders under pressure, and when the control system is turned on, it is passed through a pressure regulator and used to actuate the control elements of the missile.

There are two versions of a pneumatic actuator: one with distribution valves and the other with a jet tube. The schematic diagram of a pneumatic actuator, in which the flow of the gas is controlled by valves, is analogous to the diagram of the hydraulic actuator, shown in figure 7.17. The deflection y of the valve produces a pressure difference on the piston and the latter is displaced.

The schematic diagram of a pneumatic actuator with a jet tube is shown in figure 7.19. When the jet tube is in the middle position, the pressure on both sides of the operating cylinder is the same and it remains at rest. When the end of the jet tube is displaced by an amount y, pressure equilibrium is disturbed and the piston is placed into motion. Comparing these two constructions of a pneumatic actuator, we note that the control of a jet tube requires less force than the control of the valve, because there is a gap between the jet tube and the receiving tubes and dry friction is absent. However, gas consumption in the case of a jet tube is substantially greater than in the case of an actuator with valves, because a large part of the gas flows out into the atmosphere during the entire operation of the actuator. In an actuator with a valve, the gas consumption is limited by the volume ejected from the cylinder cavity connected to the atmosphere by the displacement of the piston. /237

The processes which occur in pneumatic actuators are complicated by the effect of gas compressibility, by the sharp variations in the gas flow through small orifices when the pressure changes in the volumes which are connected by these orifices, etc. Therefore, a detailed calculation of pneumatic actuators is difficult. Below we present a simple equation of motion for a pneumatic actuator. In spite of the structural differences between the two versions of

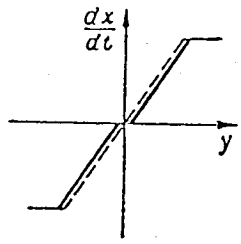

Figure 7.18. Static characteristics of hydraulic actuator.

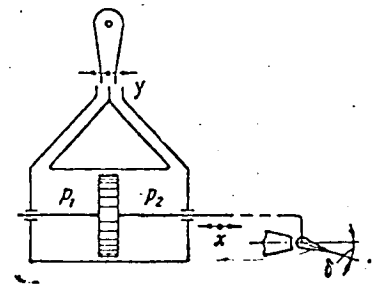

Figure 7.19. Schematic diagram of pneumatic actuator.

the pneumatic actuator (figures 7.17 and 7.19), their motion may be described by analogous equations. In deriving the differential equations for a pneumatic actuator, the following assumptions are usually made:

(1) the air pressure at the entrance to the valve or the jet tube is constant;

(2) the coefficients of gas consumption are constant.

Under these assumptions, the equation for the moving parts of a pneumatic actuator may be written /238

$$m\frac{d^2x}{dt^2} = S\Delta p - k_f\frac{dx}{dt} - k_1 x, \tag{7.24}$$

where m is the mass of the piston and the coupling rod, and also the reduced mass of all moving parts attached to the coupling rod; x is the displacement of the piston; S is the area of the piston; Δp is the pressure drop in the cavities of the cylinders; k_f is the coefficient characterizing the forces of viscous friction; and k_1 is the coefficient which characterizes the loading due to aerodynamic forces acting on the control surface (hinge moment).

The equation for the pressure differential at the piston has the form

$$T\frac{d\Delta p}{dt} + \Delta p = k_1 y - k_2\frac{dx}{dt}, \tag{7.25}$$

where T is the time constant; k_1 is the transfer constant; and k_2 is a constant which characterizes the variation in the specific weight of the gas when the piston is displaced.

The time constant T and the transfer constant are functions of pressure, gas flow and the specific weight of the gas. In the calculations we take the

average values of these parameters. If we eliminate the pressure drop Δp from equations (7.24) and (7.25), we obtain an equation for a pneumatic actuator

$$\frac{mT}{S}\frac{d^3x}{dt^3}+\left(\frac{m}{S}+\frac{k_f}{S}T\right)\frac{d^2x}{dt^2}+\left(\frac{k_f}{S}+\frac{k_1}{S}T+k_2\right)\frac{dx}{dt}+ \\ +\frac{k_1}{S}x=k_1y. \tag{7.26}$$

Equation (7.26) may be used to take into account the dynamic properties of a pneumatic actuator incorporated into some closed loop system with high dynamic properties. From the standpoint of using a pneumatic actuator for controlling missiles when the processes take place rather slowly, if we consider the total control loop, equation (7.26) may be simplified even further. In these simplifications we neglect the first and last term in the left side of the equation. The coefficient mT/S is small and may be set equal to zero. The loading produced by aerodynamic forces may also be made quite small by properly selecting the position of the suspension axis for the control surface. Therefore, the coefficient k_1/S may also be made quite small and assumed to be equal to zero.

As a result of these simplifications, expression (7.26) assumes the form /239

$$T_d\frac{d^2x}{dt^2}+\frac{dx}{dt}=k_dy, \tag{7.27}$$

(subscript d = driver)

where $T_d=\frac{m+k_TT}{k_T+k_2S}$ is the time constant of the driver; $k_d=\frac{k_1S}{k_T+k_2S}$ is the the amplification factor of the driver.

Since the angle of rotation of the control surface and the linear displacement of the piston are associated by the transfer ratio i, we may use equation (7.27) and write the equation of motion for the entire actuator

$$T_{ds}\frac{d^2\delta}{dt^2}+\frac{d\delta}{dt}=k_{ds}y, \tag{7.28}$$

(subscript ds = driving system)

where $T_{ds}=T_d$ is the time constant of the driving system; $k_{ds}=\frac{k_d}{i}$ is the amplification factor of the driving system.

On the basis of equation (7.28) we obtain the transfer function for the pneumatic drive

$$W_{ds}(p)=\frac{k_{ds}}{(T_{ds}p+1)p}. \tag{7.29}$$

CHAPTER 8. MATHEMATICAL DESCRIPTION OF MOTION /240

Section 8.1. Systems of Coordinates

The equations of a missile are written for a specific system of coordinates. In aerodynamics several coordinate systems are used and are selected in such a way as to simplify the solution of a given problem. Below we determine the system of coordinate axes used in aerodynamics and which we use in the present book.

1. The System of Earth Axes. The system of Earth axes x_g, y_g, z_g (fig. 8.1) is rigidly fixed with respect to Earth. The y_g axis is directed vertically up, while the x_g and z_g axes have an arbitrary position in the horizontal plane forming a right-hand system of coordinates. In analyzing the motion of the missile it is desirable to use the launching point as the center of coordinates and to place the x_g axis in the vertical plane passing through this point.

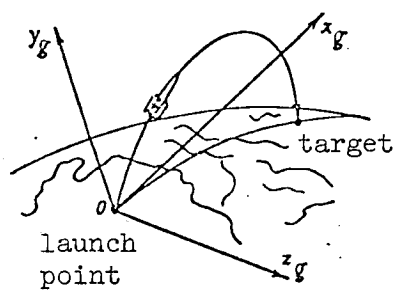

Figure 8.1. Earth coordinate axes.

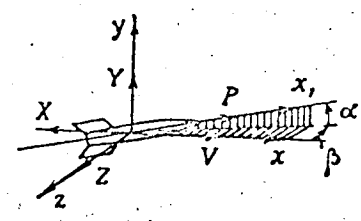

Figure 8.2. Flow coordinate axes.

2. The System of Flow Axes. The origin of the system of flow (velocity) axes is at the center of gravity of the moving body (missile). The x axis (drag forces) coincides with the flight velocity direction (fig. 8.2). The y axis (lift force) lies in the missile's plane of symmetry and is turned counter- /241
clockwise by an angle of 90° with respect to the x axis. The z axis (lateral force) is perpendicular to the plane x or y and directed to the right (if we are facing into the direction of flight), and forms a right hand coordinate system with the x and y axes. (Figure 8.2 shows the components of the total aerodynamic force R which reacts on the missile in flight, along the coordinate axes: the drag force X, the lift force (when the angle of attack is α) Y and a lateral force (when the slip angle β is positive) Z.

3. The system of Body Axes. As the name implies, this coordinate system is rigidly attached to the moving body (missile). The origin of this system is at the center of gravity of the missile (fig. 8.3). The x_1 axis (longitudinal axis) lies in the missile's plane of symmetry and is directed from the tail to the nose parallel to its axis or to the chord of its wing. The y_1 axis (the normal axis) lies in the missile's plane of symmetry and is rotated counterclockwise by an angle of 90° with respect to the x_1 axis. The z_1 axis (transverse axis) is perpendicular to the plane x_1oy_1 and is directed to the right (if we face in the flight direction).

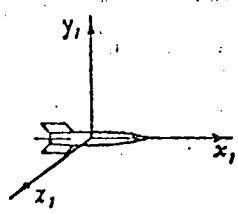

Figure 8.3. System of body axes.

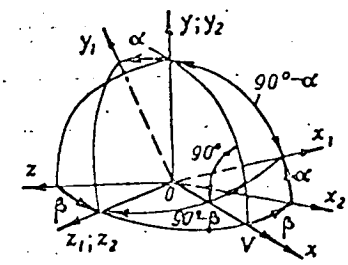

Figure 8.4. Angles between coordinate systems using flow axes, semifixed body axes and fixed body axes.

4. A System of Semifixed Body Axes. When aerodynamic coefficients are determined experimentally, it is common to use a semifixed system of aerodynamic axes. This is dictated by the construction of balances used to measure the aerodynamic coefficients in a wind tunnel. The semifixed body axes differ from the flow axes because the x_2 axis is directed along the projection of the velocity in the missile's plane of symmetry. Thus, semifixed body axes may be obtained from flow axes by rotation through the slip angle β around the axis of the lift force.

TABLE 8.1. COSINES OF ANGLES BETWEEN EARTH AND BODY COORDINATE AXES. /242

	x_1	y_1	z_1
x_g	$\cos\psi\cos\vartheta$	$-\cos\gamma\cos\psi\sin\vartheta+$ $+\sin\gamma\sin\psi$	$\cos\gamma\sin\psi+$ $+\sin\gamma\cos\psi\sin\vartheta$
y_g	$\sin\vartheta$	$\cos\gamma\cos\vartheta$	$-\sin\gamma\cos\vartheta$
z_g	$-\sin\psi\cos\vartheta$	$\sin\gamma\cos\psi+$ $+\cos\gamma\sin\psi\sin\vartheta$	$\cos\gamma\cos\psi-$ $-\sin\gamma\sin\psi\sin\vartheta$

TABLE 8.2. COSINES OF ANGLES BETWEEN BODY AND FLOW COORDINATE AXES.

	x	y	z
x_1	$\cos\alpha\cos\beta$	$\sin\alpha$	$-\cos\alpha\sin\beta$
y_1	$-\sin\alpha\cos\beta$	$\cos\alpha$	$\sin\alpha\sin\beta$
z_1	$\sin\beta$	0	$\cos\beta$

TABLE 8.3. COSINES OF ANGLES BETWEEN EARTH AND SEMI-FIXED BODY COORDINATE AXES.

	x_2	y_2	z_2
x_g	$\cos\theta\cos\psi$	$-\cos\gamma\cos\psi\sin\theta + \sin\gamma\sin\psi$	$\sin\gamma\sin\theta\cos\psi + \cos\gamma\sin\psi$
y_g	$\sin\theta$	$\cos\gamma\cos\theta$	$-\sin\gamma\cos\theta$
z_g	$-\cos\theta\sin\psi$	$\sin\gamma\cos\psi + \cos\gamma\sin\psi\sin\theta$	$\cos\gamma\cos\psi - \sin\gamma\sin\psi\sin\theta$

TABLE 8.4. COSINES OF ANGLES BETWEEN BODY AND SEMI-FIXED BODY COORDINATE AXES.

	x_2	y_2	z_2
x_1	$\cos\alpha$	$\sin\alpha$	0
y_1	$-\sin\alpha$	$\cos\alpha$	0
z_1	0	0	1

Figure 8.4 shows this transformation as well as the mutual position of the axes and also the position of the body axes x_1, y_1, z_1. The same figure shows /243 that the axes of the semifixed body system y_2 coincides with the axis of the lift force y, while the z_2 axis coincides with the transverse axis of the body system z_1. The angle $x_1 o x_2$, i.e., the angle formed by the body axis x_1 with the

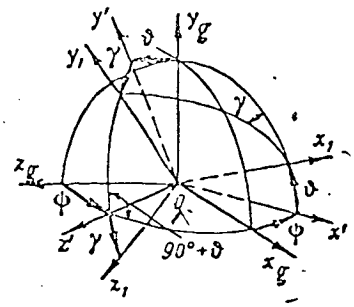

Figure 8.5. Angles between fixed body coordinate system and Earth coordinate system.

projection of the velocity and the missile's plane of symmetry is the angle of attack α. The angle zoz_1, or the angle formed by the velocity vector and the missile's plane of symmetry, is the slip angle β. The positive directions of angles α and β are also shown in figure 8.4. The positive angles of rotation of system x_1, y_1, z_1 with respect to the system x, y, z, are obtained from the general rule for right-hand coordinate systems.

Figure 8.5 shows the angles formed between the body coordinate system and the Earth coordinate system. For convenience, the origins of both coordinate systems coincide. The angle ϑ formed by the x_1 axis with the horizontal plane $x_g o z_g$ is called the pitch angle. The angle Ψ formed by the projection of the x_1 axis on the horizontal plane $x_g o z_g$ with the x_g axis is called the angle of yaw. The angle γ formed by the z_1 axis in the horizontal plane $x_g o z_g$ is called the tilt angle. The positive directions of these angles are given in figure 8.5.

Tables 8.1 - 8.4 show the direction cosines for transforming from one system of coordinates to another.

Section 8.2. General Equations of Motion of a Missile Assuming that it is a Rigid Body

The general formulation of the problem concerning the motion of a missile, even when the latter is not guided, is very complex. To simplify this problem a whole series of assumptions has to be made. In the first of these assumptions the elastic deformations of the missile are neglected, so that the latter can be considered a rigid body.

The motion of a rigid body of variable mass may be determined by using the laws of momentum and of the moments of momentum for the center of gravity of the

body. The law of momentum in this case has the form /244

$$m\frac{d\bar{V}}{dt} = \bar{R} + \bar{P}, \tag{8.1}$$

where m is the mass of the body which varies due to the combustion of the fuel; $\bar{V}$ is the velocity of the center of gravity;[1] $\bar{R}$ is the resultant of the external forces acting on the center of gravity. $\bar{P} = \bar{U}\, dm/dt$ is the resultant of the reactive forces applied at the center of gravity, and $\bar{U}$ is the relative velocity of the added (or removed) mass (mass of the fuel).

For bodies of variable mass, the law of the moments of momentum has the form

$$\frac{d^*\bar{K}}{dt} = \bar{M} + \bar{N}, \tag{8.2}$$

where $\bar{K}$ is the moment of momentum in relative motion with respect to the center of gravity of the body; $\bar{M}$ is the moment of external forces with respect to the center of inertia, and $\bar{N}$ is the moment of reactive forces with respect to the center of inertia.

The asterisk in the derivative indicates that the moment of momentum of a body may be considered constant during differentiation.

Equations (8.1) and (8.2) are valid for a fixed system of coordinates. The concept of a fixed coordinate system is conditional, because it is always necessary to specify another coordinate system with respect to which the system used in a given problem is fixed. For most of the problems encountered in this book the fixed coordinate system will be the Earth coordinate system. In problems where the motion of the Earth must be taken into account when considering the flight of the missile, this will be specified.

The forces and moments which occur in the right sides of equations (8.1) and (8.2) can be expressed most conveniently by using a system of coordinates fixed with respect to the missile, rather than with respect to Earth. Therefore, it becomes necessary to transform equations (8.1) and (8.2) to one of these systems. The transformation from a fixed system of coordinates to a moving system of coordinates is based on the following general lemma

$$\frac{d\bar{a}}{dt} = \frac{d\tilde{a}}{dt} + [\bar{\omega}\bar{a}], \tag{8.3}$$

---

[1]Strictly speaking, $\bar{V}$ is not the velocity of the center of gravity, but is the transport velocity of that point in the body through which the center of gravity passes at a given instant of time. The center of gravity does not occupy a fixed position in the body. However, the relative velocity of the center of gravity in a body may be neglected compared with the transport velocity of the body (of the missile).

where $d\bar{a}/dt$ is the derivative of the vector $\bar{a}$ in the fixed system of coordinates; $d\tilde{a}/dt$ is the derivative of the vector $\bar{a}$ in the moving system of coordinates, and $\bar{\omega}$ is the angular velocity of the moving system with respect to the fixed system.

On the basis of (8.3) it is possible to transform from the Earth (fixed) axes to flow axes, to fixed body axes and to semifixed body axes. To obtain the equations of motion of the missile in the form generally accepted in aerodynamics, it is desirable to write equations (8.1) and (8.2) in a semifixed body system of coordinates. Applying (8.3) to these equations, we find /245

$$m\frac{d\bar{V}}{dt} = m\frac{d\tilde{V}}{dt} + m[\bar{\omega}'\bar{V}] = \bar{R} + \bar{P}, \tag{8.4}$$

$$\frac{d^*\bar{K}}{dt} = \frac{d\tilde{K}}{dt} + [\bar{\omega}'\bar{K}] = \bar{M} + \bar{N}, \tag{8.5}$$

where $\bar{\omega}'$ is the angular velocity of the semifixed system of coordinates with respect to the Earth system of coordinates.

If we project the vector equations (8.4) and (8.5) on the axes of the semifixed system, we obtain two systems of equations

$$\left.\begin{aligned} m\frac{dV_{x2}}{dt} + m\omega'_{y2}V_{z2} &= R_{x2} + P_{x2}, \\ m\left(\omega'_{z2}V_{x2} - \omega'_{x2}V_{z2}\right) &= R_{y2} + P_{y2}, \\ m\frac{dV_{z2}}{dt} - m\omega_{y2}V_{x2} &= R_{z2} + P_{z2}, \end{aligned}\right\} \tag{8.6}$$

$$\left.\begin{aligned} \frac{d^*K_{x2}}{dt} + \left(\omega'_{y2}K_{z2} - \omega'_{z2}K_{y2}\right) &= M_{x2} + N_{x2}, \\ \frac{d^*K_{y2}}{dt} + \left(\omega'_{z2}K_{x2} - \omega'_{x2}K_{z2}\right) &= M_{y2} + N_{y2}, \\ \frac{d^*K_{z2}}{dt} + \left(\omega'_{x2}K_{y2} - \omega'_{y2}K_{x2}\right) &= M_{z2} + N_{z2}. \end{aligned}\right\} \tag{8.7}$$

Equations (8.6) take into account that in the semifixed system of coordinates the y_2 axis is perpendicular to the missile flight velocity V. Therefore, the projection of the velocity on this axis (V_{y2}) is identically equal to zero.

The projection of the moment of momentum on the axes of the semifixed system, which enter into equations (8.7), for a body of variable mass are determined by equations

$$\left.\begin{aligned} K_{x2} &= J_{x2}\omega_{x2} - J_{xy2}\omega_{y2}, \\ K_{y2} &= J_{y2}\omega_{y2} - J_{xy2}\omega_{x2}, \\ K_{z2} &= J_{z2}\omega_{z2}. \end{aligned}\right\} \tag{8.8}$$

where J_{x2}, J_{y2}, J_{z2} are the axial moments of inertia of the missile in this semifixed system of coordinates; J_{xy2} is the centrifugal moment of inertia of the missile, and ω_{x2}, ω_{y2}, ω_{z2} are the projections of the angular velocity of the missile on the axes of the semifixed system.

The derivation of equation (8.8) takes into account the fact that the missile has a plane of symmetry and, therefore, the centrifugal moments of inertia J_{yz2} and J_{zx2} are equal to zero. In addition, we should point out that the angular velocity of the missile $\overline{\omega}$ is different from the angular velocity of the semifixed system $\overline{\omega}'$, because this system is not rigidly fixed with the missile and may move with respect to the missile (together with the projection of the velocity vector on the plane of symmetry). It is also obvious that the moments of inertia in equations(8.8) are not constant quantities. The variation in these moments of inertia is due both to the variation in the mass of the missile caused by fuel consumption and due to the mobility of the semifixed axes with respect to the missile. /246

Substituting into equation (8.7) the values for the projections of the moment of momentum on the axes of semifixed system (8.8), and noting that the derivatives contain the asterisk, we obtain

$$\left.\begin{aligned} J_{x2}\frac{d^*\omega_{x2}}{dt} - J_{y2}\omega_{y2}\omega'_{z_2} + J_{z2}\omega'_{y2}\omega_{z2} + J_{xy2}\left(\omega_{x2}\omega'_{z_2} - \frac{d^*\omega_{y2}}{dt}\right) &= M_{x2} + N_{x2}, \\ J_{y2}\frac{d^*\omega_{y2}}{dt} - J_{z2}\omega'_{x_2}\omega_{z2} + J_{x2}\omega_{x2}\omega'_{z_2} - J_{xy2}\left(\omega_{y2}\omega'_{z_2} + \frac{d^*\omega_{x2}}{dt}\right) &= M_{y2} + N_{y2}, \\ J_{z2}\frac{d^*\omega_{z2}}{dt} - J_{x2}\omega_x\omega'_y + J_{y2}\omega_{y2}\omega'_{y_2} + J_{xy2}\left(\omega_{y2}\omega'_{y_2} - \omega_{x_2}\omega'_{x_2}\right) &= M_{z2} + N_{z2}. \end{aligned}\right\} \tag{8.9}$$

The asterisk in the derivatives for the projections of the angular velocities on the axes of the semifixed system indicates that these derivatives are computed by assuming that the axes x_2, y_2, z_2 are fixed with respect to the missile.

It is necessary to point out that the projections of the angular velocity of the missile and of the semifixed system of coordinates on the axes x_2 and y_2 of this system are equal to each other. This is explained by the fact that system x_2, y_2, z_2 may rotate in the missile only with respect to the z_2 axis. Only the

projections with respect to this axis (ω_{z2} and ω'_{z2}) may differ from each other in principle. Taking this into account, we rewrite equations (8.6) and (8.9) in a simpler form

$$\left.\begin{aligned} m\frac{dV_{x2}}{dt} + m\omega_{y2}V_{z2} &= R_{x2} + P_{x2}, \\ m\left(\omega'_{z2}V_{x2} - \omega_{x2}V_{z2}\right) &= R_{y2} + P_{y2}, \\ m\frac{dV_{z2}}{dt} - m\omega_{y2}V_{x2} &= R_{z2} + P_{z2}. \end{aligned}\right\} \tag{8.10}$$

$$\left.\begin{aligned} J_{x2}\frac{d^*\omega_{x2}}{dt} - J_{y2}\omega_{y2}\omega'_{z2} + J_{z2}\omega_{z2}\omega_{y2} + J_{xy2}\left(\omega_{x2}\omega'_{z2} - \frac{d^*\omega_{y2}}{dt}\right) &= M_{x2} + N_{x2}, \\ J_{y2}\frac{d^*\omega_{y2}}{dt} - J_{z2}\omega_{x2}\omega_{z2} + J_{x2}\omega_{x2}\omega'_{z2} - J_{xy2}\left(\omega_{y2}\omega'_{z2} + \frac{d^*\omega_{x2}}{dt}\right) &= M_{y2} + N_{y2}, \\ J_{z2}\frac{d^*\omega_{z2}}{dt} - J_{x2}\omega_{x2}\omega_{y2} + J_{y2}\omega_{y2}\omega_{x2} + J_{xy2}\left(\omega_{y2}^2 - \omega_{x2}^2\right) &= M_{z2} + N_{z2}. \end{aligned}\right\} \tag{8.11}$$

To determine the linear coordinates of the missile's center of gravity in the fixed system, and also to determine the semifixed angular coordinates in this system, it is necessary to write six more kinematic equations. From table 8.3, the relation between the projections of flight velocity in the fixed and semifixed systems has the form /247

$$\left.\begin{aligned} \frac{dx_g}{dt} &= V_{x2}\cos\theta\cos\psi + V_{z2}(\sin\gamma\sin\theta\cos\psi + \cos\gamma\sin\psi), \\ \frac{dy_g}{dt} &= V_{x2}\sin\theta - V_{z2}\sin\gamma\cos\theta, \\ \frac{dz_g}{dt} &= -V_{x2}\cos\theta\sin\psi + V_{z2}(\cos\gamma\cos\psi - \sin\gamma\sin\theta\sin\psi). \end{aligned}\right\} \tag{8.12}$$

Figure 8.6 shows the components of the anglular velocity vector in the semifixed coordinate system $\overline{\omega}'$ as products of Euler angles. From geometric considerations we obtain the kinematic equations which relate to these components

$$\left.\begin{aligned} \frac{d\gamma}{dt} &= \omega_{x2} - \omega_{y2}\operatorname{tg}\theta\cos\gamma + \omega'_{z2}\operatorname{tg}\theta\sin\gamma, \\ \frac{d\psi}{dt} &= \frac{\omega_{y2}\cos\gamma - \omega'_{z2}\sin\gamma}{\cos\theta}, \\ \frac{d\theta}{dt} &= \omega_{y2}\sin\gamma + \omega'_{z2}\cos\gamma. \end{aligned}\right\} \tag{8.13}$$

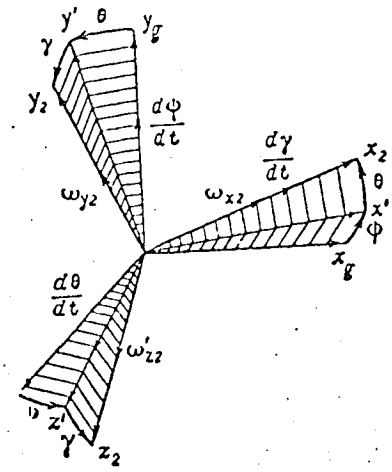

Figure 8.6. Geometric relations for angular velocities.

To these equations we must add the following kinematic relationships used below

$$\vartheta = \theta + \alpha; \quad \frac{d\vartheta}{dt} = \omega_{y2} \sin\gamma + \omega_{z2} \cos\gamma. \tag{8.14}$$

The system of equations which contains equations (8.10) - (8.14) is a complete system describing the motion of the missile. In principle it may be solved if we determine the forces and moments acting on the missile during flight.

Section 8.3. Reduction of Generation Equations of Motion of a Missile to a Simpler Form

The system of equations (8.10) - (8.14) obtained in the preceding section is a complex nonlinear system with variable coefficients which does not have a general solution. These equations are also complicated by the fact that the forces and moments contained on the right side of equations (8.10) and (8.11) are, in turn, nonlinear functions of missile motion parameters (functions of the angular and linear coordinates of the missile and of the derivatives of these coordinates). Although the system of equations (8.10) - (8.14) may be solved for specific numerical values of the missile parameters by means of computers, this approach is not considered suitable in investigating the motion of guided missiles and in selecting control parameters. A solution using specific values of control system parameters does not make it possible to select the optimum values of these parameters, since it does not establish a clear relationship between these parameters and the motion of the missile. Therefore, the most rational method to obtain simple, although approximate, analytical expressions for the motion of the missile involves a simplification of the problem. Following the accepted practice in the aerodynamics of airplanes, we simplify the problem by separating the true motion of the missile into a longitudinal and lateral component. The longitudinal motion refers to the motion of the center /249

of gravity in the vertical plane $x_g o y_g$ and a rotation around axis z_2. The lateral motion covers the motion of the center of gravity in the incline plane $x_2 o z_g$ and the rotation with respect to axes x_2 and y_2.

The separation of missile motion into longitudinal and lateral components is based on the assumption that the parameters determining longitudinal motion, $\left(\frac{dx_g}{dt}, \frac{dy_g}{dt}, V_{x2}, \vartheta, \dot{\vartheta}, \omega_{z2}, \omega'_{z2}\right)$, are considered to be constants in the equations for lateral motion, while the parameters which determine lateral motion, $\left(\frac{dz_g}{dt}, V_{z2}, \gamma, \psi, \omega_{x2}, \omega_{y2}\right)$, are considered to be constant in the equations for the longitudinal motion. As a result of this assumption, the general system of equations (8.10) - (8.14) is divided into two systems describing the isolated longitudinal and lateral motions. We note that when the missile moves strictly in a vertical plane, this approach is not an approximation, because in this case the parameters of lateral motion are indeed constant and equal to zero. For the lateral motion of the missile, the approach always introduces a certain error, because during this motion the parameters of longitudinal motion vary somewhat, which is not taken into account by the isolated equations of lateral motion. The error will be smaller if the variation in the parameters of longitudinal motion is smaller during the time when the lateral motion of the missile is investigated. /249

However, even after motion has been separated into longitudinal and lateral components, the equations are still very complex. There are two basic methods for a further simplification of the problem. The first method, known as the method of linearization, or the method of small perturbations, consists of the following. The motion of the missile is divided into perturbed motion and unperturbed motion. The unperturbed motion may cover any portion of the flight of interest to us. Let us assume that a missile whose motion was unperturbed is subject to perturbations (deflection of the control surfaces, change in engine thrust, gust of wind). Perturbed motion is any motion which is obtained after the unperturbed motion changes due to a perturbation. We assume that the deviations in the parameters of perturbed motion from their values during unperturbed motion is small. We expand all of the nonlinear functions which enter in the initial nonlinear equations in a power series of the perturbations and drop all terms which are infinitesimals of a higher order than one. The equations obtained in this manner are known as equations of the first approximation and are linear. In the general case, some of the coefficients of these equations may be functions of time.

This method of linearization is of practical significance when the unperturbed state consists of rectilinear and uniform flight. In this case, linearization is very simple, and it is for this region of flight that the method will be used in the present book. It constitutes a natural mathematical approach to the analysis of missile motion involving rectilinear and uniform flight. There are many missiles of this type whose sustainer engine operates during the entire flight trajectory or during a large portion of it. There is, however, a large class of missiles which does not have a region of constant flight velocity. This class includes missiles which have only booster engines

or sustainer engines which operate over a smaller portion of the trajectory. Also, the accelerated motion of a missile after launching cannot be described by means of linearized equations for the same reason--in this case the unperturbed operation in the form of rectilinear and uniform motion is absent. /250

If the initial equations of motion of the missile cannot be linearized, then a second method is used to simplify them, known as the method of grouping. This method is not as strict mathematically as the method of linearization but, nevertheless, produces satisfactory results in many cases. To explain the method of grouping, we note that the motion of the missile is described by parameters, including those which vary rapidly or slowly as functions of time. The rapidly varying functions may include the motion of the missile with respect to its center of gravity, while the slowly varying functions include the motion of the center of gravity of the missile. The idea of this method is to group the equations of motion in such a way and simplify them so that the group for the slowly varying functions may be integrated separately from the group for the rapidly varying functions. The results obtained by integrating the equations for slowly varying functions of time are substituted into the group of equations for rapid motion, which, as a rule, change from nonlinear equations to linear equations with variable coefficients.

In this section we present only the method of linearizing the equations of longitudinal and lateral motion. The method of grouping will be covered in subsequent sections.

To linearize the nonlinear equations (8.10) - (8.14), we take the region of rectilinear and uniform flight as the unperturbed state, when the sum of the forces and moments acting on the missile is equal to zero. We assume also that the x_g axis of the Earth coordinate system in this case coincides with the flight direction of the missile. In this case, the parameters, which determine the motion of the missile in the unperturbed state, have the following values

$$(V_{x2})_0 = V_e; \quad (V_{z2})_0 = 0; \quad \left(\frac{dx_g}{dt}\right)_0 = V_e \cos\theta_e; \quad \left(\frac{dy_g}{dt}\right)_0 = V_e \sin\theta_e;$$

$$\left(\frac{dz_g}{dt}\right)_0 = 0; \quad (\omega_{x2})_0 = (\omega_{y2})_0 = (\omega_{z2})_0 = (\omega'_{z2})_0 = 0;$$

$$(\psi)_0 = (\gamma)_0 = 0; \quad (\vartheta)_0 = \vartheta_e; \quad (\theta)_0 = \theta_e.$$

If we substitute these parameters into the system of equations (8.10) - (8.14), the latter transform into algebraic equations. From these equations we can determine the numerical values of the parameters for unperturbed flight. /251

Now let us assign small increments to all of the parameters, which shall be designated by the sign Δ in the case when the value of the parameter during the unperturbed state is different from zero. However, if it is equal to zero, then the deviation will be designated by the same symbol as the parameter. Substituting

the values of the parameters with increments into equations (8.10) - (8.14) and assuming that there is no coupling between the longitudinal and lateral motions of the missile, we obtain two systems of equations for the increments (first approximation).

The system of equations for longitudinal motion is

$$\left.\begin{aligned}
&m\frac{d\Delta V}{dt}=\Delta R_{x2}+\Delta P_{x2};\quad \frac{d\Delta x_g}{dt}=(V_e+\Delta V)\cos\theta_e-V_e\sin\theta_e\Delta\theta;\\
&mV_e\frac{d\Delta\theta}{dt}=\Delta R_{y2}+\Delta P_{y2};\quad \frac{d\Delta y_g}{dt}=(V_e+\Delta V)\sin\theta_e+V_e\cos\theta_e\Delta\theta;\\
&J_{z2}\frac{d\omega_{z2}}{dt}=\Delta M_{z2}+\Delta N_{z2};\quad \frac{d\Delta\vartheta}{dt}=\omega_{z2};\\
&\Delta\vartheta=\Delta\theta+\Delta\alpha.
\end{aligned}\right\}\qquad(8.15)$$

The system of equations for lateral motion is[1]

$$\left.\begin{aligned}
&m\frac{dV_{z2}}{dt}-m\omega_{y2}V_e=\Delta R_{z2}+\Delta P_{z2};\quad \frac{dz_g}{dt}=-V_e\psi+V_{z2};\\
&J_{x2}\frac{d\omega_{x2}}{dt}-J_{xy2}\frac{d\omega_{y2}}{dt}=\Delta M_{x2}+\Delta N_{x2};\quad \frac{d\gamma}{dt}=\omega_{x2};\\
&J_{y2}\frac{d\omega_{y2}}{dt}-J_{xy2}\frac{d\omega_{x2}}{dt}=\Delta M_{y2}+\Delta N_{y2};\quad \frac{d\psi}{dt}=\omega_{y2}.
\end{aligned}\right\}\qquad(8.16)$$

Due to the separation of motion into longitudinal and lateral components, the use of a semifixed system of coordinates as an independent system loses its meaning. For some components of motion of the missile the semifixed system has become identical to the flow system, for others it has become identical to the fixed system. Indeed, the x and y axes of the flow system and the x_2 and y_2 axes of the semifixed system, which determine the longitudinal motion of the missile's center of gravity, differ only in that the x axis is situated along the velocity vector, while the x_2 axis is along the projection of the velocity vector on the missile's plane of symmetry. Since the effect of lateral parameters on longitudinal motion is not taken into account, it was assumed in the investigation of this motion that the slip angle (parameter of lateral motion) is equal to zero. In this case, the velocity vector is situated in the plane of symmetry and coincides with its projection on this plane. Consequently, for longitudinal motion the x_2 and y_2 axes of the semifixed system are identical to the x and y axes of the flow system. We shall assume that the first two equations of system (8.15) are in the system of flow axes. /252

[1] In equation (8.16) we have dropped the asterisk for convenience.

The third equation of (8.15) and the first three equations of (8.16) turn out to be in the fixed system of coordinates. This is obvious with respect to the third equation of system (8.15), because the z_1 and z_2 axes coincide in the body of the missile (fig. 8.4). As far as equation (8.16) are concerned, when we consider only lateral motion, the x_2, y_2, z_2 axes become fixed with respect to the missile. The mobility of the semifixed system is due only to the variation in the angle of attack of the missile. When we consider isolated lateral motion, the angle of attack does not enter into this system of equations as a parameter of longitudinal motion. Therefore, the semifixed axes change from moving axes to stationary axes, i.e., axes fixed with respect to the missile. Now, the difference in the x_1, y_1, z_1 axes and the x_2, y_2, z_2 axes consists only of the presence of the angle of attack between the x_1 and x_2 axes and between y_1 and y_2 axes. If we take into account this angle, we can replace the semifixed axes x_2, y_2, z_2 for the lateral motion by fixed axes x_1, y_1, z_1, by changing, respectively, the designations for the moments of inertia and the angular velocities of the missile. We shall also replace the z_2 axis by the z_1 axis in the same way in the first equation of system (8.16). In doing this we note that, due to the rotation of the axes by an angle α_e, a term $mV_{y1}\omega_{x1}$ will appear in the first equation of (8.16), which, in the semifixed system of coordinates, was equal to zero due to the identity $V_{y2} \equiv 0$. The components of the velocity along the y_1 and z_1 axes are conveniently taken into account in terms of the angles of attack and angle of slip together with equations

$$V_{y1} = -V_e \cos\beta_e \sin\alpha_e \approx -V_e\alpha_e,$$
$$V_{z1} = V_e \sin\beta \approx V_e\beta.$$

To simplify the equations we shall also neglect the centrifugal moment J_{xy}, which usually has an insignificant value. As a result of above transformations, the system of equations (8.15) and (8.16) may be written in a slightly different form. The system of equations for longitudinal motion is

$$\left.\begin{aligned}
&m\frac{d\Delta V}{dt} = \Delta R_x + \Delta P_x; \quad \frac{d\Delta x_g}{dt} = (V_e + \Delta V)\cos\theta_e - V_e \sin\theta_e \Delta\theta;\\
&mV_e\frac{d\Delta\theta}{dt} = \Delta R_y + \Delta P_y; \quad \frac{d\Delta y_g}{dt} = (V_e + \Delta V)\sin\theta_e + V_e\cos\theta_e\Delta\theta;\\
&J_z\frac{d\omega_z}{dt} = \Delta M_z + \Delta N_z; \quad \frac{d\Delta\vartheta}{dt} = \omega_z;\\
&\Delta\vartheta = \Delta\theta + \Delta\alpha.
\end{aligned}\right\} \qquad (8.17)$$

/253

The system of equations for lateral motion is

$$\left.\begin{aligned}
&mV_e\frac{d\beta}{dt}-mV_e\alpha_e\omega_x-mV_e\omega_y=\Delta R_z+\Delta P_z;\quad \frac{dz_g}{dt}=V_e(\beta-\psi);\\
&J_x\frac{d\omega_x}{dt}=\Delta M_x+\Delta N_x;\quad \frac{d\gamma}{dt}=\omega_x;\\
&J_y\frac{d\omega_y}{dt}=\Delta M_y+\Delta N_y;\quad \frac{d\psi}{dt}=\omega_y.
\end{aligned}\right\}\qquad(8.18)$$

Now the subscripts of the corresponding parameters merely indicate the selection of a specific axis in a given system. They do not show the selection of any particular system, because this problem was previously solved and it is known for each of equations (8.17) and (8.18) in which coordinate system it was constructed.

Let us analyze the right sides of equations for the projections of force and moments, which enter into systems (8.17) and (8.18), in order to obtain the final form of these equations.

Section 8.4. Equations for the Longitudinal Motion of the Missile Obtained by the Method of Linearization and their Analysis

To obtain equations for longitudinal motion, it is necessary to find an analytical expression for the increments of forces and moments which enter into the system of equations (8.17).

Figure 8.7 shows the forces and moments which act on a missile during longitudinal motion.

These forces and moments are nonlinear functions of a series of arguments

$$X=X(\alpha,V,M,\rho);$$
$$Y=Y(\alpha,V,M,\rho);$$
$$P=P(\delta_{tc},M,p,T);$$
$$M_z=M_z\left(\delta_{el},\alpha,\frac{d\alpha}{dt},\frac{d\vartheta}{dt},V,M,\rho\right),$$

where $M = V_e/\alpha_e$ (α_e is the velocity of sound at the flight altitude); ρ is the air density; δ_{tc} is the angle of rotation of the thrust control member; p is air pressure; T is the absolute air temperature, and δ_{el} is the deflection angle of the elevator. /254

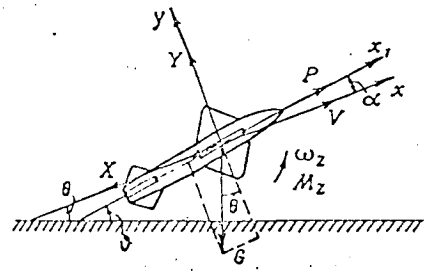

Figure 8.7. Forces and moments which act on missile undergoing longitudinal motion. x, y--axes of flow system of coordinates; ϑ--pitch angle of missile; θ--slope of missile's trajectory; α--angle of attack assuming that longitudinal axis and chord of wing coincide in direction. P--thrust developed by engine; we assume that it passes through center of gravity of missile; therefore, moment of reactive forces N is identically equal to zero; X--drag whose direction is opposite to that of the velocity vector; Y--lift force perpendicular to velocity vector; G--weight of missile; M_z--moment of aerodynamic forces with respect to transverse axis z_1.

The projections of the forces on the x and y axes of the flow system are determined from figure 8.7 by means of the following expressions

$$R_x + P_x = -X - G\sin\theta + P\cos\alpha; \tag{8.19}$$

$$R_y + P_y = Y - G\cos\theta + P\sin\alpha. \tag{8.20}$$

The initial unperturbed state of motion in the vertical plane may be obtained if all forces and moments acting on the missile are equal to zero. Consequently, for this state the following system of equations is valid

$$\left.\begin{aligned} -X_e - G\sin\theta_e + P_e\cos\alpha_e &= 0, \\ Y_e - G\cos\theta_e + P_e\sin\alpha_e &= 0, \\ M_z(\delta_{el}, \alpha_e, 0, 0, V_e, M_e, \rho_e) &= 0, \\ \vartheta_e = \theta_e + \alpha_e. \end{aligned}\right\} \tag{8.21}$$

In the system of equations (8.21) two quantities, the thrust P_e and the angle of deflection of the elevator δ_{el}, depend on the position of the actuators /255

which control the engine and the elevator. Therefore, these two quantities are contained in the equations of motions as functions of time. These functions must either be known or definitely related to the flight parameters. These relations characterize the operation of the missile control system. In equations (8.21), which describe the unperturbed state, these quantities must be constant and must be known.

If the thrust and the deflection angle of the control surface are known, in the system of equations (8.21) there will be four remaining unknown flight parameters,[1] V_e, θ_e, ϑ_e and α_e, which characterize the unperturbed motion and which can be determined in principle by solving this system of equations.

We shall now assign small increments to these parameters and to the flight altitude and expand the nonlinear functions X, Y, P and M_z in a power series of these increments. If we limit ourselves to the linear approximation and take into account equation (8.21), we obtain the following expressions for the increments in the forces and moments during longitudinal motion.

$$\left.\begin{aligned}
&\Delta R_x + \Delta P_x = -X^V\Delta V - X^M\Delta M - X^\alpha\Delta\alpha - X^\rho\rho^y\Delta y_g - \\
&- G\cos\theta_e\Delta\theta + P^M\cos\alpha_e\Delta M - P_e\sin\alpha_e\Delta\alpha + P^\rho\cos\alpha_e\rho^y\Delta y_g + \\
&+ P^T\cos\alpha_e T^y\Delta y_g + P^\delta\cos\alpha_e\Delta\delta_{tc}, \\
&\Delta R_y + \Delta P_y = Y^V\Delta V + Y^M\Delta M + Y^\alpha\Delta\alpha + Y^\rho\rho^y\Delta y_g + G\sin\theta_e\Delta\theta + \\
&+ P^M\sin\alpha_e\Delta M + P_e\cos\alpha_e\Delta\alpha + P^\rho\sin\alpha_e\rho^y\Delta y_g + \\
&+ P^T\sin\alpha_e T^y\Delta y_g + P^\delta\sin\alpha_e\Delta\delta_{tc}, \\
&\Delta M_z = M_z^\delta\Delta\delta_{el} + M_z^\alpha\Delta\alpha + M_z^{\dot\alpha}\frac{d\alpha}{dt} + M_z^\vartheta\frac{d\vartheta}{dt} + M_z^V\Delta V + \\
&+ M_z^M\Delta M + M_z^{\rho,y}\Delta y_g.
\end{aligned}\right\} \qquad (8.22)$$

The various terms with superscripts designate the partial derivatives of these quantities with respect to the parameter given by the respective superscript. For example, $X^V = \partial X/\partial V$, $X^\alpha = \partial X/\partial\alpha$ etc.

---

[1] If we consider the horizontal flight of the missile or if we do not take into account the variation in the air density ρ as a function of altitude; if we take into account this variation, then, in these equations we must add expressions which relate flight altitude y_g to angle θ_e and to flight velocity V_e, and also the air density as a function of altitude; we shall do this below.

Let us consider briefly the method of determining individual components of forces and moments which enter into these expressions. The variation in the drag X, in the lift force Y and in the moment M_z as a function of velocity V and air density ρ follows directly from these equations: /256

$$X = c_x S \frac{\rho V^2}{2}, \tag{8.23}$$

$$Y = c_y S \frac{\rho V^2}{2}, \tag{8.24}$$

$$M_z = m_z S b_A \frac{\rho V^2}{2}, \tag{8.25}$$

where $c_x = c_x(M,\alpha)$ is the drag coefficient; $c_y = c_y(M, \alpha)$ is the coefficient of lift; $m_z = m_z(\delta_{el}, \alpha, d\alpha/dt, d\vartheta/dt, M)$ is the coefficient of moment M_z; S is the area of the missile's wings or some other area (e.g., the area of the mid-frame of the missile), and b_A is the average aerodynamic chord.

Thus, the partial derivatives of the forces and of the moment with respect to V and ρ may be obtained indirectly by differentiating expressions (8.23) - (8.25). We note that the partial derivatives $M_z = m_{ze} S b_A \rho_e V_e$ and $M_z^\rho = m_{ze} S b_A \frac{V_e^2}{2}$ are equal to zero because the moment coefficient m_{ze} is equal to zero. This coefficient corresponds to unperturbed rectilinear flight for which $M_z = 0$. The partial derivatives of the forces and moments with respect to the angle of attack α and the M (Mach) number are determined graphically from the characteristics of the missile, which are shown approximately in figures 8.8, 8.9 and 8.10. The other necessary relationships for the missile--$m_z = m_z(\delta_{el}, d\alpha/dt, d\vartheta/dt)$ and for the engine $P = P(\delta_{tc} M, \rho, T)$ are also presented graphically or analytically. The derivatives with respect to the density ρ, the pressure p and the absolute air temperature T are determined from data on the variation in atmospheric parameters with altitude as shown in table 8.5. The reference quantities in these tables are as follows: $\rho_0 = 1.22\ 554$ kg x m $^{-3}$, $p_0 = 760$ mm Hg, $T_0 = 288^\circ$C.

As an illustration, figure 8.11 shows the graphs ρ/ρ_0 and p/p_0 as functions of altitude constructed on the basis of data given in table 8.5.

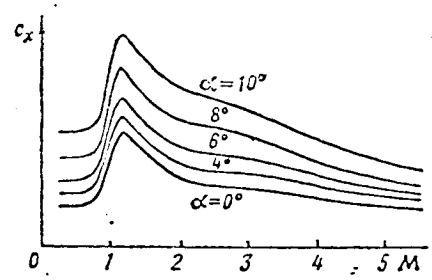

Figure 8.8. Variation in drag coefficient as function of Mach number M.

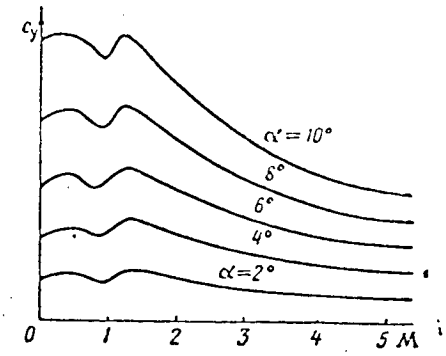

Figure 8.9. Variation in lift coefficient as function of Mach number M.

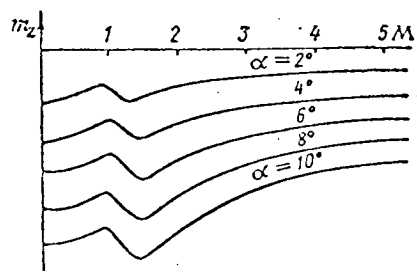

Figure 8.10. Variation in moment coefficient m_z as function of M.

Let us clarify the physical meaning of individual incremental components of the moment ΔM_z. The moment $M_z^{\delta}\Delta\delta_{el}$ is the control moment produced by the elevator of the missile. The moment $M_z^{\alpha}\Delta\alpha$ is called the static stability moment. /257

This moment is produced because the aerodynamic focus of the missile does not coincide with its center of gravity. It determines the static stability, i.e., stability with respect to the perturbation of the angle of attack which is considered without the other components of moment M_z during perturbed motion. If the aerodynamic force is applied behind the center of gravity, $M_z^{\alpha}\Delta\alpha < 0$ in the missile is statically stable. As the angle of attack is increased, the aerodynamic force also increases and produces a moment which decreases the angle of attack. When the angle of attack decreases, the picture is reversed. If the aerodynamic force is applied in front of the center of gravity, the missile will be statically unstable with respect to the angle of attack. Finally, when the point of application of the aerodynamic force coincides with the center of gravity, the missile is statically neutral with respect to changes in the angle of

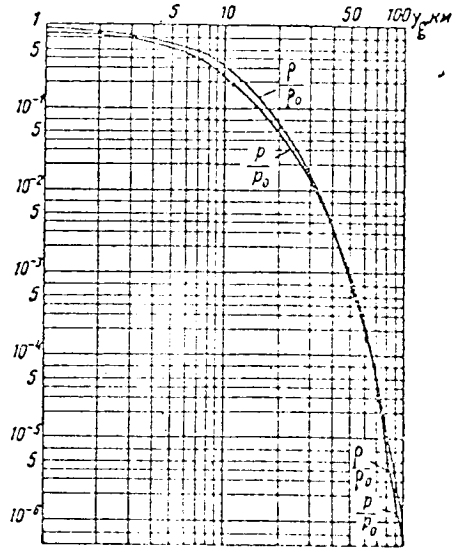

Figure 8.11. Variation in air pressure and air density as function of altitude.

attack. Under actual conditions, the variation in the angle of attack always produces a moment $M_z A\alpha$, and also a series of other moments which also affect the flight stability of the missile, but to a lesser degree than the moment $M_z^{\alpha}\Delta\alpha$. Therefore, the moment of static stability is only one of the factors affecting the stability and dynamic properties of the missile.

TABLE 8.5. VARIATION IN ATMOSPHERIC PARAMETERS AS A FUNCTION OF ALTITUDE[1]

Altitude, km	$\frac{p}{p_0}$	$\frac{\rho}{\rho_0}$	$\sqrt{\frac{T_0}{T}}$
0	1.0	1.0	1.0
1	0.885	0.902	1.01
2	0.78	0.813	1.021
5	0.527	0.586	1.054
10	0.258	0.323	1.118
15	0.118	0.152	1.133
20	$0.543 \cdot 10^{-1}$	$0.697 \cdot 10^{-1}$	1.133
25	$0.251 \cdot 10^{-1}$	$0.316 \cdot 10^{-1}$	1.121
30	$0.118 \cdot 10^{-1}$	$0.145 \cdot 10^{-1}$	1.109
35	$0.653 \cdot 10^{-2}$	$0.679 \cdot 10^{-2}$	1.098
40	$0.283 \cdot 10^{-2}$	$0.302 \cdot 10^{-2}$	1.034
50	$0.878 \cdot 10^{-3}$	$0.764 \cdot 10^{-3}$	0.933
100	$0.580 \cdot 10^{-6}$	$0.8 \cdot 10^{-6}$	1.176

[1] V. I. Feodos'yev and G. B. Sinyarev. Introduction to Rocket Engineering, Oborongiz, 1961.

The moment $M_z^{\alpha} \frac{d\Delta\alpha}{dt}$ is due to a lag in the measurement of the flow taper on the wing. This lag is due to the propagation time of the perturbation from the wing to the horizontal stabilizer, and it increases with an increase in the rate of change of the angle of attack. The moment $M_z^{\alpha} \frac{d\Delta\alpha}{dt}$ is always negative.

The moment $M_z^{\vartheta} d\vartheta/dt = M_z^{\omega_z} \omega_z$ is called the damping moment. The damping moment is produced by the variation in the angle of attack when the missile rotates. The auxiliary angle of attack at any point on the missile is due to its rotation with respect to the center of gravity. It increases with increase in the angular velocity of the missile ω and in the distance from this point to the center of gravity. Therefore, the principal part of the damping moment is produced by the variation in the angle of attack of the stabilizer, because the stabilizer has a substantial lever arm with respect to the center of gravity. /259

The moment $M_z^M \Delta M$ is produced by the displacement of the point of application of aerodynamic forces (aerodynamic focus) during high flight speeds when the compressibility of the air becomes significant. The position of this point is determined by the Mach number. As the Mach number increases, the aerodynamic focus, as a rule, is displaced to the rear, producing a negative moment. Consequently, in this case $M_z^M \Delta M < 0$. The moments $M_z^V \Delta V$ and $M_z^{\rho} \rho^y \Delta y_g$ are equal to zero, as shown above.

We substitute into equation (8.17) the values for the increments of forces and of the moment given by expressions (8.22). In this case the terms with the unknown parameters of longitudinal motion are transferred to the left sides of the equations, and transformations are carried out to give these equations a more suitable form for future use. As a result we obtain linearized equations for the longitudinal motion of the missile

$$\left.\begin{aligned}
&a_\theta \Delta\theta + a_\alpha \Delta\alpha + \frac{d\Delta V}{dt} + a_V \Delta V + a_y \Delta y_g = a_\delta \Delta\delta_{tc};\\
&\frac{d\Delta\theta}{dt} - b_\theta \Delta\theta - b_\alpha \Delta\alpha - b_V \Delta V + b_y \Delta y_g = b_\delta \Delta\delta_{tc};\\
&\frac{d^2\Delta\vartheta}{dt^2} + c_\vartheta \frac{d\Delta\vartheta}{dt} + c_\alpha \frac{d\Delta\alpha}{dt} + c_\alpha \Delta\alpha + c_V \Delta V = c_\delta \Delta\delta_{el},\\
&\frac{d\Delta x_g}{dt} = (V_e + \Delta V)\cos\theta_e - V_e \sin\theta_e \Delta\theta;\\
&\frac{d\Delta y_g}{dt} = (V_e + \Delta V)\sin\theta_e + V_e \cos\theta_e \Delta\theta; \quad \Delta\alpha + \Delta\theta = \Delta\vartheta.
\end{aligned}\right\} \qquad (8.26)$$

The coefficients contained in equation (8.26) have the following values

$$
\left.
\begin{aligned}
&a_\theta = g\cos\theta_e;\\
&a_\alpha = \frac{V_e}{2\tau_e}\left(c_x^\alpha - c_{ye}^{\,r} + \frac{2G\cos\theta_e}{S\rho_e V_e^2}\right);\\
&a_V = \frac{1}{\tau_e}\left(c_{xe} + c_x^M\frac{M_e}{2} - \frac{P^M\cos\alpha_e}{S\rho_e V_e a_e}\right);\\
&a_y = \frac{V_e}{2\tau_e\rho_e}\left(c_{xe}\rho^y - \frac{2P^P\cos\alpha_e\rho^y}{SV_e^2} - \frac{2P^T\cos\alpha_e T^y}{SV_e^2}\right);\\
&a_\delta = \frac{P^\delta}{m}\cos\alpha_e;\\
&b_\theta = \frac{g\sin\theta_e}{V_e};\\
&b_\alpha = \frac{1}{2\tau_e}\left(c_y^\alpha + c_{xe} + \frac{2G\sin\theta_e}{S\rho_e V_e^2}\right);\\
&b_V = \frac{1}{\tau_e V_e}\left(c_{ye} + c_y^M\frac{M_e}{2} + \frac{P^M\sin\alpha_e}{S\rho_e V_e a_e}\right);\\
&b_y = -\frac{1}{2\tau_e\rho_e}\left(c_{ye}\rho^y + \frac{2P^P\sin\alpha_e\rho^y}{SV_e^2} + \frac{2P^T\sin\alpha_e T^y}{SV_e^2}\right);\\
&b_\delta = \frac{P^\delta\sin\alpha_e}{mV_e};\\
&c_{\dot\theta} = -\frac{m_z^{\omega_z}}{J_z}b_A S\frac{\rho_e V_e^2}{2} = -\frac{m_z^{\bar\omega_z}}{2\tau_e\bar r_z^2};\\
&c_{\dot\alpha} = -\frac{m_z^{\dot\alpha}}{J_z}b_A S\frac{\rho_e V_e^2}{2} = -\frac{m_z^{\bar{\dot\alpha}}}{2\tau_e\bar r_z^2};\\
&c_\alpha = -\frac{m_z^\alpha\mu_d}{2\tau_e^2\bar r_z^2};\quad c_V = -\frac{m_z^M M_e\mu_d}{2V_e\tau_e^2\bar r_z^2};\quad c_\delta = \frac{m_z^\delta\mu_d}{2\tau_e^2\bar r_z^2};\\
&\tau_e = \frac{m}{S\rho_e V_e};\quad \mu_d = \frac{m}{\rho_e b_A S};\quad \bar\omega_z = \frac{b_A}{V_e}\omega_z;\\
&\bar r_z^2 = \frac{J_z}{b_A^2 m};\quad \bar{\dot\alpha} = \frac{b_A}{V_e}\frac{d\Delta\alpha}{dt}.
\end{aligned}
\right\}
\tag{8.27}
$$

The coefficient μ_d is known as the relative density of the missile in the longitudinal motion, while the coefficient $\bar r_z$ is known as the relative radius of inertia; the bars over ω_z and $d\Delta\alpha/dt$ indicate that these quantities are dimensionless. All the partial derivatives in equation (8.27) for the control coefficients of longitudinal motion are computed when the value of the argument corresponds to the unperturbed state. /260

In equation (8.26) the angles are expressed in radians and the distances in meters, while the velocity is given in m/sec. Sometimes it is desirable to express the angles in degrees. To do this it is sufficient to change the following coefficients: $a_\theta^\circ = a_\theta/57.3$; $a_\alpha^\circ = a_\alpha/57.3$; $a_\delta^\circ = a_\delta/57.3$; $b_V^\circ = 57.3b_V$; $b_y^\circ = 57.3b_V$ by; $c_V = 57.3c_V$. The remaining coefficients of equations (8.26) do not change when /261

we transform from radians to degrees. The equation for the vertical component of the missile's velocity when transforming to degrees must be written in the form

$$\frac{d\Delta y_g}{dt} = \frac{V_e}{57,3}\Delta\theta^\circ.$$

The system of equations for the linear approximation (8.26) is obtained by taking into account a large number of factors affecting the motion of the missile. The fact that the role of some of these factors is small was not considered and, consequently, it was not considered that the corresponding coefficient in equation (8.26) is small. If we take this situation into account, the behavior of the missile without the control system described by equation (8.26) may be represented quite simply.

Let us consider the stability of rectilinear flight with constant velocity, assumed to be unperturbed when we linearized the initial equations. In this investigation the last two equations of (8.26) drop from the system, because the stability of the missile's flight without a control system does not depend on the coordinate x_g of its center of gravity and depends very little on the coordinate y_g. The coefficients a_y and b_y are small compared with the other coefficients in the first two equations; therefore, for simplicity we shall assume that they are equal to zero. As a result the following equations are left for the analysis of the stability of rectilinear uniform motion of a missile without a control system

$$\left.\begin{aligned}
&a_\theta\Delta\theta + a_\alpha\Delta\alpha + \frac{d\Delta V}{dt} + a_V\Delta V = a_\delta\Delta\delta_{tc},\\
&\frac{d\Delta\theta}{dt} - b_\theta\Delta\theta - b_\alpha\Delta\alpha - b_V\Delta V = b_\delta\Delta\delta_{tc},\\
&\frac{d^2\Delta\theta}{dt^2} + c_\theta\frac{d\Delta\theta}{dt} + c_\alpha\frac{d\Delta\alpha}{dt} + c_\alpha\Delta\alpha + c_V\Delta V = c_\delta\Delta\delta_{el},\\
&\Delta\theta + \Delta\alpha = \Delta\vartheta.
\end{aligned}\right\} \qquad (8.28)$$

The characteristic polynomial for a system of equations (8.28) has the form

$$A(p) = p^4 + a_1p^3 + a_2p^2 + a_3p + a_4, \qquad (8.29)$$

where

$$\left.\begin{aligned}
a_1 &= a_V + b_\alpha - b_\vartheta + c_\vartheta + c_{\dot\alpha};\\
a_2 &= c_1 + b_\alpha c_\vartheta + c_\alpha + (c_\vartheta + c_{\dot\alpha})(a_V - b_\vartheta);\\
a_3 &= c_\alpha (a_V - b_\vartheta) + c_\vartheta c_3 + (c_\vartheta + c_{\dot\alpha}) c_2 - a_\alpha c_V;\\
a_4 &= c_\alpha c_2 - c_V c_4;\\
c_1 &= c_2 + c_3;\\
c_2 &= a_\vartheta b_V - a_V b_\vartheta;\\
c_3 &= a_V b_\alpha - a_\alpha b_V;\\
c_4 &= a_\vartheta b_\alpha - a_\alpha b_\vartheta.
\end{aligned}\right\} \qquad (8.30)$$

The polynomial A(p) usually consists of a pair of large and a pair of small roots. The large roots are determined primarily by coefficients a_1 and a_2, while the small roots are determined by coefficients a_3 and a_4. The large roots of the polynomial A(p) characterize the short period motion of the missile, i.e., motion associated with the establishment of the angle of attack $\Delta\alpha$ after some perturbation. The small roots characterize the long term motion of the missile which, as a rule, represents oscillations with a large period and low damping of the velocity increment ΔV and the trajectory slope increment $\Delta\theta$ with a practically constant angle of attack. The long period oscillations are sometimes known as Phugoid oscillations. /262

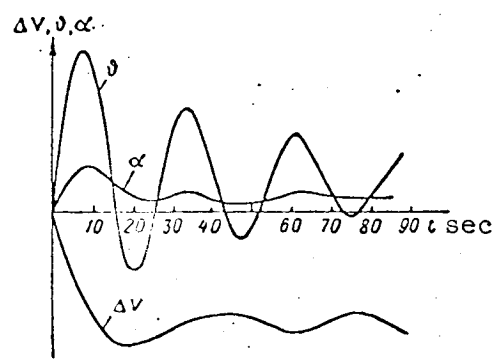

Figure 8.12. Curves showing variation in parameters of longitudinal motion of missile when elevator is displaced.

The basic perturbing force for guided missiles is produced by deflection of the control surfaces. The deflection of the elevator by some constant angle changes all of the parameters in equation (8.28). In this case, due to the separation of the roots of polynomial A(p), we may distinguish between two stages in the variation of these parameters. The first stage lasting several seconds is the stage of motion with short period. During this stage there is rapid variation in the angles $\Delta\theta$, $\Delta\vartheta$ and $\Delta\alpha$ (fig. 8.12), and at the end of the period an almost constant angle of attack is established. The second stage lasts several

tens or sometimes several hundreds of seconds and corresponds to the long period motion. During the period of the second stage, there is slow variation in the angles $\Delta\theta$, $\Delta\vartheta$ and in velocity ΔV. Figure 8.12 shows an approximate variation in the parameters of the longitudinal motion of a missile when the elevators are displaced.

We can obtain an approximate description of the short period motion of the missile, and also an approximation for the value of the large roots of the polynomial if, in the system of equations (8.28), we let $\Delta V = b_\theta = 0$, i.e., if we neglect the variation in the flight velocity and assume that flight is horizontal. As a result the first equation of this system becomes isolated from the others and the system assumes the form

$$\left.\begin{aligned} &\frac{d\Delta\theta}{dt} - b_\alpha \Delta\alpha = 0, \\ &\frac{d^2\Delta\vartheta}{dt^2} + c_\vartheta \frac{d\Delta\vartheta}{dt} + c_\alpha^{\cdot} \frac{d\Delta\alpha}{dt} + c_\alpha \Delta\alpha = c_\delta \Delta\delta_{el}, \\ &\Delta\alpha + \Delta\theta = \Delta\vartheta. \end{aligned}\right\} \tag{8.31}$$

The characteristic polynomial for system (8.31) has the form

$$A_1(p) = p\,[p^2 + a_1 p + a_2], \tag{8.32}$$

where

$$\left.\begin{aligned} a_1 &= b_\alpha + c_\alpha^{\cdot} + c_\vartheta; \\ a_2 &= b_\alpha c_\vartheta + c_\alpha. \end{aligned}\right\} \tag{8.33}$$

The zero root of this polynomial indicates that the missile is neutral with respect to angles $\Delta\theta$ and $\Delta\vartheta$. To have stability of short period motion without control system, the coefficients a_1 and a_2 must be greater than zero. The coefficient a_1 is always positive because its components are always positive: b_α, c_α and $c_\alpha^{\cdot}$. Coefficient a_2 may become negative because we have $c_\alpha < 0$ for static instability of the missile. The value of this coefficient depends substantially on the flight velocity and, as result, the missile which is statically stable at normal flight velocity amy become statically unstable at low velocity, i.e., during launching. The missile with $a_2 = b_\alpha c_\vartheta + c_\alpha < 0$ is called unstable with respect to its angle of attack.[1] In this case stability may be achieved by using an automatic control system.

---

[1] Sometimes these missiles are referred to as being unstable with respect to the load factor.

Equation (8.31) will be widely applied in analyzing the angular motions of the missile with respect to its center of gravity.

To give an approximate description of the long period of motion and to find the approximate values of the small roots of the polynomial A(p), we must make an assumption concerning the instantaneous balancing of the missile with respect to the z_1 axis. Indeed, after the short period motion terminates, the rapid variations in angles $\Delta\vartheta$ and $\Delta\alpha$ stop, and the terms with the products of these angles in the third equation of system (8.28) may be neglected. This is the same as assuming that the missile is balanced instantaneously /264

$$c_\alpha \Delta\alpha + c_V \Delta V = c_\delta \Delta\delta_{el}. \tag{8.34}$$

As a result the system of equations (8.28) is simplified and assumes the form

$$\left.\begin{aligned} &a_\theta \Delta\theta + a_\alpha \Delta\alpha + \frac{d\Delta V}{dt} + a_V \Delta V = a_\delta \Delta\delta_{tc}, \\ &\frac{d\Delta\theta}{dt} - b_\theta \Delta\theta - b_\alpha \Delta\alpha - b_V \Delta V = b_\delta \Delta\delta_{tc}, \\ &c_\alpha \Delta\alpha + c_V \Delta V = c_\delta \Delta\delta_{el}. \end{aligned}\right\} \tag{8.35}$$

The characteristic polynomial for the system of equations (8.35) is equal to

$$A_2(p) = p^2 + a_1 p + a_2, \tag{8.36}$$

where

$$\left.\begin{aligned} a_1 &= a_V - b_\theta - a_\alpha \frac{c_V}{c_\alpha}; \\ a_2 &= c_2 - c_4 \frac{c_V}{c_\alpha}. \end{aligned}\right\} \tag{8.37}$$

The values of coefficients c_2 and c_4 are shown in equation (8.30). If one of the coefficients a_1 or a_2 is negative, the long period motion of the missile without a control system becomes unstable, i.e., any of the parameters of this motion ΔV, $\Delta\theta$ or $\Delta\vartheta$ will deviate in time without limit from the value which it had during the initial unperturbed state. Coefficients a_1 and a_2 can take on negative values in the following cases:

(1) for small or negative value of c_2, which takes place when $a_2 < 0$; such a case is possible when $c_y^M < 0$, because this coefficient enters in the equation for b_V;

(2) for very large values of c_V associated with a large displacement of the aerodynamic focus when flight velocity changes; in this case both a_1 and a_2 may become negative;

(3) for negative values of a_V, which may occur for large values of the derivative P^M; in this case $a_1 < 0$;

(4) for large values of b_θ, which increases with the slope of the trajectory θ during pitching; due to the large value of b_θ, a_1 and a_2 may become negative; during diving, $b_\theta < 0$ and the stability of the missile will increase. In all these cases, the stability of the missile may be achieved by a suitable selection of the control system parameters.

Equation (8.35) will be used to analyze the motion of the missile's center of gravity.

Section 8.5. Equations and Analysis for the Lateral Motion of a Missile Obtained by the Method of Linearization

To obtain the equations of lateral motion it is necessary to find an analytical expression for the increments of the force and moments entering into equation (8.18). First we shall consider the equations of lateral motion for a missile with plane wings, because lateral motion in this case is more complex. After solving this problem, it is easy to find the equations of lateral motion for a missile with cruciform wings. Figure 8.13 shows the forces[1] and moments which act on a missile with plane wings during lateral motion.

The force Z and the moment M_x and M_y are given by equations

$$Z = c_z S \frac{\rho V^2}{2} + G \sin \gamma; \tag{8.38}$$

$$M_x = m_x l S \frac{\rho V^2}{2}; \tag{8.39}$$ /266

$$M_y = m_y l S \frac{\rho V^2}{2}, \tag{8.40}$$

where l is the wing span; $c_z = c_z(\beta, M)$ is the coefficient of lateral force; $m_x = m_x(\delta_{ai}, \delta_{cr}, \omega_x, \omega_y, \beta, M)$ is the moment coefficient M_x; $m_y = m_y(\delta_{ai}, \delta_{cr},$

[1]Since it was assumed that the thrust of the engine passes through the center of gravity of the missile, the projections of the moment of this force on the axis are also equal to zero, i.e., $\Delta N_x = \Delta N_y = 0$.

ω_x, ω_y, β, M) is the coefficient of moment M_y; δ_{cr} is the angle of deflection of the course rudder, and δ_{ai} is the angle of deflection of the ailerons.

Equations (8.38) - (8.40) show that the forces and moments are nonlinear functions of a series of arguments[1]

$$Z = Z(\beta, \gamma); \quad M_x = M_x(\delta_{ai}, \delta_{cr}, \omega_x, \omega_y, \beta);$$

$$M_y = M_y(\delta_{ai}, \delta_{cr}, \omega_x, \omega_y, \beta).$$

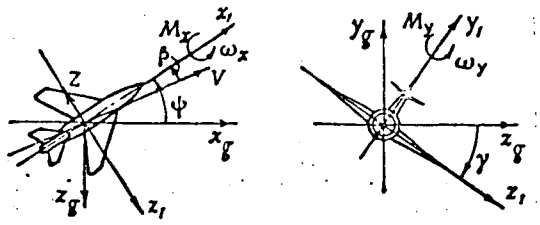

View from top View from rear

Figure 8.13. Force and moments acting on missile during lateral motion. x_1, y_1, z_1, are the axes of the fixed system of coordinates, γ is the tilt angle, Ψ is the pitch angle, β is the slip angle, Z is the lateral force, M_x is the moment of aerodynamic forces with respect to the x_1 axis; M_y is the moment of aerodynamic forces with respect to the y_1 axis.

In the initial unperturbed state of rectilinear uniform flight all parameters for the lateral motion and, consequently, force Z and moments M_x and M_y are equal to zero. During the deviation from the unperturbed state, the increment in force ΔZ and in moments ΔM_x, and ΔM_y, as in the case of longitudinal motion, are determined by the first terms in the expansion of these functions in powers of their arguments

---

[1] From equations (8.38) - (8.40) we see that the force Z and the moments M_x and M_y depend also on ρ, V and M; however, since these quantities pertain to the parameters of longitudinal motion, their effect cannot be taken into account in analyzing the isolated lateral motion by the method of linearization.

$$\left.\begin{aligned}\Delta Z &= Z^{\beta}\beta + Z^{\gamma}\gamma,\\ \Delta M_x &= M_x^{\delta_{ai}}\delta_{ai} + M_x^{\delta_{cr}}\delta_{cr} + M_x^{\omega_x}\omega_x + M_x^{\omega_y}\omega_y + M_x^{\beta}\beta,\\ \Delta M_y &= M_y^{\delta_{ai}}\delta_{ai} + M_y^{\delta_{cr}}\delta_{cr} + M_y^{\omega_x}\omega_x + M_y^{\omega_y}\omega_y + M_y^{\beta}\beta.\end{aligned}\right\} \tag{8.41}$$

The partial derivative Z is given directly by equation (8.38). To determine the partial derivatives Z^{β}, $M_x^{\delta_{ai}}$, $M_x^{\delta_{cr}}$, etc. the required relations for coefficients c_z, m_x, and m_y as a function of corresponding quantities are obtained analytically or by modeling in wind tunnels. Some of these relations are shown in figures 8.14 - 8.18. It is obvious that all characteristics must be recorded at the Mach number 2, corresponding to the initial unperturbed state.

Let us clarify the physical meaning of the individual components of moments ΔM_x and ΔM_y. The moments $M_x^{\delta_{ai}}\delta_{ai}$ and $M_y^{\delta_{cr}}\delta_{cr}$ are the basic control moments of the control surfaces--ailerons and course rudder. The moments $M_x^{\delta_{cr}}\delta_{cr}$ and $M_y^{\delta_{ai}}\delta_{ai}$ are parasitic moments which produce undesirable reactions on the missile when the control surfaces are displaced. The moment $M_x^{\delta_{cr}}\delta_{cr}$ produces a tilt of the missile when the course rudder is deflected, while the moment $M_y^{\delta_{ai}}\delta_{ai}$ tends to rotate the missile with respect to the normal axis y_1 when the ailerons are deflected. Usually these moments are very small and are shown here as part of the presentation. In most problems these moments can be neglected.

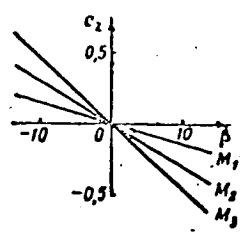

Figure 8.14. Variation in coefficients of lateral force as function of slip angle.

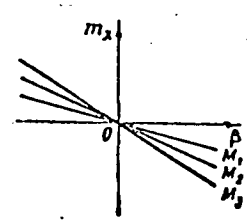

Figure 8.15. Variation in coefficients of moment m_x as function of slip angle.

The damping transverse moment $M_x^{\omega_x}\omega_x$ and the spiral twisting moment $M_y^{\omega_x}\omega_x$ appear during the rotation of the missile with respect to the x_1 axis when one wing is dropped and the other is raised. The angle of attack and the lift force

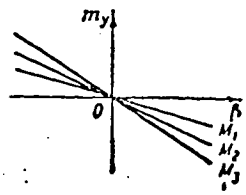

Figure 8.16. Variation in coefficient of moment m_y as function of slip angle.

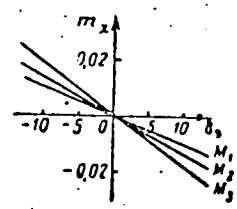

Figure 8.17. Variation in coefficient of moment m_x as function of angular displacement of ailerons.

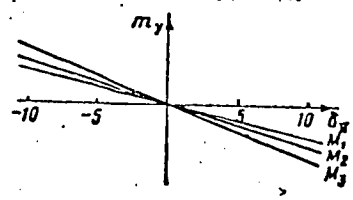

Figure 8.18. Variation in coefficient of moment m_y as function of angular deflection of course rudder.

on the dropped wing increase, while on the lifted wing they decrease. As a result, a moment $M_x^{\omega_x}\omega_x$ appears, proportional to the angular velocity of the missile ω_x and directed against this velocity ($M_x^{\omega_x} < 0$). The variation in the drag of the lowered and raised wing leads to a twisting moment $M_y^{\omega_x}\omega_x$ around the y_1 axis, proportional to the angular velocity ω_x. For small angles /268 of attack, this moment is usually negative ($M_y^{\omega_x} < 0$), i.e., it tends to rotate the missile in the negative direction (to the right) with respect to the y_1 axis when the angular velocity ω is positive (the right wing drops).

The damping twisting moment $M_y^{\omega_y}\omega_y$ appears due to the variation in the slip angle when the missile rotates with respect to the y_1 axis. As in the case of the damping moment, $M_z^{\omega_z}\omega_z$, the origin of moment $M_y^{\omega_y}\omega_y$ during longitudinal

motion is due to the effect of the stabilizer--in this case the vertical stabilizer. The moment $M_y^{\omega_y}\omega_y$ is negative ($M_y^{\omega_y} < 0$).

The moment $M_x^{\omega_y}\omega_y$ is called the transverse spiral moment. The rotation of the missile with respect to the y_1 axis increases the air velocity and, consequently, the lift on the external wing and decreases it on the internal wing. As a result, the moment $M_x^{\omega_y}\omega_y$ around the x_1 axis appears and is proportional to the angular velocity ω_y. This moment is negative ($M_x^{\omega_y} < 0$), i.e., it tends to produce a tilt on the left wing when the angular velocity ω_y is positive (to the left).

The moment $M_x^{\beta}\beta$ is the moment of the transverse static stability. It produces a tilt of the missile when the slip angle appears. The missile has lateral static stability when $M_x^{\beta} < 0$. This means that the slipping, which occurs during the tilt of the missile, produces a moment with respect to the x_1 axis which tends to decrease the tilt.

The moment $M_y^{\beta}\beta$ is called the moment of zero--torque stability. This moment is analogous to the moment of static stability during longitudinal motion. It is produced because the resulting lateral force (from the fuselage and from the vertical stabilizer, and in the case of cruciform wings also from the vertical wing), which appeared when the missile had a slip angle, does not pass through the center of gravity. If the point of application of this force is behind the center of gravity, then $M_y^{\beta} < 0$, and the missile has zero-torque stability. The moment $M_y^{\beta}\beta$ in this case tends to decrease slip angle β. During the tilt of the missile, the lowered wing slips. The missile with zero-torque stability rotates in the direction of the dropped wing and decreases the slip angle.

Let us substitute into equation (8.18) the values of the force and of the moments given by expression (8.41). We transpose the unknown parameters of lateral motion to the left sides of equations and reduce these equations to a more convenient form. As a result we obtain a system of equations which describes the lateral motion in the linear approximation /269

$$
\left.
\begin{aligned}
&\frac{d\beta}{dt} + k_\beta\beta - \frac{d\psi}{dt} - \alpha_e\frac{d\gamma}{dt} - k_\gamma\gamma = 0,\\
&\frac{d^2\gamma}{dt^2} + l_{\dot\gamma}\frac{d\gamma}{dt} + l_{\dot\psi}\frac{d\psi}{dt} + l_\beta\beta = l_{\delta_{ai}}\delta_{ai} + l_{\delta_{cr}}\delta_{cr},\\
&\frac{d^2\psi}{dt^2} + n_{\dot\psi}\frac{d\psi}{dt} + n_{\dot\gamma}\frac{d\gamma}{dt} + n_\beta\beta = n_{\delta_{ai}}\delta_{ai} + n_{\delta_{cr}}\delta_{cr},\\
&\frac{dz_g}{dt} = V_e(\beta - \psi),
\end{aligned}
\right\} \qquad (8.42)
$$

where α_e is the value of the angle of attack in the unperturbed state.

The coefficients contained in equation (8.42) have the following values

$$
\left.
\begin{aligned}
&k_\beta = -\frac{c_z^\beta}{2\tau_e};\quad k_\gamma = \frac{g}{V_e};\quad l_{\dot\gamma} = -\frac{m_x^{\bar\omega_x}}{\tau_e i_x};\quad l_{\dot\psi} = -\frac{m_x^{\bar\omega_y}}{\tau_e i_x};\\
&l_\beta = -\frac{m_x^\beta}{\tau_e^2 i_x}\mu_6;\quad l_{\delta_{ai}} = \frac{m_x^{\delta_{ai}}}{\tau_e^2 i_x}\mu_6;\quad l_{\delta_{cr}} = \frac{m_x^{\delta_{cr}}}{\tau_e^2 i_x}\mu_6;\\
&n_{\dot\psi} = -\frac{m_y^{\bar\omega_y}}{\tau_e i_y};\quad n_{\dot\gamma} = -\frac{m_y^{\bar\omega_x}}{\tau_e i_y};\quad n_\beta = -\frac{m_y^\beta}{\tau_e^2 i_y}\mu_6;\\
&n_{\delta_{ai}} = \frac{m_y^{\delta_{ai}}}{\tau_e^2 i_y}\mu_6;\quad n_{\delta_{cr}} = \frac{m_y^{\delta_{cr}}}{\tau_e^2 i_y}\mu_6;\quad \bar\omega_x = \frac{\omega_x}{2V_e}l;\quad \bar\omega_y = \frac{\omega_y}{2V_e}l;\\
&\mu_6 = \frac{2m}{\rho_e S l};\quad \tau_e = \frac{m}{\rho_e S V_e};\quad i_x = \frac{4J_x}{ml^2};\quad i_y = \frac{4J_y}{ml^2}.
\end{aligned}
\right\} \qquad (8.43)
$$

The coefficient μ_d is known as the relative density of the missile in lateral motion, while i_x and i_y are coefficients of the moment of inertia of the missile with respect to the x_1 and y_1 axes; the bars over ω_x and ω_y indicate that these quantities are dimensionless. All partial derivatives in equation (8.43) are computed for the values of arguments corresponding to the unperturbed state.

In the system of equations (8.42), all angles are expressed in radians. If it becomes necessary to measure the angles in degrees, the coefficients of the first three equations remain unchanged, because they contain only the angular parameters of lateral motion. When the angles are measured in degrees, the last equation must be written in the form

$$\frac{dz_g}{dt} = \frac{V_e}{57.3}(\beta^\circ - \psi^\circ).$$

To analyze the lateral motion of a missile with cruciform wings or of a missile with angular wings, equation (8.42) must be slightly changed. Usually /270

missiles of this type are stabilized with respect to their longitudinal axis in a definite position. Assuming that the stabilization system of the missile tilt works sufficiently well, we may assume that the tilt angles and the derivatives of these angles are small and, therefore, assume that they are equal to zero in the second and third equations of system (8.42). As a result, the system will be divided into two parts. The first part will contain equations describing the lateral motion of the missile's stabilized tilt

$$\left.\begin{aligned} &\frac{d\beta}{dt} + k_\beta \beta - \frac{d\psi}{dt} = 0, \\ &\frac{d^2\psi}{dt^2} + n_{\dot\psi}\frac{d\psi}{dt} + n_{\dot\beta}\frac{d\beta}{dt} + n_\beta \beta = n_\delta \delta_{cr}, \\ &\frac{dz_g}{dt} = V_e(\beta - \psi). \end{aligned}\right\} \tag{8.44}$$

The appearance of the term $n_{\dot\beta}\, d\beta/dt$ in the second equation of (8.44) is associated with the tapering of the flow at the stabilizer. This term has the same origin as the term $C_{\dot\alpha}\, d\Delta\alpha/dt$ in equations (8.26), i.e., it is due to the interference between the wing and the stabilizer. In equations for the lateral motion of a missile with plane wings, this term is absent because there are no wings in the x_1Oy_1 plane. The value of coefficient $n_{\dot\beta}$ is equal to

$$n_{\dot\beta} = -\frac{m_y^{\bar{\dot\beta}}}{\tau_e i_y}, \tag{8.45}$$

where

$$\bar{\dot\beta} = \frac{l}{2V_e}\frac{d\beta}{dt}.$$

The second part consists of one equation which must be utilized in designing the control system or the system for stabilizing the tilt[1]

$$\frac{d^2\gamma}{dt^2} + l_{\dot\gamma}\frac{d\gamma}{dt} = l_{\delta_{ai}}\delta_{ai}. \tag{8.46}$$

Let us investigate the stability of the missile's lateral motion without a control system. Equation (8.44) for the lateral motion of a missile with cruciform wings and with a stabilized tilt angle are entirely identical to the /271

[1] In equations (8.44) and (8.46) the terms $l_{cr}\,\delta_{cr}$ and $n_{ai}\,\delta_{ai}$ are dropped, because they are small compared with the remaining terms of the corresponding equations.

simplified equation (8.31) for the horizontal longitudinal motion with constant velocity. The third of equations (8.44) is not taken into account in the analysis of stability, because the coordinate of the center of gravity z_g has no effect on flight stability. The characteristic polynomial for the two first equations of system (8.44) has the form

$$A(p) = p(p^2 + a_1 p + a_2), \tag{8.47}$$

where

$$\left.\begin{aligned} a_1 &= k_\beta + n_{\dot\beta} + n_{\dot\psi}, \\ a_2 &= k_\beta n_{\dot\psi} + n_\beta. \end{aligned}\right\} \tag{8.48}$$

From the structure and the physical meaning of individual terms, coefficients a_1 and a_2 of polynomial (8.47) coincide with the coefficients of polynomial (8.32), which were determined from equation (8.33). Therefore, the analysis of the values of coefficients (8.33) and conclusions concerning the stability of short period longitudinal motion, presented in section 8.4, may be applied to the polynomial (8.47) and to the stability of the lateral motion of a missile with cruciform wings whose angle of tilt is stabilized. We should only bear in mind that coefficients b_α, c_α, $c_\alpha^\cdot$ and $c_\vartheta^\cdot$ of the longitudinal motion are equivalent (for a missile with cruciform wings) to coefficients k_β, n_β, $n_\beta^\cdot$ and $n_\psi^\cdot$ of the lateral motion, respectively.

Equation (8.42), which describe the lateral motion of a missile with plane wings without a control system, turn out to be somewhat more complex than for the case of a missile with cruciform wings. If we drop the last equation (8.42), because it refers to the motion of the center of gravity, we obtain a system consisting of three equations. The characteristic polynomial for this system has the form

$$A_1(p) = p^4 + a_1 p^3 + a_2 p^2 + a_3 p + a_4, \tag{8.49}$$

where

$$\left.\begin{aligned} a_1 &= k_\beta + l_\gamma^\cdot + n_{\dot\psi}^\cdot; \\ a_2 &= l_{\dot\psi}^\cdot n_\gamma^\cdot + l_\gamma^\cdot n_{\dot\psi}^\cdot + k_\beta(l_\gamma^\cdot + n_{\dot\psi}^\cdot) + n_\beta + \alpha_e l_\beta; \\ a_3 &= k_\beta(l_\gamma^\cdot n_{\dot\psi}^\cdot - n_\gamma^\cdot l_{\dot\psi}^\cdot) + k_\gamma l_\beta + l_\gamma^\cdot n_\beta - n_\gamma^\cdot l_\beta + \alpha_e(l_\beta n_{\dot\psi}^\cdot - l_{\dot\psi}^\cdot n_\beta); \\ a_4 &= k_\gamma(l_\beta^\cdot n_{\dot\psi}^\cdot - l_{\dot\psi}^\cdot n_\beta). \end{aligned}\right\} \tag{8.50}$$

When we derived the characteristic polynomial (8.49), we took the unknown functions γ, β and $d\psi/dt$ in the first three equations of system (8.42), because, without a control system, the missile is neutral with respect to angle ψ.

The coefficient a_4 of the characteristic polynomial (8.49), as a rule, is a rather small positive or negative quantity. As a result, the polynomial (8.49) has one small real root, which is approximately equal to minus (a_4/a_3). The second real root is very large and is approximately equal to coefficient a_1 /272 taken with a negative sign. This large negative root characterizes the intensely damped motion of the missile with respect to its tilt, since the basic component a_1 is the coefficient of the tilt damping moment $l_{\dot{\gamma}}$. The remaining two roots are usually complex conjugates with a small real part. If the small root is positive $(a_4 < 0)$, while the large root and the real parts of the complex roots are negative, it is possible to have the spiral instability of the lateral motion of the missile. Since the positive root is small, the parameters which characterize lateral motion (γ, β and $d\psi/dt$) will increase slowly, so that the missile will move along a spiral. If, on the other hand, the complex roots have a positive real part, oscillatory instability occurs: the missile will roll from wing to wing with increasing amplitudes in the oscillations of the tilt angle and the slip angle. All these phenomena, which are not permissible, are removed by the missile control system with a proper selection of its parameters.

Missiles which possess complete (or almost complete) aerodynamic symmetry do not change their motion during rotation with respect to the longitudinal axis. Therefore, it is not necessary to stabilize the tilt, and they can rotate slowly during flight due to some inaccuracy in fabrication of the glider. It is obvious that such missiles have no ailerons. In describing the lateral motion of such missiles, it is rational to use the flow axes (rather than the fixed axes), which are fixed with respect to the trajectory and not with respect to the missile and which, therefore, do not rotate together with the missile in space.

The motion of missiles, which rotate around the longitudinal axis with high velocity, cannot be divided into its longitudinal and transverse components. These missiles are subjected to a series of additional forces, which are not considered in this chapter. Therefore, in the motion of such missiles we cannot use the equations presented here. The present book does not consider rotating missiles.

Section 8.6. Equations for the Longitudinal Motion of a Missile Obtained by the Method of Grouping

Let us derive the equations for the isolated longitudinal motion of a missile. We make use of figure 8.7 showing the forces and moments acting on the missile during this motion. We write the equations for the projection of the forces using the flow axes x and y and the moment about the z_1 axis fixed with /273 respect to the missile. These equations have the form

$$
\left.\begin{aligned}
&m\frac{dV}{dt} = -X - G\sin\theta + P\cos\alpha,\\
&mV\frac{d\theta}{dt} = Y = G\cos\theta + P\sin\alpha,\\
&J_z\frac{d^2\vartheta}{dt^2} = M_z,\\
&\vartheta = \theta + \alpha,\\
&\frac{dx_g}{dt} = V\cos\theta,\\
&\frac{dy_g}{dt} = V\sin\theta.
\end{aligned}\right\} \tag{8.51}
$$

If we substitute into (8.51) the values of drag X, lift Y and moment M_z, obtained from equations (8.23) - (8.25) and transpose the terms with unknown functions to the left side, we obtain two groups of equations

$$
\left.\begin{aligned}
&m\frac{dV}{dt} + c_x S\frac{\rho V^2}{2} = -G\sin\theta + P\cos\alpha;\\
&\frac{dx_g}{dt} = V\cos\theta;\ \frac{dy_g}{dt} = V\sin\theta;
\end{aligned}\right\} \tag{8.52}
$$

$$
\left.\begin{aligned}
&mV\frac{d\theta}{dt} - c_y^\alpha S\frac{\rho V^2}{2}\alpha + G\cos\theta - P\sin\alpha = 0;\\
&J_z\frac{d^2\vartheta}{dt} - m_z^{\bar{\omega}_z} S b_A^2\frac{\rho V}{2}\frac{d\vartheta}{dt} - m_z^{\dot{\bar{\alpha}}} S b_A^2\frac{\rho V}{2}\frac{d\alpha}{dt} -\\
&- m_z^\alpha S b_A\frac{\rho V^2}{2}\alpha = m_z^M S b_A\frac{\rho V^3}{2a} + m_z^\delta S b_A\frac{\rho V^2}{2}\delta_{el},\\
&\vartheta = \theta + \alpha.
\end{aligned}\right\} \tag{8.53}
$$

The group of equations (8.52) contains equations whose terms are determined primarily by the motion of the missile's center of gravity, i.e., by motion which is substantially slower than the motion with respect to the center of gravity. We make definite assumptions concerning angles θ and α[1] and determine the flight velocity of the missile V from the first equation of (8.52). Since this equation is nonlinear and has variable coefficients (m, c_x, α, θ, depending on time), its solution may be obtained most simply by numerical or graphic means. Following this, x_g and y_g are determined from the second and third equation. /274

[1] For example, the approximate value of these angles as a function of time, as we shall show below, may be obtained from trajectories constructed only on the basis of the kinematics of missile motion.

After the flight velocity has been determined, its value as a function of time is substituted into equations (8.53), which, as a result, transform into linear equations with variable coefficients. The nonlinear functions of cos θ and sin θ, which remain in the first equation of (8.53), are linearized by means of some assumption. For example, when flight is close to horizontal, we may assume that $\cos\theta \approx 1$; when the angle of attack is small, we may assume that $\sin\alpha \approx \alpha$. If necessary, we may also take into account in these equations the variation in air density with altitude as a function of time, because the variation in the altitude y_g as a function of time is determined by the third equation of (8.52). The relation between the altitude and air density is given graphically (fig. 8.11). In the same way, by considering the operation of the engine, we may determine approximately the variation in the mass of the missile m and the moment of inertia J_z.

The system of linear equations with variable coefficients obtained in this way can be analyzed by any of the methods presented in section 2.4.

Section 8.7. Equations for the Lateral Motion of a Missile Obtained by the Method of Grouping

Let us formulate equations for the isolated lateral motion of a missile with plane wings with respect to the fixed axes. For this purpose we use figure 8.13. Assuming that the fixed axes are the principal axes of inertia, and neglecting all terms which contain the parameters of longitudinal motion, we obtain a system of equations for lateral motion[1]

$$\left.\begin{aligned} mV\frac{d\beta}{dt} - mV\frac{d\psi}{dt} &= Z, \\ J_x\frac{d^2\gamma}{dt^2} &= M_x, \\ J_y\frac{d^2\psi}{dt^2} &= M_y, \\ \frac{dz_g}{dt} &= V(\sin\beta - \sin\psi). \end{aligned}\right\} \qquad (8.54)$$

Substituting into (8.54) the values of the lateral force Z and of the moments M_x and M_y, using equation (8.41) and transposing terms with unknown functions to the left side, we obtain /275

[1] The moments due to reactive forces are not taken into account, because it was assumed that the thrust passes through the center of gravity.

$$
\left.\begin{aligned}
& mV\frac{d\beta}{dt} - mV\frac{d\psi}{dt} - c_z^{\beta}S\frac{\rho V^2}{2}\beta - G\sin\gamma = 0,\\
& J_x\frac{d^2\gamma}{dt^2} - m_x^{\bar{\omega}}S\frac{l^2}{2}\frac{\rho V}{2}\frac{d\gamma}{dt} - m_x^{\bar{\omega}}S\frac{l^2}{2}\frac{\rho V}{2}\frac{d\psi}{dt} - m_x^{\beta}Sl\frac{\rho V^2}{2}\beta = m_x^{\delta}Sl\frac{\rho V^2}{2}\delta_{ai},\\
& J_y\frac{d^2\psi}{dt^2} - m_y^{\bar{\omega}}S\frac{l^2}{2}\frac{\rho V}{2}\frac{d\psi}{dt} - m_y^{\bar{\omega}}S\frac{l^2}{2}\frac{\rho V}{2}\frac{d\gamma}{dt} - m_y^{\beta}Sl\frac{\rho V^2}{2}\beta = m_y^{\delta}Sl\frac{\rho V^2}{2}\delta_{cr}.\\
& \frac{dz_g}{dt} = V(\sin\beta - \sin\psi).
\end{aligned}\right\} \qquad (8.55)
$$

The first equation has one nonlinear function of $\sin\gamma$. In the overwhelming majority of cases, the angle of tilt of missiles with plane wings is limited to values such that for all practical purposes $\sin\gamma = \gamma$. In this case, the first equation becomes linear. Thus, in system (8.55) the first three equations are linear with variable coefficients. The variation with time in flight velocity V and, when necessary, in air density ρ and in missile mass m are taken from results obtained by solving the equations of longitudinal motion. When the mass of the missile varies, we can compute approximately the variations in the moments of inertia J_x and J_y as functions of time. As far as the fourth equation of (8.55) is concerned, it is isolated and can be integrated after the functions $\beta(t)$ and $\psi(t)$ are obtained from the first three equations. However, if it turns out that it is connected with other equations through the control system, then, when we investigate the system to obtain an analytical solution, this equation must be linearized by means of some assumption. The simplest assumptions concern the small values of angles β and ψ, in which case we let $\sin\beta \approx \beta$ and $\sin\psi \approx \psi$.

If the missile has cruciform wings and is stabilized with respect to its angle of tilt, the system of equations (8.55) can be separated into two isolated groups. The first group contains the equations of motion with respect to the y_1 axis and along the z_g axis

$$
\left.\begin{aligned}
& m\frac{d\beta}{dt} - m\frac{d\psi}{dt} - c_z^{\beta}S\frac{\rho V}{2}\beta = 0,\\
& J_y\frac{d^2\psi}{dt^2} - m_y^{\bar{\omega}_y}S\frac{l^2}{2}\frac{\rho V}{2}\frac{d\psi}{dt} - m_y^{\bar{\beta}}S\frac{l^2}{2}\frac{\rho V}{2}\frac{d\beta}{dt} - m_y^{\beta}Sl\frac{\rho V^2}{2}\beta = m_y^{\delta}Sl\frac{\rho V^2}{2}\delta_{cr},\\
& \frac{dz_g}{dt} = V(\sin\beta - \sin\psi).
\end{aligned}\right\} \qquad (8.56)
$$

The second group contains the equations of rotation with respect to the x_1 axis, which are used in designing the stabilization system for the tilt of the missile /276

$$
J_x\frac{d^2\gamma}{dt^2} - m_x^{\bar{\omega}_x}S\frac{l^2}{2}\frac{\rho V}{2}\frac{d\gamma}{dt} = m_x^{\delta}Sl\frac{\rho V^2}{2}\delta_{ai}. \qquad (8.57)
$$

In sections 8.6 and 8.7 the method of grouping has been used to obtain equations with variable coefficients describing the longitudinal and lateral movements of a missile with variable velocity. These equations will be used to analyze various methods for selecting the parameters of missile guidance systems.

CHAPTER 9. THE STRUCTURE OF AUTOMATIC PILOTS /277

Section 9.1. General Information

An automatic pilot of a missile is a device which receives signals from different sensors and by transforming these signals actuates the control surfaces of the missile. Thus, the automatic pilot is one of the principal components of a missile control system. Figure 9.1 shows the functional diagram of an automatic pilot. This diagram includes the sensors, the computer and the actuators.

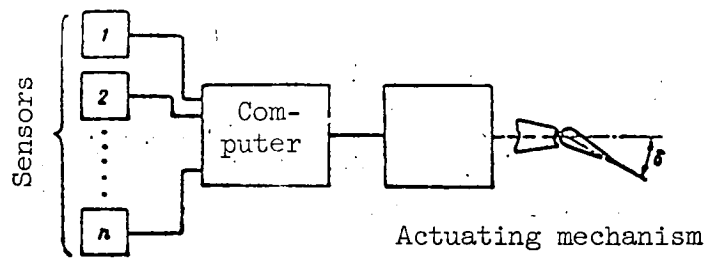

Figure 9.1. Functional diagram of automatic pilot.

The sensors which feed their signals into the computer measure the values of those parameters of missile motion which are necessary to provide the necessary guidance and the necessary dynamic properties of the control system. Such parameters include various angular coordinates characterizing the position of the missile with respect to the target and the surface of the Earth, the derivatives of these coordinates and sometimes the linear coordinates of the missile's center of gravity with respect to a given trajectory and the derivatives with respect to these coordinates. Special equipment, described in Chapters 3-5, is used to measure some of these parameters. Other parameters are measured by sensors which are common to all missiles, such as gyroscopes, manometers, accelerometers, etc. /278

Some of the devices which pertain to sensors (fig. 9.1) may be very complex elements of the control system, containing closed loop automatic control systems, tracking systems and computer elements. Such complex devices include the homing heads of missiles, radar receivers for developing control signals during beam guidance, gyro-inertial systems for determining the coordinates of missiles with self-contained guidance and many other control elements.

The computer of an automatic pilot in the simplest case represents a summation device which adds the signals from the sensors in a required proportion.

In the general case, the computer may perform any operations on the signals which it receives. The basic operations of the computer are described in Chapter 6. When the signals are transformed, it is frequently necessary to amplify their voltage or power, which is accomplished by the amplifiers of various types considered in Chapter 7. A computer shapes the control signal u, which is fed to the actuator of the automatic pilot. The latter represents a device which moves the control surfaces of the missile.[1] The driving units used aboard missiles may be electric, pneumatic or hydraulic. These forms of actuators are described in Chapter 7. Thus, all elements contained in an automatic pilot of a missile have been described in previous chapters. In the present chapter we shall consider the more common functional diagrams of automatic pilots.

Section 9.2. Functional Diagrams of Automatic Pilots

According to figure 9.1, the sensors in the computer shape the control signal which must be utilized by the actuating mechanism of an automatic pilot. One way of classifying automatic pilots is by the structure of their actuating mechanisms. To clarify this structure, let us consider the functional diagram of this mechanism, shown in figure 9.2. As we can see, the actuating mechanism in the general case represents a closed loop automatic control system for the control surfaces. The driver with a power amplifier, characterized by the transfer function $W_{\delta/\Delta u}(p)$, rotates the control surface by means of a reducer or without it, /279

and the deflection of the control surface is measured by some sensor. The signal from this sensor moving along a feedback path with transfer function $W_{u_1\delta}(p)$ is

fed to the input of the system, where it is compared with control signal u. From the form of the transfer function for the feedback loop $(W_{u_1/\delta}(p))$ it is custom-

ary to distinguish between automatic pilots with fixed feedback and automatic pilots with rate feedback or without feedback and, finally, automatic pilots with isodromic feedback.

1. Automatic Pilot with Fixed Feedback. In automatic pilots with fixed feedback the transfer function of the feedback network is constant, i.e.,

$$W_{u_1/\delta}(p) = k_c. \tag{9.1}$$

Most automatic pilots use electrical signals in the signal shaping networks. In this case, fixed feedback is accomplished in the form of some signal generator (potentiometer, selsyn) which transforms the angular deflection of the control surface into an electric voltage.

The transfer functions of drivers (electric, hydraulic, pneumatic) in the region of their linear characteristics are the same and have the form (see equations (7.15), (7.23) and (7.29))

---

[1] The actuator of an automatic pilot is frequently called the control surface mechanism.

$$W_{\delta/\Delta u}(p) = \frac{k_d}{p(T_d p + 1)}, \tag{9.2}$$

where k_d is the amplification factor of the drive equal to the ratio of the angular velocity of the control surface to the voltage Δu at the output, and T_d is the time constant for turning on the driver which produces the lag and the driving force.

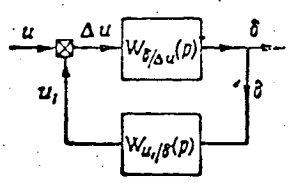

Figure 9.2. Functional diagram of actuating mechanism of automatic pilot.

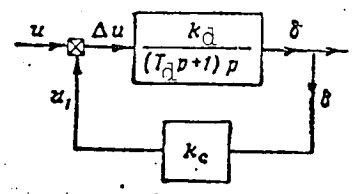

Figure 9.3. Functional diagram of actuating mechanism of automatic pilot with fixed feedback.

The functional diagram of an actuating mechanism of an automatic pilot with fixed feedback is shown in figure 9.3. On the basis of this functional diagram we obtain the differential equation which describes the dynamics of the actuating mechanism of an automatic pilot /280

$$\frac{T_d}{k_d k_c}\frac{d^2\delta}{dt^2} + \frac{1}{k_d k_c}\frac{d\delta}{dt} + \delta = \frac{1}{k_c}u. \tag{9.3}$$

The actuators of automatic pilots are designed in such a way that the start time T_d is as short as possible, and in any case, is less than one second. This time constant is divided into the product of coefficients k_d/k_c, which usually has a value of 3-10 1/sec. For these reasons, the coefficient in front of the second derivative turns out to be very small and at this time can be neglected. As a result, we obtain a differential equation of the first order

$$T_a\frac{d\delta}{dt} + \delta = i_a u, \tag{9.4}$$

where $T_a = 1/k_d k_c$ is the time constant of the actuator of the automatic pilot, and $i_a = 1/k_c$ is the transfer factor (amplification factor) of the actuating mechanism of the automatic pilot.

The value of the time constant T_a in modern automatic pilots is equal to (0.1 to 0.3) sec, while the control time for the most rapid motions of the missile involving variation in the tilt angle and the pitch angle is 1.5 - 3.0 sec. The control time of the yaw angle and particularly of the linear coordinates of the missile is substantially greater. These data make it possible to neglect the time constant of the automatic pilot when selecting the parameters of the missile control system (make it possible to neglect the transfer factors of the automatic pilot with respect to specific parameters fed into the computer). As a result of this assumption, the differential equation of the automatic pilot (9.4) is transformed into an algebraic equation

$$\delta = i_a u. \tag{9.5}$$

Equation (9.5) is the equation of an ideal automatic pilot, i.e., one without inertia.

As we can see from the functional diagram in figure 9.1, the control signal u, in general, is the sum of several signals. Thus, for example, when stabilizing the tilt angle of a missile, the control signal may be expressed in the following manner

$$u = k_\gamma \gamma + k_{\dot\gamma} \frac{d\gamma}{dt}, \tag{9.6}$$

where γ and $d\gamma/dt$ is the tilt angle of the missile and its angular velocity respectively. /281

Substituting this value of u into equation (9.5) we obtain

$$\delta = i_\gamma \gamma + i_{\dot\gamma} \frac{d\gamma}{dt}, \tag{9.7}$$

where $i_\gamma = i_a k_\gamma$ is the transfer factor of the automatic pilot with respect to tilt, and $i_{\dot\gamma} = i_a k_{\dot\gamma}$ is the transfer function of the automatic pilot with respect to the angular velocity of tilt.

The final equation of the automatic pilot (9.7) will not change if equations (9.5) and (9.6) are written in the following form

$$\delta = u, \tag{9.8}$$

$$u = i_\gamma \gamma + i_{\dot\gamma} \frac{d\gamma}{dt}. \tag{9.9}$$

In practice it is more convenient to represent the automatic pilot by means of transfer numbers (i_γ, $i_{\dot\gamma}$, etc.) with respect to different signals, as done in equation (9.9), than to take into account the transfer number of actuating mechanism of the automatic pilot i_a and portions of the signals (k_γ, $k_{\dot\gamma}$, etc.) as is

done in equations (9.5) and (9.6). Therefore, the equation of an ideal automatic pilot will be written in the form (9.8) for convenience. As we can see from expression (9.8), the ideal automatic pilot with fixed feedback produces an angular deflection of the control surface equal to the control signal.

It is necessary to point out that the equations for an idealized automatic pilot can be used only when the parameters of the control system are selected in the manner indicated. In analyzing the operation of the actuating mechanism itself, the complete equation (9.3) should be used. This is particularly important when investigating the effect of various nonlinearities in the actuating mechanism (free play, zone of insensitivity, dry friction), which were not taken into account in deriving equation (9.3), but which may produce a substantial effect on the proper operation of this mechanism. This pertains not only to an automatic pilot with fixed feedback, but to all of the automatic pilots considered below.

2. Automatic Pilot with Rate Feedback or Without Feedback. To form rate feedback, it is necessary to obtain a signal which is proportional to the angular velocity of the control surface, i.e., to the derivative of the angular displacement of the control surface. In this case, the transfer function of the feedback network has the form /282

$$W_{u_1\delta}(p) = k\,p. \tag{9.10}$$

To obtain this signal, a tachometer is usually used, with voltage proportional to the angular velocity of the control surface.

The functional diagram of an actuating mechanism of an automatic pilot with proportional feedback is shown in figure 9.4. On the basis of this functional diagram we obtain a differential equation which describes the dynamics of the actuating mechanism of an automatic pilot

$$T_a \frac{d^2\delta}{dt^2} + \frac{d\delta}{dt} = i_a u, \tag{9.11}$$

where

$$\left.\begin{aligned} T_a &= \frac{T_d}{1 + k_d k_c}; \\ i_a &= \frac{k_d}{1 + k_d k_c}. \end{aligned}\right\} \tag{9.12}$$

If rate feedback is not introduced ($k_c = 0$), we obtain a diagram of an actuating mechanism of an automatic pilot without feedback, whose equation has the same form as equation (9.11) of an automatic pilot with rate feedback, but the values of the time constant and of the transfer number are determined by expressions

$$\left.\begin{aligned} T_a &= T_d, \\ i_a &= k_d. \end{aligned}\right\} \tag{9.13}$$

A comparison of expressions (9.12) and (9.13) for the time constant and the transfer number of the actuating mechanism of automatic pilots with rate feedback and without it shows that the introduction of rate feedback leads to a decrease of both these quantities by a factor $(1 + k_d k_c)$. As we have already stated, the value of the time constant T_d is usually small, and the introduction of rate feedback is not necessary in these cases. Therefore, the automatic pilots of this scheme are most frequently designed without rate feedback. If in equation (9.11) we neglect the lag in the actuating mechanism of the automatic pilot due to the small value of the time constant T_a, we obtain an equation for the ideal automatic pilot with rate feedback or without feedback. /283

$$\frac{d\delta}{dt} = i_a u. \tag{9.14}$$

From the analogy with equation (9.8), equation (9.14) may also be conveniently written in the form

$$\frac{d\delta}{dt} = u, \tag{9.15}$$

by referring the transfer number of the actuating mechanism of the automatic pilot to the transfer number of the entire automatic pilot with respect to

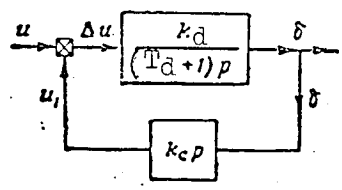

Figure 9.4. Functional diagram of actuating mechanism of automatic pilot with rate feedback.

individual signals. Thus, equation (9.15) shows that for an ideal automatic pilot with rate feedback or without feedback, the angular velocity of the control surface is equal to the control signal.

3. Automatic Pilot with Isodromic Feedback. In purely mechanical automatic control systems (e.g., in a centrifugal regulator of angular velocity), a device known as an isodrome was used to realize astaticism. The diagram of an isodrome is shown in figure 9.5. The input quantity of the isodrome is the displacement y of the control lever connected with the piston rod, while the output quantity is the displacement x of the isodrome cylinder. During a sudden displacement of the

lever's end by y, the cylinder with the piston behaves like a rigidly connected body, and the piston obtains a displacement x proportional to y. The spring is compressed and, due to the pressure difference, the liquid in the connecting tube begins to flow from one cavity to the other until the piston assumes an equilibrium position (x = 0). The transfer function of an isodrome has the form

$$W_{x/y}(p) = k_c \frac{T_i p}{T_i p + 1}, \tag{9.16}$$

where T_i is the time constant of the isodrome, which depends on the cross section area of the cylinder and of the connecting tube and also on the rigidity of the spring; and k_c is the factor of proportionality equal to the ratio of the arms of the driving lever.

As shown in Chapter 6, the transfer function analogous to expression (9.16) is characteristic of an RC differentiating network (equation (1) in table 2.5). Therefore, to achieve isodromic feedback in an automatic pilot with electric signals, the control surface must be displaced to cause the potentiometer to generate a signal and to feed this signal voltage to the RC network. /284

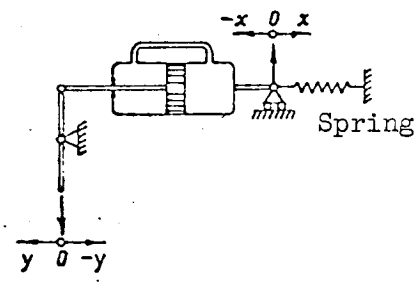

Figure 9.5. Schematic diagram of isodrome.

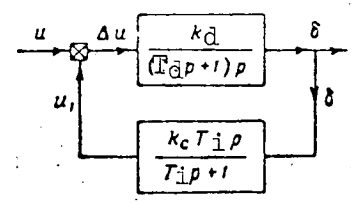

Figure 9.6. Functional diagram of actuating mechanism of automatic pilot with isodromic feedback.

The functional diagram of an actuating mechanism with isodromic feedback is shown in figure 9.6. On the basis of this functional scheme we obtain the differential equation

$$\frac{T_i T_d}{1 + k_d k_c T_i} \cdot \frac{d^3\delta}{dt^3} + \frac{T_i + T_d}{1 + k_d k_c T_i} \frac{d^2\delta}{dt^2} + \frac{d\delta}{dt} = \frac{k_d T_i}{1 + k_d k_c T_i} \frac{du}{dt} + \frac{k_d}{1 + k_d k_c T_i} u. \tag{9.17}$$

Since the quantity $(1 + k_d k_c T_i)$ is usually much greater than unity, the coefficients in front of the third and second derivatives with respect to the angular deflection of the control surface turn out to be quite small. To select the parameters of the control system we can neglect these terms in equation (9.17) and obtain an equation for the ideal automatic pilot in the form

$$\frac{d\delta}{dt} = i_a T_i \frac{du}{dt} + i_a u,$$

where $i_a = \frac{k_d}{1 + k_d k_c T_i}$ is the transfer number of the actuating mechanism of the automatic pilot.

As in the preceding cases, the coefficient i_a may be referred to the transfer numbers of the automatic pilot for different signals. As a result, the equation of an ideal automatic pilot with isodromic feedback takes the form

$$\frac{d\delta}{dt} = T_i \frac{du}{dt} + u. \tag{9.19}$$

Equation (9.19) shows that in this automatic pilot the rate of control surface deflection is proportional to the control signal as well as to its derivative. /285

Section 9.3. Examples of Automatic Pilot Systems for Controlling Missiles

As an example of an automatic pilot with fixed feedback we consider the automatic pilot of an airplane-missile which is guided to the target by means of a radio navigation system (hyperbolic or circular, see section 4.4). Figure 9.7 shows the functional diagram of such an automatic pilot,[1] while figure 9.8 shows its individual blocks and their interaction.

In the vertical plane the missile is controlled by elevators, while in the horizontal plane it is controlled by means of the tilt angle produced by ailerons. The rudder is designed only to eliminate slipping, which may occur during the evolutions of the missile. The slip angle (β) is measured by means of a special sensor. The stabilization of the missile with respect to the pitch angle (ϑ) and the tilt angle (γ) is accomplished by signals from the gyrovertical. To improve the dynamic characteristics of the stabilization process according to these parameters, signals are transmitted from the rate gryoscopes, which give the angular velocities of pitch ($d\vartheta/dt$) and tilt ($d\gamma/dt$). The stabilization of altitude

---

[1]The solid lines between the blocks of the diagram in figure 9.7 correspond to electric couplings, while the broken lines show mechanical couplings.

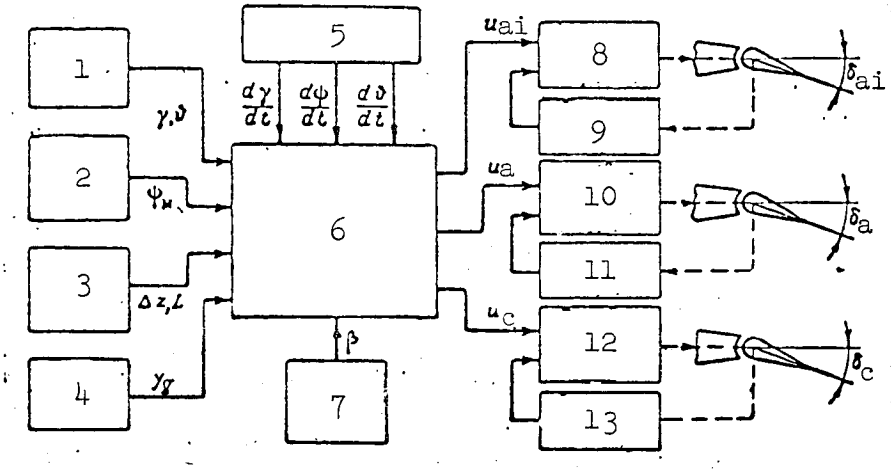

Figure 9.7. Functional diagram of automatic pilot with fixed feedback. 1--gyrovertical; 2--magnetic course sensor; 3--radio navigation unit; 4--altitude sensor; 5--rate gyros; 6--computer; 7--slip; 8--aileron actuator; 9--feedback sensor; 10--altitude control surface actuator; 11--feedback sensor; 12--course rudder actuator; 13--feedback sensor; (subscripts ai = aileron, a = altitude, c = course).

is accomplished by an altitude sensor (y_g). The stabilization of the missile on a given trajectory is accomplished by a signal showing the deviation of the center of gravity of the missile from this trajectory (Δz), which is produced by the element of the radio navigation system. To improve the dynamic characteristics of the stabilization process along the trajectory, the signals from the magnetic course sensor (ψ_m) and from the rate gyroscope for yaw ($d\psi/dt$) are used. The radio navigation system measures the range to the target (L), and when the desired range is obtained, it sends a signal (ϑ_3) to put the missile into a dive towards the target.

All sensors of an automatic pilot produce their signals in the form of electric voltages and transmit them to the computer. Here, the signals are processed, smoothed out to the desired degree and fed to actuating mechanisms of all three control surfaces. Due to fixed feedback, the angle of deflection of the control surface is proportional to the control signal fed to the input of the actuator. By applying the coefficient of proportionality to each component of this signal we obtain an equation of an automatic pilot with fixed feedback in the form $\delta = u$. The computer provides for the execution of all evolutions of the missile in the horizontal plane without slip and without loss of altitude. A detailed analysis of the dynamics of a missile with automatic pilot for various control systems is presented in Chapters 10 and 11. /287

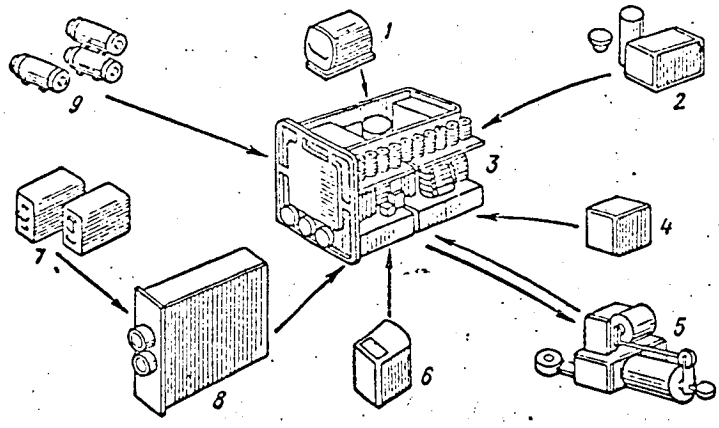

Figure 9.8. Component parts of automatic pilot with fixed feedback. 1--gyrovertical; 2--equipment for obtaining magnetic course (sensor, gyroscope, amplifier); 3--computer and power amplifier; 4--slip angle sensor; 5--one of three hydraulic actuators; 6--altitude sensor; 7--transceiver of the radio navigation system; 8--communication unit between automatic pilot and radio navigation equipment; 9--rate gyroscopes for pitch, yaw and tilt.

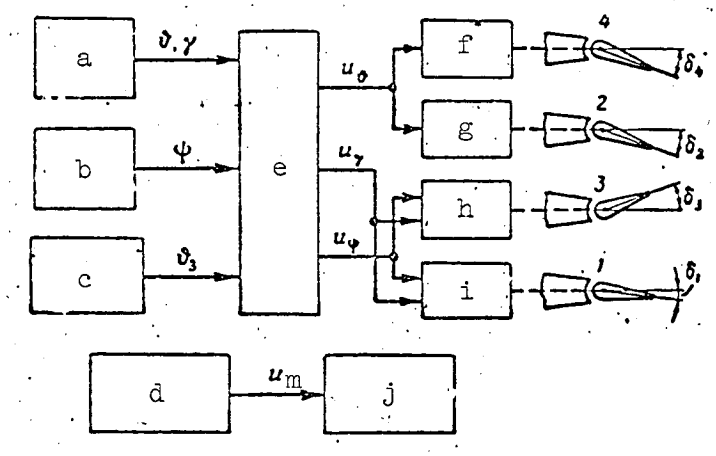

Figure 9.9. Functional diagram of automatic pilot without feedback. a--gyrovertical; b--course gyro; c--programming mechanism; d--sensor for turning on the motor; e--computer; f--control actuator; g--control actuator; h--control actuator; i--control actuator; j--valve for turning on motor; (subscript m = motor).

As an example of an automatic pilot without feedback we consider the automatic pilot of a ballistic missile. The rocket is controlled only over the active region of its trajectory, when the engine develops a thrust substantially in excess of its weight. Since the rocket has no wings, the control force which varies the flight trajectory is obtained by moving the frame of the rocket with respect to its center of gravity, as a result of which the thrust produces a component which is normal to the initial flight direction (figure 1.8). Figure 9.9 shows the block diagram of an automatic pilot used in a ballistic missile.

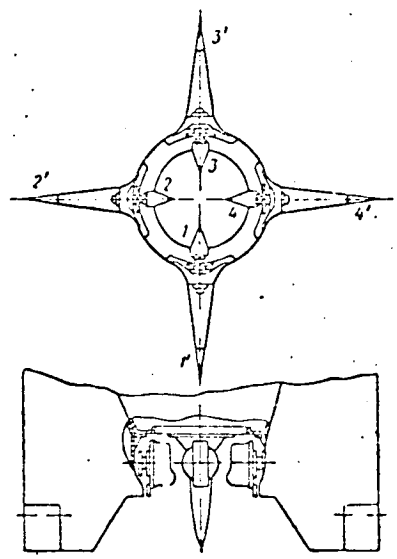

Figure 9.10. Position of rocket control surfaces. 1, 2, 3, 4--jet control surfaces; 1', 2', 3', 4'--aerodynamic control surfaces.

The stabilization of the missile in space is achieved by signals from the gyrovertical (pitch angle ϑ and tilt angle γ) and from the course gyroscope (the yaw angle ψ). To obtain the desired trajectory along the active region (fig. 1.21) in accordance with a preestablished program, the value of the pitch angle (ϑ_3) of the rocket is changed. To achieve this, a special programming mechanism is used. The flight velocity of the rocket is controlled from the Earth by means of a radar system using the Doppler principle. When the rocket achieves a preassigned velocity value, a signal (u_e) is sent from the Earth to turn off the engine.

The principal function of a computer of the automatic pilot without feedback is to obtain the first and second derivatives of the signals showing the mismatches in the pitch, tilt and yaw angles. These signals are obtained by means of the differentiating network described in Chapter 6. The necessity of introducing signals of the first and second derivatives with respect to the angular coordinates of the rocket, when using an automatic pilot without feedback, is shown in Chapter 10.

The rocket is controlled by four aerodynamic control surfaces and four control surfaces placed in the gas jets which exit from the nozzle of the engine. The position of the control surfaces along the cross section of the nozzle is shown schematically in figure 9.10 (view from the rear).[1] The aerodynamic control surfaces operate only in the dense regions of the atmosphere and are auxiliary. Each of the four control surfaces in the gas jets is actuated hydraulically and has no mechanical coupling with the other control surfaces. Control surfaces 2 and 4 are situated in a plane perpendicular to the firing plane and control the pitch angle. Control surfaces 1 and 3 are situated in the firing plane and operate as elevons. When both control surfaces are deflected in the same direction they control the yaw angle of the rocket and when they are deflected in opposite directions, they stabilize the angle of tilt. Since the control surface actuators have no feedback, the velocity of the control surface is proportional to the control signal. By applying the coefficients of proportionality to the individual components of this signal, we obtain an equation for an automatic pilot without feedback in the form $d\delta/dt = u$. /288

Section 9.4. Automatic Pilot Using Relays

As an example we describe an automatic pilot using relays, diagramatically shown in figure 9.11. The operation of this automatic pilot is based on the principle of the vibratory linearization of a relay system by delayed feedback in the amplifier (see section 2.6). The deviations from a given course are measured by the position gyroscope G with a potentiometric sensor P_1. Sensor P_1 and the potentiometer of the control surface P_2 form a bridge, which is fed by an AC current through transformer T_1. The amplifier is a tube amplifier using tubes L_1, L_2, L_3 and relay amplifiers R_1 and R_2, linearized by vibration. Tubes L_1 and L_2 are used for the amplifying stages, while tube L_3 serves as a phase discriminator. The actuator consists of an electric servomotor running at a constant velocity with an electromagnetic friction clutch controlled by relays R_1 and R_2. Sensor P_2 is the negative feedback potentiometer.

Let us consider the principle of vibratory linearization for this case. The windings of R_1 and R_2 are connected to the plate circuits of tube L_3. In addition to the contacts which control the servomotor, each relay has contacts for controlling the feedback loop. A positive voltage is fed to the R_2C network through contacts C_{11} and C_{21} and resistance R_1.

---

[1] V. I. Feodos'yev and G. V. Sinyarev. Introduction to Rocket Engineering, Oborongiz, 1960.

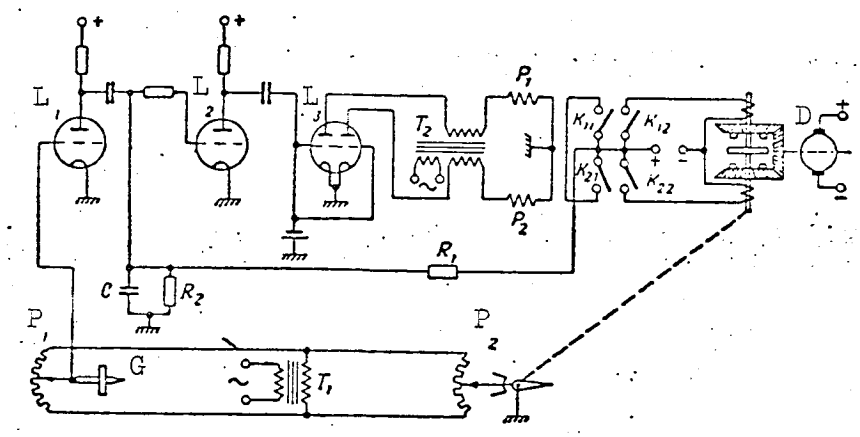

Figure 9.11. Automatic pilot using relays.

The operation of the system takes place in the following manner. When an input signal appears, one of the triodes of tube L_3 conducts and the plate current operates the relay. Depending on the sign of the deflection, either relay R_1 or /289 relay R_2 operates and turns on the storage cell R_2C. The condenser C charges and in this way the positive potential increases on the grid of tube L_2. The operating point on the grid characteristics is displaced into the region of saturation, the amplification factor of the tube decreases, the AC voltage on the grid of tube L_3 decreases and the relay opens. After the relay opens, condenser C discharges, the positive potential on the grid of tube L_2 decreases, its amplification factor increases and the relay again closes, etc. The system undergoes self-sustained oscillations. When one sign deviates, only one relay pulsates. If the input signal is absent, there are no oscillations in the system. The actuator consists of a driver D, which rotates the gears attached to it in opposite direction. In this case the control surface is not actuated. When a current appears in one of the windings of the electromagnetic clutch, rotation is transmitted to the control surface. The direction of rotation depends on the clutch which is actuated by the current. If the clutch is de-energized (the contacts of the relay are open), the position of the control surface is fixed by electromagnetic brakes, not shown in figure 9.11. When the axes of the missile are deflected from the assigned position, the control surface is displaced into a new position during several pulsations of relays R_1 or R_2. The angle of rotation of the control surface is proportional to the deviation of the corresponding axis from the assigned position.

CHAPTER 10. CONTROL OF MOTION OF A MISSILE WITH RESPECT TO ITS CENTER OF GRAVITY /290

Section 10.1. General Information

As we have pointed out in Chapter 1, the ultimate purpose of a missile control system is to maintain the trajectory of the missile so that it passes through the target or close to it. The missile control system is sufficiently complicated and, therefore, its analysis to select various parameters which determine this system is carried out in several stages. The first stage provides for adequate control of the missile with respect to its center of gravity. This motion produces the force which controls the missile.[1]

The present chapter is concerned with the methods of controlling the motion of various missiles with respect to their center of gravity. This analysis will be based on the equations of longitudinal and lateral missile motion presented in Chapter 8. When using these equations, it is necessary to bear in mind one important situation. Strictly speaking, if we use the equations obtained by the method of linearization or the method quasifixation of the coefficients, we can only establish the stability or instability of the system described by initial nonlinear equations or by equations with variable coefficients. However, in the present book these equations will be used to investigate the dynamics of the system by constructing the transient processes or by using the frequency characteristics.

This approach is justified in most of the problems concerned with the motion of the missile, if the nonlinear functions which describe its motion do not have characteristics close to discontinuities, or if the rate of variation of the coefficients is not too great. The criterion for the suitability of this approach involves a sufficient coincidence of the dynamic characteristics of missiles obtained by means of the simplified equations and the exact equations, when the /291
exact equations are solved by computers.

Section 10.2. Lateral Motion of a Missile with Cruciform Wings When the Control Surface is Deflected

As shown in Chapter 1 most of the missiles are controlled by the rotation of the missile frame around the center of gravity by means of control surfaces. The control surfaces may be aerodynamic surfaces or jet surfaces. Sometimes it is

---

[1]There is only a narrow class of missiles which does not require the preliminary rotation of the missile frame with respect to the center of gravity.

necessary to rotate the combustion chamber of a reactive engine to produce the desired moment with respect to the missile's center of gravity.

Let us consider a simple problem of varying the trajectory of the missile by deflecting its control surfaces. Let us assume that the missile moves in a straight line with constant velocity. It is necessary to determine its parameters of motion after the control surface has been deflected, neglecting the change in its flight speed, i.e., considering that the perturbed motion of the missile takes place at constant velocity. To make the problem even simpler, we consider the lateral motion of a missile with cruciform wings. In this case, the forces of gravity do not affect the missile. Finally, we shall consider a missile whose angle of tilt is stabilized.

To analyze the motion of a missile under these conditions, we use the first two equations of the linear approximation (8.44) for the lateral motion of a missile. The third equation is not considered, because the coordinate of the center of gravity is not contained in the first two equations. If, in a missile moving in a straight line, we deflect the control surface or use some other method to produce a moment with respect to the center of gravity, the frame of the missile will start to turn. An angle of attack will appear together with a control force which will vary the direction of the missile's velocity vector. Figure 10.1 shows the forces and moments acting on the missile with cruciform wings when the control surface is deflected.

Taking into account the obvious relation $\psi = \theta_b + \beta$, we can transform the first two equations of (8.44) so that the equations for the slip angles and the rotation of the trajectory will be

$$\frac{d^2\beta}{dt^2} + (k_\beta + n_\beta + n_\psi)\frac{d\beta}{dt} + (k_\beta n_\psi + n_\beta)\beta = n_{\delta_{cr}}\delta_{cr}, \tag{10.1}$$

$$\frac{d^2\theta_b}{dt^2}(k_\beta + n_\beta + n_\psi)\frac{d^2\theta_b}{dt^2} + (k_\beta n_\psi + n_\beta)\frac{d\theta_b}{dt} = k_\psi n_{\delta_{cr}}\delta_{cr}. \tag{10.2}$$

The two equations are linear with constant coefficients and their integration therefore poses no difficulty. The value of the coefficients contained in these equations is associated with aerodynamic and structural characteristics of the missile and is given by (8.43). /292

With a sudden deflection of the course rudder by an angle δ_{cr}, the integral of equation (10.1) has the form

$$\beta = \beta_{st}\left(1 - \frac{p_1 e^{p_2 t} - p_2 e^{p_1 t}}{p_1 - p_2}\right), \tag{10.3}$$

(subscript st = stabilized),

where $\beta_{st} = \frac{n_{\delta_{cr}}\delta_{cr}}{k_\beta n_\psi + n_\beta}$ is the steady state value of the slip angle obtained after the transient process ends; p_1 and p_2 are the roots of the characteristic equation

$$p^2 + (k_\beta + n_{\dot\beta} + n_{\dot\psi})p + k_\beta n_{\dot\psi} + n_\beta = 0. \tag{10.4}$$

It is more convenient to apply this equation in normalized form, which is common to any differential equation of the second order

$$p^2 + 2\zeta\Omega_0 p + \Omega_0^2 = 0, \tag{10.5}$$

where ζ is the relative damping coefficient, and Ω_0 is the natural or resonance angular frequency of the system.

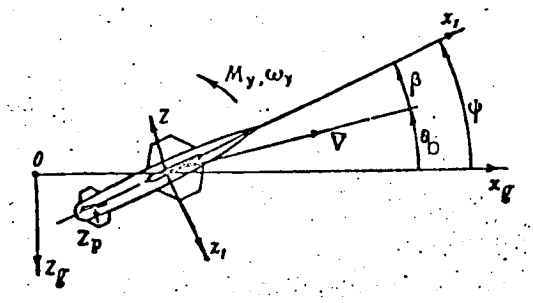

Figure 10.1. Forces and moments which act on missile with cruciform wings during lateral motion. x_1, z_1--body axes; x_g, z_g--Earth axes; V--velocity of missile; ψ--angle of yaw; ω_y--angular velocity of yaw; β--slip angle (analogous to the angle of attack); θ_b--angle of rotation of trajectory (analogous to slope of trajectory during longitudinal motion); Z--lateral force (analogous to lift); Z_p--lateral force of course rudder which produces moment due to course rudder M_δ; M_y--sum of remaining moments which act on missile when it turns with respect to Oy_1 axis.

These newly derived parameters ζ and Ω_0 can be expressed in terms of the characteristic equation (10.4) in the following manner /293

$$\zeta = \frac{k_\beta + n_{\dot\beta} + n_{\dot\psi}}{2\sqrt{k_\beta n_{\dot\psi} + n_\beta}}, \tag{10.6}$$

$$\Omega_0 = \sqrt{k_\beta n_\psi + n_\beta}. \tag{10.7}$$

If $\zeta \geq 1$, the roots of the characteristic equation (10.5) are real

$$p_{1,2} = \left(-\zeta \pm \sqrt{\zeta^2 - 1}\right)\Omega_0. \tag{10.8}$$

For the case $\zeta < 1$ the roots are complex

$$p_{1,2} = \left(-\zeta \pm j\sqrt{1-\zeta^2}\right)\Omega_0. \tag{10.9}$$

In this case, the solution of differential equation (10.1) may be conveniently expressed in the form

$$\beta = \beta_{st}\left[1 - \frac{e^{-\zeta\Omega_0 t}}{\sqrt{1-\zeta^2}}\sin\left(\sqrt{1-\zeta^2}\,\Omega_0 t + \xi\right)\right], \tag{10.10}$$

where

$$\xi = \operatorname{arc\,tg}\frac{\sqrt{1-\zeta^2}}{\zeta}. \tag{10.11}$$

Both solutions (10.3) and (10.10) of equation (10.1) show that when the control surface is deflected a slip angle is produced which, after the transient process, assumes some stationary value proportional to the angle of deviation of the control surface. When an angle of slip is present, a lateral force Z is produced, which is perpendicular to the flight velocity, and the missile in its steady state must move along a circumference. This physical consideration is confirmed by the analytical solution of equation (10.2) for the angular displacement of the trajectory

$$\theta_b = k_\beta \beta_{st}\left[t + \frac{p_1 + p_2}{p_1 p_2} + \frac{p_2 e^{p_1 t_1}}{p_1(p_1 - p_2)} - \frac{p_1 e^{p_2 t}}{p_2(p_1 - p_2)}\right], \tag{10.12}$$

where p_1 and p_2 are the roots of the characteristic equation in form (10.4) or (10.5).

After the transient process is over, an angular displacement of the trajectory has the value

$$\theta_b = k_\beta \beta_{st}\left(t + \frac{p_1 + p_2}{p_1 p_2}\right). \tag{10.13}$$

Expression (10.13) shows that in the steady state the angular displacement of the trajectory varies according to a linear law, which means that the /294

missile can fly only along a circle if its speed is constant. Indeed, the steady state value of the angular velocity of the velocity vector on the basis of (10.13) is equal to

$$\left(\frac{d\vartheta_b}{dt}\right)_{st} = k_3\beta_{st} = \frac{k_\beta n_{\delta cr}\delta_{cr}}{k_\beta n_\psi + n_\beta}. \tag{10.14}$$

Equation (10.14) also shows that for a slow deflection of the control surface, when the transient time for the establishment of the slip angle may be neglected compared with the time during which the control surface moves, the steady state value of the slip angle as well as the angular rate of change of the missile's velocity vector are proportional to the angular deflection of the control surface.

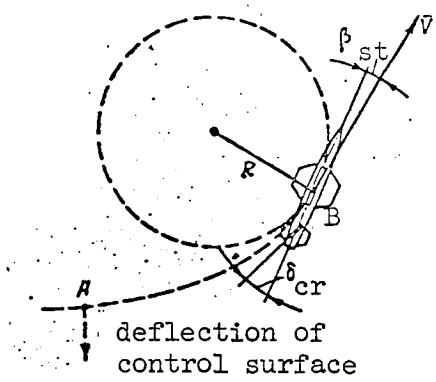

Figure 10.2. Trajectory of missile after deflection of control surface.

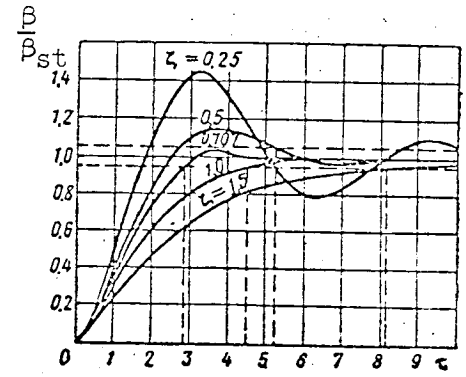

Figure 10.3. Curves showing variation in slip angle after sudden deflection of course rudder.

Figure 10.2 shows the trajectory of a missile, which had been moving in a straight line, after the control surface is deflected by an angle δ_{cr} at point A. The region AB may be called the transient trajectory during which a steady value of the slip angle is established. The possible nature of this process, when the relative damping varies as a function of dimensionless time $\tau = \Omega_0 t$, is shown in figure 10.3. The curves in figure 10.3 reflect the solution of (10.1). It is obvious that since these curves are constructed in relative units, they are suitable for the analysis of the solution of any second order equation with constant coefficients. The duration of the transient process in terms of the dimensionless time τ is determined as the time during which the value of the slip angle achieves a specified deflection from its steady state value. Thus, for example, if this /295 deflection is 0.05 of β_{st}, when ζ = 0.25, 0.5, 0.707, 1.0 and 1.5, we obtain the values τ = 10.2, 5.3, 2.8, 4.5 and 8.2, respectively. The true control time is

determined by means of equation (2.9). Thus, for any damping ζ, the time for the establishment of the slip angle is determined by the natural frequency of the missile Ω_0.

To establish the effect of missile parameters and of flight parameters on the natural frequency and relative damping, it is necessary to substitute the values of coefficients from (8.43) into equations (10.6) and (10.7). As a result, we obtain the expressions

$$\Omega_0 = \sqrt{\frac{\rho_e V_e^2}{2J_y}\left(\frac{c_z^\beta m_y^{\bar{\omega}_y} \rho_e S^2 l^2}{4m} - m_y^\beta S l\right)}, \tag{10.15}$$

$$\zeta = -\frac{\sqrt{\rho_e}\left[\frac{c_z^\beta S}{m} + \frac{S l^2}{2J_y}\left(m_y^{\bar{\beta}} + m_y^{\bar{\omega}_y}\right)\right]}{2\sqrt{\frac{2}{J_y}\left(\frac{c_z^\beta m_y^{\bar{\omega}_y} \rho_e S^2 l^2}{4m} - m_y^\beta S l\right)}}. \tag{10.16}$$

Let us analyze these expressions. Let us remember that coefficients c_z^β, $m_y^{\bar{\beta}}$ and $m_y^{\bar{\omega}_y}$ are always less than zero; consequently, we always have $\zeta > 0$. The coefficient m_y^β for the missile has a static zero-torque stability less than zero. When this coefficient increases, the natural frequency of the missile Ω_0 increases, but there is a simultaneous decrease in the slip angle (equation (10.3), coefficient n_β) for the same angular displacement of the control surface, i.e., the controllability of the missile deteriorates. A missile which is statically neutral ($m_y^\beta = 0$) will have a low value of Ω_0 and a long control time, if it has no control system. A missile which is statically unstable also becomes dynamically unstable for some value $m_y^\beta > 0$, if $\Omega_0^2 < 0$.[1] In this case, when there is some random displacement of the missile from rectilinear flight (even when the course rudder is not deflected) the slip angle will increase continuously until it reaches a critical value. After this, the uniform flow around the missile is disrupted and the flight of the missile becomes random in nature. Thus, the normal flight of a dynamically unstable missile is impossible without a control system. /296

[1] When $\Omega_0^2 < 0$ we must substitute the absolute value of the natural frequency into the expression for the damping coefficient, i.e., this coefficient should be written in the form $2\zeta|\Omega_0|$.

Expression (10.15) also shows that the natural frequency of the missile Ω_0 increases with flight velocity V_e and decreases when the flight altitude increases due to a decrease in $\sqrt{\rho_e}$. It is precisely the last condition which explains the fact that at high altitudes the transient time for the establishment of a new slip angle after the control surface is deflected becomes very long.

We note that the first term contained in the brackets of equation (10.15), as a rule, is substantially less than the second term, and in the overwhelming majority of cases it may be neglected. Therefore, the natural frequency of a missile for given flight conditions is determined almost entirely by the coefficient of static stability m_y^β. The relative damping coefficient equation (10.16) decreases with an increase in altitude, due to $\sqrt{\rho_e}$, which deteriorates the damping of the missile with respect to its center of gravity. As we shall show the control system may be used substantially to decrease the effect of flight conditions on the dynamic characteristics of the missile.

Let us also consider the effect of flight characteristics on the effectiveness of the control surface. This effectiveness may be evaluated from the value of the proportionality coefficient between the values of the steady state slip angle and the deflection angle of the control surface equation (10.3). Instead of coefficients $n_{\delta_{cr}}$, k_β, n_β and n_ψ, let us substitute their values from (8.43). We have

$$\beta_{st} = \frac{m_{y\,cr}^{\delta}}{-m_y^\beta + \frac{1}{4m} c_z^\beta m_y^{\bar{\omega}_y} \rho_e S l} \cdot \delta_{cr}. \tag{10.17}$$

Equation (10.17) shows that when the flight altitude increases (due to a decrease in ρ_e), the slip angle β_{st} will increase for this angular displacement of the control surface δ_{cr}, i.e., the effectiveness of the control surface in the above sense increases. However, this effective altitude for most missiles is negligibly small. This is explained by the small value of the second term of the denominator in equation (10.17), compared with the first term for missiles with normal static zero-torque stability. The flight velocity is not contained in equation (10.17) and consequently does not affect the variation in the slip angle as a function of the angular displacement of the control surface.

It should be pointed out that all of these considerations concerning the effect of flight on the natural frequency of the missile as they pertain to damping and the effectiveness of the control surface take into account only the explicit variation in these quantities as a function of velocity. In addition, it is necessary to bear in mind that the flight velocity (more precisely, the Mach

number of flight) affects the c_z^β, m_y^β, $m_y^{\bar{\dot{\beta}}}$, $m_y^{\bar{\omega}}y$, $m_y^\delta cr$ (section 8.5). To take this situation into account when carrying out the design, we must have the corresponding characteristics of these coefficients as a function of the Mach number. /297

As shown in figure 10.2, after the missile has completed its path over the transient trajectory AB, it moves along a circle with radius R. This radius is given by the expression

$$R=\frac{V_e}{\left(\frac{d\theta_b}{dt}\right)_{st}}, \tag{10.18}$$

where $\left(\frac{d\theta_b}{dt}\right)_{st}$ is the angular rate of rotation of the missile's velocity vector in the xoz_g plane. On the basis of (10.14) this angular rate is equal to

$$\left(\frac{d\theta_b}{dt}\right)_{st}=k_\beta\beta_{st}. \tag{10.19}$$

Substituting the value of $(d\theta_b/dt)_{st}$ into equation (10.18) and taking into account the value of coefficient k_β from (8.43), we obtain an expression for the circle[1]:

$$R=-\frac{2g_S}{gc_z^\beta\rho_e\beta_{st}}, \tag{10.20}$$

where $g_S = G/S$ is the specific load on the wing.

Equation (10.20) characterizes in a definite way the maneuverability of the missile and, in particular, clearly shows that R increases with flight altitude (due to a decrease in ρ_e). However, the maneuverability of missiles is more conveniently characterized by the load factor, i.e., by the ratio of the resultant of aerodynamic forces (including the thrust) to the weight of the missile. Sometimes, however, the load factor is determined as the ratio of the acceleration of the missile due to aerodynamic forces to the acceleration due to gravity. It is obvious that both of these definitions are identical. In considering curvilinear

---

[1]The negative sign in equation (10.20) disappears after we substitute the value of c_z^β which is always negative.

flights, it is convenient to use the components of the load factor along different axes: n_x, n_y and n_z. Then the total load factor is determined by the equation

$$n = \sqrt{n_x^2 + n_y^2 + n_z^2}. \tag{10.21}$$

When evaluating the possibility of realizing some curvilinear trajectory, the turning radius R and the load factor are equivalent characteristics, because for each value of R there is a corresponding definite load factor. The advantage of the concept of the load factor for the characteristics of the missile's maneuverability consists of the fact that the strength of the missile frame and of its other component parts is determined precisely by the load factor. The proper operation of the control system is also checked at the allowable load factor. /298

In the case when flight takes place along a circle, it is easy to go from radius R to the load factor along the z_1 axis. Indeed, when the missile flies along a circle, it is subjected to a lateral acceleration

$$j_z = \frac{V_e^2}{R}. \tag{10.22}$$

If we divide the right and left sides of (10.22) by the acceleration due to gravity g and substitute the value of R from (10.20), we obtain

$$n_z = -\frac{c_z^\beta \rho_e V_e^2}{2g_S} \beta_{st}. \tag{10.23}$$

Expression (10.23) makes it possible for us to arrive at important conclusions concerning the effect of missile parameters and flight parameters on the load factor and, consequently, on the maneuverability of the missile. The load factor for a given slip angle β_{st} depends on the square of the flight velocity, while for large velocities it may reach values which are inadmissable if we consider the strength and proper operation of the control system. Therefore, in such cases it is necessary to limit the allowable values of β_{st}, by some method. On the other hand, load factors decrease when the flight altitude increases (due to ρ_e), and at high altitudes the maneuverability of the missile may become insufficient. An increase in β_{st} is permissible only up to values at which the uniform flow around the missile is disrupted. Finally, the smaller the specific load on the wing, the greater is the possible value of the load factor when all other conditions are equal. From this point of view it is desirable to have wings with large areas, but this is difficult to realize because it increases the size of the missile. As a rule, for small missiles it is easier to provide

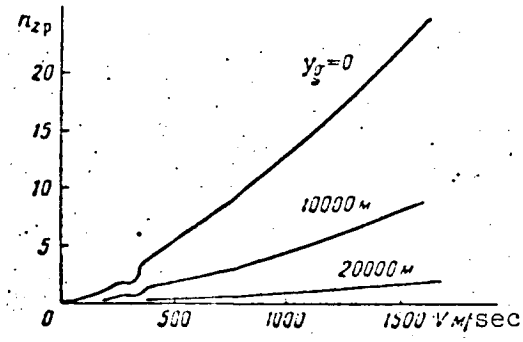

Figure 10.4. Graphs of usable load factor.

for low specific wing loading, and it is for this reason that the maneuverability of small missiles is better than the maneuverability of large missiles.

If, in equation (10.23), instead of β_{st} we substitute the value β_m, the maximum permissible slip angle for which the flow is not disrupted, we obtain the limiting load factor which characterizes the maneuverability of the missile. The graphs showing the variation in the usable load factor n_{zp} as a function of velocity for various flight altitudes are shown in figure 10.4. These graphs illustrate the conclusions made earlier concerning the effect of velocity and flight altitude on the maneuverability of a missile.

As we have already pointed out, the analysis in this section is made under the assumption that the flight velocity of the missile is constant during maneuvering, produced by the deflection of the control surface. In spite of this, the results which we have obtained are significant, even for missiles whose flight velocity is variable. Actually, the control surface of a missile is displaced continuously, and the missile does not have circular regions of trajectory for any extensive distance. If we consider the continuous slow motion of the control surface as a series of small intermittent changes following in short intervals, the velocity of the missile will not vary appreciably during the period of one interval. Consequently, for each interval the results of the analysis will be approximately correct. /299

Section 10.3. Longitudinal Motion of a Missile When the Control Surface is Deflected

In the investigation of isolated longitudinal motion, missiles with plane wings and missiles with nonrotating cruciform wings are under identical conditions: both have wings situated in the plane perpendicular to the trajectory plane. Therefore, the results presented in this section may be extended to both types of missiles. Let us assume that a missile moving uniformly and in a straight line has an elevator which is deflected by some angle. Obviously, in

this case the trajectory of the missile will become distorted. For the case of curvilinear longitudinal motion, the projections of the force of gravity on the x and y coordinate axes change constantly. This causes a variation in the flight velocity of the missile, as a result of which, in some cases, the missile again enters a rectilinear trajectory with a new slope with respect to the horizon. However, the process of establishing a new flight velocity takes a rather long time, and if we consider the initial reaction of the missile to the deflection of the control surface, we can neglect the effect of the missile's weight as well as the effect of velocity change and flight altitude over this segment of the trajectory. /300

With these limitations we analyze the variations in the angles of attack $\Delta\alpha$ and in the slope of the trajectory $\Delta\theta$, which take place when the elevator is suddenly displaced. We use the system of equations (8.31) which was derived taking into account this limitation ($\Delta V = b_\theta = 0$). In this manner we obtain the following differential equation

$$\frac{d^2\Delta\alpha}{dt^2} + (b_\alpha + c_{\dot\alpha} + c_{\dot\delta})\frac{d\Delta\alpha}{dt} + (b_\alpha c_{\dot\delta} + c_\alpha)\Delta\alpha = c_\delta \Delta\delta_t; \tag{10.24}$$

$$\frac{d^3\Delta\theta}{dt^3} + (b_\alpha + c_{\dot\alpha} + c_{\dot\delta})\frac{d^2\Delta\theta}{dt^2} + (b_\alpha c_{\dot\delta} + c_\alpha)\frac{d\Delta\theta}{dt} = b_\alpha c_\delta \Delta\delta_t. \tag{10.25}$$

Comparing equations (10.24) and (10.25) for longitudinal motion with analogous equations (10.1) and (10.2) for lateral motion we note their complete equivalence. The role of the slip angle is now played by the angle of attack of the missile, while the angular displacement of the trajectory is now the slope of the trajectory. All the conclusions made in the preceding section for lateral motion are applicable to the case of longitudinal motion, if, of course, we consider this motion under assumptions made at the beginning of the section. Therefore, without repeating the analysis carried out in section 10.2 we present only the equations for the steady state value of the variation in the angle of attack, in the natural frequency and in the damping of longitudinal motion of the missile with respect to its center of gravity, when the elevator is deflected

$$\Delta\alpha_{st} = -\frac{m_z^\delta}{m_z^\alpha + \frac{1}{2m} c_y^\alpha m_z^{\bar\omega_z} \rho_e S b_A} \Delta\delta_t; \tag{10.26}$$

$$\Omega_0 = \sqrt{-\frac{\rho_e V_e^2}{2J_z}\left(\frac{c_y^\alpha m_z^{\bar\omega_z} \rho_e S^2 b_A^2}{2m} + m_z^\alpha S b_A\right)}; \tag{10.27}$$

$$\zeta = \frac{\sqrt{\rho_e}\left[c_y^\alpha \frac{S}{m} - \frac{S b_A^2}{J_z}\left(m_z^{\bar\alpha} + m_z^{\bar\omega_z}\right)\right]}{2\sqrt{-\frac{2}{J_z}\left(\frac{c_y^\alpha m_z^{\bar\omega_z} \rho_e S^2 b_A^2}{2m} + m_z^\alpha S b_A\right)}}. \tag{10.28}$$

Section 10.4. Lateral Movement of a Tilted Missile with Plane Wings

/301

To change the trajectory of the missile in the xoz_g plane, it is necessary to produce a control force lying in this plane. If the course rudder of a missile with plane wings produces a slip angle, the lateral force is too small and the maneuverability of the missile is entirely unsatisfactory. This is explained by the fact that in a missile with plane wings there are no wings in the x_1oy_1 plane. Therefore, when slip is present, the lateral force is produced only due to the dissymmetry of the flow around the frame, and it is for this reason that the lateral force is small. To obtain a more substantial lateral force, the component of the lift Y is utilized. This component is obtained when the missile is tilted as shown in figure 10.5. Let us consider the simplest case when the turning maneuver is properly executed. In such a maneuver, the altitude, velocity and angle of tilt remain constant and slipping is absent. To make a proper turn, the missile must be given a definite tilt, and its angle of attack must be increased so that the vertical component of the lift force Y cos γ remains equal to the weight.

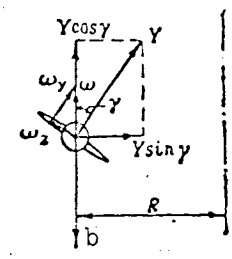

Figure 10.5. Forces acting on missile with plane wings during properly executed turn.

Let us find the basic parameters which characterize the motion of the missile when executing a proper turn. We write the equations for the center of gravity of the missile, using the axes of a natural trihedron: tangent, normal and binormal to the flight trajectory. Assuming that the velocity and flight altitude are constant, we obtain (on the basis of figure 10.5)

$$\left.\begin{aligned} 0 &= P - X; \\ 0 &= Y\cos\gamma - G; \\ mV\frac{d\theta_b}{dt} &= Y\sin\gamma, \end{aligned}\right\} \qquad (10.29)$$

where γ is the tilt angle during the turn, and θ_b is the angular displacement of the trajectory.

In a proper turn slip angle is equal to zero and the turn angle of the trajectory θ_b coincides with yaw angle ψ.

The first equation of (10.29) establishes the relation between the drag and the thrust which must be maintained so that the velocity during the turn is constant. Drag increases with the angle of attack because the lift force coefficient during turning must be increased compared with its value during rectilinear flight. From the second equation of (10.29) we obtain the following equation /302

$$c_{y_t} = \frac{c_{y_r}}{\cos\gamma}, \tag{10.30}$$

where c_{y_t} and c_{y_r}, are the lift coefficients during turning and during straight flight, respectively.

The relation between the angles of attack during turning and during rectilinear flight will be approximately the same as given by equation (10.30).

The normal load factor also increases with the tilt angle during the proper turning maneuver. From the second equation of (10.29) we obtain

$$n_y = \frac{1}{\cos\gamma}. \tag{10.31}$$

Combining the second and third equations of (10.29) we find an expression for the angular velocity and the radius of a proper turn

$$\frac{d\psi}{dt} = \frac{g}{V}\operatorname{tg}\gamma; \tag{10.32}$$

$$R_t = \frac{V^2}{g\operatorname{tg}\gamma}.$$

When the tilt angles are small (γ_{max} = 20-25°), it is permissible to take the direct value of the angle γ in equations (10.32) and (10.33) instead of tan γ, when carrying out approximate evaluations. It follows from expressions (10.32) and (10.33) that the maneuverability of a missile with plane wings can be increased by taking a turn with a large tilt angle. However, it is impossible to bring the tilt angle close to 90° for the following two reasons. In the first place, when the tilt angles are large, there is an increase in c_{y_t}, as we can see from expression (10.30). The increase in this coefficient is limited by some value $c_{y(allowable)}$, which is 10-15 percent less than $c_{y\ max}$ under given flight conditions. This limitation is associated with the break in the flow which takes place at critical

angles of attack. In the second place, it follows from equation (10.31) that the increase in the tilt angle is associated with an increase in the normal load factor, which may also be limited by some value.

Let us see how we must control the tilt angle necessary to maneuver the missile in the xoz_g plane. Obviously, in this case we must have an automatic pilot to control the ailerons of the missile. Let us consider the problem of controlling the tilt angle independently, without associating the tilt motion with other parameters of lateral motion (with the angles β, ψ, θ_b and the coordinate of the center of gravity z_g). In selecting the parameters of the automatic pilot for the tilt channel this approach is quite justified, since the variation in the tilt angle of missiles takes place much more rapidly than the variation of the other parameters mentioned before. Therefore, to select the parameters for controlling the tilt angle we use equation (8.46) /303

$$\frac{d^2\gamma}{dt^2} + l_{\dot\gamma}\frac{d\gamma}{dt} = l_{\delta_e}\delta_e. \tag{10.34}$$

(subscript e = aileron).

Equation (10.34) shows that under the assumptions used to derive it, the missile is neutral with respect to the tilt angle. For the control system we use an ideal automatic pilot with fixed feedback or without feedback. The equation of an automatic pilot with fixed feedback for controlling the tilt angle has the form

$$\delta_e = -i_{\dot\gamma}\frac{d\gamma}{dt} + i_\gamma(\gamma_3 - \gamma). \tag{10.35}$$

The equation of an automatic pilot without feedback is

$$\frac{d\delta_e}{dt} = -i_{\dot\gamma}\frac{d^2\gamma}{dt^2} - i_\gamma\frac{d\gamma}{dt} + q_\gamma(\gamma_3 - \gamma). \tag{10.36}$$

The following designations are used in equations (10.35) and (10.36): $\gamma_3 = \gamma_3(t)$ is the assigned value of the tilt angle which is physically determined by some signal sent by the control system of the missile into the tilt channel of the automatic pilot; and $i_{\dot\gamma}$, i_γ, q_γ are transfer numbers of the automatic pilot for the respective signals having the dimensions:

$$[i_{\dot\gamma}] = \text{sec};\ [i_\gamma] = 1;\ [q_\gamma] = 1/\text{sec}.$$

Combining equation (10.34) with equation (10.35) or (10.36) we obtain a general equation for the tilt control system. For an automatic pilot with fixed feedback we have

$$\frac{d^2\gamma}{dt^2} + (l_\gamma^{\cdot} + i_\gamma^{\cdot} l_{\delta_e}) \frac{d\gamma}{dt} + i_\gamma l_{\delta_e} \gamma = i_\gamma l_{\delta_e} \gamma_3. \tag{10.37}$$

For an automatic pilot without feedback we have

$$\frac{d^2\gamma}{dt^2} + (l_\gamma^{\cdot} + i_\gamma^{\cdot} l_{\delta_e}) \frac{d^2\gamma}{dt^2} + i_\gamma l_{\delta_e} \frac{d\gamma}{dt} + q_\gamma l_{\delta_e} \gamma = q_\gamma l_{\delta_e} \gamma_3. \tag{10.38}$$

Each of the coefficients in the left part of equations (10.37) and (10.38) contains one of the transfer numbers of the automatic pilot. Therefore, it is possible to select these coefficients in such a way that the dynamic characteristics of the missile with respect to the tilt angle are optimum. In this case it is convenient to apply the method of standard coefficients to select the parameters of the automatic pilot. Let us illustrate this by specific examples. /304

Example 10.1. The parameters of the missile are as follows: $l_{\dot{\gamma}} = 0.5$ 1/sec; $l_{\delta_e} = 5$ 1/sec^2. It is required to select the transfer numbers of an automatic pilot with fixed feedback in such a way that the control time for the tilt angle (t_p) (p = control) is equal to 1.5 sec.

The transfer function of the closed loop system is obtained from equation (10.37) and has the form

$$\Phi_{\gamma/\gamma_3}(p) = \frac{i_\gamma l_{\delta_e}}{p^2 + (l_{\dot{\gamma}} + i_{\dot{\gamma}} l_{\delta_e}) p + i_\gamma l_{\delta_e}}, \tag{10.39}$$

which corresponds to a typical transfer function (2.8). For this typical function the standard coefficients are shown on tables 2.1 and 2.2. Let us use table 2.2 because in this case the control time is a minimum, and the small overcontrol characteristic of these standard coefficients is not significant in the present case. On the basis of table 2.2 the standard characteristic equation has the form

$$p^2 + 1.5\Omega_0 p + \Omega_0^2 = 0. \tag{10.40}$$

If we set the coefficients of equation (10.37) or the denominator of function (10.39) equal to the coefficients of the standard equation (10.40), we find two algebraic equations

$$l_{\dot{\gamma}} + i_{\dot{\gamma}} l_{\delta_e} = 1.5\Omega_0; \tag{10.41}$$

$$i_\gamma l_{\delta_e} = \Omega_0^2. \tag{10.42}$$

On the basis of the graphs shown in figure 2.6 we obtain the value of the dimensionless control time for the second order system $\tau_p = 3$. From this it

follows that the natural frequency of the system must be equal to

$$\Omega_0 = \frac{\tau_p}{t_p} = \frac{3}{1.5} = 2\ \frac{1}{\text{sec}}.$$

Substituting this value of Ω_0 into (10.42) we obtain a transfer number for the tilt angle

$$i_\gamma = \frac{\Omega_0^2}{l_{\delta_e}} = \frac{2^2}{5} = 0.8.$$

Finally, from equation (10.4) we determine the transfer number for the angular rate of change of tilt

$$i_{\dot\gamma} = \frac{1.5\Omega_0 - i_\gamma}{l_{\delta_e}} = \frac{1.5\cdot 2 - 0.5}{5} = 0.5.$$

The transfer numbers of the automatic pilot selected in this way provide for the required dynamic characteristics of the missile with respect to the tilt channel. /305

Example 10.2. Let us assume that the missile parameters are the same as in the preceding example. Let us select the transfer numbers of the automatic pilot without feedback in such a way that the control time for the tilt angle (t_p) is equal to 1.5 sec.

The transfer function for the closed loop system obtained from equation (10.38) has the form

$$\Phi_{\gamma/\gamma_3}(p) = \frac{q_\gamma l_{\delta_e}}{p^3 + \left(i_{\dot\gamma} + i_\gamma l_{\delta_e}\right)p^2 + i_\gamma l_{\delta_e} p + q_\gamma l_{\delta_e}}. \tag{10.43}$$

As in the preceding example, this function corresponds to the typical transfer function (2.8). From table 2.2 we determine the standard characteristic equation

$$p^3 + 2.5\Omega_0 p^2 + 2.5\Omega_0^2 p + \Omega_0^3 = 0. \tag{10.44}$$

If we set the coefficients of the polynomial in the denominator of function (10.43) equal to the coefficients of the standard equation (10.44), we obtain a system of three algebraic equations

$$\left.\begin{aligned} i_{\dot\gamma} + i_\gamma l_{\delta_e} &= 2.5\Omega_0, \\ i_\gamma l_{\delta_e} &= 2.5\Omega_0\Omega_0^2, \\ q_\gamma l_{\delta_e} &= \Omega_0^3. \end{aligned}\right\} \tag{10.45}$$

From the graphs shown in figure 2.6 we find the value of the dimensionless control time for a third order system $\tau_p = 4.5$. From this it follows that the natural frequency of the system must be equal to

$$\Omega_0 = \frac{\tau_p}{t_p} = \frac{4.5}{1.5} = 3\,\frac{1}{\text{sec}}.$$

Substituting this value of Ω_0 into system (10.45), we obtain the values of the transfer numbers

$$i_{\dot{\gamma}} = 1.4 \text{ sec}; \; i_{\gamma} = 4.5; \; q_{\gamma} = 5.4\,\frac{1}{\text{sec}}.$$

These values of the transfer numbers are very large, and if they are used, the linear region of operation of the automatic pilot over the tilt channel is sharply reduced. In some cases this may be undesirable. To decrease the transfer numbers, it is necessary to increase the control time for the angle of tilt. Thus, for example, if we let this time (t_c) be equal to 3 secs after carrying out the calculations in a similar fashion we obtain acceptable values for the transfer numbers: $i_{\dot{\gamma}} = 0.55$ sec; $i_{\gamma} = 1.125$; $q_{\gamma} = 0.675$ 1/sec.

Section 10.5. Control of the Yaw Angle of a Missile with Cruciform Wings

The tilted motion of a missile with a deflected control surface was considered in sections 10.2 - 10.4 to present a clear picture of these simple control maneuvers of a missile. Actually, the control system of a missile consists of several circuits which, as a rule, cover the control surface elements and the tilt control channel of the missile. Of these the simplest circuits are the ones for controlling the angular position of the missile: the angle of yaw in lateral motion and the pitch angle in longitudinal motion. In the present section, we consider the circuit for controlling the angle of yaw of a missile with cruciform wings. It is assumed in this analysis that the tilt angle of the missile is rigidly stabilized by a special channel of the automatic pilot, which controls the ailerons and remains equal to zero during the entire flight period of the missile. The method of selecting the parameters of an automatic pilot for stabilizing the yaw angle does not differ in any way from the method presented in the preceding section for selecting the parameters of the automatic pilot which controls the tilt angle. The automatic pilot which controls the tilt angle will maintain this angle equal to zero, if we let $\gamma_3 = 0$. /306

To select the parameters of an automatic pilot which controls the yaw angle of a missile with cruciform wings, it is necessary to analyze the system of equations which describe the motion of the controlled object and the operation of the automatic pilot. To describe the controlled object--the missile with cruciform wings--we make use of the first two equations of system (8.44)

$$\left.\begin{aligned}&\frac{d\psi}{dt}-\frac{d\beta}{dt}-k_\beta\beta=0;\\&\frac{d^2\psi}{dt^2}+n_{\dot\psi}\frac{d\psi}{dt}+n_{\dot\beta}\frac{d\beta}{dt}+n_\beta\beta=n_{\delta_{cr}}\delta_{cr}+\frac{\Delta M_p}{J_y}\end{aligned}\right\}\tag{10.46}$$

The right side of the second equation contains the perturbing moment M_p (perturbing), which takes into account the possible aerodynamic dissymmetry of the missile with respect to the y_1 axis caused by the dissymmetry of the frame or of the thrust. In future calculations we shall assume that this moment is constant. We do not consider the third equation of system (8.44), because it describes the motion of the center of gravity, and the automatic pilot, which controls only the yaw angle of the missile, does not react to changes in the coordinates of the center of gravity.

By eliminating the variable β from system (10.46) we obtain an equation for the yaw angle of the missile

$$\frac{d^3\psi}{dt^3}+a_1\frac{d^2\psi}{dt^2}+a_2\frac{d\psi}{dt}=b_1\frac{d\delta_{cr}}{dt}+b_2\delta_{cr}+\frac{1}{J_y}\frac{d\Delta M_p}{dt}+\frac{k_\beta}{J_y}\Delta M\tag{10.47}$$

where

$$\left.\begin{aligned}&a_1=k_\beta+n_{\dot\beta}+n_{\dot\psi},\\&a_2=k_\beta n_{\dot\psi}+n_\beta,\\&b_1=n_{\delta_{cr}},\\&b_2=k_\beta n_{\delta_{cr}}.\end{aligned}\right\}\tag{10.48}$$

Of the various types of automatic pilots, the most common is the automatic pilot with fixed feedback. Therefore, we shall analyze it first. /307

The ideal automatic pilot, with fixed feedback used for controlling the angular movement of the missile, is usually described by the following equation

$$\delta_{cr}=-i_{\dot\psi}\frac{d\psi}{dt}+i_\psi(\psi_3-\psi),\tag{10.49}$$

where $\psi_3=\psi_3(t)$ is the assigned value of the missile's yaw angle, i.e., the control signal; and i_ψ and $i_{\dot\psi}$ are the transfer numbers of the automatic pilot for the angle of yaw and for the angular rate of change of yaw which have the following dimensions: $[i_\psi]=1$; $[i_{\dot\psi}]=\text{sec}$.

Combining expressions (10.47) and (10.49) we obtain a general equation for the control system

$$\frac{d^3\psi}{dt^3} + (a_1 + i_{\dot\psi} b_1)\frac{d^2\psi}{dt^2} + (a_2 + i_{\dot\psi} b_2 + i_\psi b_1)\frac{d\psi}{dt} + i_\psi b_2 \psi = \tag{10.50}$$

$$= i_\psi b_1 \frac{d\psi_3}{dt} + i_\psi b_2 \psi_3 + \frac{1}{J_y}\frac{d\Delta M_p}{dt} + \frac{k_3}{J_y}\Delta M_p.$$

By analyzing the structure of equation (10.50) we can make certain significant conclusions. This equation shows that from the standpoint of the control signal $\psi_3(t)$ the system missile--automatic pilot with fixed feedback is astatic and, in the steady state when perturbations are absent ($\Delta M_p = 0$), we have $\psi = \psi_3 = \text{const}$. On the other hand, this system is static with respect to a constant perturbing moment produced by aerodynamic dissymmetry. The error in the yaw angle produced by this moment is equal to

$$\psi_{st} = \frac{k_3 \Delta M_p}{J_y i_\psi b_2}. \tag{10.51}$$

From the structure of equation (10.50) we can also see that the selection of the automatic pilot parameters ($i_{\dot\psi}$ and i_ψ) cannot be carried out conveniently by the method of standard coefficients, because the number of variable automatic pilot parameters is equal to two, while the number of coefficients in the equation to be selected is equal to three. Therefore, to select these parameters it will be necessary to use both the method of standard coefficients and of the logarithmic amplitude--frequency characteristics.

In order to have a clear concept of the system which we are investigating it is desirable to make up its functional diagram. On the basis of equation (10.47), the transfer function for the ratio of the yaw angle to the angular deflection of the control surface is written in the form /308

$$W_{\psi/\delta_{cr}}(p) = \frac{b_1 p + b_2}{p(p^2 + a_1 p + a_2)}, \tag{10.52}$$

where the values of coefficients a_1, a_2, b_1 and b_2 are given by equation (10.48).

The transfer function for the ratio of the yaw angle to the perturbing moment ΔM_p has the form

$$W_{\psi/\Delta M_p}(p) = \frac{b_1 p + b_2}{p(p^2 + a_1 p + a_2)} \cdot \frac{1}{n\delta_{cr} J_y}. \tag{10.53}$$

For convenience in preparing the structural diagram, it is desirable that the transfer functions of the missile be the same for both the controlling signal and the perturbing signal. To make these functions the same, it is necessary to reduce the perturbation to the control surface, i.e., to replace ΔM_p by a new perturbation measured in angular units and given by the expression

$$\Delta F_p = W_p(p)\Delta M_p. \tag{10.54}$$

By comparing (10.53) and (10.54) we see that the transfer function $W_p(p)$ must be equal to

$$W_p(p) = \frac{1}{J_y n_{\delta_{cr}}} = \frac{2}{m_y^{\delta}{}_{cr}\, S l \rho_e V_e^2}. \tag{10.55}$$

The functional diagram of the system for controlling the yaw angle which takes into account the equation of the automatic pilot (10.47) is shown in figure 10.6. To select the first parameter, the transfer number for the angular rate of yaw ($i_{\dot\psi}$), the functional diagram may be represented in the form shown in figure 10.7. The perturbation ΔM_p is not shown, since it does not affect the dynamic properties of the system and does not enter into the picture when we compute the parameters of the automatic pilot.

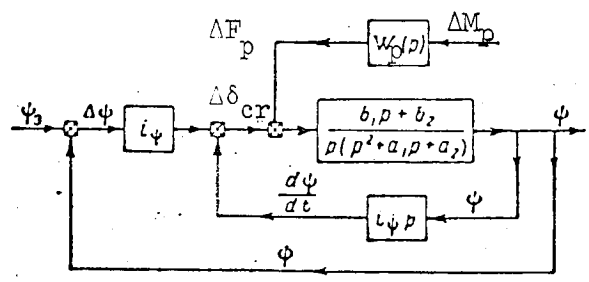

Figure 10.6. Functional diagram of yaw control system using automatic pilot with fixed feedback.

Let us select a transfer number $i_{\dot\psi}$ from the condition that the transient process in the inner circuit takes place in a minimum time ($\zeta = \sqrt{2}/2$). If we consider this circuit independently, it represents the control process for the angular rate of change of yaw.

The characteristic equation for the closed loop inner circuit has the form

$$p^2 + (a_1 + i_{\dot\psi} b_1)\, p + a_2 + i_{\dot\psi} b_2 = 0. \tag{10.56}$$

On the basis of equation (10.56) the relative damping is equal to /309

$$\zeta = \frac{a_1 + i_{\dot\psi} b_1}{2\sqrt{a_2 + i_{\dot\psi} b_2}}. \tag{10.57}$$

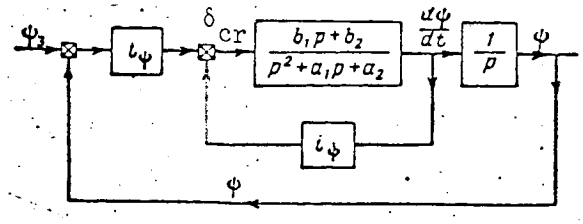

Figure 10.7. Transformed functional diagram of figure 10.6, used to select parameters of automatic pilot.

If we let $\zeta = \sqrt{2}/2$ we find the required value of the transfer number $i_\psi^{\cdot}$ from expression (10.57). For convenience we do not express this number in terms of coefficients a_1, a_2, b_1 and b_2, but rather in terms of the initial parameters of the missile

$$i_\psi^{\cdot} = \frac{1}{n_{\delta_{cr}}} \left[\sqrt{2(n_\beta - k_\beta n_\beta^{\cdot}) - k_\beta^2} - (n_\beta^{\cdot} + n_\psi^{\cdot}) \right]. \tag{10.58}$$

After the selection of $i_\psi^{\cdot}$, the transfer function of the inner loop (fig. 10.7) is reduced to a normal form

$$W_{\omega_y/\delta_{cr}}(p) = \frac{(T_V p + 1) k_c}{T_\omega^2 p^2 + 2\zeta T_\omega p + 1}, \tag{10.59}$$

where

$$T_V = \frac{b_1}{b_2}; \; k_c = \frac{b_2}{a_2 + i_\psi^{\cdot} b_2}; \; T_\omega = \frac{1}{\sqrt{a_2 + i_\psi^{\cdot} b_2}}; \; \zeta = \frac{a_1 + i_\psi^{\cdot} b_1}{2\sqrt{a_2 + i_\psi^{\cdot} b_2}}. \tag{10.60}$$

Now this functional diagram can be represented in the form shown in figure 10.8. As we have already mentioned in section 2.3, in order to obtain a satisfactory transfer function, it is necessary that the cutoff frequency occur over the region of the logarithmic amplitude--frequency characteristics, which has a slope of 20 db/sec. This is the criterion for selecting the total amplification factor of the system $i_\psi k_c$ and, consequently, of the transfer number i_ψ, because the value of k_c must be known.

Table 10.1 shows the parameters of two missiles with different characteristics. The assigned values are k_β, n_β, $n_\beta^{\cdot}$, $n_\psi^{\cdot}$ and $n_{\delta_{cr}}$, while the remaining parameters are computed by means of equations (10.48) and (10.60). The table

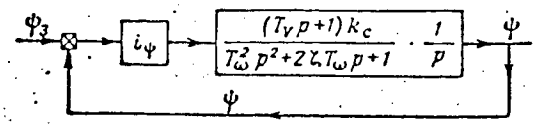

Figure 10.8. Transformed functional diagram of figure 10.7.

also shows the values of the transfer number for the angular rate of change of yaw ($i_{\dot{\psi}}$) computed by means of equation (10.57). The negative value of $i_{\dot{\psi}}$ for missile No. 1 shows that the natural damping of the missile is large, and to obtain the optimum damping ($\zeta = \sqrt{2}/2$) it is necessary to introduce negative damping

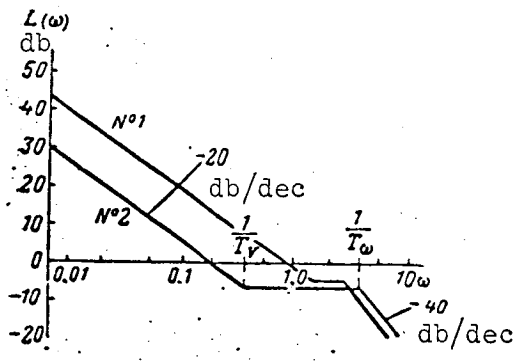

Figure 10.9. Logarithmic amplitude--frequency characteristics of missiles whose parameters are shown in table 10.1.

artificially. Since a certain amount of increase in damping does not produce much effect on the short period motion of the missile, in future calculations for missile No. 1 we shall assume that $i_{\dot{\psi}} = 0$. /311

Figure 10.9 shows the logarithmic amplitude-frequency characteristics for both missiles. For missile No. 1, $i_{\dot{\psi}} = 1.0$ and for missile No. 2, $i_{\dot{\psi}} = 1.5$. It is undesirable to decrease the value of $i_{\dot{\psi}}$ because in this case the transient process is prolonged. However, an increase in this value leads to substantial oscillations.

Figure 10.10 shows the transient functions for the yaw angle. From these graphs we can see that if the method of selecting the transfer number $i_{\dot{\psi}}$ for missile No. 1 led to the desired result (rapid transient process with small

TABLE 10.1. DYNAMIC CHARACTERISTICS OF MISSILES

Missile No.	Characteristic													
	k_β	n_β	$n_{\dot\psi}$	$n_{\dot\psi}$	$n_{\delta_{cr}}$	a_1	a_2	b_1	b_2	$l_{\dot\psi}$	T_V	k_c	T_ω	ζ
	1/sec	1/sec^2	1/sec	1/sec	1/sec^2	1/sec	1/sec^2	1/sec^2	1/sec^2	sec	sec	1/sec	sec	
1	1.6	5.3	1.5	2.5	5.8	5.6	9.3	5.8	9.3	—0.6	0.625	1.0	0.328	0.92
2	0.34	13.5	0.1	0.205	5.6	0.645	13.6	5.6	1.9	0.865	2.95	0.124	0.256	0.707

overshoot), the transient process for missile No. 2 becomes unsatisfactory. This is explained by the fact that the third root of the characteristic polynomial of differential equation (10.50) has turned out to be much smaller than the two other complex roots. This value of the root is due to an excessively large value of constant T_V and small value of coefficient k_c. The transient process for missile No. 2 is divided into two periods. The first period is determined by the large complex roots and ends quickly. The second period is determined by the small root and produces a long "tail" on the curve of the transient function. This result shows that for certain types of missiles an automatic pilot using the simplest law for controlling the yaw is unsuitable.

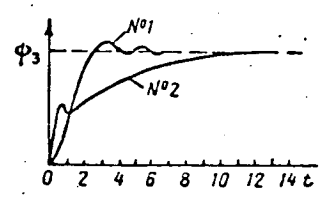

Figure 10.10. Curves showing transient functions of missiles whose parameters are presented in table 10.1.

Let us consider the possibility of using an automatic pilot with fixed feedback and with integral control for missile No. 2. The control law for such an automatic pilot may be written in the form /312

$$\delta_{cr} = -i_{\dot\psi}\frac{d\psi}{dt} + i_\psi(\psi_3 - \psi) + q_\psi\int_0^t(\psi_3 - \psi)\,dt \qquad (10.61)$$

or in symbolic form

$$\delta_{cr} = -i_{\dot\psi}p\psi + q_\psi\frac{T_\psi p + 1}{p}(\psi_3 - \psi), \qquad (10.62)$$

where q_ψ is the integral transfer number for the mismatch signal $(\psi_3 - \psi)$, having a dimension $[q_\psi] = 1/\text{sec}$; and $T_\psi = i_\psi/q_\psi$.

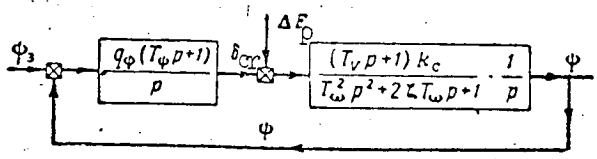

Figure 10.11. Structural diagram of system for controlling yaw with automatic pilot described by equation (10.61).

The functional diagram of the system for the automatic control of the yaw angle using the integral law is shown in figure 10.11. Since the functional diagram in figure 10.11 contains an integrating element, the system has become astatic with respect to the constant perturbation ΔM_p = const. The transfer function of a closed loop system which corresponds to this functional diagram and to equations (10.46) of the missile and (10.61) of the automatic pilot is given by

$$\Phi_{\psi/\psi_3}(p)=\frac{(T_V p+1)(T_\psi p+1)q_\psi b_2}{p^4+(a_1+i_\psi b_1)p^3+(a_2+i_\psi b_1+i_{\dot\psi} b_2)p^2+(i_\psi b_2+q_\psi b_1)p+q_\psi b_2}. \qquad (10.63)$$

The diagram in figure 10.11 shows the series connection of the "controlled object,"[1] all of whose parameters are given and the equation of the "regulator" (automatic pilot), whose parameters q_ψ and i_ψ (or T_ψ) must be selected. To select these parameters, we use the method of logarithmic amplitude-frequency characteristics. Figure 10.12 shows the logarithmic amplitude-frequency characteristics of the "controlled object," of the "regulator" and of the compensated system. The logarithmic amplitude-frequency characteristics of the regulator are constructed in such a way that the cutoff frequency in the compensated system is equal to unity (ω_c = 1.0), while T_ψ = 0.555 sec. In this case, the transfer numbers of the automatic pilot are equal to q_ψ = 2.6 1/sec; $i_\psi = q\,T_\psi$ = 1.45.

The transient function for the control system of missile No. 2 is a line in figure 10.3. If we compare it with the transient function shown in figure 10.10 for the automatic pilot with fixed feedback, we can see that by using integral control we have been able to provide good dynamic properties when controlling the angle of yaw of missile No. 2.

---

[1]In this case the parameters of the controlled object contain the transfer number of the automatic pilot for the angular rate of change of yaw ($i_{\dot\psi}$), which determines the parameters T_ω k_c and ζ (equation (10.60)).

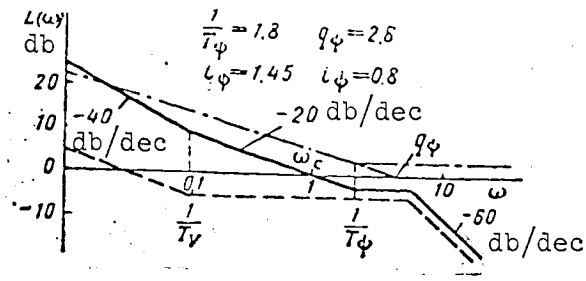

Figure 10.12. Logarithmic amplitude--frequency characteristics of missile, of automatic pilot and of entire control system. -----logarithmic amplitude--frequency characteristics of controlled object (missile); -.-.-.-.logarithmic--amplitude--frequency characteristics of regulator (automatic pilot);———logarithmic amplitude--frequency characteristics of system.

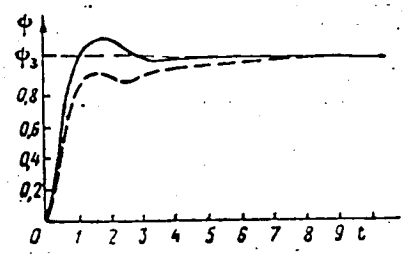

Figure 10.13. Transient functions of systems whose logarithmic amplitude--frequency characteristics are shown in figure 10.12.

To control the angular position of the missile's frame (in this case the yaw angle) we can also utilize an automatic pilot without feedback. In this case, the control law must contain the second derivative of the angle, which is controlled by the automatic pilot. In the case of the yaw angle, the control law for the automatic pilot has the form

$$\frac{d\delta_{cr}}{dt} = -i_{\dot\psi}\frac{d^2\psi}{dt} - i_{\psi}\frac{d\psi}{dt} + q_{\psi}(\psi_3 - \psi). \qquad (10.64)$$

The designations of the transfer numbers are determined by their dimensions /314

$$[i_{\dot\psi}] = \text{sec}; [i_{\psi}] = 1; \quad [q_{\psi}] = 1/\text{sec}.$$

By combining the equation for the automatic pilot without feedback (10.64) with the equation of the missile (10.47), we obtain the transfer function of the closed loop system for controlling the angle of yaw.

$$\Phi_{\psi/\psi_3}(p) = \frac{(T_V p + 1) q_\psi b_2}{p^4 + (a_1 + i_\psi b_1) p^3 + (a_2 + i_\psi b_1 + i_\psi b_2) p^2 + (i_\psi b_2 + q_\psi b_1) p + q_\psi b_2}. \tag{10.65}$$

The difference between the transfer function (10.65) and the transfer function (10.63) is that the former does not have the term $(T_\psi p + 1)$ in the numerator. The absence of this term produces some lag in the end of the turning transient process, as shown by the broken line in figure 10.13.

Section 10.6. Control of the Pitch Angle of a Missile

The analysis of the pitch angle control system (for a missile with plane wings or cruciform wings) may be simplified and reduced to the problem considered in the preceding section, concerning the control of yaw in a missile with cruciform wings.

Equations(8.31) are usually applicable for selecting the parameters of the automatic pilot which controls the pitch angle. These equations describe approximately the longitudinal short period motion of the missile

$$\left.\begin{aligned} &\frac{d\Delta\vartheta}{dt} - \frac{d\Delta\alpha}{dt} - b_\alpha \Delta\alpha = 0; \\ &\frac{d^2\Delta\vartheta}{dt^2} + c_\vartheta \frac{d\Delta\vartheta}{dt} + c_\alpha \frac{d\Delta\alpha}{dt} + c_\alpha \Delta\alpha = c_\delta \Delta\delta_p + \frac{\Delta M_p}{J_z}. \end{aligned}\right\} \tag{10.66}$$

We introduce a perturbing moment ΔM_p in the right side of the second equation. This moment takes into account the possible aerodynamic dissymmetry of the missile with respect to the z_1 axis.

By eliminating the variable $\Delta\alpha$, from (10.66) we obtain an equation for the pitch angle of the missile

$$\frac{d^3\Delta\vartheta}{dt^3} + a_1 \frac{d^2\vartheta}{dt^2} + a_2 \frac{d\Delta\vartheta}{dt} = b_1 \frac{d\Delta\delta_p}{dt} + b_2 \Delta\delta_p + \frac{1}{J_z}\frac{d\Delta M_p}{dt} + \frac{b_\alpha}{J_z}\Delta M_p, \tag{10.67}$$

where

$$\left.\begin{aligned} a_1 &= b_\alpha + c_\alpha + c_\vartheta; \\ a_2 &= b_\alpha c_\vartheta + c_\alpha; \\ b_1 &= c_\delta; \\ b_2 &= b_\alpha c_\delta. \end{aligned}\right\} \tag{10.68}$$

Comparing equation (10.67), which describes the variation of the pitch angle during the longitudinal short period motion of the missile, with equation (10.47) for the yaw angle of a missile with cruciform wings, we note that they are completely analogous. This reflects the analogy between the lateral motion of a missile with cruciform wings and the longitudinal motion of any missile with wings. The coefficients a_1, a_2, b_1 and b_2 shown by equations (10.48) and (10.68) /315

also have exactly the same structure. Therefore, all of the equations, conclusions and recommendations obtained in the preceding section for controlling the yaw angle of a missile with cruciform wings may be utilized in the analysis of the pitch angle control of a winged missile. In utilizing the equations of the preceding section, it is necessary to replace the functions and parameters for the lateral motion of a missile with cruciform wings with the functions and parameters of longitudinal motion by using the following table

ψ	δ_{cr}	J_y	k_β	n_β	$n_{\dot\beta}$	$n_{\dot\psi}$	$n_{\delta_{cr}}$	$i_{\dot\psi}$	i_ψ	q_ψ	T_ψ
$\Delta\vartheta$	$\Delta\delta_p$	J_z	b_α	c_α	$c_{\dot\alpha}$	$c_{\dot\vartheta}$	c_δ	$i_{\dot\vartheta}$	i_ϑ	q_ϑ	T_ϑ

In concluding this section we consider the control of the pitch angle taking into account the force of gravity as it affects the angular motions of the missile. In this case, a system of equations which describes the short period motions of the missile, has the form

$$\left.\begin{aligned} &\frac{d\Delta\vartheta}{dt} - \frac{d\Delta\alpha}{dt} - b_\theta\Delta\theta - b_\alpha\Delta\alpha = 0, \\ &\frac{d^2\Delta\vartheta}{dt^2} + c_{\dot\vartheta}\frac{d\Delta\vartheta}{dt} + c_{\dot\alpha}\frac{d\Delta\alpha}{dt} + c_\alpha\Delta\alpha = c_\delta\Delta\delta_p + \frac{\Delta M_p}{J_z}. \end{aligned}\right\} \qquad (10.69)$$

This system differs from the system of (10.66) only by the presence of the term $b_\theta\Delta\theta$ in the first equation. It is this term that takes into account the effect of gravity because, from equation (8.27) $b^\theta = g \sin\theta_e/V_e$. During horizontal flight $\theta_e = \sin\theta_e = 0$. For small values of θ_e the coefficient b_θ is also small, but for substantial slopes of the trajectory it may have a significant effect on the motion of the missile. /316

If we eliminate from system (10.69) all of the variables except $\Delta\vartheta$, we obtain an equation for the pitch angle which takes into account the force of gravity

$$\frac{d^3\Delta\vartheta}{dt^3} + a_1\frac{d^2\Delta\vartheta}{dt^2} + a_2\frac{d\Delta\vartheta}{dt} + a_3\Delta\vartheta = b_1\frac{d\Delta\delta_p}{dt} + b_2\Delta\delta_p + \frac{1}{J_z}\frac{d\Delta M_p}{dt} - \frac{b_\theta}{J_z}\Delta M_p, \qquad (10.70)$$

$$\left.\begin{aligned} a_1 &= b_\alpha - b_\theta + c_\alpha + c_\vartheta; \\ a_2 &= b_\alpha c_\vartheta + c_\alpha - b_\theta (c_\alpha + c_\vartheta); \\ a_3 &= - b_\theta c_\alpha; \\ b_1 &= c_\delta; \\ b_2 &= c_\delta (b_\alpha - b_\theta); \end{aligned}\right\} \tag{10.71}$$

Comparing equations (10.67) and (10.70), we note that the latter contains a term with a zero derivative of the pitch angle. When $\theta_e > 0$, the coefficient $a_3 < 0$, and when $\theta_e < 0$, the coefficient $a_3 > 0$. It follows from this that the missile will be unstable in any flight with a pitch angle (without a control system). This result is explained by the fact that in the analysis of the short-period motion, one of the equations of system (8.28) is dropped, and the flight velocity is assumed to be constant. If we take into account the entire system of equations for longitudinal motion, the stability of flight without a control system may not be disrupted during pitching (equations (8.37)).

Coefficients a_1 and a_2 will also vary as functions of the magnitude and sign of the trajectory slope (due to the coefficient b_θ) and may become negative under some flight conditions (for example, when the velocity is low at launching).

Let us write the general equation for the pitch angle control system, using an automatic pilot with fixed feedback. We combine equation (10.49) of the automatic pilot and the equation of the missile (10.70) by replacing in the former the parameters of lateral motion with the parameters of longitudinal motion, taken from table 10.2. As a result we obtain the general equation

$$\begin{aligned} \frac{d^3\Delta\vartheta}{dt^3} + (a_1 + i_\vartheta b_1)\frac{d^2\Delta\vartheta}{dt^2} + (a_2 + i_\vartheta b_1 + i_\vartheta b_2)\frac{d\Delta\vartheta}{dt} + (a_3 + i_\vartheta b_2)\Delta\vartheta = \\ = i_\vartheta b_1 \frac{d\vartheta_3}{dt} + i_\vartheta b_2 \vartheta_3 + \frac{1}{J_z}\frac{d\Delta M_p}{dt} - \frac{b_\theta}{J_z}\Delta M_p. \end{aligned} \tag{10.72}$$

The structure of the coefficients of equation (10.72) shows that the control system for the pitch angle which uses an automatic pilot with fixed feedback is static, if we take into account the force of gravity, not only with respect to external perturbation (ΔM_p), but also with respect to the assigned value of the pitch angle. This value of the pitch angle is processed by the control system with an error equal to /317

$$\Delta\vartheta_{st} = \frac{i_\vartheta b_2}{a_3 + i_\vartheta b_2}\vartheta_3. \tag{10.73}$$

As the slope angle of the trajectory increases, b_θ, a_3 and $\Delta\vartheta_{st}$ also increase. For horizontal flight $a_3 = b_\theta = 0$, and the error $\Delta\vartheta_{st}$ is also equal to zero.

If we use an automatic pilot without feedback or with the integral control law, the control system for the pitch angle becomes astatic in spite of the force of gravity or the constant external perturbation ΔM_p.

Section 10.7. Control of a Yaw Angle of a Missile with Plane Wings

It was pointed out in section 10.4 that the effective control of a missile with plane wings in the xoz_g plane required tilt. In the same section the basic relationships characterizing flight with tilt were obtained; however, the dynamics of lateral curvilinear controlled motion was not considered. To analyze these dynamics, it is necessary to combine equations for the lateral motion of a plane-winged missile (8.42) with the equations of an automatic pilot for some system. The system of equations which is obtained in this manner is quite complex. Therefore, in selecting the transfer numbers of an automatic pilot, it is desirable to make certain assumptions which simplify the problem.

Let us divide this problem into two problems not associated with each other:

(1) the stabilization (more accurately, the liquidation) of the slip angle by means of the course rudder;

(2) control of the yaw angle and stabilization of tilt by means of ailerons.

In solving the first problem we use the first and second equations of (8.42), neglecting in them the terms which contain the tilt angle and its derivatives. As a result we obtain equations which describe the isolated motion with respect to the y_1 axis /318

$$\left.\begin{aligned} &\frac{d\beta}{dt} + k_\beta\beta - \frac{d\psi}{dt} = 0; \\ &\frac{d^2\psi}{dt^2} + n_\psi \frac{d\psi}{dt} + n_\beta\beta = n_{\delta_{cr}}\delta_{cr} + \frac{\Delta M_p}{J_y}. \end{aligned}\right\} \qquad (10.74)$$

The second equation contains an external moment with respect to the y_1 axis, due to the aerodynamic dissymmetry of the missile. The equation of the automatic pilot with fixed feedback designed to eliminate slipping has the form

$$\delta_{cr} = -i_\psi \frac{d\psi}{dt} - i_\beta\beta. \qquad (10.75)$$

A signal proportional to the angular rate of change of the pitch angle ($d\psi/dt$) is introduced into the control law to provide for the necessary damping of the system.

Combining equations (10.74) and (10.75), we find the general equation for the stabilization of the slip angle by the automatic pilot with fixed negative feedback.

$$\frac{d^2\beta}{dt^2} + (k_\beta + n_\psi + i_\psi n\ \delta_{cr} \qquad \frac{d\beta}{dt} + (k_\beta n_\psi + n_\beta + i_\psi k_\beta n_\delta{}_{cr} + i_\beta n \delta_{cr} \qquad \beta = \frac{\Delta M_p}{J_y} \tag{10.76}$$

The structure of equation (10.76) permits us to draw the following conclusions:

(1) the transfer numbers of the automatic pilot can be best selected by the method of standard coefficients because each coefficient has a transfer number which we are free to control;

(2) the external perturbation moment produces a constant slip angle equal to

$$\Delta\beta_{st} = \frac{\Delta M_p}{J_y(k_\beta n_\psi + n_\beta + i_\psi k_\beta n_\psi + i_\beta n\ \delta_{cr}}; \tag{10.77}$$

(3) when the missile executes a turn with a constant angular velocity $d\psi/dt$ = const, a constant slip angle is produced equal to

$$\Delta\beta_p = -\frac{n_\psi + i_\psi n \delta_{cr}}{n_\beta + i_\beta n \delta_{cr}} \cdot \frac{d\psi}{dt}. \tag{10.78}$$

If the last two situations are significant for a specific type of missile, to obtain a system astatic with respect to constant perturbation and to the turn with constant angular velocity, it is necessary to use an automatic pilot with fixed feedback and with integral control /319

$$\delta_{cr} = -i_\psi \frac{d\psi}{dt} - i_\beta \beta - q_\beta \int_0^t \beta dt. \tag{10.79}$$

Combining equations (10.74) and (10.79), we find the general solution for the stabilization of the slip angle by the automatic pilot with integral control

$$\frac{d^3\beta}{dt^3} + (k_\beta + n_\psi + i_\psi n\ \delta_{cr} \qquad \frac{d^2\beta}{dt^2} + (k_\beta n_\psi + n_\beta + i_\psi k_\beta n\ \delta_{cr} + \\ + i_\beta n\ \delta_{cr} \qquad \frac{d\beta}{dt} + q_\beta n\ \delta_{cr} \qquad \beta = 0. \tag{10.80}$$

When an automatic pilot with integral control is used, the errors during the steady state produced by the moment during turning with constant velocity

are equal to zero. The selection of the transfer numbers in the system described by equation (10.80) should be carried out by the method of standard coefficients for the reasons stated for equation (10.76).

Example 10.3. The given parameters of the missile are as follows: $k_\beta = 0.08$ 1/sec; $n_\beta = 3.2$ 1/sec^2; $n_\psi = 0.1$ 1/sec; $n_{\delta_{cr}} = 1.3$ 1/sec^2. It is required to use the method of standard coefficients and determine the transfer numbers of the automatic pilot with fixed feedback for the stabilization of the slip angle. The control time (t_c) must be equal to 1.5 sec.

On the basis of (10.76) the characteristic equation for this system has the form

$$p^2 + (k_\beta + n_\psi + i_\psi n_{\delta_{cr}})\, p + k_\beta n_\psi + n_\beta + i_\psi k_\beta n_{\delta_{cr}} + i_\beta n_{\delta_{cr}} = 0. \qquad (10.81)$$

The standard characteristic equation for this case (on the basis of table 2.2) will have the form

$$p^2 + 1.5\Omega_0 p + \Omega_0^2 = 0. \qquad (10.82)$$

By equating the coefficients of equation (10.81) to the standard coefficients, we obtain two equations with two unknowns

$$\left.\begin{aligned} k_\beta + n_\psi + i_\psi n_{\delta_{cr}} &= 1.5\Omega_0, \\ k_\beta n_\psi + n_\beta + i_\psi k_\beta n_{\delta_{cr}} + i_\beta n_{\delta_{cr}} &= \Omega_0^2. \end{aligned}\right\} \qquad (10.83)$$

From the graphs in figure 2.6 we find the value of the dimensionless control time $\tau_c = 3$ (for n = 2). From this it follows that the natural frequency of the system must be equal to

$$\Omega_0 = \frac{\tau_c}{t_c} = \frac{3}{1.5} = 2\ \frac{1}{\text{sec}}.$$

Substituting this value of Ω_0 and the numerical values of missile parameters /320 into (10.83) and solving this system with respect to i_ψ and i_β, we obtain their values

$$i_\psi = 2.17 \text{ sec}; \quad i_\beta = 0.44.$$

The same method can be used to select the transfer numbers of the automatic pilot with integral control.

After selecting the parameters of the system for stabilizing the slip angle (the course rudder channel), we can select the parameters for the system controlling the yaw angle and stabilizing the tilt angle (aileron channel). In this case

we let $\dot{\beta} = d\beta/dt = 0$ in the system of equations for the lateral motion of a plane-winged missile (8.42). As a result of this assumption we have the first and second equation of this system to describe the controlled object. The third equation drops out of the system, while the fourth equation describing the motion of the center of gravity is not associated with the first three. Thus we obtain

$$\left.\begin{aligned} &\frac{d\psi}{dt} + \alpha_e \frac{d\gamma}{dt} + k_\gamma \gamma = 0; \\ &\frac{d^2\gamma}{dt} + l_{\dot\gamma} \frac{d\gamma}{dt} + l_\psi \frac{d\psi}{dt} = l_{\delta_e} \delta_e + \frac{\Delta M_p}{J_x}. \end{aligned}\right\} \tag{10.84}$$

In the right side of the second equation we introduce the external moment with respect to the x_1 axis, due to the aerodynamic dissymmetry of the missile.

The equation of the automatic pilot with fixed feedback designed to control the yaw angle by producing a tilt, has the form

$$\delta_e = -i_{\dot\gamma} \frac{d\gamma}{dt} - i_\gamma \gamma - i_\psi (\psi_3 - \psi), \tag{10.85}$$

where $i_{\dot\gamma}$ is the transfer number for the angular rate of change of tilt; i_γ is the transfer number for the tilt angle; and i_ψ is the transfer number of the mismatch in the yaw angle to the ailerons (cross coupling).

The introduction into the control law (10.85) of a signal for the tilt angle is due to the necessity of stabilizing this angle at the zero value when other signals are absent. The signal for the angular rate of change of the tilt is introduced to improve the tilt motion. Finally, the signal $(\psi_3(t) - \psi)$ is the mismatch signal in the control system for the yaw angle. The negative sign of this angle is necessary because of the coupling between tilt and yaw: to turn the missile over a positive yaw angle (to the left), it is necessary to produce a negative tilt (tilt of the left wing).

Combining equations (10.84) and (10.85), we obtain the general equations for the system which controls the yaw angle and stabilizes the pitch angle by means of an automatic pilot with fixed feedback /321

$$\begin{aligned} &\frac{d^3\psi}{dt^3} + (l_{\dot\gamma} - \alpha_e l_{\dot\psi} + i_{\dot\gamma} l_{\delta_e}) \frac{d^2\psi}{dt^2} + (-k_\gamma l_{\dot\psi} + i_\gamma l_{\delta_e} + i_\psi \alpha_e l_{\delta_e}) \frac{d\psi}{dt} + \\ &+ i_\psi k_\gamma l_{\delta_e} \psi = i_\psi \alpha_e l_{\delta_e} \frac{d\psi_3}{dt} + i_\psi k_\gamma l_{\delta_e} \psi_3 - \frac{\alpha_e}{J_x} \frac{d\Delta M_p}{dt} - k_\gamma \frac{\Delta M_p}{J_x}. \end{aligned} \tag{10.86}$$

Each of the coefficients of equation (10.86) has one of the transfer numbers of the automatic pilot which does not enter into the other coefficients. Therefore, to select the values of these transfer numbers, it is rational to utilize the method of standard coefficients. To determine the natural frequency of the present system for controlling the yaw angle of a missile, it is desirable to use

the following approximate data: the time of additional turn must be 5-15 sec,[1] and it increases with the dimensions and weight of the missile. To provide a short time for the additional turns, they must be carried out with substantial tilts. Therefore, the transfer ratio from the yaw angle to the pitch angle must be 5-10. To satisfy this requirement, it is necessary that the ratio of the transfer numbers i_ψ/i_γ be within these same limits.

It follows from equation (10.86) that the automatic pilot with fixed feedback does not provide for astaticism when the external moment is present and when the turn is properly executed. If these shortcomings are substantial for a given missile, as in the case of slip angle stabilization, it is necessary to introduce a signal into the control law of the automatic pilot proportional to the integral of the yaw angle. In this case, to select the parameters of the control system we can use the method of standard coefficients.

Section 10.8. Control of Motion with Respect to the Center of Gravity of a Missile with Variable Velocity

Every missile, when it is launched, changes its velocity from zero to a nominal or maximum value during a rather short period of time (units or tens of sec). For certain types of missiles (ballistic missiles) the final stage of retarded motion is very significant. This motion occurs after the missile has traveled at a very high altitude and enters the lower, denser layers of the atmosphere. Therefore, the analysis of missile motion with variable velocity is of definite interest.

The method of grouping the motions, which makes it possible in a given case to investigate the motion of a missile with variable velocity, is presented in sections 8.6 and 8.7. Here we consider the application of this method to the calculation of angular motions of guided missiles traveling with variable velocity. The lateral motion of a missile with cruciform wings stabilized with respect to its angle of tilt is described by the simplest equations. /322

To investigate the angular motion of a missile, we should take the first two equations of (8.56)

$$\left.\begin{aligned} &\frac{d\beta}{dt}-\frac{d\psi}{dt}-\frac{1}{m}c_z^\beta S\frac{\rho V}{2}\beta=0;\\ &J_y\frac{d^2\psi}{dt^2}-m_y^{\bar{\omega}_y}S\frac{l^2}{2}\frac{\rho V}{2}\frac{d\psi}{dt}-m_y^{\bar{\dot{\beta}}}S\frac{l^2}{2}\frac{\rho V}{2}\frac{d\beta}{dt}-m_y^\beta Sl\frac{\rho V^2}{2}\beta=\\ &\quad=m_y^\delta Sl\frac{\rho V^2}{2}\delta_{cr}\end{aligned}\right\}\qquad(10.87)$$

[1] We have in mind the additional turn by an angle such that the system does not depart from the state where its elements are linear.

First let us analyze the effect of missile velocity variation on the nature of the short period motion of the missile without a control system. This problem is of interest for several flight stages of the missile. For example, when a missile is launched with solid fuel boosters, the control system is sometimes not turned on while these boosters operate, and the missile moves in an uncontrolled manner. This is done because, when accelerations are high, the control system may not operate with sufficient accuracy and also because, at small velocities which exist when the missile is accelerating, its control surfaces are not effective. Therefore, even if the control system is turned on, it has little effect on the motion of the missile. Finally, along the terminal trajectory of a ballistic missile which slows down as it enters the denser layers of the atmosphere, in most cases the missile is not controlled.

If we eliminate from (10.87) the yaw angle, we obtain an equation for the slip angle of the missile[1]

$$J_y \frac{d^2\beta}{dt^2} - \left(\frac{J_y}{m} c_z^\beta S \frac{\rho V}{2} + m_y^{\bar{\omega}_y} S \frac{l^2}{2} \frac{\rho V}{2} + m_y^{\dot{\beta}} S \frac{l^2}{2} \frac{\rho V}{2}\right) \frac{d\beta}{dt} +$$
$$+ \left(\frac{1}{m} c_z^\beta m_y^{\bar{\omega}_y} S^2 \frac{l^2}{2} \frac{\rho^2 V^2}{4} - m_y^\beta S l \frac{\rho V^2}{2} - \frac{J_y}{m} c_z^\beta S \frac{\rho}{2} \frac{dV}{dt}\right) \beta = \qquad (10.88)$$
$$= m_y^\delta S l \frac{\rho V^2}{2} \delta_{cr}.$$

When a term appears in the coefficient for a zero derivative, depending on the acceleration and not on the velocity, this signifies that the thrust of the missile directed along the longitudinal axis has an effect on the lateral motion. When a slip angle occurs, this thrust produces a component perpendicular to the flight velocity, which tends to make the velocity vector coincide with the longitudinal axis of the missile.

Equation (10.88) is a linear nonstationary equation of the second order and, strictly speaking, it is impossible to evaluate the stability of the process from the coefficients of this equation. In addition, the very concept of stability (more precisely, asymptotic stability) in the sense in which it was understood for stationary linear systems also turns out to be unsuitable. Here we must speak of the stability during the terminal interval of time $t(< t \leq t_1)$. If, during the interval $t(0 < t \leq t_1)$, angle β and its derivative decrease in such a way that at the end of the interval they attain specified low values, the system is considered to be stable over the terminal interval. In the contrary case, the system is unstable. If the entire process of missile motion is contained within the /323

[1] It is necessary to bear in mind that when variables are eliminated from the control system with variable coefficients we cannot use the symbolic or operator methods because they are not applicable to such equations. In addition, in obtaining equation (10.88), the mass of the missile was considered to be constant.

interval 0 - t_1, the stability in the conventional sense, i.e., stability over an infinite interval, has no meaning. The stability of the solution of equation (10.88) over the terminal interval is subject to analysis in the case when the velocity does not change too rapidly and when the method of fixed and quasi-fixed coefficients described in section 2.4 can be applied. To apply this method, it is necessary to know the law for the variation of the flight velocity.

Let us assume that during a certain interval of time the motion of the missile takes place with equal acceleration or equal deceleration, i.e.,

$$V = V_0 \pm jt. \tag{10.89}$$

To obtain a more convenient form of this equation, we shall assume that in equation (10.89) the sign before the second term refers to the time t, rather than to the acceleration j. In this case (10.89) may be represented in the form

$$V = j(t_0 \pm t), \tag{10.90}$$

where $t_0 = V_0/j$ is a substantially positive quantity.

The plus sign in the brackets pertains to acceleration, while the minus sign pertains to deceleration. In addition, the bracket as a whole cannot become negative. The second assumption means that over this region of time we neglect the variation in time of all the other characteristics of the missile (J_y, m) and of the atmosphere (ρ).

Substituting the value of V into equation (10.88) we obtain

$$\begin{gathered} J_y \frac{d^2\beta}{dt^2} - S\frac{\rho j}{2}\left(\frac{J_y}{m} c_z^\beta + m_y^{\bar{\omega}_y}\frac{l^2}{2} + m_y^{\bar{\beta}}\frac{l^2}{2}\right)(t_0 \pm t)\frac{d\beta}{dt} + \\ + \left[Sl\frac{\rho j^2}{2}\left(\frac{1}{m} c_z^\beta m_y^{\bar{\omega}_y} S\frac{l\rho}{4} - m_y^\beta\right)(t_0 \pm t)^2 - \frac{J_y}{m} c_z^\beta S\frac{\rho j}{2}\right]\beta = \\ = m_y^\delta Sl\frac{\rho j^2}{2}(t_0 \pm t)\,\delta_{\text{cr}}. \end{gathered} \tag{10.91}$$

Generally speaking, equation (10.91) may be integrated by means of power series.[1] However, the form of such a solution is insufficiently illustrative, and to obtain purely qualitative results we use the method of fixed and quasi-fixed coefficients. Let us write equation (10.91) in a more compact form

$$\frac{d^2\beta}{dt^2} + a_1(t_0 \pm t)\frac{d\beta}{dt} + [a_2(t_0 \pm t)^2 + a_3]\beta = b(t_0 \pm t)^2\delta_{\text{cr}}, \tag{10.92}$$

---

[1] V. I. Smirnov. A Course in Higher Mathematics, Gostekhizdat, 1948.

where

$$a_1 = -S\frac{\rho j}{2J_y}\left(\frac{J_y}{m}c_z^\beta + m_y^{\bar{\omega}y}\frac{l^2}{2} + m_y^{\dot{\bar{\beta}}}\frac{l^2}{2}\right);$$

$$a_2 = Sl\frac{\rho j^2}{2J_y}\left(\frac{1}{m}c_z^\beta m_y^{\bar{\omega}y}S\frac{l\rho}{4} - m_y^\beta\right);$$

$$a_3 = -\frac{J_y}{m}c_z^\beta S\frac{\rho j}{2}; \quad b = m_y^\delta Sl\frac{\rho j^2}{2J_y}.$$

We note that coefficients a_1, a_3 and b are positive for any missile (c_z^β, $m_y^{\bar{\omega}y}$, $m_y^{\dot{\bar{\beta}}}$ are negative), while the coefficient a_2 for a statically stable missile ($m_a^\beta < 0$). /324

To go from equation (10.92) to the equation with fixed coefficients, it is sufficient to let: $t = 0$; $t_0 = V_0/j = \text{const}$. As a result, from (10.92) we obtain

$$\frac{d^2\beta}{dt^2} + a_1 t_0\frac{d\beta}{dt} + (a_2 t_0^2 + a_3)\beta = bt_0^2\delta_{cr}. \tag{10.93}$$

From equation (10.93) we obtain a formula for the natural frequency and for the relative damping of the missile ζ

$$\left.\begin{aligned} \Omega_0 &= \sqrt{a_2 t_0^2 + a_3}; \\ \zeta &= \frac{a_1 t_0}{2\sqrt{a_2 t_0^2 + a_3}}. \end{aligned}\right\} \tag{10.94}$$

It follows from equation (10.94) that for very small flight velocities ($V_0 \to 0$ and $t_0 \to 0$) the damping of the missile's motion tends to zero ($\zeta \to 0$). Equation (10.93) describes the motion of the missile without a control system. However, at small flight velocities the control system using conventional aerodynamic control surfaces cannot control the missile, because the moment produced by the control surface $M_\delta = bt_0^2\delta_{cr}$ has an insignificant value. Therefore, the conclusions which we have reached retain their validity for missiles with a control system over the initial region of acceleration.

As the flight velocity increases, $a_2 t_0^2$ becomes much greater than a_3 and, therefore, from equation (10.94) we obtain

$$\left.\begin{aligned} \Omega_0 &\approx t_0\sqrt{a_2}, \\ \zeta &\approx \frac{a_1}{2\sqrt{a_2}}. \end{aligned}\right\} \tag{10.95}$$

Expression (10.95) shows that the natural frequency Ω_0 will increase with time and, consequently, with an increase in flight velocity, whereas the relative damping ζ does not depend on these arguments. The opposite picture takes place when the flight velocity is decreased, because in this case the value $t_0 = V_0/j$ will decrease.

If we analyze the motion of the missile described by equations with variable coefficients and use the method of quasistationary coefficients, we shall obtain, by using table 2.6, from equation (10.92)

$$\frac{d^2\beta}{dt^2} + \left(a_1 t_0 \pm \frac{a_2 t_0}{a_2 t_0^2 + a_3}\right)\frac{d\beta}{dt} + \left(a_2 t_0^2 + a_3\right)\beta = b t_0^2 \delta_{1\,cr}. \tag{10.96}$$

Comparing equations (10.93) and (10.96), we note that the effect of flight acceleration taken into account in the first approximation, as permitted by the method of quasifixed coefficients, has led to the appearance of an auxiliary term $\pm a_2 t_0/(t_0^2 + a_3)$ in the damping coefficient. The plus sign refers to ac- /325 celerated motion of the missile, while the minus sign refers to decelerated motion of the missile. This auxiliary term increases damping during acceleration and decreases it during deceleration. Its value first increases from zero and then decreases when t_0 increases, i.e., when the velocity V_0 increases. At high flight velocities, the effect of this term becomes insignificant.

To show how the analysis is complicated if we take into account the variation of the flight velocity, we consider the system for controlling the yaw angle of a missile with cruciform wings, which uses an automatic pilot with fixed feedback. Combining the equations of the missile (10.87) and of the automatic pilot (10.49), we find the general equation for the yaw angle control system

$$\frac{d^3\psi}{dt^3} + (a_1 + i_\psi b_1)\frac{d^2\psi}{dt^2} + (a_2 + i_\psi b_2 + i_\psi b_1)\frac{d\psi}{dt} + (i_\psi b_2 + a_3)\psi = \tag{10.97}$$
$$= i_\psi b_1 \frac{d\psi_3}{dt} + i_\psi b_2 \psi_3.$$

The resemblance of expression (10.97) to equation (10.50) considered in section 10.5 is purely external. This becomes obvious if we compare the values of the coefficients of equation (10.50) given by equations (10.48) with the coefficients of equation (10.97) shown below

$$
\left.
\begin{aligned}
a_1 &= -\frac{1}{J_y}\left[\left(m_y^{\bar{\omega}y} + m_y^{\bar{\beta}}\right) S \frac{l^2}{2} \frac{\rho V}{2} + \frac{J_y}{m} c_z^{\beta} S \frac{\rho V}{2} + \frac{J_y}{V} \frac{dV}{dt}\right]; \\
a_2 &= -\frac{1}{J_y}\left(\frac{1}{m} c_z^{\beta} m_y^{\bar{\omega}y} S^2 \frac{l^2}{2} \frac{\rho^2}{4} + m_y^{\beta} S l \frac{\rho}{2}\right) V \frac{dV}{dt} + \\
&+ S \frac{l^2 \rho}{4 J_y}\left(m_y^{\bar{\omega}y} + m_y^{\bar{\beta}}\right)\left(\frac{dV}{dt} + \frac{1}{m} c_z^{\beta} S \frac{\rho V^2}{2}\right); \\
b_1 &= m_y^{\delta} S l \frac{\rho V^2}{2 J_y}; \\
b_2 &= -m_y^{\delta} S l \frac{\rho V}{2 J_y}\left(\frac{1}{m} c_z^{\beta} S \frac{\rho V^2}{2} - \frac{dV}{dt}\right).
\end{aligned}
\right\} \qquad (10.98)
$$

As in the preceding problems of the present section, the mass of the missile was considered to be constant in the derivation of equation (10.97). If we had taken into account the variation in the mass of the missile, it would have produced a further complication of equations (10.98). However, in the present case, equations (10.98) for the coefficients of equation (10.97) have turned out to be so complex that they do not even lend themselves to qualitative analysis.

Therefore, the rational path for selecting the transfer numbers of an automatic pilot in this system consists of the following. Since the characteristics of the missile and the variation of velocity with time must be known beforehand, after they are introduced into equation (10.97) we obtain specific values of its coefficients. Then, by using fixed or quasifixed coefficients, we must use the method of standard coefficients or the logarithmic amplitude-frequency characteristics to determine the optimum value of the transfer numbers for several flight conditions. Having selected some average value, we should check to see /326 what the dynamic properties of the missile will be under different flight conditions. If it becomes impossible to use the same transfer numbers of the automatic pilot and provide for the necessary properties of the missile under different flight conditions, we should seek the technical possibility of changing these numbers in the course of the flight into functions of velocity, velocity head or, more simply, into functions of time.

The material presented in this paragraph pertains to the lateral motion of a missile. However, the considerations and recommendations made here are valid for longitudinal motion.

Section 10.9. Control of the Tilt Angle of a Missile by Means of Relay Automatic Pilots

As a first example, showing the application of a relay automatic pilot, we shall consider a system for stabilizing the angle of tilt of a missile. The simplified schematic of an automatic pilot is shown in figure 10.14. The entire device consists of a block of gyroscopes and a pair of spoilers for tilt control. The spoilers may be situated on the lift surfaces of the missile. The

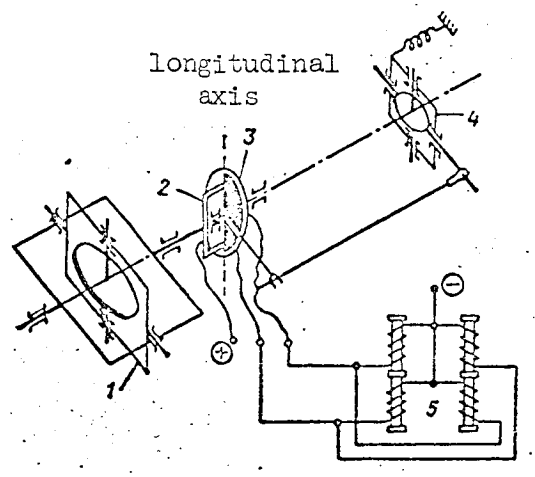

Figure 10.14. Electrokinematic diagram of relay automatic pilot. 1--position gyroscope; 2--brush; 3--disk; 4--damping gyroscope; 5--spoilers.

spoilers are extended in opposite directions and produce a rotating moment of either sign with respect to the longitudinal axis of the missile. The block of gyroscopes consists of a position gyroscope 1 and a damping gyroscope 4. The axes of rotation of both gyroscopes are both normal with respect to the longitudinal axis of the missile. The axis of the external frame of gyroscope 1 has brushes 2 which slide along the contact disk 3, which has two current-carrying sectors. The contact disk is connected to the frame of the missile. In addition, it may be rotated with respect to the frame of the missile through the lever transmission by the damping gyroscope. When the missile rotates with respect to its longitudinal axis, the sliding contacts associated with the external frame of the gyroscope remain fixed. The contact disk, on the other hand, turns together with the missile. As a result, one of the segments of the disk falls under the sliding contact and switches on the windings of the spoiler /327 electromagnets 5. This causes the spoiler to move out in such a way that the moment which it produces rotates the missile towards its original position and eliminates tilt angle γ. The damping gyroscope rotates the contact disk by an angle proportional to the angular velocity of rotation of the missile around its longitudinal axis ($\omega = d\gamma/dt$). If the missile returns to its initial position under the action of the spoilers, the disk undergoes an additional rotation towards the sliding contacts.

Let us consider the motion of the missile around the longitudinal axis, when it is subjected to a moment developed by the spoilers which control the tilt angle. If, for some reason or other, the tilt becomes different from zero, the motion of the missile may be described with a sufficient degree of accuracy by the following equation

$$J_x \frac{d^2\gamma}{dt} + M_x^{\omega}{}_x \frac{d\gamma}{dt} = M_x, \qquad (10.99)$$

where J_x is the moment of inertia of the missile with respect to its longitudinal axis; $M_x^{\omega_x}$ is the aerodynamic damping moment; and M_x is the moment produced by the tilt spoilers.

The absolute value of the moment developed by the spoilers is a constant quantity, i.e.,

$$|M_x| = M_{xm} = \text{const}.$$

If we take into account the variation in flight velocity and altitude, the quantities $M_x^{\omega_x}$ and M_{xm} are variables. However, the variation in these quantities during the flight of the missile takes place at a much slower rate than the occurrence of transient processes associated with the stabilization of the missile with respect to its longitudinal axis. Therefore, we shall consider expression (10.99) as an equation with constant coefficients.

First, let us consider the operation of the scheme shown in figure 10.14 without taking into account the damping gyroscope. In this case, contact disk 3 will be rigidly attached to the frame of the missile. If we assume that the operating time of the spoiler electromagnets is equal to zero and that there is no delay in the occurrence of the aerodyanmic moment, then, when there is a change in the sign of the tilt angle, there is an instantaneous change in the sign of the moment produced by the spoilers. Then, similar to (2.66),

$$M_x = -M_{xm}\,\text{sign}\,(\gamma). \tag{10.100}$$

The minus sign in the right side shows that the moment developed by the spoilers always tends to decrease the tilt angle. Combining (10.99) and (10.100), we find the equation for the system controlling the position of the missile with respect to its longitudinal axis

$$J_x \frac{d^2\gamma}{dt^2} + M_x^{\omega_x} \frac{d\gamma}{dt} + M_{xm}\,\text{sign}\,(\gamma) = 0. \tag{10.101}$$

The expression we obtained is analogous to equation (2.70), which was considered in section 2.6. If we assume that the switching of spoilers cannot take place instantaneously, the last term in equation (10.101) will be delayed, and the equation will be written in the following form

$$J_x \frac{d^2\gamma}{dt^2} + M_x^{\omega_x} \frac{d\gamma}{dt} + M_{xm}\,\text{sign}_{t_3}(\gamma) = 0. \tag{10.102}$$

Introducing such new variables as the relative magnitude of the tilt angle /328

$$\bar{y} = \frac{\gamma\left(M_x^{\omega_x}\right)^2}{J_x M_{xm}},$$

the dimensionless time $\tau = t \cdot \frac{M_x^{\omega_x}}{J_x}$ and the dimensionless delay time $\Delta\tau = t_3 \frac{M_x^{\omega_x}}{J_x}$, we reduce equation (10.102) to form (2.80)

$$\frac{d^2\bar{y}}{d\tau^2} + \frac{d\bar{y}}{d\tau} + \operatorname{sign}_{\Delta\tau}(\bar{y}) = 0. \tag{10.103}$$

As shown in section 2.6, such a relay system with delay will always undergo self-sustained oscillations whose amplitude may become too large and whose frequency may become too low, making the system inoperative. To eliminate self-sustained oscillations in the system, a compensating device is used, which has the form of a damping gyroscope 4 (fig. 10.14), which turns the contact disk by an additional angle proportional to the angular velocity of rotation of the missile.

The equation for the stabilization of the missile taking into account the effect of the damping gyroscope will have the form

$$J_x \frac{d^2\gamma}{dt^2} + M_x^{\omega_x} \frac{d\gamma}{dt} + M_{xm} \operatorname{sign}_{t_3}\left(\gamma + b \frac{d\gamma}{dt}\right) = 0. \tag{10.104}$$

By introducing relative units, we reduce this equation to equation (2.97) considered in section 2.5.

$$\frac{d^2\bar{y}}{d\tau^2} + \frac{d\bar{y}}{d\tau} + \operatorname{sign}_{\Delta\tau}\left(\bar{y} + \zeta \frac{d\bar{y}}{d\tau}\right) = 0. \tag{10.105}$$

All of the conclusions made during the analysis of equations (2.80) and (2.97) are valid for the dynamics of the processes stabilizing the missile with respect to its longitudinal axis.

By using the theory of relay systems presented in section 2.6, we can submit recommendations for the selection of the characteristics of the damping gyro when the structural-aerodynamic parameters of the missile J_x, $M_x^{\omega_x}$ and M_{xm} are known. To obtain the most suitable transient process with a sufficiently low amplitude of oscillations, it is necessary to select the coefficient of rate feedback ζ in accordance with equation (2.98). In the present case ζ is a dimensionless value of coefficient b in equation (10.104), i.e.,

$$\zeta = b \frac{M_x^{\omega_x}}{J_x}.$$

From this it follows that

$$b = \zeta \frac{J_x}{M_x^{\omega_x}}. \tag{10.106}$$

Having selected the optimum value of ζ on the basis of equation (2.98), we obtain from equation (10.106) the basic characteristic of the damping gyroscope--the angle of deviation of its moving system b per unit angular velocity of rotation of the missile with respect to its longitudinal axis. /329

Example 10.4. The missile has the following specifications:

(1) the moment of inertia with respect to the longitudinal axis is J_x = 31.4 kg x m^2;

(2) the coefficient of aerodynamic damping is $M_x^{\omega_x}$ = 274 kg x m^2 sec^{-1};

(3) the maximum moment developed by the spoilers is M_{xm} = 5880 j;

(4) the pick-up time of the spoiler electromagnet t_{pu} = 4 x 10^{-3} sec;

(5) the switching time of the spoilers (from one extreme position to the other) t_{switch} = 12 x 10^{-3} sec.

On the basis of these data we can determine the amplitude and the period of self-sustained oscillations of a missile without a damping gyroscope. The equivalent delay is equal to

$$t_d = t'_{pu} + \frac{t'_{SW}}{2} = 4 \cdot 10^{-3} + \frac{1}{2} 12 \cdot 10^{-3} = 10 \cdot 10^{-3} \text{ sec.}$$

(subscript d = delay).

The delay in dimensionless units is equal to

$$\Delta\tau = t_d \frac{M_x^{\omega_x}}{J_x} = \frac{10 \cdot 10^{-3}}{31.4} \cdot 274 = 0.0875.$$

With this delay we use the curves shown in figure 2.37 to obtain $\overline{z}_m$ = 0.480; $\frac{1}{\theta}$ = 0.5; θ = 2.0; $\overline{y}_m$ = 0.12. In units with dimensions:

(1) the period of oscillations of the missile with respect to the longitudinal axis is equal to $\theta \frac{J_x}{M_x^{\omega_x}} = 2.0 \frac{31.4}{274} = 0.228$ sec; (the frequency of self-sustained oscillations is 3.6 cps.);

(2) the amplitude of oscillations of the tilt angle is equal to

$$\bar{y}_m \cdot \frac{J_x M_{xm}}{(M_x^{\omega_x})^2} = \frac{0.12 \cdot 31.4 \cdot 5880}{274^2} = 0.294 \text{ radius} = 16.8^\circ.$$

On the basis of expression (2.98) we select the basic characteristic of the damping gyroscope

$$\zeta = 1 - \ln 2 \cdot e^{-\Delta\tau} = 1 - \ln 2 \cdot e^{-0.0875} = 0.365.$$

To obtain this value for the coefficient ζ, we must have

$$b = \zeta \frac{J_x}{M_x^{\omega_x}} = 0.365 \cdot \frac{31.4}{274} = 0.0417 \text{ sec.}$$

When $\Delta\tau = 0.0875$ and $\zeta = 0.365$, we use the curves in figure 2.43 to find the value of $z_2 = 0.015$. The remaining parameters of the self-sustained oscillatory process are determined from equations analogous to (2.82) -- (2.84)

$$\bar{z}_m = 1 - (1 - \bar{z}_2)\, e^{-\Delta\tau},$$
$$\bar{y}_m = \ln \frac{1}{1 - z_2} - z_2 (1 - \zeta),$$
$$\theta = 4 (\Delta\tau + z_2).$$

Substituting the values for z_2 and $\Delta\tau$ into these equations, we obtain $\bar{y}_m$ = 0.0055; θ = 0.410 or in units with dimensions. /330

The period of oscillations is

$$\theta \frac{J_x}{M_x^{\omega_x}} = 0.410 \frac{31.4}{274} = 0.0467 \text{ sec;}$$

and the amplitude of oscillations is

$$\bar{y}_m \frac{J_x M_{xm}}{(M_x^{\omega_x})^2} = 0.0055 \frac{31.4 \cdot 5880}{274^2} \cdot 57.3 = 0.77^\circ = 46.5'.$$

Thus, the introduction of a damping gyroscope reduces the amplitude of the oscillations to 46.5 angular minutes and increases the switching frequency of the spoilers by almost a factor of 7. Obviously, such oscillations will have no effect on the control of the missile, while oscillations with an angular amplitude of 16.3 degrees and a frequency of 3.6 cps. must be considered inadmissible.

The system which we have considered for the stabilization of the tilt angle of the missile may also be used to control the tilt. For this purpose, brushes 2 (fig. 10.14) must also be coupled with a device which receives the command signals for controlling the tilt, and which converts these signals into proportional mechanical displacements of the brushes 2. In this case, the axis of the external frame of the gyroscope and of the actuating roller must be connected to a differential arrangement.

As a second example for the application of relay control, let us consider the vibratory-linearized system for controlling the tilt of a missile. As before, we shall be concerned with a system operating with an electromagnetic driver. The self-sustained oscillations will be damped by using the vibratory linearization produced by forced oscillations. The system for controlling the tilt of a missile is shown in figure 10.15. It consists of the following: position gyroscope 11, contact disk 10, rigidly attached to the external frame of the gyroscope, an electromagnetic relay 6, polarized relay 12 and spoilers 13 and 14. One half of the contact disk is a conductor, while the other half is an insulator. The axis of the external frame, which contains the disk, coincides with the longitudinal axis of the missile. Brushes 9-9 slide over the contact disk and are used to connect the windings of a two-position relay 12. The controlling relay, by means of its contacts, turns on the windings of the electromagnetic tilt spoilers. The windings of the spoiler electromagnets are connected to the contacts of relay 12 in such a way that for any position of its moveable contact the spoilers are displaced in opposite directions.

When the brushes 9-9 rotate with respect to the disk 10, there will always be a switching of the spoilers and a discontinuous variation in the moment which rotates the missile with respect to its longitudinal axis. If the brushes are rigidly attached to the frame of the missile, then we have a tilt stabilization system similar to the one considered before (fig. 10.14). To control the tilt, a device is used rotating the brushes with respect to the frame of the missile. This device is an electromagnetic relay, 6, whose frame rotates the brushes, 9-9, through the given angle by means of a pair of gears, 7 and 8. The moving system of the electromagnetic relay has two coils, 5, which turn in the field of the constant magnet 4, when current passes through them and overcome the restoring force of two spiral springs, 3. The neutral position of the moving system of relay 6, and consequently of the brushes, corresponds to the zero tilt angle of the missile. The windings of relay 6 are connected to the contacts of the polarized relay 2 at the output of receiver 1. The moveable contact of this relay is switched at a frequency of 10-15 cps and alternately switches in the windings of the electromagnetic relay.

If the control signal is equal to zero, both windings are fed with constant voltage pulses of the same duration. The moving system of the relay will oscillate about its neutral position. If the control signal is different /331 from zero, the duration of the pulses in windings 5 will be different, which will produce some average moment on coil 5, proportional to the magnitude of the control signal. This average moment will rotate the moving system by an angle at which it will be counterbalanced by the spiral springs 3. Thus, the average angle of rotation of the relay's frame and of the brushes 9-9 turns out to be proportional to the control signal. By turning the sliding contacts, any tilt angle may be imparted to the missile.

The moving system of relay 6 will always oscillate with the switching frequency of relay 2 contacts. The oscillations will take place with respect to the average angular position, which is assigned by the control signal. The brushes 9-9 will also undergo angular oscillations with the same frequency and with a definite amplitude. A moving system of the electromagnetic relay

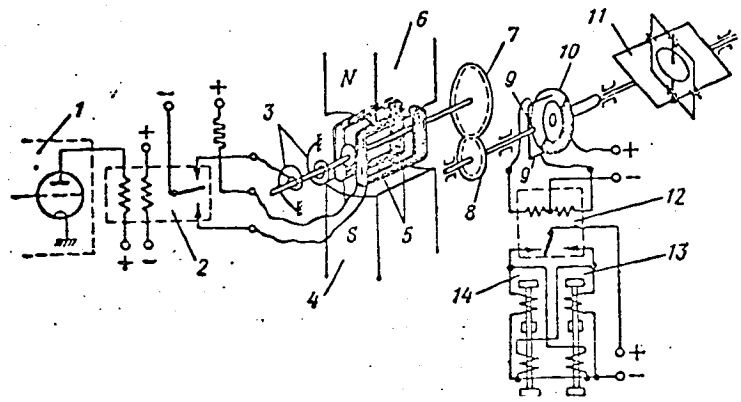

Figure 10.15. Electrokinematic schematic diagram of relay automatic pilot with vibratory linearization. 1--receiver; 2--polarized relay; 3--spiral springs; 4--permanent magnet; 5--coils; 6--electromagnetic relay; 7 and 8--gear drive; 9--sliding contacts; 10--contact disk; 11--position gyroscope; 12--two-positioned relay; 13 and 14--spoilers.

is designed so that it has sufficient mass. The coils are wound on a copper form, which produces a short-circuited turn and its motion in the magnetic field is considerably damped. Due to this, the oscillations of the moving system and of the sliding contacts near some average position are almost sinusoidal when the exciting periodic moment has a rectangular form. The law of motion of brushes 9-9, which are connected to the frame of the electromagnetic relay, may be written in the following form

$$\psi = \psi_0(t) + \psi_m \sin \omega t,$$

where $\psi_0(t)$ is the assigned law for the variation in the tilt angle; and ψ_m and ω are the amplitude and frequency of oscillations of brushes 9-9 with respect to the angle $\psi_0(t)$.

In this case $\psi_0(t)$ as well as the tilt angle $\gamma(t)$ must be slowly varying functions compared with $\psi_m \sin \omega t$. Equation (10.99), which described the variation of the tilt angle of the missile, will also be valid in this case, however, the moment M_x produced by the spoilers will be a function of the /332 mismatch $\epsilon = \psi_0 - \gamma$. If the relay and the electromagnets operate instantaneously, this relationship will have the following form

$$M_x = M_{xm} \operatorname{sign}(\varepsilon) = M_{xm} \operatorname{sign}[\psi_m \sin \omega t + \psi_0(t) - \gamma]. \qquad (10.107)$$

Combining equations (10.99) and (10.107), we obtain an equation which describes the control process for the tilt angle of the missile

$$J_x \frac{d^2\gamma}{dt^2} + M_x^{\omega_x} \frac{d\gamma}{dt} = M_{xm} \operatorname{sign} [\psi_m \sin \omega t + \psi_0 (t) - \gamma]. \tag{10.108}$$

If, for simplicity, we assume that

$$\psi_0 (t) = \text{const} = 0,$$

we can rewrite equation (10.108):

$$J_x \frac{d^2\gamma}{dt^2} + M_x^{\omega_x} \frac{d\gamma}{dt} + M_{xm} \operatorname{sign} (\gamma - \psi_m \sin \omega t) = 0. \tag{10.109}$$

Expression (10.109) shows that the argument of the nonlinear function sign contains a periodic component. Since γ is a slowly varying function compared with $\psi_m \sin \omega t$, it may be considered constant over several periods $2\pi/\omega$.

The function sign $n(\gamma - \psi_m \sin \omega t)$ will be periodic only when $|\gamma| < \psi_m$. The switching frequency of the spoilers ω is usually selected so that it is quite high (10-15 cps), so that the oscillations of the missile around the longitudinal axis produced by the periodic component will have an insignificant amplitude.

Thus, in this relay system linearization is accomplished by sinusoidal oscillations. Consequently, in this case equation (2.105) is applicable

$$K = \frac{2}{\pi} \arcsin \frac{\gamma}{\psi_m}. \tag{10.110}$$

The relationship $K = K(\gamma)$ is given by the graph in figure 2.47b. When γ/ψ_m are small

$$K = \frac{2}{\pi} \frac{1}{\psi_m} \gamma. \tag{10.111}$$

Expression (10.111) shows that the amplification factor of the relay amplifier is equal to $\frac{2}{\pi} \frac{1}{\psi_m}$ for slowly varying signals. If $|\epsilon| < \psi_m$, we can write the equation which describes the variation in the tilt angle when the input signal $\psi_0(t)$ is variable

$$J_x \frac{d^2\gamma}{dt^2} + M_x^{\omega_x} \frac{d\gamma}{dt} + M_{xm} \frac{2}{\pi\psi_m} \cdot \gamma = M_{xm} \frac{2}{\pi\psi_m} \psi_0 (t). \tag{10.112}$$

Expression (10.112) represents the equation for an oscillating member

$$\frac{d^2\gamma}{dt^2} + 2\zeta\Omega_0 \frac{d\gamma}{dt} + \Omega_0^2 \gamma = \Omega_0^2 \psi_0(t), \tag{10.113}$$

where

$$\left.\begin{aligned} \Omega_0^2 &= \frac{2}{\pi} \cdot \frac{M_{xm}}{J_x \psi_m}; \\ \zeta &= \frac{M_x^{\omega_x}}{2} \sqrt{\frac{\pi}{2} \cdot \frac{\psi_m}{J_x M_{xm}}}. \end{aligned}\right\} \tag{10.114}$$

Expression (10.114) shows that the natural frequency of oscillations of the system Ω_0 is inversely proportional, while the degree of damping ζ is directly proportional to the square root of ψ_m. /333

In the region where $|\psi_0 - \gamma| > \psi_m$, the tilt angle must be computed by means of the following equation

$$J_x \frac{d^2\gamma}{dt^2} + M_x^{\omega_x} \frac{d\gamma}{dt} = \pm M_{xm}.$$

In this case the spoilers are completely extended in the same direction, and a constant moment M_{xm} acts on the missile. The amplitude of the fundamental frequency of oscillations of the missile in the stationary state ($\epsilon = 0$) may be obtained as a specific solution of equation

$$J_x \frac{d^2\gamma}{dt^2} + M_x^{\omega_x} \frac{d\gamma}{dt} = \frac{4}{\pi} M_{xm} \sin \omega t. \tag{10.115}$$

The solution of this equation gives us the unknown amplitude

$$\gamma_m = \frac{4}{\pi} \frac{M_{xm}}{\omega \sqrt{J_x^2 \omega^2 + (M_x^{\omega_x})^2}}. \tag{10.116}$$

The frequency $\omega = \frac{2\pi}{T_1 + T_2}$ must be selected in such a way that the amplitude of oscillations of the missile is insignificant. Linear equations for describing the behavior of the system in the zone of spoiler vibrations were obtained under the assumption that the delay is $t_3 = 0$. As we stated in section 2.6, for $t_3 = 0$ and for a Z-type variation in the moment as a function

of the tilt angle, self-sustained oscillations will not take place in the system. Actually, $t_3 \neq 0$, and self-sustained oscillations will inevitably occur in the system. However, if the input of the system is subjected to oscillations $\psi_m \sin \omega t$ of sufficiently high frequency and with an amplitude which provides for reliable operation of the relay and of the electromagnets, the self-sustained oscillations will be suppressed. Then, in the stationary state, the spoilers will be switched with frequency ω, and the oscillations of the missile with respect to its longitudinal axis will take place with the same frequency.

To suppress the self-sustained oscillations, the frequency of the external forced oscillations must be several times greater than the possible frequency of self-sustained oscillations. The increase in the frequency of external oscillations ω is limited by the capability of all relay elements of the system to reproduce this frequency. For example, electromagnets are capable of switching the spoilers with a frequency ω only if their operate time will be less than the half period of oscillations $t_{operate} < \frac{\pi}{\omega}$. The relay delay t_3 has an insignificant effect on the nature of the transient process in the region of proportionality; therefore, equation (10.112) remains approximately valid even if we take into account delay t_3.

Example 10.5. Let us assume that the following parameters of the missile and of the control system are known: /334

(1) the moment of inertia $j_x = 155$ kg wt·m^2;

(2) the coefficient for the moment of aerodynamic damping $M_{xm} = 677$ kg wt·m^2 sec^{-1};

(3) the maximum moment developed by the spoilers, $M_{xm} = 2130$ j;

(4) the delay introduced by the relay and the spoilers, $23 \cdot 10^{-3}$ sec.

Let us determine the frequency and amplitude of the oscillations of the missile with respect to its longitudinal axis, when linearizing oscillations are absent. When the relative delay is equal to

$$\Delta\tau = \frac{t_3}{J_x} \cdot M_x^{\omega} x = \frac{0.023}{155} \cdot 677 = 0.1$$

we use the curves shown in figure 2.37 to determine

$$\bar{y}_m = 0.14 \quad \text{and} \quad \frac{1}{\theta} = 0.47.$$

Thus the amplitude of oscillations of the tilt angle is equal to

$$\gamma_m = \bar{y}_m \cdot \frac{J_x}{M_x^{\omega_x}} \cdot \frac{M_{xm}}{M_x^{\omega_x}} = 0.14 \frac{155 \cdot 2130}{677^2} 57.3 = 5.8^\circ,$$

and the frequency of oscillations is equal to

$$\frac{M_x^{\omega_x}}{\theta J_x} = \frac{677}{155} \cdot 0.47 = 2.13 \text{ cps}.$$

Oscillations with this frequency and amplitude make it very difficult to control the missile.

Now let us place the brushes into an oscillatory angular motion in accordance with the law $\psi_m \sin \omega t$. Let us assume that the amplitude of the angular oscillations is $\psi_m = 25^\circ$ and that the frequency is $f = \omega/2\pi = 10$ cps. Obviously, in this case, self-sustained oscillations will be suppressed and the spoilers will be switched with a frequency ω.

The amplitude of the angular oscillations of the missile is determined from equation (10.116)

$$\gamma_m = \frac{4}{\pi\omega} \cdot \frac{M_{xm} \cdot 57.3}{\sqrt{J_x^2\omega^2 + (M_x^{\omega_x})^2}} = \frac{4 \cdot 2130 \cdot 57.3}{\pi \cdot 62.8 \sqrt{155^2 \cdot 62.8^2 + 677^2}} = 0.255^\circ.$$

The transient process during the adjustment of some assigned tilt angle in the region of proportionality may be determined from equation (10.113).

The degree of damping in the region of proportionality will be equal to

$$\zeta = \frac{M_x^{\omega_x}}{2} \sqrt{\frac{\pi}{2} \frac{\psi_m}{J_x M_{xm}}} = \frac{69}{2} \sqrt{\frac{\pi \cdot 25}{2 \cdot 57.3 \cdot 2130 \cdot 155}} = 0.352.$$

The degree of damping turns out to be rather small and the transient process when the tilt angle is adjusted in the region of proportionality will have an oscillatory nature. We can increase ζ by increasing ψ_m. However, in order to obtain, for example, $\zeta = 0.7$, the amplitude of oscillations must be raised to a value $\psi_m = 99^\circ$. This may be impossible to do. Therefore, we can increase the damping by introducing a damping gyroscope into the control system for the tilt angle.

Section 10.10. Self-Adaptive Missile Guidance Systems /335

To stabilize the dynamic characteristics of guided missiles when flight conditions change, it is possible to change the transfer characteristics of the automatic pilot as a function of the velocity head. To achieve this, the equipment aboard the missile must have means for measuring the velocity head. With a given program for the unperturbed state, as in the case of the active region of ballistic missiles, the transfer characteristics of an automatic pilot may be varied with time. However, there is a more advanced method of stabilizing the dynamic characteristics of guided missiles by means of self-adaptive systems or by self-adaptive automatic pilots. Self-adaptive automatic control systems may have:

(1) optimalizing compensating networks or transfer numbers of the automatic pilot;

(2) a high amplification factor and nonlinear characteristics.

The functional diagram of the first system is shown in figure 10.16. In addition to the regulator on the controlled object, the system includes an analog (model) of the missile with the desired dynamic characteristics and an optimalizing compensating network. The input of the system and of the model with the transfer function $W_a(p)$, in addition to the input signal $x(t)$, is also fed with a special test signal f_{test} (harmonic signal, sequence of pulses or some other signal). The output of the model y_a and the output of the system y are compared and a difference μ is obtained. The signal μ is fed to the optimalizing system. The optimalizing system reacts on the parameters of the compensating networks T_1, T_2, T_3, T_4 and causes a search for the minimum of μ or for some of its functionalities. When μ assumes a minimum value, the output of the reference y_a is close to the output of the system y, i.e., the transfer function of the system becomes close to the transfer function of the model, which remains constant and is selected on the basis of the requirements for the control system. Thus, there is an automatic approach of the dynamic properties of the control system to the desired reference properties. The test signal f_t is selected in such a way that its component at the output of the system lies within allowable limits. When a random signal $x(t)$, which also contains a high frequency part of the spectrum, is applied continuously at the input, it is possible to do away with the test signal.

An optimalizing system cannot instantaneously readjust the compensating network when the parameters of the controlled object change suddenly. There is a certain transient process of self-adaptation, whose duration is several times greater than the transfer function of the model $H_a(t)$. This is a dis- /336 advantage of the system and manifests itself when there is a sharp variation

in the parameters of the controlled object (e.g., in the first seconds when a ballistic missile is launched).

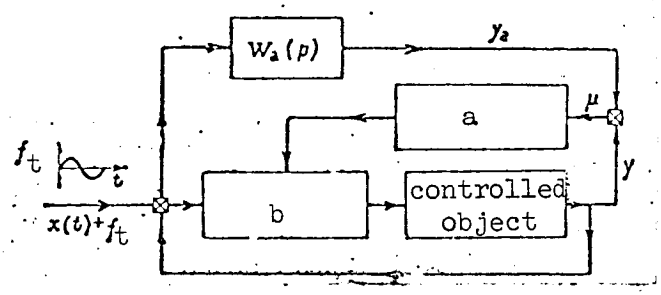

Figure 10.16. Functional diagram of optimalizing system (a); with compensating networks (b).

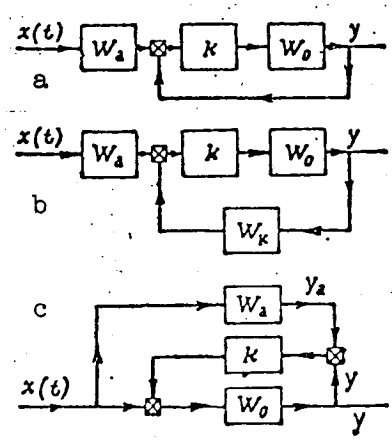

Figure 10.17. Functional diagrams of systems which are invariant with respect to properties of controlled object.

The self-adaptive system of the second type is free from this defect. This system uses some special features of a system with feedback containing an amplifier with a very high amplification factor (infinity). This amplifier may be a true physical unit or it may be produced by local positive feedback, which occurs when the invariance principle is realized in automatic control systems. Figure 10.17 shows three diagrams with feedback containing an amplifier with high gain. These three systems have the following transfer functions:

$$\Phi(p) = \frac{W_0 W_a k}{1 + W_0 k} = \frac{W_0 W_a}{\left.\frac{1}{k} + W_0\right|_{k\to\infty}} = W_a \quad \text{(fig. 10.17a)},$$

$$\Phi(p) = \frac{W_a W_0 k}{1 + W_k W_0 k} = \frac{W_a W_0}{\left.\frac{1}{k} + W_k W_0\right|_{k\to\infty}} = W_a \quad \text{(fig. 10.17b)},$$

$$\Phi(p) = \frac{W_0 + W_a W_0 k}{1 + k W_0} = \frac{\frac{W_0}{k} + W_a W_0}{\left.\frac{1}{k} + W_0\right|_{k\to\infty}} = W_a \quad \text{(fig. 10.17c)}.$$

As we can see from these expressions, in all limiting cases the dynamic properties of the system coincide with the dynamic properties of the model and do not depend on the properties of the controlled object with transfer function W_0. In other words, the properties of the system as a whole are invariant with respect to the varying properties of the controlled object. Difficulties may arrive in systems a and c, associated with the stability of the /337

system at high values of k. Therefore, the elements which form W_0 must provide for stability at high values of k. In system b, stability may be achieved by the proper selection of W_k.

As we know, infinite gain may be achieved in relay automatic control systems under ideal conditions.[1] The ideal state is obtained with relay elements which have characteristics shown in figures 10.18a and c. In the ideal state, the element with characteristic a is switched, while the relay element with characteristic c is turned on and off with an infinitely high frequency. Actually, switching rates of infinite frequency cannot be realized because a relay has some form of delay (electric, mechanical or electromechanical). For a true relay, there is a true sliding state, and the switching of the relay takes place with finite frequency. When perturbations are absent, this state will coincide with the self-sustained oscillations near the equilibrium position of the relay system. The smaller the relay delay, the higher is the frequency and the lower the amplitude of self-sustained oscillations and the higher is the amplification factor k of the relay for slowly varying signals. When the relay characteristics are those shown in figures 10.18b and d, only real sliding states may occur. The relay delay is taken into account by introducing, in series with the relay element, a transient (transport) delay with the transfer function $e^{-p\tau}$, where τ is the operate time of the relay. In this case we should note the special features associated with the description of the relay by the transfer function $e^{-p\tau}$. All periodic solutions of the relay system with frequencies greater than π/τ are dropped, because they have no physical meaning. The relay cannot be switched with a frequency greater than π/τ.

Although the ideal sliding state as well as an infinite amplification factor are not possible physically, these concepts may, nevertheless, be used when synthesizing self-adaptive systems of the second type. Systems which realize a large amplification factor by means of a relay will be called nonlinear or relay self-adaptive systems.

Now it is necessary to clarify the conditions under which a sliding state may be realized in a relay system. In other words, it is necessary to determine the conditions in a closed loop relay system when the transfer function input-output (fig. 10.19c) will be close to unity. The conditions for the sliding state are close to the conditions for the stability of equilibrium in a relay system. In its equilibrium state a relay with ideal characteristics of the form shown in figure 10.19a oscillates at an infinite frequency and has an amplification factor equal to infinity. Therefore, the stability conditions of a relay system may be obtained from the stability conditions of a system with an infinite amplification factor.

---

[1] A. A. Krasovskiy and G. S. Pospelov, The Principles of Automation and Engineering Cybernetics, Gosenergoizdat, 1962. Ya. Z. Tsypkin, The Theory of Relay Automatic Control System, Gostekhizdat, 1955.

Before introducing the stability conditions for relay systems we introduce the concept of a limit system. A limit system is formed from a relay system when the relay element and the amplifier are replaced by an infinite amplification factor.

As an example let us find the transfer functions of a limit system for the output y using the input signal x(t) and a perturbation F(t) of a relay system, whose structural diagram is shown in figure 10.19a (figures 10.19b and d show the transformed functional diagrams).

For the input x(t) we have /338

$$\Phi_x(p) = \frac{kW_1}{1 + k(W_1 + W_2)}\Bigg|_{k\to\infty} = \frac{W_1}{W_1 + W_2}.$$

For the perturbation F(t)

$$\Phi_F(p) = \frac{W_1}{1 + W_1 \dfrac{k}{1 + kW_2}} = \frac{(1 + kW_2)\,W_1}{1 + k(W_1 + W_2)}\Bigg|_{k\to\infty} = \frac{W_1 W_2}{W_1 + W_2}.$$

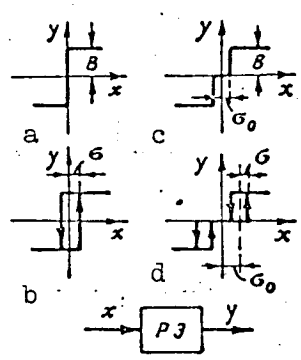

Figure 10.18. Characteristics of relay element; P3 = relay element.

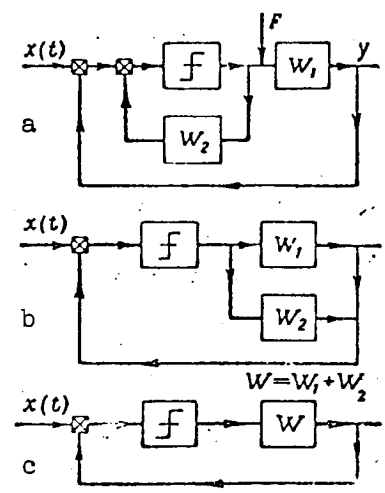

Figure 10.19. Functional diagrams with relay element.

Now let us determine the characteristic equation of the limit system. This equation is obtained if we set the denominator of the transfer function equal to zero

$$1 + kW(p) = 0, \tag{10.117}$$

where

$$W(p) = W_1(p) + W_2(p) = \frac{Q(p)}{P(p)} = \frac{b_0 + b_1 p + \ldots + b_m p^m}{a_0 + a_1 p + \ldots + a_n p^n} \tag{10.118}$$

is the transfer function for the linear part of the system.

From (10.117) and (10.118) we find two forms of the characteristic equation /339

$$P(p) + kQ(p) = 0, \tag{10.119}$$

$$\frac{1}{k} P(p) + Q(p) = 0. \tag{10.120}$$

When $k \to \infty$, we obtain the characteristic equation of the limit system

$$Q(p) = 0. \tag{10.121}$$

From expression (10.121) it follows that the limit system is stable, if all the zeros of the transfer function for the linear part of the system W(p) lie to the left of the imaginary axis of the complex plane. However, the stability of the limit system is only one of the necessary conditions for the stability of the system with high gain and for the stability of the relay system.

The degree of the characteristic equation (10.119) is equal to the degree n of the polynomial P(p). At the same time, the degree of the characteristic equation (10.121) of the limit system is equal to $m < n$. Thus, when $k \to \infty$, n-m roots of (10.119) become infinite. It is important to establish how these n-m roots will approach infinity. If they approach infinity through the left hemisphere, then, when the limit system is stable, the real system will be stable for any large but finite k. If it approaches infinity through the right hemisphere of the complex plane, the system will be unstable for high values of k, even though the limit system is stable. A series of simple criteria makes it possible to determine this condition. Thus, if the degree P(p) is not higher than two, the system will be stable for any value of k, no matter how large. Therefore, relay system may always be considered stable if P(p) has a degree not greater than two.

By using an analogy with the amplitude-phase characteristics $W(j\omega)$ of the second degree system, we obtain recommendations for the form of the amplitude-phase characteristics of the stable relay system of any degree.

The relay system is stable if the amplitude-phase characteristics of the linear part $W(j\omega)$ occur in the lower semiplane and if its form is similar to the hodograph $W(j\omega)$ of a system not greater than the second degree. This criterion is equivalent to the following[1]: all of the zeros of W(p) must lie in the left semiplane; the difference in $n - m \leq 2$; when $n - m$ 1 $d_0 > 0$, while for $n - m = 2$ $d_0 > 0$ and $d_1 < 0$; here d_0 and d_1 are the first two coefficients in the expansion for W(p) in degrees p^{-1}. This expansion of W(p) in a series has the form

$$W(p) = \frac{b_0 + b_1 p + \ldots + b_m p^m}{a_0 + a_1 p + \ldots + a_n p^n} = \frac{1}{p^{n-m}} [d_0 + d_1 p^{-1} + d_2 p^{-2} + \ldots]. \tag{10.122}$$

[1] Ya. Z. Tsypkin. The Theory of Relay Automatic Control Systems, Gostekhizdat, 1955.

where

$$d_0 = \frac{b_m}{a_n}; \tag{10.123}$$

$$d_1 = \frac{1}{a_n^2}[b_{m-1}a_n - a_{n-1}b_m]. \tag{10.124}$$

Since

$$d_0 = \dot{H}(0), \quad \text{and} \quad d_1 = \ddot{H}(0) \quad \text{when} \quad n - m = 1 \quad \text{and} \quad H(0) = 0;$$

$$\text{and } d_0 = \ddot{H}(0), \quad \text{and} \quad d_1 = \dddot{H}(0) \quad \text{when} \quad n - m = 2 \quad \text{and} \quad H(0) = \dot{H}(0) = 0,$$

where H(t) is the transfer function of the linear part, a third formulation of the stability of the relay system occurs: the relay system must be stable and the following conditions must be satisfied

$$\dot{H}(0) > 0 \quad \text{when} \quad H(0) = 0;$$
$$\ddot{H}(0) > 0, \quad \dddot{H}(0) < 0 \quad \text{when} \quad H(0) = \dot{H}(0) = 0.$$

The conditions for the existence of a continuous sliding state are more rigid than the conditions for the stability of a relay system. The sliding state takes place when we have a stable limit system and when n - m = 1 for $d_0 > 0$ or $\dot{H}(0) > 0$ for $H(0) = 0$. /340

After these remarks we can proceed with the design of a self-adaptive automatic pilot. Figure 10.20 shows the relay scheme for controlling the pitch angle. The relay controls a servomotor with isodromic feedback, whose transfer function is

$$W_g(p) = \frac{T_g p + 1}{T_{g1} p + 1} \frac{k_g}{p} \approx \frac{T_g p + 1}{p} k_g. \tag{10.125}$$

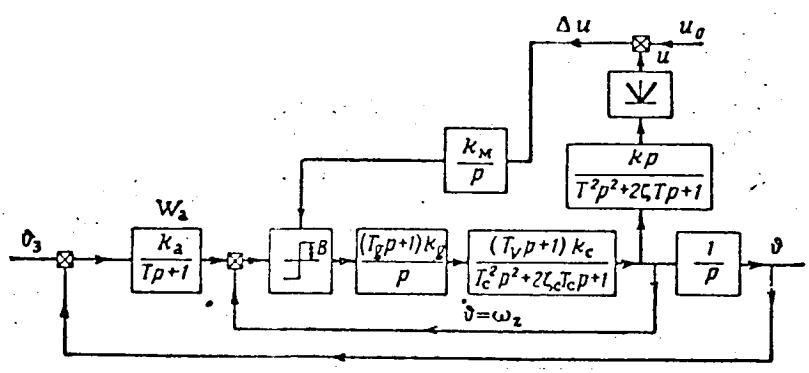

Figure 10.20. Functional diagram of self-adaptive automatic pilot.

The time constant T_{g1} can be made sufficiently small and can be neglected. The transfer function for the linear part of the relay system has the form

$$W(p) = \frac{(T_g p + 1)(T_\gamma p + 1) k_c k_g}{(T_c^2 p^2 + 2\zeta_c T_c p + 1) p}. \tag{10.126}$$

As we can see from expression (10.126), the stability conditions for the limit system are satisfied. The condition n - m = 3 - 2 = 1 is also satisfied. Thus, in the system represented in figure 10.20, we have a sliding state, and amplification in the circuit for the angular velocity ω_z will be equal to unity. These conditions are also satisfied for flight outside the atmosphere when the transfer function for the angular velocity is equal to k_c/p. When the amplification of the angular velocity circuit is equal to unity, the transfer function of the closed loop system for the pitch angle assumes the form

$$\Phi(p) = \frac{k_a}{T_a p^2 + p + k_a}. \tag{10.127}$$

For the selected reference transfer function, the transfer properties of the system are equivalent to the transfer properties of the oscillating element. The coefficients k_a and T_a are selected in such a way that the natural frequency $\sqrt{k_a/T_a}$ and the damping coefficient $\zeta = \frac{1}{2\sqrt{k_a T_a}}$ have the desired values. /341 Since k_a and T_a refer to the properties of the model, the dynamic properties of the system for controlling the pitch angle are fixed and independent of the dynamic properties of the missile. We should bear in mind that the conclusion is valid when the amplification factor and the switching frequency of the relay element are equal to infinity. Actually, the delay produced by the relay, the unaccounted nonlinearities and dynamic elements with small parameter values, e.g., T_{g1} in equation (10.125), lead to high frequency self-sustained oscillations. The amplification factor of the relay will be less than infinity, and certain effects of the dynamic properties of the controlled object may affect the dynamic properties of the entire system. This effect will be manifested by the variation in the frequency and amplitude of oscillations due to the change in the properties of the controlled object. The frequency of self-sustained oscillations must be sufficiently large and must exceed substantially the resonance frequency of the controlled object $1/T_c = \omega_0$. At high frequency, the amplitude of oscillations of the angular velocity must be small and must lie within the limits permitted for the controlled object.

A sufficiently high frequency of oscillations is achieved by means of a compensating network in the angular velocity loop of the missile. In this case it turns out that the frequency of self-sustained oscillations is practically independent of the properties of the missile, i.e., of coefficients T_V, k_c T_c and ζ_c. The variation in the properties of the missile or in the flight conditions changes only the amplitude of oscillations of the angular velocity. In order that the amplitude of self-sustained oscillations be stable for all flight conditions, a special amplitude stabilization loop is formed (fig. 10.20). The output signal of the angular velocity is applied to a bandpass filter with a transfer function.

$$\frac{kp}{T^2p^2 + 2\zeta Tp + 1},$$

where $\omega = 1/T$ is the frequency of self-sustained oscillations of the missile, which remains practically constant for all flight conditions. After passing through the bandpass filter, the signal is detected and compared with the master signal u_0. The difference $\Delta u = u_0 - u$ causes the operation of a servomotor with transfer function k_M/p, which changes the parameter B of the relay system. By changing the magnitude of the master signal, u_0, we may assign the necessary value to the amplitude of self-sustained oscillations. Variable gain amplifiers are also used in place of the relay element. The amplification factor of the amplifier is changed by means of a servomotor, as shown in figure 10.20.

The application of an amplifier with a large and variable amplification factor instead of a relay eliminates self-sustained oscillations completely, and we can design a system which, under all conditions, will maintain a fixed degree of stability in the angular velocity loop. A system with a given degree of stability does not require the adjustment of the automatic pilot for every type of missile to eliminate self-sustained oscillations. Obviously, the transfer function for the angular velocity loop will not be equal to unity in this case. However, the bandpass of this circuit will remain large and the necessary invariance of the dynamic pitch angle loops with respect to flight conditions will be retained.

CHAPTER 11. CONTROL OF THE MOTION OF THE CENTER OF GRAVITY OF A MISSILE WITH RESPECT TO A GIVEN TRAJECTORY /342

Section 11.1. General Information

In some cases the guidance of a missile to its target is limited to the assignment of a fixed trajectory passing through the target. When a trajectory is assigned, it is necessary to measure the lateral displacement of the center of gravity of a missile from this trajectory. As we have mentioned in Chapters 3-5, the trajectory may be assigned by the equisignal zone of a radio beam and by various methods of self-contained radio navigation. Regardless of the technical methods used to assign the trajectory and, consequently, regardless of the methods used to measure the deviation of the missile from this trajectory, a specific problem in dynamics occurs--the problem of automatically stabilizing the center of gravity of the missile along the trajectory. It is necessary to establish which signals must be introduced into the automatic pilot, how these signals must be transformed and how the transfer numbers of the automatic pilot must be selected, so that the missile is returned to its trajectory as quickly as possible.

The present chapter will consider the dynamic properties of the automatic control system for maintaining the center of gravity of a missile on the assigned trajectory. As in the preceding chapters, the lateral and longitudinal motions of the missile are considered separately.

Section 11.2 Control of the Center of Gravity of a Missile with Cruciform Wings during Lateral Motion

When the dynamics of the missile are complex, the selection of the control system parameters is carried out in several stages. The complex multiloop functional diagram of the system is divided into several simpler loops. This division is not always possible. It can be made only after a very careful study of the dynamic properties of the missile. It has been pointed out many times in Chapter 8 that the motion of the missile with respect to its center of gravity takes place much more rapidly (by a factor of 5-10) than the motion /343 of the center of gravity. This situation makes it possible to select separately the parameters of the automatic pilot for controlling the motion of the center of gravity of the missile and for controlling motion with respect to the center of gravity. The second problem is considered in sections 10.5-10.8.

As a first example we consider a missile with cruciform wings whose angle of tilt is stabilized. This problem is clarified in figure 11.1. Let us assume that MN is the assigned rectilinear trajectory along which the missile moves. In this case, the assigned value of the coordinate of the missile's center of gravity along the oz_g axis is $z_3 = z_0$.

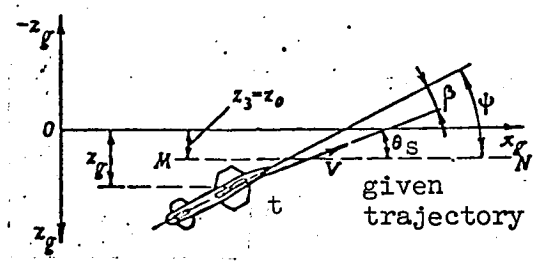

Figure 11.1. Diagram of angular and linear coordinates, characterizing position of missile with respect to rectilinear trajectory during lateral motion.

Chapter 14 considers the case when the assigned trajectory is displaced uniformly and parallel to itself. This means that $z_3 = k_1 t$ where k_1 = const. Other forms of z_3 as functions of time may be used as approximations for controlling the missile with respect to a curvilinear trajectory, because in the region where the linear equations are valid, the acceleration of the missile may be assumed to be equal to d^2z_g/dt^2. The process of guiding the missile by means of a radio beam may be considered as the stabilization of a missile with respect to assigned curvilinear trajectories. The method of generating the functions $z_3(t)$ for this case will be presented in Chapter 16. In any case, the input functions of the form $z_3 = z_0$, $z_3 = k_1 t$ and $z_3 = k_2 t^2$ may be considered as the first terms of a series used to expand a more complex function $z_3(t)$. The position of the missile during lateral motion is characterized by the linear coordinate of the center of gravity z_g and by angular coordinates ψ and β. We assume that the sensor of the control system measures the error $z = z_3 - z_g$ and the angular coordinate ψ.

In a simplified investigation of the dynamics of the control process we assume that the missile is instantaneously balanced. Under this assumption /344
the equation of moments, the second equation in system (8.44), is transformed into an algebraic equation which associates the slip angle with the angular deflection of the control surface. Thus the equations for the controlled object have the form [1]

[1] In the assumed system of coordinates (fig. 11.1), the positive angle θ_s leads to a negative value in the lateral velocity dz_g/dt. However, since the sign of the output coordinate z_g is of no significance when considering only plane motion, the minus sign in the left side of the last equation of system (11.1) is dropped.

$$\left.\begin{aligned} &\frac{d\theta_s}{dt} - k_\beta\beta = 0; \\ &n_\beta\beta = n_{s_{cr}}\delta_{cr}, \\ &\frac{dz_g}{dt} = V_e\theta_s, \end{aligned}\right\} \tag{11.1}$$

where

$$\theta_s = \psi - \beta.$$

To form the control loop for lateral motion in system (11.1), it is necessary to add the equations for the control system and for the automatic pilot, which we shall initially take in the simplest form

$$\delta_{cr} = i_z(z_3 - z_g), \tag{11.2}$$

where i_z is the transfer number of the deviation in rad/m or deg/m.

Figure 11.2 represents the functional diagram of a system defined by equations (11.1) and (11.2).

The functional diagram shows that the single loop network of this system contains two integrating elements. Such a system is unstable; therefore, the simplest control law (11.2) cannot be used. To obtain a stable system for controlling the center of gravity, the control law (11.2) must be augmented with compensating signals. Such a signal may be the signal proportional to the derivative of the deviation $z = z_3 - z_g$, or the signal produced by angle /345 θ_s, which is proportional to the derivative of the input quantity z_g when there is no lateral wind and when the missile velocity is constant. In place of angle θ_s we may take angle ψ between the direction of the trajectory and the longitudinal axis of the missile. The control laws, which correspond to these two cases of compensating signals, have the form

$$\delta_{cr} = i_z(z_3 - z_g) + i_{\dot z}\left(\frac{dz_3}{dt} - \frac{dz_g}{dt}\right); \tag{11.3}$$

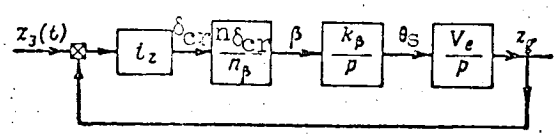

Figure 11.2 Functional diagram for controlling center of gravity, defined by equations (11.1) and (11.2).

$$\delta_{cr} = i_z(z_3 - z_g) - i_\psi \psi, \tag{11.4}$$

where i_z is the transfer number of the derivative of the deviation in radian·sec/m or degree·sec/m, and i_ψ is the transfer number for the yaw angle.

The functional diagrams for the system operating with control laws (11.3) and (11.4) are presented in figure 11.3b and a, respectively. In the first case stability is achieved by a signal which is a derivative of the deviation, while in the second case it is achieved by using fixed feedback in one of the integrating elements.

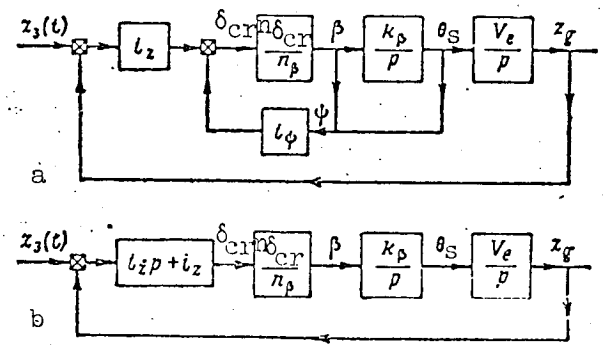

Figure 11.3. Functional diagram of control system for center of gravity using control laws (11.3) and (11.4).

By combining the equations of the missile (11.1) and of the automatic pilot (11.3) and eliminating all variables, except z_g, we obtain the general equation for the entire system

$$\frac{d^2 z_g}{dt^2} + a_1 \frac{dz_g}{dt} + a_2 z_g = a_1 \frac{dz_3}{dt} + a_2 z_3, \tag{11.5}$$

where /346

$$a_1 = \frac{i_z k_\beta n_{\delta_{cr}} V_e}{n_\beta};$$

$$a_2 = \frac{i_z k_\beta n_{\delta_{cr}} V_e}{n_\beta}.$$

In the same way, the system with control law (11.4) is described by equation

$$a_0 \frac{d^2 z_g}{dt^2} + a_1 \frac{dz_g}{dt} + a_2 z_g = a_2 z_3 + b_1 \frac{dz_3}{dt}, \tag{11.6}$$

where

$$a_0 = 1 + \frac{n_{\delta cr}}{n_\beta} i_\psi;$$

$$a_1 = \frac{n_{\delta cr}}{n_\beta} k_\beta i_\psi + \frac{n_{\delta cr}}{n_\beta} i_z V_e;$$

$$a_2 = \frac{n_{\delta cr}}{n_\beta} k_\beta i_z V_e;$$

$$b_1 = \frac{n_{\delta cr}}{n_\beta} i_z V_e.$$

As we can see from the structure of equations (11.5) and (11.6), and from their coefficients, the extent of fixed stabilization of the missile along the trajectory, characterized by the value of the natural frequency of oscillation $\Omega_0 = \sqrt{a_2/a_0}$, is determined by the transfer number i_z. However, the damping coefficient for the oscillations of the missile along the trajectory $\zeta = a_1/2a_0\Omega$ is determined in one case by the transfer number $i_z^{\cdot}$, while in the other case it is determined by the transfer number i_ψ.

We can use another simplified approach to consider the problem of controlling the center of gravity of a missile. Let us assume that the automatic pilot, which controls the yaw angle, is in the missile, and that its parameters are selected in accordance with the method presented in section 10.5. If we neglect the time that it takes a missile to turn by a given angle of yaw, compared with the time of controlling the center of gravity, and if we let $\beta \approx 0$ then, instead of the equation of moments and the equation of the automatic pilot, we obtain a simple relationship

$$\psi = \psi_3. \tag{11.7}$$

The simplest law for the variation in the yaw angle when controlling lateral deflection will have the form

$$\psi_3 = i_z (z_3 - z_g). \tag{11.8}$$

We combine the third equation of system (11.1) with expressions (11.7) and (11.8), taking into account the equality $\theta_s = \psi$, and eliminate all variables except z_g. This gives us

$$\frac{dz_g}{dt} + i_z V_e z_g = i_z V_e z_3. \tag{11.9}$$

The structure of equation (11.9) shows that the simplified system for controlling the center of gravity of a missile is described in this case by the equation of an inertial element. However, with this simplified concept some very important features of the control process are lost. The control dynamics are much better described by equations (11.5) and (11.6) and the corresponding functional diagrams shown in figure 11.3.

Let us briefly consider the reaction of the system with these functional diagrams to the control signal $z_3(t)$ and the perturbing signal. The system whose functional diagram is shown in figure 11.3b contains two integrating elements in the open circuit and is astatic two times with respect to the input signal $z_3(t)$. This means that when the input function is linear

$$z_3 = k_1 t \tag{11.10}$$

the steady state error z_{ss} will be equal to zero. The system whose functional diagram is shown in figure 11.3a will not possess these properties and will have a steady state error when $z_3 = k_1 t$.

The special solution of the nonhomogeneous equation (11.6), which describes stationary tracking, for this case has the form

$$z_g = -\frac{i_\psi}{i_z V_e} k_1 + k_1 t. \tag{11.11}$$

Thus, when the value of z_3 varies according to the law (11.10), we have an error in the lateral deflection

$$z_{ss} = z_3 - z_g = \frac{i_\psi}{i_z V_e} k_1. \tag{11.12}$$

The error in the lateral deflection, when z_3 is a quadratic function of time ($z_3 = k_2 t^2$), has the following value for the system described by equation (11.5):

$$z_{ss} = \frac{2k_2}{a_2}. \tag{11.13}$$

The system described by equation (11.6) when $z_3 = k_2 t^2$ will have a linearly increasing error in the stationary state. Therefore, for missiles designed to move along moving trajectories we should recommend a control law of type (11.3). /348

Now let us consider the system for controlling the lateral deviation of the center of gravity of a missile with cruciform wings without making any simplifications, i.e., by taking into account transient processes in the angular

motion of the missile. For this purpose we combine the equation of the missile (8.44) and the equation of the automatic pilot and write it in a sufficiently general form. As a result we obtain a system of equations

$$\left.\begin{aligned}
&\frac{d\beta}{dt}+k_{\beta}\beta-\frac{d\psi}{dt}=0,\\
&\frac{d^2\psi}{dt^2}+n_{\dot\psi}\frac{d\psi}{dt}+n_{\dot\beta}\frac{d\beta}{dt}+n_{\beta}\beta=n_{\delta_{cr}}\delta_{cr}+\frac{\Delta M_p}{J_y},\\
&\frac{dz_g}{dt}=V_e(\psi-\beta),\\
&\delta_{cr}=i_{\dot z}\left(\frac{dz_3}{dt}-\frac{dz_g}{dt}\right)+i_z(z_3-z_g)+\dot q_z\int_0^t(z_3-z_z)\,dt-\\
&-i_{\dot\psi}\frac{d\psi}{dt}-i_{\psi}\psi.
\end{aligned}\right\}\qquad(11.14)$$

The right side of the moment equation contains the perturbing moment ΔM_p. The control law for the automatic pilot in addition to the basic position signal $(z_3 - z_g)$, also has compensating signals, which are proportional to the product of this signal and the signal from the yaw angle and its derivative. Finally, the control law contains a signal proportional to the integral of the mismatch over the lateral deflection. The purpose of this signal is to make the system astatic when subjected to external reactions. As we have shown, the system whose functional diagram is shown in figure 11.3a (with the compensating signal for ψ) is less accurate compared with the system whose functional diagram is shown in figure 11.3b (with a compensating signal $\frac{dz_3}{dt} - \frac{dz_g}{dt}$). The integral term in the control law is introduced precisely to give the first system the properties (in the form of reaction to $z_3(t)$ in the stationary state) of the second system, in spite of the compensating signal for the angle ψ.

Figure 11.4 shows the schematic diagram corresponding to control system (11.14). The value of coefficients a_1, a_2, b_1, b_2 is determined by equations (10.48), while the transfer function for applying the external moment ΔM_p to the control surface is determined by equation (10.55).

If we eliminate from equation (11.14) all of the variables except z_g, we find the following general system of equations for the lateral displacement of the missile's center of gravity /349

$$\frac{d^5 z_g}{dt^5} + (a_1 + i_\psi b_1)\frac{d^4 z_g}{dt^4} + (a_2 + i_\psi b_2 + i_\psi b_1)\frac{d^3 z_g}{dt^3} +$$

$$+ (i_\psi b_2 + i_z b_2 V_e)\frac{d^2 z_g}{dt^2} + i_z b_2 V_e \frac{dz_g}{dt} + q_z b_2 V_e z_g = \tag{11.15}$$

$$= i_z b_2 V_e \frac{d^2 z_3}{dt^2} + i_z b_2 V_e \frac{dz_3}{dt} + q_z b_2 V_e z_3 - \frac{k_3 V_e}{J_y}\frac{d\Delta M_p}{dt}.$$

The structure of equation (11.15) permits us to draw the following conclusions about the properties of the system. First of all, this system is astatic with respect to the constant perturbing moment ΔM_p, since the derivative of this moment will be equal to zero. The astaticism of the system also exists with respect to the external constant signal z_3 and to the signal which depends linearly on time. Only when the external signal is proportional to the square of the time ($z_3 = k_2 t^2$) will an error appear in the stationary state. This error is given by equation

$$z_{ss} = \frac{2k_2 i_\psi}{q_z V_e}. \tag{11.16}$$

If we examine the coefficients in the left side of equation (11.15), we see that each of them contains at least one new transfer number of the automatic pilot, which makes it possible to determine these coefficients independently. Thus, the method of the standard coefficients makes it possible to

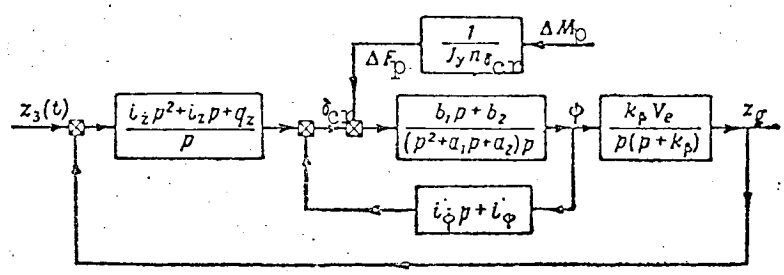

Figure 11.4. Functional diagram corresponding to control system (11.14).

determine the required values of the transfer numbers of the automatic pilot and to obtain the necessary dynamic properties of the system. The only limitation placed on the duration of the transient process will be the linear range of the individual elements of the system (the deflection angle of the control surface, allowable values of the slip angle, load factor, etc.). /350

Let us consider an example for selecting the parameters of the system for controlling the center of gravity.

Example 11.1. As the controlled object we take missile no. 2, whose parameters are presented in table 10.1. Let us assume that the velocity of the missile is $V_e = 300$ m/sec. It is necessary to select the parameters of the control system in such a way that the control time (t_c) for the motion of the center of gravity is 15 sec.[1] The transfer function for the system controlling the center of gravity is obtained from (11.15) and has the form

$$\Phi_{z_g/z_3}(p) = \frac{i_z b_2 V_e p^2 + i_z b_2 V_e p + q_z b_2 V_e}{p^5 + (a_1 + i_\psi b_1)p^4 + (a_2 + i_\psi b_2 + i_\psi b_1)p^3 + (i_\psi b_2 + i_z b_2 V_e)p^2 + \rightarrow} \tag{11.17}$$

$$\rightarrow \frac{}{+ i_z b_2 V_e p + q_z b_2 V_e}.$$

The coefficients of the numerator and denominator in front of the square of operator p differ from each other by a small quantity $i_\psi b_2 \ll i_z b_2 V_e$. Therefore we refer expression (11.17) to the typical function (2.12) and use table 2.4 to select the coefficients. From this table we obtain the characteristic equation for the differential equation of the fifth order

$$p^5 + 18\Omega_0 p^4 + 69\Omega_0^2 p^3 + 69\Omega_0^3 p^2 + 18\Omega_0^4 p + \Omega_0^5 = 0. \tag{11.18}$$

We equate the corresponding coefficients in the denominator of transfer function (11.17) to the coefficients of the characteristic equation (11.18), and obtain a system of algebraic equations

$$\left.\begin{aligned} a_1 + i_\psi b_1 &= 18\Omega_0; \\ a_2 + i_\psi b_2 + i_\psi b_1 &= 69\Omega_0^2; \\ i_\psi b_2 + i_z b_2 V_e &= 69\Omega_0^3; \\ i_z b_2 V_e &= 18\Omega_0^4; \\ q_z b_2 V_e &= \Omega_0^5. \end{aligned}\right\} \tag{11.19}$$

---

[1] It is easy to see that it is impossible to achieve a control time much less than 15 sec for missile no. 2, unless the transfer numbers are radically increased. This is associated with a decrease in the linear range of the system. There is no difficulty in obtaining a control time of more than 15 sec and, in this case, the linear range of the system increases.

The value of the natural frequency of the system Ω_0 is determined from the ratio

$$\Omega_0 = \frac{\tau_p}{t_p} = \frac{9.2}{15} = 0.613 \ 1/\text{sec}$$

where $\tau_p = 9.2$ is taken from the curve of the standard transient process for a system of fifth order having a structure analogous to that in figure 2.8.

Substituting this value of Ω_0 into equations (11.19) and solving them /351 alternately, starting with the first, we obtain the following values for the transfer numbers of the automatic pilot: $i_{\dot\psi} = 1.86$ sec; $i_\psi = 1.58$; $i_{\dot z} = 0.023$ rad·sec/m = 1.33 deg·sec/m; $i_z = 4.53 \cdot 10^{-3}$ rad/m = 0.26 deg/m; $q_z = 1.54 \cdot 10^{-4}$ rad/m·sec = $8.83 \cdot 10^{-3}$ deg/m·sec.

Let us construct the logarithmic amplitude-frequency characteristics of this system. From the functional diagram shown in figure 11.4 we find the transfer function for the open loop system

$$W_{z_g/z_3}(p) = \frac{b_2 V_e (i_{\dot z} p^2 + i_z p + q_z)}{p^2 [p^3 + (a_1 + i_{\dot\psi} b_1) p^2 + (a_2 + i_{\dot\psi} b_2 + i_\psi b_1) p + i_\psi b_2]} . \qquad (11.20)$$

If we substitute into expression (11.20) the values of the missile parameters and the transfer numbers of the automatic pilot, we obtain

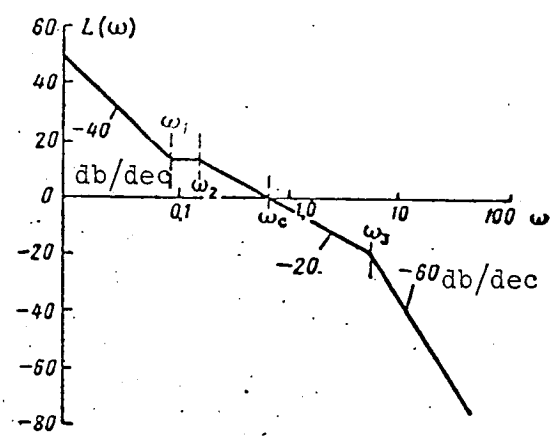

Figure 11.5. Logarithmic amplitude-frequency characteristics corresponding to transfer function (11.22).

$$W_{z_g/z_3}(p) = \frac{570\,(0.023p^2 + 4.53\cdot 10^{-3}p + 1.54\cdot 10^{-4})}{p^2\,(p^3 + 11.04p^2 + 26p + 3.34)}. \tag{11.21}$$

To construct the logarithmic amplitude-frequency characteristics it is necessary to reduce the transfer function (11.21) to the form

$$W_{z_g/z_3}(p) = \frac{k\left(T_1^2p^2 + 2\zeta_1T_1p + 1\right)}{p^2\left(T_3^2p^2 + 2\zeta_3T_3p + 1\right)(T_2p + 1)} =$$

$$= \frac{0.0265\,(12.3^2p^2 + 2\cdot 1.2\cdot 12.3p + 1)}{p^2\,(0.202^2p^2 + 2\cdot 1.1\cdot 0.202p + 1)\,(7.4p + 1)}. \tag{11.22}$$

Thus, to construct the logarithmic amplitude-frequency characteristics of the system, we have the amplification factor of the open loop system K = 0.0265 and the conjugate frequencies

$$\omega_1 = 1/T_1 = 1/12.3 = 0.079\ 1/\text{sec}; \qquad \omega_2 = 1/T_2 = 1/7.4 = 0.135\ 1/\text{sec};$$

$$\omega_3 = 1/T_3 = 1/0.202 = 4.9\ 1/\text{sec};$$

The logarithmic amplitude-frequency characteristics of the system are constructed in figure 11.5 from these data. As we see from these characteristics, high dynamic properties of the system are due to the large region of characteristics with a slope of 20 db/decade where $\omega_3/\omega_c \approx 10$. It is obvious that this high value of the ratio ω_3/ω_c can be obtained only by means of high frequency ω_3, which characterizes the rapid response of the yaw angle loop, i.e., provides for a rapid termination of the short period motions of the missile. /352

In some cases the signal proportional to the lateral displacement ($z_3 - z_g$) contains an appreciable level of high frequency noise. The missile, which acts like a smoothing filter, does not react to this noise, but will be subject to the derivative of this signal. Frequently, sufficiently high dynamic properties of the control system may be achieved without a signal which is the derivative of the lateral displacement. Figure 11.6 shows the functional diagram of a control system for the case when the automatic pilot operates in accordance with the law

$$\delta_{cr} = + i_z(z_3 - z_g) + q_z \int_0^t (z_3 - z_g)dt - i_{\dot\psi} \frac{d\psi}{dt} - i_\psi \psi. \qquad (11.23)$$

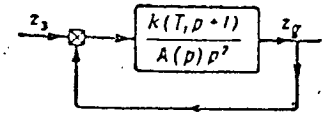

Figure 11.6. Functional diagram of system with control law (11.23).

The individual notations in figure 11.6 may be determined by means of the following equations

$$\left.\begin{aligned} k &= \frac{V_e q_z}{i_\psi} \, 1/\sec^2, \\ T_1 &= \frac{i_z}{q_z} \sec, \\ A(p) &= \frac{1}{i_\psi b_2}[p^3 + (a_1 + i_{\dot\psi} b_1)p^2 + (a_2 + i_{\dot\psi} b_2 + \\ &+ i_\psi b_1)p + i_\psi b_2]. \end{aligned}\right\} \qquad (11.24)$$

For the system shown in figure 11.6 it is not possible to select the parameters of the automatic pilot by the method of standard coefficients, as in the case of the system whose functional diagram is shown in figure 11.4. The coefficient in front of d^2z_g/dt^2 will not contain the transfer number $i_{\dot z}$, and therefore an independent selection of all transfer numbers becomes impossible. The method of standard coefficients may be used for the approximate solution, which gives the best values of transfer numbers by the method of sampling. /353

In this case, the simplest approach is to use the method of logarithmic amplitude-frequency characteristics in the following manner. The parameters of the yaw angle control loop ($i_{\dot\psi}$ and i_ψ) are determined beforehand, in accordance with recommendations presented in section 10.5. To clarify the method of selecting the remaining parameters k and T_1 and from them the transfer numbers i_z and q_z, we consider the logarithmic amplitude-frequency characteristics of a system shown in figure 11.7. To select the parameters k and T_1 it is necessary to include the corresponding position and length of the region with a slope of 20 db/dec. First of all, the conjugate frequency $\omega_1 = 1/T_1$ must satisfy

the relation $\omega_1 \leq 0.1\ \omega_3$. In addition, the conjugate frequency ω_2, which is equal to the smallest root of the polynomial A(p), must be 4-5 times greater than the cutoff frequency ω_c. To satisfy this condition for a sufficiently high cutoff frequency ω_c, which determines the response of the entire system, it is necessary to increase frequencies ω_2 and ω_3, i.e., to force the angular motions of the missile.

Let us also consider the transfer function and the logarithmic amplitude-frequency characteristics of the system without an integral element in the control law. Such a law is used in cases when a simpler control system is required, and when the small errors in the lateral displacement of the missile from the assigned trajectory do not play a substantial role.

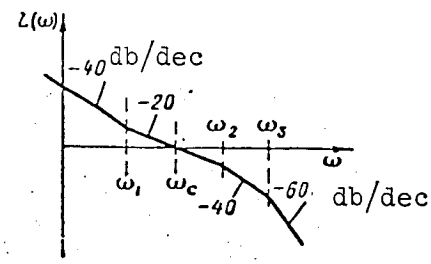

Figure 11.7. Logarithmic amplitude-frequency characteristics, corresponding to the functional diagram in figure 11.6.

The control law for the automatic pilot in this case has the form

$$\delta_{cr} = i_z(z_3 - z_g) - i_{\dot\psi}\frac{d\psi}{dt} - i_\psi\psi. \qquad (11.25)$$

The functional diagram for the control system which utilizes law (11.25) is shown in figure 11.8. The value of A(p) is determined by equation (11.24) and the quantity k is equal to /354

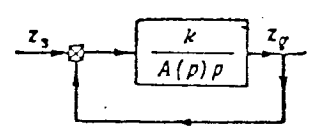

Figure 11.8. Functional diagram of system with control law (11.25).

$$k = \frac{V_c i_z}{i_\psi}. \tag{11.26}$$

Figure 11.9 shows the logarithmic amplitude-frequency characteristics corresponding to the functional diagram of figure 11.8. If the parameters of the loop which controls the yaw angle are selected beforehand, the form of the curve and the conjugate frequencies ω_2 and ω_3 remain fixed. If we vary the amplification factor, which in this system coincides with the cutoff frequency ω_c, the logarithmic amplitude-frequency characteristics will either rise or drop with respect to the axis of the abscissas.

The response of the system may be increased by increasing the cutoff frequency $\omega_c = k$. However, in this case the condition $\omega_2 \geq (4\text{-}5)\ \omega_c$ must be satisfied to obtain satisfactory transient processes in the system. As in the preceding cases, this condition may be satisfied by forcing the transient processes of the short period motion.

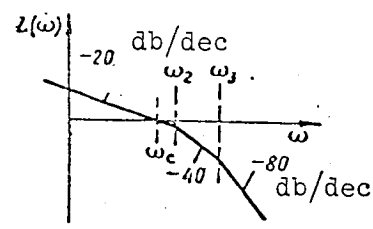

Figure 11.9. Logarithmic amplitude-frequency characteristics corresponding to functional diagram of figure 11.8.

Section 11.3. Control of the Center of Gravity of a Plane-Winged Missile during Lateral Motion

The general formulation of the problem remains the same as shown in figure 11.1. The difference in this problem is that the turning of the missile in the plane xoz_g must be carried out with tilt, because only this produces a substantial lateral force. This difference produces some special features in the method of selecting parameters for the system which controls the missile with plane wings, compared with the one considered in the preceding section. This method is clarified in the present section.

In analyzing the control system for the center of gravity of a plane-winged missile, we start with the greatest possible simplifications, which will make this problem illustrative without distorting the qualitative sides of the

process. These simplifications consist of the assumption that the system for controlling the direction rudder makes it possible to achieve the flight without slip ($\beta = d\beta/dt = 0$), and that the tilt transient processes can be neglected, /355 because the duration of these processes is at least one order of magnitude less than that of the processes for controlling the center of gravity. With these assumptions, from the general system of equations for lateral motion of a plane-winged missile (8.42) we obtain[1]

$$\left.\begin{aligned} &\frac{d\psi}{dt} - k_\gamma \gamma = 0; \\ &\frac{dz_g}{dt} = V_e \psi. \end{aligned}\right\} \tag{11.27}$$

With these simplifications, the second and third equations of (8.42) drop out. In addition, the term $a_e\, d\gamma/dt$ in the first equation is not taken into account, because in the majority of cases it is small compared with the other terms of this equation. The control law for the automatic pilot in this case degenerates into the ratio between the tilt signal and the signals which provide for the control of the center of gravity. Let us consider two possible control laws similar to (11.3) and (11.4)

$$-i_\gamma \gamma + i_{\dot z}\left(\frac{dz_3}{dt} - \frac{dz_g}{dt}\right) + i_z (z_3 - z_g) = 0 \tag{11.28}$$

and

$$-i_\gamma \gamma - i_\psi \psi + i_z (z_3 - z_g) = 0. \tag{11.29}$$

The systems with the control laws (11.28) and (11.29) coincide completely with those systems whose control laws are (11.3) and (11.4). They have the same reaction to the control force $z_3(t)$. Several insignificant features distinguish the system with law (11.4) from the system with law (11.29), because in the latter case $\beta = 0$ and $\psi = \theta_s$.

The general equation for the system controlling the center of gravity, when the control law is given by (11.28), has the form

---

[1] We drop the minus sign in front of the derivative of z_g for the same reason as in equation (11.1); in addition, instead of the tilt angle, it is more convenient to consider its negative value.

$$\frac{d^2z_g}{dt^2} + g\frac{i_z}{i_\gamma}\frac{dz_g}{dt} + g\frac{i_z}{i_\gamma}z_g = g\frac{i_z}{i_\gamma}\frac{dz_3}{dt} + g\frac{i_z}{i_\gamma}z_3. \qquad (11.30)$$

It follows from expression (11.30) that under these assumptions and with control law (11.28), the motion of the missile's center of gravity is described by a differential equation of the second order, such that the coefficients of this equation do not depend on the flight velocity and flight altitude. Consequently, the transient time of processes along the z_g coordinate depend on /356 these parameters. The path travelled during the transient process is directly proportional to the flight velocity, and the curves of the transient process, which are constructed along the axis of the abscissas to the scale $S = V_e t$, represent the flight trajectory of the missile.

With initial conditions $z_g = z_0$; $dz_g/dt = 0$, the missile is guided to the assigned trajectory by means of the double additional turn (fig. 11.10). Depending on the scale along the axis of the abscissas, the curve of figure 11.10 may be either the graph of the transient process $[z_g = f(t)]$ or the missile trajectory $[z_g = f(S)]$. The name of the maneuver shown in figure 11.10 shows that over the initial region of the trajectory the missile undergoes an additional turn in one direction with a definite tilt angle, and after the inflection point P the direction of the additional turn and the sign of the tilt angle assume an opposite value.

For the control law (11.29) the general equation for the system which controls the center of gravity of the missile is obtained in the following form

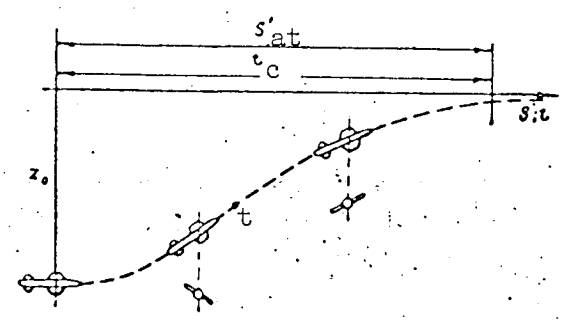

Figure 11.10. Schematic diagram of double turning of missile to achieve assigned trajectory; subscripts at = additional turning, c = control.

$$\frac{d^2z_g}{dt^2} + \frac{gi_\psi}{V_e i_\gamma}\frac{dz_g}{dt} + \frac{gi_z}{i_\gamma} z_g = \frac{gi_z}{i_\gamma} z_3. \tag{11.31}$$

In equation (11.31) the damping coefficient depends on the flight velocity and decreases as the flight velocity increases. This relationship is easily explained, if we note that the damping in the system is determined by angle ψ, contained in the control law (11.29). At the same time, from the second equation of (11.27) it follows that

$$\psi = -\frac{1}{V_e}\frac{dz_g}{dt}. \tag{11.32}$$

Thus, for a given velocity the variation in the deviation dz_g/dt angle ψ will become smaller when the flight velocity V_e increases. /357

The nature of the missile's trajectory in the case of the control system given by equation (11.31) is the same as in the case of the control system corresponding to equation (11.30). The graph in figure 11.10 remains valid for equation (11.31), except that in this case, when the flight velocity varies, the variation in the scale along the axis of the abscissas ($S = V_e t$) will be accompanied by the variation in the nature of the curve, because the damping coefficient will depend on the velocity.

Now let us proceed with the analysis of the system for controlling the movement of the center of gravity of a plane-winged missile with respect to a given trajectory by taking into account the true characteristics of the motion with respect to the x_1 axis, i.e., by taking into account the delay in the establishment of a given tilt angle. In this case, to describe the controlled object, it is necessary to take the following equations from system (8.42):[1]

$$\left.\begin{aligned} &\frac{d\psi}{dt} - a_e\frac{d\gamma}{dt} - k_\gamma\gamma = 0;\\ &\frac{d^2\gamma}{dt^2} + l_\gamma\frac{d\gamma}{dt} = l_{\delta ai}\delta_{ai} + \frac{\Delta M_p}{J_x};\\ &\frac{dz_g}{dt} = V_e\psi. \end{aligned}\right\} \tag{11.33}$$

[1] The control system (11.33) is obtained from (8.42) under the assumption that $\beta = d\beta/dt = 0$, i.e., that the slip angle is eliminated by the direction rudder; also the negative value of the tilt angle is considered and the minus sign before the derivative z_g is dropped.

The external perturbing moment with respect to the x_1 axis is introduced into the second equation of (11.33).

Let us consider the properties of the control system when we have different control laws for its automatic pilot. For the first law we select the following

$$\delta_{ai} = -i_{\dot\gamma}\frac{d\gamma}{dt} - i_\gamma\gamma + i_z\left(\frac{dz_3}{dt} - \frac{dz_g}{dt}\right) + i_z(z_3 - z_g). \qquad (11.34)$$

The signal which is proportional to the angular rate of change of tilt $d\gamma/dt$ is introduced into law (11.34) to improve damping with respect to the x_1 axis. The signal which is proportional to the tilt angle γ is the basic feedback signal in the tilt control loop, which is compared with the position signals and stabilizing signals, which in turn are proportional to the lateral deviation of the center of gravity $(z_3 - z_g)$ and its derivative $(dz_3/dt - dz_g/dt)$.

Figure 11.11 shows the functional diagram of the system for controlling the center of gravity whose control law is (11.34). Combining the equations of the missile (11.33) with the equations of the automatic pilot (11.34), we obtain a general differential equation for this system /358

$$\frac{d^4 z_g}{dt^4} + (l_{\dot\gamma} + i_{\dot\gamma}\, l_{\delta_{ai}})\frac{d^3 z_g}{dt^3} + (i_\gamma l_{\delta_{ai}} + i_z V_e l_{\delta_{ai}}\alpha_e) \times$$
$$\times \frac{d^2 z_g}{dt^2} + V_e(i_z\, l_{\delta_{ai}}\, k_\gamma + i_z l_{\delta_{ai}}\, \alpha_e)\frac{dz_g}{dt} + i_z l_{\delta_{ai}}\, k_\gamma V_e z_g =$$
$$= i_z\, l_{\delta_{ai}}\, V_e\alpha_e\frac{d^2 z_3}{dt^2} + V_e(i_z\, l_{\delta_{ai}} k_\gamma + i_z l_{\delta_{ai}}\, \alpha_e)\frac{dz_3}{dt} +$$
$$+ i_z l_{\delta_{ai}}\, k_\gamma V_e z_3 + \frac{\alpha_e V_e}{J_x}\frac{d\Delta M_p}{dt} + \frac{k_\gamma V_e}{J_x}\Delta M_p. \qquad (11.35)$$

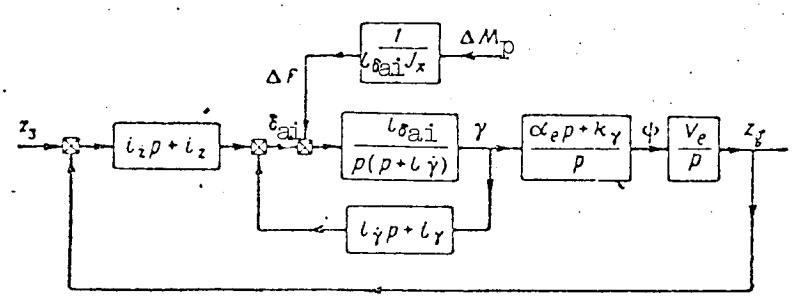

Figure 11.11. Functional diagram of system with control law (11.34).

The structure of equation (11.35) permits us to draw the following conclusions concerning the control system with law (11.34). This system is astatic with respect to the change in the assigned value of lateral deviation with constant velocity ($z_3 = kt$) and astatic with respect to the constant perturbing moment ΔM_p. The selection of the transfer numbers of the automatic pilot may be accomplished by the method of standard coefficients. It is obvious that, as in the case of the missile with cruciform wings, the increase in the response of the system described by equation (11.35) is limited, first of all by the limitation of the tilt angle. As the natural frequency of the system $\Omega = \sqrt{i_z k_i V_e l_{\delta ai}}$ increases, its response will increase. However, this will take place only in the range of $(z_3 - z_g)$ variation, for which the tilt angle is not limited by an assigned value. Obviously, this range will become narrower /359
when the natural frequency and the response of the system increase.

As an example, figure 11.12 shows the curves which characterize the variation in deviation $\Delta z = z_3 - z_g$ of the yaw angle and the tilt angle, when this system is used to control the center of gravity of a plane-winged missile.

If the generation of the signal derivative, proportional to the lateral deviation, is associated with technical difficulties caused by the high noise level in this signal, we may apply the following control law for the automatic pilot

$$\delta_{ai} = -i_1 \frac{d\gamma}{dt} - i_\gamma \gamma - i_\psi \psi + i_z (z_3 - z_g). \qquad (11.36)$$

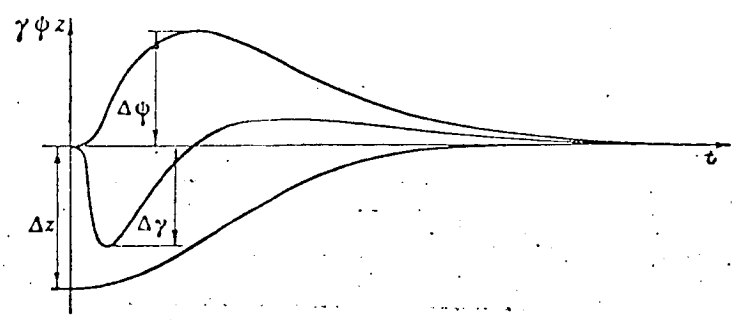

Figure 11.12. Graphs of transient process when center of gravity is controlled in lateral direction.

The functional diagram of a system with control law (11.63) is shown in figure 11.13.

Combining the missile equations (11.33) and the equations of the automatic pilot (11.36), we obtain a general equation for the system controlling the center of gravity

$$\frac{d^4 z_g}{dt^4} + (l_{\dot\gamma} + i_{\dot\gamma}\, l_{\delta_{ai}})\frac{d^3 z_g}{dt^3} + (i_\gamma l_\delta + i_\psi l_{\delta_{ai}}\, \alpha_e)\frac{d^2 z_g}{dt^2} + \tag{11.37}$$

$$+ (i_\psi l_{\delta_{ai}}\, k_\gamma + i_z l_{\delta_{ai}}\, \alpha_e V_e)\frac{dz_g}{dt} + i_z l_{\delta_{ai}}\, k_\gamma V_e z_g =$$

$$= i_z l_{\delta_{ai}}\, \alpha_e V_e \frac{dz_3}{dt} + i_z l_{\delta_{ai}}\, k_\gamma V_e z_3 + \frac{\alpha_e V_e}{J_x}\frac{d\Delta M_p}{dt} + \frac{k_\gamma V_e}{J_x}\Delta M_p .$$

Unlike equation (11.35) where the coefficients of the zero and first derivative increase proportionally to the flight velocity, in equation (11.37) the principal part of the coefficient in front of the first derivative ($i_\psi\, l_{\delta_{ai}} k_\gamma \gg i_z l_{\delta_{ai}} a_e V_e$) does not depend on the velocity, while the coefficient in front of the zero derivative is proportional to this velocity. Thus, as in the case of the simplified problem with control law (11.36), the damping of the system decreases as the flight velocity increases. In addition, the system described by equation (11.37) is static with respect to the external signal, which varies with a constant velocity ($z_3 = kt$). As we have pointed out, the system described by equation (11.35) is astatic with respect to this type of signal.

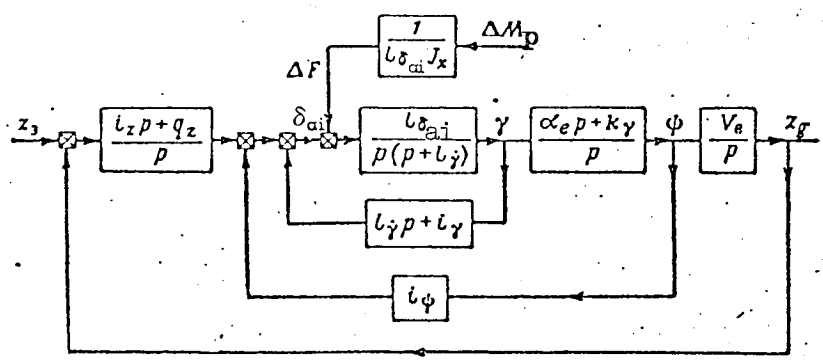

Figure 11.13. Functional diagram of system with control law (11.36).

In both systems, the constant external moment produces an error given by equation

$$Z_{ss} = \frac{\Delta M_p}{i_z l_{\delta_{ai}} J_x} . \tag{11.38}$$

To eliminate the error produced by the external moment, it is necessary to introduce the integral of the mismatch in lateral deviation into the control law

$$\delta_{ai} = -i_\gamma \frac{d\gamma}{dt} - i_\gamma \gamma - i_\psi \psi + l_z (z_3 - z_g) + q_z \int_0^t (z_3 - z_g)\, dt. \qquad (11.39)$$

The functional diagram of the system with control law (11.39) is shown in figure 11.14. Combining the missile equations (11.33) with the equations of the automatic pilot (11.39), we obtain the general equation of the system

$$\begin{gathered}
\frac{d^4 z_g}{dt^4} + (l_\gamma + i_\gamma l_{\delta_{ai}}) \frac{d^3 z_g}{dt^3} + (i_\gamma l_{\delta_{ai}} + i_\psi l_{\delta_{ai}} \alpha_e) \frac{d^2 z_g}{dt^2} + \\
+ (i_\psi l_{\delta_{ai}} k_\gamma + i_z l_{\delta_{ai}} \alpha_e V_e) \frac{d^2 z_g}{dt^2} + V_e (i_z l_{\delta_{ai}} k_\gamma + q_z l_{\delta_{ai}} \alpha_e) \frac{dz_g}{dt} + \\
+ q_z l_{\delta_{ai}} k_\gamma V_e z_g = i_z l_{\delta_{ai}} \alpha_e V_e \frac{d^2 z_3}{dt^2} + V_e (i_z l_{\delta_{ai}} k_\gamma + \\
+ q_z l_{\delta_{ai}} \alpha_e) \frac{dz_3}{dt} + q_z l_{\delta_{ai}} k_\gamma V_e z_3 + \frac{\alpha_e V_e}{J_x} \frac{d^2 \Delta M_p}{dt^2} + \\
+ \frac{k_\gamma V_e}{J_x} \frac{d\Delta M_p}{dt}.
\end{gathered} \qquad (11.40)$$

The structure of equation (11.40) shows that the introduction of the integral term into the control law has made the system for controlling the center of gravity astatic with respect to the constant external moment ΔM_p and with respect to the external signal, which is a linear function of time ($z_3 = kt$). /361

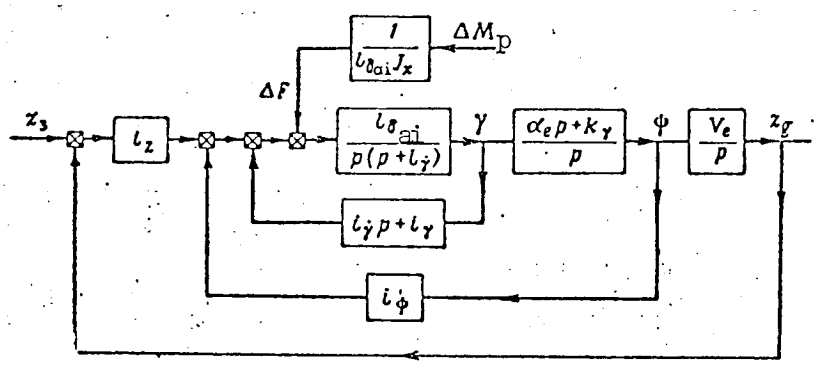

Figure 11.14. Functional diagram of system with control law (11.39).

The selection of transfer numbers in systems described by equations (11.37) and (11.40) may be carried out most simply by using the method of standard coefficients. The selection of a particular control law from those considered in this section is determined by the specific requirements assigned to a system for controlling the center of gravity of a plane-winged missile.

In this section we did not consider the use of an accelerometer, which measures the lateral acceleration of the missile to produce compensating signals. Such a signal, which is proportional to $V\, d\theta_s/dt$, and also the integral and derivative of this signal may be conveniently used in the system for controlling the center of gravity of a missile.

Section 11.4. Control of the Longitudinal Motion of the Missile's Center of Gravity /362

The problem of controlling the longitudinal motion of a missile's center of gravity with respect to a fixed trajectory is similar to the problem, considered in section 11.2, of controlling the center of gravity of a missile with cruciform wings in the lateral motion. For some flight conditions (for example, for horizontal flight), the longitudinal motion of the center of gravity may be reduced to lateral motion (for a missile with cruciform wings), as carried out in section 10.6 for the angular motions of the missile, if we assume that the flight velocity is constant. It is only necessary to replace the parameters of lateral motion in the equations with the corresponding parameters of longitudinal motion.

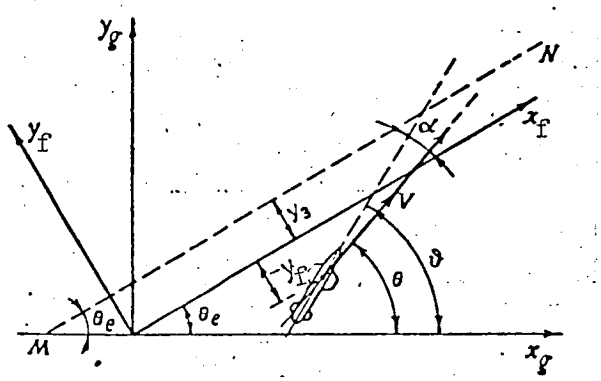

Figure 11.15. Angular and linear coordinates which characterize position of missile with respect to its rectilinear trajectory during longitudinal motion; subscript f = fixed.

However, if the missile has an inclined trajectory, terms appear in the equations for longitudinal motion, which are new compared with the lateral terms, and these may produce a substantial effect on the nature of the motion. In addition, in the problem of longitudinal motion we can take into account the variation in the missile's flight velocity during the period of perturbed motion, which cannot be done in the problem of lateral motion when the latter has the form described in this book.

The formulation of the problem of controlling the motion of the center of gravity with respect to an assigned trajectory is clarified in figure 11.15. Let us assume that the straight line MN is the assigned trajectory

with a slope θ_e. In the general case it may not coincide with the fixed incline /363
system of coordinates x_{fixed}, y_{fixed}, which is introduced to distinguish it from the Earth system x_g, y_g. If the assigned trajectory is curvilinear, then, as shown in section 11.2, we can determine y_3 as a function of time, if we know its shape and the velocity of the missile.

The system of equations for longitudinal motion, if we take into account the fact that we must separate the linear deviation of the missile from the assigned incline trajectory, is obtained from (8.26) and has the form

$$\left.\begin{aligned}
&a_\theta\Delta\theta + a_\alpha\Delta\alpha + \frac{d\Delta V}{dt} + a_V\Delta V + a_y\Delta y_g = a_\delta\Delta\delta_e;\\
&\frac{d\Delta\theta}{dt} - b_\theta\Delta\theta - b_\alpha\Delta\alpha - b_V\Delta V + b_y\Delta y_g = b_\delta\Delta\delta_e;\\
&\frac{d^2\Delta\vartheta}{dt^2} + c_\delta\frac{d\Delta\vartheta}{dt} + c_\alpha\frac{d\Delta\alpha}{dt} + c_\alpha\Delta\alpha + c_V\Delta V = c_\delta\Delta\delta_{el};\\
&\frac{d\Delta y_g}{dt} = V_e\sin\theta_e + \frac{dy_f}{dt}\cos\theta_e;\\
&\frac{dy_f}{dt} = V_e\Delta\theta;\\
&\Delta\vartheta = \Delta\theta + \Delta\alpha.
\end{aligned}\right\} \qquad (11.41)$$

(subscript e = engine)

The equation for $d\Delta x_g/dt$, which entered into equation (8.26), is not introduced into system (11.41), because it is isolated and may be integrated separately after system (11.14) has been solved and we have obtained $\Delta\theta=\Delta\theta(t)$. Without introducing a substantial error, the system of equations (11.41) may be simplified in the following manner. Because the coefficients a_y and b_y are usually small, the terms with these coefficients in the first and second equations may be neglected (when the slopes of the trajectory are small). If this assumption produces a substantial error (when the slopes of the assigned trajectory are large), then, if we know the velocity of the missile, we may compute $\Delta y(t)$ approximately as a function of time and transpose the terms with Δy into the right part, assuming that they are given functions of time. In both of these cases the fourth equation drops out.

Let us consider as an example the first of these methods for simplifying the problem. We obtain a system of equations[1]

[1]The right sides of the first two equations of system (11.42), unlike those of system (11.41) which has been written for the general case, become equal to zero, because we assume that the engine of the missile is not controlled, i.e., $\Delta\delta_e = 0$. The third equation contains the external moment ΔM_p.

$$
\left.
\begin{aligned}
& a_\vartheta \Delta\vartheta + a_\alpha \Delta\alpha + \frac{d\Delta V}{dt} + a_V \Delta V = 0; \\
& \frac{d\Delta\vartheta}{dt} - b_\vartheta \Delta\vartheta - b_\alpha \Delta\alpha - b_V \Delta V = 0; \\
& \frac{d^2\Delta\vartheta}{dt^2} + c_\vartheta \frac{d\Delta\vartheta}{dt} + c_\alpha \frac{d\Delta\alpha}{dt} + c_\alpha \Delta\alpha + c_V \Delta V = c_\delta \Delta\delta_{el} + \frac{\Delta M_p}{J_z}; \\
& \frac{dy_f}{dt} = V_e \Delta\theta; \\
& \Delta\vartheta = \Delta\theta + \Delta\alpha.
\end{aligned}
\right\} \qquad (11.42)
$$

The fourth equation of system (11.42) is isolated and may be considered separately. However, this situation prevails only as long as we are studying the motion of the missile without a control system. When we take into account the control system, this equation becomes associated with the remaining equations. /364

If we neglect the variation in velocity and the effect of weight ($\Delta V = \frac{d\Delta V}{dt} = b_\theta = 0$) in system (11.42), then, as we pointed out at the beginning of this section, the equations for the longitudinal motion will become completely analogous to the equations for the lateral motion of a missile with cruciform wings (8.44). The problem of controlling the center of gravity in this case is considered in detail in section 11.2.

Let us consider the special features which occur in the problem of controlling the center of gravity, when we take into account the variation in velocity and the effect of the gravity force. First we simplify this problem as much as possible. For this purpose we assume, as in section 8.4, that the missile is instantaneously balanced. In this case, the equation of moments is transformed into an algebraic system (11.42) and takes the form

$$
\left.
\begin{aligned}
& a_\theta \Delta\theta + a_\alpha \Delta\alpha + \frac{d\Delta V}{dt} + a_V \Delta V = 0; \\
& \frac{d\Delta\theta}{dt} - b_\theta \Delta\theta - b_\alpha \Delta\alpha - b_V \Delta V = 0; \\
& c_\alpha \Delta\alpha + c_V \Delta V = c_\delta \Delta\delta_{el} + \frac{\Delta M_p}{J_z}; \\
& \frac{dy_f}{dt} = V_e \Delta\theta.
\end{aligned}
\right\} \qquad (11.43)
$$

Let us take an automatic pilot with the simplest control law

$$
\Delta\delta_{el} = i_y (y_3 - y_f). \qquad (11.44)
$$

By combining the equations of the missile (11.43) with the equations of the automatic pilot (11.44) we obtain a general equation of the system for controlling the center of gravity of a missile with respect to an inclined trajectory /365

$$\frac{d^3y_f}{dt^3}+a_1\frac{d^2y_f}{dt^2}+\left(a_2+i_yV_e\frac{b_\alpha c_\delta}{c_\alpha}\right)\frac{dy_f}{dt}+i_yV_ec_3\frac{c_\delta}{c_\alpha}y_f=$$
$$=i_yV_e\frac{b_\alpha c_\delta}{c_\alpha}\frac{dy_3}{dt}+i_yV_ec_3\frac{c_\delta}{c_\alpha}y_3+\frac{b_\alpha V_c}{J_zc_\alpha}\frac{d\Delta M_p}{dt}+\frac{c_3V_e\Delta M_p}{J_zc_\alpha}. \quad (11.45)$$

The values of coefficients a_1 and a_2 are determined by equations (8.37). Equation (11.45) shows that if the missile is stable without a control system ($a_1>0$ and $a_2>0$), then, with the simplest control law, we can control the lateral deviation of its center of gravity with respect to the inclined trajectory in the vertical plane. This result differs in principle from the one which was obtained when we considered the lateral motion of a missile with cruciform wings, whose system for controlling the center of gravity in the case of the simplest control law (11.2) turned out to be unstable.

In section 8.4 it was pointed out that for some missiles during different flight conditions (for example, during pitching), coefficients a_1 and a_2 may become negative. If a_1 becomes negative, motion with a control system will also become unstable, as follows from equation (11.45). When a_2 is negative, the question of stability is solved by the Horwitz inequalities.

If $a_2 < i_yV_e\frac{b_\alpha c_\delta}{c_\alpha}$, then the system retains its stability.

Equation (11.45) shows that when the simplest control law is used it is difficult to provide for the desired dynamic properties of the system, because we can control only two coefficients of this equation and can do this only by means of one transfer number i_y. In addition, the system described by equation (11.45) is static with respect to the external perturbing moment ΔM_p.

Let us introduce a series of compensating signals into the control law including an integral signal for eliminating staticism. In this case we take the total system of equations (11.42) for controlling the object. Therefore, we must also introduce compensating signals in the control law for motion with respect to the center of gravity. Taking these remarks into account, we obtain a control law in the form

$$\Delta\delta_p=-i_{\dot\delta}\frac{d\Delta\vartheta}{dt}-i_\vartheta\Delta\vartheta-i_{\dot\theta}\frac{d\Delta\theta}{dt}-i_\theta\Delta\theta+i_y(y_3-y_f)+ \quad (11.46)$$
$$+q_y\int_0^t(y_3-y_f)\,dt.$$

The signals proportional to the deviation of the trajectory slope and to the derivative of this angle are introduced in the control law in place of the stabilizing signals as the first and second derivatives of the linear deviation y_f. These signals may be obtained by means of an accelerometer. The signal of the accelerometer is proportional to $V\frac{d\Delta\theta}{dt}$, while its integral is proportional to $V\Delta\theta$. To compensate for the acceleration components produced by the inclined trajectory, it is necessary to introduce a compensating signal from the position gyroscope through the sine-cosine potentiometer. /366

Combining the missile equations (11.42) with the equations of the automatic pilot (11.46), we obtain a general equation for this system[1]

$$\begin{gathered}\frac{d^6y_f}{dt^6}+a_1\frac{d^5y_f}{dt^5}+a_2\frac{d^4y_f}{dt^4}+a_3\frac{d^3y_f}{dt^3}+\\+a_4\frac{d^2y_f}{dt^2}+a_5\frac{dy_f}{dt}+a_6y_f=b_1\frac{d^2y_3}{dt^2}+a_5\frac{dy_3}{dt}+a_6y_3+\\+\frac{b_aV_e}{J_z}\frac{d^2\Delta M_p}{dt^2}+\frac{c_3V_e}{J_z}\frac{d\Delta M_p}{dt},\end{gathered}\tag{11.47}$$

where

$$\left.\begin{aligned}
&a_1=a_V+b_\alpha-b_\theta+c_\vartheta+c_\alpha+i_\vartheta c_\delta;\\
&a_2=c_1+b_\alpha c_\vartheta+c_\alpha+i_\vartheta c_\delta+(c_\vartheta+c_\alpha+\\
&+i_\vartheta c_\delta)(a_V-b_\theta)+(i_\theta+i_\vartheta)b_\alpha c_\delta;\\
&a_3=(c_\alpha+i_\vartheta c_\delta)(a_V-b_\theta)+(c_\vartheta+i_\vartheta c_\delta)c_3+\\
&+(c_\vartheta+c_\alpha+i_\vartheta c_\delta)c_2-a_\alpha c_V+i_\vartheta c_\delta b_\alpha+\\
&+i_\theta b_\alpha c_\delta+i_\theta c_\delta c_3;\\
&a_4=(c_\alpha+i_\vartheta c_\delta)c_2-c_Vc_4+i_\vartheta c_\delta c_3+\\
&+i_yb_\alpha c_\delta V_e+i_\vartheta c_\delta c_3;\\
&a_5=q_yb_\alpha c_\delta V_e+i_yc_\delta c_3V_e;\\
&a_6=q_yc_\delta c_3V_e;\\
&b_1=i_yb_\alpha c_\delta V_e.
\end{aligned}\right\}\tag{11.48}$$

The expressions for the coefficient of equation (11.47) show that each of these coefficients contains at least one new transfer number of the /367

[1]The values of coefficients c_1, c_2, c_3 and c_4 are determined by means of equations (8.30).

automatic pilot, and for this reason the required values of these coefficients can be selected by the method of standard coefficients. Because we have introduced the integral term into the control law, the system has become astatic with respect to the constant perturbing moment ΔM_p. In addition to this, the system is also astatic with respect to the control signal which depends linearly on time ($y_3 = kt$).

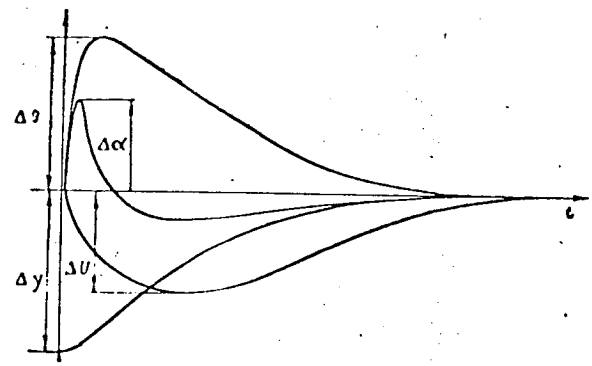

Figure 11.16. Graphs of transient process when controlling center of gravity during longitudinal motion.

If the requirements for the system which controls the missile's center of gravity can be lowered, the control law may be simplified, which will make the entire system less complex.

For example, if the deviations from the assigned trajectory produced by the external moment are not significant or if this moment is very small, we may reject the integral term in the control law, which will bring the order of equation (11.47) down to unity. We can also attempt to achieve the desired dynamic properties of the system by using only the signal for the pitch angle ($\Delta\vartheta$), neglecting the signal for the trajectory slope ($\Delta\theta$), etc.

As an example, figure 11.16 shows curves which characterize the variation in the linear deviation $\Delta_y = y_3 - y_f$, the variations in the angles of attack $\Delta\alpha$, in the slope of the trajectory $\Delta\theta$ and also in the velocity ΔV, when the center of gravity of the missile is controlled in the vertical plane.

Section 11.5. Control of the Center of Gravity when the Velocity of the Missile is Variable

In most cases of practical importance, the control of the center of gravity of the missile with respect to the assigned trajectory takes place when there is a rather large variation in flight speed. This situation occurs when the

missile is placed on the radio beam right after launching, when ballistic missiles are controlled over the active region of the trajectory, when the airplane-missiles take off, etc. Therefore, it is rational to consider the special features of the control system for the center of gravity in cases when the flight velocity of the missile is variable. Initially, this velocity is computed as a function of time from the condition that the missile must be maintained exactly on the assigned trajectory. /368

As an example, let us consider the control of the lateral motion of the center of gravity of a missile with cruciform wings stabilized with respect to the longitudinal axis. As in the preceding sections, we make a series of assumptions to simplify the problem as much as possible, which is particularly necessary in the present case since the motion of the missile is now described by linear equations with variable coefficients. To simplify the system of equations (8.56) which describe the lateral motion of the missile whose velocity is variable, we assume that the missile is balanced instantaneously, i.e., we neglect the time of transient processes during the short period motion. In addition, we shall assume that the variation in angles β and ψ is small and, consequently, $\sin\beta$ and $\sin\psi$ are replaced by the angles themselves. Taking into account these simplifications and the accepted rule for the signs, the system of equations (8.56) takes on the form

$$\left.\begin{aligned} &\frac{d\psi}{dt}-\frac{d\beta}{dt}-c_z^{\beta}S\frac{\rho V}{2m}\beta=0;\\ &\beta=\frac{m_y^{\delta}}{m_y^{\beta}}\delta_f;\\ &\frac{dz_g}{dt}=V(\psi-\beta). \end{aligned}\right\} \tag{11.49}$$

For the equations of the missile we use an automatic pilot with the following control law

$$\delta_f=i_z\left(\frac{dz_3}{dt}-\frac{dz_g}{dt}\right)+i_z(z_3-z_g). \tag{11.50}$$

Combining the equations of the missile (11.49) and of the automatic pilot (11.50) and eliminating all of the variables except z_g, we obtain the general equation for this system[1]

$$\begin{aligned} &\frac{d^2z_g}{dt^2}+\left[-\frac{1}{V}\frac{dV}{dt}+i_z c_z^{\beta}S\frac{\rho V^2}{2m}\frac{m_y^{\delta}}{m_y^{\beta}}\right]\frac{dz_g}{dt}+i_z c_z^{\beta}S\frac{\rho V^2}{2m}\times\\ &\times\frac{m_y^{\delta}}{m_y^{\beta}}z_g=i_z c_z^{\beta}S\frac{\rho V^2}{2m}\frac{m_y^{\delta}}{m_y^{\beta}}\frac{dz_3}{dt}+i_z c_z^{\beta}S\frac{\rho V^2}{2m}\frac{m_y^{\delta}}{m_y^{\beta}}z_3. \end{aligned} \tag{11.51}$$

[1]In obtaining equation (11.51), the mass of the missile was considered constant.

Since $c_z^\beta < 0$ and $m_y^\beta < 0$, when the condition

$$i_z c_z^\beta S \frac{\rho V^2}{2m} \frac{m_y^\beta}{m_y^\beta} > \frac{1}{V} \frac{dV}{dt} \tag{11.52}$$

is satisfied, equation (11.51) corresponds to the stable system for controlling the center of gravity. Obviously, in the case of very small flight velocity (with acceleration), one of the components $(1/V \quad dV/dt)$ of the coefficient in front of the first derivative of z_g may become large, and since it has a negative sign the motion of the center of gravity of the missile will be unstable. However, when the missile is accelerating very rapidly, it may pass this instability stage so quickly that there is no time for any substantial deviation to take place from the assigned law for the motion of the center of gravity. At high velocities this component becomes small, while the second component increases as the square of the flight velocity. Under these conditions, the first term may be neglected. /369

As in the case of section 10.8, when we considered the short period motion of a missile which travels with a variable velocity, we shall assume that over a limited region the velocity varies uniformly, i.e., $V = j(t_0 \pm t)$, where the plus sign refers to accelerated motion, while the minus sign refers to decelerated motion. Let us substitute this value of velocity in equation (11.51) and analyze it by the method of quasifixed coefficients. After substitution equation (11.51) takes the form

$$\begin{aligned} \frac{d^2 z_g}{dt^2} + \left[\mp \frac{1}{t_0 \pm t} + i_z j^2 b (t_0 \pm t)^2 \right] \frac{dz_g}{dt} + i_z j^2 b (t_0 \pm t)^2 z_g = \\ = i_z j^2 b (t_0 \pm t)^2 \frac{dz_3}{dt} + i_z j^2 b (t_0 \pm t)^2 z_3, \end{aligned} \tag{11.53}$$

where

$$b = c_z^\beta S \frac{\rho}{2m} \frac{m_y^\delta}{m_y^\beta}.$$

Applying the method of quasistationary coefficients to equation (11.53), we obtain from table 8.5

$$\frac{d^2 z_g}{dt^2} + i_z j^2 b t_0^2 \frac{dz_g}{dt} + i_z j^2 b t_0^2 z_g = i_z j^2 b t_0^2 \frac{dz_3}{dt} + i_z j^2 b t_0^2 z_3. \tag{11.54}$$

Comparing equations (11.53) and (11.54), we see that, due to the introduction of corrections from table 8.5 into the coefficient in front of the first derivative, the first term of this coefficient has vanished. This term took into account the effect of acceleration on the damped lateral motion of the center of gravity.

Equation (11.54) gives us an expression for the natural frequency

$$\Omega_0 = jt_0\sqrt{i_z b} \tag{11.55}$$

and an expression for the relative damping coefficient

$$\zeta = \frac{i_z\sqrt{b}}{2\sqrt{i_z}} jt_0. \tag{11.56}$$

Equations (11.55) and (11.56) show that in this control system for a missile moving with acceleration or deceleration the natural frequency and the relative damping coefficient are directly proportional to the instantaneous velocity $V_0 = jt_0$. When the velocity increases, these characteristics increase, and when it /370 decreases, they decrease.

The analysis of the longitudinal motion of the center of gravity of a missile which travels at a variable velocity is somewhat more complex than the analysis of the lateral motion because equations (8.52), which describe this motion, contain additional terms due to the effect of weight in the projection of the thrust along the longitudinal axis on the missile. However, from the qualitative standpoint the effect of variable flight velocity on the longitudinal motion of the missile's center of gravity is the same as the effect on the lateral motion considered in this section.

CHAPTER 12. THE MOTION OF A MISSILE IN A DISTURBED ATMOSPHERE /371

Section 12.1. General Information

The analysis of missile motion carried out in the preceding chapters assumed that the atmosphere through which the missile moves is fixed with respect to Earth. This assumption is quite valid for the solution of many problems associated with the control dynamics of missiles. Such problems include the selection of parameters for the missile control system and the determination of the basic components of its motion.

However, in the exploitation of guided missiles, problems arise which require that we take into account the possible movement of the air with respect to the Earth's surface. First of all, this covers problems of the scattering of guided missile trajectories produced by wind. The principal role is played here by regular and mainly horizontal airstreams. These streams are produced by the nonuniform distribution of atmospheric pressure (pressure gradient) along regions extending for tens or hundreds of kilometers. In other problems associated with the selection of the factor of safety for the missile frame and with determining the resistance of equipment to vibration, the principal role is played by atmospheric turbulence. Turbulence is the chaotic movement of air with individual portions extending from several kilometers to several meters. Gusts of very small duration (of the order of one meter or less), although they occur in the atmosphere, have a low intensity and they react with high frequency on the missile moving at a high speed. Therefore, they produce no noticeable effect on the characteristics of motion.

The turbulence of the atmosphere is due to the process of vortex formation, associated with the absorption and scattering of energy which take place continuously when large masses of air are displaced in any direction. As experiments have shown, the turbulent gusts of air, starting with an altitude of several hundred meters above the surface of the Earth, are isotropic, i.e., they have no preferred directions.

The present chapter presents a method for taking into account the effect /372
of air motion, with respect to the ground, on the flight of guided missiles.

Section 12.2. Mathematical Description of a Disturbed Atmosphere

When a missile flies in an atmosphere at rest, the vectors for its airspeed and ground speed coincide. If a missile, whose ground speed is equal to $\overline{V}$, moves in an atmosphere which has velocity $\overline{W}$ with respect to the ground, its air velocity is given by equation (subscript B = air)

$$\overline{V}_B = \overline{V} - \overline{W}. \tag{12.1}$$

Relationship (12.1) is clarified in figure 12.1. The negative sign in front of the wind velocity vector in equation (12.1) is explained by the fact that the aerodynamics of missiles consider the velocity vector of the missile with respect to the air, rather than the opposite velocity vector of the air with respect to the missile. In accordance with what has been presented in section 12.1, the air velocity vector with respect to the Earth or simply the wind vector is considered to have two components

$$\overline{W} = \overline{W}_0 + \overline{W}_c. \tag{12.2}$$

where $\overline{W}_0$ is the constant component of wind velocity, which takes into account the orderly streams of air of large extent; and $\overline{W}_c$ is the variable (random) component of the wind velocity, which takes into account the turbulent air gusts. The mathematical description of the constant wind velocity component is obviously not very complicated. The constant wind velocity vector may be resolved along the axes of the coordinates which are used to describe the motion of the missile and can be taken into account when the equations of motion are formulated.

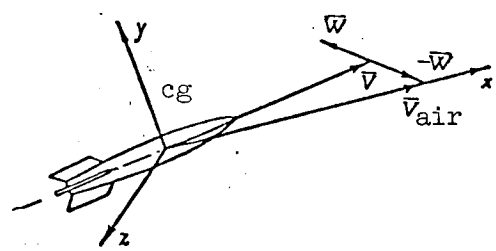

Figure 12.1 Velocity triangle of wind, ground speed and missile air speed; cg = center of gravity.

Experiments have shown that the variable component of the wind is a random function of coordinates x, y, z of a given point in the atmosphere and of time t. /373
To analyze this component we resolve the vector $\overline{W}_c$ (x, y, z, t) along the axes of the coordinates, which are associated by an arbitrarily oriented fixed system

$$\overline{W}_c(x, y, z, t) = iw_{cx}(x, y, z, t) + jw_{cy}(x, y, z, t) + kw_{cz}(x, y, z, t),$$

where w_{cx}, w_{cy}, w_{cz} are the projections of $\overline{W}_c$ along the corresponding axes; and

i, j, k are unit vectors along the xyz axes.

The projection of the vector $\overline{W}_c$ (x, y, z, t) is a random function of the same arguments as the vector itself.

To simplify the description of missile motion under the action of a random wind component, we make the following assumptions:

(1) we assume that the velocity of the random wind component is the same at all points on the surface of the missile; such an assumption is quite admissable for missiles whose dimensions are not too large;

(2) the random wind component is due to the turbulence of the atmosphere, which is assumed to be isotropic. This is valid for altitudes from 500 - 1000 m and up.

On the basis of assumptions concerning the isotropic nature of atmospheric turbulence we can maintain that the random functions w_{cx}, w_{cy}, w_{cz} must be identical in the probability sense. Therefore, the probability characteristics obtained for any one of the functions may be considered valid for the other two functions.

If we examine the turbulent atmosphere to evaluate its effect on a high speed missile, we can make a series of simplifications when we describe the random wind component mathematically. Because the projections of the random wind w_{cx}, w_{cy}, w_{cz} are small compared with the velocity of the missile, the velocity field of turbulent gusts can be reduced to a frozen fixed model in space. In the case of this field, there is a single-valued relation between the coordinates x and t which is determined by the velocity of the missile

$$x = Vt.$$

In addition, based on these assumptions, we shall neglect the variation in the velocity of random wind as a function of coordinates y and z within the limits of the missile's dimensions. All these simplifications make it possible to consider the random wind vector as a function of only one variable: coordinate x or time t. On the basis of this, in place of (12.3) we obtain

$$\begin{aligned}\overline{W}_c(x) = \overline{W}_c(t) &= i w_{cx}(x) + j w_{cy}(x) + k w_{cz}(x) = \\ &= i w_{cx}(t) + j w_{cy}(t) + k w_{cz}(t).\end{aligned} \tag{12.4}$$

To illustrate the nature of the random functions w_{cx}. w_{cy}, w_{cz}, fig. 12.2 /374 shows the experimental curve for $w_{cx}(x)$.[1] Many experiments[2] show that within the limits of several tens and sometimes several hundreds of kilometers, the meteorological conditions remain more or less unchanged, and the considered function

---

[1]Yu. P. Dobrolenskiy, The Turbulence of the Atmosphere as a Source of Perturbations for Airplane Automatic Control Systems, Izv. AN SSSR, "Energetics and Automation" 1961, No. 5.

[2]H. Press, M. T. Meadows and I. Hadlock, A Reevaluation of Data on Atmospheric Turbulence and Airplane Gust Loads for Application in Spectral Calculations, NACA Report No. 1272, 1956.

for the velocity of random wind is a stationary random function. In this case, the probability characteristics of this function do not depend on time t and consequently, do not depend on coordinate x.

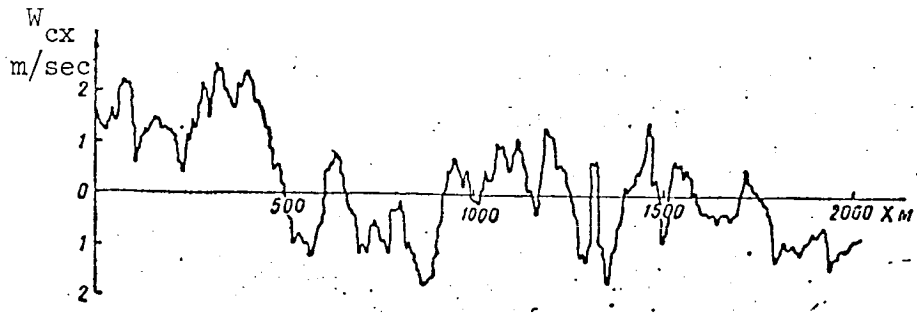

Fig. 12.2. Oscillogram of random wind component which coincides with direction of flight.

The concepts of correlation function and spectral density considered in section 2.5 are applied with success to the analysis of stationary random processes. We present here the corresponding equations with the variables which will be used

$$R(\varkappa) = \int_0^\infty S(\Omega) \cos \Omega \varkappa d\Omega; \tag{12.5}$$

$$S(\Omega) = \frac{2}{\pi} \int_0^\infty R(\varkappa) \cos \Omega \varkappa d\varkappa; \tag{12.6}$$

$$\sigma_w^2 = R(0) = \int_0^\infty S(\Omega)\, d\Omega, \tag{12.7}$$

where χ is an independent variable which describes the increase in the linear spatial coordinate x which coincides with the direction of flight and which is measured in m; and Ω is the spatial angular frequency measured in rad/m and associated with the angular frequency ω by the relation /375

$$\Omega = \frac{\omega}{V} \tag{12.8}$$

The use of spatial angular velocity Ω instead of time angular velocity ω in equations (12.5) - (12.7) is based on the concepts concerning the velocity field of turbulent gusts as constituting a frozen, fixed model in space. The advantage of this approach to the problem consists of the possibility of determining this velocity field of turbulent gusts by means of spatial coordinates. This concept makes the analytic expression for the field of turbulent velocities universal, thus suitable for investigating the dynamics of a missile flying at any velocity.

The theory of isotropic turbulence contains analytical expressions for correlation functions and spectral densities for the components of random wind vector. The experimental data on the turbulence of the atmosphere agree well with theoretical results.

The theory of isotropic turbulence[1] shows that it is sufficient to have two correlation functions (or two spectral densitites) to describe all the components of random wind. The meaning of these functions and the difference between them is clarified in figure 12.3., from which it follows that

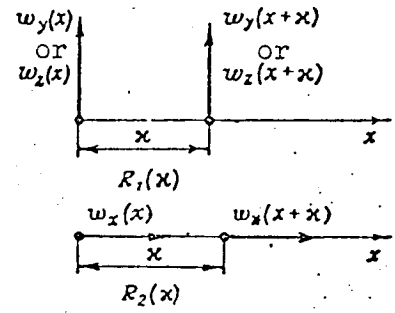

Figure 12.3. Position of two components of random wind with respect to flight direction.

$R_1(\varkappa)$ is the correlation function for the wind velocity projection normal to the direction of the coordinate x, along which the correlation is investigated;

$R_2(\varkappa)$ is the correlation function for the projection of the wind velocity coinciding with the direction of the x coordinate.

Consequently, we must use the correlation function $R_2(\varkappa)$ for the wind projection $w_{cx}(\varkappa)$ and the correlation function $R_1(\varkappa)$ for the projection of $w_{cy}(\varkappa)$ and $w_{cz}(\varkappa)$.

The analytic expressions for these equations have the form /376

$$R_1(\varkappa) = \sigma_\omega^2 (1 - \varkappa/2L) e^{-\varkappa/L}; \tag{12.9}$$

$$R_2(\varkappa) = \sigma_\omega^2 e^{-\varkappa/L}. \tag{12.10}$$

---

[1]John Batchelor, Theory of Homogeneous Turbulence, I.L., 1955.

Equations (12.9) and (12.10) have two parameters: the average value for the square of the random wind velocity (dispersion) σ_w^2, which characterized the turbulence intensity, and the so-called turbulence scale L which is proportional to the average dimension of the atmosphere.

Using these equations, graphs are constructed in figure 12.4 for normalized correlation functions $R_1(\varkappa)/\sigma_w^2$ and $R_2(\varkappa)/\sigma_w^2$. The graphs in figure 12.4 show that turbulence scale L characterizes the damping of correlation for the velocity of random wind.

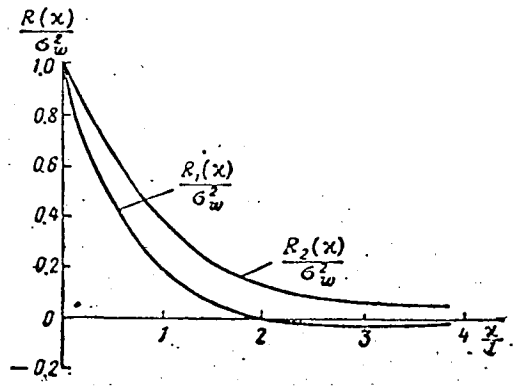

Figure 12.4. Graphs of normalized correlation functions for random components of wind.

The presence of analytic expressions for correlation functions $R_1(\varkappa)$ and $R_2(\varkappa)$ makes it possible to obtain from equation (12.7) analytical expressions for the corresponding spectral densities. These spectral densities are given by equations.

$$S_1(\Omega) = \sigma_w^2 \frac{L}{\pi} \frac{1 + 3\Omega^2 L^2}{(1+\Omega^2 L^2)^2} \tag{12.11}$$

$$S_2(\Omega) = \sigma_w^2 \frac{L}{\pi} \frac{2}{1 + \Omega^2 L^2}. \tag{12.12}$$

The graphs of normalized spectral densities $S_1(\Omega)/\sigma_w^2$ and $S_2(\Omega)/\sigma_w^2$ are shown /377 in figures 12.5 and 12.6, respectively.

Equations (12.11) and (12.12) contain the same parameters as equations (12.9) and (12.10); σ_ω^2 and L. It is obvious that turbulence scale L must depend on weather conditions and on the altutude of the missile. However, we do not have sufficient experimental data on this question at the present time. Therefore, we shall use the most probable value L = 300 m.[1]

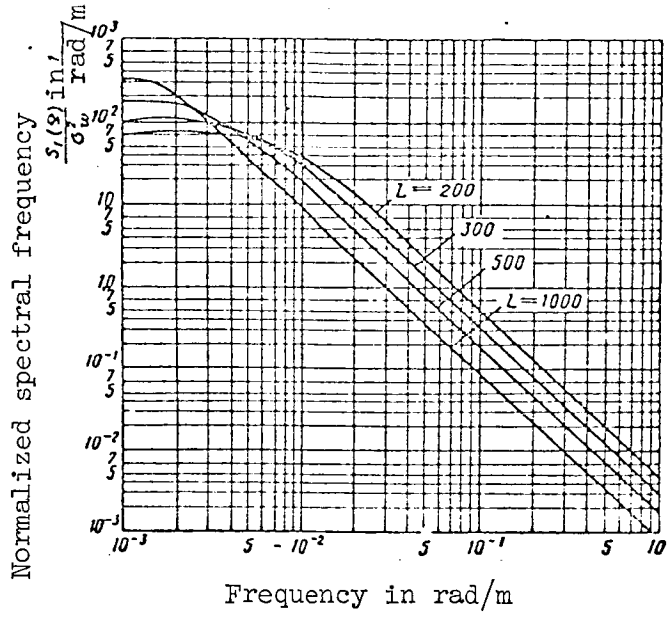

Figure 12.5. Graphs of normalized spectral density for random wind component constructed in accordance with equation (12. 1).

For the constant turbulence scale L the state of the atmosphere is characterized by one parameter--the root-mean-square value of random wind σ_w. It is sufficient to determine how quantity σ_w depends on weather conditions and flight altitude to obtain complete data on the state of the turbulent atmosphere. At the present time there is not enough experimental material available which would make it possible to obtain a reliable variation in σ_w as a /378 function of weather conditions and flight altitude. For illustration we present data which are available on this question.[1]

---

[1]See footnote[2] on page 366.

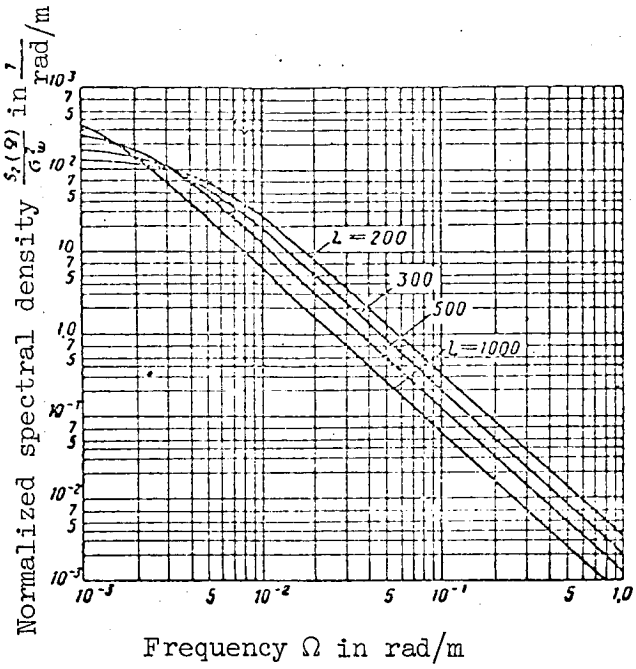

Figure 12.6. Graphs showing normalized spectral density for random component of wind constructed in accordance with equation (12.12).

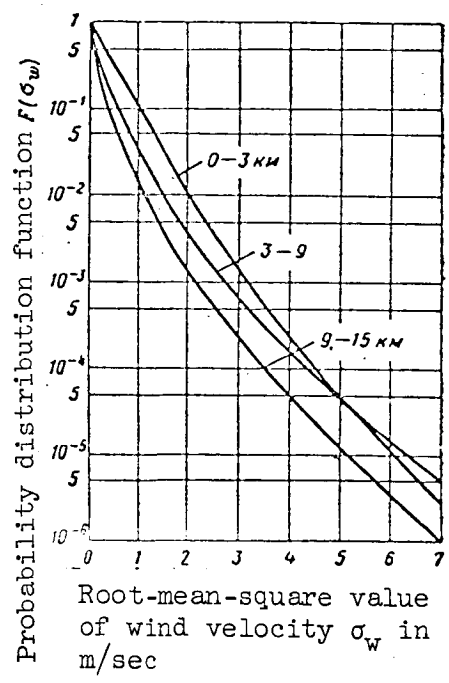

Figure 12.7. Curves for probability distribution function of root-mean-square value of random wind for various altitudes.

Figure 12.7 shows the probability distribution functions for the root-mean-square value of random noise at different flight altutudes. These curves give the probability for exceeding the given value σ_w. A comparison of the curves for the probability distribution functions for various altitudes makes it possible to draw the following conclusion. As the altitude increases, the time of flight in relatively quiet atmosphere increases substantially. For example, the period of flight in a practically calm atmosphere ($\sigma_w < 0.5$ m/sec) for altitude 0-3 km consititutes approximately 70 percent of the total flight time, while for an altitude of 9-15 km it is approximately 93 percent. The flight time in a highly perturbed atmosphere ($\sigma_w > 2.5$ m/sec) for flight altitudes of 0-3 km is approximately 0.4 percent, while for altitudes of 9-15 km it is equal to only 0.05 percent, i.e., approximately ten times less.

To consider the effect of weather on the mean square value of the random wind velocity, we introduce the following basic characteristics for the turbulence of the atmosphere: /379

(1) atmosphere practically at rest ($\sigma_w < 0.5$ m/sec);

(2) the turbulence of clear weather;

(3) the turbulence of cumulus clouds;

(4) thunderstorm turbulence.

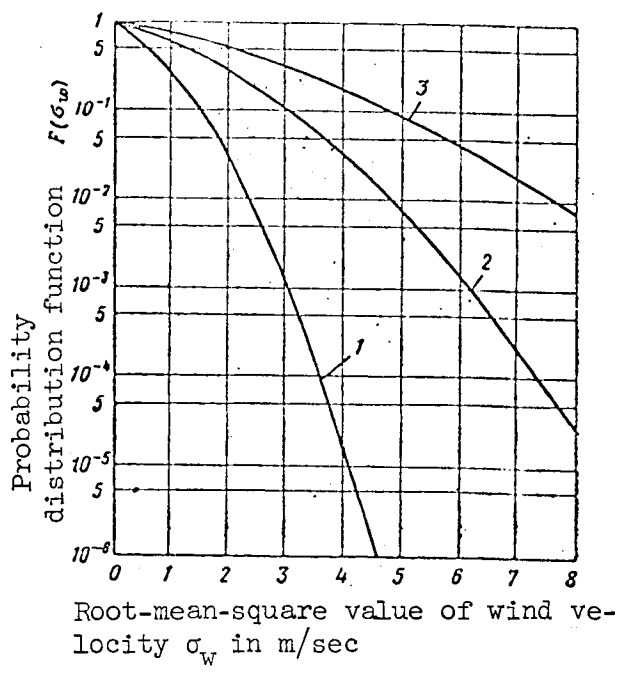

Figure 12.8. Probability distribution functions of root-mean-square value of random noise for various weather conditions. 1--clear weather; 2--cumulus clouds; 3--thunderstorm conditions.

/382

$$
\left.
\begin{aligned}
& m\frac{dV_x}{dt} - m\omega_z' V_y = -X - G\sin\theta + P\cos\alpha; \\
& m\frac{dV_y}{dt} + m\omega_z' V_x = Y - G\cos\theta + P\sin\alpha; \\
& J_z\frac{d^2\vartheta}{dt^2} = M_z; \\
& \vartheta = \theta + \alpha; \\
& \frac{dx_g}{dt} = V_e\cos\theta_2; \\
& \frac{dy_g}{dt} = V_e\sin\theta_2; \\
& \theta_2 = \theta + \alpha_в; \\
& V = \sqrt{V_x^2 + V_y^2}; \\
& \alpha_в = \operatorname{arc\,tg}\frac{w_y}{V_x + w_x}; \\
& \omega_z' = \frac{d\theta}{dt}.
\end{aligned}
\right\} \qquad (12.13)
$$

In these equations V_x and V_y are projection of the ground speed and not the air speed, because the inertial forces are determined by the acceleration of the missile with respect to Earth. However, the aerodynamic forces and moments (X, Y, M_Z) depend on the air speed of the missile. Before grouping the equations contained in system (12.13), we take into account several relationships between the quantities which they contain in order to introduce possible simplifications.

First of all we assume that the wind velocity $\overline{W}$ is substantially less than the velocity of the missile (both the air velocity and the ground velocity). This assumption makes it possible to introduce a series of approximate relations which substantially simplify the system of equations (12.13). Such relations include

$$
\left.
\begin{aligned}
& \alpha_в = \operatorname{arc\,tg}\frac{w_y}{V_x + w_x} \approx \operatorname{arc\,tg}\frac{w_y}{V} \approx \frac{w_y}{V}; \\
& V_y = V_x \operatorname{tg}\alpha_в \approx w_y; \\
& V_x = \sqrt{V^2 - V_y^2} \approx V; \\
& V_в \approx V - w_x.
\end{aligned}
\right\} \qquad (12.14)
$$

The assumption that the wind velocity is small compared with the velocity of the missile permits us to neglect the second term in the left side of the first equation of (12.13), compared with the first term. /383

Figure 12.8 shows graphs of the distribution functions for the mean square values of random noise σ_w for the indicated weather conditions. These graphs have the same meaning as those in figure 12.7. By comparing the curves in figure 12.8 we may conclude that for the same value of the probability, the root-mean-square values of the wind velocity σ_w for cumulus clouds is approximately twice as large as its value for clear weather, while for thunderstorm clouds it is approximately three times greater. The reduction of statistical data shows that the time of flight under thunderstorm conditions is approximately 0.05 percent of the entire flight time, while the flight time in cumulus clouds is 1 percent. The flight time under conditions of turbulence in clear weather in 10 percent, while the remaining 88.95 percent is occupied by flight in an atmosphere practically at rest.

All of the data presented above on the variation in the root-mean-square value of random wind as a function of flight altitude and weather conditions are obtained from the processing of a large amount of statistical information collected by U.S. airlines.[1] Therefore, these data are valid only when a specific method adapted by these airlines is used to plan flights and does /380 not reflect with sufficient objectivity the state of the atmosphere. Therefore, as we have pointed out, these data must be looked upon only as illustrative material, showing which characteristics of the turbulent atmosphere must be obtained.

Section 12.3. Controlling the Motion of a Missile in a Disturbed Atmosphere

Provision for wind in the equations of motion of a missile is made in a different manner for various coordinate axes which are used to describe this motion. If we use the flow axes, the equations contain additional terms, which take into account the " mobility" of this system due to the wind. When body axes are used, these terms are absent. The aerodynamic forces and moments /381 are obviously dependent on the air speed which is associated with the wind velocity by relation (12.1).

On the basis of these general considerations we obtain the equations for the longitudinal and lateral motion of a missile in a disturbed atmosphere.

1. The Equation for the Longitudinal Motion of a Missile in a Disturbed Atmosphere. Figure 12.9 shows the forces which act on a missile during its longitudinal motion when wind is present, and which are used to derive the equations for the coordinate system.

When the missile moves with a variable velocity in an atmosphere at rest, the longitudinal motion is described by equations (8.51). When the movement of the air is taken into account, these equations take the form

---

[1] See footnote [2] on page 366.

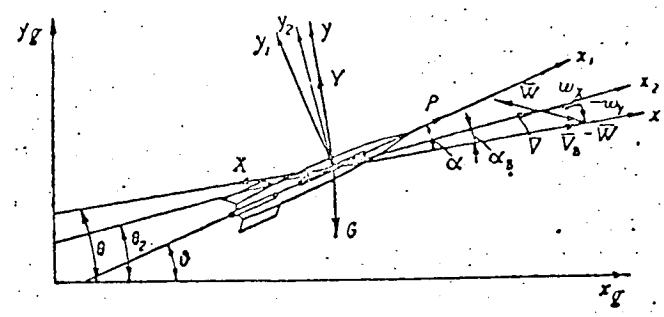

Figure 12.9. Forces acting on missile during longitudinal motion when wind is present and the utilized coordinate systems $\alpha_B = \alpha_{wind}$; $\bar{V}_B = \bar{V}_{air}$. $x_\sigma = Y_\sigma$--fixed or Earth axes; horizontal axis x_g is directed along course of missile, y_g axis is vertical; x, y--flow axes; x-axis is directed along the air velocity of the missile, the y-axis is perpendicualr to it; x_1, y_1--body axes fixed with respect to missile; x_1-axis is directed along chord of wing, y_1-axis is perpendicular to it; x_2, y_2 are associated axes; x_2-axis is directed along ground velocity of missile, i.e., along tangent to its trajectory with respect to Earth; y_2-axis is directed along normal to this trajectory; G--weight of the missile; P--thrust of engine; $\bar{V}$--ground speed of missile; $\bar{V}_B$--air velocity of missile (velocity with respect to ground); $\bar{W}$--velocity of air with respect to ground. The figure also shows components of vector $\bar{W}$ which must be taken into account when adding velocities of missile and wind as pointed out; ϑ--pitch angle; θ--slope of air speed vector; θ_2--slope of trajectory; α--angle of attack; α_B--component of total angle of attack α due to wind.

Taking into account (12.14) and the last assumption and replacing the values of X, Y, and M_z by their expressions from equations (8.23) - (8.25), we group the equations in system (12.13). The group of equations which describe the motion of the missile's center of gravity in a disturbed atmosphere has the form

$$
\left.
\begin{aligned}
& m\frac{dV}{dt} - c_x S\rho V w_x + c_x S\frac{\rho V^2}{2} = -G\sin\theta + P\cos\alpha; \\
& \frac{dx_g}{dt} = V\cos\theta_2; \\
& \frac{dy_g}{dt} = V\sin\theta_2; \\
& \theta_2 = \theta + \frac{w_y}{V}.
\end{aligned}
\right\} \qquad (12.15)
$$

The components in wind velocity w_x and w_y contained in equations (12.15) as well as the engine thrust P are considered to be known[1], i.e., in the solution of system (12.15) they must be given as functions of time. Solving the first of equations (12.15) by the methods recommended in section 2.4, we find the flight velocity as a function of time. Then, from the fourth equation we determine the slope of the trajectory θ_2 and, finally, if necessary, we can use the second and third equation to obtain the coordinates of the missile's center of gravity with respect to the Earth axes $x_g 0 y_g$.

The group of equations which describes the motion of the missile with respect to its center of gravity, taking into account the wind, has the form

$$
\left.
\begin{aligned}
& mV\frac{d\theta}{dt} - c_y^{\alpha} S\frac{\rho V^2}{2}\alpha + G\cos\theta - P\sin\alpha = \\
& = -c_y S\rho V w_x - m\frac{dw_y}{dt}; \\
& J_z\frac{d^2\vartheta}{dt^2} - m_z^{\bar{\omega}_z} S b_A^2\frac{\rho(V-w_x)}{2}\frac{d\vartheta}{dt} - m_z^{\dot{\alpha}} S b_A^2\frac{\rho(V-w_x)}{2}\frac{d\alpha}{dt} - \\
& - m_z^{\alpha} S b_A\frac{\rho(V-w_x)^2\alpha}{2} = m_z^{M} S b_A\frac{\rho(V-w_x)^3}{2a} + \\
& + m_z^{\delta} S b_A\frac{\rho(V-w_x)^2}{2}\delta_{\text{в}}; \\
& \vartheta = \theta + \alpha.
\end{aligned}
\right\} \qquad (12.16)
$$

Since the ground velocity of missile V is determined from equations (12.15), while the components of the wind velocity w_x and w_y must be assigned, /384 after linearizing the functions $\cos\theta$ and $\sin\alpha$ by means of some assumption, the entire system of equations (12.16) is transformed into a linear system

[1] In equations (12.15) and below, the effect of wind on the thrust of the engine is not taken into account.

with variable coefficients. In spite of some complexity, this system makes it possible, in principle, to analyze the effect on wind on the flight of a missile whose velocity is variable.

The equations for the longitudinal motion of the missile, taking into account the wind, which are obtained by the method of linearization, are somewhat simpler. Without repeating all of the considerations on the effect of the moving atmosphere, which have already been used in deriving equations (12.15) and (12.16), we show only the final form of the linearized equation

$$\left.\begin{aligned}
&a_\theta\Delta\theta + a_\alpha\Delta\alpha + \frac{d\Delta V}{dt} + a_V\Delta V + a_y\Delta y_g = a_V w_x + a_i\Delta\delta_{tc};\\
&\frac{d\Delta\theta}{dt} - b_\theta\Delta\theta - b_\alpha\Delta\alpha - b_V\Delta V + b_y\Delta y_g =\\
&= -b_V w_x - \frac{1}{V_e^*}\frac{dw_y}{dt} + b_i\Delta\delta_{tc};\\
&\frac{d^2\Delta\vartheta}{dt^2} + c_\vartheta\frac{d\Delta\vartheta}{dt} + c_\alpha^{\cdot}\frac{d\Delta\alpha}{dt} + c_\alpha\Delta\alpha + c_V\Delta V = c_V w_x + c_i\Delta\delta_в;\\
&\frac{d\Delta x_g}{dt} = (V_e + \Delta V)\cos\theta_e - V_e\sin\theta_e\Delta\theta;\\
&\frac{d\Delta y_g}{dt} = (V_e + \Delta V)\sin\theta_e + V_e\cos\theta_e\Delta\theta_2;\\
&\Delta\vartheta = \Delta\theta + \Delta\alpha;\\
&\Delta\theta_2 = \Delta\theta + \frac{w_y}{V_e}.
\end{aligned}\right\} \qquad (12.17)$$

The coefficients of equations (12.17) are determined by means of equations (8.27).

2. The Equations for the Lateral Motion of a Missile in a Disturbed Atmosphere. Figure 12.10 shows the coordinate systems used for deriving the equations for the lateral motion of a missile when wind is present.

As in the preceding subsection of this section, we consider first the more general case of motion in a disturbed atmosphere when the missile has a variable velocity. When a missile with variable velocity moves in a fixed atmosphere, the lateral motion of a plane-winged missile is described by equations (8.54).

If we take into account the movement of air, these equations must be written in the following form:

$$
\left.
\begin{aligned}
& mV\frac{d\beta}{dt} - mV\frac{d\beta_{\text{в}}}{dt} - mV\frac{d\psi}{dt} = Z; \\
& J_x\frac{d^2\gamma}{dt} = M_x; \\
& J_y\frac{d^2\psi}{dt^2} = M_y; \\
& \frac{dz_g}{dt} = -V\sin\theta_{\text{б}_2}; \\
& \theta_{\text{б}_2} = \psi - \beta + \beta_{\text{в}}; \\
& \beta_{\text{в}} = -\frac{w_z}{V}.
\end{aligned}
\right\} \qquad (12.18)
$$

/385

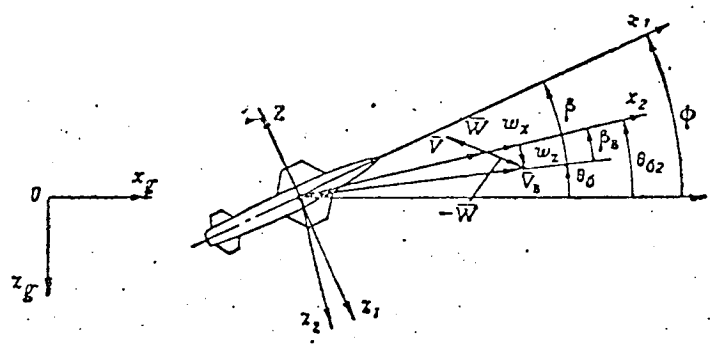

Figure 12.10. Forces acting on missile during its lateral motion in presence of wind. x_σ, z_g--Earth axes; horizontal axis x_g is directed along course of missile; x_1, z_1--fixed axes; x_2, z_2 are associated axes; $\overline{V}$--ground velocity of missile; $\overline{V}_B$--air velocity of missile; $\overline{W}$--velocity of wind with respect to ground; ψ--yaw angle; $\theta_б$--angle of rotation of air velocity vector; $\theta_{б2}$--angular rotation of the trajectory; β--slip angle; β_B--component of slip angle due to wind; Z--lateral force perpendicular to longitudinal axis.

Equations (12.18), in the form in which they are written, contain only the ground velocity of the missile. The second term in the first expression appears because the force of inertia is determined by the acceleration of the missile with respect to the ground

$$\frac{dV_z}{dt} = V\frac{d}{dt}[\sin(\beta - \beta_{\text{в}})] \approx V\frac{d\beta}{dt} - V\frac{d\beta_{\text{в}}}{dt}.$$

However, the force Z and the moments M_x and M_y depend on the air speed of the missile. Using the approximate expression (12.14), which determines this velocity from (12.18), we obtain the expended equations for a plane-winged missile

$$\left.\begin{aligned}
&mV\frac{d\beta}{dt} - mV\frac{d\psi}{dt} - c_z^{\beta} S\frac{\rho(V-w_x)^2}{2}\beta - G\sin\gamma = -m\frac{dw_z}{dt};\\
&J_x\frac{d^2\gamma}{dt^2} - m_x^{\bar{\omega}_x} S\frac{l^2}{2}\frac{\rho(V-w_x)}{2}\frac{d\gamma}{dt} - m_x^{\bar{\omega}_y} S\frac{l^2}{2}\frac{\rho(V-w_x)}{2}\frac{d\psi}{dt} -\\
&- m_x^{\beta} Sl\frac{\rho(V-w_x)^2}{2}\beta = m_x^{\delta} Sl\frac{\rho(V-w_x)^2}{2}\delta_{ai};\\
&J_y\frac{d^2\psi}{dt^2} - m_y^{\bar{\omega}_y} S\frac{l^2}{2}\frac{\rho(V-w_x)}{2}\frac{d\psi}{dt} - m_y^{\bar{\omega}_x} S\frac{l^2}{2}\frac{\rho(V-w_x)}{2}\frac{d\gamma}{dt} -\\
&- m_y^{\beta} Sl\frac{\rho(V-w_x)^2}{2}\beta = m_y^{\delta} Sl\frac{\rho(V-w_x)^2}{2}\delta_{cr};\\
&\frac{dz_g}{dt} = -V\sin\theta_{\sigma_z};\\
&\theta_{\sigma_z} = \psi - \beta - \frac{w_z}{V}.
\end{aligned}\right\} \qquad (12.19)$$

After linearization with respect to the function sin γ on the basis of some assumption, the first three equations become linear with variable coefficients. The flight velocity V must be known from the solution of equations for longitudinal motion (12.15), while the velocity components of the wind w_x and w_z must be assigned.

For a missile with cruciform wings with a stabilized tilt angle, the equations for the lateral motion in a disturbed atmosphere have the form

$$\left.\begin{aligned}
&mV\frac{d\beta}{dt} - mV\frac{d\psi}{dt} - c_z^{\beta} S\frac{\rho(V-w_x)^2}{2}\beta = -m\frac{dw_z}{dt};\\
&J_y\frac{d^2\psi}{dt^2} - m_y^{\bar{\omega}_y} S\frac{l^2}{2}\frac{\rho(V-w_x)}{2}\frac{d\psi}{dt} - m_y^{\bar{\beta}} S\frac{l^2}{2}\frac{\rho(V-w_x)}{2}\frac{d\beta}{dt} -\\
&- m_y^{\beta} Sl\frac{\rho(V-w_x)^2}{2}\beta = m_y^{\delta} Sl\frac{\rho(V-w_x)^2}{2}\delta_{cr}.\\
&\frac{dz_g}{dt} = -V\sin\theta_{\sigma_z};\\
&\theta_{\sigma_z} = \psi - \beta - \frac{w_z}{V}.
\end{aligned}\right\} \qquad (12.20)$$

In the investigation of the lateral motion of a missile in a disturbed atmosphere by means of linearized equations, the flight velocity V_e is considered constant. Therefore, it is possible to take into account only the

wind velocity component w_z normal to the given flight direction. We present /387

the final formulas of these equations for the case of flight in a disturbed atmosphere. For a plane-winged missile[1]

$$\left.\begin{aligned}
&\frac{d\beta}{dt} + k_\beta\beta - \frac{d\psi}{dt} - \alpha_e\frac{d\gamma}{dt} - k_\gamma\gamma = -\frac{1}{V_e}\frac{dw_z}{dt};\\
&\frac{d^2\gamma}{dt^2} + l_{\dot\gamma}\frac{d\gamma}{dt} + l_{\dot\psi}\frac{d\psi}{dt} + l_\beta\beta = l_{\delta_{ai}}\delta_{ai} + l_{\delta_{cr}}\delta_{cr};\\
&\frac{d^2\psi}{dt^2} + n_{\dot\psi}\frac{d\psi}{dt} + n_{\dot\gamma}\frac{d\gamma}{dt} + n_\beta\beta = n_{\delta_{ai}}\delta_{ai} + n_{\delta_{cr}}\delta_{cr};\\
&\frac{dz_g}{dt} = V_e(\beta - \psi) + w_z.
\end{aligned}\right\} \qquad (12.21)$$

For a missile with cruciform wings and with a stabilized angle of tilt[1]

$$\left.\begin{aligned}
&\frac{d\beta}{dt} + k_\beta\beta - \frac{d\psi}{dt} = -\frac{1}{V_e}\frac{dw_z}{dt};\\
&\frac{d^2\psi}{dt^2} + n_{\dot\psi}\frac{d\psi}{dt} + n_{\dot\beta}\frac{d\beta}{dt} + n_\beta\beta = n_{\delta_{cr}}\delta_{cr};\\
&\frac{dz_g}{dt} = V_e(\beta - \psi) + w_z.
\end{aligned}\right\} \qquad (12.22)$$

The coefficients of equations (12.21) and (12.22) are determined by equations (8.43) and (8.45).

Section 12.4. The Effect of the Constant Wind Component on the Motion of a Missile

1. Missiles with Variable Flight Velocity. As shown by equations (12.15), (12.16), (12.19) and (12.20), it is impossible to analyze the effect of the wind on the motion of missiles with variable velocity in a general form. In the case of a specific missile, the necessary calculations can be carried out, the corresponding functions of time can be obtained and these equations can be used to determine the effect of wind on the missile trajectory. However, if the problem is simplified as much as possible, it is then possible to make interesting qualitative conclusions concerning the effect of wind when the flight velocity is variable.

---

[1] In equations (12.21) and (12.22), the sign for dz_g/dt is determined by the kinematic relationships of the problem; the variation of this sign will be discussed later.

Let us consider three problems which differ in principle. In the first problem we shall take an uncontrolled missile which has static stability. Let us assume that this missile moves in a straight line with acceleration $\bar{j}$ (fig. 12.11a): The acceleration $\bar{j}$ is due to the excess of the thrust over the drag and is directed along the axis of the missile. At some instant of time, when /388

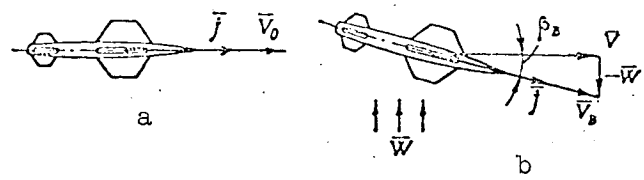

Figure 12.11. Diagram showing effect of lateral wind on stability of unguided missile.

the missile velocity is $\bar{V}_0$, it enters an air stream which is perpendicular to its direction of travel and which has a velocity $\bar{W}$. Since the missile is stable after the transient process produced by the lateral wind is over, the axis of the missile will coincide with the direction of the air velocity vector V_B, given by expression (12.1). If, for simplification, we neglect the period of this transient process, then immediately after the missile has entered the stream of air it will assume a new position, shown in figure 12.11b due to its stability.

Actually, the missile will turn by an angle which is somewhat smaller than β_B and the lateral force will appear, which will cause the vector of the ground velocity to rotate in the direction of the wind until the drift velocity of the missile becomes equal to the wind velocity. At the end of this turn, the longitudinal axis of the missile will occupy a position in space shown in figure 12.11a. The rotation of the ground velocity vector takes place very slowly and may not be completed during the flight time of the missile to the target. While the axis of the missile is deflected from its original direction, the missile is subjected to an acceleration $\bar{j}$, perpendicular to this direction. The missile will deviate from the initial trajectory against the wind direction under the action of this component. If the flight time of the missile to the target is less or is close to the turn time of the ground speed vector, its trajectory, when it moves with substantial acceleration, may be deflected from the initial direction against the wind, in spite of the drift. Missiles which move with a constant velocity or which are decelerated are always deflected from the initial trajectory in the direction of the wind when they are subjected to a lateral wind.

In the second problem, we consider a missile whose control system ideally maintains the fixed position of its longitudinal axis in space. The position of such a missile, after it has entered a lateral air stream, is shown in figure 12.12. A slip angle β_B due to the lateral wind has occurred between the longitudinal axis of the missile and the air velocity vector V_B. Due to this slip angle, a lateral force Z will occur, which will cause the ground speed vector of the missile to deflect from its initial direction into the direction of the wind vector. The indicated direction of drift will take place for any law governing the variation in the flight velocity of the missile. The action of the lateral force and, consequently, the rotation of the ground velocity vector, will cease when the drift velocity becomes equal to the wind velocity. /389

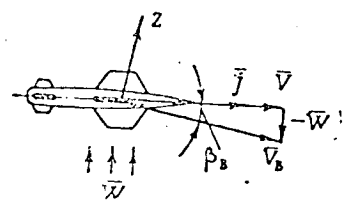

Figure 12.12. Diagram showing action of lateral wind on missile whose longitudinal axis is ideally stabilized in space.

The third problem refers to the case when the missile control system tries to maintain the missile's center of gravity along a definite fixed trajectory. Systems of this type were considered in Chapter 11. In this case, the wind will play the role of a perturbing force and will produce a static error in the position of the center of gravity on this trajectory, if special measures are not taken to eliminate this error.

2. The Motion of Missiles with Constant Flight Velocity. Since the motion of missiles with constant flight velocity is described by linear differential equations with constant coefficients, it is possible to analyze this motion in a disturbed atmosphere in a general form. The equations presented in section 12.3 for the motion of the missile will be combined with equations of the automatic pilot and will make it possible to determine the variation in any of the parameters of missile motion when the missile flies in a distrubed atmosphere. We present several examples of such investigations.

Let us consider the lateral motion of a missile with cruciform wings, which carries an automatic pilot with fixed feedback for controlling the yaw angle of the missile. Combining the first two equations of (12.22) with the equations of the automatic pilot (10.49), we obtain the following system

$$\left.\begin{aligned}
&\frac{d\beta}{dt}+k_{\dot\beta}\beta-\frac{d\psi}{dt}=-\frac{1}{V_e}\frac{dw_z}{dt};\\
&\frac{d^2\psi}{dt^2}+n_{\dot\psi}\frac{d\psi}{dt}+n_{\dot\beta}\frac{d\beta}{dt}+n_\beta\beta=n_{\delta_{cr}}\delta_{cr};\\
&\delta_{cr}=-i_{\dot\psi}\frac{d\psi}{dt}+i_\psi(\psi_з-\psi).
\end{aligned}\right\}\qquad(12.23)$$

On the basis of this system of equations we find the transfer functions for all the angular parameters of lateral motion when there is a lateral wind w_z /390

$$W_{\psi/w_z}(p)=\frac{(n_{\dot\beta}p+n_\beta)p}{V_eA(p)};\qquad(12.24)$$

$$W_{\beta/w_z}(p)=-\frac{[p^2+(n_{\dot\psi}+i_{\dot\psi}n_{\delta_{cr}})p+i_\psi n_{\delta_{cr}}]p}{V_eA(p)};\qquad(12.25)$$

$$W_{\delta_{cr}w_z}(p)=\frac{[p^2+(n_{\dot\beta}+n_{\dot\psi}+i_{\dot\psi}n_{\delta_{cr}})p+n_\beta+i_\psi n_{\delta_{cr}}]p}{V_eA(p)};\qquad(12.26)$$

The denominator A(p) in transfer functions (12.24)--(12.26) has the following form

$$A(p)=p^3+(a_1+i_{\dot\psi}b_1)p^2+(a_2+i_{\dot\psi}b_2+i_\psi b_1)p+i_\psi b_2,$$

where the coefficients a_1, a_2, b_1 and b_2 are determined by equations (10.48)

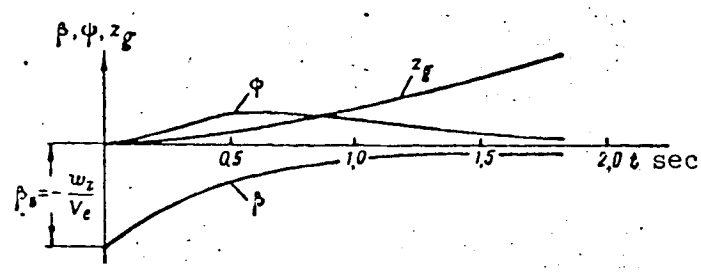

Figure 12.13. Graphs for variation in lateral deviation of slip angles and yaw angles when missile with cruciform wings enters lateral stream of air.

With these transfer functions we can analyze the behavior of a missile with an automatic pilot which controls the yaw angle, when there is a lateral stream

of air with velocity w_z (for example, a jet stream). Figure 12.13 shows the nature of variations in parameters β, ψ and Z_g, when the missile enters a lateral stream with a constant velocity (w_z = const). As follows from the graphs in this figure, slip angle β increases in a discontinuous fashion to a value $-w_z/V_e$ and then drops to zero. The deviation of angles ψ and θ_{σ} from assigned values also tend to zero, [see equations (12.24) and (12.26)]. After the transient process is over, only the angle of rotation of the trajectory $\theta_{\sigma 2}$ differs from zero and is equal to $-w_z/V_e$. As a result, as follows from the third equation of system (12.22), the missile will drift in the direction of /391 the wind with a velocity equal to the wind velocity

$$\frac{dz_g}{dt} = w_z. \tag{12.27}$$

Let us see how a constant wind reacts on a missile whose center of gravity is stabilized along an assigned trajectory by means of a control system.

If we take the simplified equations for a missile with cruciform wings (11.1) and take into account the lateral wind, it will turn out that this wind does not produce perturbations in the motion of the missile's center of gravity. This result is explained by the nature of assumptions made in deriving equation (11.1). Since the motion of the missile with respect to the center of gravity is assumed to be without inertia, when it enters a lateral wind of constant force the missile instantaneously turns by a slip angle produced by the wind and continues to move along the assigned trajectory. Thus, the assumption used to derive equation (11.1) is unsuitable for analyzing the behavior of the missile subjected to a lateral wind, because in this case the result is qualitatively incorrect.

If we utilize the second method for simplifying the problem, in which the turning of the missile is accomplished without inertia, but by means of an automatic pilot which controls the angle of yaw [see equations (11.7) and 11.8)], the result becomes quite different. In this case, the motion of the missile with an automatic pilot is described by a system of equations[1]

$$\left.\begin{aligned}
&\frac{d\beta}{dt} + k_\beta\beta - \frac{d\psi}{dt} = -\frac{1}{V_e}\frac{dw_z}{dt};\\
&\frac{dz_g}{dt} = V_e(\psi - \beta) - w_z;\\
&\psi = \psi_з;\\
&\psi_з = i_z(z_{ai} - z_g).
\end{aligned}\right\} \tag{12.28}$$

[1]As in Chapter 11 in equations (12.28), the derivative z_g is taken with a reversed sign.

The functional diagram shown in figure 12.14 corresponds to these equations. This special feature of this diagram is that the action of the wind on the missile is introduced at two points.

If we eliminate all variables from the system of equations (12.28) except z_g, we obtain the following equation

$$\frac{d^2 z_g}{dt^2} + k_\beta \frac{dz_g}{dt} + i_z k_\beta V_e z_g = i_z k_\beta V_e z_{ai} + k_\beta w_z. \tag{12.29}$$

From this it follows that the established deviation of the missile from the assigned trajectory produced by lateral wind is equal to /392

$$z_B = z_{ai} - z_g = \frac{w_z}{i_z V_e}. \tag{12.30}$$

The nature of the trajectory of the missile's center of gravity when it hits a lateral wind may be quite diverse. It is determined by the roots of the characteristic equation of differential equation (12.29). Since the damping coefficient in equation (12.29) does not depend on the parameters of the control system, efforts to decrease the deviations z_B by increasing i_z lead to a decrease in the relative damping of the system and, consequently, to oscillations of the center of gravity of the missile. This situation is illustrated in figure 12.15, which shows the trajectories of the missile with various values of the transfer number i_z, which have entered the lateral wind at the point $x_g = 0$.

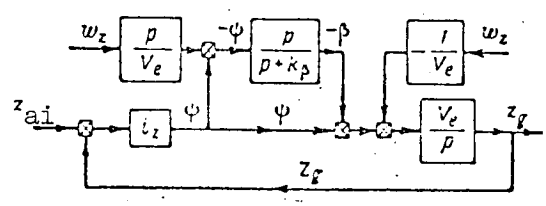

Figure 12.14. Functional diagram of system for controlling center of gravity of missile with cruciform wings corresponding to equations (12.28).

Finally, let us consider, without simplifications, the problem of a missile with cruciform wings with a system for controlling the motion of the center of gravity, when this missile enters a lateral stream of air which has a velocity w_z. For this purpose, we change the sign in front of dz_g/dt and combine the

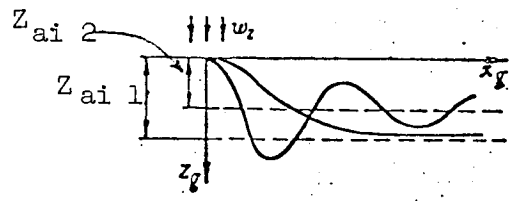

Figure 12.15. Trajectory of center of gravity determined by equations (12.28) and control law (12.31).

system of equations (12.22) with the equation for the automtic pilot, which has a sufficient general control law[1] /393

$$\delta_{cr} = i_{\dot z}\left(\frac{dz_{ai}}{dt} - \frac{dz_g}{dt}\right) + i_z(z_{ai} - z_g) + q_z\int_0^t (z_{ai} - z_g)\,dt - \\ - i_{\dot\psi}\frac{d\psi}{dt} - i_\psi\psi. \tag{12.31}$$

Figure 12.16 shows the functional diagram corresponding to this system. The transfer function of this system for lateral deviation when

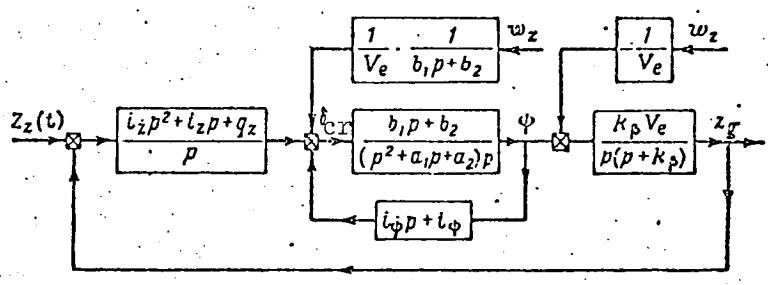

Figure 12.16. Functional diagram of system for controlling center of gravity of missile corresponding to equations (12.22) and(12.31).

subjected to a lateral wind, is obtained on the basis of equations (12.22) and (12.31) and has the form

$$W_{z_g/w_z}(p) = -\frac{k_\beta\left[p^2 + (n_{\dot\psi} + i_{\dot\psi}n_\delta)p + i_\psi n_\delta\right]p}{A(p)}, \tag{12.32}$$

[1] An automatic pilot with such a control law has already been used in a system of equations (11.14).

where A(p) is a complete polynomial of the fifth degree identical with the characteristic polynomial of equation (11.15).

On the basis of the structure of the transfer function (12.32) we can make the following conclusions concerning the motion of the center of gravity of a missile with cruciform wings when it enters a lateral air stream.

After the damping of the transient process, the center of gravity will move along the assigned trajectory, i.e., the system is astatic with respect to the lateral wind of constant velocity. If we select the parameters of the control system in accordance with recommendation given during the analysis of equ tion (11.15), the transient process produced by entry into the lateral air stream will have an optimum nature. Figure 12.17 shows the trajectory of the center of gravity of a missile with an automatic pilot operating with control law (12.31) when it enters a lateral air stream. /394

The behavior of a plane-winged missile when it enters a lateral air stream of constant velocity differs from the behavior of a missile with cruciform wings considered in this section. In principle, this difference is that all the lateral movements are accompanied by a variation in the tilt angle. By using equation (12.21), which describes the lateral motion of a plane-winged missile, taking into account the lateral wind and also the equations of the automatic pilot with various control laws presented in section 11.3, we obtain a general differential equation or transfer functions for the lateral deviation z_g when there is a lateral wind. From these data we can represent the total characteristics of the

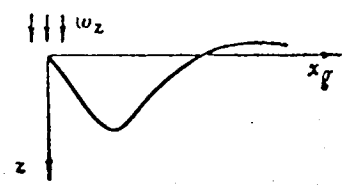

Figure 12.17. Trajectory of missile's center of gravity when control law (12.31) is used.

missile with any control system. As an example, we shall consider the simplified equations of the lateral motion of a missile with plane wings (11.27), but which are written taking into account the lateral wind

$$\left.\begin{aligned} &\frac{d\psi}{dt} - k_\gamma \gamma = 0; \\ &\frac{dz_g}{dt} = V_e \psi - w_z. \end{aligned}\right\}$$

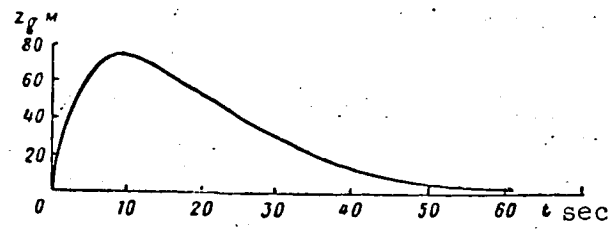

Figure 12.18. Trajectory of center of gravity of missile with transfer function (12.33).

Combining these equations with the equation of the automatic pilot (11.28), we obtain a transfer function for the lateral deviation under the action of lateral wind

$$W_{z_g/w_z}(p) = -\frac{p}{A(p)}, \tag{12.33}$$

where A(p) is the complete polynomial of the second order identical with the characteristic polynomial of differential equation (11.30). The trajectory for the center of gravity of a missile with transfer function (12.33), when it enters a lateral stream of constant velocity w_z, is shown in figure 12.18.

The longitudinal motion of a missile, when it enters a vertical (ascending or decending) stream, does not differ in any way from the lateral movement of a missile with cruciform wings in a lateral stream considered before. On the basis of system (12.17) and the equation of the corresponding automtic pilot, it is easy to find the transfer functions for any of the parameters of longitudinal motion. We note that in investigating the effect of wind there is no necessity for using the equation for longitudinal motion (12.17). In the overwhelming majority of cases, it is possible to use simplified equations for short period motion (10.66) or (10.69), and also the simplified equations presented in section 11.4. It is obvious that all of these equations must contain additional terms, which take into account the effect of wind on missile flight. /395

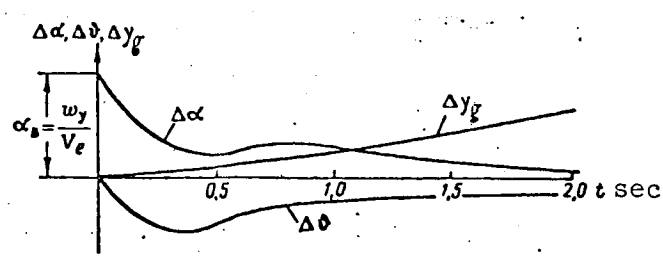

Figure 12.19. Graphs showing variation in altitude and angles of attack and pitch when missile enters vertical stream of air.

As an example of longitudinal motion in a disturbed atmosphere, figure 12.19 shows the graphs for the variation in the angles of pitch ($\Delta\vartheta$) and angles of attack ($\Delta\alpha$) with flight altitude (Δy_g), produced by the entry of the missile into a vertical stream of constant velocity. The missile is equipped with an automatic pilot which controls the pitch angle. These graphs are similar to the graphs in figure 12.13, which illustrate the lateral motion of a missile with cruciform wings and an automatic pilot which controls the yaw angle when a lateral air stream is encountered. All the results obtained for missiles with cruciform wings, and with an automatic pilot which controls the position of the center of gravity with respect to the assigned trajectory, remain valid for the case of longitudinal motion due to the vertical wind. /396

The new feature in longitudinal motion is the possiblility of taking into account the wind component directed along the trajectory of the missile. It is necessary to investigate this question in more detail. Let us examine the behavior of a missile which enters a favorable wind or a head wind with a constant velocity w_x = cost. To simplify this problem, we neglect the transient processes of short period motion, which is equivalent to the assumption that the missile is balanced instantaneously. We assume that the missile has no system for controlling its speed. Finally, we consider the equation of the missile without a control system because it will be shown below that the control system will not affect the results which will be obtained after the analysis is carried out. On the basis of these assumptions we find from system (12.17) the following equations for analyzing the behavior of the missile, after it enters a favorable or head stream of air

$$\left.\begin{aligned} &a_\vartheta\Delta\theta + a_\alpha\Delta\alpha + \frac{d\Delta V}{dt} + a_V\Delta V = a_V w_x;\\ &\frac{d\Delta\theta}{dt} - b_\theta\Delta\theta - b_\alpha\Delta\alpha - b_V\Delta V = -b_V w_x;\\ &c_\alpha\Delta\alpha + c_V\Delta V = c_V w_x. \end{aligned}\right\} \qquad (12.34)$$

The system of equations (12.34) makes it possible to obtain the transfer function for the parameters of longitudinal motion, when a favorable wind or a head wind is encountered.

The transfer function for the variation in the ground speed is

$$W_{\Delta V/w_x}(p) = \frac{b_1 p + a_2}{c_\alpha p^2 + a_1 p + a_2}, \qquad (12.35)$$

where

$$\left.\begin{aligned} a_1 &= a_V c_\alpha - b_\theta c_\alpha - a_\alpha c_V;\\ a_2 &= c_\alpha c_2 - c_4 c_V;\\ b_1 &= a_V c_\alpha - a_\alpha c_V. \end{aligned}\right\} \qquad (12.36)$$

The value of coefficient c_2 and c_4 is determined by equations (8.30).

On the basis of the transfer function (12.35) we may conclude that in the stationary state (p = 0), $W_{\Delta V/\omega_x}(p) = 1$ and, consequently, $\Delta V = \omega_x$. Thus the ground velocity of the missile will increase exactly by the value of the favorable wind velocity or will decrease by the value of the head wind velocity. The air speed of the missile will retain its initial value.

We obtain the following transfer function for the slope of the trajectory /397

$$W_{\Delta\theta/\omega_x}(p) = \frac{p\,(b_\alpha c_V - b_V c_\alpha)}{c_\alpha p^2 + a_1 p + a_2}. \tag{12.37}$$

Finally, the transfer functio for the angle of attack has the form

$$W_{\Delta\alpha/\omega_x}(p) = \frac{p\,(p - b_\theta) c_V}{c_\alpha p^2 + a_1 p + a_2}. \tag{12.38}$$

The presence of the factor p in the numerator of the transfer functions (12.37) and (12.38) shows that in the steady state (p = 0) the variation in the slope of the trajectory and in the angle of attack will be equal to 0. It is

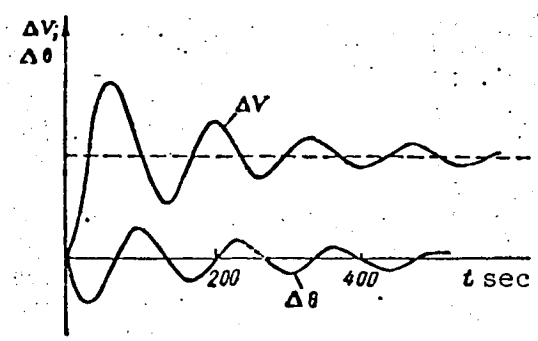

Figure 12.20. Graphs showing variation in ground velocity and slope of trajectory when missile enters favorable stream of constant velocity.

precisely these results that have made it possible to carry out the analysis without taking into account the control system, because the inclusion of this system merely complicates the system of equations (12.34) and gives nothing new for the characteristics of the steady state flight in a favorable or in a head stream. The control system would obviously have a substantial effect on the nature of the transient processes.

Figure 12.20 shows the nature of variation in the ground speed and in the slope of the trajectory produced by the entry of the missile into a favorable

air stream with constant velocity w_x. The weak damping of the oscillations is explained by the fact that this missile has no control system and, in this case, the long period motion usually has the nature of slowly damped oscillations with a large period.

Section 12.5. The Effect of a Random Wind Component on the Motion of the Missile /398

We shall consider the effect of a random wind component only on missiles with constant flight velocity, because when a missile flies with variable speed, it is very difficult to take into account the effect of a random wind component. In the latter case, the simplest approach consists of using the method of fixed or quasifixed coefficients, as a result of which the problem is reduced to the analysis of ordinary differential equations with constant coefficients, i.e., to mathematical methods used to describe the motion of missiles with constant velocity.

Section 12.3 derived equations(12.17) for longitudinal and equations (12.21) and (12.22) for lateral motion of the missile, taking into account the effect of wind. These equations are valid both for a constant as well as a random wind component. However, in analyzing the effect of a random component, special mathematical methods are used; therefore, this question requires additional analysis, which is presented in the present section.

The problem of practical interest consists of determining the effect of the random wind components normal to the plane which contains the wings of the missile. For plane-winged missiles this component will be w_{cy}, while for cruciform wings it will be w_{cy} and w_{cx}. These components produce a variation in the angle of attack or in the slip angle (for a missile with cruciform wings), and thereby change the basic control force--lift force or lateral force. The longitudinal component of the random wind w_{cx}, due to the large inertia of missiles, produces no noticeable effect on their flight. The transverse component w_{cz} also produces no substantial effect on plane-winged missiles, since the lateral force produced by the slip angle due to wind w_{cz} is small for these missiles.

Thus, for both types of missiles it is of interest to establish the effect of a random wind component w_{cy} and for missiles with cruciform wings also to determine component w_{cz}. On the basis of these considerations we examine the longitudinal motion of the missile and of the effect produced by the normal component of the random wind vector w_{cy}.

After the usual simplification, we obtain from equations (12.17) a system of equations which describe the longitudinal motion of the missile when subjected to a random wind component w_{cy}[1]:

$$\left.\begin{aligned}
&a_\theta \Delta\theta + a_\alpha \Delta\alpha + \frac{d\Delta V}{dt} + a_V \Delta V = 0;\\
&\frac{d\Delta\theta}{dt} - b_\theta \Delta\theta - b_\alpha \Delta\alpha - b_V \Delta V = -\frac{1}{V_e}\frac{dw_y}{dt};\\
&\frac{d^2\Delta\vartheta}{dt^2} + c_{\dot\vartheta}\frac{d\Delta\vartheta}{dt} + c_{\dot\alpha}\frac{d\Delta\alpha}{dt} + c_\alpha \Delta\alpha + c_V \Delta V = c_\delta \Delta\delta_в;\\
&\Delta\vartheta = \Delta\theta + \Delta\alpha.
\end{aligned}\right\} \qquad (12.39)$$ /399

In studying the reaction of the missile to the random wind component, which characterizes the succession of random gusts of arbitrary form, the effect of the variation in the ground speed is small. Therefore, without introducing an appreciable error, we may neglect these variations and let $\Delta V = 0$. As a result of this assumption, the first equation of system (12.39) drops out and the system assumes the form

$$\left.\begin{aligned}
&\frac{d\Delta\theta}{dt} - b_\theta \Delta\theta - b_\alpha \Delta\alpha = -\frac{1}{V_e}\frac{dw_y}{dt};\\
&\frac{d^2\Delta\vartheta}{dt^2} + c_{\dot\vartheta}\frac{d\Delta\vartheta}{dt} + c_{\dot\alpha}\frac{d\Delta\alpha}{dt} + c_\alpha \Delta\alpha = c_\delta \Delta\delta_в;\\
&\Delta\vartheta = \Delta\theta + \Delta\alpha.
\end{aligned}\right\} \qquad (12.40)$$

On the basis of equations (12.40) we can obtain transfer functions for any parameters of longitudinal motion without a control system, when the wind action is normal to the flight direction. For example, the transfer function for the pitch angle has the form

$$W_{\Delta\theta/\omega_y}(p) = -\frac{(c_{\dot\alpha}\, p + c_\alpha)\, p}{V_e\,(p^3 + a_1 p^2 + a_2 p + a_3)}, \qquad (12.41)$$

where the values of coefficients a_1, a_2, a_3 are determined by equations (10.71).

The transfer function for the slope of the wind air velocity is equal to

---

1 This system of equations and all subsequent equations are valid both for a random as well as for a constant component of normal wind; therefore, in these equations the subscript "c" of the wind component is dropped.

$$W_{\Delta\vartheta/w_y}(p) = -\frac{[p^2 + (c_\alpha^{\cdot} + c_{\dot\vartheta})p + z_\alpha]p}{V_e(p^3 + a_1p^2 + a_2p + a_3)}. \tag{12.42}$$

To determine the value of the normal load factor which occurs when the missile flies in a turbulent atmosphere, it is necessary to establish the relationship between the load factor and the parameters of longitudinal motion contained in the system of equations (12.17). The acceleration which acts in the vertical plane, normal to the direction of flight, may be represented by the following equation when wind is present /400

$$\frac{d^2y_{cr}}{dt^2} = V_e\frac{d\Delta\theta_2}{dt} = V_e\frac{d\Delta\theta}{dt} + \frac{dw_y}{dt}. \tag{12.43}$$

From this we establish the normal load factor

$$n_y = \frac{1}{g}\frac{d^2y_{cr}}{dt^2} = \frac{V_e}{g}\frac{d\Delta\theta}{dt} + \frac{1}{g}\frac{dw_y}{dt}. \tag{12.44}$$

Combining equation (12.44) with system (12.40) we obtain the transfer function for the normal load factor, when the normal component of the wind is acting (missile without a control system)

$$W_{n_y/w_y}(p) = \frac{1}{g}\frac{[(b_\alpha - b_{\dot\vartheta})p^2 + (a_2 - c_\alpha)p + a_3]p}{p^3 + a_1p^2 + a_2p + a_3}. \tag{12.45}$$

We note that the application of transfer functions (12.41), (12.42) and (12.45) to the study of the missile's reaction to the constant component of the normal wind is limited, due to the assumption that the ground speed is constant ($\Delta V = 0$), which was made when these equations were derived. When we investigate the motion of the missile under the action of constant wind, we should find the corresponding transfer functions on the basis of a complete system of equations for longitudinal motion (12.39). The transfer functions (12.41), (12.42) and (12.45) may be used only to describe the initial stage of motion under the action of a constant wind, during which the short period motion is practically terminated.

Let us find the transfer functions for the parameters of longitudinal motion under the action of normal wind in the case when the missile has an automatic pilot controlling the pitch angle. Combining the equation of the atuomatic pilot

$$\Delta\delta_в = -i_{\dot\vartheta}\frac{d\Delta\vartheta}{dt} + i_\vartheta(\Delta\vartheta_з - \Delta\vartheta). \tag{12.46}$$

with the system of equations (12.40), we obtain a transfer function for the pitch angle in the presence of a normal wind

$$W_{\Delta\vartheta/w_y}(p) = -\frac{(c_\alpha^{\cdot}p + c_\alpha)p}{V_e[p^3 + (a_1 + i_{\dot\vartheta}b_1)p^2 + (a_2 + i_\vartheta b_1 + i_{\dot\vartheta}b_2)p + a_3 + i_\vartheta b_2]}, \tag{12.47}$$

where the coefficients a_1, a_2, a_3, b_1 and b_2 are determined by equations (10.71).

The transfer function for the load factor has the form /401

$$W_{n_y/\omega_y}(p) = \frac{1}{g}\frac{[(b_\alpha - b_\theta)p^2 + (a_2 - c_\alpha + i_\vartheta b_2)p + a_3 + i_\vartheta b_2]p}{p^3 + (a_1 + i_\vartheta b_1)p^2 + (a_2 + i_\vartheta b_1 + i_\vartheta b_2)p + a_3 + i_\vartheta b_2}. \tag{12.48}$$

If we note that the load factor and the linear deviation normal to the flight direction are associated by the relation

$$y_{cr} = g\int_0^t\int_0^t n_y dt dt, \tag{12.49}$$

we can find from equations (12.44), (12.45), and (12.48) the transfer functions for the linear deviations of the missile from the trajectory of unperturbed flight:

missile without control system

$$W_{y_{cr}/\omega_y}(p) = \frac{(b_\alpha - b_\theta)p^2 + (a_2 - c_\alpha)p + a_3}{p(p^3 + a_1p^2 + a_2p + a_3)}; \tag{12.50}$$

missile with an automatic pilot which controls the pitch angle

$$W_{y_{cr}/\omega_y}(p) = \frac{(b_\alpha - b_\theta)p^2 + (a_2 - c_\alpha + i_\vartheta b_2)p + a_3 + i_\vartheta b_2}{p[p^3 + (a_1 + i_\vartheta b_1)p^2 + (a_2 + i_\vartheta b_1 + i_\vartheta b_2)p + a_3 + i_\vartheta b_2]}. \tag{12.51}$$

From the structure of the transfer functions (12.50) and (12.51) we may assert that the flight altitude of a missile without a control system and with an automatic pilot which controls the pitch angle will vary continuously under the action of a normal wind with constant velocity.

Finally, let us find the transfer function for the linear deviation from the assigned trajectory produced by the action of normal wind on a missile, which has a system for controlling the center of gravity. In this problem we use the complete equations for the longitudinal motion of the missile (11.42), in which the variation in the ground speed has been considered. Terms which take into account the normal wind component should be introduced into the right side of the second and fourth equation of this system. In addition, the equation of the automatic pilot (11.46) should be added to equations (11.42). The transfer function for the system which controls the center of gravity during deviation from the trajectory y_H under the action of normal wind is determined from these equations

$$W_{y_{cr}/\omega_y}(p) = \frac{(b_1p^3 + b_2p^2 + b_3p + b_4)p}{p^6 + a_1p^5 + a_2p^4 + a_3p^3 + a_4p^2 + a_5p + a_6}, \tag{12.52}$$

where

$$\left.\begin{aligned}
b_1 &= b_\alpha - b_0;\\
b_2 &= c_1 - b_0 c_\delta + c_\delta (b_\alpha - b_0) + b_\alpha c_\delta (i_\delta + i_\delta) -\\
&\quad - i_\delta b_0 c_\delta,\\
b_3 &= c_1 (c_\delta + i_\delta c_\delta) - b_0 c_\alpha + i_\delta c_\delta (b_\alpha - b_0) +\\
&\quad + c_2 c_\alpha + c_3 i_\delta c_\delta + i_\delta b_\alpha c_\delta,\\
b_4 &= c_1 i_\delta c_\delta + c_2 c_\alpha + c_3 i_\delta c_\delta - c_4 c_V.
\end{aligned}\right\} \qquad (12.53)$$ /402

The values of the coefficients in the denominator of transfer function (12.52) are determined by means of equations (11.48), while the coefficients c_1, c_2, c_3 and c_4 are determined by equations (8.30).

The presence of factor p in the numerator of the transfer function (12.52) indicates that the automatic pilot with integral control [see equation (11.46)] provides for the astaticism of the system with respect to the normal wind. Under the action of the normal wind of constant velocity, the missile with such an automatic pilot will move along the assigned trajectory after the termination of the transient process.

The transfer functions obtained above for different parameters of longitudinal motion make it possible to determine the values of these parameters from the spectral density of the wind component normal to the flight direction. In this case, it is necessary to use the well-known relations (2.39) between the spectral density of the input and output quantity in a linear system

$$S_y(\omega) = |W_y(j\omega)|^2 S_x(\omega). \qquad (12.54)$$

From the spectral density of the output quantity and from equations (12.5) and (12.7) we can obtain the correlation function and the dispersion or the output quantity.

In the practical application of equations (12.11) and (12.12) for the spectral density of the random wind components, it is necessary to transform from one independent variable--the spatial angular frequency Ω, to another--the time angular frequency ω which is used in the transfer functions of a missile. The relationship between these variables is given by equation (12.8). Let us establish the relationship between the functions of spectral density for the random wind expressed in terms of these angular frequencies. On the basis of dispersion equation (12.7) we obtain the identity

$$\sigma_\omega^2 = \int_0^\infty S(\Omega)\, d\Omega = \int_0^\infty S(\omega)\, d\omega. \qquad (12.55)$$

Taking into account relation (12.8) we obtain from identity (12.55)

$$S(\omega) = \frac{1}{V_e} S(\Omega). \tag{12.56}$$

Equation (12.8) and (12.56) make it possible to transform to the variable ω in expressions (12.11) and (12.12) for the spectral density /403

$$S_1(\omega) = \sigma_\omega^2 \frac{L}{\pi V_e} \cdot \frac{1 + 3(\omega L/V_e)^2}{[1 + (\omega L/V_e)^2]^2}, \tag{12.57}$$

$$S_2(\omega) = \sigma_\omega^2 \frac{L}{\pi V_e} \cdot \frac{2}{1 + (\omega L/V_e)^2}. \tag{12.58}$$

Let us substitute the value for the spectral density of the normal wind component (12.57), which we obtained in the basic relationship (12.54)

$$S_y(\omega) = \sigma_\omega^2 \cdot \frac{L}{\pi V_e} \left| W_y(j\omega) \right|^2 \cdot \frac{1 + 3(\omega L/V_e)^2}{[1 + (\omega L/V_e)^2]^2}. \tag{12.59}$$

Finally, by means of equation (12.7) we find the expression for the dispersion of the input quantity, when the normal random wind component acts on the missile

$$\sigma_y^2 = \sigma_\omega^2 \frac{L}{\pi V_e} \int_0^\infty |W_y(j\omega)|^2 \frac{1 + 3(\omega L/V_e)^2}{[1 + (\omega L/V_e)^2]^2} d\omega. \tag{12.60}$$

Depending on the transfer function which is substituted into equation (12.60), we obtain the dispersion of the pitch angle of the missile with an automatic pilot or without one, load factors or the linear deviation of the center of gravity from the assigned trajectory. We present an example to clarify the method used in solving this problem.

Example 12.1. It is required to determine the root-mean-square value of the load factor due to the normal random wind component, experienced by a missile which flies horizontally at an altitude:

$y_g = 5000$ м ($\rho_e = 0.736$ кг·м$^{-3}$) with velocity V_e = 500 m/sec.

The parameters of the missile are as follows: m = 10,000 kg; S = 16 m^2; b_A = 3 m; c_y^α = 5.0; b_α = 1.5; b_θ = 0; c_α = 6.1 1/sec^2; $c_{\dot\alpha}$ = 1.0 1/sec; $c_{\dot\vartheta}$ = 2.1 1/sec; c_δ = 6.2 1/sec^2; μ_n = 290.

The turbulence scale L is assumed to be equal to 300 m. The load factor must be determined for two cases: flight without a control system and flight with an automatic pilot controlling the pitch angle. The transfer numbers of the automatic pilot are $i_{\dot{\vartheta}} = 0$; $i_{\vartheta} = 1.0$.

We now consider the first case. The transfer function for the load factor of the missile without a control system is given by expression (12.45). By using equations (10.71) and substituting the values of the coefficients of this function and noting that $a_3 = 0$, we obtain

$$W_{n_y/w_y}(p) = \frac{1}{9.8} \cdot \frac{1.5p^2 + 3.15p}{p^2 + 4.6p + 9.25}. \tag{12.61}$$

The square of the modulus of the complex transfer function according to (12.61) is equal to /404

$$|W_{n_y/w_y}(j\omega)|^2 = \frac{1}{9.8^2} \frac{2.25\omega^4 + 10\omega^2}{(9.25 - \omega^2)^2 + 21.3\omega^2}. \tag{12.62}$$

The spectral density of the normal random wind component according to equation (12.57) is given by expression

$$S_{w_y}(\omega) = \sigma^2_{w_y} \frac{300}{\pi 500} \frac{1 + 1.08\omega^2}{(1 + 0.36\omega^2)^2}. \tag{12.63}$$

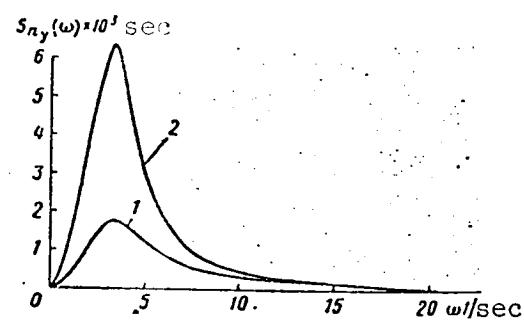

Figure 12.21. Graphs for spectral density of normal load factor produced by random wind.

Substituting the value of the square of the modulus of transfer function (12.62) and spectral density (12.63) into equation (12.60), we find an expression for the dispersion of the normal load factor

$$\sigma^2_{n_y} = \sigma^2_{w_y} \cdot 1.98 \cdot 10^{-3} \int_0^\infty \frac{2.25\omega^4 + 10\omega^2}{(9.25 - \omega^2)^2 + 21.3\omega^2} \frac{1 + 1.08\omega^2}{(1 + 0.36\omega^2)^2} d\omega. \tag{12.64}$$

The functions under the integral sign are represented in figure 12.21 (curve 1) and take into account the constant factor. We compute numerically the value of the definite integral (12.64) and obtain the following expression for the dispersion of the normal load factor

$$\sigma_{n_y}^2 = 0.0104\sigma_{w_y}^2.$$

Finally, by taking the root of both parts of this expression we find the mean square value of the normal load factor

$$\sigma_{n_y} = 0.102\sigma_{w_y}. \tag{12.65}$$

Equation (12.65) shows that the root-mean-square value of the normal load factor of the missile without a control system constitutes 0.102 g's for each unit of the root-mean-square value of the normal wind velocity component.

If we have an automatic pilot controlling the pitch angle, the transfer function of the missile for a normal load factor is given by equation (12.48). After computing the values of the coefficients by means of equations (10.71) we obtain /405

$$W_{n_y/w_y}(p) = \frac{1}{g} \cdot \frac{(1.5p^2 + 3.15p + 9.3)p}{p^3 + 4.6p^2 + 15.45p + 9.3}. \tag{12.66}$$

Leaving out the intermediate steps we write down the expression for the dispersion of the normal load factor of the missile with an automatic pilot which controls the pitch angle

$$\sigma_{n_y}^2 = \sigma_{w_y}^2 \cdot 1.98 \cdot 10^{-3} \int_0^\infty \frac{(9.3 - 1.5\omega^2)^2\omega^2 + 10\omega^4}{(9.3 - 4.6\omega^2)^2\omega^2 + (15.45 - \omega^2)\omega^2} \times \frac{1 + 1.08\omega^2}{(1 + 0.36\omega^2)^2} d\omega. \tag{12.67}$$

The function under the integral sign which takes into account the constant factor is shown in figure 12.21 (curve 2). Having computed the definite integral by means of equation (12.67), we obtain the dispersion of the normal load factor

$$\sigma_{n_y}^2 = 0.0258\sigma_{w_y}^2.$$

Taking the roots of both sides of this expression, we find the root-mean-square value of the normal load factor

$$\sigma_{n_y} = 0.16\sigma_{w_y}. \tag{12.68}$$

Comparing expressions (12.65) and (12.68), we see that in this example the automatic pilot which stabilizes the fixed pitch angle of the missile leads to an increase in the load factor produced by the normal random wind component. In most cases, the effect of the automatic pilot is opposite to this.

The same method may be used to obtain the root-mean-square values for the oscillations of other parameters of longitudinal motion due to the normal component of random wind. The action of the random wind component, which coincides with the flight direction, may also be evaluated by this method. For this purpose it is necessary to obtain transfer functions for some parameters of longitudinal motion and to use expression (12.58) for the spectral density of random wind. However, as we have pointed out, due to the large kinetic energy of the missile, the action of random wind on longitudinal motion of the missile is insignificant.

This method, where the normal wind component acts on the longitudinal motion, is completely applicable to the case of lateral motion. Due to the isotropic nature of atmospheric turbulence, the equation for spectral density (12.57), which describes the random component w_y, must also be used for describing the /406 spectral density of component w_z, which is normal to the flight direction during lateral motion. All of the transfer functions for the parameters of the lateral motion of a missile with cruciform wings, when the wind acts, may be used to analyze the effect of the random component. The action of the random component w_z on the plane-winged missiles, as indicated above, is small.

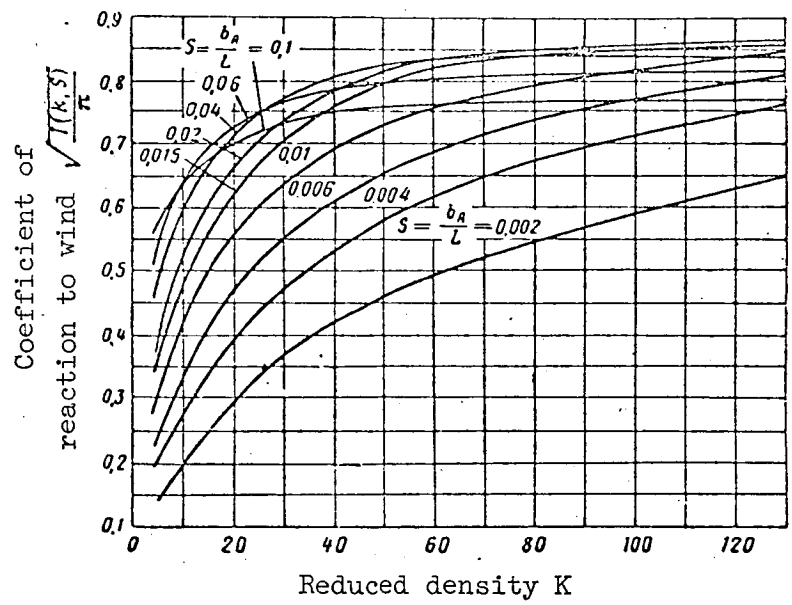

Figure 12.22. Graph of coefficient for reaction of missile to wind which is normal with respect to trajectory of missile.

In concluding this section we present an approximate equation for determining the root-mean-square value of the normal load factor in terms of the

root-mean-square value of the normal wind component and the parameters of the missile[1]

$$\sigma_{n_y} = \sigma_{w_y} \frac{c_y^{\alpha} \rho_e S V_e}{2G} \sqrt{\frac{I(k, \lambda)}{\pi}}, \tag{12.69}$$

(subscript n = density),

where $\sqrt{\frac{I(k, \lambda)}{\pi}}$ is the coefficient of missile reaction to the normal wind;

$k = \mu_n / c_y^{\alpha}$ is the reduced value of the relative density of the missile; and

$\lambda = \frac{b_A}{L}$ is the ratio of the average aerodynamic chord of the missile to the /407

turbulence scale.

The variation in the reaction coefficient to the normal wind as a function of parameters k and λ is given by the graphs in figure 12.22. In deriving equations (12.69) the following assumptions were made.

(1) the oscillations of the missile with respect to the center of gravity produced by the wind were not considered;

(2) the wing of the missile was assumed to be rigid and to have an infinite span;

(3) in considering the nonstationary nature of the flow around the wing due to the random components, the compressibility of the air was not taken into account.

In addition, we should remember that equation (12.69) is valid for missiles with a conventional aerodynamic form, i.e., a frame with a sufficiently developed lift surface. We cannot use expression (12.69) to take into account the presence of a control system aboard the missile. In spite of these limitations, this expression in many cases can be used successfully to make an approximate evaluation of the load factors experienced by a missile subjected to the normal component of random wind. We give an example which shows how to calculate the load factors by means of equation (12.69).

Example 12.2. It is required to use equation (12.69) and to determine the root-mean-square value of the normal load factor experienced by a missile, whose flight conditions and parameters are given in example 12.1. First let us find

---

[1] See footnote[2] on page 366.

the value of the wind reaction coefficient. The parameters which determine this coefficient have the following values $k=\mu_n/c_y^\alpha=59$; $\lambda=b_A/L=0.01$.

From the graphs in figure 12.22 we find the value of the coefficient for the reaction of the missile to the wind $\sqrt{I(k,\lambda)/\kappa}=0.76$.

Substituting this value and also the values of all missile parameters into equation (12.69) we obtain

$$\sigma_{n_y}=\sigma_{w_y}\cdot\frac{5\cdot 0.736\cdot 16\cdot 500}{2\cdot 10000\cdot 9.81}\cdot 0.76=0.114\sigma_{w_y}.$$

Let us compare the value of the normal load factor with its values obtained by a more accurate method and given by expressions (12.65) and (12.68). This comparison shows that the load factor determined by means of the approximate equation (12.69) is greater than the load factor of the missile without a control system, and is less than the load factor of a missile with an automatic pilot stabilizing the pitch angle. Since all three values of the load factor differ little from each other, we may assume that the results of calculations carried out by means of equation (12.69) are quite satisfactory.

CHAPTER 13. DYNAMICS OF HOMING MISSILES /408

Section 13.1 Kinematic Trajectories of Homing Guidance

Homing guidance may be achieved by several methods. These methods determine the nature of the missile trajectories. A guidance method provides for the variation in the angular position of the velocity vector of the missile as it approaches the target. In addition to determining the form of trajectory, the guidance method determines the angle at which the missile hits the target, the distribution of the load factor along the trajectory, the maximum load factor along the trajectory and the time required for the missile to hit the target. There are many methods of homing guidance.[1]

The most common methods of guidance are as follows:

(1) the pursuit method;

(2) pursuit with lead;

(3) guidance to the instantaneous impact point or the method of parallel approach.

A great deal of useful information on the possibilities and properties of various methods may be obtained by analyzing the kinematic trajectories of homing missiles. The kinematics of homing guidance assume that there is an ideal control of the missile's velocity vector.

1. The Pursuit Method. In the ideal realization of this method the velocity vector of missile $\overline{V}$ always coincides with the line joining the missile and the target (the line $C_{\text{Target}} = T$ in figure 13.1). If the velocity of the missile $\overline{V}$ is greater than the velocity of the target $\overline{V}_T$ under the indicated orientation of $\overline{V}$, the target will always be reached by the missile. /409
Using the symbols shown in figure 13.1 we write the kinematic equations

---

[1] L. S. Gutkin, Radio Control of Pilotless Objects, "Sovetskoye Radio," 1959; A. S. Lokk, Guided Missiles, GTTI, 1957; V. M. Tipugin, V. V. Veytsel', Remote Radio Control, "Sovetskoye Radio," 1962.

equation for approach velocity

$$\frac{dL}{dt} = V_T \cos\varphi - V \tag{13.1}$$

equation for angular velocity of line C_T

$$\frac{d\varphi}{dt} = -\frac{1}{L} V_T \sin\varphi. \tag{13.2}$$

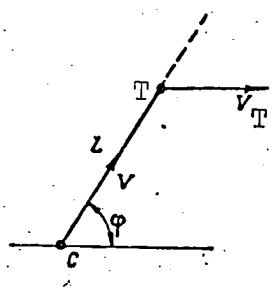

Figure 13.1. Relative position of missile and target in pursuit method.

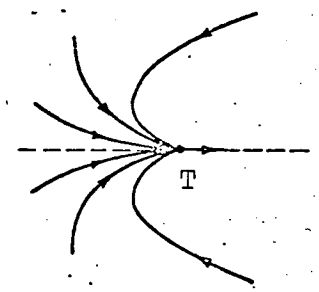

Fig. 13.2. Kinematic trajectory of missile in relative motion during pursuit.

If we divide the first equation by the second equation we obtain

$$\frac{dL}{d\varphi} = L\left(\frac{q}{\sin\varphi} - \operatorname{ctg}\varphi\right), \tag{13.3}$$

where

$$q = \frac{V}{V_T} > 1.$$

The quantity q must always be greater than unity, because only in this case $\frac{dL}{dt} < 0$ and the missile always approaches the target. After the variables are separated equation (13.3) is integrated. As a result we obtain the expression

$$L = L_0 \left(\frac{\sin\varphi}{\sin\varphi_0}\right)^{q-1} \cdot \left(\frac{1+\cos\varphi_0}{1+\cos\varphi}\right)^{q}. \tag{13.4}$$

Range L becomes equal to zero only when $\varphi = 0$. This means that for any initial conditions φ_0 and L_0 the missile hits the target from its tail. Expression (13.4) represents the trajectory of the missile in polar coordinates fixed with respect to the target. The trajectory constructed by means of this equation will be observed at the target. In other words, equation (13.4)

makes it possible to construct the trajectory in relative motion. Figure 13.2 shows a family of relative trajectories which are obtained for various initial conditions L_0 and φ_0. /410

To construct the trajectory of the missile for absolute motion (with respect to the Earth) we must find $L = L(t)$ and $\varphi = \varphi(t)$. This is quite difficult. However, it is quite simple to construct the trajectory graphically. To do this, it is sufficient to plot the position of the target by points T_0, T_1, T_2, ... at equal intervals of time Δt and to connect these points by straight lines to the successive positions of the missile C_0, C_1, C_2, ..., which are situated on these straight lines (fig. 13.3). The uniform curve which passes through C_0, C_1, C_2, ..., is the trajectory of the missile or the pursuit path. In the same simple manner the pursuit curve may be constructed for relative motion, i.e., in a coordinate system fixed with respect to the target. This construction is shown in figure 13.4. From point C_0 in the direction L_0 a line segment or vector $\overline{C_0 b_1}$ of length $V\Delta t$ is drawn. From point b_1 we draw the vector $\overline{b_1 C_1} = -V_T\,\Delta t$, whose length is equal to $V_T\,\Delta t$. The point C_1, which is the end of the vector $\overline{b_1 C_1}$, belongs to the pursuit curve in relative motion. In the same way the remaining points C_2, C_3, ..., which belong to the pursuit curve, are obtained. It is clear that graphical construction for a target undergoing maneuvers, when $V_T \neq$ const and when the velocity of the missile is also not constant, is obtained in a similar manner. The graphic construction of /411

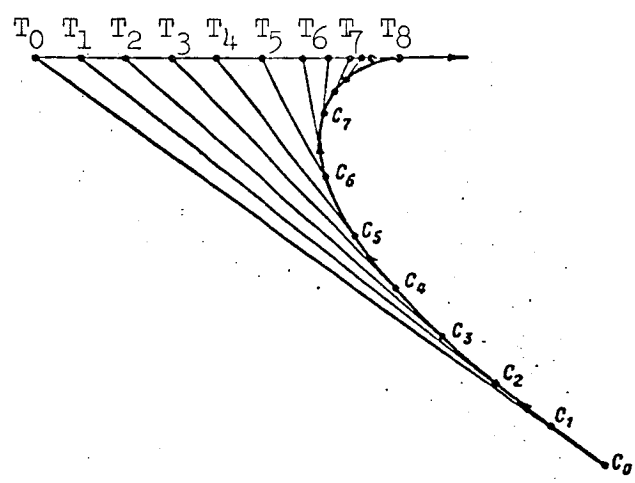

Figure 13.3. Example showing construction of kinematic trajectory of missile in absolute motion for pursuit method.

the trajectory also determines the time from the beginning of motion along the pursuit curve to the time of impact at the target, as well as the boundary at which the impact occurs.

The load factor $n = \frac{1}{g} V\dot{\varphi}$, which is proportional to the angular velocity $\dot{\varphi} = d\varphi/dt$ and which must be produced by the control system of the missile as the latter moves along the pursuit curve, is very significant. The expression for the angular velocities is obtained from (13.2) and (13.4)

$$\dot{\varphi} = -\frac{V_T}{L_0}\frac{(\sin\varphi_0)^{q-1}}{(\sin\varphi)^{q-2}}\cdot\left(\frac{1+\cos\varphi}{1+\cos\varphi_0}\right)^q. \tag{13.5}$$

Let us find the angular velocity at the instant when the missile hits the target.

When $1 < q < 2$

$$\lim_{\varphi\to 0}\dot{\varphi} = -\frac{V_T}{L_0}\frac{(\sin\varphi_0)^{q-1}}{(1+\cos\varphi_0)^q}\lim_{\varphi\to 0}(1+\cos\varphi)^q(\sin\varphi)^{2-q} = 0;$$

for $q = 2$

$$\lim_{\varphi\to 0}\dot{\varphi} = -\frac{V_T}{L_0}\frac{\sin\varphi_0}{(1+\cos\varphi_0)^2}\lim_{\varphi\to 0}(1+\cos\varphi)^2 =$$

$$= -\frac{4V_T}{L_0}\frac{\sin\varphi_0}{(1+\cos\varphi_0)^2};$$

for $q > 2$ /412

$$\lim_{\varphi\to 0}\dot{\varphi} = -\frac{V_T(\sin\varphi_0)^{q-1}}{L_0(1+\cos\varphi_0)^q}\lim_{\varphi\to 0}\frac{(1+\cos\varphi)^q}{(\sin\varphi)^{q-2}} = -\infty.$$

The load factor or the angular velocity has a maximum along the trajectory when $1 < q < 2$. To determine the maximum we differentiate the expression for $\dot{\varphi}$ with respect to φ, equation (13.5). From equation

$$\frac{d\dot{\varphi}}{d\varphi} = 0$$

we find that the maximum angular velocity occurs when $\varphi = \arccos\frac{q}{2}$. The maximum value of the angular velocity is equal to

$$|\dot{\varphi}|_{max} = \frac{V_T}{L_0}\frac{(\sin\varphi_0)^{q-1}}{(1+\cos\varphi_0)^q}\cdot\left(1+\frac{q}{2}\right)^q\cdot\left(1-\frac{q^2}{4}\right)^{1-\frac{q}{2}}. \tag{13.6}$$

When $q \geq 2$, the angular velocity does not have a maximum, for $q = 2$ the angular velocity increases from 0 to $\frac{4V_T}{L_0}\frac{\sin\varphi_0}{(1+\cos\varphi_0)^2}$ at the target; for $q > 2$, $\dot{\varphi} \to \infty$ in the region of the target.

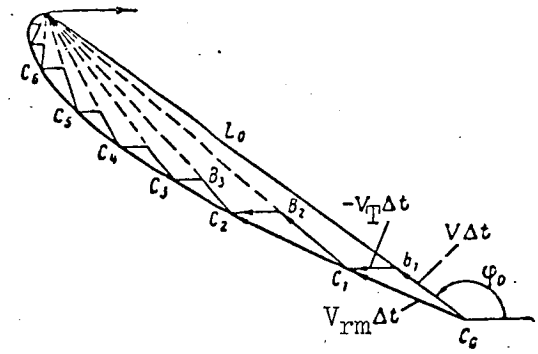

Figure 13.4. Example showing construction of kinematic trajectory for relative motion (rm).

From the equations for the angular velocity we can see that the load factor along the trajectory, including its maximum value, is inversely proportional to the initial range L_0. Therefore, it is desirable to initiate homing as far away from the target as possible.

For $1 < q < 2$, we may use equations (13.6) to construct the region of possible attack or to assume a maximum permissible load factor n_{max}, which can be experienced by the missile. In polar coordinates fixed with respect to the target, the boundary of the region of possible attacks is constructed from equation

$$L = \frac{V_T V}{n_{max}\, g}\left(1 + \frac{q}{2}\right)^q \cdot \left(1 - \frac{q^2}{4}\right)^{1-\frac{q}{2}} \cdot \frac{(\sin\varphi_0)^{q-1}}{(1+\cos\varphi_0)^q}. \qquad (13.7)$$

When the missile is fired towards the target from the region of possible attacks, the load factor will not be greater than the assigned value n_{max}. When we construct the boundary for the region of possible attacks, φ_0 assumes values from π to 0. It follows from (13.7) that when $\varphi_0 = \arccos \frac{q}{2}$, the boundary of the region is transformed into the pursuit curve with an initial radius $L_{01} = \frac{V_T V}{n_{max}\, g}\left(1 - \frac{q^2}{4}\right)^{\frac{1}{2}}$ and an initial angle $\arccos \frac{q}{2}$. This region of the boundary may be constructed graphically using the method discussed before. Figure 13.5 shows the regions of possible attacks for $q = 1.2$ and 1.8 and $\frac{V_T V}{n_{max}\, g} = 25$. In the same way, by using the maximum available load factor and /413
the permissible miss, we can construct the region of possible attacks when $q > 2$, although in this case the load factor of the missile approaches infinity when the target is hit.

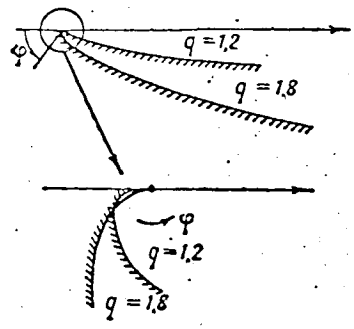

Figure 13.5. Regions of possible attacks.

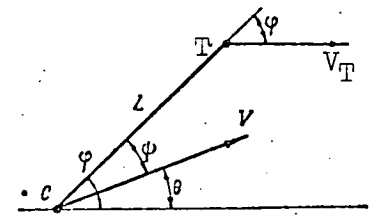

Figure 13.6. Relative position of missile and target during pursuit with a lead angle.

2. Pursuit with Lead. During pursuit with lead, a definite angle ψ (fig. 13.6) is maintained between the line CT and the missiles velocity vector. In the general case, the lead angle may be a function of many variables: $\psi = \psi(L, \dot{L}, \varphi, \dot{\varphi}, t)$. The simplest case occurs when ψ = const. For pursuit with lead the kinematic equations will have the form

$$\left.\begin{aligned} \frac{dL}{dt} &= V_T \cos\varphi - V\cos\psi, \\ L\frac{d\varphi}{dt} &= -V_T \sin\varphi + V\sin\psi \end{aligned}\right\} \tag{13.8}$$

or

$$\frac{dL}{L} = \frac{\cos\varphi - q\cos\psi}{-\sin\varphi + q\sin\psi}\, d\varphi. \tag{13.9}$$

Integrating expression (13.9) for ψ = const, we obtain the trajectory equation for relative motion[1] with a constant lead angle /414

$$L = L_0\left(\frac{\sin\varphi - q\sin\psi}{\sin\varphi_0 - q\sin\psi}\right)^{\frac{q\cos\psi}{\sqrt{1-q^2\sin^2\psi}}-1} \times$$

$$\times\left(\frac{1 - q\sin\psi\sin\varphi_0 + \cos\varphi_0\sqrt{1-q^2\sin^2\psi}}{1 - q\sin\psi\sin\varphi + \cos\varphi\sqrt{1-q^2\sin^2\psi}}\right)^{\frac{q\cos\psi}{\sqrt{1-q^2\sin^2\psi}}}. \tag{13.10}$$

[1] A. S. Lokk, Guided Missiles, Gostekhizdat, 1957.

In expression (13.10) $q^2 \sin^2 \psi < 1$. For $q^2 \sin^2 \psi = 1$

$$L = L_0 \left(\frac{1 - \sin \varphi_0}{1 - \sin \varphi} \right) e^{q \cos \psi \left\{ \operatorname{tg}\left(\frac{\varphi_0}{2} + \frac{\pi}{4}\right) - \operatorname{tg}\left(\frac{\varphi}{2} + \frac{\pi}{4}\right) \right\}}. \tag{13.11}$$

Where $q^2 \sin^2 \psi \leq 1$ the missile collides with the target. Where $q^2 \sin^2 \psi > 1$ the trajectory becomes a spiral with an infinite number of loops near the target. The condition $q^2 \sin^2 \psi \leq 1$ is satisfied both for $\psi < \frac{\pi}{2}$ and for $\psi > \frac{\pi}{\psi}$. However, when $\psi > \frac{\pi}{2}$, it follows from the first equation of (13.8) that the approach velocity $\dot{L}$ will be positive, and homing guidance becomes impossible. Thus we are left with the case $\psi \leq \frac{\pi}{2}$.

In expression (13.10) the exponent $\frac{q \cos \psi}{\sqrt{1 - q^2 \sin^2 \psi}} - 1 > 0$ when $\psi < \frac{\pi}{2}$, while the product $q^2 \sin^2 \psi < 1$, therefore L becomes equal to 0 when $\sin \varphi = q \sin \psi$. This means that the target is hit at some angle $\varphi_k = \arcsin (q \sin \psi)$. In this case the missile can approach the target from two possible directions. The first direction is given by angle $\varphi_k < \frac{\pi}{2}$, while the second direction is given by angle $\pi - \varphi_k > \frac{\pi}{2}$ (fig. 13.7). The condition $\sin \varphi_k = q \sin \psi$ is satisfied for both directions. To determine the actual direction from which the missile will approach the target, it is necessary to investigate both of the directions for stability. In relative motion the plane L, φ represents a phase plane, where the point T (target) is a singularity of (13.8). In this case the equations have two singular points $T_1(0, \varphi_k)$ and $T_2(0, \pi - \varphi_k)$ which are the foci /415 of the phase plane φ, L.

It is necessary to determine which of the foci is stable and which is unstable. The investigation of stability is carried out by the usual method. We shall assume that the motion of the missile along directions 1, 2, 3 and 4 (fig. 13.7) will be unperturbed, and we shall find equations in terms of small deviations with respect to the assumed unperturbed directions. For unperturbed motion $\varphi_0 = \varphi_k$.

The initial equations (13.8) for unperturbed motion will be

$$\dot{L} = V_T (\cos \varphi_k - q \cos \psi) = -V_{сб}; \tag{13.12}$$

(subscripts сб = approach),

$$L\dot{\varphi} = V_{\text{T}}(-\sin\varphi_k + q\sin\psi) = 0, \tag{13.13}$$

where $V_{\text{сб}} = -V_{\text{T}}(\cos\varphi_k - q\cos\psi) = \text{const}$.

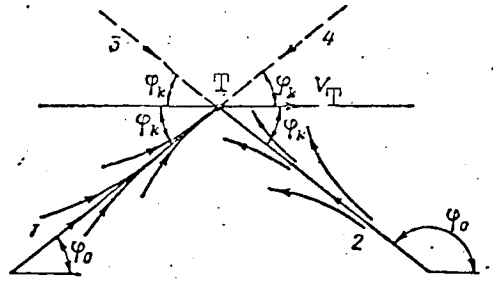

Figure 13.7. Stable and unstable direction for approach of missile to target.

If we assume that $\varphi_0 = \varphi_k$, the condition $\sin\varphi_k = q\sin\psi$ is satisfied, and $\dot{\varphi} = 0$ and $\varphi = \varphi_k$ during the entire approach time. In this case $\dot{L} = -V_{\text{сб}} = \text{const}$ and consequently $L = L_0 - V_{\text{сб}}t$.

We introduce the parameters of the unperturbed state $\varphi_e = \varphi_k$, $L_e = L_0 - V_{\text{сб}}t$, $\dot{L}_e = -V_{\text{сб}}$. Next we let $L = L_e + \Delta L$ and $\varphi = \varphi_e + \Delta\varphi$ in equations (13.8)

$$\dot{L}_e + \Delta\dot{L} = V_{\text{T}}[\cos(\varphi_e + \Delta\varphi) - q\cos\psi]; \tag{13.14}$$

$$(L_e + \Delta L)\Delta\dot{\varphi} = V_{\text{T}}[-\sin(\varphi_e + \Delta\varphi) + q\sin\psi]. \tag{13.15}$$

Assuming that the deviations $\Delta\varphi$, $\Delta\dot{\varphi}$ and ΔL are small and taking into account the equations for the unperturbed state, we obtain from (13.14) and (13.15) the equations for small deviations /416

$$\Delta\dot{L} = -(V_{\text{T}}\sin\varphi_e)\Delta\varphi; \tag{13.16}$$

$$L_e\Delta\dot{\varphi} = -V_{\text{T}}\cos\varphi_e\Delta\varphi. \tag{13.17}$$

The question of stability of the unperturbed state is solved only on the basis of equation (13.17), because equation (13.16) makes it possible only to

determine the correction $\Delta L(t)$, after $\Delta\varphi(t)$ is determined from equation (13.17). To eliminate time in the investigation of stability, we consider (13.17) together with the expression

$$\dot{L}_e = - V_{c\delta}. \tag{13.18}$$

Dividing (13.18) by (13.17), we obtain

$$\frac{d\Delta\varphi}{\Delta\varphi} = k_V \frac{dL_e}{L_e}, \tag{13.19}$$

where

$$k_V = \frac{V_T \cos\varphi_e}{V_{c\delta}}. \tag{13.20}$$

The solution of equation (13.19) leads to the expression

$$\Delta\varphi = \Delta\varphi_0 \left(\frac{L_e}{L_{e0}}\right)^{k_V} = \Delta\varphi_0 \left(\frac{L_0 - V_{c\delta} t}{L_0}\right)^{k_V}, \tag{13.21}$$

where $\Delta\varphi_0$ and $L_{e0} = L_0$ are the values of the variables at the initial instant of time.

As we can see from expression (13.21), when $k_V > 0$ the deviation from the unperturbed state $\Delta\varphi$ decreases continuously and when $t = L_0/V_{c\delta}$ it becomes equal to 0. Consequently, when $k_V < 0$, the unperturbed state is stable. On the other hand, when $k_V > 0$, the unperturbed state is unstable. However, $k_V > 0$ for $\varphi_e = \varphi_k < \frac{\pi}{2}$ and $k_V < 0$ for $\varphi_e = \pi - \varphi_k > \frac{\pi}{2}$, consequently the stable directions are 1 and 2 in the tail sector of the target. All of the trajectories of the missile for any initial conditions will be drawn together to the directions 1 and 2 in the tail sector of the target (fig. 13.8).

When $q \sin\psi = \sin\varphi_k = 1$ and when the trajectory is determined by the expression (13.11), the boundary directions $\varphi_k = \pm\frac{\pi}{2}$ are neutrally stable, because in these cases $k_V = 0$ and $\Delta\varphi$ is always equal to its initial value $\Delta\varphi_0$.

If we wish to determine the load factors during homing guidance with a constant lead angle, we must determine the angular velocity $\dot{\varphi}$ from the second equation (13.8) and from the expression for L (13.10). Since the lead angle is constant, $\dot{\varphi}$ is also the angular rate of change of the velocity vector. For this reason the load factor is $n = V\dot{\varphi}/g$, as on the pursuit curve. /417

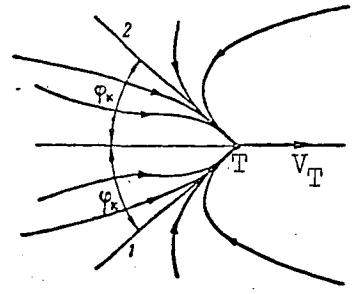

Figure 13.8. Kinematic trajectory of missile in relative motion for pursuit with lead angle.

Thus, from (13.8) and (13.10), we find

$$\dot{\varphi} = -\frac{V_T}{L_0}\frac{(\sin\varphi_0 - q\sin\psi)^{\nu-1}}{(\sin\varphi - q\sin\psi)^{\nu-2}}\cdot\frac{(1 - q\sin\psi\sin\varphi + \cos\varphi\sqrt{1-q^2\sin^2\psi})^{\nu}}{1 - q\sin\psi\sin\varphi_0 + \cos\varphi_0\sqrt{1-q^2\sin^2\psi}}, \tag{13.22}$$

where $\nu = \frac{q\cos\psi}{\sqrt{1-q^2\sin^2\psi}}$.

For target impact, when $\sin\varphi = q\sin\psi$, the angular velocity is equal to 0 when $\nu < 2$ and is equal to infinity when $\nu > 2$. Thus, the load factor has a maximum along the trajectory when $1 < \nu < 2$. The angle φ, for which the load factor is a maximum, is the root of the transcendental equation

$$\cos^2\varphi - \frac{(\nu-2)(1-q\sin\psi)}{2\sqrt{1-q^2\sin^2\psi}}\cos\varphi + \frac{q\sin\psi_0\nu}{2}\sin\varphi - \frac{\nu}{2} = 0. \tag{13.23}$$

When the lead angle is constant, the load factors required to realize the trajectory, as a rule, decrease. During attacks in the front hemisphere, the homing guidance time is decreased substantially and the target is hit along an earlier boundary. In addition, the constant lead angle makes it possible to attack the target along the assigned course $\sin\varphi_k$, which is quite important in many cases.

The lead angle $\psi = \psi(L, \dot{L}, \varphi, \dot{\varphi}, t)$, which changes in the process of homing guidance, opens up wide possibilities for constructing trajectories which are optimum in various respects. For example, we may consider a trajectory which provides for minimum homing guidance time and also a trajectory where the load factor has a more uniform distribution. In this case the load factor required for homing will be a minimum for the given initial conditions, φ_0 and L_0. The formulation of the problem concerning optimum trajectories achieved with a variable lead angle is quite complicated and is not considered in the present book. To illustrate the effect of variable /418

lead angle, let us consider the case of a small lead angle when $\sin\psi \approx \psi$ and $\cos\psi = 1$ ($\psi \leq 20\text{-}25^{\circ}$) and when this lead angle is proportional to the angular velocity of the line MT, i.e., let us assume that

$$\psi = -k\dot{\varphi}. \tag{13.24}$$

The minus sign (13.24) makes it possible to obtain a lead angle ψ, because it follows from the second equation (13.8) that $\dot{\varphi} < 0$ when $\psi \to 0$. If we assume that the lead angle is small, the kinematic equations (13.1) and (13.2) take the form

$$\dot{L} = V_{\mathrm{T}}(\cos\varphi - q); \tag{13.25}$$

$$(L + kV)\dot{\varphi} = -V_{\mathrm{T}}\sin\varphi. \tag{13.26}$$

If we introduce the new variable $(L + kV) = x$, and if $\dot{L} = \dot{x}$, we obtain the kinematic equations of the pursuit curve in terms of the x, φ coordinates.

$$\dot{x} = V_{\mathrm{T}}(\cos\varphi - q); \tag{13.27}$$

$$x\dot{\varphi} = -V_{\mathrm{T}}\sin\varphi. \tag{13.28}$$

Equations (13.27) and (13.28) have a solution of the form (13.4)

$$x = x_0\left(\frac{\sin\varphi}{\sin\varphi_0}\right)^{q-1}\left(\frac{1+\cos\varphi_0}{1+\cos\varphi}\right)^{q}. \tag{13.29}$$

For the variable L, expression (13.29) takes the form

$$L = -kV + (L_0 + kV)\left(\frac{\sin\varphi}{\sin\varphi_0}\right)^{q-1}\cdot\left(\frac{1+\cos\varphi_0}{1+\cos\varphi}\right)^{q}. \tag{13.30}$$

By comparing equations (13.4) and (13.30) we see that the introduction of a small lead angle proportional to $\dot{\varphi}$, is equivalent to increasing the homing guidance range by a constant quantity kV.

When $\psi = k\dot{\varphi}$, the method of constructing the trajectory follows from equations (13.29) and (13.30). We construct the pursuit curve $x = f(\varphi)$ - the curves P_0, P_1, P_2, . . . in figures 13.9 and 13.10. The points C_0, C_1, C_2, . . . , which are at a distance kV from the points P_0, P_1, P_2, . . . are marked on the rays P_0T_0, T_1, P_2T_2. The points C_0, C_1, C_2, . . . belong to the unknown /419
trajectory of homing guidance with a lead angle. We note that the points T_1,

C_1, P_1 are always on one straight line, and consequently the points P_0, P_1, P_2, . . . may be regarded as the successive positions of the missile control point which moves along the pursuit curve. The missile is controlled in such a way that it always remains on the sighting line T_1P_1. This is known as the combined control method and will be considered in detail in the next chapter.

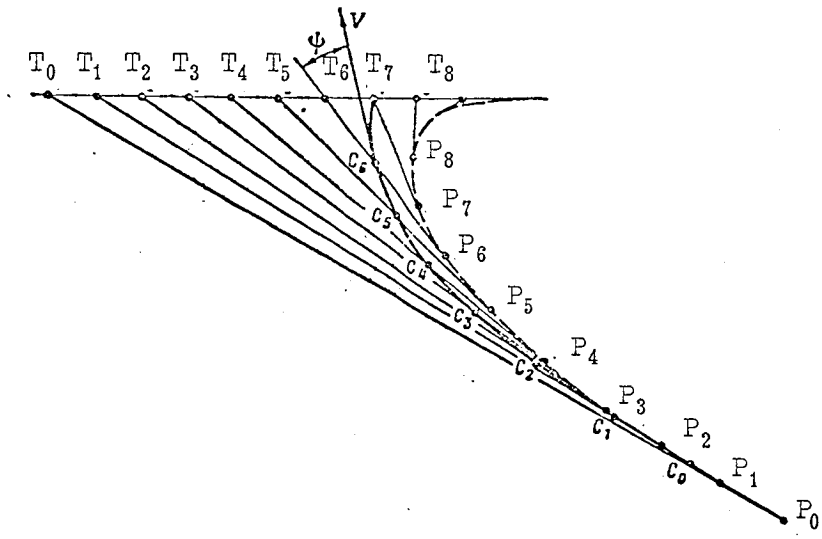

Figure 13.9 Kinematic trajectory of missile for absolute motion when pursuit is carried out with lead angle.

In the present case there is no control point and the trajectory P_0, P_1, P_2,... is a fictitious trajectory, which is required to construct the true trajectory of the missile in this method of homing guidance. However, it follows from our discussion that it is technically possible to realize this method not only by rotating the velocity vector in the lead direction by $k\dot{\varphi}$, but also by a fictitious lengthening of the distance to the target by a constant value. This realization is possible, for example, in guiding a missile to a target using radar with circular scan (Chapter 14).

We see from the graphs shown in figures 13.9 and 13.10, as well as from the analysis of equation (13.30), that the homing guidance time and the load factors along the trajectory are substantially reduced when pursuit takes place with a lead angle $\psi = k\dot{\varphi}$. The angle at which the missile encounters the target is equal to $\varphi_k + k\dot{\varphi}_k$, where φ_k is the angle given by equation (13.30) when L = 0, and $\dot{\varphi}_k$ is the angular velocity of the line CT determined from expressions (13.26) and (13.30) when L = 0. To compute the load factor /420

we must determine the angular rate of change of the velocity vector, which in this case is equal to (fig. 13.6)

$$\dot{\theta} = \dot{\varphi} - \dot{\psi} = \dot{\varphi} + k\ddot{\varphi}.$$

In this case

$$\dot{\varphi} = -\frac{V_T(\sin\varphi_0)^{q-1}}{x_0(1+\cos\varphi_0)^q} \cdot \frac{(1+\cos\varphi)^q}{(\sin\varphi)^{q-2}}. \tag{13.31}$$

To compute $\ddot{\varphi}$ we differentiate (13.28) and use equation (13.27) to find

$$\ddot{\varphi} = -\frac{V_T(2\cos\varphi - q)}{x}\dot{\varphi},$$

from which it follows that

$$\dot{\theta} = \left[1 - \frac{kV_T(2\cos\varphi - q)}{x}\right]\dot{\varphi}. \tag{13.32}$$

Equation (13.32) shows that by using this method the load factor experienced by the missile (proportional to $\dot{\theta}$), is smaller than in the case when the missile moves along the pursuit curve without a lead angle. In the latter case, the load factor is proportional to $\dot{\varphi}$. /421

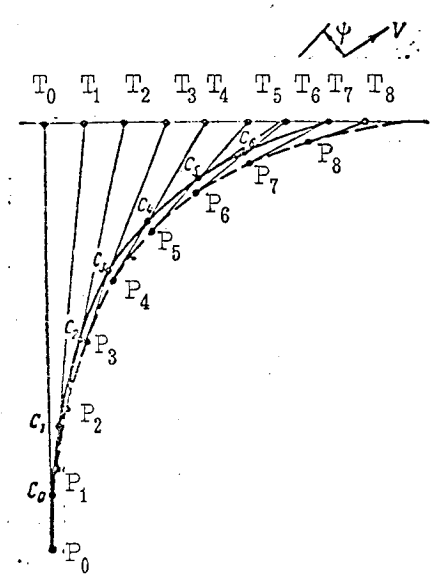

Figure 13.10. Kinematic trajectory of missile in absolute motion during pursuit with load angle.

3. The Method of Parallel Approach. When we analyzed the guidance of a missile to the target which moves with a velocity $\overline{V}_T$ = const, using the method of pursuit with a constant lead angle ψ, we established that for the initial angle $\varphi_0=\varphi_k$, where $\sin\varphi_k=q\sin\psi$, the approach to the target takes place along a straight line. A straight trajectory is rather attractive, because in this case the process of homing guidance takes place without lateral accelerations. Unfortunately, when ψ = const, trajectories of this type are possible only for two initial angles $\varphi_0 = \pm\varphi_k$, and the probability of realizing this motion is therefore, equal to 0. In order to have the trajectory a straight line for any initial conditions, the lead angle must be a function of the initial angle φ_0 and a function of the ratio of the missile velocity to the target velocity.

In other words, the lead angle must satisfy the condition.

$$\sin\psi=\frac{1}{q}\sin\varphi_0=\frac{V_T}{V}\sin\varphi_0 \tag{13.33}$$

or

$$\frac{\sin\psi}{V_T}=\frac{\sin\varphi_0}{V}=\frac{\sin\psi_T}{V}, \tag{13.34}$$

where $\psi_T = \pi - \varphi_0$.

Condition (13.33) or (13.34) means that $\dot{\varphi} = 0$, i.e., the line CT will be displaced parallel to itself. Since the quantities ψ, φ_0, V_T and V are constant, the approach velocity is also constant

$$\dot{L}=-V_{c\delta}=V_T(\cos\varphi_0-q\cos\psi).$$

The homing guidance time is equal to

$$t_c=\frac{L_0}{V_{c\delta}}.$$

Condition (13.34) shows that the vectors $\overline{L}_0$, $\overline{L}_T$ and $\overline{L}_c$ form a triangle (fig. 13.11a). The vector's $\overline{V}_{c\delta}$, $\overline{V}$ and $\overline{V}_T$ (figs. 13.11b and c) also form triangles, because $L_T = t_c V_T$ and $L_c = t_c V$. The method of parallel approach both from the front and from the rear hemisphere is realized when $q = V/V_T > 1$, and also when $q = V/V_T < 1$ (figs.13.11b and c). The vectors $\overline{L}_T$ and $\overline{L}_c$ meet at the apex of the triangle T, where the missile hits the target. /422

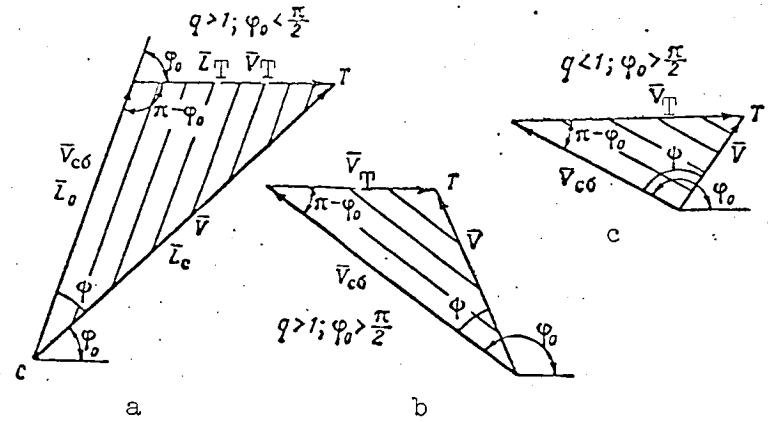

Figure 13.11. Construction of kinematic trajectories for method of parallel approach.

The point T is the impact point of the missile at the target. This point is unique for given initial conditions if $\overline{V}_T$ = const and $\overline{V}_c$ = const. If the latter conditions are not satisfied, while the conditions for parallel approach (13.34) are satisfied for instantaneous values V, V_T φ and ψ, we have a multiplicity of impact points T forming the trajectory of the impact points. For each instant of time there is a definite impact point. This instantaneous impact point is the apex of the triangle formed by the instantaneous values of vectors $\overline{L}$, $\overline{L}_T$ and $\overline{L}$.

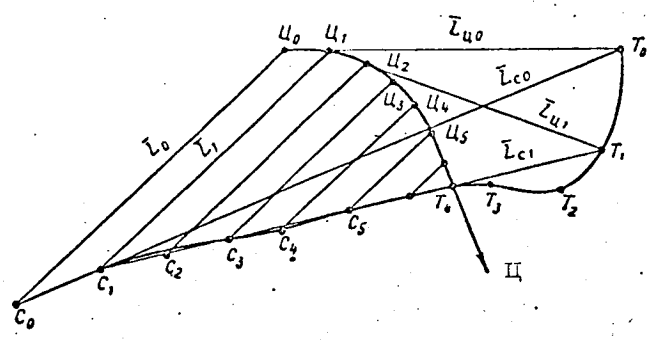

Figure 13.12. Kinematic trajectory of missile guided by method of parallel approach when target undergoes maneuvers ; ц = T.

Figure 13.12 shows the trajectory of a target which has started its maneuvers at point T_1. At point T_5 the target again begins to move in a straight line. The instantaneous positions of the target and of the missile at the

same instant of time are connected by parallel straight lines C_0T_0, C_1T_1, C_2T_2. Figure 13.12 shows two "instantaneous" triangles $C_0T_0P_0$ and $C_1T_1P_1$ and the trajectory formed by the instantaneous impact points P_0, P_1, P_2, P_3 and P_4.

If the velocity vectors of the target and of the missile are constant, the load factor of the missile is equal to 0 after parallel approach is realized[1]. If these conditions are violated the missile trajectory will not be a straight line, and the missile will be subjected to lateral load factors. /423

Let us determine the load factor of the missile when the target moves along a curvilinear path when V_T = const and V = const. Figure 13.13 shows the triangle of parallel approach and the angles θ and θ_T determining the flight direction of the missile and of the target with respect to the reference directions 0 - 0.

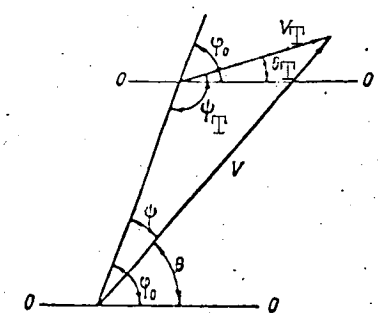

Figure 13.13. Triangle of parallel approach.

For this case the condition of parallel approach will have the form

$$V_T \sin(\varphi_0 - \theta_T) = V \sin(\varphi_0 - \theta). \tag{13.35}$$

Because the $\dot{\varphi} = 0$, $\varphi = \varphi_0$ = const. The angular position of the target vector $\theta_T = \theta_T(t)$ is a given function of time. From equation (13.35) we determine the value θ under which parallel approach takes place

$$\theta = \varphi_0 - \arcsin \frac{\sin(\varphi_0 - \theta_T)}{q}. \tag{13.36}$$

[1]The load factor is necessary to place the missile in the state of parallel approach--to establish the required angle ψ. However, this problem is not related to the kinematics.

Differentiating (13.36) with respect to time and introducing the load factors $n_c = \frac{V\dot{\theta}}{g}$ and $n_T = \frac{V_T\dot{\theta}_T}{g}$ instead of the angular velocities $\dot{\theta}$ and $\dot{\theta}_T$, we obtain

$$n_c = \frac{\sqrt{1 - \sin^2(\varphi_0 - \theta_T)}}{\sqrt{1 - \frac{\sin^2(\varphi_0 - \theta_T)}{q^2}}} n_T, \qquad (13.37)$$ /424

where $q = \frac{V}{V_T}$.

When $q > 1$, the load factor of the missile is always less than the load factor of the target. When $q = 1$, the load factor of the missile is equal to the load factor of the target. Finally, when $q < 1$, the load factor of the missile is greater than the load factor of the target. In addition, when $q < 1$, the maneuvers of the target may produce a condition whereby $\sin(\varphi_0 - \theta_T)/q$ becomes greater than unity. In this case expression (13.37) loses its meaning,

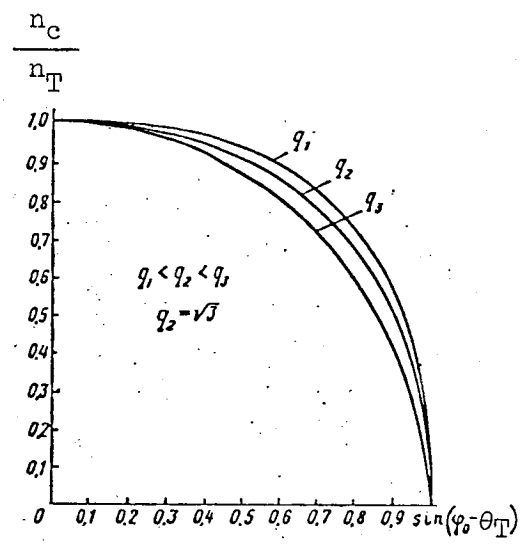

Figure 13.14. Graphs of function.

because condition (13.35) is no longer satisfied. The state of parallel approach will be disrupted and the target will not be hit.

Figure 13.14 shows the graphs of the function n_c/n_T, when $q > 1$, constructed in accordance with equation (13.37). It follows from these graphs that the maximum load factor during maneuvers of the target occurs when $\varphi_0 - \theta_T$ is close to 0 or π. From this we obtain a rule for the evasive maneuvers of the target: the target must turn with the maximum possible

acceleration, such that $\varphi_0 - \theta_T \begin{matrix} \rightarrow 0 \\ \rightarrow \pi \end{matrix}$. Consequently, when attack takes place from the rear hemisphere, the target must turn away from the missile, and when the attack takes place from the front hemisphere, the target must turn towards the missile. The same maneuvers of the target when $q < 1$ may cause a disruption in the homing guidance of the missile.

In concluding this section we note several special features of the kinematics of homing guidance. The kinematic examination of the problem assumes an instantaneous orientation of the velocity vector, due to this particular /425 method of guidance. However, in the actual control of a missile we can only vary the lateral force which causes the velocity vector of the missile to rotate. Therefore, the data obtained from the kinematic analysis with respect to load factors in the region of the target, and particularly with respect to the impact accuracy, becomes inaccurate. As we shall show, the question of hit accuracy is solved by investigating the dynamics of homing guidance. The kinematic analysis gives us general information on the nature of the trajectory, makes it possible for us to compute the homing guidance time and gives us a sufficiently accurate concept about the required load factors along the trajectory, except in the region close to the target. In general, the further the missile is from the target, the more accurate is the information on the required load factors obtained from the kinematic analysis. In the kinematic analysis the placement of the missile on the parallel approach from a random initial position of the velocity vectors of the target in the missile is obtained instantaneously, because the direction of the missile flight velocity varies instantaneously.

Under actual conditions an instantaneous orientation of the velocity vector is impossible, and the placement of the missile in the state of parallel approach presents a rather complex problem. However, this is a problem of dynamics, because there is no other way of entering the parallel approach except by applying a force to the missile and producing an angular velocity $\dot{\theta}$.

Since φ must be equal to 0 in the state of parallel approach, we can enter this state by varying $\dot{\theta}$ (or the lateral force) according to the law

$$\dot{\theta} = k\,\dot{\varphi}, \tag{13.38}$$

where k is the coefficient of proportionality. The higher the value of k, the more rapidly will the state of parallel approach be established.

In some sources[1] the control of the missile in accordance with the law $\dot{\theta} = k\dot{\varphi}$ is considered as a special guidance method and is called the method of proportional navigation.

---

[1] A. S. Lokk, Guided Missiles, Gostekhizdat, 1957.

Section 13.2. The Equation of Motion for Missiles with Homing Guidance

1. Equations for the Two-Dimensional Motion of the Missile. Equations of motion of missiles with homing guidance consist of three groups: the equations of motion of missile, the equations of kinematics relations between the missile and the target and the equations of the control systems.

The equations of the missile (8.53) moving with a variable velocity[1], are written in the following form /426

$$\left.\begin{aligned} & T_V \frac{d\theta}{dt} - \alpha + \frac{T_V g}{V} \cos\theta = 0; \\ & \frac{d^2\vartheta}{dt^2} + c_{\dot\vartheta} \frac{d\vartheta}{dt} + c_{\dot\alpha} \frac{d\alpha}{dt} + c_\alpha \alpha = c_\delta \delta; \\ & \vartheta = \theta + \alpha, \end{aligned}\right\} \tag{13.39}$$

where $T_V = \dfrac{mV}{c_y^\alpha S \dfrac{\rho V^2}{2} + P}$;

and the coefficients $C_{\dot\vartheta}$, $C_{\dot\alpha}$, C_α and C_δ are determined by means of equations (8.27).

In accordance with figure 13.13 the kinematic coupling equations are obtained in the following form

$$\frac{dL}{dt} = V_T \cos(\varphi - \theta_T) - V \cos(\varphi - \theta); \tag{13.40}$$

$$L \frac{d\varphi}{dt} = -V_T \sin(\varphi - \theta_T) + V \sin(\varphi - \theta); \tag{13.41}$$

If we assume that the control system of the missile is linear, we can write its equation in the general form

$$P_\delta(p)\,\delta = F(\psi, \alpha, \dot\vartheta, \dot\varphi, L, \ldots), \tag{13.42}$$

where $P_\delta(p)$ is a polynomial $p = d/dt$, which characterizes the delay in the control system associated with the formulation of the control laws; $F(\psi, \alpha, \dot\vartheta, \dot\varphi, \ldots L)$ is a linear function of the arguments ψ, α, $\dot\vartheta$, $\dot\varphi$, ... and may be a nonlinear function of the range L.

---

[1] Velocity $V = V(t)$ may be determined from equations (8.52) and from the kinematic trajectory of homing guidance.

The arguments ψ, α, $\dot{\vartheta}$, $\dot{\varphi}$, . . . , may be established under action of polynomial $Q(p)$, whose degrees are equal to or less than the degree of $P_\delta(p)$. The number of arguments $F(\psi, \alpha, \dot{\vartheta}, \dot{\varphi}, \ldots, L)$ is determined by the collection of available technical means for measuring and forming the signals ψ, α, $\dot{\vartheta}$, $\dot{\varphi}$, . . . The form of the function $F(\psi, \alpha, \dot{\vartheta}, \dot{\varphi}, \ldots, L)$, obtained for a given selection of signals ψ, α, . . ., determines the particular method of guidance.

Equations (13.39) - (13.42) do not lend themselves to investigation for the purpose of selecting a reliable form of equation (13.42) and, consequently, for selecting a guidance method which takes into account the existing technical means. Therefore, to analyze the dynamics of homing guidance we shall consider the motion of the missile with respect to some unperturbed rectilinear motion of the missile and target with constant values $V = V_e$ and $V = V_{Te}$ and carry /427

out the corresponding linearization of equations (13.39) - (13.41). However, before proceeding with the linearization of these expressions, we shall consider the concept of missile miss.

2. The Miss of a Missile. This concept is associated with firing unguided missiles at the target (mobile or fixed). The miss is the minimum distance L_{min} between the trajectories of the target and of the missile. Figure 13.15 shows the instantaneous position of target T and of missile M for some instant of time. If, beginning with this instant of time, the velocity vectors of the missile and of the target remain constant, we shall experience a certain miss L_{min}, shown by symbol χ in figure 13.15. To determine the miss it is convenient to consider relative motion. For this purpose we draw a vector $-V_T$ from the end of the missile vector $\overline{V}$. The sum of vectors $\overline{V}$ and $-\overline{V}_T$ forms a vector for the relative velocity of the missile $\overline{V}_{OTH}$, i.e.,

$$\overline{V}_{OTH} = \overline{V} - \overline{V}_T . \tag{13.43}$$

(subscript OTH = relative).

The missile will move in the direction $\overline{V}_{OTH}$ and at point α_1 the distance between the target and the missile will be a minimum, i.e., equal to the miss χ. If the vectors $\overline{V}_T$ and V are constant, the miss is also constant. If $\overline{V}_T \neq$ const and $V \neq$ const, the miss vector is a continuously variable quantity. We note that in parallel approach the miss is obviously equal to 0.

Let us express the miss in terms of the basic kinematic parameters L and $\dot{\varphi}$. The miss χ in figure 13.15 is represented by segment $\overline{\alpha_1 T}$, equal to segment $\overline{\alpha_4 \alpha_5}$. Let us designate by t_c the time of motion of the missile to the range $L = \chi$. Then

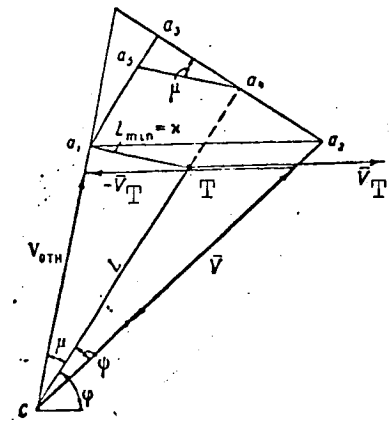

Figure 13.15. Instantaneous position of target and of missile.

$$t_c V_{отн} = Ca_1 = L\cos\mu. \tag{13.44}$$

Furthermore, element $\overline{\alpha_3\alpha_4}$ is equal to /428

$$\overline{a_3a_4} = t_c\,[V_T \sin\varphi - V\sin\psi] = -t_c L\dot{\varphi}\ .$$

Consequently, the miss χ will be equal to

$$x = -t_c L\dot{\varphi}\frac{1}{\cos\mu}. \tag{13.45}$$

Eliminating the time t_c from equations (13.44) and (13.45), we find

$$x = -\frac{L^2\dot{\varphi}}{V_{отн}}, \tag{13.46}$$

where

$$V_{отн} = V\cos(\psi+\mu) - V_T\cos(\varphi+\mu). \tag{13.47}$$

Angle μ may be considered as the angular miss or the angular sighting error. The sighting error is always small, i.e., under normal conditions angle μ cannot be very large. For this reason we may assume

$$V_{отн} \approx V_{сб} = V\cos\psi - V_T\cos\varphi. \tag{13.48}$$

3. Linearization of Equations of Motion for Missiles with Homing Guidance. As we have already mentioned, we consider unperturbed motion to be the one for which the velocity vectors of the missiles and of the target remain constant during the entire approach process. This form of unperturbed motion is realized for all quidance methods considered in section 1., i.e., when guidance is carried out with a constant lead angle and with parallel approach. Any deviations of the velocity vector of the target from some constant value $\overline{V}_{Te}$ and of the values of the missile velocity from V_e will appear as some additional perturbing forces, which act on the homing guidance system of the missile. In the pursuit method the lead angle is equal to 0 and unperturbed motion will take place when the missile flies with angles $\varphi_e = \begin{cases} 0 \\ \pi \end{cases}$.

Let us assume that $L = L_e + \Delta L$; $\varphi = \varphi_e + \Delta\varphi$; $\theta_e = \theta + \Delta\theta$; $\theta_T = \theta_{Te} + \Delta\theta_T$ $V_T = V_{Te} + \Delta V_T$; $V = V_e + \Delta V$. Here the quantities with the subscript e represent the parameters of the unperturbed state (in this case $\theta_{Te} = 0$). For the unperturbed state the following relations are valid.

$$\left.\begin{aligned} \frac{dL_e}{dt} &= V_{Te} \quad \cos\varphi_e - V_e\cos(\varphi_e - \theta_e) = -V_{c\delta} = \text{const}; \\ 0 &= -V_{Te} \quad \sin\varphi_e + V_e\sin(\varphi_e - \theta_e). \end{aligned}\right\} \tag{13.49}$$

Substituting the variables $L = L_e + \Delta L$, $\varphi = \varphi_e + \Delta\varphi$ in equations (13.40) and (13.41), taking into account the equation of the unperturbed state (13.49) and dropping terms which are infinitesimals of the second order, we obtain linear equations for small deviations from the unperturbed state /429

$$\frac{d\Delta L}{dt} = -V_e\sin(\varphi_e - \theta_e)\Delta\theta + f_L(t); \tag{13.50}$$

$$\frac{L_e}{V_{c\delta}}\frac{d\Delta\varphi}{dt} - \Delta\varphi = -k_V\Delta\theta + f_\varphi(t); \tag{13.51}$$

where

$$L_e = L_0 - V_{c\delta}t; \quad k_V = \frac{V_e\cos(\varphi_e - \theta_e)}{V_{c\delta}};$$

$$f_L(t) = \cos\varphi_e\Delta V_T - \cos(\varphi_e - \theta_e)\Delta V + V_{Te} \quad \sin\varphi_e\Delta\theta_T, \tag{13.52}$$

$$f_\varphi(t) = \frac{1}{V_{c\delta}}[V_{Te} \quad \cos\varphi_e\Delta\theta_T - \sin\varphi_e\Delta V_T + \sin(\varphi_e - \theta_e)\Delta V]. \tag{13.53}$$

Equation (13.50) will not be required in the future. It can be used to refine $L = L(t)$ after $\Delta\theta$ is obtained, because $L = L_e + \Delta L$. However, this refinement of the law for range variation has no special meaning.

Equation (13.51) may be written with respect to the miss χ. Comparing the derivatives of the expression for the miss (13.46) and expression (13.51) we obtain

$$\frac{d\chi}{dt} = L_e k_V \frac{d\Delta\theta}{dt} - L_e \dot{f}_\varphi(t). \tag{13.54}$$

Equations (13.51) and (13.54) are equations with a variable coefficient $L_e = L_0 - V_{c\delta}\, t$.

The missile equations (13.39) are also equations with variable coefficients T_v, V, m_ω, $m_{\dot\alpha}$, m_α and m_δ. However, the laws for the variation in the coefficients of the missile equation and in the coefficient L_e of the kinematic equation (13.51) or (13.54) differ in principle. The coefficient L_e becomes equal to 0 when $t = L_0/V_{c\delta}$, while the coefficients of the missile equations do not become equal to 0 (with perhaps the exception of m_α), and their variation is not associated in any way with the fact that the missile approaches the target. The variation in the coefficient L_e during the process of homing guidance is significant. For this reason we shall assume that the coefficients of equation (13.99) are constant, but different for various flight conditions of the missile.

If we assume that the deviations in the flight direction of the missile from the unperturbed direction are small, the last term in the first equation (13.39) may be assumed to be constant or to be a very slowly varying quantity, so that its derivative can be neglected. Furthermore, in expression (13.39) we should take the deviations $\Delta\vartheta$ and $\Delta\theta$ in place of ϑ and θ. Thus, instead of equation (13.39) we obtain the following group of equations /430

$$\left.\begin{aligned} &T_V \frac{d\Delta\theta}{dt} - \chi = -\frac{T_V g}{V_e}\cos\theta_e; \\ &\frac{d^2\Delta\vartheta}{dt^2} + c_{\dot\vartheta}\frac{d\Delta\vartheta}{dt} + c_{\dot\alpha}\frac{d\Delta\alpha}{dt} + c_\alpha \Delta\alpha = c_\delta \Delta\delta; \\ &\Delta\vartheta = \Delta\theta + \Delta\alpha. \end{aligned}\right\} \tag{13.55}$$

Now we can obtain expression for the miss

$$\frac{d\chi}{dt} = L_e \frac{k_V}{T_V}\chi + f_\chi(t), \tag{13.56}$$

where

$$f_\chi(t) = -L_e \dot{f}_\varphi(t) - \frac{g L_e k_V}{V_e}\cos\theta_e. \tag{13.57}$$

We can introduce the load factor developed by the missile in expression (13.56) in place of the angle of attack a.

Section 13.3. The Dynamics of Missile Homing Guidance During Parallel Approach

1. The Equations of the Dynamics of Homing Guidance for Various Control Laws. At the initial instant of guidance, when the missile is launched or the control system is turned on, there is always some initial miss χ_0. The control system of the missile is designed to decrease the initial miss χ_0 to 0 or to some minimum value, so that when the warhead of the missile explodes it will destroy the target. The purpose of investigating the dynamics of homing guidance is to study the laws for the variation in miss and the selection of missile control system which would reduce the miss to 0 or to some necessary minimum value.

Expression (13.56) clearly shows the type of law which must be used to vary the angle of attack of the missile or its laod factor to provide for an asymptotic decrease in the initial miss. Indeed if we require that

$$a = -\frac{k_x}{L_e} x, \tag{13.58}$$

we obtain the equation for miss in the form

$$\frac{dx}{dt} + kx = f_x(t). \tag{13.59}$$ /431)

The solution of equation (13.59) when $f_x(t) = 0$ has the well-known form

$$x = x_0 e^{-kt},$$

where $k = k_v k_x / T_V$. We should select k_x in such a way that $3/k$ [sec] is less than the guidance time. If $f_x(t) = f_x = \text{const}$, the solution of equation (13.59) will take the form

$$x = x_0 e^{-kt} + \frac{f_x}{k}(1 - e^{-kt}). \tag{13.60}$$

As we can see, the constant perturbing force f_x produces a miss f_x/k. The constant component f_x is determined by the gravity force [see equation (13.57)]. However, since the missile flight direction θ_e is known approximately, we can always introduce a constant signal into the control law which

compensates the effect of missile weight. The perturbation f_x is also produced by the maneuvers of the target. Indeed, the term $\dot{L}_e \dot{f}_\varphi(t)$ in expression (13.57) has the following value when V = const

$$L_e\left(\frac{\cos\varphi_c}{V_{c6}} V_{Te} \quad \Delta\dot{\theta}_T - \frac{\sin\varphi_e}{V_{c6}} \Delta\dot{V}_T\right). \tag{13.61}$$

From this we can see that the longitudinal load factor of the target $\Delta\dot{V}_T$ and the lateral load factor of the target $V_{Te}\Delta\dot{\theta}_T$ produce a perturbing force f_x.

To increase the accuracy of guidance and lower the miss when the perturbations are constant or vary slowly, it is neccessary to increase the order of astaticism of the system, i.e., to augment the control law or to allow for the variation in the angle of attack (13.58) by the integral term

$$\alpha = -\frac{k_x}{L_e} x - \frac{q_x}{L_e} \int_0^t x dt. \tag{13.62}$$

In this case the equation with respect to the miss would be of the second order

$$\frac{d^2x}{dt^2} + 2\zeta\Omega_0 \frac{dx}{dt} + \Omega_0^2 x = \dot{f}_x(t), \tag{13.63}$$

where

$$2\zeta\Omega_0 = \frac{k_x k_V}{T_V} \quad \text{and} \quad \Omega_0^2 = \frac{q_x k_V}{T_V}.$$

If $f_x(t)$ = const, the right side of the equation is equal to 0 and the effect of f_x does not produce a miss. In the same way, during the slow variation of $f_x(t)$ the miss will be small because $\dot{f}_x(t) = df_x/dt$ is small. The coefficient use of q_x is selected in such a way that $3/\Omega_0 \leq t_c$, where t_c is the homing guidance time. The coefficient k_x determines the relative damping coefficient ζ which must be taken equal to $\sqrt{2}/2$ (we note that for this value of the damping coefficient we obtain an optimum transient process with a control time $t_p \approx \frac{3}{\Omega_0}$) . /432

The equations for homing guidance (13.59) and (13.63) have constant coefficients due to the special control laws (13.58) and (13.62) which contain

the instantaneous value of the range to the target. Expanding the value of the miss in equation (13.58) we obtain

$$a = + k_x \frac{L_e \dot{\varphi}}{V_{c\delta}}. \tag{13.64}$$

As we can see from expression (13.64), to form the control law we must measure the range L to the target, the approach velocity $V_{c\delta} = \left|\frac{dL_e}{dt}\right|$, the angular velocity of the line joining the missile to the target $\dot{\varphi}$ and use a computer for generating signals in accordance with equation (13.64).

It is rather difficult to realize a range measuring channel aboard the missile. Also, as a rule, radars for measuring range are not too well protected against interference. Therefore it is undesirable to use signals L_e and $V_{c\delta}$. Certain difficulties are encountered in carrying out the multiplication and division operations due to the requirements of the control law (13.64).

For this reason in the parallel approach method the following laws are used[1]

$$a = - k_{\dot{\varphi}} \dot{\varphi} \tag{13.65}$$

and

$$a = - k_{\dot{\varphi}} \dot{\varphi} - q_{\dot{\varphi}} \int_0^t \dot{\varphi} dt. \tag{13.66}$$

For control law (13.65) we have an equation for the miss having the form

$$\frac{dx}{dt} + \frac{k}{l_0 - t} x = f_x, \tag{13.67}$$

where $l = l_0 - t = \frac{L_e}{V_{c\delta}} - t$ - the range to the target in seconds; /433

$$k = \frac{k_V}{T_V} k_{\dot{\varphi}}; \quad l_0 = \frac{L_0}{V_{c\delta}}. \tag{13.68}$$

For integral control (13.66) the equation for the miss has the form

$$\frac{1}{l} \frac{dx}{dt} + \frac{k}{l^2} + q \int_0^t \frac{x}{l^2} dt = \frac{1}{l} f_x(t), \tag{13.69}$$

[1]The minus sign in equation (13.46) must be dropped when the control laws are written in this manner.

where

$$k = \frac{k_V}{T_V} k\dot{\varphi}; \quad q = \frac{k_V}{T_V} q\dot{\varphi}.$$

After differentiation we obtain

$$l^2 \frac{d^2x}{dt^2} + (k+1) l \frac{dx}{dt} + (lq + 2k) x = l^2 \dot{f}_x(t) + l f_x(t). \tag{13.70}$$

Expressions (13.67) and (13.70) contain a variable coefficient $l = l_0 - t$; they are, therefore, nonstationary linear equations. These equations have one special feature--their solution has a singularity when $t = l_0$. The singularity corresponds to the instant of time when the missile hits the target. Before continuing the analysis of missile guidance dynamics for parallel approach, we consider briefly the properties of linear nonstationary equations with singularities.

2. Nonstationary Linear Equations of the Second Order with Singularities. The following equation represents a sufficiently general form of linear equations of second order with singularities

$$t^2 \frac{d^2x}{dt^2} + P(t) t \frac{dx}{dt} + Q(t) x = 0, \tag{13.71}$$

where

$$P(t) = a_0 + a_1 t + a_2 t^2 + \ldots$$

and

$$Q(t) = b_0 + b_1 t + b_2 t^2 + \ldots$$

are series or polynomials of t.

The solution of equation (13.71) is sought in the form of a series

$$x = t^\rho \sum_{s=0}^{\infty} k_s t^s. \tag{13.72}$$

Substituting expression (13.72) into equation (13.71) and setting to 0 the coefficients in front of the same degrees of t, we obtain a series of equations which can be used to determine ρ and k_s (s = 0, 1, 2 . . .): /434

$$\left.\begin{aligned}
&[\rho(\rho-1) + a_0\rho + b_0] k_0 = 0,\\
&[(\rho+1)\rho + a_0(\rho+1) + b_0] k_1 + a_1\rho k_0 + b_1 k_0 = 0,\\
&[(\rho+2)(\rho+1) + a_0(\rho+2) + b_0] k_2 + a_1(\rho+1) k_1 +\\
&+ a_2\rho k_0 + b_1 k_1 + b_2 k_0 = 0,\\
&\ldots\ldots\ldots\ldots\ldots\ldots\ldots\ldots
\end{aligned}\right\} \tag{13.73}$$

In the first equation (13.73) $k_0 \neq 0$ and may be taken as an arbitrary value (in particular equal to 1). Consequently, the exponent ρ is determined from the first equation

$$\rho(\rho-1)+a_0\rho+b_0=0. \tag{13.74}$$

Equation (13.74) used to determine the exponent ρ is called the characteristic equation. This equation is quadratic and has two routes ρ_1 and ρ_2. If the difference between the roots $\rho_1 - \rho_2$ is not equal to a whole positive number or to 0, solution of (13.71) will have the following form

$$x=c_1 t^{\rho_1}\sum_{s=0}^{\infty} k_s t^s + c_2 t^{\rho_2}\sum_{s=0}^{\infty} h_s t^s, \tag{13.75}$$

where c_1 and c_2 are arbitrary constants determined by the initial conditions; k_s are coefficients determined successively from equations (13.73) where $\rho = \rho_1$; and h_s are coefficients determined from the same system of equations when $\rho = \rho_2$.

If the difference in the values of the roots of the characteristic equation is equal to a whole positive number or to 0, the terms of (13.75) lose their linear independence and the solution of (13.71) has the form

$$x=c_1 t^{\rho_1}\sum_{s=0}^{\infty} k_s t^s + c_2\left[\left(t^{\rho_1}\sum_{s=0}^{\infty} k_s t^s\right)\lg x + t^{\rho_2}\sum_{s=0}^{\infty} h_s x^s\right]. \tag{13.76}$$

Quite frequently an equation of the form (13.71) is called a Bessel equation

$$t^2\frac{d^2x}{dt^2}+t\frac{dx}{dt}+(t^2-\nu^2)=0, \tag{13.77}$$

where ν is a constant number (parameter).

The series in solutions (13.75) and (13.76) for equation (13.77) are called Bessel or cylindrical functions. If ν is not whole or is not half of a whole odd number, the solution of (13.77) has the form

$$x=c_1 I_\nu(t)+c_2 I_{-\nu}(t), \tag{13.78}$$

where $I_\nu(t)$ is a Bessel function of the first type of order ν.

If ν is a whole number n or 0, the terms in (13.78) lose their linear independence and the solution of (13.77) will be

$$x = c_1 I_n(t) + c_2 K_n(t), \tag{13.79}$$

where $K_n(t)$ is a Bessel function of the second type of order n.

Bessel functions are well known and tabulated.[1] For this reason the analysis of processes described by equation (13.77) is not difficult. When the parameter ν is equal to 1/2 of a whole odd number, the Bessel functions are expressed in terms of elementary functions. /435

Let us note one other important case of equation (13.71)

$$t^2 \frac{d^2x}{dt^2} + (b - t) t \frac{dx}{dt} - atx = 0$$

or

$$t \frac{d^2x}{dt^2} + (b - t) \frac{dx}{dt} - ax = 0. \tag{13.80}$$

Expression (13.80) is a degenerate hypergeometric equation satisfied by the degenerate hypergeometric functions

$$F_1(a, b, t) = 1 + \frac{a}{b} t + \frac{a(1+a)}{b(1+b)} t^2 + \frac{a(1+a)(2+a)}{b(1+b)(2+b)} t^3 + \ldots$$

If b is not a whole number, the solution of (13.80) has the form

$$x = c_1 F_1(a, b, t) + c_2 t^{1-b} F_1(a - b + 1, 2 - b, t). \tag{13.81}$$

Hypergeometric functions are not tabulated or investigated as thoroughly as the Bessel functions. The graphs of the functions for various values of a and b may be found in the book of E. Janke and F. Emde.[1]

When parameter b is equal to a whole number, the terms in equation (13.81) lose their linear independence. To obtain a solution in this case we use a hypergeometric function of the second type $F_2(a, b, t)$, which is constructed according to the second term in expression (13.76). Figure 13.16 shows graphs of functions $F_1(a, b, t)$ and $F_2(a, b, t)$ for b = 2 and a = -4, a = -9. We

[1] E. Janke and F. Emde, Tables of Functions with Equations and Curves, Fizmatgiz, 1959.

note that if a = -n, where n is a natural number, $F_1(a, b, t)$ and $F_2(a, b, t)$ are transformed into polynomials and $F_1(a, b, t)$ is equal to the generalized Chebyshev-Lager polynomial.

As we can see from these graphs, when the arguments have large values, both functions have a monotonic nature and when the values of the arguments are small, these functions have an oscillatory nature. The function $F_2(a, b, t)$ approaches infinity when $t \to 0$. One of the solutions (13.75), (13.78) or (13.81) approaches infinity when t = 0. This can be determined by considering the roots of the characteristic equation. If the root $\rho_2 < 0$, then obviously the second term in (13.75) approaches infinity when t = 0.

For the Bessel equation the characteristic equation has the form

$$\rho(\rho - 1) + \rho - \nu^2 = 0$$

or

$$\rho^2 - \nu^2 = 0,$$

from which it follows that

$$\rho_1 = \nu \quad \text{and} \quad \rho_2 = -\nu.$$

Thus, the second solution of the Bessel equation and consequently the Bessel functions of the second type always have an infinite value when t = 0.

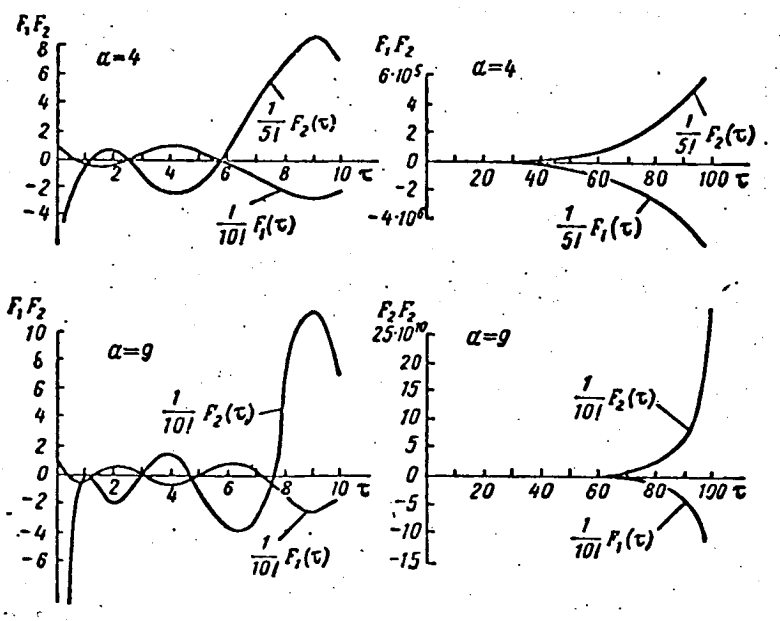

Figure 13.16. Graphs of functions $F_1(\tau)$ and $F_2(\tau)$.

For the hypergeometric equation the defining equation is written in the form /436

$$\rho(\rho - 1) + b\rho = 0.$$

Consequently $\rho_1 = 0$ and $\rho_2 = 1 - b$, and the second solution of the hypergeometric equation approaches infinity for all $b > 1$, which can also be seen from equation (13.81).

3. The Analysis and Comparison of Parallel Approach Laws. Parallel approach with control laws (13.58) and (13.62) leading to stationary equations was investigated in the first subsection of this section.

Now let us consider equation (13.67). This equation, as well as expressions (13.59), (13.63) and (13.69), is an equation of a closed loop automatic control system for the miss χ. In this case the error of the system is the negative value of the miss χ. The functional diagrams corresponding to equations (13.67) and (13.69) are shown in figures 13.17a and b.

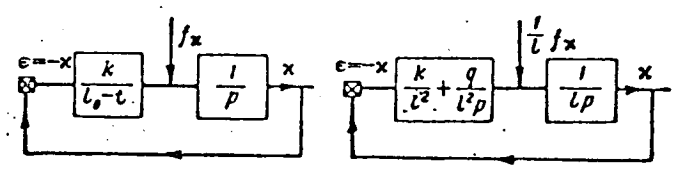

a b

Figure 13.17. Functional diagrams corresponding to equations (13.67) and (13.69).

We should note that the transformation and convolution laws for the functional diagrams of linear stationary systems are not applicable to functional diagrams whose elements have variable parameters. However, it is still possible to draw certain conclusions about the general properties of nonstationary systems from their functional diagrams. For example, in the diagram shown in /437 figure 13.17a there is an amplifying element with coefficient $\frac{k}{l_0 - t}$ which approaches infinity when $t = l_0$. From this we can conclude that the perturbation f_x, which is limited in modulus, must not lead to a miss in this case. The validity of this conclusion is confirmed by the solution of equation (13.67) when $f_x = \text{const}$

$$x = x_0\left(\frac{l}{l_0}\right)^k + \frac{f_x}{k-1}\, l\left[1 - \left(\frac{l}{l_0}\right)^{k-1}\right]. \tag{13.82}$$

We can see from this solution that the miss component due to the perturbation becomes equal to 0 when $l = 0$. Therefore, it would seem that there is no necessity for having an integral law (13.66). However, this is not exactly true. The fact is that guidance must be stopped at a certain distance from the target L_{min} (or l_{min}), because the target coordinator goes blind. For this reason the miss must be reduced to a minimum at a range L_{min} rather than at zero range. From this point of view the requirement for the integral law still holds. From the same considerations the quantity k in expression (13.82) is significant. The quantity k is determined by selecting the coefficient of proportionality in the control law (13.65). If we set a requirement that the miss must decrease to 5 percent of its initial value, when $l = l_{min}$ is reached, we have

$$k = \frac{\lg 20}{\lg \frac{l_0}{l_{min}}}. \tag{13.83}$$

Since l_{min} is assigned, we can see from equation (13.83) that when the initial range is large we shall have the same accuracy when the gain of the system is less. Since the coefficient k cannot be made too large, it turns out that homing guidance cannot be started when the initial range is too /438 small. A large initial range is advantageous from all points of view: the initial miss has enough time to decrease and the amplification factor may be large. When the amplification factor is small, the missile becomes unstable to high frequency interference which, in particular, is determined by the fluctuations in the signal reflected by the target.

If we compare the control laws satisfying the miss (13.58) and the angular velocity (13.65), we may conclude that the control law based on the angular velocity provides for homing guidance from any ranges, and if we neglect noise interference, it provides a higher hit accuracy; for the control law based on the miss there is an exponential decrease in the miss and, therefore, the guidance time must always be greater than the control time. If we take into account noise interference, the difference between the two laws from the standpoint of accuracy becomes insignificant. The control law based on the miss, as we have stated, is more difficult to realize than the control law based on the angular velocity.

Therefore, the basic advantage is in the control law based on the angular velocity. In section 1 of this Chapter we stated that the control law based on the angular velocity is called the Law of Proportional Navigation in some references.

Now let us consider the integral law based on the angular velocity. We consider equation (13.70) when $f_x = f_x = 0$ and introduce a new independent variable $l = l_0 - t$.

Equation (13.70) takes the form

$$l^2 \frac{d^2\chi}{dl^2} - (k+1)\frac{d\chi}{dl} + (ql + 2k)\chi = 0. \tag{13.84}$$

First let us check the value of the miss when l = 0. To do this we formulate the characteristic equation

$$\rho(\rho - 1) - (k+1)\rho + 2k = 0.$$

The roots of the characteristic equation $\rho_1 = k$ and $\rho_2 = 2$ are positive, so that when l = 0, the miss is also equal to zero according to expression (13.75).

By making the substitutions $\tau = 2\sqrt{gl}$ and $y = \chi l^{-\frac{k+2}{2}}$, equation (13.84) is transformed into the Bessel equation of the order $\nu = k - 2$. Consequently the solution of equation (13.84) will have the form

$$\chi = l^{\frac{k+1}{2}} \left[C_1 I_{k-2}(2\sqrt{ql}) + C_2 I_{-(k-2)}(2\sqrt{ql})\right], \tag{13.85}$$

where C_1 and C_2 are arbitrary constants.

For the initial conditions $\chi\Big|_{l=l_0} = 0$, $\frac{d\chi}{dl}\Big|_{l=l_0} = 0$ the constants C_1 and C_2 /439

are given by the following expressions

$$C_1 = \frac{\chi_0}{l_0^{\frac{k+2}{2}}} \cdot \frac{I'_{k+2}(\tau_0)}{I_{k-2}(\tau_0) I'_{k+2}(\tau_0) - I'_{k-2}(\tau_0) I_{-k+2}(\tau_0)}, \tag{13.86}$$

$$C_2 = \frac{\chi_0}{l_0^{\frac{k+2}{2}}} \cdot \frac{I'_{k-2}(\tau_0)}{I_{k-2}(\tau_0) I'_{k+2}(\tau_0) - I'_{k-2}(\tau_0) I_{-k+2}(\tau_0)}, \tag{13.87}$$

where

$$I'_\nu(\tau_0) = \frac{d}{d\tau} I_\nu(\tau)\Big|_{\tau=\tau_0}.$$

The following equation is valid for the derivatives of Bessel functions

$$\frac{dI_\nu(\tau)}{d\tau} = I_{\nu-1}(\tau) - \frac{1}{\tau} I_\nu(\tau). \tag{13.88}$$

If k - 2 is a whole number n the functions $I_{-k+2}(\tau)$ in expressions (13.85), (13.86) and (13.87) should be replaced by a function of the second type $K_n(\tau)$. Equation (13.88) remains valid for functions of the second type.

Bessel functions of any order ν represent oscillations with a variable period which are almost undamped. As we can see from solution (13.85), the damping of the oscillations in the instantaneous value of the miss are determined by the quantity k. When k becomes greater, the damping of the oscillations also becomes greater. The coefficient q (a portion of the integral control) determines the periods of the oscillatory motion. For the same values k and q, the nature of the miss oscillations depends to a large degree on the initial range L_0 (or l_0). The greater the range, the greater is the oscillatory nature of the miss decrease process. In figure 13.18 curves computed by means of equation (13.85) are shown for the variation in the miss when q = 1.0 1/sec and when k assumes different values with l_0 = 160 sec and l_0 = 30 sec. The behavior of the curves shows that the decrease of the initial miss at long range has a more oscillatory nature. The variation in the damping as a function of range may be obtained by analyzing equation (13.70). The variable coefficient l is frozen for different instants of time. Let us write the homogeneous equation (13.70) in normalized form, assuming that l is a parameter

$$\frac{d^2\varkappa}{dt^2} + 2\zeta\Omega_0 \frac{d\varkappa}{dt} + \Omega_0^2\varkappa = 0, \tag{13.89}$$

where

$$\Omega_0 = \frac{q}{l} + \frac{2k}{l^2}; \quad 2\Omega_0 = \frac{k+1}{l}; \quad \zeta = \frac{k+1}{2\sqrt{ql+2k}}.$$

As the target is approached, the natural frequency of oscillations increases and the coefficient of relative damping also increases. /440

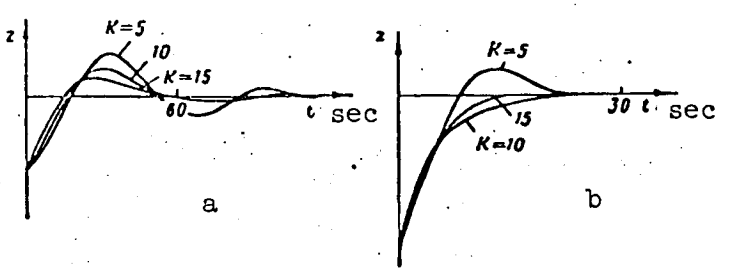

Figure 13.18. Curves showing variations in miss.

4. The Effect of Delay in Establishing the Control Force in the Process of Parallel Approach. The control laws given by expressions (13.58), (13.62), (13.65) and (13.66) assume that the angle of attack and the lateral control force are proportional and follow the variations in the total control signal without delay. However, actually there is a delay in the control signals when

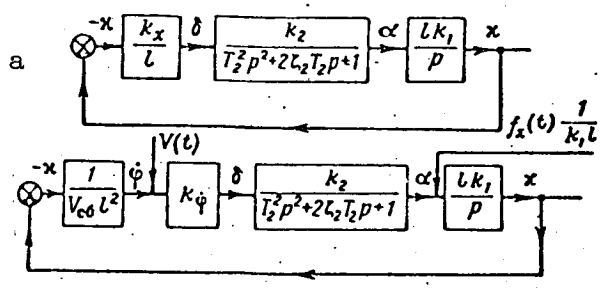

Figure 13.19. Functional diagrams corresponding to control laws (13.58) and (13.65).

they are amplified and transformed by the control system aboard the missile, and, in addition, for missiles with fixed wings there is a delay between the deflection of the control surfaces and the angle of attack. The latter delay is most appreciable. It is known that the relationship between the angle of attack and the deflection angle of the control surface, for the case of linear approximation, is characterized by the transfer function of the oscillating element. Figures 13.19a and b show the functional diagrams corresponding to control laws (13.58) and (13.65), which take into account the true relationship between the angle of attack and the deflection angle of the control surface (delay in the control system is disregarded). The functional diagrams contain the following designations

$$k_1 = \frac{V_{c6} k_V}{T_V} [м/sec^2], \quad k_2 = \frac{m_\delta}{m_\alpha + \frac{m_\alpha}{T_V}}; \quad T_2^2 = \frac{1}{m_\alpha + \frac{m_\omega}{T_V}},$$

$$2\zeta_2 T_2 = \frac{\dot{m}_\omega + m_\alpha + \frac{1}{T_V}}{m_\alpha + \frac{m_\omega}{T_V}}.$$

To investigate the effect of delay within the scope of the well-known linear equations of the second order, we approximate the oscillating element and functional diagrams in figure 13.19 by an inertial element. This approximation is possible when the damping coefficient $\zeta > 1.0$. In this case both real poles of the oscillating element differ substantially. We neglect the large pole and obtain an inertial element in place of an oscillating element. The delay in the control force which has this form is also characteristic for missiles in which the lateral force is controlled directly. Such missiles include those which have rotatable wings and those with a lateral reactive thrust. /441

The equations of homing guidance which take into account the delay in the control system have the following form for both control laws.

for controlling the miss

$$\left.\begin{aligned} &\frac{dx}{dt} = lk_1\alpha + f_x(t), \\ &T_2\frac{d\alpha}{dt} + \alpha = k_2\delta, \\ &\delta = -k_x\frac{1}{l}x; \end{aligned}\right\} \tag{13.90}$$

for controlling the angular rate of change of the line joining the missile and the target /442

$$\left.\begin{aligned} &\frac{dx}{dt} = lk_1\alpha + f_x(t), \\ &T_2\frac{d\alpha}{dt} + \alpha = k_2\delta, \\ &\delta = -k_{\dot\varphi}\dot\varphi, \\ &\dot\varphi = \frac{1}{V_{c\delta}l^2}x, \end{aligned}\right\} \tag{13.91}$$

(see footnote on p 26).

Eliminating variables α and δ from equation (13.90), we obtain a second order equation for the miss

$$\begin{aligned} &T_2\frac{d^2x}{dt^2} + \left(\frac{T_2}{l} + 1\right)\frac{dx}{dt} + kx = \\ &= \left(1 + \frac{T_2}{l}\right)f_x(t) + T_2\dot f_x(t), \end{aligned} \tag{13.90a}$$

where

$$k = k_1k_2k_x\left[\frac{1}{\text{sec}}\right].$$

Thus, we obtain an equation for the miss from system (13.91)

$$\begin{aligned} &T_2\frac{d^2x}{dt^2} + \left(\frac{T_2}{l} + 1\right)\frac{dx}{dt} + \frac{k}{l}x = \\ &= \left(\frac{T_2}{l} + 1\right)f_x(t) + T_2\dot f_x(t), \end{aligned} \tag{13.91a}$$

where

$$k = k_1 k_2 k_{\dot{\varphi}} \frac{1}{V_{c6}}.$$

First, let us consider the value of the miss for both cases when $l = 0$. We investigate the homogeneous equations (13.90a) and (13.91a), introducing a new independent variable l

$$\frac{d^2\varkappa}{dl^2} - \left(\frac{1}{l} + \frac{1}{T_2}\right)\frac{d\varkappa}{dl} + \frac{k}{T_2}\varkappa = 0, \tag{13.90b}$$

$$\frac{d^2\varkappa}{dl^2} - \left(\frac{1}{l} + \frac{1}{T_2}\right)\frac{d\varkappa}{dl} + \frac{k}{T_2 l}\varkappa = 0. \tag{13.91b}$$

Let us multiply both equations by l^2 and find the characteristic equations which are the same for both cases /443

$$\rho(\rho - 1) - \rho = 0.$$

One of the roots of the characteristic equations is equal to 0, while the other is equal to 2. Consequently, for both cases when $l = 0$ the miss is also equal to 0. However, the conclusion that the missile will hit the target because $\chi = 0$ when $l = 0$ is premature.

In addition to the law for the variation of the miss, when the target is approached, it is necessary to study the behavior of the other coordinates of the system, such as the angle of attack or the deflection angle of the control surface. Let us consider equation (13.91b) first. By using the substitution

$$\varkappa(\tau) = \tau^2 w(\tau),$$

where

$$\tau = \frac{l}{T_2},$$

equation (13.91b) is reduced to a degenerate hypergeometric equation when $b = 3$ and $a = -(k - 2)$; see equation (13.80)

$$\tau\frac{d^2w}{d\tau^2} + (3 - \tau)\frac{dw}{d\tau} + (k - 2)w = 0. \tag{13.91c}$$

Except for the constant factor, the value of w in equation (13.91c), as we can see from system (13.91), is equal to the deflection angle of the control surface δ and to the angular rate of change of the line joining the missile and the target $\dot{\varphi}$. If we eliminate all of the variables except α from equation (13.91), we also obtain a hypergeometric equation with the same parameter a and with parameter $b = 2$

$$\tau\frac{d^2\alpha}{d\tau^2} + (2 - \tau)\frac{d\alpha}{d\tau} + (k - 2)\alpha = 0, \tag{13.91d}$$

where, as before,

$$\tau = \frac{l}{T_2} = \frac{l_0 - t}{T_2}.$$

The characteristic equations for (13.91c) and (13.91d) have one zero root and one negative root: [ρ_2 = -3 for (13.19c) and ρ_2 = - 2 for (13.91d)]. Thus, all coordinates $\dot{\varphi}$, δ and α near the target approach infinity, even though the miss becomes equal to 0. It would be more correct to say that the target can be hit alternately when the angle of attack has an infinite value or when the lateral control force is infinite. Since the latter is impossible, homing guidance should be stopped when the angle of attack (or the load factors) reach certain limiting values.

In the guidance process the angle of attack will vary in accordance with the curves representing the hypergeometric functions. At the initial instant of time, when the range is large, the angle of attack will decrease, and the missile will go into a state of parallel approach. The selection of the initial miss and decrease in the angle of attack are more pronounced when the amplification factor k is high. As the target is approached, the hypergeometric functions assume an oscillatory nature, and any perturbation leads to an oscillatory increase in the angle of attack. Homing guidance should be turned off until the oscillations can be exited and after the state of parallel approach is established and the angle of attack is practically equal to zero. After homing guidance is turned off, the flight of the missile becomes uncontrollable, and we must consider the presence of inevitable interference. The shorter the range, at which homing guidance is turned off, the shorter will be the time of uncontrolled flight and the shorter will be the miss. From the curves of hypergeometric functions we can find the value $\tau = t_{turnoff}$, at which homing guidance should be turned off. Because $\tau = \frac{l}{T_2} = \frac{r}{V_{c\delta}T_2}$, the turnoff range will be equal to /444

$$L_{turnoff} = \tau_{turnoff} V_{c\delta} T_2. \qquad (13.92)$$

Expression (13.92) shows that as delay decreases, $L_{turnoff}$ decreases and the miss decreases (during uncontrolled flight), while the probability of target distruction increases. Thus, the response of the control system is the determining factor for increasing the probability of target destruction. In this case the response of the system refers to the response of the entire loop for the angular motions of the missile which contains the control system and the oscillating member which establishes the relation between the angle of attack and the angle of deflection of the control surface. The response of this loop may be increased by increasing the natural frequency of oscillations Ω_0 of the oscillating element, while retaining the optimum damping coefficient ζ. An increase in the natural frequency of oscillations requires the use of

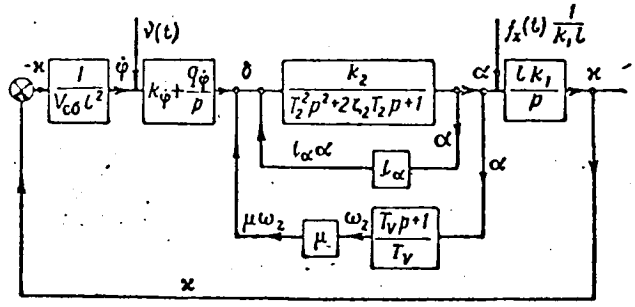

Figure 13.20. Functional diagram corresponding to control law 13.93).

the signal for the angle of attack or for the load factor. The necessary damping is provided by signal $\omega_z = \dot{\vartheta}$, obtained from the rate gyroscope. Thus, the law for the control surface of the missile during parallel approach will have the following form

$$\delta = -\mu\omega_z - i_\alpha \alpha - k_{\dot{\varphi}}\dot{\varphi} - q_{\dot{\varphi}}\int_0^t \dot{\varphi}\,dt. \qquad (13.93)$$

When we have ideal sensors for the angular velocity $\omega_z = \dot{\vartheta}$ and for the /445

load factor (or the angle of attack) α, the functional diagram for homing guidance with control law (13.93) has the form represented in figure 13.20.

Now let us consider the control of miss whose dynamics is given by a group of equations (13.90). The equation for the relative angle of attack in this case will have the form

$$\tau\frac{d^2\alpha}{d\tau^2} + (1-\tau)\frac{d\alpha}{d\tau} + (T_2 k\tau - 1)\alpha = 0,$$

where as before $\tau = \frac{l}{T_2}$.

Both roots of the characteristic equation are equal to zero. Therefore, the angle of attack will not increase when $l \to 0$. From this point of view the control law in terms of the miss has an advantage over the control law in terms of the angular velocity. We can recommend a combined use of both laws: in the initial stage we can control the angular velocity, and as the target is approached we can decrease the amplification factor $k_{\dot{\varphi}}$ proportionately to the range

l, [equations (13.90) and (13.91)]. If the range cannot be measured, we can decrease the amplification factor as a function of time, because we do not require a particularly high accuracy. We can use the same procedure for the integral law (13.93) by changing both coefficients $k_{\dot{\varphi}}$ and $q_{\dot{\varphi}}$ correspondingly.

Section 13.4. The Dynamics of Homing Guidance in the Pursuit Method

Let us consider the dynamics of homing guidance for the pursuit methods without lead angle and also with a constant lead angle, and a lead angle proportional to the angular velocity of the line joining the missile and the target.

1. The Dynamics of Homing Guidance for the Pursuit Method Without Lead Angle and With a Constant Lead Angle. As in the preceding case, the unperturbed state is assumed to be the one in which the velocity vectors of the missile and the target are constant, and constant lead angle $\psi=\varphi_e-\theta_e$ is chosen so that in the unperturbed state the angular velocity of the line joining the missile and the target $\dot{\varphi}_e$ is equal to zero. For homing guidance without a lead angle in the unperturbed state, the velocity vecotrs of the target and the missile are situated on one line. Their direction is either the same or opposite. /446

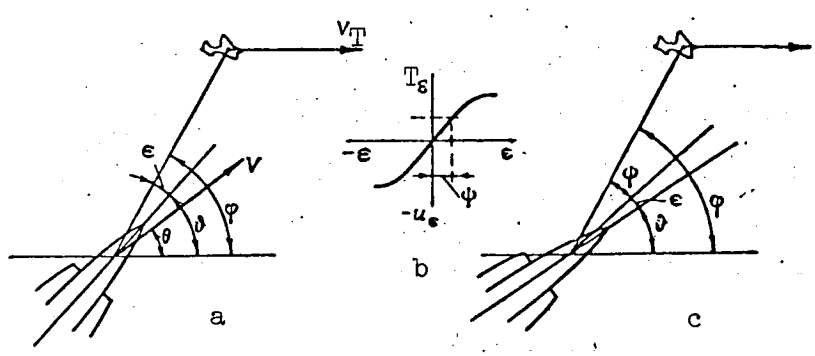

Figure 13.21. Homing guidance using pursuit method without lead angle and with lead angle.

Thus, the linearized kinematic equations and the expressions for the miss, which were derived earlier (see section 13.2), remain valid for the present case.

In homing guidance using the pursuit method without a lead angle, the simplest target coordinators are used (homing guidance heads), which produce an electric signal proportional to angle ϵ between the line joining the missile and the target and the optical axis of the target coordinator (fig. 13.21a). It is quite natural to use the signal for angle ϵ as the basic signal for guiding the missile in the pursuit method. This signal reacts on the control surfaces of the missile in such a way that angle ϵ is reduced to zero. The optical axis of the coordinator coincides either with the longitudinal axis of the missile or with the flight direction (with the velocity vector of the missile). In this case the homing method is called "feathered." To achieve feathered homing guidance, the target coordinator is oriented along the incident

airstream, or the total signal which reacts on the control surface contains a signal proportional to the angle of attack. /447

During homing guidance, using the pursuit method, with a constant lead angle (fig. 13.21b), we can also use the simplest target coordinators which are used in homing guidance without a lead angle. A constant lead angle is assigned when the missile is launched and may be recorded aboard the missile by two methods:

(1) by means of the position gyroscope of the target coordinator, whose axis coincides with the longitudinal axis of the missiles;

(2) by means of a rotating target coordinator.

In the first case a constant signal is fed to the control members of the missile from the position gyroscope. This signal is balanced by the signal from the target coordinator, which produces the necessary lead angle ψ. To realize this method, it is necessary to have a relatively wide region for the proportional characteristic of the coordinator $\mu_\varepsilon = f_{(\varepsilon)}$ (fig. 13.21c), with a curvature independent of range. In the second method this region may be substantially less.

In homing guidance using the pursuit method with constant lead angle, the signal acting on the control surfaces is the signal which measures angle ε between the optical axis of the homing guidance head and the direction of the line joining the missile and the target, displaced by the constant lead angle ψ. Feathered guidance is also possible in homing guidance with constant lead angle.

Thus, angle ε for nonfeathered guidance is expressed in the following manner

$$\varepsilon = \varphi - \psi - \vartheta,$$

while for feathered guidance it is expressed by

$$\varepsilon = \varphi - \psi - \theta.$$

If we express φ, θ and ϑ in terms of their unperturbed values φ_e, θ_e, and ϑ_e and increments $\Delta\varphi$, $\Delta\theta$ and $\Delta\vartheta$, and note that in the first case $\varphi_e-\psi-\vartheta_e=0$, while in the second case $\varphi_e-\psi-\theta_e=0$, we obtain, respectively

$$\varepsilon = \Delta\varphi - \Delta\vartheta = \Delta\varphi - \Delta\theta - \Delta\alpha, \tag{13.95}$$

$$\varepsilon = \Delta\varphi - \Delta\theta. \tag{13.96}$$

If we note that the expression for the angle ε contains the angle φ (or $\Delta\varphi$) the kinematic equation for the coupling between the target and the missile

should be taken in the form (13.51). When constructing the functional diagram it is more convenient to consider the negative value of $\Delta\varphi$--the quantity $\Delta\varphi^* = \Delta\varphi$. In this case $\varepsilon = -\Delta\varphi^* - \Delta\theta$. Taking this into account, the system of equations of motion of the missile has the following form[1] /448

$$\left.\begin{aligned}
&l\frac{d\Delta\varphi}{dt} - \Delta\varphi = +k_V\Delta\theta,\\
&T_V\frac{d\Delta\theta}{dt} = \alpha,\\
&T_2^2\frac{d^2\alpha}{dt^2} + 2\zeta_2 T_2\frac{d\alpha}{dt} + \alpha = k_2\delta,\\
&\Delta\vartheta = \alpha + \Delta\theta,\\
&\delta = k_\varepsilon\varepsilon,\\
&\varepsilon = \Delta\psi_0 - \Delta\varphi - \Delta\vartheta
\end{aligned}\right\} \qquad (13.97)$$

or for the case of feathered guidance

$$\varepsilon = \Delta\psi_0 - \Delta\varphi - \Delta\theta.$$

The second, third and fourth equations of system (13.97) are the well-known equations of missile dynamics with constant velocity. The fifth and sixth equations of this group are the equations of an ideal control system. The signal $\Delta\psi_0$ = const in the last equation represents the possible error in setting lead angle ψ, or the angular error in setting the target coordinator when guidance is performed without a lead angle.

The functional diagrams corresponding to equations (13.97) for feathered and unfeathered homing guidance are shown in figure 13.22. Expressions (13.97) and functional diagrams are valid both for guidance with a constant lead angle as well as for guidance without a lead angle.

The coefficient k_V depends on the different directions of homing guidance with a constant lead angle

$$k_V = \frac{V}{V_{c\delta}}\cos(\varphi_e - \theta_e) = \frac{V}{V_{c\delta}}\cos\psi. \qquad (13.98)$$

This coefficient is contained in the first equation of (13.97). Thus, when the attack takes place from the rear without a lead angle $k_V > 1.0$, and when the attack takes place from the front, $k_V < 1$. When a stationary target is

[1]The unperturbed value of the angle of attack $\alpha_e = 0$. The sign (*) for $\Delta\varphi$ in the equations and in the functional diagrams is dropped.

attacked $k_V = 1.0$. The coefficient k_V is positive, because the lead angle $\psi > \frac{\pi}{2}$ is difficult to realize and is not required.

To investigate the dynamics of homing guidance with an accessible method we neglect the delay in the establishment of the angle of attack and consider the following system of equations /449

$$\left.\begin{aligned} & l\frac{d\Delta\varphi}{dt} - \Delta\varphi = +k_V\Delta\theta, \\ & T_V\frac{d\Delta\theta}{dt} = \alpha, \\ & \Delta\vartheta = \alpha + \Delta\theta, \\ & \alpha = k_\varepsilon\varepsilon, \\ & \varepsilon = \Delta\psi_0 - \Delta\varphi - \Delta\nu \end{aligned}\right\} \qquad (13.99)$$

or for feathered guidance

$$\varepsilon = \Delta\psi_0 - \Delta\varphi - \Delta\theta.$$

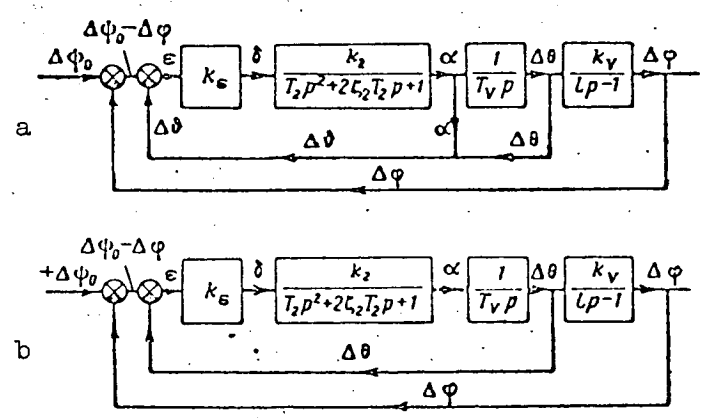

Figure 13.22. Functional diagram corresponding to equations (13.97). a--for unfeathered guidance; b-- for feathered guidance.

The coefficient k_ε in the fourth equation (13.99), unlike in the fifth equation (13.97), is a portion of the angle of attack per unit angle ε.

First let us analyze the case of unfeathered homing guidance. Eliminating variables $\Delta\theta$, $\Delta\alpha$, $\Delta\vartheta$ and ε from equations (13.99), we obtain an expression for $\Delta\varphi$

$$l\frac{d^2\Delta\varphi}{dt^2}+\left(\frac{k_{\varepsilon 1}}{T_V}l-2\right)\frac{d\Delta\varphi}{dt}+\frac{k_{\varepsilon 1}}{T_V}(k_V-1)\Delta\varphi=\frac{k_V k_{\varepsilon 1}}{T_V}\Delta\psi_0, \qquad (13.100)$$ /450

where

$$k_{\varepsilon 1}=\frac{k_\varepsilon}{k_\varepsilon+1}.$$

We can see from equation (13.100) that, in the first place, the error in the establishment of the lead angle $\Delta\psi_0$ produces a deviation of the missile's trajectory from the unperturbed states; in the second place, an increase in the amplification factor does not affect the dynamics of homing guidance, and, in the third place, expression (13.100) is a degenerate hypergeometric equation of type (13.80) with parameters b = 2 and a = $-(k_V - 1)$[1]. In this case there will be an increase in the coordinate $\Delta\varphi$ in the region of the target. We should also add that the increase in coordinate $\Delta\varphi$ will be most pronounced when attacks take place from the front hemisphere, when $k_V < 1$ and the last coefficient of equation (13.100) is negative. For the "frozen" coefficients of equation (13.100) the case $k_V < 1$ means that stability is lost, because one of the roots of the characteristic equation becomes positive. In the same way, in the solution of the equation with variable coefficients, i.e., in the solution of equation (13.100), as it stands, when $k_V < 1$, there will be a component which increases with time. With an unfavorable combination of initial conditions $\Delta\varphi_0$ and $\Delta\dot{\varphi}_0$, this component may become most significant, in which case there will be a monotonic increase in the deviation $\Delta\varphi$ from the beginning of guidance.

Let us consider this equation in more detail and establish the combination of initial conditions described by equation (13.100) which will be particularly undesirable. Let us "freeze" the coefficients of equation (13.100). In this case the solution of the homogeneous equation with given initial values $\Delta\varphi_0$ and $\Delta\dot{\varphi}_0$ will have the form

$$\Delta\varphi=-\frac{\Delta\dot{\varphi}_0\pm\Delta\varphi_0\eta}{\sigma\mp\eta}e^{-\sigma t}+\frac{\Delta\dot{\varphi}_0+\Delta\varphi_0\sigma}{\sigma\mp\eta}e^{\mp\eta t}, \qquad (13.101)$$

where σ is the absolute value of the large root of the characteristic equation $p_1 = -\sigma$; and η is the absolute value of the small root of the characteristic equation.

---

[1]We can prove this by introducing a new independent variable $\tau=l\frac{k_{\varepsilon 1}}{T_V}=\left(l_0-l\right)\frac{k_{\varepsilon 1}}{T_V}$.

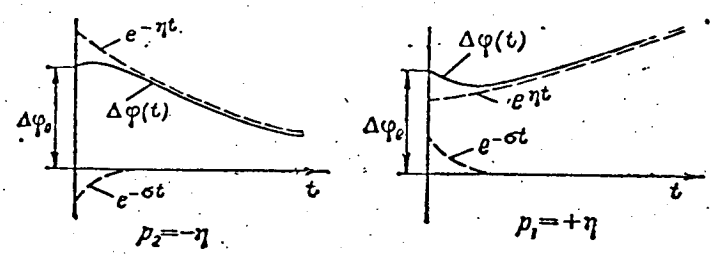

Figure 13.23. Graphs constructed by means of equation (13.101).

When $k_V > 1$, the small root is negative ($p_2 = -\eta$), while when $k_V < 1$, it is positive ($p_2 = \eta$). As we can see from (13.101) the combination of initial conditions $\Delta\dot{\varphi}_0 = 0$, $\Delta\varphi_0 \neq 0$ refers to the unfavorable case, because the significant component in this case is determined by the small root. Figure 13.23 shows the process given by expression (13.101) with a small positive and negative root $p_2 = \pm\eta$ for the above initial conditions. /451

As we can see from figure 13.23, the initial deviation damps very slowly when $p_2 = -\eta$ and begins to increase almost immediately when $p_2 = \eta$. For the zero root $p_2 = 0$.

$$\Delta\varphi = \frac{\Delta\dot{\varphi}_0}{\sigma}(1 - e^{-\sigma t}) + \Delta\varphi_0. \tag{13.102}$$

The initial deviation will vary from $\Delta\varphi_0$ to $\Delta\varphi_0 + \frac{\Delta\dot{\varphi}_0}{\sigma}$, when $t \to \infty$. Now let us see how the angular velocity $\Delta\dot{\varphi}$ will vary. After differentiating (13.101) we find

$$\Delta\dot{\varphi} = \frac{\Delta\dot{\varphi}_0 \pm \Delta\varphi_0\eta}{\sigma \mp \eta}\sigma e^{-\sigma t} \mp \eta\frac{\Delta\dot{\varphi}_0 + \Delta\varphi_0\sigma}{\sigma \mp \eta}e^{\mp\eta t}. \tag{13.103}$$

For initial conditions $\Delta\varphi_0 = 0$, $\Delta\dot{\varphi}_0 \neq$ we have

$$\Delta\dot{\varphi} = \frac{\Delta\dot{\varphi}_0}{\sigma \mp \eta}[\sigma e^{-\sigma t} \mp \eta e^{\mp\eta t}]. \tag{13.104}$$

With this combination of initial conditions the small root (positive or negative) has no practical effect on the decrease in the angular velocity.

The small root of the characteristic equation means that the value of coefficient $\frac{k_{\varepsilon 1}}{T_V}(k_V - 1)$ in equation (13.100) is small. Therefore, the analysis which we have conducted is entirely valid with respect to the initial stage of the solution given by nonstationary equations of type (13.100). From (13.100) we proceed to the equation for the miss χ. We differentiate equation (13.100) and note that /452

$$\frac{d\Delta\varphi}{dt} = -\frac{1}{V_{c0} l^2}\chi. \tag{13.105}$$

After differentiating (13.100), making use of (13.105) and transforming to an independent variable l, we obtain

$$l^2 \frac{d^2\chi}{dl^2} - l\left[1 + \frac{k_{\varepsilon 1}}{T_V} l\right]\frac{d\chi}{dl} + \frac{k_{\varepsilon 1} k_V}{T_V} l\chi = \tag{13.106}$$
$$= -\frac{V_{c0} k_V k_{\varepsilon 1}}{T_V} l^3 \frac{d\Delta\bar{\psi}_0}{dl}.$$

We see from equation (13.106) that the constant error $\Delta\overline{\psi}_0$ does not produce a miss. The characteristic equation for (13.106) has no negative roots. Consequently, in spite of the increase in the angle $\Delta\varphi$, the initial miss will be selected up to zero. However, this decrease in the miss to zero is accompanied not only by the increase in the coordinate $\Delta\varphi$, but also by an increase in the angle of attack, and the natural zero value of miss takes place only when the angle of attack is infinitely large which, of course, is impossible.

By eliminating the unnecessary variables from expressions (13.99) we find the equation for the angle of attack (when $\Delta\psi_0=0$)

$$l\frac{d^2\alpha}{dl^2} + \left(\frac{k_{\varepsilon 1}}{T_V} l - 2\right)\frac{d\alpha}{dt} + \frac{k_{\varepsilon 1}}{T_V}(k_V - 2)\alpha = 0. \tag{13.107}$$

This relationship is also a degenerate hypergeometric equation of type (13.80). The equation of the miss (13.106) may have a small value for the last coefficient $\frac{k_{\varepsilon 1}}{T_V} k_V$, while the equation for the angle of attack (13.107), like equation (13.100), may have a negative value for this coefficient. However, the miss is proportional to $d\Delta\varphi/dt$ and the angle of attack is proportional to $d\Delta\theta/dt$, while for angular velocities according to (13.104) the effect of the small last coefficient in the equation is insignificant. Thus, for the miss and for the angle of attack the process at the initial stage of guidance will converge rapidly. For angles $\Delta\varphi$ and $\Delta\theta$, as indicated by (13.101), the process may converge slowly ($k_V > 1$), or diverge ($k_V < 1$). However, this is insignificant, because this result merely means that angles $\Delta\varphi$ and $\Delta\theta$ are indeterminate when the missisle approaches the target.

Now let us consider the case of feathered homing guidance. From equations (13.99) and (13.96) we obtain the respective expressions for deviation $\Delta\varphi$, miss χ and angle of attack α /453

$$\left.\begin{aligned}
&l\frac{d^2\Delta\varphi}{dt^2}+\left(\frac{k_\varepsilon}{T_V}l-2\right)\frac{d\Delta\varphi}{dt}+\frac{k_\varepsilon}{T_V}(k_V-1)\Delta\varphi=\frac{k_Vk_\varepsilon}{T_V}\Delta\psi_0,\\
&l\frac{d^2\chi}{dt^2}-l\left[1+\frac{k_\varepsilon}{T_V}l\right]\frac{d\chi}{dt}+\frac{k_\varepsilon k_V}{T_V}l\chi=V_{c6}\frac{k_Vk_\varepsilon}{T_V}l^2\frac{d\Delta\psi_0}{dt},\\
&l\frac{d^2\alpha}{dt^2}+\left(\frac{k_\varepsilon}{T_V}l-2\right)\frac{d\alpha}{dt}+\frac{k_\varepsilon}{T_V}(k_V-2)\alpha=0.
\end{aligned}\right\}\qquad(13.108)$$

Equation (13.108) does not differ in any way from the corresponding equations of unfeathered homing guidance. However, the amplification factor k (unlike $k_{\varepsilon 1}=\frac{k_\varepsilon}{k_\varepsilon+1}$ for the unfeathered guidance) may be assigned any desirable value. Consequently, by selecting k_ε we may realize a desirable rate of decrease in the deviations and the miss along the initial region of homing guidance. Thus, feathered guidance may provide for higher hit accuracy precisely because k_ε can be controlled. Regarding the unfavorable phenomena which can occur in the motion of the missile when $k_V < 1$ (for the angle $\Delta\varphi$), the picture for feathered homing guidance remains the same as for unfeathered homing guidance.

2. The Dynamics of Homing Guidance for the Pursuit Method with an Auxiliary Lead Angle, Proportional to the Angular Velocity of the Line Joining the Missile and the Target. Let us require that the lead angle for any deviation from the unperturbed state increase by a value proportional to the angular velocity of the line joining the missile and the target.

To achieve this effect we must send a signal to the control surfaces proportional to $d\varphi/dt = d\Delta\varphi/dt$. If we neglect the process for the establishment of the angle of attack, the angle of attack must satisfy the law

$$\alpha=k_\varepsilon\varepsilon+k_{\dot\varphi}\frac{d\Delta\varphi}{dt}.\qquad(13.109)$$

From the first three equations of (13.99), from equation (13.95) and from the control law (13.109), after eliminating the corresponding variables, we obtain an expression for $\Delta\varphi$

$$l\frac{d^2\Delta\varphi}{dt^2}+\left[\frac{k_{\varepsilon 1}}{T_V}l-\left(2-\frac{k_Vk_{\dot\varphi}}{T_V(1+k_\varepsilon)}\right)\right]\frac{d\Delta\varphi}{dt}+\frac{k_V-1}{T_V}k_{\varepsilon 1}\Delta\varphi=0,\qquad(13.110)$$

where /454

$$k_{\varepsilon 1} = \frac{k_\varepsilon}{k_\varepsilon + 1}.$$

After we replace t by $\tau = \frac{k_{\varepsilon 1}}{T_V} l = \frac{k_{\varepsilon 1}}{T_V} (l_0 - l)$, equation (13.110) transforms into the hypergeometric equation (13.80) with parameters

$$b = 2 - \frac{k_V k_{\dot\varphi} k_\varepsilon}{T_V}$$

and

$$a = -(k_V - 1).$$

One of the roots of the characteristic equation is equal to zero, while the second is equal to $\rho = 1 - b$. By properly selecting $k_{\dot\varphi}$ we can always satisfy the condition $b < 1$ (or $\rho > 0$) and, consequently, prevent the increase in the coordinate $\Delta\varphi$ near the target. The same conclusion is obtained with respect to the angle of attack.

By comparing expressions (13.110) and (13.100) , we see that by introducing the signal $d\Delta\varphi/dt$ into the control law we can increase the damping properties of the system (because by selecting the coefficient $k_{\dot\varphi}$ we can change the value of the coefficient in front of the first derivative). The last coefficient of the equation did not change when the additional signal $d\Delta\varphi/dt$ was introduced with a portion of $k_{\dot\varphi}$. Therefore, everything we have said concerning the behavior of the coordinate $\Delta\varphi$ remains valid in the present case.

To realize the control law (13.109) it is necessary to measure the angular velocity of the line joining the missile and the target. When going over to parallel approach it is sufficient to let the coefficient k_ε be zero in the control law (13.109). In this case equation (13.110) is transformed into an equation of the first order with respect to $\dot\varphi = d\Delta\varphi/dt$.

3. The Dynamics of Homing Guidance Using the Pursuit Method When Attacking a Stationary Target (With and Without a Lead Angle). When the target is stationary, $k_V = 1$ and all of the equations for the angle of attack and the miss considered in subsections 1 and 2 of the present section degenerate into equations of the first order, because these quantities are, respectively, proportional to the angular velocities $d\Delta\theta/dt$ and $d\Delta\varphi/dt$. It has already been pointed out that in this case angles $\Delta\theta$ and $\Delta\varphi$ are indeterminate when the missile approaches the target. First, let us show how the equations for the miss (13.106) degenerate into equations of the first order. We multiply this equation by l^{-3} and write in terms of the variable t. /455

$$l^{-1}\frac{d^2\chi}{dl^2} + \left(l^{-2} + \frac{k_{\varepsilon 1}}{T_V} l^{-1}\right)\frac{d\chi}{dl} + \frac{k_{\varepsilon 1}}{T_V} l^{-2}\chi = 0. \qquad (13.111)$$

By making a check we see that equation (13.111) is an equation of the first order, which has been differentiated once after it was first multiplied by $l^{-1} = \frac{1}{l_0 - t}$.

$$\frac{dx}{dt} + \frac{k_{\varepsilon 1}}{T_V} x = 0, \tag{13.112}$$

Thus, the miss incurred in attacking the stationary target varies in accordance with the solution of the first order equation with constant coefficients, specifically

$$x = x_0 e^{-\frac{k_{\varepsilon 1}}{T_V} t}. \tag{13.113}$$

The smaller the value of T_V and the greater $k_{\varepsilon 1}$, the more intense is the decrease in the miss. For feathered guidance $k_{\varepsilon 1}$ must be replaced by k_ε, and the intensity of miss decrease may be increased.

Turning to equation (13.107) for the angle of attack when $k_V = 1$, we have

$$l \frac{d^2 x}{dt^2} + \left(\frac{k_{\varepsilon 1}}{T_V} l - 2 \right) \frac{dx}{dt} - \frac{k_{\varepsilon 1}}{T_V} \alpha = 0. \tag{13.114}$$

Similar to expression (13.111), this equation becomes a once differentiated equation of the first order

$$l \frac{d\alpha}{dt} + \left(\frac{k_{\varepsilon 1}}{T_V} l - 1 \right) \alpha = 0. \tag{13.115}$$

Equation (13.115) may be solved by separating the variables

$$\alpha = \alpha_0 \frac{l_0}{l_0 - t} e^{-\frac{k_{\varepsilon 1}}{T_V} t}. \tag{13.116}$$

In accordance with equation (13.116) the angle of attack will first decrease, because the term $e^{-\frac{k_{\varepsilon 1}}{T_V} t}$ increases. Towards the end of homing guidance /456 the picture changes and the term $\frac{l_0}{l_0 - t}$ increases more rapidly, while the term $e^{-\frac{k_{\varepsilon 1}}{T_V} t}$ is almost constant. As a result, when $t \to l_0$, the angle of attack $\alpha \to \infty$. Thus, the exponential damping of the miss is achieved only when the angle of

attack has an infinite value in the region close to the target. Since this is impossible, homing guidance must be stopped at some distance from the target.

According to expression (13.116), the angle of attack has a minimum. Let us find this minimum and the time when it occurs. After differentiating equations (13.116) and setting the derivative equal to zero, we have

$$l_{\min} = l_0 - \frac{T_V}{k_{\varepsilon 1}} \tag{13.117}$$

and

$$\alpha_{\min} = \alpha_0 l_0 \frac{k_{\varepsilon 1}}{T_V} e^{-\left(\frac{k_{\varepsilon 1}}{T_V} l_0 - 1\right)}. \tag{13.118}$$

According to equation (13.113), the miss is damped to a value equal to 5 percent of its initial value after $3\frac{T_V}{k_{\varepsilon 1}}$. This value of the miss coincides with the minimum value of the angle of attack, when the initial range is $l_0 = 4\frac{T_V}{k_{\varepsilon 1}}$. If we assume that T_V = 1.0 sec, $k_\varepsilon = 2\left(k_{\varepsilon 1} = \frac{2}{3}\right)$, then l_0 = 4 3/2 = 6 sec, which, for example, when the velocity is 200 m/sec, will be 1200 m. When the initial range is greater than $4V\frac{T_V}{k_{\varepsilon 1}}$, the miss will become 5 percent of its initial value, before the angle of attack reaches its minimum value. This minimum value is smaller when the initial range $l_0 = \frac{L_0}{V}$ is longer. Let us now see the minimum value of the angle of attack, when $l_0 = 4\frac{T_V}{k_{\varepsilon 1}}$:

$$\alpha_{\min} = \alpha_0 4 e^{-3} \approx 0.2\alpha_0.$$

Thus, at the instant of time when the miss is reduced to 5 percent of its initial value, the angle of attack will be reduced to 20 percent of its initial value. This value of the angle of attack is determined in terms of the initial value of the miss. To establish this relationship, we write down the system of initial equations for a stationary target (for example, for feathered guidance) /457

$$\left.\begin{aligned} l\frac{d\Delta\varphi}{dt} &= \Delta\varphi - \Delta\theta, \\ T_V\frac{d\Delta\theta}{dt} &= \alpha, \\ \alpha &= k_\varepsilon \varepsilon, \\ \varepsilon &= \Delta\varphi - \Delta\theta - \alpha. \end{aligned}\right\} \tag{13.119}$$

From the last two equations we find

$$\frac{1}{k_{\varepsilon 1}}\alpha = \Delta\varphi - \Delta\theta. \tag{13.120}$$

Furthermore, for a stationary target we obtain the following expression from equation (13.105)

$$\frac{d\Delta\varphi}{dt} = -\frac{1}{Vl^2}x. \tag{13.121}$$

Comparing the first equation of (13.119) and expressions (13.120) and (13.121), we find an expression for the miss which is characteristic for this case

$$x = -\frac{Vl}{k_{\varepsilon 1}}\alpha = -\frac{L}{k_{\varepsilon 1}}\alpha. \tag{13.122}$$

From this we obtain the initial value of the angle of attack for a given initial miss

$$\alpha_0 = -\frac{k_{\varepsilon 1}}{L_0}x_0. \tag{13.123}$$

We note that the equation for the angle of attack (13.115) may be obtained directly from system (13.119). Then, by using relationship (13.123), we can obtain the equation for the miss.

Let us also consider the effect of the signal proportional to the angular velocity $d\Delta\varphi/dt$ in the control law (13.109). If we replace the third expression in system (13.119) by equation (13.109), we obtain an equation for the angle of attack

$$l\frac{d\alpha}{dt} + \left(\frac{k_{\varepsilon 1}}{T_V}l - 1 + \frac{k_{\varepsilon 1}k_{\dot\varphi 1}}{T_V} - \frac{k_{\dot\varphi 1}}{l + k_{\dot\varphi 1}}\right)\alpha = 0, \tag{13.124}$$

where /458

$$k_{\varepsilon 1} = \frac{k_\varepsilon}{k_\varepsilon + 1} \quad \text{and} \quad k_{\dot\varphi 1} = \frac{k_{\dot\varphi}}{k_\varepsilon}.$$

In this case the miss expressed in terms of the angle of attack will have the following form

$$x = -\frac{Vl^2\alpha}{k_{\varepsilon 1}(l + k_{\dot\varphi 1})}. \tag{13.125}$$

Using this expression we obtain an equation for the miss from (13.124)

$$\frac{dx}{dt} + \frac{k_{\varepsilon 1}}{T_V}\frac{l + k_{\dot\varphi 1}}{l}x = 0. \tag{13.126}$$

Both equations are solved by the separation of variables

$$\alpha = \alpha_0 \frac{l + k_{\dot{\varphi}} l}{l_0 + k_{\dot{\varphi}} l} \left(\frac{l}{l_0}\right)^{b-2} e^{-\frac{k_{\varepsilon l}}{T_V} t} \tag{13.127}$$

and

$$\varkappa = \varkappa_0 \left(\frac{l}{l_0}\right)^{b} e^{-\frac{k_{\varepsilon l}}{T_V} t}, \tag{13.128}$$

where

$$b = \frac{k_{\varepsilon l} k_{\dot{\varphi} l}}{T_V} = \frac{k_{\dot{\varphi}}}{T_V (k_\varepsilon + 1)}.$$

As we can see from these expressions the decrease in the miss take place more rapidly than the exponential law, and the angle of attack for $b > 2$ will not have a minimum, and when $t = l_0$ it will be equal to zero like the miss.

Therefore, additional control of the angular velocity produces favorable results.

Let us compare law (13.109) with the law of parallel approach when attacking a stationary target. To guide the missile by the method of parallel approach, it is sufficient to set $k_\varepsilon = 0$ in expression (13.109)

$$\alpha = k_{\dot{\varphi}} \frac{d\Delta\varphi}{dt}. \tag{13.129}$$

Using the first two equations of (13.119) and equation (13.129), we obtain the expression for the miss and for the angle of attack /459

$$l \frac{d\varkappa}{dt} + \frac{k_{\dot{\varphi}}}{T_V} \varkappa = 0 \tag{13.130}$$

and

$$l \frac{d\alpha}{dt} + \left(\frac{k_{\dot{\varphi}}}{T_V} - 2\right) \alpha = 0. \tag{13.131}$$

From the solution of these equations we obtain

$$\varkappa = \varkappa_0 \left(\frac{l}{l_0}\right)^{\frac{k_{\dot{\varphi}}}{T_V}}, \tag{13.132}$$

and

$$\alpha = \alpha_0 \left(\frac{l}{l_0}\right)^{\frac{k_{\dot{\varphi}}}{T_V} - 2}. \tag{13.133}$$

Comparing expressions (13.128) and (13.132), we note that in the first case the decrease in the miss due to the exponential factor takes place more intensely. From this point of view the combined law (13.109) is more effective than the law of parallel approach.

CHAPTER 14. THE DYNAMICS OF EXTERNALLY GUIDED MISSILES /460

Section 14.1. Formulation of the Problem

Externally guided missiles are directed to the target by signals from the control point. The simplest method is the method of beam guidance. We recall that in this method target and missile are sighted continuously from the control point.

Guidance consists of keeping the missile on the target sighting line (fig. 14.1). If the missile is maintained on the sighting line, the three points--control point, missile point and target point--always lie on one straight line. The mismatch signal represents the angular μ or linear ϵ deviation of the missile from the sighting line. The angular mismatch is taken into account by the visual control of the missile and the target. In this case the human operator sends signals over the guidance link to deflect the control surfaces of the missile. The measurement of the linear deviation ϵ may be realized by means of a radio beam. In this case its equisignal zone coincides with the line joining the control point and the target (cp-T).

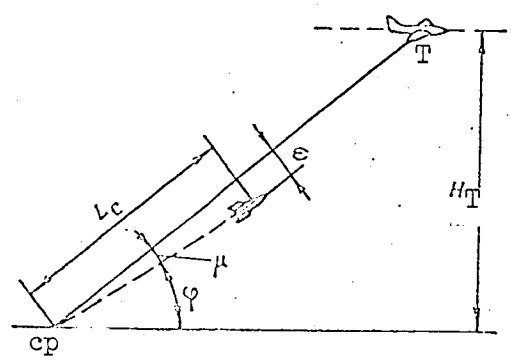

Figure 14.1. Schematic diagram of beam guidance; cp = control point; C = missile; T = target.

In the general case, when the coordinates of the target and the missile are measured at the control point, computers may be used to obtain the most diverse methods for guiding missiles to the target. In particular, all of the methods of homing guidance considered in Chapter 13 may be applied. In this case the dynamics of missiles with homing guidance and with external guidance will coincide. The difference will only be in the engineering methods of realizing any of the guidance techniques. In homing guidance the control signals are formed at the missile, while in external guidance they are formed /461

at the control point and are transmitted to the missile over the remote control link.

In this chapter we consider the kinematics and dynamics of the beam method and also some other methods of guiding missiles to surface and aerial targets, achieved by means of external guidance.

Section 14.2. The Kinematic Trajectories of the Beam Method

In the general case, the target and the control point are displaced with velocities V_T and V_{cp}. This general case corresponds to guidance of air-to-air missiles by the beam method. The missile velocity V is usually greater than velocity V_{cp} of the airplane which launches and controls this missile. Important specific cases are as follows: (1) $V_{cp} = 0$--guidance of the surface-to-air missile and (2) $V_T = 0$--guidance of the air-to-surface missile.

Let us write the kinematic equations for the pairs target-control point and target-missile, assuming that the missile is situated exactly on the target sighting line (fig. 14.2). The equations of the target-control point have the form

$$\left.\begin{aligned} \dot{L}_{cp} &= V_T \cos\varphi - V_{cp}\cos(\varphi - \theta_{cp}) \\ L_{cp}\,\dot{\varphi} &= -V_T \sin\varphi + V_{cp}\sin(\varphi - \theta_0), \end{aligned}\right\} \tag{14.1}$$

while the equations for the target-missile have the form

$$\left.\begin{aligned} \dot{L} &= V_{cp} \cos\varphi - V\cos(\varphi - \theta), \\ L\dot{\varphi} &= -V_{cp}\sin\varphi + V\cos(\varphi - \theta). \end{aligned}\right\} \tag{14.2}$$

The values of the angles in equations (14.1) and (14.2) are shown in figure 14.2. The equations are written for rectilinear target motion, and the quantities V_T, V, V_{cp}, and θ_{cp} must be assigned as functions of time. Because in the kinematic formulation of the problem the missile is always maintained on the sighting line, the angular velocities and the instantaneous angular positions of the segments cp-T and C-T (fig.14.2) always coincide. This is reflected in equations /462

(14.1) and (14.2) by the introduction of quantities φ and $\dot{\varphi}$, common to both control methods.

To establish the trajectory of the missile and the necessary handling analytically, it is necessary to solve equations (14.1) first and to find $\varphi = \varphi(t)$, and then to use the solution of equations (14.2) and find $L = L(t)$, $\theta = \theta(t)$. The analytical solution of equations (14.1) and (14.2) may be obtained only in the form of series; therefore, graphical methods are used to

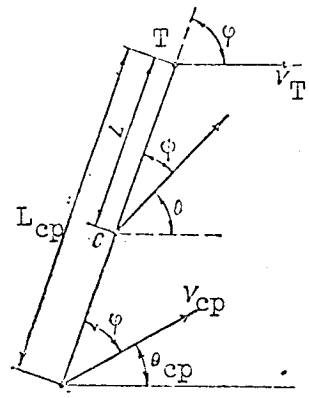

Figure 14.2. Geometric configuration of target, missile and control point in beam method.

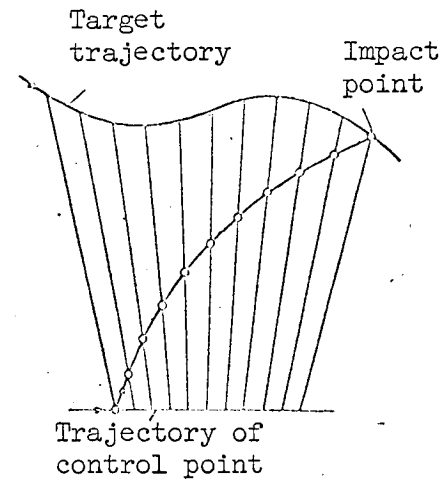

Figure 14.3. Construction of kinematic trajectory for beam method.

obtain the kinematic trajectory and the guidance time. These graphical methods are very simple (an example is shown in figure 14.3. In regard to the necessary handling or the angular velocities of the missile velocity vector, they can be obtained analytically in special cases. Thus, for the case of a surface-to-air missile, we have the following analytical expression for the angular velocity of the missile's velocity vector[1]

$$\dot{\theta} = \frac{2V_T \sin^2\varphi}{H_T}\left(1 + \frac{L_c \operatorname{ctg}\varphi}{\sqrt{\frac{k^2}{\sin^4\varphi} - L_c}}\right), \tag{14.3}$$

where H_T is the constant altitude of the target; $L_c = L_{cp} - L$ is the distance from the control point to the missile; and $k = \frac{V}{T}$.

This equation is valid for H_T = const, V_T = const and V = const. /463

In the guidance of air-to-air missiles it is possible to reduce the load factors of the missile by maneuvering the airplane which controls the missile. When $\overline{V}_T$ = const, the control point may be maneuvered to obtain a rectilinear missile flight. The flight of the airplane, controlling the missile when it makes a parallel approach to the target, permits least load factors of the missile when the target undergoes maneuvers, and reduces the handling to zero when attacking a target not undergoing evasive maneuvers. Indeed, during the

[1]A. S. Lokk, Guided Missiles, Gostekhizdat, 1957.

flight of the airplane with the control point, $\dot{\varphi} = 0$ and $\varphi = \text{const}$ during a parallel approach. Both of these conditions are also satisfied for the missile. Consequently, the missile also goes to the target along the parallel approach, i.e., in the most economical way from the standpoint of load factors. Thus, when the airplane with the control point undergoes optimum maneuvers, the beam guidance method is reduced to homing guidance with parallel approach, considered in Chapter 13.

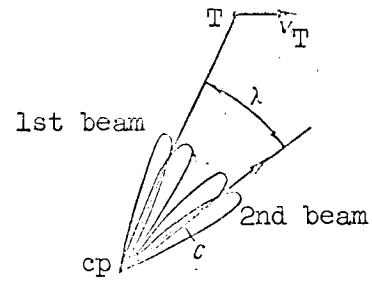

Figure 14.4. Schematic diagram showing beam guidance of missile by using second radar to track target.

We note that in any case the beam guidance problem is reduced to a homing guidance problem with a lead angle ψ, which is a function of time and of various quantities depending on the homing guidance method. For the beam guidance of surface-to-air missiles we can obtain the parallel approach of the missile to the target. However, because the control point in this case is stationary, the parallel approach may be realized by means of two beams (fig. 14.4). One of the beams tracks the target, while the second beam is used to guide the missile. The angle λ between the beams can be varied in any manner by rotating the second beam. This is done in such a way that we achieve a parallel approach of the target by the missile. However, regardless of how angle λ varies, at the instant of time when the missile hits the target angle λ must be zero, and the axes of both beams must coincide.

In the present chapter we shall describe other variations of the external guidance systems by which any methods of guidance can be realized, including the method of parallel approach.

Section 14.3. Dynamics of Guiding the Missile Along the Beam /464

An investigation of the dynamics of a missile moving along a beam will clarify the structure of the missile guidance system which holds the missile on the beam, as well as the accuracy of this operation or the accuracy of maintaining the kinematic trajectory.

First let us consider the dynamics of a missile in the simplest case, i.e., when the beam is stationary in space. The beam may become nonstationary when the target velocity vector and the control point velocity vector

coincide with the sighting line or with the equisignal zone of the beam, or when the velocities of the target and of the control point are equal to zero. This situation occurs when the target is attacked by an air-to-air missile directly at its tail or its head, or when a stationary target is attacked from a stationary control point.

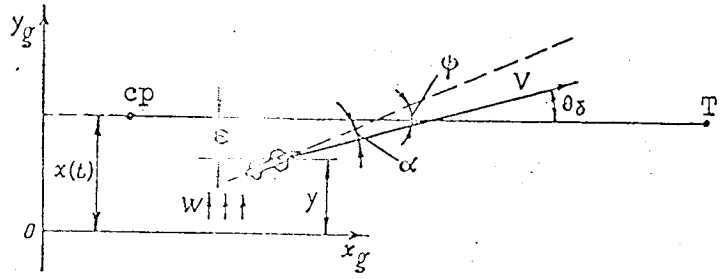

Figure 14.5. Position of missile with respect to target sighting line.

Figure 14.5 shows the general case for the position of a missile with respect to the target sighting line, which in this case becomes the given trajectory. The missile deviates from this trajectory and has a nonzero initial velocity dyg/dt. In addition, the missile may be subjected to a side wind. In the present chapter we also consider the dynamics of plane motion. Because in this case motion may take place in the vertical, horizontal or any other plane, the output coordinate of the system will be designated by y (in Chapter 11 this is designated by z_g and y_g), the input coordinate will be designated by x(t) (in Chapter 11 it was designated by $z_3(t)$ and $y_3(t)$, the error will be designated by $\varepsilon = x(t) - y(t)$, the angle between the velocity vector and the direction of the given trajectory will be designated by θ_δ, and the angle between the longitudinal axis of the missile and the direction of the given trajectory will be designated by ψ. The control of the motion experienced by the missile's center of gravity, both in a calm atmosphere as well as in the presence of wind, is considered in detail in Chapters 11 and 12. These chapters present the diagrams of control systems for the center of gravity, which operate on the basis of various principles and give recommendations for selecting the parameters of these control systems.

Let us consider the special features associated with the motion of the center of gravity when the missile must move along a moving beam. Precisely this case is of most interest. /465

Chapter 12 presents general information on errors occurring when the missile moves along moving and curvilinear trajectories, and also presents methods for eliminating these errors. It is precisely these cases that are of most practical interest in beam guidance.

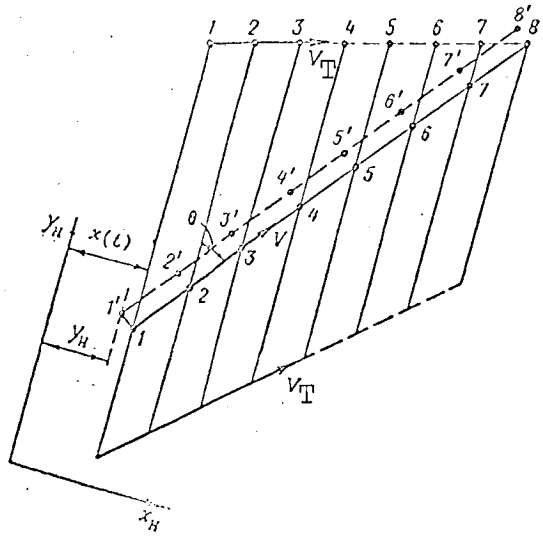

Figure 14.6. Trajectory of missile guided with beam by method of parallel approach; subscript H = fixed.

Let us consider an example which clarifies the use of these data in studying the motion of missiles along a beam. We consider the simplest case, when the beam is displaced in space parallel to itself. As we already mentioned, the beam will move in this manner if the control point moves towards the target according to the law of parallel approach.

If the fixed system of coordinates is situated as shown in figure 14.6, the assigned value of a coordinate will vary according to the law

$$x(t) = kt.$$

In Chapter 11 we pointed out that for a given control law the missile may move, when the coordinate x(t) varies according to this law, either exactly along the beam or with an error obtained from the differential equation of the missile control system. The solid line in figure 14.6, which passes through points 1, 2, 3, . . ., is the trajectory for the stationary motion of the missile which has no static error for the law x(t) = kt. Point 8 is the impact point of the missile and the target. /466

The broken trajectory 1', 2', 3',. . ., is the trajectory of a missile moving with a systematic error. This trajectory occurs when the control laws do not include an integral term. Since the missile moves with an error, at the moment when the target has approached po nt 8 the missile has approached point 8'. As we can see, in this case the missile misses its target. Whether we have an error or not, a constant lead angle θ_{lead} is established between the beam and the missile velocity vector (similar to the drift angle caused by wind). This angle

corresponds to conditions for the parallel approach of the missile to the target.[1]

For curvilinear kinematic trajectories, when any control laws are used, an error will be observed, i.e., the deviation of the missile from the kinematic trajectory. This deviation may be determined, if we compute the initial acceleration necessary to realize the kinematic trajectory (Chapter 16).

Section 14.4. Dynamics of the Beam Method During Visual Sighting

At the present time various systems are used to isolate targets, using some contrast feature of the target which separates it from its background.[2] These systems use the radiation or reflection of some form of energy by the target. The visual recognition of a target is still widely used in the guidance of missiles. The visual guidance of missiles is sometimes simpler and more reliable than the use of complex radar or infrared guidance systems. Visual methods may be used to guide the air-to-surface, surface-to-air and air-to-air missiles (when the velocities are small) and also to guide surface-to-surface missiles used at the battlefield.

The beam method is the natural method for guiding missiles visually. The operator observes the position of the missile and of the target through a sight and sends control signals to the missile attempting to keep it on the sighting line. In the case of ideal guidance the image of the missile in the sight coincides with the image of the target.

The control signals sent to the missile are obtained by means of a special /467
control lever. The kinematics and construction of the control lever are determined by the aerodynamic shape of the missile. In the guidance of missiles with cruciform wings, which are controlled in the Cartesian system of coordinates, the control lever may move in mutually perpendicular directions "right-left" and "up-down." Figure 14.7 shows the guidance of an air-to-surface missile. The up and down movement of the control lever produces a proportional displacement of the missile's altitude control surfaces. The right and left movement of the lever (normal to the plane in the drawing in figure 14.7) produces a proportional deflection of the rudders. To prevent the interchange of the two controls, the missile must be stabilized with respect to its longitudinal axis when it moves toward the target. Any missile with cruciform wings guided by a beam is stabilized in this way.

---

[1] When the missile moves with an error, angle θ_{lead} corresponds to conditions for the parallel approach to the point situated behind the target at a certain constant distance.

[2] V. I. Marisov and I. K. Kucherov, Guided Missiles, Voyenizdat, 1959.

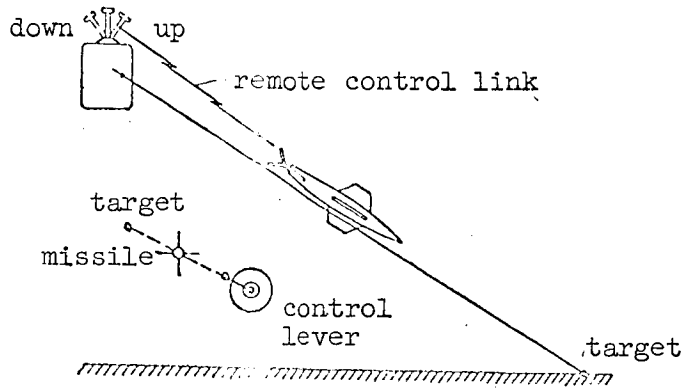

Figure 14.7. Guidance of an air-to-surface missile with cruciform wings by means of control lever.

The guidance of missiles with plane wings is accomplished by using a polar system of coordinates. As shown in figure 14.8, the control lever rotates about the longitudinal axis and is displaced from its vertical position in any direction. The displacement of the lever around the longitudinal axis changes the tilt angle and produces the same rotation of the missile around its longitudinal axis. The displacement of the lever from its vertical position produces a proportional deflection of the altitude control surfaces. Whether Cartesian control or polar control is used, the operator follows the same procedure: when the image of the missile is displaced from the image of the target, he must displace the control lever in the direction of the line joining the missile and the target. In the case of Cartesian control this leads to the required ratio in the displacement of the direction and altitude control surfaces, while in the case of polar control this leads to the coincidence of the missile's plane of symmetry with the line joining the missile and the target, and to the corresponding deflection of altitude control surfaces.

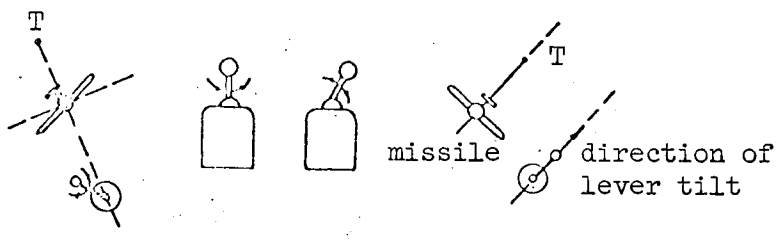

Figure 14.8. Control of missiles with plane wings by means of control lever.

In this control method the operator is directly included in the missile control loop. For visual guidance the operator controls the missile, depending on the angular deviation μ of the missile from the target sighting line (fig. 14.1). /468

When μ is small we have

$$\varepsilon = L_c \mu, \tag{14.4}$$

where ε is the deviation of the missile from the beam in the vertical plane; and L_c is the distance from the control point to the missile. When the missile moves away from the control point with constant velocity, $L_c = V_e t$, where V_c is the velocity at which the missile moves away from the control point.

Assuming that V_c = const, we differentiate (14.4)

$$\frac{d\varepsilon}{dt} = V_c t \dot{\mu} + V_c \mu. \tag{14.5}$$

Assuming that in this case $V\theta + W = d\varepsilon/dt$, we obtain

$$t\dot{\mu} + \mu = \frac{V}{V_c}\theta + \frac{W}{V_c}, \tag{14.6}$$

where θ is the deviation of the velocity vector from the beam, and W is the normal wind component.

If we know the relation between angle μ and angle θ, we can construct the schematic diagram for the visual control of a missile shown in figure 14.9. The transfer function which relates angle μ to angle θ consists of an inertial element with a continuously increasing time constant. During the guidance process the operator must develop a transfer function providing for the stability of the control loop (fig. 14.9); he must also maintain sufficient accuracy and

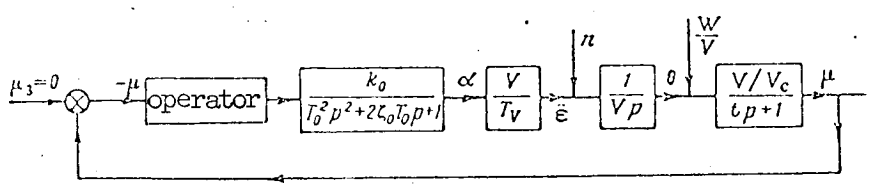

Figure 14.9. Schematic representation of system for visual control of missile.

rigidity in the stabilization process in the presence of perturbations in the form of lateral wind or excessive handling, which occurs when the missile moves along a curvilinear trajectory. It is well known that the operator can most easily perform the function of a simple amplifier. In this case, according to extensive experimental data, the transfer function of the operator has the form /469

$$W_{op}(p) = \frac{e^{-p\tau_{op}}}{T_{op}p + 1} k_{op}, \tag{14.7}$$

(subscript op = operator),

where $\tau_{op} \approx 0.25$ sec and $T_{op} = 0.1 - 0.3$ sec.

It follows from expression (14.7) that the amplification of the signal by factor k_{op} is accompanied by transfer delay τ_{op}, experienced by the operator, as well as by a delay which corresponds to that of an inertial element with the time constant T_{op}. However, in the control loop shown in figure 14.9 the transfer function of the operator which has the form of a simple amplifier is obviously quite insufficient. The operator must realize a transfer function of the type

$$W_{op}(p) = \frac{(T_{1op}\, p + 1)\, e^{-p\tau_{op}}}{T_{2op}\, p + 1}\, k_{op}, \tag{14.8}$$

where $T_{1op} \gg T_{2op}$.

It is difficult for the operator to realize this transfer function, and he can only do this after extensive training. However, under complex combat conditions even an experienced operator can lose control of a missile.

To improve the effectiveness of control, it is necessary to remove the operator from the control loop without losing the advantages associated with the visual detection of a target. This can be achieved by dividing the channels for the sighting of the target and of the missile. The channel for sighting the target remains under the control of the operator. The channel for sighting the missile is automated by an automatic missile tracking system at the control point. The automatic tracking system of a missile is not complicated, because the missile may contain a responder to signals from the control point. The problem encountered by the operator now becomes considerably simpler. He is only required to maintain the target at the crosshairs by displacing the moveable plate with the crosshairs with respect to the sighting plane. The signal picked up by the sensors on the plate will be equal to the bearing ϵ_T from the control point to the target. The signal which is picked up by the sensor of the automatic tracking system will be the bearing to the missile ϵ_c. The difference $\epsilon_T - \epsilon_c = \epsilon$ is the unknown angle between the direction to the target and the direction to the missile from the control point. Because signal ϵ is now electric, it may be transformed in any required manner. In particular, if we multiply ϵ by the L_c we obtain y_f, which is the lateral displacement of the missile from the beam. If we have signal y_f, we can construct any of these beam control systems. The operator is now outside the control loop, and his property of identifying the target is fully retained. /470

Section 14.5. Placing the Missile on the Beam

As a rule the launching point of a missile does not coincide with the axis of the beam. Therefore the missile is launched towards the beam, and the control system must place the missile on the axis of the beam. The missile control system is turned on under certain nonzero initial conditions $y\big|_{t=0} = y_0$ and $\frac{dy}{dt}\Big|_{t=0} = V\sin\theta_0 = V\theta_0$ (fig. 14.10). The missile must be placed on the beam under these conditions. The deviation signal obtained aboard the missile is always a nonlinear function of the deviation proper y. A typical form of this nonlinear function is shown in figure 14.10. The nonlinear function has a linear region $-m \le y \le m$, and it is only in this region that the linear equations and structural schemes presented in Chapters 11 and 12 are valid. In all these structural schemes with integral control the transfer functions will definitely exhibit overcontrol. It is known that the transient function as a reaction to /471

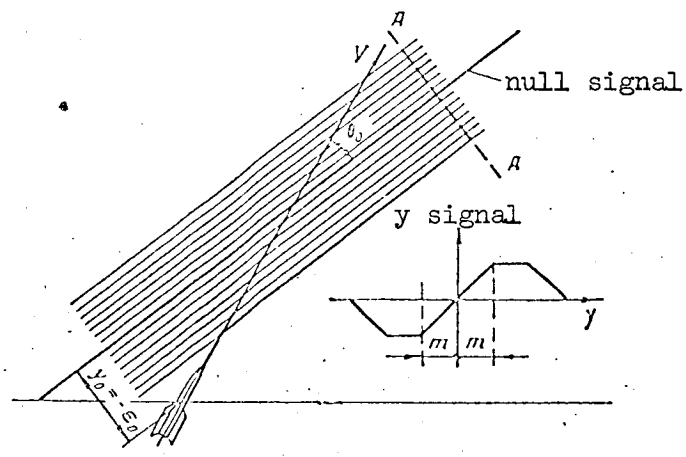

Figure 14.10. Position of missile with respect to radio beam.

step signal $y_0\,1(t)$ represents a mirror image with respect to the axis of the abscissas of the transient process with initial conditions $y(0) = y_0$; $\dot{y}(0) = \ddot{y}(0) = \ldots = 0$, and is displaced by amount y_0 (fig. 14.11).

If $\dot{y}(0) = \ddot{y}(0) = \dddot{y}(0) = \ldots = 0$, when the missile control system is turned on and $|y_0| \le m$, i.e., the missile is in the proportional band, the transient process will be brought to a satisfactory conclusion, in the sense that the missile enters the beam because overcontrol Δy_{oc} is always less than y_0. We must

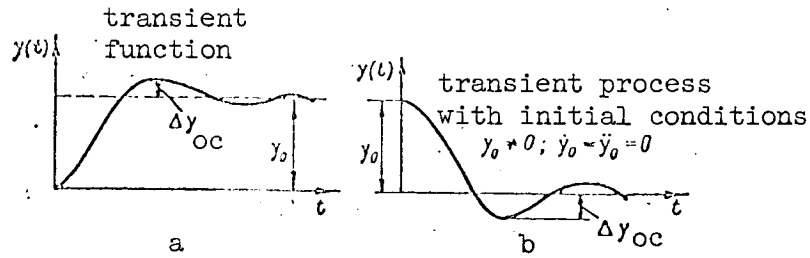

Figure 14.11. Graph of transient function; (a) and of transient process; (b) under specified initial conditions; oc = overcontrol.

always remember that when the control system is switched on, the initial velocity of the missile with respect to the beam $\dot{y}(0) = \dot{y}_0$ is not equal to zero, but is equal to $V\theta_0$ (fig. 14.10). In this case the sign of $\dot{y}_0$ is always such that it leads to an increase in overcontrol. If we take into account the effect of y_0, it may turn out that $\Delta y_{oc} > m$, i.e., there is danger that the missile might leave the beam and that control will be lost. To reduce this danger to a minimum, the parameters of the system must be selected such that the overcontrol property of the transfer function is as small as possible. However, in the functional schemes considered in Chapter 11, a decrease in overcontrol is achieved by increasing the control time. Consequently this method is undesirable. There are other ways of solving the problem of placing a missile on the beam, which do not produce an increase in the control time. By using modern computer elements we can obtain an optimum method for placing the missile on the beam. /472

As an example let us consider a simplified system with integral control (fig. 14.12). In this system the lateral control force and acceleration $\ddot{y}$, which is proportional to it, are established without delay and are proportional to the total control signal.

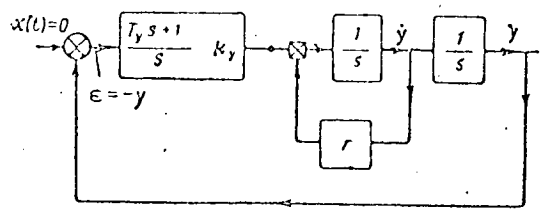

Figure 14.12. Simplified diagram of system with integral control.

Therefore, for the scheme shown in figure 14.12 we shall have

$$\ddot{y} = -r\dot{y} - k_y T_y y - k_y \int_0^t y\,dt,$$

where r is the feedback coefficient proportional to the transfer factor of the automatic pilot i_{ϑ}.

The transfer function for the closed loop input-output system has the following form for this scheme[1]

$$\Phi(s) = \frac{(T_y s + 1) k_y}{s^3 + rs^2 + T_y k_y s + k_y}. \tag{14.9}$$

Since this transfer function has a zero equal to $-1/T_y$, the transfer function will always exhibit overcontrol (fig. 14.11a). We obtain the Laplace transform of this function if we multiply $\Phi(s)$ by y_0/s

$$H^*(s) = \Phi(s) \cdot \frac{y_0}{s}.$$

In the same way the Laplace transform of the process y(t) with initial conditions $y_0 \neq 0$; $\dot{y}_0 = \ddot{y}_0 = 0$ (fig. 14.11b) will have the form

$$Y^*(s) = \frac{y_0}{p} - H^*(s) = \frac{s^2 + rs}{s^3 + rs^2 + T_y k_y s + k_y} y_0. \tag{14.10}$$

If, in addition, $\dot{y}_0 \neq 0$, we have /473

$$Y^*(s) = \frac{s^2 + \left(r + \frac{\dot{y}_0}{y_0}\right) s}{s^3 + rs^2 + T_y k_y s + k_y} \cdot y_0. \tag{14.11}$$

In this case overcontrol increases due to $\dot{y}_0$ when y_0 and $\dot{y}_0$ have opposite signs, and decreases when the signs of y_0 and $\dot{y}_0$ are the same. So that the value of overcontrol is not too great when the transfer function has the form (14.9), the roots of the characteristic polynomial

$$A(s) = s^3 + rs^2 + T_y k_y s + k_y$$

are selected so that they are real and are distributed in arithmetic progression (table 2.3). However, as we have pointed out, this increases the control time. However, if the roots of A(s) are selected so that they are multiples, we obtain inadmissible overcontrol, although the control time will be shortened. Bearing this in mind, let us select the roots of A(s) so that they are multiples. Then

---

[1] Here and in the future s is the parameter of the Laplace transform.

$$A(s) = (s + \sigma)^3 = s^3 + 3\sigma s^2 + 3\sigma^2 s + \sigma^3,$$
$$r = 3\sigma, \quad T_y k_y = 3\sigma^2, \quad \sigma^3 = k_y.$$

We note that for all real roots of the characteristic polynomial and for the case of a transfer function with the form

$$\Phi(s) = \frac{k_y}{A(s)}, \tag{14.12}$$

where $A(0) = k_y$, the transient function will not exhibit overcontrol. If for this constant $A(0) = k_y$ we assume that all of the roots of $A(s)$ are multiples, the control time be less than for any other real roots. This situation is the reason why the roots of the characteristic polynomial are selected as multiples.

Let us take a homogeneous differential equation

$$\dddot{y} + 3\sigma\ddot{y} + 3\sigma^2\dot{y} + \sigma^3 y = 0. \tag{14.13}$$

For $y_0 \neq$; $\dot{y}_0 = \ddot{y}_0 = 0$ its solution has the form

$$y = y_0 e^{-\sigma t}\left(1 + \sigma t + \frac{\sigma^2 t^2}{2}\right). \tag{14.14}$$

The graph of function (14.14) is shown in figure 14.13. This figure also represents /474

$$\dot{y}(t) = -y_0 \sigma e^{-\sigma t}\left(\frac{\sigma^2 t^2}{2}\right) \quad \text{and} \quad \ddot{y}(t) = y_0 \sigma^2 e^{-\sigma t}\left(\frac{\sigma^2 t^2}{2} - \sigma t\right).$$

The maximum value of velocity $\dot{y}(t)$ and the zero of acceleration $\ddot{y}(t)$ take place when $t_1 = 2/\sigma$. The maximum value of the derivative will be $\dot{y}(t_1) = -y_0 2\sigma e^{-2}$. At this instant of time the deviation is equal to $y(t_1) = 5y_0 e^{-2}$.

Let us assume that from the instant of time t_1 the curve $y(t)$ is the reference curve $y_r(t)$, which is used to place the missile on the beam axis. Such a curve is shown in figure 14.13 by the double line. Let us find the transform of this curve, assuming that time is measured from t_1. To obtain the transform of the curve we must carry out the Laplace transformation of equation (14.13) under the following initial conditions

$$y(0) = y_{01}, \quad \dot{y}(0) = -\dot{y}_{01} \quad \text{and} \quad \ddot{y}(0) = 0$$

$$Y_r^*(s) = \frac{s^2 + \left(3\sigma - \frac{\dot{y}_{01}}{y_{01}}\right)s - 3\sigma\frac{\dot{y}_{01}}{y_{01}} + 3\sigma^2}{(s+\sigma)^3}\, y_{01}.$$

Since $y_{01} = y(t_1)$, and $\dot{y}_{01} = -\dot{y}(t_1)$ and $\dot{y}_{01}/y_{01} = 2/5\,\sigma$, we drop index "1" and obtain the final expression for the transform of the curve which guides the missile to the beam

$$Y_r^*(s) = \frac{s^2 + \left(3 - \frac{2}{5}\right)\sigma s + \frac{9}{5}\sigma^2}{(s+\sigma)^3}\, y_0. \tag{14.15}$$

At the same time, when the roots are multiples, the following transform is obtained from equation (14.11) /475

$$Y^*(s) = \frac{s^2 + \left(3 + \frac{\dot{y}_0}{\sigma y_0}\right)\sigma s}{(s+\sigma)^3}\, y_0. \tag{14.16}$$

Expression (14.15) represents the Laplace transform of the required or reference curve $y_r(t)$ without overcontrol. The transform (14.16) corresponds to a curve with overcontrol, which in this case is quite large. By comparing (14.16)

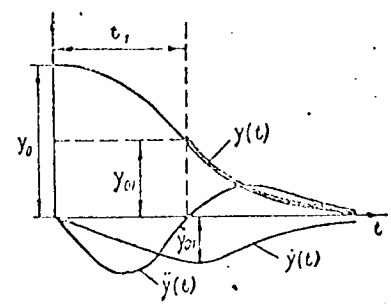

Figure 14.13. Graphs of function (14.14) with first and second derivatives.

and (14.15) we can see the terms required in the numerator of (14.16) to make the curve coincide with the reference curve. Let us see if we can achieve these terms (14.16) by feeding step signal $y_0 1(t)$ to the system through specially selected filters.

The step signal, which has passed through the filter, may be applied to the input of the system or, e.g., at point a of the scheme shown in figure 14.12. Let us consider the last variation. Let us find the transfer function of the system which can be applied at point a

$$\Phi_a(s) = \frac{\dfrac{1}{(s+r)s}}{1+\dfrac{(T_y s+1)k_y}{(s+r)s^2}} = \frac{s}{s^3+rs^2+T_y k_y s+k_y}$$

or, when the roots of the characteristic equation are multiples,

$$\Phi_a(s) = \frac{s}{(s+\sigma)^3}. \tag{14.17}$$

The form of the transfer function (14.17) shows that to form the term $\frac{\frac{9}{5}\sigma^2}{(s+\sigma)^3} y_0$ in the transform (14.15) it is sufficient to introduce a step signal $y_0 1(t)$ at point a (whose transform is y_0/s through an amplifier with a gain of $9/5\ \sigma^2$. Furthermore, if the transform of the process in the diagram in figure 14.12 is to be identical to (14.15), an additional signal must be introduced at point a. The value of this signal must be

$$-\left(\frac{2}{5}\sigma+\frac{\dot{y}_0}{y_0}\right) y_0 \delta(t). \tag{14.18}$$

Because it is impossible to realize a reaction in the form $\delta(t)$, we must be satisfied with a reaction of the step signal $y_0 1(t)$ through a real dif- /476
ferentiating network with a transfer function

$$W(p) = \frac{s}{Ts+1}.$$

If, in addition, $T \ll 1/\sigma$, the approximation to the reaction of the $\delta(t)$ function will be quite satisfactory.

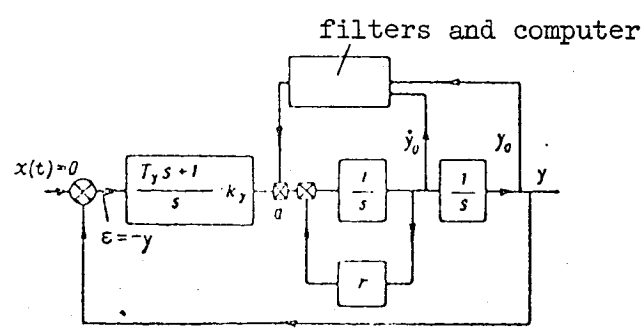

Figure 14.14. Functional diagram of system with additional signal dictated by initial conditions.

Figure 14.14 shows the functional diagram of a missile control system with additional reaction produced by a static signal whose magnitude is determined by the initial conditions. We can see from figure 14.14 that the signals due to initial conditions y_0 and $\dot{y}_0$ are transformed by the filters and by the computer into a signal acting on the system. We may call this negative feedback, which is determined from the initial conditions.

In this case the following signal is fed at point a

$$\left[\frac{6}{5}\sigma^2 - \left(\frac{2}{5}\sigma + \frac{\dot{y}_0}{y_0}\right)\frac{s}{Ts+1}\right] y_0 1(t). \tag{14.19}$$

To generate this signal we must measure y_0 and $\dot{y}_0$ and operate on them as indicated by expression (14.19). The operations which are attributed to expression (14.19) may be carried out by a digital computer aboard the missile. If the missile does not have a computer of this type, the operations may be performed by suitable passive filters and amplifiers. When digital computer techniques are used to generate the step signal, the initial conditions y_0 and $\dot{y}_0$ are stored in the memory of the machine during the entire period of time in which the missile is being placed on the beam. If a digital computer is not present, the conditions y_0 and $\dot{y}_0$ may be memorized by means of an integrating device with a shorttime, negative feedback.

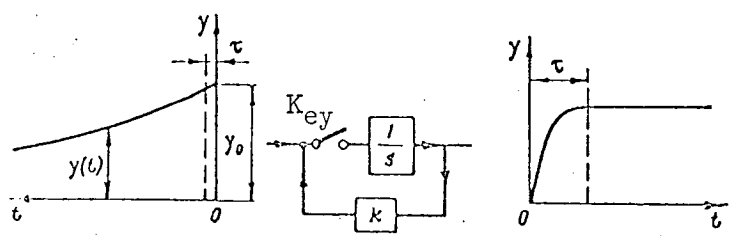

Figure 14.15. Functional diagram and graphs which clarify operation of memory-storage device.

Figure 14.15 shows the schematic diagram of such a memory device and its principle of operation. When the control system aboard the missile is turned on, the key k_{ey} of the integrator is closed for a short period of time τ, during which the coordinate y(t) remains substantially unchanged. When the key is closed, the integrator is transformed into a servosystem with a coupling coefficient k in the feedback loop. If we assume that $3/k < \tau$, the output /477

signal y_0 will be completely processed by the servosystem during the time τ and can be picked off from its output sensor. After the key k_{ey} is open, this signal, as before, will be read as a constant value or as $y_0 1(t)$ of this sensor.

We have considered the application of feedback, determined by the initial conditions in the linear system which places the missile on the beam. It is not difficult to apply these feedbacks in a nonlinear system where the relation between deviation y and signal y_s is a nonlinear function, shown in figure 14.10. In this case it is necessary to turn the system on when y_s passes through a maximum and begins to decrease. Until this instant of time the missile is not controlled, and aboard the missile only coordinate y is controlled according to quantity $\dot{y}_s$ and approach velocity $\dot{y}$. Instead of measuring velocity $\dot{y}$, we measure angle ϑ between the longitudinal axis of the missile and the beam axis. This angle can be measured by means of a position gyro oriented along the beam axis.

Section 14.6. Missile Guidance by Means of Radar Stations and Radio Navigation Systems

Surface radar stations with circular scan and equipped with computers may be used to guide surface-to-surface and surface-to-air missiles with wings, and also to guide interceptor-pursuit planes. Systems of radio navigation may be used to guide surface-to-surface missiles. /478

Radar stations can determine the coordinates of the target as well as the coordinates of the missile. As we have already pointed out in section 14.1, in this case computers may be used to realize any laws or methods of guiding missiles to their target. However, in such missile control systems there is one significant feature: radar stations measure the coordinates by sampling, rather than continuously. During each revolution of the antenna system the coordinates of the missile or the target are obtained once in the form of pulses, whose duration is insignificant compared with the period of rotation of antenna T. This discontinuity in the feeding of information concerning the coordinates of the target and the missile is the most significant feature in the use of radar stations with circular scan for missile guidance. Instead of continuous missile guidance systems, we achieve sampled-data systems.

To clarify the operation of sampled-data guidance systems we consider first the guidance of surface-to-surface missiles.

1. The Guidance of Surface-to-Surface Winged Missiles. To guide missiles of this type it is necessary to know the mutual coordinates of the target and the tracking station.

Let us place the radar at the origin of a polar coordinate system fixed with respect to Earth. It is most convenient to use a polar system of coordinates when a radar station is used, because the radar station measures the range L and the bearing φ to the missile or the target. Figure 14.16 shows the trajectory of a missile. Due to the rotation of the antenna with a frequency $1/T_{cp}$, the coordinates of the range and the azimuth are measured and are stored for the entire period of rotation of the antenna T_{cp}. As a result, $\varphi = \varphi(t)$ as well as $L = L(t)$ become step functions consisting of a sequence of rectangular pulses.

To guide the missile to a surface target, it is necessary to assign a trajectory which passes through the target and through the launching site of the missile. To hold the missile on the specified trajectory, we must measure the deviations ϵ from this trajectory and transmit them as signals to the missile.

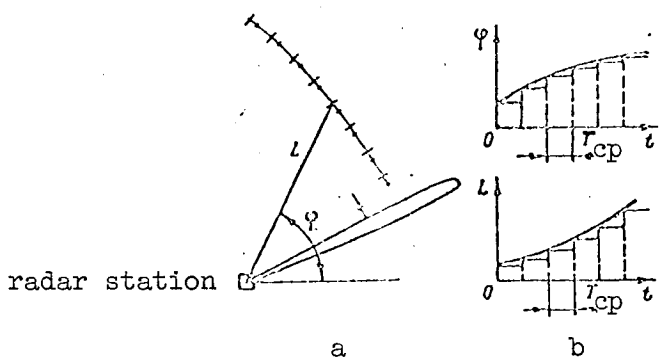

Figure 14.16. System with circular scanning used for guidance (a) and graphs showing range and bearing of missile (b).

Any rectilinear trajectory is completely determined by the length of the perpendicular L_0 to this trajectory and the polar angle of this perpendicular φ_0, or by the approach angle of this trajectory $\psi_0 = \varphi_0 - \pi/2$ (fig. 14.17).

Figure 14.17 shows that the lateral deviation from the assigned trajectory is equal to /479

$$\varepsilon = L_0 - L \sin(\varphi - \psi_0). \tag{14.20}$$

The computer at the radar station computes the deviation ϵ for each revolution of the antenna. If we compute the values of ϵ and fix ϵ for a period of one antenna revolution, we obtain the step function $\epsilon = \epsilon[t]$. By sending the signals $\epsilon = \epsilon[t]$ to the missile, we obtain a sampled-data stabilization of the missile along the assigned trajectory.

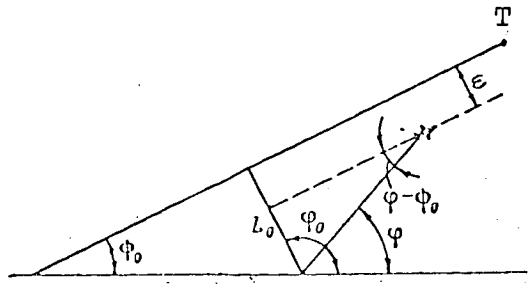

Figure 14.17. Relative position of missile and assigned trajectory.

The functional diagram of a sampled-data missile control system for guiding the missile along an assigned trajectory is shown in figure 14.18. The functional diagram is constructed for a winged missile, when the slip is equal to zero and when the missile reacts instantaneously to commands from the channel controlling its tilt. To achieve functional stability, fixed feedback is used for the deviation of the missile's course angle ψ from the course of the trajectory ψ_0. The signal ψ is measured by a position gyroscope oriented along the assigned trajectory. The orientation of the gyroscope is achieved by a special command from the ground when the trajectory is assigned.[1] The sampling /480

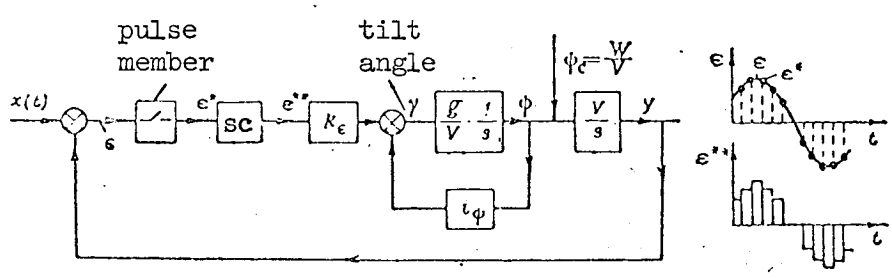

Figure 14.18. Functional diagram for sampled-data missile control system; sc = shaping circuit.

of the deviation ϵ is characterized by a pulse element which generates the $\delta(t)$ functions. In this case the intensity of the $\delta(t)$ function is equal to the value of the error $\epsilon = x(t) - y$ at the nth instant of time, i.e.,

$$\epsilon_n = \int_{nT_n}^{\infty} \delta(t - nT_n)\, dt$$

Following this, a succession of $\delta(t)$ functions is fed to the shaping circuit of the first order. This shaping circuit transforms each $\delta(t)$ pulse into a rectangular pulse, whose height is equal to ϵ_n. The $\delta(t)$ pulse element

[1]For this orientation the missile must contain a course system.

and the shaping circuit simulate the radar and the computer quite accurately in measuring the deviation or the error $\epsilon = -y$ (when $x(t) = 0$). However, the delay $\tau \ll T_n$ is not taken into account. This delay is due to the necessity of reducing the measured φ and L and computing $\epsilon = -y$ by means of equation (14.20). The computation time is of the order of a fraction of a second, while T_n--the period of revolution of the antenna--may be 4-10 sec. Because each $\delta(t)$ pulse is transformed by the shaping circuit into a rectangular pulse, the Laplace transform of a rectangular pulse of unit height will also be transfer function of the shaping circuit.[1] The transform of the rectangular pulse is equal to the difference between the two step functions 1(t) which are displaced by T_n, i.e., /481

$$W_\Phi(s) = \frac{1 - e^{-sT_n}}{s} = \frac{z-1}{z} \cdot \frac{1}{s},$$

where $z = e^{sT_n}$.

The transfer function of all continuous members and the transfer function of the shaping circuit, form the transfer function of the continuous part of the system W(p). In this case

$$W(s) = \frac{z-1}{z} \cdot \frac{1}{s} \cdot \frac{k}{(T_\psi s + 1)s}, \tag{14.21}$$

where

$$k = \frac{k_z}{i_\psi} V\left[\frac{1}{\text{sec}}\right], \quad T_\psi = \frac{V}{g i_\psi}\,[\text{sec}].$$

The continuous part with the transfer function W(s) and the $\delta(t)$ pulse element (pe) form a single loop sampled-data automatic control system (fig. 14.19). To analyze this system, it is rational to transform the continuous transform function W(s) with an argument $s = \sigma \pm j\omega$ into a discrete transfer function W(z) with an argument $z = e^{sT_n}$. This transformation may be accomplished by means of corresponding tables for the transfer functions of elementary members.[2] When the transfer function (14.21) is broken down into elementary fractions or members, it takes the form of

$$W(s) = kT_\psi \cdot \frac{z-1}{z}\left[-\frac{1}{s} + \frac{1}{T_\psi} \cdot \frac{1}{s^2} + \frac{1}{s + 1/T_\psi}\right]. \tag{14.22}$$

---

[1] The construction of this circuit can be analogous to that of a memory cell shown in figure 14.15.

[2] G. S. Pospelov, Sampled-data Control Systems, Collected Articles "Automatic Control and Computer Engineering," Mashgiz, No. 3, 1960.

We have the following relations /482

$$\frac{1}{s} \div\!\!\succ \frac{z}{z-1}, \quad \frac{1}{s^2} \div\!\!\succ \frac{zT_n}{(z-1)^2} \quad \text{and} \quad \frac{1}{s+1/T_\psi} \div\!\!\succ \frac{z}{z-a},$$

where

$$a = e^{-\frac{T_n}{T_\psi}}.$$

By using these relationships we obtain

$$W[z] = \lambda_2 \frac{(\lambda_1 + a - 1)z + 1 - a(\lambda_1 + 1)}{z^2 - (a+1)z + a}, \tag{14.23}$$

where

$$\lambda_1 = \frac{T_n}{T_\psi}; \qquad \lambda_2 = kT_\psi.$$

The transfer function (14.23) is the transfer function of an open loop system. To obtain the transfer function for a closed-loop system we use the relationship between these functions, which is analogous to the corresponding expression for continuous systems

$$\Phi[z] = \frac{W[z]}{1 + W[z]} = \frac{d_1 z + d_0}{z^2 + b_1 z + b_0}, \tag{14.24}$$

where

$$d_1 = (\lambda_1 + a - 1)\lambda_2, \quad d_0 = [1 - a(\lambda_1 + 1)]\lambda_2,$$
$$b_0 = d_0 + a, \quad b_1 = d_1 - (a+1).$$

The denominator of the transfer function (14.24) is the characteristic equation of the difference equation which describes the behavior of the output coordinate y at discrete points $t = 0;\ 2T_n, \ldots, nT_n$. The homogeneous equation itself in terms of finite differences has the form

$$y_{n+2} + b_1 y_{n+1} + b_0 y_n = 0, \tag{14.25}$$

where

$$y_n = y(t)\big|_{t=nT_n}.$$

Equation (14.25) is a recurrent relationship with which we can compute all the values of y_n, beginning with y_2, from the assigned initial conditions y_0 and y_1.

In order that the system be stable, i.e., in order that $y_n \to 0$ for $n \to \infty$, it is necessary and sufficient that the modulus of the roots of characteristic equation

$$z^2 + b_1 z + b_0 = 0$$

be less than unity. It is obvious that the roots and their distribution in a unit circle on plane z will determine the nature of the transient processes. /483

The transfer function (14.24), as in the case of continuous systems, is the transform[1] of the system's pulse reaction. To obtain the pulse reaction we expand $\Phi(z)$ in power series of z^{-1} [2]

$$\Phi[z] = \sum_{n=0}^{\infty} f_n z^{-n} = \sum_{n=0}^{\infty} f_n e^{-nT_n p}. \tag{14.26}$$

As we can see from expression (14.26) the coefficients of the series, which in the present case are known as the weighting coefficients, represent the ordinates of the system's pulse reaction at points $t = 0, T_n, 2T_n, 3T_n \ldots, nT_n$.

To obtain the transient function we must expand the expression $\Phi[z]\frac{z}{z-1}$ in a series

$$\Phi[z]\frac{z}{z-1} = \sum_{n=0}^{\infty} H_n z^{-n}. \tag{14.27}$$

Here H_n is the ordinate of the transient function ($n = 0, 1, 2, \ldots$).

The transient function $H(t)$ of this system is a continuous function. By using this method it is possible to determine the values of this function at discrete points $t = 0, T_n, 2T_n \ldots, nT_n$ (fig. 14.20). Requirements imposed on the transient function are analogous to requirements imposed on continuous transient functions, when a beam is used for guidance.

These methods for using radar to guide surface-to-surface missiles may be used in their general form to guide this class of missiles by various radio navigation systems. By using a radio navigation system and a computer, which in this case is located aboard the missile, the trajectory passing through the target is assigned. To maintain the missile on the assigned trajectory, signals of deviation of the missile's center of gravity from the

---

[1] The z-transform or a discrete transform.

[2] The series expansion may be achieved by a successive division of the numerator $\Phi(z)$ by the denominator.

assigned trajectory are used. These are obtained by means of the radio navigation system. The methods of obtaining control signals are considered in Chapter 4.

2. The Guidance of a Surface-to-Surface Winged Missile and of Interceptor Fighters by Means of Radar. The computer of the surface radar permits us to realize any method of guiding a missile. Let us consider the method of parallel approach. During each revolution of the antenna the radar measures the bearing of missile φ_c, the range to missile L_c, the bearing of the target /484

φ_T and the range to the target L_T (fig. 14.21). From these data it is possible

to determine the position of the target and of the missile in the assigned system of coordinates, the velocity vectors of the target and of the missile, to compute the distance between the target and the missile, to determine the value of the angular velocity of the line joining the missile and the target, etc.

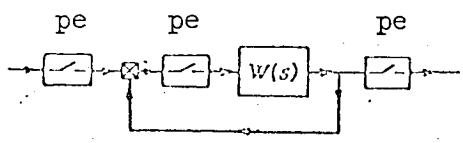

Figure 14.19. Schematic diagram of single-loop sampled-data automatic control system; pe = pulse element.

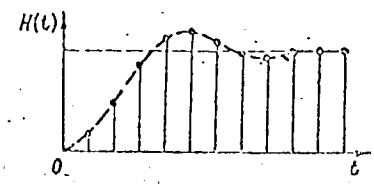

Figure 14.20. Discrete value of transfer function.

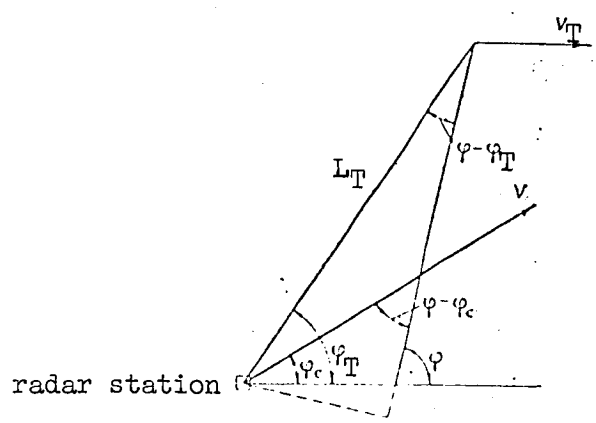

Figure 14.21. Geometric relationships when missile is guided by surface radar.

Finally, by making use of expression (13.46) we can determine the indicated miss y. Like the deviation from the trajectory y in the preceding case, the miss is determined once during each revolution of antenna T_n and

remains fixed for the entire period. The indicated miss, which may be obtained, will be represented in the form of the same step curve as φ and L in figure 14.16.

Now let us assume that a control signal is generated in accordance with expression (13.58) and is transmitted to the missile along the guidance link. The signal $\nu(t) = -ky/kc\,\chi$ will also represent a succession of rectangular pulses. Since the relation between the miss and the angle of attack is given by expression (13.56), we obtain a sampled-data control system of the first order. The functional diagram of this system is shown in figure 14.22. The transfer function of the continuous part in this case will have the form /485

$$W(s) = \frac{z-1}{z} \cdot \frac{k}{s^2}.$$

In the same way the transfer function of the argument z must be written in the form

$$W[z] = \frac{kT_n}{z-1}.$$

From this it follows that the transfer function of the closed loop system is

$$\Phi[z] = \frac{kT_n}{z-(1-kT_n)} = \frac{1-a}{z-a}, \tag{14.28}$$

where $1 - kT_n = a$.

The system is stable and the miss decreases if $|a| < 1$. The equation in terms of finite differences, corresponding to the transfer function, has the form

$$x_{n+1} - ax_n = 0$$

or

$$x_{n+1} = ax_n. \tag{14.29}$$

If the initial miss was x_0, then

$$\begin{gathered} x_1 = ax_0, \qquad x_2 = ax_1 = a^2x_0, \\ x_n = a^nx_0 \\ n = (0,\ 1,\ 2, \ldots, \infty). \end{gathered} \tag{14.30}$$

The last expression is the solution of the difference equation (14.29), because it determines the valuesof the miss during the nth antenna rotation in terms of the initial miss and the system parameter $a = 1-kT_n$. From this expression we can also see that $x_n \to 0$ only if $|a| < 1$. In this case the miss decreases more rapidly as $|a|$ becomes smaller. Expression (14.30) shows that the miss decreases according to the law of geometric progression. This means that

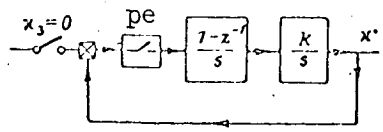

Figure 14.22. Functional diagram of sampled-data control system of first order.

the envelope of the miss ordinates will be an exponential curve with an exponent $-\frac{1}{T_n}\ln\frac{1}{a}$. As we can see from the functional diagram shown in figure 14.22, rectangular pulses are fed to the input of the integrating element. /486
This means that, within the limits of T_n, the output of the integrating element or the miss χ will vary according to a linear law.

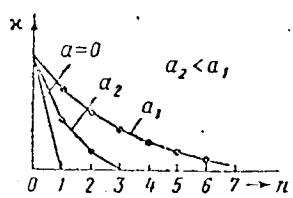

Figure 14.23. Graph showing variation and miss as function of positive values of parameter a less than unity.

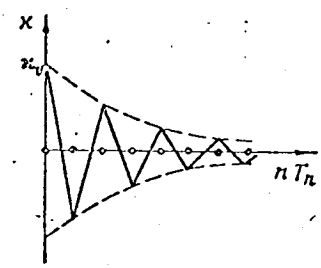

Figure 14.24. Variation in miss for negative values of parameter α.

Figure 14.23 shows the graphs for the variation in χ for two positive values of α less than unity. As we have already mentioned, as α decreases, the miss χ decreases more rapidly. From the expression for $\alpha=1-kT_n$, we can see that by selecting the quantity k we can make $\alpha = 0$. In this case miss χ will become equal to zero during one period of recurrence T_n (the case $\alpha = 0$ in figure 14.23). However, when the values of α is equal to zero or close to zero, there will be an unfavorable reaction of the system to noise and interference. Therefore, these values of α cannot always be recommended. Negative values of α are also not recommended. According to equation (14.30) a negative α (less than unity) leads to a variation in the miss having the form of damped oscillations. The frequency of these oscillations is equal to $1/2\ T_n$. The graph showing the variation in the miss for negative values of α is shown in figure 14.24.

Equation (14.29) is obtained through the formal application of the theory of sampled-data control systems. The same expression may be obtained directly. Indeed, instead of the differential equation (13.56) let us write the equation in terms of the finite differences corresponding in essence to the sampled-data control of the missile

$$\frac{\Delta x_n}{T_n} = L_{en} \frac{k_V}{T_V} \alpha_n, \tag{14.31}$$

where

$$\Delta x_n = x_{n+1} - x_n;$$

L_{en} is the range at the instant of time $t = n\,T_n$; and α_n is the angle of attack at the time instant $t = nT_n$.

Let us require that /487

$$\alpha_n = -\frac{k_y}{L_{en}} x_n. \tag{14.32}$$

Then from equation (14.31) we obtain

$$\Delta x_n + kT_n x_n = 0, \tag{14.33}$$

where

$$k = \frac{k_y k_V}{T_V}.$$

Since $\Delta x_n = x_{n+1} - x_n$ we go from equation (14.33) to equation (14.29).

The use of a computer to obtain the miss involves a rather complex operation. We shall limit ourselves to the calculation of $\dot{\varphi}$. In addition, as we have pointed out in Chapter 13, the variation of the angle of attack as a function of $\dot{\varphi}$ is somewhat more advantageous than its variation as a function of miss. The angular velocity $\dot{\varphi}$ may be determined in terms of the increment in the angle φ during one rotation of the antenna, i.e.,

$$\dot{\varphi}_n = \frac{\Delta\varphi_n}{T_n} = \frac{\varphi_{n+1} - \varphi_n}{T_n}. \tag{14.34}$$

The angle φ for each revolution of the antenna is computed by means of a computer using the equation

$$\varphi_n = \operatorname{arc\,tg} \frac{L_{Tn} \sin \varphi_{Tn} - L_{cn} \sin \varphi_{cn}}{L_{Tn} \cos \varphi_{Tn} - L_{cn} \cos \varphi_{cn}}, \tag{14.35}$$

where L_{cn}, L_{Tn} is the range to the missile and the target; and φ_{cn}, φ_{Tn} are the bearings of the missile and the target.

Now let us require that $\alpha_n = -k\dot{\varphi}_n$. In this case, by considering the relation between the miss χ_n and $\dot{\varphi}_n$ and equation (14.31), we obtain an equation in terms of finite differences which has the form

$$\frac{\Delta z_n}{T_n} + \frac{k}{l_0 - nT_n} z_n = 0$$

or

$$z_{n+1} = \left(1 - \frac{kT_n}{l_0 - nT_n}\right) z_n. \tag{14.36}$$

Equation (14.36) as well as the differential equation (13.67) are equations with variable coefficients. The solution of (14.36) may be represented in the form /488

$$z_n = z_0 \prod_{i=0}^{n-1} \left(1 - \frac{k}{l_0/T_n - i}\right). \tag{14.37}$$

Table 14.1 shows the results of the calculations carried out by means of equation (14.37) for

$$l_0/T_n = 9.5, \quad k = 6 \quad \text{and} \quad k = 2.$$

TABLE 14.1. RESULTS OF COMPUTING MISS BY MEANS OF EQUATION (14.37).

n	i	$k=6$			$k=2$		
		$\frac{6}{9.5-i}$	$1-\frac{6}{9.5-i}$	z_n	$\frac{2}{9.5-i}$	$1-\frac{2}{9.5-i}$	z_n
0	—	—	—	1	—	—	1
1	0	0.63	0.37	0.37	0.210	0.790	0.790
2	1	0.706	0.294	0.109	0.235	0.765	0.605
3	2	0.8	0.2	0.0216	0.267	0.733	0.442
4	3	0.925	0.075	$0.162 \cdot 10^{-2}$	0.308	0.692	0.306
5	4	1.09	−0.09	$-0.146 \cdot 10^{-3}$	0.364	0.636	0.195
6	5	1.33	−0.33	$0.48 \cdot 10^{-4}$	0.445	0.555	0.109
7	6	1.72	−0.72	$-0.346 \cdot 10^{-4}$	0.572	0.428	0.0465
8	7	2.4	−1.4	$0.485 \cdot 10^{-4}$	0.8	0.2	$0.93 \cdot 10^{-2}$
9	8	4	−3.0	$-0.145 \cdot 10^{-3}$	1.33	−0.33	$-0.307 \cdot 10^{-2}$
10	9	12	−11	$0.18 \cdot 10^{-2}$	4	−3	$0.92 \cdot 10^{-2}$

If in a continuous system for any value of k the initial miss χ given by (13.82) always becomes equal to zero when l = 0, in a sampled-data system this

is not observed. The miss cannot become equal to zero nor can it change its sign in the region of the target.[1] Thus, the impact accuracy in the case of sampled-data control is always less than in the case of continuous control.

[1]In a particular case when for some n $\frac{k}{l_0/T_n'-i}$ becomes equal to 1.0, the miss beginning with this interval becomes equal to zero.

CHAPTER 15. THE DYNAMICS OF MISSILES WITH SELF-CONTAINED GUIDANCE SYSTEMS

/489

Section 15.1. Control and Guidance of Airplane Missiles by Means of Inertial Systems

1. Rectilinear Flight to the Target. In guiding airplane-missiles to a surface target it is necessary to know either the geographic coordinates of the target or the range and bearing of the target with respect to the launching site. Sometimes another reference point is used instead of the launching point and the position and velocity of the missile are measured with respect to this point. When the range and target bearing are given, the flight trajectory may be taken as the arc of the great circle which takes into account the rotation of the Earth. One of the accelerometers A_x is oriented along the arc of the great circle, while the second accelerometer A_z is normal to the plane of the great circle.

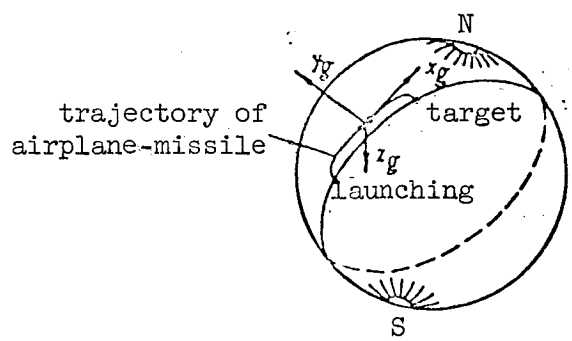

Figure 15.1. Flight trajectory of airplane-missile along arc of great circle.

The range control (15.1) is quite simple. The output of the second integrator of the inertial system records the travelled path L. This travel path is compared with the given programed value of the target range L_3, which is stored beforehand aboard the rocket in the programing mechanism or in a computer. When x becomes equal to L_3, the airplane-missile goes into a dive towards the target and if there is a homing system, a signal turns it on. With

this type of range control it becomes necessary to stabilize the trajectory with respect to lateral motion.

The coordinate z (fig. 15.1) is maintained at zero[1] during the entire flight /490
flight period. The functional diagram of the inertial stabilization system for the airplane-missile is shown in figure 15.2. It is further assumed that the airplane-missile flies without slipping, and that the transient processes associated with the tilt may be neglected. The functional diagram of an inertial system shown in figure 15.2 is equivalent to the functional diagram shown in figure 5.27, because $z/R = \beta_c$ and $\dot{z}_g/R = \dot{\beta}_g$ Accelerometer A is subjected to the total lateral acceleration $\ddot{z}$ due to the tilting of the missile $g\gamma$ and due to the wind $\dot{w}$, as well as due to the component of gravity gz/R. To achieve stabilization

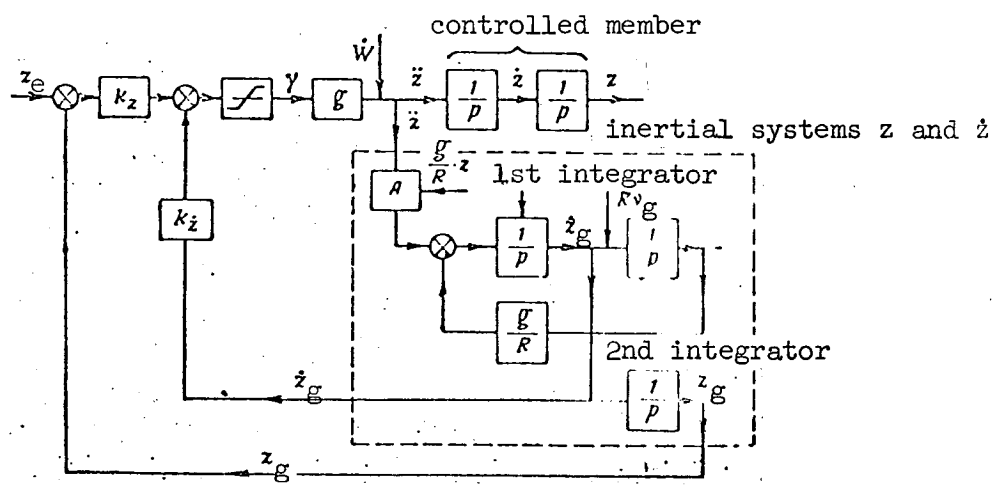

Figure 15.2. Functional diagram of inertial stabilization system for airplane-missile.

along the trajectory, the channel for controlling the tilt receives the signals $z_g = z + \eta$ and $\dot{z}_g = \dot{z} + \dot{\eta}$, where z and $\dot{z}$ are the true deviations of the rocket from the assigned trajectory and the rate of this deviation, z_g and $\dot{z}_g$ are the same quantities, but measured by the inertial system, and η, $\dot{\eta}$ are the errors in measuring the lateral velocity and the lateral displacement. These errors were considered in Chapter 5. For an undamped and uncompensated stable platform errors η and $\dot{\eta}$ contain harmonic components with the Schuler period. Due

[1]As we shall show, this is not absolutely necessary if it becomes desirable to maneuver the rocket.

to the drift of the platform with constant velocity, error η will contain a component which increases linearly. Let us assume that not all errors of the inertial system are taken into account by errors η and $\dot{\eta}$. Specifically, these errors are associated with the threshold values of the accelerometers and of the integrators and with the deviations in the transfer characteristics of integrators from ideal characteristics with a transfer function 1/p. We note that in the controlled member the members 1/p are always ideal because they characterize the kinematic relation between acceleration and velocity and also between velocity and the coordinate. In addition to measuring accelerations, the basic problem of inertial systems is to simulate the ideal members 1/p of the controlled member as accurately as possible.

In the functional diagram shown in figure 15.2 the restriction of the tilt is shown in the tilt control signal circuit. For small deviations from a given trajectory and in the proportionality zone for the tilt limiter we have the following system of equations

$$\left.\begin{aligned} &\dot{z} = V\theta_b + W; \\ &V\dot{\theta}_b = g\gamma; \\ &\gamma = k_z(z_3 - z_g) - k_{\dot{z}}\dot{z}_g; \\ &z_g = z + \eta; \\ &\dot{z}_g = \dot{z} + \dot{\eta}, \end{aligned}\right\} \qquad (15.1)$$

where V is the air speed of the rocket which is assumed to be constant; W is the wind velocity normal to the trajectory; $z_3 = z_3(t)$ is the signal from the programing mechanism to displacing the rocket from its trajectory, if this is necessary. If it is not necessary, then $z_3 = 0$, and θ_b is the angle between the given trajectory and the air velocity vector of the airplane.

If we eliminate V and θ_b from the first two equations we obtain an expression for the acceleration

$$\ddot{z} = g\gamma + \dot{W}, \qquad (15.2)$$

which is the one realized in the functional diagram shown in figure 15.2. The construction of a functional diagram which takes into account expression (15.2) is valid only when the inertial system is placed into operation before the missile is launched. Only in this case is perturbation W applied in front of the second integrator of the member (see system (15.1), first equation), equivalent to perturbation $\dot{W} = dW/dt$, applied in front of the first integrator of the member, as shown in figure 15.2. If, for example, the inertial system is turned on after launching, which takes place when there is a /492

constant side wind, the transformation of perturbation W into $\dot{W}$ is incorrect, because in this case the accelerometer of the inertial system will not sense any acceleration associated with the uniform motion of the air mass.

The equation (15.1) is reduced to one equation of the second order in terms of the coordinate z

$$\ddot{z} + a_1 \dot{z} + a_0 z = a_0 z_3 + \dot{W} - a_0 \eta - a_1 \ddot{\eta}, \tag{15.3}$$

where

$$a_0 = gk_z \quad \text{and} \quad a_1 = gk_{\dot{z}}.$$

The parameters k_z and $k_{\dot{z}}$ may be selected by proceeding from the assigned damping coefficient $\zeta = a_1/2\sqrt{a_0}$ and control time $t_{p(\text{control})}$. When we have an optimum damping coefficient $\zeta = \sqrt{2/2}$ the control time $t_p = \pi/\sqrt{a_0} = \pi/\sqrt{gk_z}$,

from which it follows that

$$k_z = \frac{57.3}{t_p^2}\left[\frac{\text{degree tilt}}{\text{meter}}\right].$$

The time t_p is usually 20-60 sec. It is difficult to realize a shorter control time due to nonlinearity and limitations in the automatic pilot. When the damping coefficient is $\zeta = \sqrt{2/2}$ the portion of the signal due to the derivative is equal to

$$k_{\dot{z}} = 25.8\frac{1}{t_p}\left[\frac{\text{degree tilt}}{\text{misec}}\right].$$

Let us consider the reaction of the system to the perturbation of the function in the right side of equation (15.3). When $Z_3 = Z_{30} 1(t)$, where Z_{30} = const, the flight trajectory will be displaced laterally by z_0 (15.3a). If fuel supply permits, the signal $z_3(t)$ may be used to produce a counter-zenith maneuver over some region of the trajectory. The maneuver will be most effective in the case when $z_3(t)$ is a random function of time. A maneuver away from the zenith achieved by means of generating $z_3(t)$ will have no effect on the operation of the range channel of the inertial system, because the x-axis of this system is oriented towards the target. When the airplane-missile at the time

t_1 encounters a side wind with constant velocity, we obtain the following equation from (15.3)[1]

$$\ddot{z} + a_1\dot{z} + a_0 z = W_0\delta(t), \tag{15.4}$$

where W_0 is the velocity of the side wind $\delta(t) = \frac{d}{dt}1(t)$.

Due to the action of pulse $\delta(t)$ the airplane-missile first deviates and then again returns to the assigned trajectory (fig. 15.3b). The maximum ejection from the trajectory will be less when the coefficients k_z and $k_{\dot{z}}$ are greater, i.e., the smaller the control time t_p during reaction to the step signal $1(t)$. With equation (15.3) we can determine the reaction of the missile /493

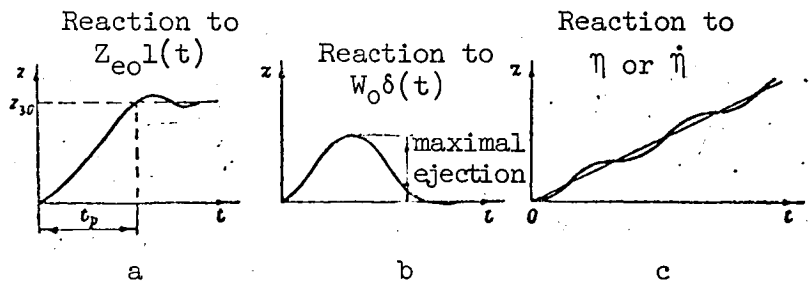

Figure 15.3. Curves showing reaction of system to perturbing function.

to errors $\dot{\eta}$ and η, which for the system under consideration are the perturbing functions; as we have already pointed out, errors η and $\dot{\eta}$ contain a sinusoidal component with the angular Schuler frequency $\sqrt{g/R}$ and a constant and linearly increasing component. The angular frequency of the natural oscillations of the airplane-missile during the control period, for example, during 31.4 sec is equal to 0.1 1/sec, while the Schuler angular frequency is equal to 0.0393 1/sec. Therefore, the trajectory of the airplane-missile will actually follow the laws for the variation in errors η and $\dot{\eta}$ without distortion (fig. 15.3c). As we can see, the drift of the stable platform will produce a gradual deviation of the airplane-missile from the assigned flight trajectory. This deviation may be prevented only by compensating the inertial system.

---

[1] In the equation, time t_1 is taken as the beginning of the reading, i.e., it is assumed that $t_1 = 0$.

2. Introducing Initial Conditions. Flight Along a Programed Trajectory. The problem of introducing initial conditions occurs if the airplane-missile is not on the assigned trajectory when the control system is turned on, or if the trajectory itself must be suddenly changed. These situations may occur when an inertial guidance system is used in the surface-to-air missiles or when the airplane-missiles are not properly aimed.

The initial conditions may be introduced by means of additional sources of information (radar, radio navigational or others). Let us assume, for example, that the missile was directed to target T_1, along a straight line P_1T_1 (fig.15.4).

Let us also assume that the missile was tracked from the control point continuously or episodically, for example, by means of radar. At the moment when the missile is at point P_1 a decision is made to aim the missile to target T_2 along the straight line P_2T_2. With respect to the straight line P_2T_2 the missile has the initial conditions $\dot{Z}_0$ and $\dot{Z}_0 = V\lambda$, where λ is the angle between the trajectories P_1T_1 and P_2T_2. (In this example angle λ is small; therefore the same system of coordinates may be used to measure z for both trajectories.) The values of Z_0 and $\dot{Z}_0$ must be determined by external sources of information and introduced to the input of the second and the input of the first integrator. /494

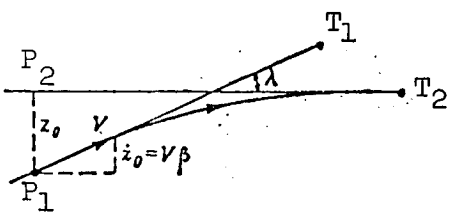

Figure 15.4 Flight trajectory of missile when it is overaimed.

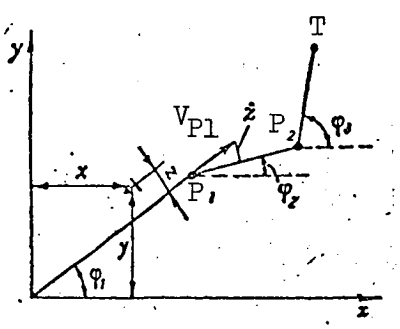

Figure 15.5 Broken programed trajectory of missile.

Before introducing the initial conditions, the integrator should be disconnected from the accelerometer and the automatic pilot and should be placed in the zero position, i.e., the accumulated readings at the output should be

dropped. After the initial conditions are introduced, the entire system is again turned on. Similar operations must be carried out with the system recording the distance to the target. The accuracy which is achieved in determining the initial conditions by external sources of information determines the accuracy of the new specified trajectory and the accuracy of pursuing the new target.

The introduction of initial conditions is also necessary when flight must take place along a broken programed trajectory (fig. 15.5). Let us assume that the missile must travel from P_0 along the broken trajectory $P_0P_1P_2T$. The accelerometers are oriented in the rectilinear system of coordinates along axes x and y. Consequently the inertial system makes it possible to obtain the signals x,y and $\dot{x},\dot{y}$. To realize the flight along the straight line, which does not coincide with the coordinate axes x and y, a computer is required. If the straight line along which the missile must move passes through the origin of the coordinates, its position is determined completely by angle φ_1. The traveled path L and the velocity V along the straight line are computed by means of equations

$$L = x\cos\varphi_1 + y\sin\varphi_1; \tag{15.5}$$

$$V = \dot{L} = \dot{x}\cos\varphi_1 + \dot{y}\sin\varphi_1. \tag{15.6}$$

The deviation from the assigned trajectory z and its velocity are also determined by a computer by means of equations /495

$$z = y\cos\varphi_1 - x\sin\varphi_1, \tag{15.7}$$

$$\dot{z} = \dot{y}\cos\varphi_1 - \dot{x}\sin\varphi_1. \tag{15.8}$$

The signals z and $\dot{z}$ (more precisely z_g and $\dot{z}_g$) are introduced into the channel of lateral control for stabilizing the motion of the center of gravity. Furthermore, when the signal L achieves a value assigned by the programing device (or stored in the memory unit of the computer) determined by the length of segment P_0P_1, a transition to the new trajectory P_1P_2 must take place. In this case it is rational to zero both of the second integrators (this is equivalent to moving the coordinates to point P_1). Flight along the new straight line P_1P_2 will commence with the initial conditions $z_0 = 0$ and $\dot{z}_0 = V_{\text{contact point 1}} \sin(\varphi_1 - \varphi_2)$, where $V_{\text{contact point 1}}$ is the velocity computed by means of equation (15.6) at point P_1. From the known value z_0 and φ_2 the values of $\dot{y}_0$ and $\dot{x}_0$ are computed and introduced at the inputs of the first integrators. When the missile arrives at the point P_2, all operations are repeated.

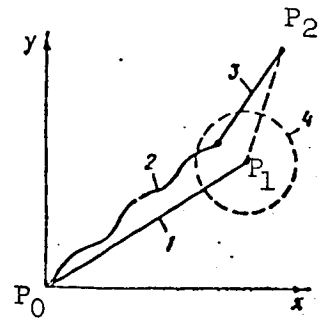

Figure 15.6. Actual and programed trajectory of missile.

The intermediate points P_1, P_2. . . . may be situated in regions where the position of the missile may be refined by means of other sources of information (surface or astronomical reference points, etc.). In this case the trajectory at each new bend should be assigned by taking into account the actual position of the missile (fig. 15.6).

Section 15.2. The Flight Trajectory of a Short Range Ballistic Rocket (L = 500 - 1000 km)

For this range it is not necessary to take into account the curvature of the Earth, and it is permissible to consider the vector of the acceleration due to gravity to be constant. The flight trajectory of a ballistic rocket is divided into active and passive regions (fig. 15.7). At the end of the active region the guidance system and the engine have provided the rocket with the velocity V_a (subscript a = burnout) and a flight direction θ_a. When the velocity is V_a and the slope angle is θ_a the engine is turned off and the passive region starts. Even for a short range rocket we may assume that the passive region lies outside the Earth's atmosphere. At the end of the passive region the rocket again returns into the atmosphere. It is rational to subdivide the passive region into the ballistic region with a range $L_{b(\text{ballistic})}$ and terminal region with a range $L_{K(\text{terminal})}$. Along the ballistic region the only force which acts on /496 the rocket is the force due to Earth's gravity. Therefore, the equations of motion of a rocket along the ballistic region will have the following form if a rectilinear system of coordinates x,y is used

$$\left.\begin{aligned} \ddot{x} &= 0, \\ \ddot{y} &= -g, \end{aligned}\right\} \qquad (15.9)$$

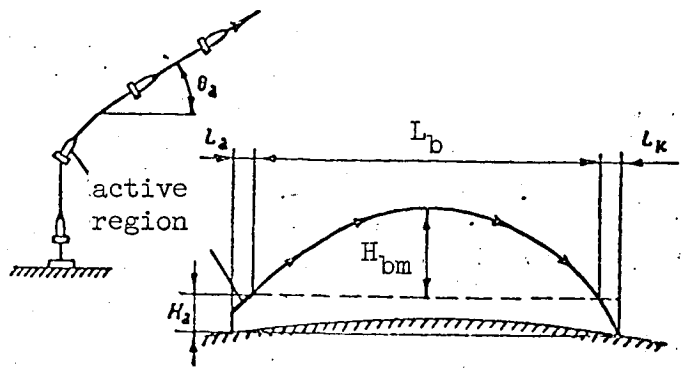

Figure 15.7. Flight trajectory of ballistic rocket; subscripts a = burnout, b = ballistic, K = terminal.

For initial conditions $x_0 = y_0 = 0$

$$\dot{x}_0 = V_a \cos\theta_a, \qquad \dot{y}_0 = V_a \sin\theta_a.$$

The solution of equation (15.19) gives us

$$x = (V_a \cos\theta_a)\, t,$$
$$y = (V_a \sin\theta_a)\, t - \frac{gt^2}{2}.$$

By eliminating time we obtain an equation for a parabolic trajectory

$$y = x \operatorname{tg}\theta_a - \frac{gx^2}{2V_a^2 \cos^2\theta_a} \tag{15.10}$$

and its parameters of maximum altitude

$$H_{bm} = \frac{V_a^2 \sin^2\theta_a}{2g} \tag{15.11}$$

and range

$$L_b = \frac{V_a^2}{g} \sin 2\theta_a. \tag{15.12}$$

The maximum range L_{bm} is obtained when $\theta_a = 45^\circ$. Therefore, for a ballistic missile θ_a is usually close to 45 degrees. If $\theta_a = 45^\circ$, then H_{bm} and L_{bm} are associated by the relation /497

$$H_{bm} = \frac{L_{bm}}{4} \tag{15.13}$$

The basic component of the rocket's range is the ballistic range, so that errors in the ballistic range are most significant. As we can see from equation (15.12), to obtain the desired range it is necessary to maintain definite values of velocity and of the angle θ_a. An error in velocity ΔV and an error in slope $\Delta\theta$ will produce an error in range ΔL_b. If we take into account the possible errors, equation (15.12) takes the form

$$(L_{bm} + \Delta L_{bm}) = \frac{(V_a + \Delta V)^2}{g} \cdot \sin 2(\theta_a + \Delta\theta). \tag{15.14}$$

If we limit ourselves to terms which are infinitesimals of the first order in the right side of equation (15.14), we obtain

$$\frac{\Delta L}{L_b} = 2\frac{\Delta V}{V_a} + 2\operatorname{ctg} 2\theta_b \Delta\theta^\circ \frac{1}{57.3}. \tag{15.15}$$

As we can see from equation (15.15), an error in the angle $\Delta\theta$ (by $2 - 3^\circ$) in the case of an optimum trajectory ($\theta_a = 45^\circ$) produces practically no error in the range because $\operatorname{ctg} 90^\circ = 0$. The range error is determined completely by the flight speed error. The relative range error is equal to twice the relative velocity error. Thus, when a missile is fired over a distance of 1000 km, a velocity error equal to 1 percent produces a miss of 20 km.

It is necessary to point out that, although the error in the angle does not lead to practical errors in the ballistic range L_b, nevertheless, due to the displacement of the end of the active region and the beginning of the ballistic region the angular error may produce a noticeable range miss component. When $\theta_a \approx 45^\circ$, this miss is equal to

$$\Delta L = 2\frac{H_h}{57.3}\Delta\theta^\circ, \tag{15.16}$$

where H_h is the altitude of the slope of the active region in km. Thus, for

example, an error of one degree in $\Delta\theta$ for $H \approx 30$ km gives a miss of approximately 1 km.

For very short ranges the assumption that the passive region begins outside the atmosphere may be incorrect. The validity of this proposition may be verified, if we know the values of H_a and V_a by evaluating the magnitudes of the /498

aerodynamic forces. The aerodynamic forces may be evaluated from the coefficients c_x and c_y, from the dimensions of the rocket and from the parameters of the atmosphere at the altitude H_a.

Figures 8.8 and 8.9 show the characteristics $c_y = c_y(\alpha, M)$ and $c_x = c_x(\alpha, M)$, referred to the maximum cross section of the rocket. Table 8.5 presents data on the atmosphere up to an altitude of 100 km.

Section 15.3. Flight Trajectories of Long-range Ballistic Rockets (L>1000 km)

For long-range flights it is not possible to neglect the Earth's curvature or to consider the center of gravity as constant and independent of altitude. Before obtaining an equation of motion for the rocket along the passive region let us consider two extreme cases of rocket flight: (1) a flight with an angle $\theta_a=0$; (2) flight with an angle $\theta_a=\pi/2$. For the first case we find the value of velocity V_a, for which the rocket will orbit the Earth along a circular orbit. During flight along a circular orbit the centrifugal force tends to move the rocket away from the Earth, but it is balanced out by the force of gravity, i.e.,

$$m\frac{V_a^2}{R_0} = mg. \tag{15.17}$$

From equality (15.17) we determine the value of velocity $V_a = V_{K1}$, for which flight along an orbit close to the Earth is achieved

$$V_{K1} = \sqrt{R_0 g_0} = \sqrt{6\,370\,000 \cdot 9.81} = 7912 \approx 8 \text{ km/sec.}$$

The velocity V_{K1} is known as the first cosmic velocity.

Thus, when the first cosmic velocity is achieved the rocket becomes an Earth satellite with a circular orbit. The period of revolution of this satellite around the Earth will be equal to

$$T = \frac{2\pi R_0}{V_{K_1}} = \frac{2\pi R_0}{\sqrt{R_0 g_0}} = 2\pi\sqrt{\frac{R_0}{g_0}} = 84.5 \text{ min.}$$

As we can see, the satellite orbits the Earth with a period equal to the period of oscillations of the Schuler pendulum (section 5.9). For the second case let us determine the altitude reached by a rocket whose initial velocity is V_a.

We write the expression for the variation in the kinetic energy of a rocket

$$\frac{mV^2}{2} - \frac{mV_a^2}{2} = -\int_{R_0}^{R_0+H} F dR, \tag{15.18}$$

where $R = R_0 + H$ is the distance from the rocket to the center of the Earth; /499

$F = k\frac{m \cdot M}{R^2}$ is the force attracting the rocket towards the Earth; M is the mass of the Earth; and k is the gravitational constant.

At the Earth $F=mg_0$, consequently, $kM=g_0R_0^2$. From this we obtain other expressions

for the force of attraction

$$F = mg_0 \frac{R_0^2}{R^2}. \tag{15.19}$$

for the Earth's acceleration

$$g = g_0 \frac{R_0^2}{R^2}.$$

Substituting equality (15.19) into (15.18) and integrating we find

$$\frac{V^2 - V_a^2}{2} = -g_0R_0^2\left[\frac{1}{R_0} - \frac{1}{R_0+H}\right]. \tag{15.20}$$

At the maximum altitude velocity V becomes zero. Assuming that in equation (15.20) V=0, we find the maximum altitude achieved by the rocket

$$H_m = \frac{V_a^2}{2g_0 - \frac{V_a^2}{R_0}}. \tag{15.21}$$

When $\frac{V_a^2}{R_0} \ll 2g_0$ we obtain the well-known equation of Galileo

$$H_m = \frac{V_a^2}{2g_0}. \tag{15.22}$$

When $V_a^2 = 2g_0R_0$ or when

$$V_a = V_{\kappa 2} = \sqrt{2g_0R_0} \tag{15.23}$$

altitude H_m becomes infinite, the rocket overcomes the Earth's gravity and flies into cosmic space. The velocity V_{K2} is called the second cosmic velocity. The second cosmic velocity is greater than the first cosmic velocity by a factor $\sqrt{2}$ and is equal to 11180 m/sec≈11 km/sec. Both cosmic velocities are constants of our planet. The equations of motion of a long range rocket may be formulated conveniently by using polar coordinates R,φ with their origin at the center of the Earth (15.8). To derive the equations of the rocket trajectory, we make use /500 of expression (15.20) and replace R_0+H by R and R_0 by R_0^1, where $R_0^1 > R_0$. As a result we obtain expression

$$V^2 - V_a^2 = -2g_0R_0\left[\frac{R_0}{R_0^1} - \frac{R_0}{R}\right] = -V_{\kappa 2}^2\left[\frac{R_0}{R_0^1} - \frac{R_0}{R}\right]. \tag{15.24}$$

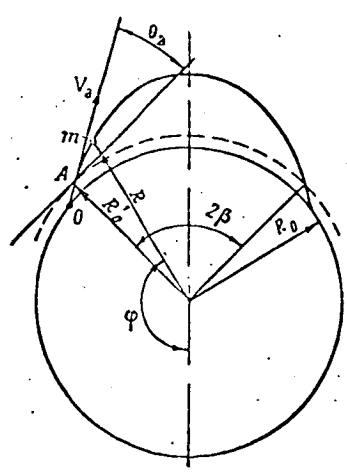

Figure 15.8. Flight trajectory of ballistic missile in polar coordinates.

In addition, we use Kepler's law

$$R^2\dot{\varphi} = C, \tag{15.25}$$

where C=const.

From the initial conditions (t=0) $R=R_0^1$ and $\dot{\varphi}_0=\frac{V_a \cos\theta_a}{R_0^1}$, we find the value of the constant in equation (15.25): $C = R_0^1 V_a \cos\theta_a$. Therefore,

$$R^2\dot{\varphi} = R_0^1 V_a \cos\theta_a = C. \tag{15.26}$$

We write the value for the square of the velocity V in polar coordinates

$$V^2 = \left(\frac{dR}{dt}\right)^2 + R^2\dot{\varphi}^2 = \left[\left(\frac{dR}{d\varphi}\right)^2 + R^2\right]\dot{\varphi}^2. \tag{15.27}$$

By means of equation (15.26) we eliminate $\dot{\varphi}$ from (15.27)

$$V^2 = (R_0^1)^2 V_a^2 \cos^2\theta_a \left[\frac{1}{R^4}\left(\frac{dR}{d\varphi}\right)^2 + \frac{1}{R^2}\right]. \tag{15.28}$$

Finally, by eliminating V from expressions (15.24) and (15.28), we obtain a differential equation for the trajectory of the rocket in polar coordinates.

After separation of variables this equation takes the form /501

$$d\varphi = \frac{C\,dR}{R^2\sqrt{V_a^2 - \frac{2g_0R_0^2}{R_0^1} - \frac{C^2}{R^2} + \frac{2g_0R_0^2}{R}}}. \tag{15.29}$$

By introducing a new variable $y=\frac{C}{R} - \frac{g_0R_0^2}{C}$ equation (15.29) is reduced to the form

$$d\varphi = -\frac{dy}{\sqrt{a^2 - y^2}}, \tag{15.30}$$

where

$$a^2 = V_a^2 - \frac{2g_0R_0^2}{R_0^1} + \frac{g_0^2 R_0^4}{k^2}.$$

Integration of equation (15.30) gives us

$$\varphi - \varphi_0 = \arccos \frac{y}{a} - \arccos \frac{y_0}{a}. \tag{15.31}$$

In the specific case when $\cos \theta_a = 1$ and $y_0 = a$ the second term in (15.31) becomes zero and in this case

$$R = \frac{p}{1 + \epsilon \cos(\varphi - \varphi_0)}, \tag{15.32}$$

where

$$p = \frac{R_0^1 V_a^2}{g_0 R_0^2} \quad \text{and} \quad \epsilon = \frac{R_0^1 V_a^2}{g_0 R_0^2} - 1.$$

Equation (15.32) is the equation of conic sections in polar coordinates with eccentricity ϵ. In the more general case, by using an equation for the sum of the arc cosines, we obtain from expression (15.31)

$$\frac{y y_0}{a^2} + \sqrt{1 - \frac{y^2}{a^2}} \sqrt{1 - \frac{y_0^2}{a^2}} = \cos(\varphi - \varphi_0).$$

Returning to the initial variable, we also obtain an equation for conic sections from this equality

$$R = \frac{p}{1 \pm \epsilon \cos(\varphi - \varphi_0 \mp \psi_0)}, \tag{15.33}$$

where

$$p = \frac{(R_0^1)^2 V_a^2 \cos^2 \theta_a}{g_0 R_0^2};$$

$$\psi_0 = \operatorname{arctg} \frac{\sqrt{a^2 - y_0^2}}{y_0} = \operatorname{arctg} \frac{0.5 V_a^2 \sin 2\theta_a}{V_a^2 \cos^2 \theta_a - \frac{g R_0^2}{R_0^1}};$$

$$\epsilon = \sqrt{1 - \frac{2 V_a^2 R_0^1 \cos^2 \theta_a}{g_0 R_0^2} + \frac{V_a^4 (R_0^1)^2 \cos^2 \theta_a}{g_0^2 R_0^4}}.$$

/502

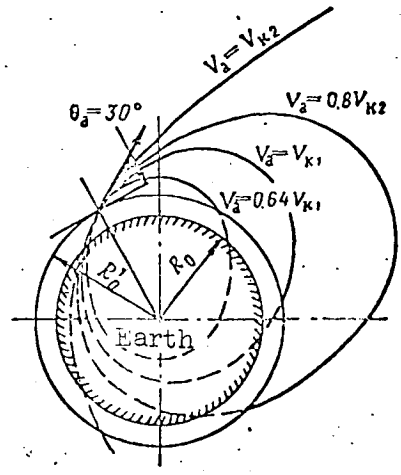

Figure 15.9. Trajectory of ballistic rocket for different burnout velocities.

If the rocket is launched from the surface of the Earth, then $R_0^1 \approx R_0$ is the radius of the Earth. In this case we obtain the following expressions for p and ϵ

$$p = \frac{V_a^2 \cos^2 \theta_a}{g_0}; \qquad \psi = \operatorname{arc\,tg} \frac{0.5 V_a^2 \sin^2 \theta_a}{V_a^2 \cos^2 \theta_a - V_{K1}^2};$$

$$\epsilon = \sqrt{1 - \frac{2V_a^2 \cos^2 \theta_a}{g_0 R_0} + \frac{V_a^4 \cos^2 \theta_a}{g_0^2 R_0^2}} = \tag{15.34}$$

$$= \sqrt{1 + \frac{V_a^2 \cos^2 \theta_a \left[V_a^2 - V_{K2}^2\right]}{V_{K1}^4}}.$$

Depending on the value of eccentricity ϵ, various rocket trajectories are formed. For $\epsilon < 1$ when $V_a < V_{K2}$, the rocket trajectory will be an ellipse. For $\epsilon = 1$ when $V_a = V_{K2}$ the rocket trajectory will be a parabola.[1] For $\epsilon > 1$ when $V_a > V_{K2}$, the rocket trajectory is a hyperbola. Finally, for $\epsilon = 0$, the trajectory of the rocket is a circle. /503

The rocket may enter a circular trajectory only when $\theta_a = 0$. Therefore, for $\epsilon = 0$ from (15.34)

$$V_{K1}^4 = -V_a^2 \left[V_a^2 - V_{K2}^2\right].$$

[1]This parabola differs from the parabola of (15.10).

However, since $V_{K2}^2 = 2V_{K1}^2$, consequently, $(V_{K1}^2 - V_a^2)^2 = 0$.

Thus, for $\epsilon = 30^\circ$, $V_a = V_{K1}$ which has already been obtained before from other considerations.

Fig. 15.9 shows the trajectories of rockets when $\theta_a = 30^\circ$ for different burn-out velocities.

Section 15.4. The Range of a Ballistic Rocket

To compute the range of a ballistic rocket it is first necessary to compute the central angle 2β between the end of the trajectory and the beginning of the trajectory (fig. 15.8). When the trajectory is symmetric, it is sufficient to find half of the central angle, i.e., β. The initial angle φ_0 in equation (15.33) may be selected arbitrarily. Let us assume that it is equal to 0. Then

$$R = \frac{p}{1 + \epsilon \cos(\varphi \mp \psi_0)}. \tag{15.35}$$

For an elliptic trajectory ($\epsilon < 1$) radius R achieves a maximum value when φ achieves a value of β

$$R_{max} = \frac{p}{1 - \epsilon}. \tag{15.36}$$

This maximum occurs when $\cos(\varphi \mp \psi_0) = -1$ or $\beta \mp \psi_0 = \pi$. From this it follows that

$$\beta = \pi \pm \psi_0. \tag{15.37}$$

Utilizing only the lower sign in (15.37) and expanding the expression for ψ_0, we obtain

$$\beta = \pi - \arccos \frac{\frac{p}{R_0^1} - 1}{\epsilon}$$

or

/504

$$\beta = \pi - \arccos \frac{\frac{V_a^2 R_0^1}{g_0 R_0^2} \cos^2 \theta_a - 1}{\sqrt{1 - \frac{2V_a^2 R_0^1 \cos^2 \theta_a}{g_0 R_0^2} + \frac{V_a^4 (R_0^1)^2 \cos^2 \theta_a}{g_0^2 R_0^4}}} \tag{15.38}$$

If we set the derivative $d\beta/d\cos^2\theta_a$ to 0, we can determine the burnout angle θ_a which provides for a maximum angle β and a maximum range with a given velocity V_a

$$(\cos^2\theta_a)\ \text{opt} = \left.\frac{1}{2-\dfrac{V_a^2 R_0^1}{g_0 R_0^2}}\right|_{R_0^1 \sim R_0} = \frac{1}{2-\dfrac{V_a^2}{V_{K1}^2}}.$$

for $V_a < V_{K1}$ $(\theta_a)_{opt} \approx 45^\circ$.

The nature of the function $(\theta_a)_{opt} = f(V_a/V_{K1})$ is shown in fig. 15.10. The optimum burnout angle decreases when V_a increases and for $V_a = V_{K1}$ becomes equal to 0, as required for the circular orbit of a rocket.

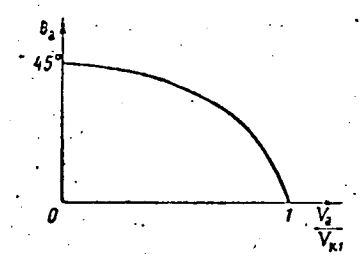

Figure 15.10. Curve showing variation in optimum burnout angle as function of burnout velocity.

The range, or more precisely, the angle β, in the case of the optimum burnout angle is given by equation

$$\beta = \pi - \arccos\frac{-2\sqrt{1-\dfrac{V_a^2 R_0^1}{g_0 R_0^2}}}{2-\dfrac{V_a^2 R_0^1}{g_0 R_0^2}} \qquad (15.39)$$

or for

$$R_0^1 \approx R_0.$$

$$\beta = \pi - \arccos\frac{-2\sqrt{1-\left(\dfrac{V_a}{V_{K1}}\right)^2}}{2-\left(\dfrac{V_a}{V_{K1}}\right)^2}. \qquad (15.40)$$ /505

The total flight range along the surface of the Earth is equal to

$$L = L_a + L_b + L_K, \tag{15.41}$$

where L_a is the range along the active region of the trajectory; L_b is the range along the ballistic region of the trajectory; and L_K is the range along terminal region of the trajectory.

The ballistic range is determined by the expression

$$L_b = 2\beta R_0. \tag{15.42}$$

As we can see from expression (15.42), for a given β the ballistic range does not depend on the altitude of the active region $H_a = R_0^1 - R_0$. The equations for the trajectory were obtained without taking into account the rotation of the Earth. The rotation of the Earth affects the trajectory of the rocket in two directions:

(1) As its component the velocity vector $\overline{V}_a$ contains the vector of the peripheral velocity due to the Earth's rotation, whose modulus is equal to $V_{per} = \omega_3 R_0 \cos \varphi$, where φ is the altitude of the place, and $\omega_3 = 0.251$ rad/hour = 725 x 10 rad/sec is the angular velocity of the Earth. The component due to the velocity of the Earth's rotation changes both the magnitude of the velocity at the end of the active region V_a and also the direction of the rocket flight (the firing plane);

(2) Due to the rotation of the Earth, during its flight time t_b the rocket will drop to the west of the impact point for the case of a fixed Earth by a distance $t_b V_{per\ impact}$ where $V_{per\ impact} = \omega_3 R_0 \cos \varphi_{impact}$ is the peripheral velocity of the Earth at latitude where the rocket hits. To compute L_K in equation (15.41) we may assume that over this region the trajectory is also elliptic. The length L_a is determined from the calculation of the active region of the trajectory.

Section 15.5. Errors in Range of Long-Range Ballistic Missiles

The actual range differs from the required range as specified by equation (15.41), first by the magnitude of the error accumulated over three regions of the flight and secondly by the value of the purely computational error $\Delta L_{computational}$, which occurs due to the inaccuracy in determining the mutual

position of the launching place and the impact point. Thus,

$$L_{\Phi} = (L_a \pm \Delta L_a) + (L_b \pm \Delta L_b) + (L_K \pm \Delta L_K) + \Delta L_{\text{computational}}. \qquad (15.43)$$

Let us consider in detail all the component range errors. /506

1. The error in the distance to the termination of the active region of the trajectory (ΔL_a) depends on launching conditions, the state of the atmosphere, the accuracy of rocket stabilization over the active region and the deviation of rocket parameters (weight, aerodynamic characteristics, thrust of the engine, etc.) from the design values. All these deviations along the active region in addition to the error in range ΔL_a (15.11) change the parameters at the end of the active region V_a, θ_a and H_a;

2. An error in the range of the ballistic region of the trajectory (ΔL_b) is determined in terms of the error in angle β, i.e.,

$$\Delta L_b = 2\Delta\beta R_0.$$

In accordance with equation (15.38), angle β is a function of V_a, θ_a and $H_a = R_0^1 - R_0$, i.e., of the parameters at the end of the active region of the trajectory:

$$\beta = f(V_a, \theta_a, R_0^1).$$

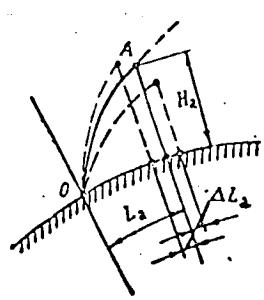

Figure 15.11. Range Error at End of Active Region.

The occurrence of deviations ΔV_a, $\Delta\theta_a$, ΔR_0^1 from the design values V_a, θ_a and R_0^1 (or H_a) leads to an error $\Delta\beta$

$$\beta + \Delta\beta = f\,(V_a + \Delta V_a,\quad \theta_a + \Delta\theta_a,\quad R_0^1 + \Delta R_0^1). \tag{15.44}$$

By expanding expression (15.44) in a power series of deviations and considering only the linear terms of the series, we find

$$\Delta\beta = f^V \Delta V_a + f^\theta \Delta\theta_a + f^R \Delta R_0^1, \tag{15.45}$$

where

$$f^V = \frac{\partial f}{\partial (V_a + \Delta V_a)}\bigg|_{\Delta V_a = \Delta\theta_a = \Delta R_0^1 = 0;}$$

$$f^\theta = \frac{\partial f}{\partial (\theta_a + \Delta\theta_a)}\bigg|_{\Delta\theta_a = \Delta V_a = R_0^1 = 0;}$$

$$f^R = \frac{\partial f}{\partial (R_0' + \Delta R_0^1)}\bigg|_{\Delta V_a = \Delta\theta_a = \Delta R_0^1 = 0}$$

To compute coefficients f^V, f^θ and f^R it is necessary to take the partial derivatives of expression (15.38).

For an optimum trajectory, according to equation (15.39) the error in the slope to the first approximation will not lead to an error in the ballistic range. Figure 15.12 illustrates the effect of errors ΔV_a and $\Delta R_0^1 = \Delta H_a$ on the error in the ballistic range. /508

3. The error in the range of the terminal region of the trajectory (ΔL_K) depends on the parameters at the termination of the ballistic region, and on the stabilization of the rocket in the dense layers of the atmosphere and on the deviation of the weight and aerodynamic drag of the rocket from design values.

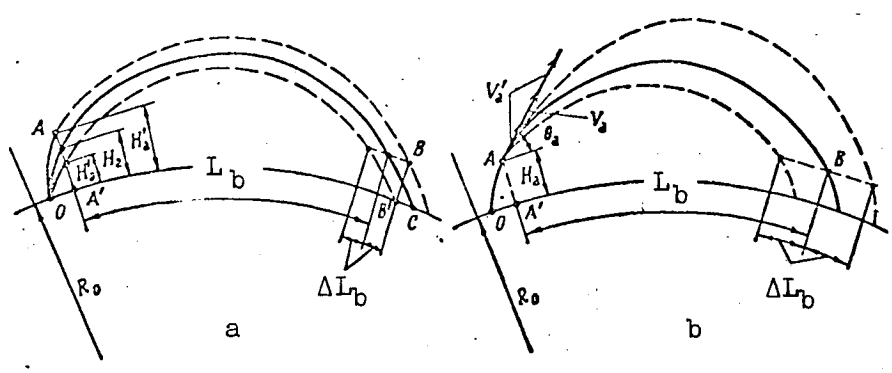

Figure 15.12. Graphs illustrating effect of errors in altitude and in velocity at termination of active region on ballistic range.

Of all the component range errors the most significant one is the error ΔL_b, due primarily to the deviation of V_a from the design value.

Section 15.6. The Active Region of the Ballistic Rocket Trajectory

In computing the ballistic region we need not consider the Earth's curvature, because L_a is small compared with L_b. The equations for the longitudinal motion of the rocket along the active region in this case assume the well-known form (fig. 15.13)

$$\left.\begin{aligned} m\frac{dV}{dt} &= P\cos\alpha - X - mg\sin\theta, \\ mV\frac{d\theta}{dt} &= Y + P\sin\alpha - G\cos\theta, \\ J_z\frac{\partial^2\vartheta}{\partial t^2} &= M_z(\alpha, \beta, V, \delta, t), \\ \theta + \alpha &= \vartheta, \end{aligned}\right\} \tag{15.46}$$

where $P(V,\rho,t)$ is the thrust of the engine; m is the mass of the rocket; $Y = c_y S\frac{\rho V^2}{2}$, $c_y = c_y(M,\alpha)$ is the lift force and its coefficient; $X = c_x S\frac{\rho V^2}{2}$, $c_x = c_x(M,\alpha)$ is the resistance and its coefficient; J_z is the moment of inertia of the rocket with respect to the transverse axis; $M = \frac{Y}{a}$ is the number M (a is the velocity of sound at the altitude where the density is equal to ρ); and M_z is the moment with respect to the transverse axis, which depends on angle of attack α, air density ρ, velocity V and the deflection angle of the control surface (gas or aerodynamic or both).

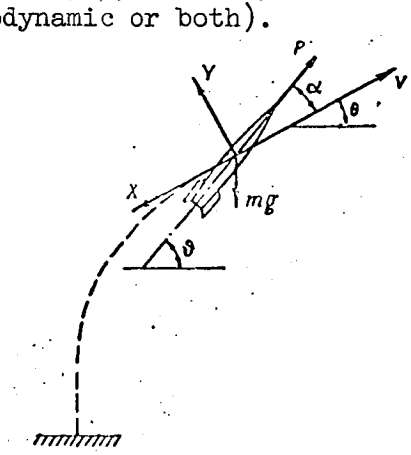

Figure 15.13. Forces which act on rocket in active region.

The moment M_z is also a function of time, because as the fuel is consumed, the distance between the center of gravity of the rocket and the center of thrust Y changes. The mass m and the moment of inertia I_z are also functions of time.

To compute the law for the variation of velocity V, of altitude H and of the range along the active region L_a, we may use the programed variation in the slope of the trajectory $\theta_3 = \theta_3(t)$. In this case V, H and L_a are obtained by the numerical integration of the system of equations

$$\left.\begin{aligned} m\frac{dV}{dt} &= p - x - mg\sin\theta_3, \\ \frac{dH}{dt} &= V\sin\theta_3, \\ \frac{dL}{dt} &= V\cos\theta_3. \end{aligned}\right\} \qquad (15.47)$$

In solving equation (15.47) to the first approximation, we may assume that the angle of attack is equal to 0. Furthermore, we may refine the solution by determining the required angle of attack $\alpha = \alpha(t)$ and using the value of $\alpha = \alpha(t)$, thus obtained, in the iterative solution of equation (15.47). After determining the velocity and the flight altitude as functions of time (from the solution of the system of equations (15.47)), we obtain from the last three equations (15.46) the equations for small deviations of angles α, θ and ϑ. /509

If we take into account the action of aerodynamic and reactive control surfaces, these equations have the following form

$$\left.\begin{aligned} mV\frac{d\Delta\theta}{dt} &= \left(c_y^{\alpha}s\frac{\rho V^2}{2} + P\right)\alpha \mp c_y^{\delta_a}s\frac{\rho V^2}{2}\delta_a \mp P^{\delta}g_{\delta_g} - G\cos\theta_e, \\ J_z\frac{d^2\Delta\vartheta}{dt^2} + M_z^{\omega}\frac{d\Delta\vartheta}{dt} + M_z^{\alpha}\alpha &= M_z^{\delta_a}\delta_a + M_z^{\delta_g}\delta_g, \\ \Delta\vartheta &= \Delta\theta + \alpha, \end{aligned}\right\} \qquad (15.48)$$

where δ_a is the deflection of the aerodynamic control surface; and δ_g is the deflection of the reactive control surface.

In the first equation (15.48) we have taken into account the components of the lateral force produced by the deflection of the control surfaces. The upper sign refers to the rear and the lower sign to the front position of the control

surfaces. All the coefficients in equations (15.48) as well as m, V, c_y^α, ρ, P, $c_y^\delta a$, $P^\delta g$, I_z, M_z^α, $M_z^\delta a$, $M_z^\delta g$ are functions of time. These functions are determined from the solution of (15.47).

Let us consider the stages of motion of a rocket whose angular oscillations may be described by equations (15.48).

1. Motion in the Earth's atmosphere with a velocity for which the effect of aerodynamic forces is substantial. Equations (15.48) for this case will be written in the form

$$\left.\begin{aligned} &T_V \frac{d\Delta\theta}{dt} = \alpha \mp c^{\delta_a}\delta_a \mp c^{\delta_g}\delta_g - \frac{T_V g}{V}\cos\theta_c, \\ &\frac{d^2\Delta\vartheta}{dt^2} + m^\omega \frac{d\Delta\vartheta}{dt} + m^\alpha \alpha = m^{\delta_a}\delta_a + m^{\delta_g}\delta_g, \\ &\Delta\vartheta = \Delta\theta + \alpha, \end{aligned}\right\} \qquad (15.49)$$

where

$$T_V = \frac{mV}{c_y^\alpha s \frac{\rho V^2}{2} + P}\,[\text{sec}]; \quad c^{\delta_a} = \frac{c_y^{\delta_a} s \frac{\rho V^2}{2}}{c_y^\alpha s \frac{\rho V^2}{2} + P}; \qquad /510$$

$$c^{\delta_g} = \frac{p^{\delta_g}}{c_y^\alpha s \frac{\rho V^2}{2} + P}; \quad m^\omega = \frac{M^\omega{}_z}{J_z}; \quad m^\alpha = \frac{M_z^\alpha}{J_z};$$

$$m^{\delta_a} = \frac{M_z^{\delta_a}}{J_z}; \quad m^{\delta_g} = \frac{M_z^{\delta_g}}{J_z}.$$

2. Motion outside the atmosphere or in highly rarefied layers of the atmosphere, where the effect of aerodynamic forces is insignificant and therefore $m^\omega = m^\alpha = c\delta a = m\delta a = 0$, while $T_V = mV/P$. The equations for this case take the form

$$\left.\begin{aligned} &T_V \frac{d\Delta\theta}{dt} = \alpha \mp c^{\delta_g}\delta_g - \frac{T_V g}{V}\cos\theta_c, \\ &\frac{d^2\Delta\vartheta}{dt^2} = m^{\delta_g}\delta_g \\ &\Delta\vartheta = \Delta\theta + \alpha. \end{aligned}\right\} \qquad (15.50)$$

Equations (15.50) are valid for the launching of the rocket when the aerodynamic forces and moments are small due to low flight velocity.

The most general are equations (15.49), which are transformed smoothly into equations (15.50) or vice versa.

If we fix ("freeze") the coefficients (15.49) for different instants of time, we may obtain transfer functions for the angles $\Delta\vartheta$, $\Delta\theta$ and α in terms of the angular deflection of the control surface (it does not matter which one - δ_g or δ_a)

/511

$$\left.\begin{aligned}
W_\theta(p) &= \frac{\mp \frac{c^\delta g}{T_V}(p^2 + m^\omega p + m^\alpha) + \frac{m^\delta g}{T_V}}{p^3 + \left(m^\omega + \frac{1}{T_V}\right)p^2 + \left(m^\alpha + \frac{m^\omega}{T_V}\right)p};\\
W_\alpha(p) &= \frac{\pm \frac{c^\delta g}{T_V}(p + m^\omega) + m^\delta g}{p^2 + \left(m^\omega + \frac{1}{T_V}\right)p + \left(m^\alpha + \frac{m^\omega}{T_V}\right)};\\
W_{\Delta\vartheta}(p) &= \frac{\left(p + \frac{1}{T_V}\right)m^\delta g \mp \frac{c^\delta g}{T_V}m^\alpha}{p^3 + \left(m^\omega + \frac{1}{T_V}\right)p^2 + \left(m^\alpha + \frac{m^\omega}{T_V}\right)p}.
\end{aligned}\right\} \quad (15.51)$$

In the same way from equation (15.50) we have

$$\left.\begin{aligned}
W_{\Delta\theta}(p) &= \frac{\mp c_y^\delta g + m^\delta g}{(T_V p + 1)p^2};\\
W_\alpha(p) &= \frac{\pm c_y^\delta g\, p + T_V m^\delta g}{(T_V p + 1)p};\\
W_{\Delta\vartheta}(p) &= \frac{m^\delta g}{p^2}.
\end{aligned}\right\} \quad (15.52)$$

Figure 15.14 shows the logarithmic amplitude-frequency characteristics for the pitching angle of the ballistic rocket constructed on the basis of transfer function $W_{\Delta\vartheta}(p)$. The logarithmic amplitude-frequency characteristics are constructed in accordance with (15.51) for two values of the parameters, corresponding to different values of the coefficients at different stages of the active region of the trajectory, while (15.52) is used to construct these characteristics for one value of $m^\delta g$.

Equation (15.49) describes the behavior of the nonstationary linear dynamic system. By fixing or "freezing" the coefficients for different instants of time, we obtain in this manner a series of stationary systems for each of which we can write the transfer functions. However, for the nonstationary linear systems as well as for stationary ones there is also a concept of the pulse transfer function and the pulse transient function. If we undertake the operation to eliminate the variables, for example, from equations (15.49) we obtain one equation in terms of some one unknown /512

$$A(t,p)x = B(t,p)\delta, \tag{15.53}$$

where p = d/dt and in the general case

$$A(t,p) = a_n(t)p^n + a_{n-1}(t)p^{n-1} + \ldots + a_1(t)p + a_0(t); \tag{15.54}$$

$$B(t,p) = b_m(t)p^m + b_{m-1}(t)p^{m-1} + \ldots + b_1(t)p + b_0(t). \tag{15.55}$$

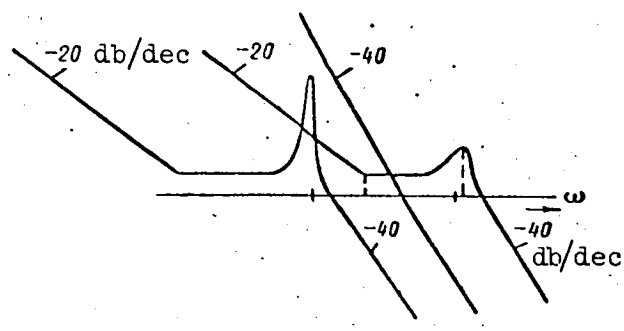

Figure 15.14. Logarithmic amplitude-frequency characteristics of the pitching angle loop of ballistic rocket.

It can be shown that the transfer function of a nonstationary system is the solution of some linear equation with variable coefficients having the same order as equation (15.53)

$$\begin{gathered}\alpha_n(t)\frac{d^n}{dt^n}W(t,s) + \alpha_{n-1}\frac{d^{n-1}}{dt^{n-1}}W(t,s) + \ldots \\ \ldots + \alpha_1(t)\frac{d}{dt}W(t,s) + A(t,s)\cdot W(t,s) = B(t,s),\end{gathered} \tag{15.56}$$

where s--a complex number--is the Laplace transform,

$$\alpha_k(t) = \frac{1}{k!}\frac{\partial^k A(t,s)}{ds^k} \qquad (k = 1, 2, \ldots).$$

If we fix the coefficients of equation (15.53), all derivatives of W(ts) will become equal to 0. Then, from equation (15.56) we shall obtain the first approximation of the transfer function of a nonstationary system as functions of the complex parameter s

$$W_1(t, s) = \frac{B(t, s)}{A(t, s)}. \tag{15.57}$$

The transfer function (15.57) has the same meaning as transfer functions (15.51) and (15.52), i.e., it also has different coefficients for different instants of time. However, it is somewhat more accurate than transfer functions (15.51) and (15.52), which may be clarified in the following manner. The transfer function (15.57) was obtained from equation (15.53) after its coefficients were fixed at different instants of time. Equation (15.53) itself is obtained from a system of nonstationary equations by excluding the variables which are of no interest. As far as the transfer functions (15.51) or (15.52) are concerned, they were obtained from a system of equations whose coefficients were fixed. /513

The complete solution of equation (15.56), which gives the refined values for the transfer function, is represented in the form of a series

$$W(t, s) = \sum_{\mu=1}^{\infty} W_\mu(t, s), \tag{15.58}$$

and the μth term of the series is computed by means of the recurrent equation

$$W_\mu = -\frac{1}{A(t, s)}\left[a_n(t) W_{\mu-1}^{(n)} + \ldots + a_1(t)\dot{W}_{\mu-1}\right].$$

The slower the variation in the coefficients of the initial equation (15.53), the faster is the convergence of series (15.58) and the closer is the true value of W(t,s) to its first approximation $W_1(t,s)$. From transfer function W(ts), considering t as a parameter, we may use the inverse Laplace transform to obtain the pulse transfer and pulse transient functions. The pulse transfer function has the form

$$\dot{H}(\tau, t) = \frac{1}{2\pi j}\int_{c-j\infty}^{s+j\infty} W(t, s)\, e^{s\tau}\, ds, \tag{15.59}$$

the transient function has the form

$$H(\tau, t) = \frac{1}{2\pi j}\int_{s-j\infty}^{s+j\infty} W(t, s)\, \frac{e^{s\tau}}{s}\, ds. \tag{15.60}$$

In expressions (15.59) and (15.60) parameter t represents the instant of time when reactions $\delta(t)$ is applied for (15.59) and $1(t)$ for (15.60). We can obtain the approximate values of the transfer functions, if in equations (15.59) and (15.60) we replace the exact value $W(t,s)$ with an approximate value in the form $W_1(t,s)$ or in the form of transfer functions (15.51) and (15.52). Again,

the slower the variations in the coefficients of the initial equations, the closer will be the approximate solution to the true one. However, because the transients functions are not subject to extremely rigid requirements,[1] even in the case of relatively rapid variation in the parameters which takes place along the active region of the ballistic missile trajectory, the computation of transient functions on the basis of transfer functions(15.51) and (15.52) is quite adequate. This means that the same transfer functions may be used to select the parameters of the rocket control system along the active region. /514

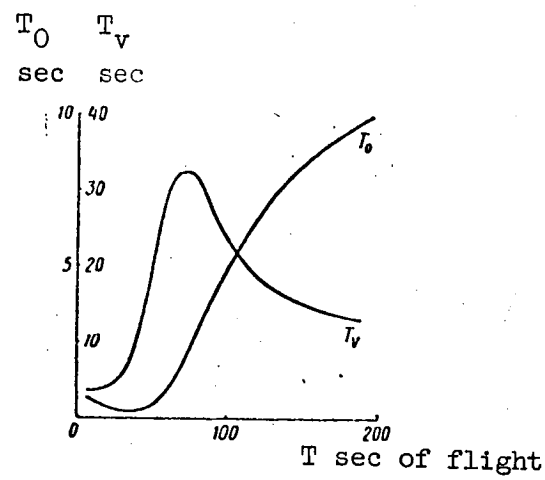

Figure 15.15. Variation in coefficients of transfer function of ballistic missile along active region.

Figure 15.15 shows the curves $T_V = T_V(t)$, $T_0 = T_0(t)$ for the active region of some arbitrary ballistic rocket, showing the nature of the variation in the coefficients of the ballistic rocket transfer function. The transfer function, in terms of the pitching angle, is taken in the form

$$W(p) = \frac{(T_V p + 1)\, k_0}{(T_0^2 p^2 + 2\zeta_0 T_0 p + 1)\, p}, \qquad (15.61)$$

[1]Thus, for example, in a second order system it is quite permissible to assume that the variation in the coefficient with respect to damping is from 0.4-0.9.

where

$$k_0 = \frac{m^{\delta}}{\left(m^{\alpha} + \frac{m^{\omega}}{T_V}\right) T_V}; \quad T_0 = \left(m^{\alpha} + \frac{m_{\omega}}{T_V}\right)^{-\frac{1}{2}};$$

$$2\zeta_0 T_0 = \frac{m^{\omega} + \frac{1}{T_V}}{m^{\alpha} + \frac{m^{\omega}}{T_V}}, \quad \zeta_0 = \frac{m^{\omega} + \frac{1}{T_V}}{2\sqrt{m^{\alpha} + \frac{m^{\omega}}{T_V}}}.$$

The amplification factor k_0 and the attenuation factor ζ_0 remain approximately constant[1] $k_0 \approx 0.8 \frac{1}{\text{sec}}$ and $\zeta \approx 0.05 - 0.01$. As we can see from the graphs, constant T_V varies most intensely between the 40th and the 50th second of flight /515 time, when the slope of the increase in T_V reaches a value of ≈ 1.3 sec/sec. If we require that the duration of the transient function of the pitching angle be approximately 5 sec, then $T_V = 11$ sec to $T_V = 17.5$ sec during the period of the transient process (beginning with the 40th second). It is obvious that even in this rigid case the variation in T_V (and also T_0) will not affect the nature of the transient function from the standpoint of effective stabilization of the rocket's pitch angle.

Equations (15.49) determine the dynamic properties of the rocket during longitudinal motion (motion in the firing plane).[2] The equation for the lateral motion of the ballistic missile will be the same as equations (15.49), if the gravity force is set equal to 0.

$$\left.\begin{aligned} T_V \frac{d\theta_b}{dt} &= \beta \mp c^{\delta_a} \delta_a \mp c^{\delta_g} \delta_g, \\ \frac{d^2\psi}{dt^2} + m^{\omega} \frac{d\psi}{dt} + m^{\alpha}\beta &= m^{\delta_a} \delta_a + m^{\delta_g} \delta_g; \\ \psi &= \theta_b + \beta. \end{aligned}\right\} \qquad (15.62)$$

---

[1]For the given case.

[2]The firing plane is the vertical plane passing through the launching point and the target.

where ψ is the angular deviation o the rocket's longitudinal axis from the firing plane; θ_b is the deviation in the rocket velocity vector from the same plane; and β is the angle of attack in lateral motion.

Because of the rocket's symmetry, the control coefficients (15.62) have the same numerical values as the control coefficients given by (15.49).

In addition to expressions (15.49) and (15.62), we must also bear in mind the control of rotation (tilt angle) of the rocket with respect to the longitudinal axis

$$J_x \frac{d^2\gamma}{dt^2} + M_x^{\omega_x} \frac{d\gamma}{dt} = M_x^{\delta_g} \delta_g + M_x^{\delta_a} \delta_a,$$

where γ is the tilt angle; J_x is the moment of inertia of the rocket with respect to the longitudinal axis; $M_x^{\omega}x$ is the coefficient of the damping moment; δ_g δ_a are the deflections of the jet and aerodynamic control surfaces which produce moments around the longitudinal axis; and $M_x^{\delta}g$, $M_x^{\delta}a$ are the coefficients of these moments. The damping moment $M_x^{\omega}x\frac{d\gamma}{dt}$ is rather small in ballistic missiles /516 and may be neglected.

Section 15.7. Automatic Control of Rocket Flight Over the Active Region

The purpose of controlling the flight of the rocket along the active region is to assure that the rocket flies in the firing plane and to maintain a programed value for the slope of the trajectory $\theta_3(t)$.[1] In the case of self-contained guidance, these problems are solved by the automatic pilot on the basis of information obtained from the gyroscopes and the inertial system of navigation. First let us consider the control of the missile by means of gyroscopic devices involving gyroscopes with 3 and 2 degrees of freedom. Figure 9.10 shows the position of the rocket's control surfaces and the description of their operation.

Since the tilt angle of the rocket is stabilized, the position of the control surfaces in space remains fixed. The stabilization of the tilt angle γ and

[1]The problem of automatic control is, of course, also concerned with range control. This question will be considered briefly in section 15.9.

the course angle ψ is accomplished by signals from a gyroscope with 3 degrees of freedom. The axis of the gyroscope's rotor is situated along a normal to the firing plane. The gyroscope has pendulum compensation which is disconnected before the rocket is launched. These signals ψ and γ for stabilizing the rocket are taken from the potentiometers of the gyroscope. The second gyroscope with three degrees of freedom produces signals for the pitch control surfaces 2 - 4. The axis of its rotor is horizontal and lies in the firing plane. The gyroscope has pendulum compensation which is turned off before the rocket is launched. The potentiometer, whose brush picks up and sends signals to the control surfaces 2 - 4, is connected with a programing mechanism which programs the slope of the trajectory.

It follows that the control of the rocket is reduced to the stabilization of angle ψ and γ ($\psi_3 = 0, \gamma_3 = 0$) and the tracking of the pitch angle to assure that it has the programed value $\vartheta_3(t) = \theta_3(t)$. To solve these problems, it is rational to use an astatic automatic pilot (an automatic pilot without feedback or an isodromic automatic pilot). To use an automatic pilot without feedback, it is necessary to have methods of measuring the signals for the angular velocity $\dot{\vartheta}$ ($\dot{\psi}$ and $\dot{\gamma}$, respectively) and the angular acceleration $\ddot{\vartheta}$ ($\ddot{\psi}$ and $\ddot{\gamma}$, respectively). However, it is not necessary to measure these signals, if we use a subsequent compensating network which performs double differentiation in the circuit for the signals ψ, γ and ϑ from the gyroscope's potentiometer to the control surfaces.

Figure 15.16 shows a functional diagram for the control of the pitch angle with a series compensating circuit. The series compensating network with a transfer function /517

$$\frac{(T_1 p + 1)(T_2 p + 1)}{(T_3 p + 1)(T_4 p + 1)}$$

may be either in the form of a double differentiating network, when $T_1 > T_2 > T_3 > T_4$, or in the form of an integrating-differentiating network, when $T_3 > T_1 > T_2 > T_4$. To retain the same dynamic properties in the circuit for controlling the pitch angle, it is desirable to vary the circuit parameters

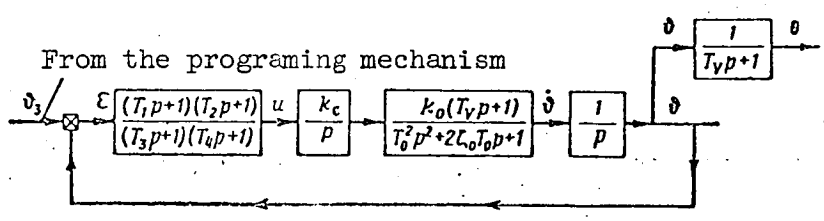

Figure 15.16. Functional diagram showing pitch angle control with series compensating network.

T_1, T_2, T_3, T_4 either as functions of time or as functions of the velocity head. The dynamic properties of the pitch angle control circuit are characterized completely by the logarithmic frequency characteristics of the open circuit and by the cutoff frequency ω_c. If the control time for the pitch angle must be within the limits 3 - 6 seconds, it is necessary to have $\omega_c = 0.5\text{-}1$ 1/sec. For small velocity heads, when the natural frequency of oscillations of the rocket $1/T_0$ is small, the cutoff frequency $\omega_c = 0.5\text{-}1.0$ turns out to be greater than the natural frequency $1/T_0$, and the compensating network in this case consists of a double differentiating circuit. At high velocity heads ω_c becomes less than $1/T_0$, and the compensating network is transformed into an integrating-differentiating circuit. During launching and during flight outside the atmosphere, the compensating network also consists of a differentiating circuit.

Figure 15.17 shows the amplitude characteristics for a large velocity head and for a small velocity head. As we have already pointed out, the variation in the parameters T_1, T_2, T_3 and T_4 and the change in the form of the circuit may be carried out by the programing mechanism as a function of time. The programing mechanism must also be used to change the total amplification factor of the circuit by changing k_c (fig. 15.16).

If the rocket has a digital computer, the functions of the compensating device may be assigned to it. Let us assume that T is the operating frequency /518 of the computer.[1] In particular, this means that the results produced by the computer are in the form of a sequence of rectangular voltage pulses, whose amplitude corresponds to the results obtained by the computer at the instants of time $t = nT$ ($n = 0, 1, 2, \ldots$). If it is necessary to program the computer to realize a compensating network with a transfer function $W(s)$, it is sufficient to find the reaction of this network at discrete instants of time $t = nT$ ($n = 0, 1, 2, \ldots$) to a rectangular pulse with duration T and with unit amplitude. The transform of a unit pulse of duration T is equal to

$$\frac{1-e^{sT}}{s} = \frac{z-1}{z} \cdot \frac{1}{s},$$

where $z = e^{sT}$.

[1]The value of T for computers aboard the missile may vary in the limits 0.05-0.3 sec.

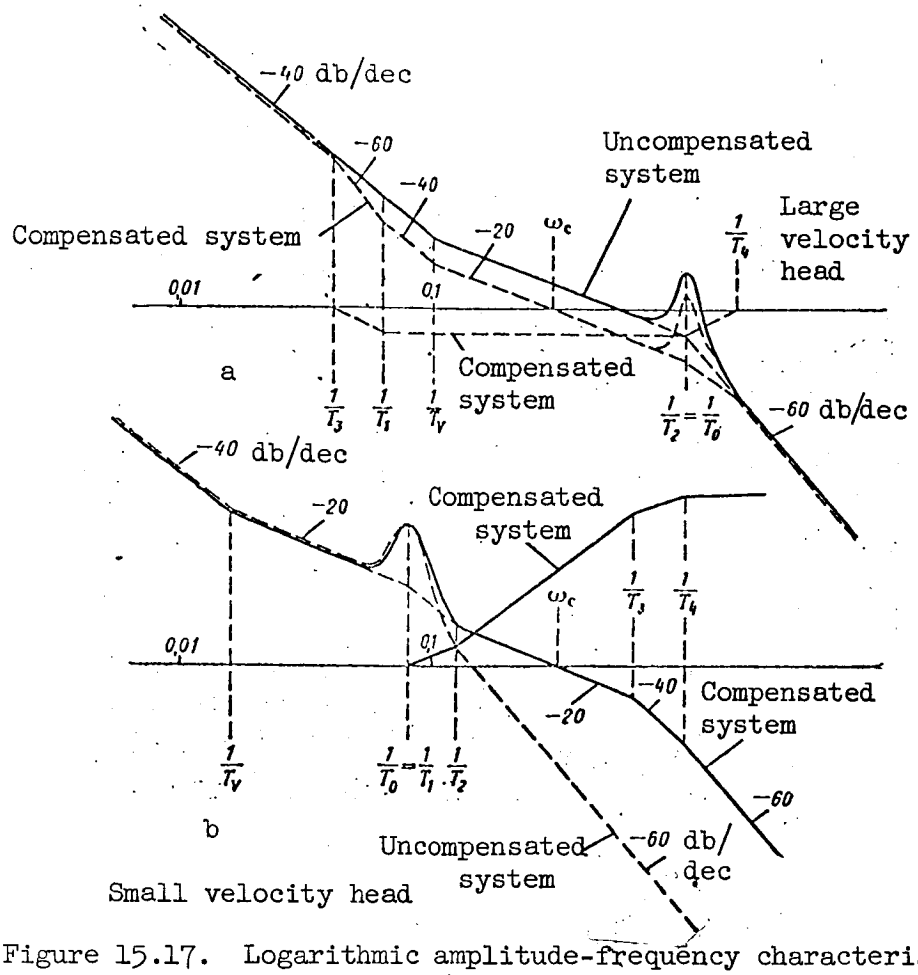

Figure 15.17. Logarithmic amplitude-frequency characteristics of circuit which controls pitch angle of ballistic missile: a, for large velocity heads; b, for small velocity heads.

Consequently, the transform of the output of the compensating network will have the form

$$u^*(s) = W(s) \cdot \frac{1}{s} \frac{z-1}{}. \tag{15.63}$$

Since we are interested in the reaction of the pulse network, we must go from transform (15.63) to a discrete transform whose parameter is $z = e^{sT}$.[1] In its discrete form the transform $u^*(s)$ is the transfer function of the computer (subscript M = computer)

$$W_M[z] = \frac{b_q z^q + b_{q-1} z^{q-1} + \ldots + b_1 z + b_0}{z^r + a_{r-1} z^{r-1} + \ldots + a_1 z + a_0}. \tag{15.64}$$

[1] G. S. Pospelov, Sampled-data Control Systems, "Automatic Control and Computer Engineering," Mashgiz, 1960, No. 3.

Since the transfer function of the computer $W_M[z]$ is the ratio of the transform at the output u and the input ϵ, the computer program follows from equation (15.64) in the form of a recurrent relationship

$$u_n = b_0\varepsilon_{n-r} + b_1\varepsilon_{n+1-r} + \ldots + b_{q-1}\varepsilon_{n+q-1-r} + b_q\varepsilon_{n+q-r} - \\ -[a_0u_{n-r} + a_1u_{n+1-r} + \ldots + a_{r-1}u_{n-1}]. \tag{15.65}$$

Let us determine the program for this case when

$$W(s) = \frac{(T_1s+1)(T_1s+1)}{(T_3s+1)(T_4s+1)}.$$

For this case

$$u^*(s) = \frac{z-1}{z}\frac{(T_1s+1)(T_2s+1)}{(T_3s+1)(T_4s+1)}\cdot\frac{1}{s} = \\ = \frac{z-1}{z}\left[\frac{c_0}{s} + \frac{c_3}{s+\frac{1}{T_3}} + \frac{c_4}{s+\frac{1}{T_4}}\right], \tag{15.66}$$

where

$$c_0 = 1, \quad c_3 = \frac{(T_3-T_1)(T_3-T_2)}{(T_4-T_3)T_3}, \quad c_4 = \frac{(T_4-T_1)(T_4-T_2)}{(T_3-T_4)T_4}.$$

From expression (15.66) by using the z-transform we find /520

$$W_M[z] = \frac{b_2z^2 + b_1z + b_0}{z^2 + a_1z + a_0}, \tag{15.67}$$

where

$$a_1 = -(z_3+z_4): \quad a_0 = z_3z_4; \quad z_3 = e^{-\frac{T}{T_3}};$$

$$z_4 = e^{-\frac{T}{T_4}};$$

$$b_2 = c_0 + c_3 + c_4, \quad b_1 = -[c_0(z_3+z_4) + c_3(z_4-1) + c_4(z_3+1)];$$

$$b_0 = c_0z_3z_4 + c_3z_4 + c_4z_3.$$

From equation (15.67) we obtain the program of the computer

$$u_n = b_0\varepsilon_{n-2} + b_1\varepsilon_{n-1} + b_2\varepsilon_n - a_0u_{n-2} - a_1u_{n-1}. \tag{15.68}$$

From expression (15.68) we can see that every nth pulse at the output of the computer is proportional to the sum of the input signal ϵ during the nth interval of time and during two preceding intervals of time, and also proportional to the sum of two output pulses during two preceding intervals of time. The coefficients b_0, b_1, b_2, a_0 and a_1 are computed and stored in the memory of the computer. Since parameters T_1, T_2, T_3 and T_4 must vary with time, the computer must replace the values of coefficients b_0, b_1, b_2, a_0 and a_1 at instants of time programed beforehand.

The system which we have considered for the control of the rocket along the active part of the trajectory by means of gyroscopic sensors has two shortcomings:

(1) the trajectory of the rocket is not stabilized in the firing plane; therefore, there is a miss $L\Delta\theta_b$, where L is the range of the rocket and $\Delta\theta_b$ is the error in stabilizing the velocity vector;

(2) the fast response of the control system to the pitching angle achieved by using compensating devices does not mean that the system reacts with the same speed to the slope of the trajectory, which is actually what we require.

Both of the shortcomings may be avoided by using an inertial system of guidance. Let us assume that the x-axis of the inertial system of the second type is oriented in the firing plane (fig. 5.33). Then the z-axis of the system will be normal to the firing plane, and from the first and second integrator of channel z of the inertial system we can obtain deviation signals z and deviation rates z of the rocket from the firing plane. By feeding these signals to the control surfaces of the rocket we obtain a stabilization system for the rocket in the firing plane, which was described in detail in section 1 of this Chapter.

The second shortcoming can be overcome by the inertial system itself, because it measures the value of the rocket's velocity vector, i.e., it determines the modulus of velocity V and the slope of the trajectory θ. Since the z-axis is normal with respect to the firing plane, we have /521

$$V = \sqrt{\dot{x}^2 + \dot{y}^2}, \tag{15.69}$$

$$\theta = \operatorname{arc\,tg} \frac{\dot{y}}{\dot{x}}, \tag{15.70}$$

where x and y are the signals from the first integrators of the $\dot{x}$ and $\dot{y}$ channels of the inertial system. Equations (15.69) and (15.70) are valid, if we do not take into account the curvature of the Earth. For the active region of the trajectory, it is permissible to neglect the curvature of the Earth.

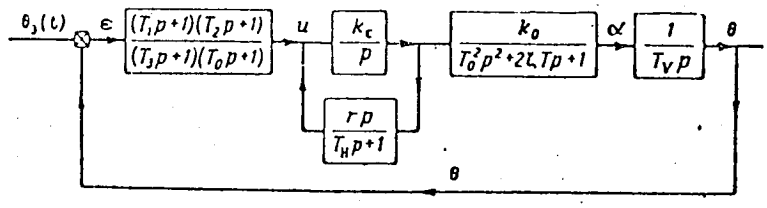

Figure 15.18. Functional diagram showing control of ballistic missile trajectory slope.

When the signal of θ is measured, it is possible to develop a circuit for controlling angle θ, rather than the pitch angle ϑ, as was true in the preceding case. The variation of the functional diagram for controlling the slope of the trajectory is shown in figure 15.18. Unlike the system which controls the pitch angle, the servomotor in this case has isodromic feedback. The transfer function of the servomotor with isodromic feedback has the form

$$W_c(p) = \frac{\dfrac{k_c}{p}}{1 + \dfrac{rk_c}{T_H p + 1}} = \frac{T_H p + 1}{T_c p + 1} \cdot \frac{k_{c1}}{p} \approx \frac{k_{c1}(T_H p + 1)}{p},$$

(subscripts c = servomotor, H = load),

where

$$k_{c1} = \frac{k_c}{1 + rk_c} \quad \text{and} \quad T_c = \frac{T_H}{1 + rk_c}.$$

Usually k_c has a sufficient value so that $T_c \ll T_H$ and we can neglect T_c.

In this case the transfer function of the servomotor is represented as a product of the ideal forcing element and the integrating element. As a whole, the functional diagram shown in figure 15.18 is identical to the functional diagram for the pitch angle shown in figure 15.16, where the role of T_V is carried out by the isodromic circuit constant T_H. The identity of these functional diagrams shows that it is possible to obtain a control system for the slope of the trajectory with as good a response time as the system involving the control of the pitch angle. To control and stabilize the rocket along the active region of the trajectory, it is quite appropriate to use adaptive automatic pilots, whose principle of operation is described in section 10.10. An adaptive automatic pilot will provide for constant dynamic characteristics of the circuits for stabilizing and controlling the rocket, even though there is a substantial variation in the dynamic properties of the rocket itself. /522

Section 15.8. Controlling the Range of a Ballistic Missile

As we have shown, the range of a rocket in the case of an optimum trajectory is determined by velocity V_a at the end of the active region. Therefore, the simplest way of controlling the range of the rocket is to turn off the rocket motor at the time when the rocket has reached the required velocity. To do this it is necessary to measure the actual flight velocity of the rocket and to track it.

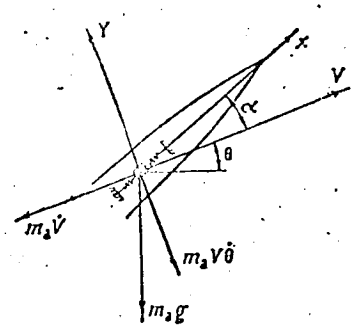

Figure 15.19. Schematic diagram showing position of accelerometer which measures longitudinal acceleration of a rocket.

The measurement of a rocket's velocity can be carried out by radar methods using the Doppler effect, or by means of devices contained aboard the rocket which integrate the rocket's acceleration. In the simplest case, an accelerometer is installed on the frame of the rocket and its mass is displaced along the longitudinal axis x of the rocket. The mass of the accelerometer m_a will be subject to the resultant force composed of the acceleration due to gravity, the longitudinal acceleration of the rocket V and the normal acceleration of the rocket $V\dot{\theta}$ (fig. 15.9). Since the accelerometer is oriented along the longitudinal axis of the rocket, the signal produced by the accelerometer will be equal to

$$j_x = \dot{V}\cos\alpha + V\dot{\theta}\sin\alpha - g\sin(\theta + \alpha). \tag{15.71}$$

If we neglect the angle of attack, then /523

$$\dot{V} = j_x - g\sin\theta. \tag{15.72}$$

The angle θ may be replaced by its known programed value, then

$$V = \int_0^t j_x\,dt - g\int_0^t \sin\theta_з(t)\,dt. \tag{15.73}$$

Thus, in order to obtain the velocity it is necessary to integrate the readings of the accelerometer and take into account the second term in expression (15.73). One method of realizing this is to use a gyroscopic integrator[1]--a device which combines an accelerometer and an integrator. This device consists of a gyroscope whose external frame axis is directed along the x-axis of the rocket and does not pass through the center of gravity of the rotor (see Chapter 5).

This method of controlling range does not take into account many factors on the range error. In particular, the error in the coordinates of the burnout point is not taken into account. The error in the burnout altitude is also quite substantial. Equation (15.38) shows how we can eliminate the effect of the error in the burnout altitude on the range error. Let us recall that in equation (15.38) $R_0^1 = R_0 + H_a$, where H_a is the altitude of the active region of the trajectory and R_0 is the radius of the Earth. Elsewhere in equation (15.38) we have a product consisting of the square of the velocity V_a and the radius R_0^1. In connection with this, if the engine is turned off when the quantity $\eta = V^2 R_0^1 = V^2(R_0+H)$ reaches its assigned value $\eta_a = V_a^2(R_0+H_a)$, the effect of the altitude error will be excluded. The quantity η must be computed continuously by means of a computer operating with an inertial system.

If we neglect the curvature of the Earth along the active region of the trajectory, we can obtain η from equation

$$\eta = (R_0 + y)(\dot{x}^2 + \dot{y}^2), \tag{15.74}$$

where

$$\dot{x}^2 + \dot{y}^2 = V^2 \quad \text{and} \quad y = H;$$

y is the output of the second integrator of channel y; $\dot{y}$ is the output of the first integrator of channel y; x is the output of the second integrator of channel x; and $\dot{x}$ is the output of the first integrator of channel x.

Equation (15.74) does not take into account the effect of several less significant factors: the error in the length of the active region of the trajectory, errors in the weight of the rocket, etc. For this reason, more accurate methods have been developed for controlling the range which are based on a continuous /524

[1] V. I. Feodos'yev and G. E. Sinyarev, Introduction to Rocket Engineering, Oborongiz, 1960.

computation of range error during the entire active region of the trajectory.[1] This error is computed by measuring the deviation of the parameters of rocket motion from the programed values. The engine is turned off when the total range error is equal to zero. However, the total range error due to the effect of many factors may not become equal to zero at any period of time, particularly if we take into account such factors as atmospheric perturbations along the active region of the trajectory. To maintain a minimum value of this instantaneous range error, it is necessary to actuate the thrust of the engine and the pitch control surfaces as a function of this error over the entire active region of the trajectory. The implementation of this idea is associated with substantial technical difficulties and requires the installation of a digital computer aboard the rocket.

---

[1] G. Tsien, T. Adamson and E. Cute, Automatic Control of Long Range Rockets, "Problems of Rocket Technology," 1953, No. 1.

CHAPTER 16. MISSILE GUIDANCE SYSTEMS AND METHODS OF EVALUATING THE FIRING ACCURACY

16.1 General Information

In the preceding chapters we considered the equipment carried aboard the missile and the dynamics of automatic missile control for various guidance methods. However, in combat the control of missiles is achieved by a whole series of facilities which form the missile guidance system. The system includes the controlled missile with its war head and launching facilities, which in general include the tracking system and the launching control system. A missile control system is developed to achieve a more effective destruction of the target. The quantitative evaluation of missile control systems is one of the problems of operations research. There are various criteria for effectiveness and various approaches for establishing these criteria. For example, in the work of Merrill and others[1] the criterion of effectiveness of the weapon and of the guidance system is assumed to be the quantity E which is determined by the equation

$$E = \frac{D}{C},$$

where D is the total damage, and C is the total cost of the system.

In particular, quantity D depends on the hit probability. The probability of hitting the target in turn depends on the accuracy of firing or on the magnitude of miss distance at the target, on the charge in the warhead and the detonator, and the initial conditions for attacking the target, and the reliability of the control system as a whole and on many other factors. In line with the subject of the present book we shall consider only one of these factors: /526
the firing accuracy of guided missiles or the miss distance at the target. The value of the miss distance at the target is a result of a whole series of random factors and cannot be evaluated without recourse to the theory of probability. We shall evaluate firing accuracy as it applies to the systems of homing guidance and external guidance.

We shall make some preliminary remarks concerning the requirements for hit accuracy. The natural requirement for minimum or zero target miss is not always

---

[1] G. Merrill, G. Goldberg, P. Helmholz, Operations Research. Combat Part. Launching of Missiles, I. L., 1958.

feasible. If this requirement makes the entire system very complicated and increases its cost, then its reliability is decreased and no useful effect is achieved by increasing the accuracy. The requirements for accuracy must always be compared with the effectiveness of the missile warehead and with the technical possibilities of realizing the control system.

16.2 Homing Guidance Systems[1]

As an example, let us consider the homing guidance system for aerial combat. The system consists of one or several missiles carried aboard a fighter, launching devices and a sight. In launching target seeking missiles, sighting is a necessary operation. Sighting makes it possible to reduce the initial miss to a minimum. The accuracy achieved in hitting the target depends substantially on the initial conditions when the missile is launched. (According to the linear theory of homing guidance presented in Chapter 13, the miss at the target is proportional to the initial miss.)

If we require that at the instant of firing the initial miss be equal to 0, the sighting scheme for a guided missile will be the same as for an unguided missile[2]. At the moment of firing the missile must move to the instantaneous collision point with the target. For this reason, the missile must be fired at the instant of time when the following condition is satisfied (see equation (13.8) and figure 13.6)

$$0 = -V_T \sin\varphi + V \sin\psi, \tag{16.2}$$

(subscript T = target)

where V is the absolute velocity of the missile; and ψ is the lead angle.

/527

On the other hand, from the conditions of approach

$$L\dot{\varphi} = -V_{Tp} \sin\varphi + V_{fp} \sin\psi, \tag{16.3}$$

where V_{fp} is the velocity of the fighter plane.

By eliminating the product $V_T \sin\varphi$ from expressions (16.2) and (16.3), we obtain the equation of sighting

$$\sin\psi = -\varphi \frac{L}{V - V_{fp}} = -\dot{\varphi}T_p. \tag{16.4}$$

(subscript p = computed).

---

[1]V. I. Marisov and I. K. Kucherov, Guided Missiles, Voyenizdat, 1959.

[2]Under the assumption that the vectors of target velocity and missile velocity are constant.

According to equation (16.4), the launching of the missile takes place at the instant of time when the sine of the lead angle is equal to the product of the angular velocity of the line joining the fighter plane and the target and the computed time $T_p = \frac{L}{V - V_{fp}}$.[1] Equation (16.4) is used by the computer to compute the required or assigned value of the lead angle $\psi_3 = \arcsin \dot{\varphi} \cdot T_p$. To compute ψ_3 it is necessary to introduce the signals φ, L, V_{fp} and V into the computer. The signals $\dot{\varphi}$ and L are measured by the sight; the velocity V_{fp} is also measured aboard the fighter plane. As far as the velocity of the missile is concerned, its proposed average value is introduced into the computer.

We describe two types of maneuvers of a fighter plane which precede the launching of a guided missile. The first one consists of the following. After the target is sighted, the computer begins to calculate the value of ψ_3. The signal ψ_3 is fed to the display of the sight. The pilot turns the airplane in such a way that the actual lead angle ψ is equal to the programed lead angle. The actual lead angle is the angle between the axis of the airplane[2] and the axis of the sighting antenna directed towards the target (fig. 16.1). In practice this may be accomplished in the following manner: the computer determines the guidance error $\Delta\psi = \psi_3 - \psi$, and this error appears on the screen of the sight as a luminous point. The position of the luminous point gives the error components in the vertical and horizontal planes $\Delta\psi_{vertical}$ and $\Delta\psi_{horizontal}$. The pilot turns the airplane in such a way that the mark is at the center of the cross hairs when the sighting error is equal to 0. The pilot continues his flight so that the mark is at the center of the cross hairs. In this case condition $\psi = \psi_3$ is always maintained, and the pilot is always ready to launch the missile. When condition $\psi = \psi_3$ is maintained, the flight takes place along the so called attack curve.

We note that the movement along the attack curve may be automated by feeding a signal $\Delta\psi = \psi_3 - \psi$ to the automatic pilot of the fighter plane. The missile may be launched after the homing guidance head of the missile has captured /528

[1]The calculations of T_p may be carried out by using more exact equations.

[2]More accurately between the velocity vector of the airplane and the axis of the sight; however, in this case, the angles of attack and the angles of slip of the airplane must be introduced into the computer.

the target, which sends in a special signal to the pilot, or before the homing guidance head of the missile has captured the target.

In the latter case, it is desirable to program the movement of the missile in accordance with the data on the motion of the target and the missile available at the time the missile is launched.

The airplane may move along the attack curve with large load factors and consequently with large angles of attack. If the suspended missile is not oriented along the velocity vector of the airplane, its angle of attack will be greater when the angle of attack of the airplane is greater (fig. 16.2). This angle of attack has a perturbing effect which, according to (13.56), corresponds to some initial miss velocity.

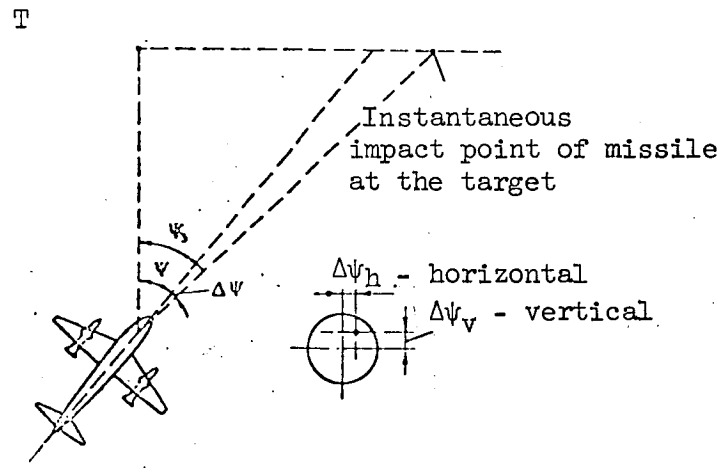

Figure 16.1. Schematic diagram showing first type of maneuver; h = horizontal, v = vertical.

To decrease the perturbation associated with the initial angle of attack of the missile, it is necessary to launch the missile when the flight of the fighter plane is almost rectilinear. To achieve this, a second maneuver is carried out in the following manner: after the target is captured by the sight, the fighter is brought into a position with respect to the target, such that the approach to /529

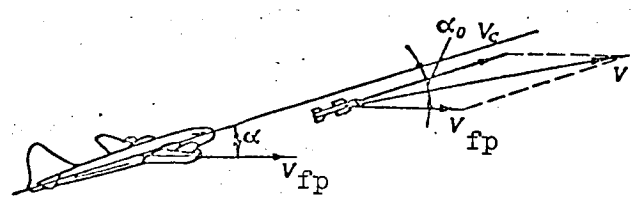

Figure 16.2. Schematic diagram of second maneuver: a, angle of attack of fighter plane at instant of launching; V_C, velocity of missile with respect to fighter plane; α_0, initial angle of attack of missile.

the target is carried out with a constant miss. This is equivalent to the fighter making a parallel approach to a hypothetic point situated behind the target. When this point is approached properly, the lead angle ψ or the angle between the distance to the target and the longitudinal axis of the fighter will decrease continuously (fig. 16.3). The computer of the sight actually compares the lead angle with a given value computed by means of equation (16.4).

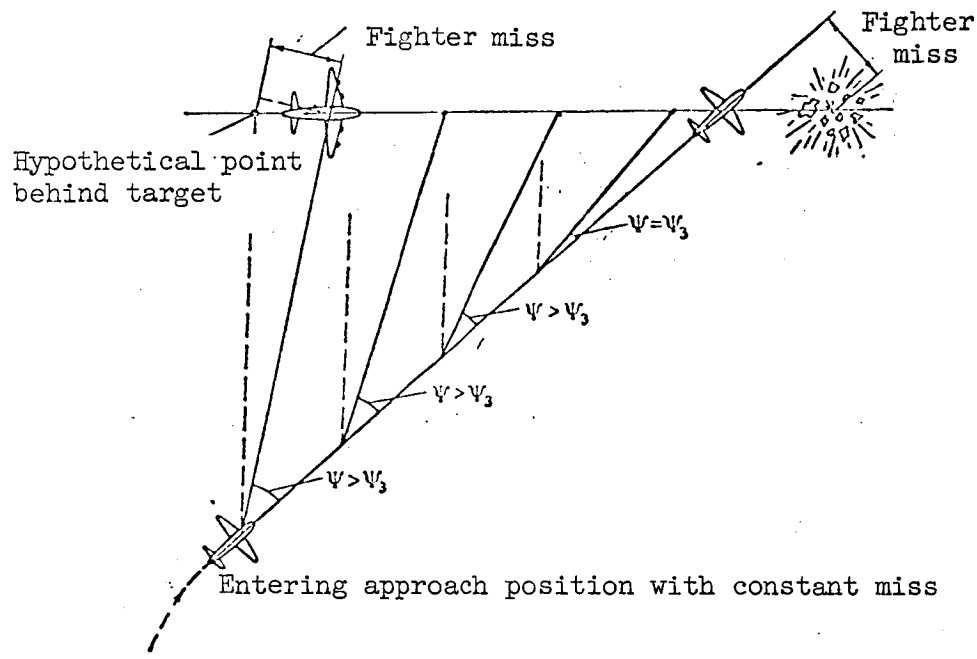

Figure 16.3. The schematic diagram showing the maneuver with constant miss.

At the instant of time when these two angles coincide the missile is launched. If the fighter plane continues to fly in a straight line after launching the missile, it will fly to the rear with an insignificant constant miss with respect to the target which is hit by the guided missile.

This short description of the guidance system points to a way for investigating the accuracy of hitting the target. As a measure of accuracy in hitting the target, we can take the root-mean-square value of the miss for a range when /530 the missile can no longer be guided due to the blinding of the homing head or when coordinates $\dot{\varphi}$, α, δ (see Chapter 13) achieve their limiting values. The value of the miss is computed by means of equation (13.46) if we assume $L = L_{tilt}$ and if $\dot{\varphi}$ and $V_{relative}$ correspond to this value of L. The miss value computed by means of equation (13.46) would be the true miss if the velocity vectors of the target and of the missile remained constant from the time when $L = L_{tilt}$. Actually the miss will differ from the value computed by means of equation (13.46) because of the maneuvers of the target. In spite of this, in the

calculations it is convenient to select the root-mean-square value of the miss for the range $L = L_{tilt}$, because it is precisely this value which characterizes

the quality of the process of controlling or guiding a missile in the linear theory of homing guidance. The miss represents a random vector quantity or a random two dimensional quantity.

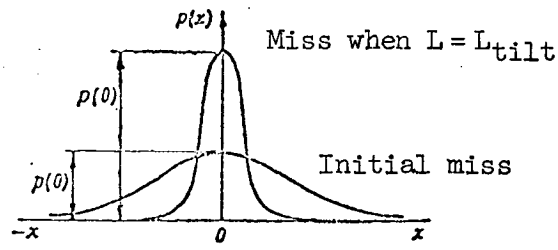

Figure 16.4. Curves showing probability density of miss in two-dimensional motion.

$$p(x) = \frac{1}{\sqrt{2\pi}\sigma_x} \exp\left(-\frac{x^2}{2\sigma_x^2}\right)$$

--probability density of miss; σ_x--mean square value of miss;

$$p(0) = \frac{1}{\sqrt{2\pi}\sigma_x}$$ --accuracy measurement.

The miss of a missile with homing guidance occurs first of all because the control system does not reduce the initial miss to zero, and in the second place because perturbations in the course of the missile's flight produce additional misses (see Chapter 8). In this connection it becomes necessary to take into account the internal noise in the control system and the external disturbances which react on the missile's control system.

Let us consider briefly both components of the miss and the methods of computing them.

The Miss Component Due to the Initial Miss or Due to the Initial Zero Conditions at the Instant of Firing.

This miss is unavoidable due to instrument errors and methodical errors associated with sights, due to perturbations at the instant of launching, due to inaccuracies in the launching equipment, due to pilot error, and due to many other factors. The many factors responsible for the initial miss make it possible to consider it as a random quantity, whose distribution follows the normal law. If we compute the sighting process by means of linear equations (see Chapter 13), the target miss will also have a distribution which follows the normal law. Figure 16.4 shows typical miss probability densities for two-dimensional motion. /531

The Miss Component Due to Noise and Perturbations

As an example, let us consider the functional diagram shown in figures 13.19 and 13.20 for missiles with a control system which provides for guidance by the method of parallel approach. The control system is subjected to noise $\nu(t)$, which is contained in the signal for the angular velocity of the line joining the missile and the target and which is of a complex nature. It is due to the fluctuations in the signal reflected by the target and the internal noise in the target coordinator. This noise has a nonstationary nature, particularly in connection with the continuously decreasing distance to the target. The perturbation due to the movements of the target is also a nonstationary random function of time in the general case. Finally we encounter a case when a nonstationary linear system is subjected to two nonstationary effects.

For statistically independent effects $\nu(t)$ and $f_x(t)$ the miss dispersion may be determined by means of equation (2.55). In this case $n = 2$; $R_{x1}(t_1,t_2)$ is the correlation function for $\nu(t)$, $R_{x2}(t_1,t_2)$ is the correlation function for $f_x(t)$; $k_1(t,\tau)$ is the pulse transfer function of the system for the noise $\nu(t)$ and $k_2(t,\tau)$ is the pulse transfer function for the perturbation.

If simultaneously we take into account the nonzero initial conditions (initial miss) and perturbations, the miss dispersion should be computed by means of equations similar to (2.57) and (2.58). These calculations are rather cumbersome. They are further complicated if we take into account the fact that the actual missile control systems are usually not linear. The principal effect on the value of the miss will be produced by nonlinearity of the limiting type.

The difficulty of computing the dispersion and the mathematical expectation of the miss forces us to use different simulation methods for determining the probability nature of miss or the hit accuracy. Let us consider briefly the simulation techniques. In this case the model of the system (whether it is purely mathematical or of a hybrid type) should be subjected simultaneously to all the random signals whose effect must be investigated. We must provide for a coincidence of the probability characteristics of these signals with the characteristics of real random perturbations which will act on the missile during its flight. After this, the firing of the missile is simulated many times for random combinations of initial conditions and possible target movements. As a result the miss is determined for each simulation process, i.e., the minimum flight distance of the missile from the center of the target. Depending on the /532 nature of the detonator used in the missile, the miss may be represented by two or three coordinates. For the case of an impact detonator the miss is characterized by two coordinates in a plane perpendicular to the trajectory of the missile in the region of the target. If the target is on the surface, the dispersion for the impact detonator must be considered in the plane which coincides with the surface of the Earth. For a proximity fuse the miss is determined by three coordinates.

As an illustration let us consider the simpler case of a missile with an impact fuse. Let us assume that n firings have been performed by the simulator,

and that the coordinates (x_1,y_1), (x_2,y_2), ... (x_n,y_n) of n flight points of the missile through the above plane have been recorded. The origin of the coordinates coincides with the target, while the axes are situated in the plane in which the dispersion is determined in the following manner: the x-axis lies in the firing plane, while the y-axis is perpendicular to it. The results of simulating the firings may be represented graphically as shown in figure 16.5.

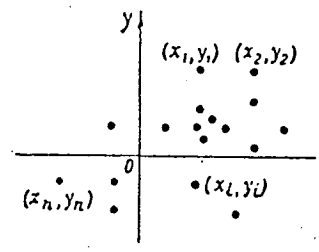

Figure 16.5. Graphic presentation of results obtained by simulating firing.

We assume that the dispersion of guided missiles is subject to the normal distribution law, as in the case of unguided missiles. This assumption is based on the fact that a deviation of the impact point of the missile from the center of the target is assumed to be due to the combined effect of a large number of relatively insignificant and independent factors. This situation is responsible for the normal distribution law describing the probability of random quantities. We shall also assume that the coordinate axes selected above are the principal axes of the dispersion ellipse. In a coordinate system of this type the abscissa and the ordinate of the flight point of the missile through the target plane are independent random quantities, and their distribution law is determined by 4 parameters: by the coordinates of the dispersion ellipse center m_x and m_y and by dispersions σ_x^2 and σ_y^2. These parameters are computed by means of the following equations.

$$m_x = \frac{\sum_{i=1}^{n} x_i}{n}; \qquad m_y = \frac{\sum_{i=1}^{n} y_i}{n};$$

$$\sigma_x^2 = \frac{\sum_{i=1}^{n} (x_i - m_x)^2}{n-1}; \qquad \sigma_y^2 = \frac{\sum_{i=1}^{n} (y_i - m_y)^2}{n-1}:$$

When we evaluate the results of the firings we must use the concept of the probable deviation E instead of the root-mean-square deviation σ. For the normal distribution law, these parameters are associated by the following relation /533

$$E = 0.675\sigma.$$

It is necessary to carry out a very large number of simulated firings (of the order of several hundred) to obtain a sufficiently accurate evaluation of

missile dispersion. If the result of the simulation indicates that the center of dispersion ellipse of the missile is at a considerable distance from the target, this points to some defects in the control system or defects in the proposed guidance method. Both of these causes must be established and eliminated. If, on the other hand, the root-mean-square or the probable deviations of the missile exceed the allowable limits, the signal circuit must be provided with additional elements, which decrease the effect of random perturbations on the flight of a guided missile or which vary to some extent the parameters of individual elements of the missile control system.

16.3 External Missile Guidance Systems

External missile guidance systems are quite diverse. They are considerably more diverse than the homing guidance systems. The external guidance system may include a homing guidance system for guiding the missile along the terminal region of its projectory when it approaches a target. Figures 16.6, 16.7 and 16.8 show three variations of external guidance systems for antiaircraft missiles. Figure 16.6 shows a missile guidance system using a beam coincidence method. The coordinates of the target (azimuth, the elevation angle $\varphi_{\text{target elevation}}$ and range) are determined by a special radar which operates as an automatic tracking device. Guidance is achieved by the guidance radar. The latter produces a signal aboard the missile for the lateral deviation from the equisignal zone of the radio beam.

The target is tracked by means of radar signals which are processed by the computer. The computer introduces a correction for the parallax which occurs because the tracking radar is separated from the guidance radar. When these two radars are sufficiently close together the parallax becomes insignificant and the need for a computer disappears. In this case the guidance antenna is locked onto the tracking antenna. /534

1--guidance radar

2--φ target guidance

3--computer

4--radar target sight

5--φ target elevation.

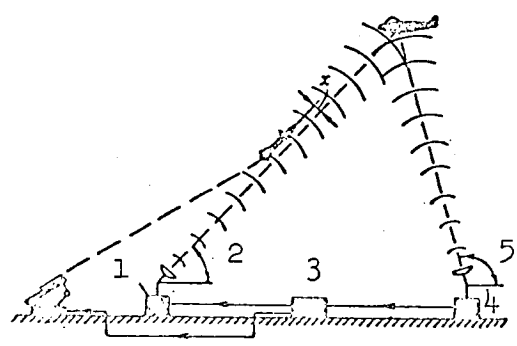

Figure 16.6. First version of missile external guidance system.

Figure 16.7 shows a system with 2 radars for tracking the target and the missile. The coordinates of the target and the missile (azimuths, elevation angles and ranges) are measured by radars and are fed to the computer. The

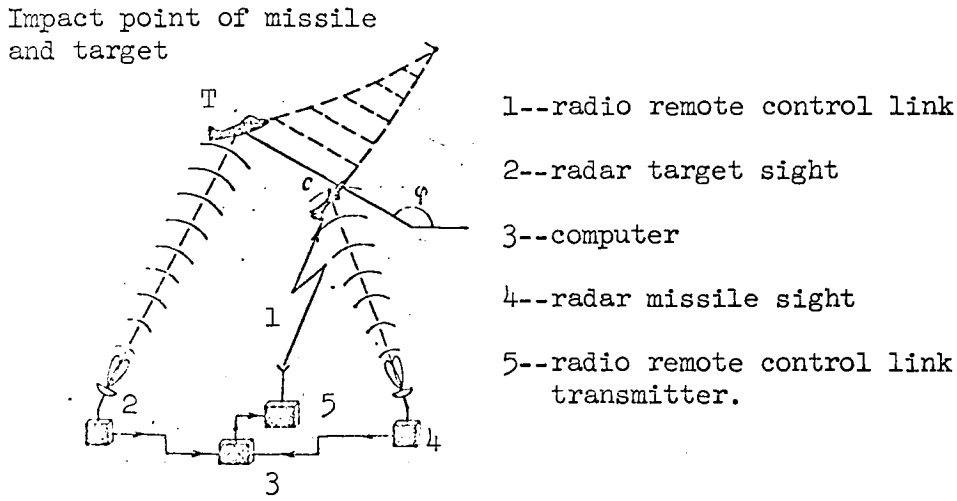

Figure 16.7. Second version of external missile guidance system.

computer develops the control commands, which are transmitted to the missile by the radio control link. The computer makes it possible to realize any method for guiding the missile to the target: pursuit, superposition, parallel approach, etc. Figure 16.7 shows the method of parallel approach. In this method the radio link is used to transmit two components of the angular velocity vector of the line joining the missile and the target obtained by the computer, or such values of pitch and course angles of the missile for which $\dot{\vec{\varphi}}$ becomes equal to 0.

The two external guidance systems which we have considered have a short range. The range is increased by using a search radar to determine the coordinates of the target and the missile. The antenna of this search radar rotates with a constant angular velocity Ω. Figure 16.8 shows the system with the search radar. In this radar, the discrete values for the coordinates of the target and the missile are recorded periodically. These coordinates are fed to the computer, which generates the control signals and transmits them over the radio link to the missile. In this case the control system is a sampled-data system. Some of the special features associated with the dynamics of sampled-data guidance systems were described in Chapter 14. It is not possible to guide /535

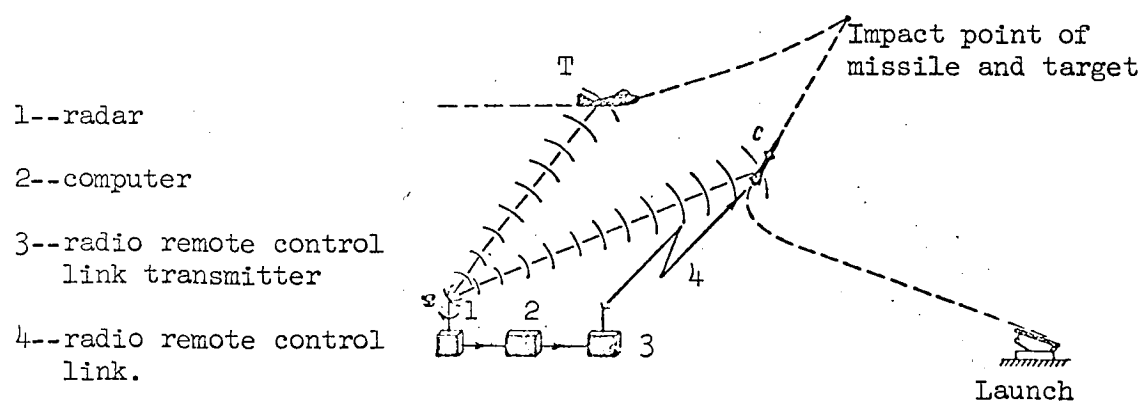

Figure 16.8. Third variation of external missile guidance system.

the missile all the way to the target by this method because of the low accuracy in determining the coordinates by means of the search radar. Indeed, if we assume, for example, that the radar beam has a width of 0.2°, then the position of the target at a distance of 300 km will be determined with an accuracy of 1.0 km. In this connection the search radars are used to guide a fighter plane, which may be piloted or pilotless. The commands from the computer guide the fighter to the region of the target where the latter can be captured either by radar equipment aboard the fighter plane or by means of a sight carried aboard the fighter plane. After this, the target is attacked with antiaircraft gunnery or with guided or unguided missiles. Pilotless fighters usually use guided missiles. A pilotless fighter may therefore be called a two-step guided missile.

In considering the accuracy of guiding missiles we shall limit ourselves to the case when the missile is guided by a radio beam (fig. 16.9). The special features of this method, which is associated with a direct measurement of the signal produced by the linear deviation from the equisignal zone, make it possible to evaluate the accuracy of guidance by using the theory for the accuracy of conventional stationary tracking systems or servomechanisms. In this case it is possible to evaluate the dynamic accuracy of guidance and the accuracy in the presence of perturbations associated primarily with the fluctuations of the equisignal zone. To evaluate the dynamic accuracy of guidance, it is necessary to determine the time function $Z_3 = Z_3(t)$, in equation (11.14). /536

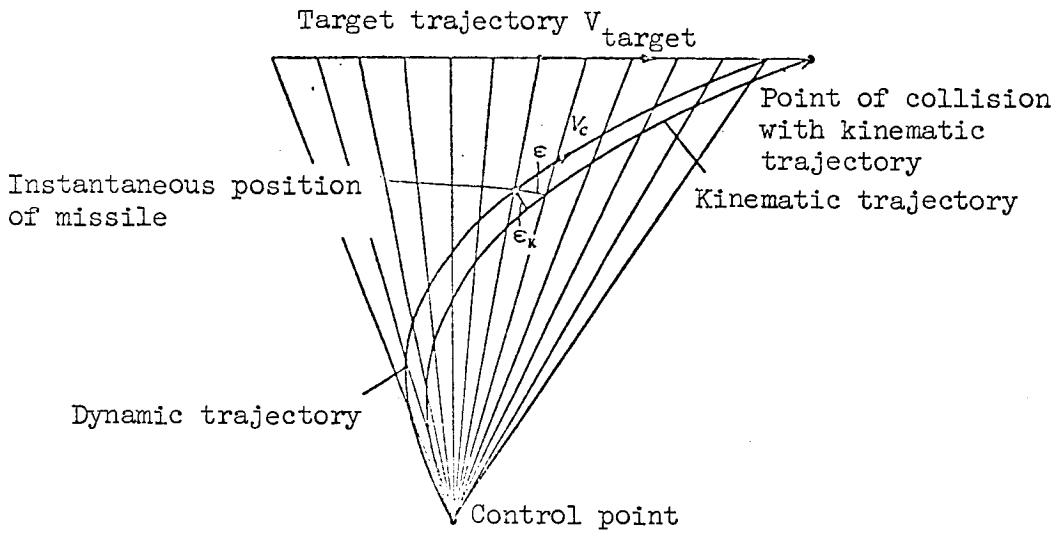

Figure 16.9. Guidance of missile by radio beam: ϵ--deviation from equisignal zone; ϵ_K--deviation from kinematic trajectory; ϵ_K--$\epsilon_{Kinematic}$

Figure 16.9 shows the instantaneous positions of the equisignal zone and also the kinematic and dynamic trajectories of the missile. From the figure it is clear that the deviation of the missile from the equisignal zone ϵ is not equal to the deviation from the dynamic trajectory from the kinematic trajectory

$\epsilon_{Kinematic}$. We can judge the miss of the missile from the values ϵ and ϵ_K, taken at the instant of time when the missile impacts the target. It is clear, however, that neither ϵ nor ϵ_K taken at this instant of time represent the true miss, but differ little from it. To obtain a refined value for the miss it would be necessary to write the beam guidance equations as a variation of homing guidance with a lead angle (see Chapter 14). However, in this case it would be impossible for us to estimate the misses by using the theory for the accuracy of stationary systems and, what is most important, to use this theory for the synthesis of the missile control system. /537

As we have pointed out in Chapter 14, to determine the accuracy by means of error ϵ_K we must first determine the normal acceleration along the kinematic trajectory as a function of time $j = j(t)$. Error ϵ_K is computed as resulting from perturbation $j(t)$, applied at a point in the functional diagram where the normal acceleration is recorded.

Let us consider the simplified functional diagrams shown in figure 14.12.[1] For simplified equations and functional diagrams it is assumed that the angles of attack of missiles with cruciform wings and plane wings are proportional (without delay) to the deflection of the control surface, or to the total output signal of the compensating network. For the lateral motion of a missile with plane wings, the simplification consists of assuming the same relationship between the tilt angle and the output signal of the compensating network. Since the force normal to the trajectory is proportional to the angles of attack and tilt, the output of the compensating network in the simplified drawings will be at the same point where the acceleration is recorded. Figure 16.10 shows simplified functional diagrams: the diagram with a series compensating device (fig. 16.10a) and the diagram with series and parallel compensating device (see fig. 16.10b, also Chapter 11). The parallel compensating device indicates that there is feedback in the course signal or in the signal for the velocity of lateral deviation $\dot{y}$. First, let us determine error ϵ_K produced by perturbation $j(t)$ for the diagram in figure 16.10a. When $x(t) = 0$, output y is equal to ϵ_K with a reversed sign. Therefore[2]

$$\epsilon_K = \frac{\frac{1}{p^2}}{1 + W(p)} j(t), \tag{16.5}$$

where

$$W(p) = \left[k\frac{T_1 p + 1}{T_2 p + 1} + \frac{q}{p}\right]\frac{1}{p^2} = \frac{kT_1 p^2 + (T_2 q + k)p + q}{(T_2 p + 1)p^3}$$

---

[1] In these diagrams $Z_3(t)$ is designated by $x(t)$.

[2] The transfer functions in this case may be written more conveniently as functions of the argument $p = d/dt$.

is the transfer function of the open loop.

Substituting W(p) into the expression for ε_K, we obtain

$$\varepsilon_K = \frac{(T_2 p + 1)\, p}{T_2 p^4 + p^3 + kT_1 p^2 + (T_2 q + k)\, p + q}\, j(t). \tag{16.6}$$

To reduce perturbation j(t) to the input, i.e., to find an x(t) which would lead to the same error, we write the expression for the error at input x(t). As we know in this case

$$\varepsilon_{xK} = \frac{1}{1 + W(p)}\, x(t) = \frac{(T_2 p + 1)\, p}{T_2 p^4 + \ldots + q}\, p^2 x(t). \tag{16.7}$$

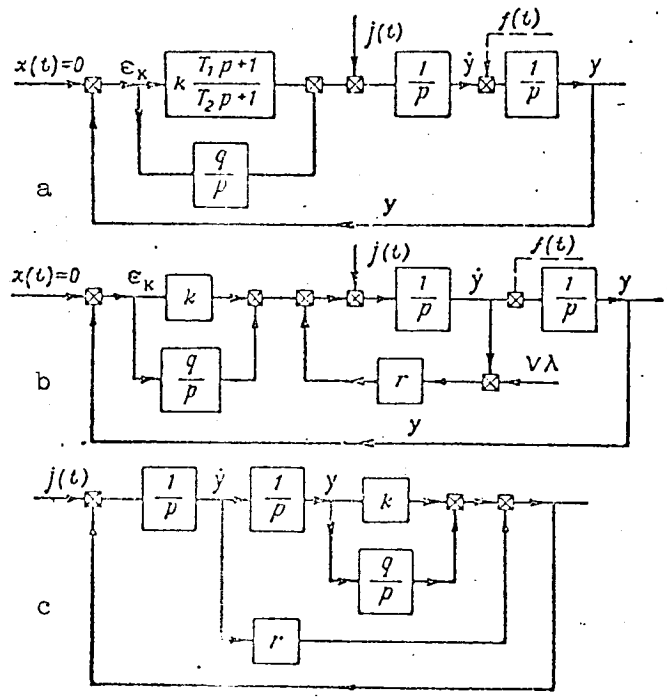

Figure 16.10. Functional diagram of external guidance system. a--with series; b--with series and parallel compensating devices; c--transformed diagram b.

Comparing expressions (16.6) and (16.7) we note that for this diagram

$$j(t) = \frac{d^2 x(t)}{dt^2}$$

or

$$x(t) = \int_0^t \int_0^t j(t)\, dt \cdot dt.$$

Now let us determine the error and the equivalent action x(t) for the diagram in figure 16.10b. As in the previous case for error ε_K, it is necessary to find output y due to perturbation j(t). It is more convenient to do this by using the transformed functional diagram shown in figure 16.10c. From this diagram we find /539

$$\varepsilon_K = \frac{\frac{1}{p^2}}{1 + W_1(p)} j(t), \tag{16.8}$$

where

$$W_1(p) = \frac{rp^2 + kp + q}{p^3},$$

and

$$\varepsilon_K = \frac{p}{p^3 + rp^2 + kp + q} j(t). \tag{16.9}$$

The error in reproducing the input signal x(t) for the diagram shown in figure 10.16b is

$$\varepsilon_K = \frac{1}{1 + W_2(p)} \cdot x(t), \tag{16.10}$$

and

$$W_2(p) = \frac{kp + q}{(p + r)\, p^2}. \tag{16.11}$$

We note that the transfer functions of the open loop system for the basic and transformed functional diagram (fig. 16.10b) are different, see equations (16.8) and (16.11). Substituting the equation into (16.10), we find

$$\varepsilon_K = \frac{(p + r)\, p^2}{p^3 + rp^2 + kp + q} \cdot x(t). \tag{16.12}$$

Comparing equations (16.9) and (16.12), we find that j(t) and x(t) are related by the operator

$$x(t) = \frac{1}{p^2 + rp} j(t).$$

In other words, when j(t) is known, function x(t) may be obtained from the solution of the differential equation

$$\ddot{x} + r\dot{x} = j(t).$$

The expressions which we have derived for the errors may be used to compute these after function j(t) is obtained from the investigation of the kinematics.

We can see from expressions (16.2) and (16.5) that the integral of the signal error in the control law (the coefficient q) makes the error equal to 0 when the acceleration is constant, i.e., when flight takes place along a circular kinematic trajectory. If, on the other hand, we let q = 0 in these expressions, /540 then a constant acceleration will lead to a stable error. Since the duration of the transient process associated with placing the missile on the beam, as a rule, is less than the flight time of the missile until it meets the target, the dynamic error may be computed by means of the error coefficients. In this case the operational transfer functions in expressions (16.6) and (16.9) or in equations (16.7) and (16.12) should be expanded in the power series of p, if x(t) is determined, i.e., it is necessary to represent the equalities (16.6) and (16.9) in the form

$$\varepsilon_\kappa = (c_0 + c_1 p + c_2 p^2 + \ldots) j(t) = \\ = \left[c_0 j(t) + c_1 \frac{dj}{dt} + c_2 \frac{d^2 j}{dt^2} + \ldots \right].$$

When $q \neq 0$, the error coefficient $c_0 = 0$ and, conversely, when $q = 0$, the error coefficient is $c_0 = \frac{1}{k}$ (for the functional diagram in figures 16.10a and b).

Now let us compute the dynamic error ϵ, which represents the deviation of the missile from the equisignal zone of the radio beam. In Chapters 11 and 14 we considered the equations of motion of a missile with respect to a stationary beam or with respect to a beam which moves parallel to its initial position. In the present case (the guidance of antiaircraft missiles), the equisignal zone of the beam rotates with a certain angular velocity $\dot{\lambda} = \dot{\lambda}(t)$ (fig. 16.11). Therefore, it is sufficient to consider the equation of kinematic coupling, the third equation in system (11.1).

Turning to figure 16.11, we write the expression for the total derivative of the deviation y or of the error ϵ for a small angle $\theta - \lambda$:

$$\frac{dy}{dt} = (\theta - \lambda) V - L\dot{\lambda}$$

or

$$\frac{dy}{dt} = V\theta + f(t), \tag{16.13}$$

where f(t) equals $-V\lambda - L\dot{\lambda}$ is the perturbation which occurs when the missile moves along a curvilinear path.

Function f(t) is computed by investigating the kinematics of guidance, which gives us the law for the angular displacement of the beam $\dot{\lambda} = \dot{\lambda}(t)$ and the distance from the guidance point to the projection of the missile on the instantaneous position of the beam. We may assume approximately that $L(t) = Vt$.

Equation (16.13) shows that in the functional diagrams shown in figure 16.10 the perturbation for f(t) is applied at the point where the derivative

dy/dt is recorded. On these functional diagrams the reactor f(t) is designated by a broken arrow to emphasize the fact that we can consider the acting perturbation j(t) or f(t).

Let us write the expression for the error in the functional diagram of figure 16.10a /541

$$\varepsilon = \frac{\frac{1}{p}}{1 + W(p)} f(t) = \frac{(T_2 p + 1) p^2 f(t)}{p^3 + \ldots + (T_2 q + k) p + q} \tag{16.14}$$

and for the diagram in figure 16.10b

$$\varepsilon = \frac{\frac{1}{p}}{1 + W_2(p)} f(t) = \frac{(p + r) p}{p^3 + r p^2 + k p + q} f(t). \tag{16.15}$$

Comparing expressions (16.14) and (16.15), we note that when f(t) is a linear function of time a stable error does not occur in the diagram of figure 16.10a, while in the diagram of figure 16.10b it does occur. This is due to the fact that the feedback signal in the diagram is picked up before the point where the perturbation is applied. The feedback signal picked up at this point means that the control law contains a signal proportional to the angle θ. We can substantially reduce the value of the steady-state error, if we introduce a programed signal $\lambda = \lambda(t)$ in the feedback loop. As far as the coupling between the perturbation f(t) and the equivalent input signal x(t) is concerned, the following expression will be valid for both diagrams $x(t) = \int_0^t f(t)\,dt$.

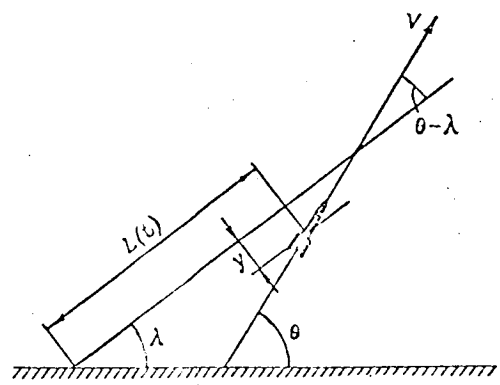

Figure 16.11. Geometry of guiding missile by means of beam.

The miss of a missile guided by a beam depends not only on dynamic errors, but also on the fluctuations of the equisignal zone of the radio beam. The fluctuations of the equisignal zone are produced by the fluctuations in the signal reflected by the target and by noise in the transceivers of the system.

Fluctuations of the equisignal zone represent noise which is applied at the input of the functional guidance system. Thus, a sum consisting of the useful signal x(t) and interference $\nu(t)$ act at the input of the guidance system. In this case x(t) as well as $\nu(t)$ must be considered as random functions of time in the general case.

As a rule the random function $\nu(t)$ may be considered stationary. If the target flies with a constant azimuth and the control point for the antiaircraft missile is situated along the projection of the target trajectory and the Earth's surface, the beam will move in one plane. In this case the miss component of the missile normal to the beam displacement plane will depend only on the fluctuating noise $\nu(t)$. When the random function $\nu(t)$ is stationary, the root-mean-square value of this miss component is computed by means of the following equation /542

$$\sigma_x^2 = \int_0^\infty |\Phi(j\omega)|^2 S_\nu(\omega)\, d\omega,$$

where S $\nu(\omega)$ is the spectral density of the noise $\nu(t)$, and $\Phi(j\omega) = \frac{W(j\omega)}{1 + W(j\omega)}$ is the transfer function for the closed loop beam guidance system.

For the diagram in figure 16.10a

$$W(j\omega) = \frac{kT_1(j\omega)^2 + (T_2 q + k) j\omega + q}{(T_2 j\omega + 1)(j\omega)^2};$$

while for the diagram in figure 16.10b

$$W(j\omega) = \frac{k(j\omega) + q}{(j\omega + r)(j\omega)^2}.$$

If we also represent x(t) as a stationary random function, the mean-square-root value of the miss is computed by means of the following equation

$$\sigma_x^2 = \int_0^\infty |\Phi(j\omega)|^2 S_\nu(\omega)\, d\omega + \int_0^\infty |\Phi_\varepsilon(j\omega)|^2 S_x(\omega)\, d\omega,$$

where $\Phi_\varepsilon(j\omega) = \frac{1}{1 + W(j\omega)}$ is the transfer function of the errors; and $S_x(\omega)$ is the spectral density of the signal x(t).

If $x(t)$ is not represented with sufficient accuracy by the stationary random function, and if the transient processes are not damped sufficiently well by the action of stationary noise $\nu(t)$ and of the initial conditions, we should use the equations or the simulation method presented in Chapter 2 for computing the miss.

REFERENCES

/543

1. Astronavigation Control System for Long-Range Missiles (Astronavigatsionnaya sistema upravleniya snaryadov dal'nego deystviya). Voprosy Raketnoy Tekhniki, No. 4, 1958.

2. Bachelor, John. Theory of Homogeneous Turbulence (Teoriya odnorodnoy turbulentnosti). Foreign Literature Publishing House (I.L.), 1955.

3. Bonni, Ye. A., Zucrov, M.D. and Besserer, K.U. Aerodynamics, Theory of Reactive Engines, Construction and Design Practice (Aerodinamika, teoriya reaktivnykh dvigateley, konstruktsiya i praktika proyektirovaniya). Voyenizdat, 1959.

4. Bramson, M.A. and Kalikeyev, A.Ye. Infrared Engineering in Capitalistic Nations (Infrakrasnaya tekhnika kapitalisticheskikh stran). Sovetskoye Radio, 1960.

5. Braslavskiy, D.A., Logunov, S.S. and Pel'nor, D.S. Design and Construction of Aviation Instruments (Raschet i konstruirovaniye aviatsionnykh priborov). Oborongiz, 1954.

6. Burgess, E. Controlled Reactive Weapons (Upravlyayemoye reaktivnoye oruzhiye). I.L., 1958.

7. Van Horn. Simulation Method for Determining Hit Probability and the Solution of Associated Statistical Problems (Metod modelirovaniya dlya opredeleniya veroyatnosti popadeniya i resheniya svyazannykh s etim statisticheskikh zadach). Voprosy Raketnoy Tekhniki, No. 6, 1958.

8. Gutkin, L. S. Radio Control of Pilotless Objects (Printsip radioupravleniya bespilatnymi ob'yektami). Sovetskoye Radio, 1959.

9. - - - Theory of Optimium Radio Reception Methods in the Presence of Fluctuating Noise (Teoriya optimal'nykh metodov radiopriyema pri flyuktuatsionnykh pomekhakh). Gosenergoizdat, 1961.

10. Getlend, K.U. Development of Guided Missiles (Razvitiye upravlyayemykh snaryadov). I.L., 1956.

11. Dobrolenskiy, Yu. P. Atmospheric Turbulence as a Source of Perturbations for Airplane Automatic Control Systems (Turbulentnost' atmosfery kak istochnik vozmushcheniy dlya sistem avtomaticheskogo upravleniya samoletom). Izv. AN SSSR, Energetika i Avtomatika, No. 5, 1961.

12. Duncan. Analysis of an Inertial Control System (Analiz inertsial'noy sistemy upravleniya). Voprosy Raketnoy Tekhniki, No. 5, 1958.

13. Klas. Infrared Engineering Challenges the Monopoly of Radar (Infrakrasnaya tekhnika osparivayet monopoliyu radiolokatsii). Voprosy Radiolokatsionnoy Tekhniki, No. 2, 1958.

14. Krasovskiy, A.A. and Pospelov, G.S. Principles of Automation and Engineering Cybernetics (Osnovy avtomatiki i tekhnicheskoy kibernetiki). Gosenergoizdat, 1962.

15. Kolosov, S.P. Elements of Aviation Automatic Devices (Elementy aviatsionnykh avtomaticheskikh ustroystv). Oborongiz, 1958.

16. Kooy, I. and Yutenbogart, I. Rocket Dynamics (Dinamika raket). Oborongiz, 1950.

17. Krysenko, G.D. Control of Reactive Missiles (Upravleniye reaktivnymi snaryadami). Voyenizdat, 1960.

18. Loytsyanskiy, L.G. and Lur'ye, A.I. Theoretical Mechanics (Kurs teoreticheskoy mekhaniki). Vol. II, Gostekhizdat, 1954.

19. Lokk, A.S. Guided Missiles (Upravlyayemyye snaryady). Gostekhizdat, 1957.

20. Lening, John H. and Bettin, R.G. Random Processes in Automatic Control Problems (Sluchaynyye protsessy v zadachakh avtomaticheskogo upravleniya). I.L., 1958.

21. Margolin, I.A. and Rumyantsev, N.P. Principles of Infrared Engineering (Osnovy infrakrasnoy tekhniki). Gosenergoizdat, 1955.

22. Marisov, V.I. and Kucherov, I.K. Guided Missiles (Upravlyayemyye snaryady). Voyenizdat, 1959.

23. Meyerov, M.V. Automatic Control of Electrical Equipment (Osnovy abtomaticheskogo regulirovaniya elektricheskikh mashin). Gosenergoizdat, 1952.

24. Merrill, G., Goldberg, G. and Helmholtz, P. Operations Research, Combat Units, Missile Launching (Issledovaniye operatsiy, boyevyye chasti, pusk snaryadov). I.L., 1959.

25. Met'yuz. Analytical Determination of Guided Missile Flight Parameters (Analiticheskoye opredeleniye velichiny proleta upravlyayemogo snaryada). Voprosy Raketnoy Tekhniki, No. 3, 1958. /544

26. Muller, F. Remote Control (Teleupravleniye). I.L., 1957.

27. Ostoslavskiy, I.V. Aerodynamics of the Airplane (Aerodinamika samoleta). Oborongiz, 1957.

28. Pospelov, G.S. Automatic Pulse Control Systems, Collected Works "Automatic Control and Computer Engineering" (Impul'snyye sistemy avtomaticheskogo regulirovaniya, Sb. statey "Avtomaticheskoye upravleniye i vychislitel'naya tekhnika"). Mashgiz, No. 3, 1960.

29. - - - Special Methods for Increasing the Quality of the Control Process (Spetsial'nyye priyemy povysheniya kachestva protsessa regulirovaniya). Izv. AN SSSR, Energetika i Avtomatika, No. 3, 1960.

30. Pospelov, G.S. and Dobrolenskiy, Yu.P. The Method of Standard Coefficients for Selecting the Parameters of a Linear Control System (Metod standartnykh koeffitsiyentov dlya vybora parametrov lineynykh sistem avtomaticheskogo regulirovaniya). Collected Articles on Automation and Electrical Engineering, Izd. AN SSSR, 1956.

31. Pospelov, G.S. Vibratory Linearization of Relay Automatic Control Systems. Reaction of Relay Systems to Slowly Varying Perturbations. (Vibratsionnaya linearizatsiya releynykh sistem avtomaticheskogo regulirovaniya, reaktsiya releynykh sistem na medlenno menyayushchiyesya vozmushcheniya). Proceedings of the Second All-Union Conference of the Theory of Automatic Control. Izd. AN SSSR, 1955.

32. Russel. Inertial Control Systems for Reactive Missiles (Inertsial'nyye sistemy upravleniya reaktivnykh snaryadov). Voprosy Raketnoy Tekhniki, No. 6, 1958.

33. Ril. Requirements for Guided Missile Control Systems. Stabilization and Guidance. (Trebovaniya k sistemam upravleniya snaryadami. Stabilizatsiya i navedeniye). Voprosy Raketnoy Tekhniki, No. 4, 1958.

34. Rosser, D., Newton, P. and Gross, G. Mathematical Theory of Uncontrolled Rockets (Matematicheskaya teoriya poleta neupravyayemykh raket). I.L., 1950.

35. Slomyanskiy, G.A. and Pryadilov, Yu.N. Floating Gyroscopes and Their Application (Poplavkovyye giroskopy i ikh primeneniye). Oborongiz, 1958.

36. Smirnoff, V.I. Course in Higher Mathematics (Kurs vysshey matematiki). Gostekhizdat, 1948.

37. Smit, R., Jones, F. and Chesmer, R. Detection and Measurement of Infrared Radiation (Obnaruzheniye i izmereniye infrakrasnogo izlucheniya). I.L., 1959.

38. Solodov, A.B. Linear Automatic Control Systems with Variable Parameters (Lineynyye sistemy automaticheskogo upravleniya s peremennymi parametrami). Fizmatgiz, 1962.

39. Solodnikov, V.V. Statistical Dynamics of Linear Automatic Control Systems (Statisticheskaya dinamika lineynykh sistem avtomaticheskogo upravleniya). Fizmatgiz, 1960.

40. Handbook of Automatic Control under the Editorship of John Traxel (Spravochnaya kniga po tekhnike avtomaticheskogo regulirovaniya, pod redaktsiy Dzh. Traksela). Gosenergoizdat, 1962.

41. Stepanov, B.M. Radar Survey (Radiolokatsionnyy obzor). Voyenizdat, 1959.

42. Tsien, G., Adamson, T., and Cute, E. Automatic Control of Long Range Missiles (Avtomaticheskoye upravleniye raketami dal'nego deystviya). Voprosy Raketnoy Tekhniki, No. 1, 1953.

43. Tipugin, V.N. and Veytsel', V.V. Remote Radio Control (Radioteleupravleniye). Sovetskoye Radio, 1962.

44. Guided Missiles (Upravlyayemyye snaryady). I.L., 1960.

45. Feodos'yev, V.I. and Sinyarev, G.B. Introduction to Rocket Engineering (Vvedeniye v raketnuyu tekhniku). Oborongiz, 1960.

46. Fridlender, G.O. and Kozlov, M.S. Aviation Gyroscope Devices (Aviatsionnyye giroskopicheskiye pribory). Oborongiz, 1961.

47. Tsypkin, Ya. Z. Theory of Automatic Control Relay Systems (Teoriya releynykh sistem avtomaticheskogo regulirovaniya). Gostekhizdat, 1955.

48. Shtol'tse. Principal Characteristics of Long-Range Ballistic Missiles (Osnovnyye kharakteristiki dal'nykh ballisticheskikh raket). Voprosy Raketnoy Tekhniki, No. 5, 1958.

49. Shchukin, A.N. Dynamic and Fluctuation Errors of Controlled Objects (Dinamicheskiye i flyuktuatsionnyye oshibki upravlyayemykh ob"yektov). Sovetskoye Radio, 1961.

50. Elements of Inertial Guidance Systems (Elementy inertsial'nykh navigatsionnykh sistem). Voprosy Raketnoy Tekhniki, No. 2, 1959.

51. Janke, E. and Emde, F. Tables of Functions with Equations and Curves (Tablitsy funktsiy s formulami i krivymi). Fizmatgiz, 1959.

52. Press, H., Meadows, M. T. and Hadlock, I.A. Reevaluation of Data on Atmospheric Turbulence and Airplane Gust Loads for Application in Spectral Calculations. NACA Report No. 1272, 1956.

53. Grensted, P.E.W. Stability Criteria for Linear Equations with Time-Varying Coefficients, RAS, No. 3, 1956.

Translated for the National Aeronautics and Space Administration by John F. Holman and Co. Inc.